NOVA SCHOOL OF SCIENCE & TECHNOLOGY

DEPARTAMENT OF EARTH SCIENCES

PLEISTOCENE VERTEBRATES FROM PORTUGAL:

Paleobiodiversity, paleoecology and quality of the fossil record.

Darío Estraviz-López

Master in Paleontology

DOCTORATE IN GEOLOGY

NOVA University Lisbon

May, 2025

DEPARTAMENT OF
EARTH SCIENCES

PLEISTOCENE VERTEBRATES FROM PORTUGAL:

PALEOBIODIVERSITY, PALEOECOLOGY AND QUALITY OF THE FOSSIL RECORD

Darío Estraviz-López

Master in Paleontology

Adviser: María Ríos Ibáñez
Researcher, NOVA University Lisbon

Co-advisers: Aurora María Grandal D´Anglade
Associate Professor, University of A Coruña

Examination Committee:

Chair: José Carlos Ribeiro Kullberg,
Full Professor, NOVA University Lisbon

Rapporteurs: Cleia Detry Cardoso e Cunha,
Assistant Professor, University of Lisbon
Alejandro Pérez-Ramos,
Postdoctoral researcher, University of Málaga

Adviser: Aurora María Grandal D´Anglade,
Associate Professor, University of A Coruña

Members: José Carlos Ribeiro Kullberg,
Full Professor, NOVA University Lisbon
Vicente Daniel Crespo Roures,
Researcher, NOVA University Lisbon

DOCTORATE IN GEOLOGY

NOVA University Lisbon
May, 2025

Pleistocene vertebrates from Portugal: Paleobiodiversity, paleoecology and quality of the fossil record.

Copyright © Darío Estraviz-López, NOVA School of Science and Technology, NOVA University Lisbon.

The NOVA School of Science and Technology and the NOVA University Lisbon have the right, perpetual and without geographical boundaries, to file and publish this dissertation through printed copies reproduced on paper or on digital form, or by any other means known or that may be invented, and to disseminate through scientific repositories and admit its copying and distribution for non-commercial, educational or research purposes, as long as credit is given to the author and editor.

This document was created with Microsoft Word text processor and the NOVAthesis Word template [1].

A mi familia, porque la familia es lo más importante.

ACKNOWLEDGMENTS

It really feels surreal to be writing this after four years of PhD, it feels more like an entire life, because actually it is what this thesis has behind it, not just the four years of this PhD, but my entire life. Paleontology has been my passion and vocation since I have memory, never ever I wanted to do something else in my life and this thesis just feels like the natural way of how this passion would eventually develop; a real dream of mine comes true. But during these four years, besides my unending passion for paleontology, everything else has changed academically for me. It has been an absolute roller-coaster since when I started the PhD grant in June of 2021 when the world was still dealing with the COVID-19. Now I am (hopefully) a much better researcher with much more knowledge (which is the objective of a PhD), but I also have very different academic and personal relationships, views, interests and approaches to work and life. I am actually reborn as a researcher, reshaping my previously existing experiences, which have resulted in an incredibly personal growth, that make me ready for the next chapter of my life. And If I am here, if this thesis exists, is because the help and support of many people and institutions, who deserve to be acknowledged:

First, I want to thank from the bottom of my heart my main PhD advisor, Dr. María Ríos. She academically rescued me in the darkest moment of my PhD journey and despite not having been from the beginning my main PhD advisor; she really understood me, my way of thinking and working. I think that it helped a lot that we knew each other since 2018… so, I am definitely super happy about going that year to excavate to Batallones-10, because I met such an academically and emotionally brilliant person, that has helped so much my personal and professional growth since then.

Second, I want to thank my marvelous co-advisor Prof. Aurora Grandal-d´Anglade. It made so much sense for her to be my co-advisor since the beginning, the best connection to my alma-mater at Galicia that I could have, being also a really accomplished specialist on the

topic of Pleistocene faunas. I wish I could have been more present in the day to day life of the lab there. You really helped me so much at so many levels (especially with molecular analyses) the time periods that I was there and, even more importantly, also from the distance.

I also want to extended my gratitude to the members of the commission accompanying my thesis: Prof. João Luis Cardoso, Dr. Ana García-Vázquez and Dr. Vicente Crespo for all the critical insights, the advice, and their expertise; as well as their help with several of the works of the thesis. I hope that we can collaborate further in the future.

Two co-authors of some of the research of this thesis also deserve special recognition, Dr. Qigao Jiangzuo and Dr. Joan Madurell-Malapeira. Huge thanks for reaching out to me about the pantherine from Algar da Manga Larga, which would result in the groundbreaking work about *Panthera uncia lusitana*. We still have more work to do on this specimen!

I also had the support of several institutions and people that deserve recognition:

First and foremost, I should thank the Fundação para a Ciência e Tecnologia (FCT) for the funding that supported me during these four years, through the PhD grant 2020.05395.BD. Furthermore, part of the research here presented has been also funded through the research unit GeoBioTec UIDB/04035/2020 and the project "LOURI-QAVE" by Museu da Lourinhã.

Professor José Carlos Kullberg, as head of the PhD program in Geology of the NOVA School of Science and Technology during most of my PhD, helped me and other PhD students to navigate several complicated problems beyond the call of duty and I will forever be grateful to him for that, as well as Professor João Almeida for his help while finishing this thesis. I also thank the staff at the Department of Earth Sciences, specially Fátima Silva, Eduarda Ferreira and Sónia Soares for always attending my requests of help with bureaucratic procedures with such a short notice.

This thesis would have not been possible without the support of the Laboratorio Nacional de Energia e Geologia (LNEG), through the team of the Geological Museum of Lisbon, that houses most of the specimens mentioned on this thesis. Because of that, and their dedication to the care of this treasure for Portuguese Paleontology that is the Geological Museum, I want to sincerely thank Rubén Dias, José Moita and Jorge Sequeira.

I am extraordinarily grateful to the team of Museu da Lourinhã. Not only it was a pleasure to work with them while I was at the direction board of the Museum during the first three years of my PhD; but they also helped me a lot with several task during my thesis, like the preparation of Pleistocene material from several sites. Huge thanks in particular to Carla Alexandra Tomás and Micael Martinho for their expertise in preparation, as well as the long list of current and former workers.

I am beyond grateful to my fellow PhD students (current and former) of the PhD program in Geology at FCT-NOVA for your friendship, unwavering support, and collaboration navigating complex issues, as well as for your help fulfilling a paleo-dream of mine during this thesis by organizing the XXI EJIP/6th IMERP at Lourinhã in April of 2023. Immense thanks to João Russo, Filippo Maria Rotatori, Francisco Costa, Alexandre Guillaume (even if you wanted to dispatch me almost every week), Simone Conti, André Saleiro, Roberta Martino, Victor López-Rojas, João Pratas, Marc Ricetto, and Arthur Maréchal.

And of course, I also have to thank for their help with a thousand different tasks, their scientific insight, and over all their friendship during these years to postdocs, paleontology master students (current and former) of FCT-NOVA, and volunteers and workers of the Museu da Lourinhã: Dr. Miguel Moreno-Azanza, Dr. Eduardo Puértolas-Pascual, Dr. Cristina Sequero-López, Dr. Alexandra Fernades, Victor Beccari, Vincent Cheng, Miguel Marx, Cátia Ribeiro, Inês Marques, Priscila Lohmann, Bruno Pereira, Ana Luz, Alexandre Audigane, Pedro Ferreira and many others more.

During this journey of the PhD I have found a lot of people that helped me along the way in unexpected ways: Huge thanks to Dr. Jan van der Made, Elpiniki Parparousi, Pavlos Piskoulis, Dr. Raquel Moyá-Costa, Dr. Juan Manuel López-García, and Pilar Alfaro-Ibáñez for their help with the Early Pleistocene sites of Portugal. Thanks to the members of the speleology group GPS (Grupo de Procteção Sicó) who saved my life several times while rescuing fossils from a cave, this thesis is only possible thanks also to the help of their former president, the late Sérgio Medeiros. I will also want to thank the staff of the National Archeological Museum of Portugal, the LARC (Laboratório de Arqueociências) of DGPC as well as Dr. Mariana Nabais and Prof. João Zilhão for entrusting me the bear fossils from Oliveira Cave as well as giving me the opportunity to dig at Gruta do Caldeirão and Gruta do Aderno. I want to specially thank Dr. Henrique Matias and Dr. John Charles Willman for their trust during this last digging: Gruta do Aderno is truly an amazing site, and I will surely come back in the future. Thanks also to Carlos Prates, Madalena Travassos and all the team of Affidea clinic of Avenida da República who CT-scanned for free the skull of the Manga Larga pantherine. Many thanks to Afonso Barrocal for always being ready to help about the state of species currently living on Portugal and also with the distribution of the snow leopard nowadays. Also, many thanks to Zé Pedro Ferreira (@Paleotuga) for his amazing paleoart that he did on such a short notice. Lastly, thanks to João Lourenço, who compiled the template of the thesis and gave it for free to everyone.

I also extend gratitude to the developers of digital tools and open-access resources that facilitated this research, like Alexandra Elbakyan.

Finally, thanks to all the marvelous human beings of Academia that I met in congresses and excavations during my PhD years, because you are also the reason why a love paleontology.

Outside of Academia, I want to say many thanks to my MMA training partners at "Miga fight team", the staff of the swimming pool of the municipality of Peniche, my friends back in Spain and everyone else that preserved my sanity during these years with their support, work, and friendship.

And last but ABSOLUTELY not least… to my family, who have cared for me all my life and to whom this thesis is dedicated, because they are actually the most important thing in my life, even if sometimes it seems that paleontology is:

To all my extended family of cousins and uncles. To my great grandmother Antonia and my grandfather José, that will see me presenting my thesis from wherever they are. To my grandparents Mariví, Josefa and Nicolás who have endured my absence with understanding for all these years. To my father Antonio, who always wants to hear my stories from Portugal and my stepmother María José. To my mother Silvia, and my stepfather Suso, who have taken care of me from the distance as much as if I was at home and always wanted to help me as much as they could. Huge thanks for being my family, huge thanks for making me so happy and understand my dream. You are the best family I could have had.

"What we know about the past record relied heavily on museum collections—the cumulation of centuries of investigation of the fossil record. The sample of past biodiversity will accumulate only with continued exploration of the fossil record … and restudy of existing collections…" - **Joseph John Sepkoski Jr.**, *"Phylogenetic and ecologic patterns in the Phanerozoic history of marine biodiversity"*

"Discipulus est prioris posterior dies." - **Publilius Syrus**, "*Sententiae*"

"Queira Deus que o passado diga alguma coisa ao presente. Se não servem de nada as suas lições a história a ninguém aproveita" - **Luís Augusto Rebelo da Silva,** *"Memoria sobre a população e a agricultura de Portugal desde a fundação da monarchia até 1865. Parte I"*

Abstract

The Pleistocene fossil vertebrates of Portugal have important implications for our understanding of modern ecosystems. This thesis aims to be a comprehensive and multidisciplinary investigation, integrating over 150 years of paleontological data with new analytical methodologies. This will help to clarify overarching questions in paleontology like the representativeness of the fossil record, as well as several questions related with individual clades. The oldest sites from Western Iberia (Early Pleistocene) are reviewed, and a new locality (Santa Margarida) is presented, including the first documented occurrences in Portugal of the voles *Victoriamys chalinei* and *Iberomys huescarensis*. This research also unexpectedly helped to disentangle the evolutionary history of the snow leopard by describing *Panthera uncia lusitana*, a new fossil subspecies of snow leopard from Portugal, revealing the key adaptations acquired during the evolution of this clade of pantherine cats. Further work with digital and molecular paleontological techniques delves deeper into the paleoecology and paleobiology of this unexpected felid. A detailed analysis of over 500 bear remains from six Portuguese localities refines our understanding of the fossil populations of this species, describing a robust Late Pleistocene population that might share analogous ecological traits to cave bears, and providing a framework for the brown bear evolution in Iberia. Finally, the first comprehensive census of Pleistocene terrestrial tetrapods in Portugal documents over 680 occurrences of 200 taxa across over 40 sites, providing data about the relationship of biodiversity with the fossil record that it leaves behind, as only 38% of modern tetrapod species in Portugal were recorded as Pleistocene fossils. This thesis improves our knowledge of the Pleistocene fossil record of Portugal, underscores the importance of interdisciplinary collaboration, and demonstrates the enduring potential for new discoveries. Future research on the lines of investigation laid on this thesis will be critical to further inform conservation strategies and better understand both the past and modern biodiversity.

Keywords: Early Pleistocene, Santa Margarida Site, *Panthera uncia lusitana*, *Ursus arctos*, Furninha Cave, Iberian Peninsula.

RESUMO

Os vertebrados fósseis do Plistocénico de Portugal têm grandes implicações para a nossa compreensão dos ecossistemas modernos. Esta tese pretende ser uma investigação abrangente e multidisciplinar, integrando mais de 150 anos de dados paleontológicos com novas metodologias analíticas. Isto ajudará a esclarecer diversas questões abrangentes na paleontologia, como a representatividade do registo fóssil, bem como diversas questões relacionadas com vários grupos. São revistos os sítios mais antigos do Oeste da Península Ibérica (Plistocénico Inferior) e apresentada uma nova localidade (Santa Margarida), incluindo as primeiras ocorrências documentadas em Portugal dos roedores *Victoriamys chalinei* e *Iberomys huescarensis*. Esta investigação ajudou também inesperadamente a desvendar a história evolutiva do leopardo-das-neves ao descrever *Panthera uncia lusitana*, uma nova subespécie fóssil de leopardo-das-neves de Portugal, mostrando as principais adaptações adquiridas durante a evolução deste clado de felinos panterinos. Trabalhos posteriores com técnicas paleontológicas digitais e moleculares aprofundam na paleoecologia e paleobiologia deste inesperado felídeo. Uma análise detalhada de mais de 500 restos de ursos procedentes de seis localidades portuguesas melhora a nossa compreensão das populações fósseis desta espécie, descrevendo uma população robusta do Pleistoceno Superior que pode partilhar características ecológicas análogas às dos ursos das cavernas e proporcionando um *framework* para a evolução do urso pardo na Península Ibérica. Por fim, o primeiro censo abrangente de tetrápodes terrestres do Plistocénico em Portugal documenta mais de 680 ocorrências de 200 taxa em mais de 40 locais, fornecendo dados sobre a relação da biodiversidade com o registo fóssil, uma vez que apenas 38% das espécies modernas de tetrápodes em Portugal foram registadas como fósseis do Plistocénico. Esta tese melhora o nosso conhecimento do registo fóssil do Pleistoceno de Portugal, sublinha a importância da colaboração interdisciplinar e demonstra o potencial duradouro para novas descobertas. Pesquisas futuras sobre as linhas

de investigação estabelecidas nesta tese serão essenciais para informar as estratégias de conservação e compreender melhor a biodiversidade passada e moderna.

Palavras chave: Plistocénico Inferior, sitio de Santa Margarida, *Panthera uncia lusitana*, *Ursus arctos*, Gruta da Furninha, Peninsula Ibérica.

CONTENTS

1 INTRODUCTION 1

1.1 History of Pleistocene vertebrate paleontology in Portugal 1

1.1.1 Context 1

1.1.2 Methodology 2

1.1.3 Chronology 2

1.1.4 Remarks about the History of Pleistocene paleontology in Portugal. 4

1.2 Main Pleistocene sites with fossil fauna from Portugal 5

1.2.1 Lorga de Dine 7

1.2.2 Fariseu 7

1.2.3 Mealhada 8

1.2.4 Condeixa 9

1.2.5 Buraca Grande 10

1.2.6 Buraca Escura 11

1.2.7 Lagar Velho 11

1.2.8 Caldeirão 13

1.2.9 Foz do Enxarrique 14

1.2.10 Lapa do Picareiro 15

1.2.11 Aroeira 15

1.2.12 Oliveira 18

1.2.13 Lapa dos Coelhos 18

1.2.14 Algar da Manga Larga 19
1.2.15 Casais Robustos & Cabeço de Morto 20
1.2.16 Algar de João Ramos 21
1.2.17 Serra de Molianos 21
1.2.18 Furninha 22
1.2.19 Casa da Moura 23
1.2.20 Gruta Nova da Columbeira 24
1.2.21 Lapa do Suão 24
1.2.22 Fontainhas 25
1.2.23 Lapa da Rainha 26
1.2.24 Pedreira e Gruta das Salemas 26
1.2.25 Pego do Diabo 27
1.2.26 Porto Covo 28
1.2.27 Algar de Cascais 29
1.2.28 Escoural 29
1.2.29 Figueira Brava 31
1.2.30 Gruta de Ibn Amar 35
1.2.31 Santa Margarida 35
1.2.32 Algoz 36
1.2.33 Goldra 38
1.2.34 Guia 38
1.2.35 Morgadinho 39
1.2.36 Vale Boi 40
1.3 Pleistocene fauna of Portugal: A synthetic overview 41
1.3.1 Herpetofauna 41
1.3.2 Avifauna 42
1.3.3 Proboscidea 44

1.3.4 Euarchontoglires....45
1.3.5 Chiroptera & Eulipotyphla....45
1.3.6 Artiodactyla....46
1.3.7 Perissodactyla....48
1.3.8 Carnivora....49
1.4 Objectives of this thesis....50
2 EARLY PLEISTOCENE (EPIVILLAFRANCHIAN) VERTEBRATES FROM PORTUGAL: AN UPDATED REVIEW....53
2.1 Introduction....53
2.2 The Epivillafranchian localities of Portugal....55
2.2.1 Algoz....55
2.2.2 Morgadinho....56
2.2.3 Santa Margarida....56
2.3 Material and methods....57
2.3.1 Material....57
2.3.2 Methods....58
2.4 Systematic paleontology....59
2.4.1 Algoz Cervidae: The medium-sized deer....59
2.4.2 Algoz Cervidae: The large-sized deer....61
2.4.3 Algoz Leporidae....67
2.4.4 The microvertebrates from Santa Margarida....68
2.5 Discussion....74
2.5.1 Chronology of the Epivillafranchian localities of Portugal....74
2.5.2 Paleoenvironment of Epivillafranchian localities from Portugal....74
2.6 Conclusions....75
3 INSIGHTS ON THE EVOLUTION AND ADAPTATION TOWARD HIGH-ALTITUDE AND COLD ENVIRONMENTS IN THE SNOW LEOPARD LINEAGE....77
3.1 Introduction....77

3.2 Materials and methods 79
3.2.1 Phylogenetic analyses 79
3.2.2 Metric and geometric morphometric analyses 79
3.2.3 Anatomical study and fossil records 80
3.2.4 Finite element analyses 80
3.2.5 Species distribution modeling 81
3.3 Results and discussion 82
3.3.1 Systematics 82
3.3.2 Ecomorphological adaptation of fossil snow leopard 84
3.3.3 Multiple out-of-Tibet dispersal and the rapid evolution of the snow leopard during the Middle and Late Pleistocene 91
3.3.4 SDM analysis of potential LGM distribution and dispersal route of the snow leopard 96
4 3D DIGITAL AND BIOGEOCHEMICAL ANALYSIS OF THE ALGAR DA MANGA LARGA PANTHERINE (*PANTHERA UNCIA LUSITANA*) 99
4.1 Introduction 99
4.1.1 The Manga Larga Pantherine: Discovery and Reassessment 99
4.1.2 Non-destructive 3D imaging in fossil analysis 100
4.1.3 Geochemical approaches for chronological and paleoecological reconstruction 101
4.1.4 Objectives 103
4.2 Material and methods 104
4.2.1 Material 104
4.2.2 Methods 105
4.3 Results 109
4.3.1 CT-scan segmentation 109
4.3.2 U-Th series dating 111
4.3.3 Nitrogen quantification 112

4.3.4 $\delta^{18}O$ and $\delta^{13}C$ analysis 113
4.4 Discussion 115
4.4.1 Endocast morphology 115
4.4.2 Isotopic analyses 116
4.5 Conclusions 118
5 PLEISTOCENE FOSSIL URSIDAE FROM PORTUGAL: MORPHOMETRY AND PALEOBIOLOGICAL INFERENCES 121
5.1 Introduction 121
5.1.1 Evolutionary history and adaptability of the brown bear (*Ursus arctos*) 121
5.1.2 The evolution and distribution of *Ursus arctos* in the Iberian Peninsula 123
5.1.3 Characterization of the Portuguese Pleistocene localities with presence of *Ursus arctos* considered on this work 125
5.2 Material and methods 127
5.2.1 Material 127
5.2.2 Methods 129
5.3 Results 132
5.3.1 Oliveira 132
5.3.2 Escoural 133
5.3.3 Caldeirão 135
5.3.4 Serra de Molianos 139
5.3.5 Fontainhas 147
5.3.6 Furninha 164
5.4 Discussion 191
5.4.1 Contextualizing Pleistocene Portuguese brown bears: observations from their sites 191
5.4.2 Body size evolution of brown bears in western Iberia. 195
5.5 Conclusions 199
6 PALEOBIODIVERSITY OF PLEISTOCENE VERTEBRATES FROM PORTUGAL 201

6.1 Introduction ... 201
6.2 Methods ... 202
6.2.1 Census of paleobiodiversity of the Pleistocene of Portugal ... 202
6.2.2 Comparison with online databases ... 203
6.2.3 Descriptive statistics of the main matrix. ... 203
6.2.4 Comparison of the Pleistocene fossil record with modern biodiversity: How representative is the fossil record? How important are caves? ... 203
6.2.5 Validation of non-parametric estimations for species number: How they perform with the Pleistocene fossil record? ... 204
6.3 Results ... 204
6.3.1 Paleobiodiversity census of the Pleistocene of Portugal ... 204
6.3.2 Evaluation of online databases ... 209
6.3.3 Descriptive statistics of the presence-absence matrix ... 211
6.3.4 Comparison of the Pleistocene fossil record with modern biodiversity: How representative is the fossil record? How important are caves? ... 214
6.3.5 Validation of non-parametric estimations for species richness: How do they perform with the Pleistocene fossil record? ... 219
6.4 Discussion ... 224
6.5 Conclusions ... 226
7 CONCLUSIONS ... 229
7.1 Conclusions of previous chapters ... 229
7.1.1 Early Pleistocene (Epivillafranchian) vertebrates from Portugal: An updated review. 229
7.1.2 Insights on the evolution and adaptation toward high-altitude and cold environments in the snow leopard lineage. ... 230
7.1.3 3D digital and biogeochemical analysis of the Algar da Manga Larga pantherine (*Panthera uncia lusitana*) ... 230
7.1.4 Pleistocene fossil Ursidae from Portugal: Morphometry and paleobiological inferences ... 231

7.1.5 Paleobiodiversity of Pleistocene vertebrates from Portugal 233
7.2 General conclusions of the thesis 234

List of Figures

Figure 1.1 — Map of main paleontological Pleistocene sites in Portugal. Dots are cave localities, squares are open-air sites. Sites are numbered roughly from North to South. Red, Early Pleistocene; blue, Middle Pleistocene; black, Late Pleistocene. 1) Lorga de Dine; 2) Fariseu; 3) Mealhada; 4) Condeixa; 5) Buraca Grande; 6) Buraca Escura; 7) Lagar Velho; 8) Caldeirão; 9) Foz do Enxarrique; 10) Lapa do Picareiro; 11) Aroeira; 12) Oliveira; 13) Lapa dos Coelhos; 14) Algar da Manga Larga; 15) Casais Robustos; 16) Algar de João Ramos; 17) Serra de Molianos; 18) Furninha; 19) Casa da Moura; 20) Gruta Nova da Columbeira; 21) Lapa do Suão; 22) Fontainhas; 23) Lapa da Rainha; 24) Pedreira e Gruta das Salemas; 25) Pego do Diabo; 26) Porto Covo; 27) Algar de Cascais; 28) Escoural; 29) Figueira Brava; 30) Gruta de Ibn Amar; 31) Santa Margarida; 32) Algoz; 33) Goldra; 34) Guia; 35) Morgadinho; 36) Vale Boi. Modified from map by Wikipedia commons user Waldyrious (2020). Scale is 100 km. 6

Figure 1.2 — Left astragalus of *Cervus elaphus* used as reference (top). Left astragalus of *Cervus elaphus* from Fariseu (bottom). Image modified from Gabriel & Béarez (2009). Scale bar equals 3 cm. 8

Figure 1.3 — *Hippopotamus* remains collected from Condeixa. MG3665, right mandible fragment (A, dorsal view; B, m3 occlusal view; C, left lateral view; D, anterior view; E, right lateral view); MG3677, left canine (F, lateral view; G, mesial view); MG25172, left I2 (H, lateral view; I, ventral view); MG25170, right M1/M2 (J, occlusal view; K, labial view); MG25175, left m3 (L, labial view; M, occlusal view; N, lingual view); MG25171 thoracic vertebra (O, anterior view). Image modified from Martino et al. (2023). All scale bars equal 3 cm. 10

Figure 1.4 — Lagar Velho rock shelter as observed from a northerly perspective, illustrating a bearded vulture pair nesting in a recess situated above the area of occupation, 29 Ka cal B.P. (A)—location of the infant burial; (B)—layer 143 from where the studied coprolites were

recovered; (C)—the Hanging Remnant, a recess preserving sediments with Upper Palaeolithic remains dated from 26 to 24 Ka cal B.P. Image modified from Sanz et al. (2023). 13
Figure 1.5 — Digital renderings of the juvenile macaque mandible ARO 934 from Gruta da Aroeira, in left lateral (a), right lateral (b), frontal (c), oblique (d), and basal (e) views. The mandibular bone is shown in semitransparent ocher, whereas tooth loci are denoted with different colors. Image modified from Alba et al. (2019). Scale bar equals 1 cm. 17
Figure 1.6 — *Panthera uncia lusitana.* Skull from Algar da Manga Larga (MG1355.0001-0002) in anterolateral view. Geological Museum, Lisbon. Image from Estraviz-López (2019). Scale equals 5 cm. 20
Figure 1.7 — Skull of *'Hyaena' prisca* from Furninha cave in dorsal view. Geological Museum, Lisbon. Image from Estraviz-López (2019). Scale bar equals 5 cm. 23
Figure 1.8 — Type specimen of *Equus ferus antunesi* (FO.I-1) in lateral view. Geological Museum, Lisbon. Image from Estraviz-López (2019). 25
Figure 1.9 — Comparison of the proximal humerus fragment assigned to *Phaisanus colchicus* from Pego do Diabo compared with the specimen from the CIPA collection, and the 1:1 scale drawing by Cohen & Serjeantson, 1996. Cranial view (left) and caudal view (right). The arrows indicate the similarities considered for taxonomic classification. Image modified from Figueiredo (2010). Scale not provided in the original. 28
Figure 1.10 — Escoural Cave and location of the test profiles excavated in 2020. Image modified from Cobo-Sánchez et al., 2024. 30
Figure 1.11 — Fragment of left hemimandible of *Cuon alpinus* with P4 and fragment of M1 from Escoural cave in lingual view. Scale bar is 35 mm. Image modified from Cardoso (1992). 31
Figure 1.12 — Plan of Figueira Brava with position of excavation trenches (Area C, 1986 to 1989 paleontological work; Areas F and SEx, 2010 to 2013 archeological excavation) and indication of main features. Image modified from Zilhão et al. (2021) 32
Figure 1.13 — *Hystrix* mandible from Figueira Brava. Lingual (top), occlusal (center) and labial (bottom) views. Image modified from Cardoso et al. (2021). Scale bar is 10 mm. 34
Figure 1.14 — *Hippopotamus* remains collected from Algoz. A, MG25769.1, femur head (A, proximal view). MG25769.2, right tibia (B, distal view; C, lateral view); MG25769.3, right calcaneus (D, posterior view; E, distal view; F, articular surface for the astragalus; G, medial view); MG25769.4, right astragalus (H, anterior view; I, lateral view; J, distal view; K, posterior view; L, medial view; M, proximal view); MG25769.10, right cuboid (N, anterior view; O, proximal view); MG25769.5, right navicular (P, proximal view; Q, anterior view; R, lateral view; S, distal view);

MG25769.6, right MTIII (T, anterior view; U, lateral view; V, posterior view; W, medial view); right phalanxes in anterior view (X, MG25769.9, third proximal phalanx; Y, MG25769.8, third middle phalanx; Z, MG25769.7, second middle phalanx). Image modified from Martino et al. (2023). Scale bars equal 3 cm. 37
Figure 1.15 — Quartzite artifact embedded in first phalanx of red deer (*Cervus elaphus*) from Vale Boi. Image modified from Manne et al., (2012). Scale bar is 20 mm. 41
Figure 2.1 — Location of Early Pleistocene (Epivillafranchian) localities from Portugal, Iberian Peninsula (credit: LNEG). Scale bar: 25 km (regional level).....54
Figure 2.2 — A-C. Distal fragment of radius of *Metacervocerus rhenanus* from Algoz (MG-25771) in palmar or posterior (A), dorsal or anterior (B), and distal (C) views. D-F. Fragment of mandible with d4 of *Metacervocerus rhenanus* from Algoz (MG-25770) in labial (D), occlusal (E), and lingual (F) views. G. Scatter plot of the distal radius mediolateral and anteroposterior diameters of the Algoz specimen compared with other European *Dama*-like deer. H. Principal component analysis showing the position of the Algoz specimen compared with the radius of other European *Dama*-like deer. Scale bars: 50 mm (A-C), 25 mm (D-F). 60
Figure 2.3 — Recovered material from the large-sized deer from Algoz, including 15 remains with different degrees of preservation from the same juvenile individual (MG-25768). A-C. Partial right hemimandible (MG-25768.1) in buccal (A), occlusal (B), and lingual (C) views. D-F. Partial right scapula (MG-25768.7) in dorsal (D) ventral (E), and distal (F) views. G, H. Right femur without epiphyses (MG-25768.8) in anterior (G) and lateral (H) views. I-K. Distal epiphysis of left tibia (MG-25768.16) in anterior or dorsal (I), distal (J), and posterior or palmar (K) views. L. Proximal epiphysis of left ulna (MG-25768.5) in lateral view. M, N. Left navico-cuboid in distal (M) and proximal (N) views. Skeletal diagram modified from ArcheoZoo.org (2003). Scale bars: 50 mm.....63
Figure 2.4 — Morphological comparison of the material from the large-sized deer from Algoz (MG-25768) with *Eucladoceros* and large Megacerini and Capreolini. A. Mandible from MG-25768 with d3 and d4 in occlusal view. B. Mandible from *E. boulei* with d3 and d4 in occlusal view. C. Mandible from *E. boulei* with d3 and d4 in occlusal view. D. Mandible from *E. montenegrensis* with d3 and d4 in occlusal view. E. Mandible from *M. novocarthaginiensis* with d3 and d4 in occlusal view. F. m1 in lingual view from MG-25768. G. m1 in lingual view from *E. montenegrensis*. H. m1 from *M. novocarthaginiensis* in lingual view. I. Navico-cuboid from MG25768 in proximal view. J. Navico-cuboid from *E. boulei* in proximal view. K. Navico-cuboid from *A. alces* in proximal view. L. Navico-cuboid from *M. giganteus* in proximal view. M. Tibia from MG25768 in distal view. N. Tibia from *E. boulei* in distal view. O. Tibia from *A. alces* in

distal view. P. Tibia from *M. giganteus* in distal view. Q. Tibia from MG25768 in posterior or palmar view. R. Tibia from *E. boulei* in posterior or palmar view. S. Tibia from *A. alces* in posterior or palmar view. T. Tibia from *M. giganteus* in posterior or palmar view. Images from: *Eucladoceros boulei*, adapted from Tong and Zhang, (2019); *Eucladoceros montenegrensis* adapted from van der Made and Dimitrijevic´, (2015); *Megaloceros novocarthaginiensis* adapted from van der Made, (2015); *Alces alces* and *Megaloceros giganteus*, adapted from Breda, (2005). Green lines: condition of the character in *Eucladoceros*; red lines: condition in *Megaloceros*; blue lines: condition in *Alces alces*. Scale bars: 50 mm 65
Figure 2.5 — Morphometric analyses of skeletal elements of the cranial and postcranial anatomy from the large-sized deer of Algoz (MG-25768) compared with several species of *Eucladoceros* and Megacerini deer. Check Appendix A for additional information. A. Principal component analysis (PCA) of d3. B. PCA of d4. C. PCA of m1. D. PCA of scapula. E. Scatter plot of transversal vs. anteroposterior diameters of the distal tibia. F. Scatter plot of the transverse diameter of the distal humerus vs. anteroposterior diameter.....66
Figure 2.6 — Microvertebrate remains from Santa Margarida, modified from Estraviz-López, (2019). A. Lacertidae, left dentary (NOVA-FCT-DCT-5377) in lingual view. B-D. Soricidae, fragment of left mandible (NOVA-FCT-DCT-5378) in occlusal (B), lingual (C), and labial (D) views. E-H. Lagomorpha, distal left humerus (NOVA-FCT-DCT-5376) in anterior (E), exterior (F), posterior (G), and medial (H) views. I. Gliridae, upper molar (NOVA-FCT-DCT-5382 (2.8)) in occlusal view. J. Muridae, first upper molar (NOVA-FCT-DCT-5381 (1.6)) in occlusal view. K. *Allocricetus bursae*, first left upper molar (NOVA-FCT-DCT-5380 (1.17)) in occlusal view. Scale bars: 1 mm (A-D, I-K), 25 mm (E-H).....69
Figure 2.7 — Arvicolinae m1s and M3s from Santa Margarida. A-E. m1s in occlusal view, modified from Estraviz-López, (2019). A: NOVA-FCT-DCT-5383; B: NOVA-FCT-DCT-5384; C: NOVA-FCT-DCT-5385 (1); D: NOVA-FCT-DCT-5385 (2); E: NOVA-FCT-DCT-5386. F. Measurements and nomenclature of arvicoline m1s (from López-García et al., 2015): a, length of the anteroconid complex; ACC, anteroconid complex; AC, anterior cap; BRA, buccal reentrant angle; BSA, buccal salient angle; c, width of the opening of triangles T4-T5; L, length; La, mean width of T4; Li, mean width of T5; LRA, lingual re-entrant angle; LSA, lingual salient angle; PL, posterior lobe; TTC, trigonid-talonid complex, T1-T7, triangles 1–7; W, width. G. Measurements and nomenclature of arvicoline M3s (adapted from Martin, 2012): LA, anterior lobe; BRA, buccal reentrant angle; BSA, buccal salient angle; L, length; LRA, lingual re-entrant angle; LSA, lingual salient angle; PC, posterior cap; T1-T5, triangles 1–5; W, width. H-M. M3s in occlusal view. H: NOVA-FCT-DCT-5387 (1.3); I: NOVA-FCT-DCT-5388 (1.5); J: NOVA-FCT-DCT-5389 (1.6); K:

NOVA-FCT-DCT-5390 (2.1); L: NOVA-FCT-DCT-5391 (2.2); M: NOVA-FCT-DCT-5392 (2.6). Scale bars: 1 mm.....71
Figure 2.8 — Morphometric analysis of the Arvicolinae m1s from Santa Margarida. A. Scatter plot of length (without posterior lobe) vs. width of the specimen NOVA-FCT-DCT-5386 compared with *Iberomys brecciensis* and *Iberomys cabrerae*. B. Scatter plot of length vs. width of the specimens NOVA-FCT-DCT-5383 and NOVA-FCT-DCT-5384 compared with specimens of *Iberomys huescarensis*, *Victoriamys chalinei*, and *Allophaiomys lavocati*. C. Scatter plot of length vs. width of the specimens NOVA-FCT-DCT-5384, NOVA-FCT-DCT-5385 (1) and NOVA-FCT-DCT-5385 (2) compared with *Iberomys huescarensis*, *Iberomys brecciensis*, and *Iberomys cabrerae*. D. Scatter plot of A/L ratio vs. C/W ratio of specimens NOVA-FCT-DCT-5383, NOVA-FCT-DCT-5384, NOVA-FCT-DCT-5385 (1) and NOVA-FCT-DCT-5385 (2) compared with *Allophaiomys lavocati*, *Victoriamys chalinei*, and *Iberomys huescarensis*. E. Scatter plot of A/L ratio vs. La/Li ratio of specimens NOVA-FCT-DCT-5383, NOVA-FCT-DCT-5384, NOVA-FCT-DCT-5385 (1) and NOVA-FCT-DCT-5385 (2) compared with *Allophaiomys lavocati*, *Victoriamys chalinei*, *Iberomys huescarensis*, *Iberomys brecciensis*, and *Iberomys cabrerae*. F. Principal component analysis comparing specimens NOVA-FCT-DCT-5383 and NOVA-FCT-DCT-5384 with *Allophaiomys lavocati*, *Victoriamys chalinei*, and *Iberomys huescarensis*. See Appendix A for more details.....72
Figure 3.1 — Fossil snow leopards from Eurasia. (A) *Panthera* aff. *pyrenaica*, IVPP V31895, Longdan, Linxia Basin, northeastern Tibet, China. (B) *Panthera pyrenaica*, E14-EFNI-1001, Aragó Cave, Southeastern France. (C) *Panthera* aff. *uncia*, Zhoukoudian Loc. 3, Beijing, China. (D) *Panthera uncia lusitana* subsp. nov., MG1355.0001-0002, Manga Larga, Portugal. (E) *Panthera uncia*, IVPP V11800.1, Niuyan Cave, Beijing, China.....83
Figure 3.2 — Craniodental ecomorphology of the snow leopard and related taxa. (A) Cranial comparison of *P. uncia* AMNH M166952 and *P. pardus* AMNH M89009, highlighting functional traits related to high/cold adaptation (green) and (prey type related) mountain life (red). (B) Finite element analyses of mandibles of modern and fossil *P. uncia*, modern *P. pardus*, and several fossil snow leopards.....86
Figure 3.3 — Functional statistical traits of *Panthera uncia* and its fossil relatives in comparison with other felids. (A) Cranial angles of felids; (A1) Angle in the lion *P. leo*; (A2) angle in the snow leopard *P. uncia*; (A3) angle α and its impact on eyesight; (A4) comparison of angle α in modern and fossil felids; (A5) comparison of angle β in modern and fossil felids; (B) comparison of the ratio of ectotympanic and ectotympanic area in modern and fossils felids; (C) comparison of angle γ in modern and fossil felids.....89

Figure 3.4 — Functional statistical postcranial traits of *Panthera uncia* in comparison with other felids. (A) Plot on tibia/femur length ratio and radius/humerus ratio. (B) Plot on pelvis/femur length ratio and scapular/humerus ratio. (C) PCA plot of 16 postcranial skeleton ratios; see the explanation in the appendix and raw data in table S3 of Appendix B. R, radius; H, humerus; T, tibia; DH, distal antero-posterior height (of long bone); DW, distal medio-lateral width (of long bone); Pe, pelvis; Sc, scapular; F, femur; L, length; MC, metacarpal; MT, metatarsal; P/p, upper/lower premolar.....90
Figure 3.5 — Phylogenetic position and morphospace of modern and fossil snow leopards. (A) Time-calibrated total evidence phylogenetic tree of pantherine cats and the morphological evolutionary rate. (B) Geometric morphometric analyses on lateral views of the cranium and mandible of the fossil snow leopard in comparison with modern species. (B1) Mandible lateral profile, (B2) cranial dorsal view, (B3) cranial lateral view, and (B4) cranial ventral view. 92
Figure 3.6 — SDM predicted suitable distribution and morphospace of the modern and fossil snow leopards. (A) The predicted probability of snow leopard presence under the LGM climate conditions. (B) Functional traits PCA morphospace, with reconstruction of fossil and modern snow leopards. Artwork by Jianhao Ye.....95
Figure 4.1 — Location of the sampled areas in the canine (MG1355.0001) (top), and in the humerus (MG1355.0003) (bottom) of the type specimen of *Panthera uncia lusitana*. Scale bars are 30 mm. 104
Figure 4.2 — Skull and mandible of *Panthera uncia lusitana* (MG1355.0001-2) undertaking CT-scanning at the Affidea clinic of Avenida da República, Lisbon. 105
Figure 4.3 — Endocast of *Panthera uncia lusitana* (MG1355.0001) before (left) and after (right) undertaking 100 hours of manual editing in a) anterior, b) posterior, c) right lateral, and, d) left lateral views. The brown areas have been more manually reconstructed than the white ones. 106
Figure 4.4 — Endocast of *Panthera uncia lusitana* (MG1355.0001) in dorsal view compared with the dorsal views of the endocast of related felids. Scale bars are 50 mm. 109
Figure 4.5 — Endocast of *Panthera uncia lusitana* (MG1355.0001) in ventral view compared with the ventral views of the endocast of modern related felids. Scale bars are 50 mm. 110
Figure 4.6 — Endocast of *Panthera uncia lusitana* (MG1355.0001) in right lateral view compared with the right lateral views of the endocast of modern related felids. Scale bars are 50 mm. 110
Figure 4.7 — Plot of $^{234U}/^{238}U$ activity ratios against $^{230}Th/^{238}U$ activity ratios for the samples of the leopard of Manga Larga (IS-1773 and IS-1773), modified after Osmond and Ivanovich

(1992). This graphical representation is for reference only and should not be construed as an interpretation of these test results..... 112
Figure 4.8 — Standard ellipse areas showing the isotopic niche space occupied by herbivores from Levels JJ and KK of Lapa do Picareiro, Level 5/6 of Valdegoba Cave and Level 20E of El Castillo Cave. The star represents the pantherine from Algar da Manga Larga. Image modified from Carvalho et al. 2022. 113
Figure 4.9 — Mean ± 1 standard deviation of δ ^{13}C (‰, VPDB) and δ ^{18}O (‰, VSMOW) values of mammalian tooth enamel from A) Punta Lucero, B) Atapuerca sites, C) Valdegoba, and D) La Paloma compared with the values of the pantherine from algar da Manga Larga (red star). Image modified from Domingo et al. (2017). 114
Figure 4.10 — Mean annual temperature (MAT) in ºC across snow leopard´s range. Data extracted from IUCN and worldclim.org 118
Figure 5.1 — Sites where Ursidae remains have been found in Portugal: Red, Pleistocene sites studied on this work; white, Pleistocene sites not studied on this work; blue, Holocene prehistoric sites; purple, Roman Imperial site; yellow, medieval site. North of green dotted line is the approximate distribution of *Ursus arctos* during the second half of the 19th century. 1, Furninha; 2, Oliveira; 3, Caldeirão; 4, Escoural; 5, Fontainhas; 6, Serra de Molianos; 7, Algar do Vale da Pena; 8, Lorga de Dine; 9, Aroeira; 10, Gruta Nova da Columbeira; 11, Algar de Cascais; 12, Pedreira das Salemas; 13, Gruta das Salemas; 14, Pego do Diabo; 15, Figueira Brava; 16, Pedreira São Bartolomeu dos Galegos; 17, Leceia; 18, Vila Nova de São Pedro; 19, Monte Molião; 20, Castle of Leiria. 126
Figure 5.2 — a) Number of *Ursus arctos* remains by site. b) Number of brown bear remains in this work by body part, from all sites considered. 128
Figure 5.3 — a) Principal Component Analysis based on the measurements of third phalanges of bears, including several Portuguese specimens. b) Third phalanx from Oliveira Cave (O17-226) in lateral view. c) Biplot of anteroposterior and transverse diameters of the proximal tibia of Cave and brown bears, including Portuguese specimens. d) Proximal left tibia of brown bear from Oliveira Cave (O16-766) in anterior (left) and lateral (right) views. All scales are 50 mm. 133
Figure 5.4 — a) Left lower first molar (Escral121966) from Escoural in occlusal view. b) Left m2 (EscGalEntrad1964) from Escoural in occlusal view. c) Right m2 (EscGal2Tal7C1) from Escoural in occlusal view. d) Biplot of length vs breadth of the m1. e) Principal component analysis of measurements of the m2. f) Biplot of length vs breadth of the m2. All scale bars are 25 mm. 134

Figure 5.5 — a) Three first phalanges from Caldeirão Cave in dorsal view, from left to right: P11 699; O14 sc 358 Jb J3 and P11 776. b) Left first metatarsal (P-11 666) from Caldeirão Cave in dorsal view. c) Second phalanx (N14-Sc341) from Caldeirão Cave in dorsal view. d) M1 (P-11 886) from Caldeirão Cave in occlusal view. All scale bars are 25 mm. 136
Figure 5.6 — a) Biplot of length vs breadth of the M1 of several Iberian brown and cave bears. b) PCA of the M1 of several Iberian brown and cave bears. c) PCA of the M1 of several Iberian brown bears. 137
Figure 5.7 — a) PCA of the first metatarsal of several Iberian brown and cave bears modified to include the specimen from Caldeirão. b) PCA of the minimum, average and maximum measurements of first phalanges from diverse Iberian brown and cave bear localities. c) PCA of the minimum, average and maximum measurements of the second phalanges from diverse Iberian brown and cave bear localities. 138
Figure 5.8 — Material from brown bears of Serra de Molianos. a) Canine SM219.34 in lateral view. b) m1 SM219.36 in occlusal view. c) m2 SM219.38 in occlusal view. d) m3 SM219.40 in occlusal view. 140
Figure 5.9 — a) Biplot of length vs breadth of the canine of several Iberian brown and cave bears. b) Biplot of length vs breadth of the m3 of several Iberian brown and cave bears. 141
Figure 5.10 — a) Distal radius SM219.32.1 from Serra de Molianos in lateral view. b) Proximal radius SM219.32.2 from Serra de Molianos in lateral view. c) Proximal radius SM219.2 from Serra de Molianos in lateral view. d) Proximal ulna SM219.4 from Serra de Molianos in lateral view. e) First metacarpal SM219.33.1 from Serra de Molianos in dorsal view. All scale bars are 25 mm. 143
Figure 5.11 — a) PCA of the proximal ulna of several Iberian brown and cave bears. b) Biplot of transverse vs anteroposterior diameters of diaphysis of ulna of several Iberian brown bears. 144
Figure 5.12 — a) Biplot of transverse vs anteroposterior diameters of the proximal radius of several Iberian brown bears. b) Biplot of transverse vs anteroposterior diameters of the distal radius of several Iberian brown bears. 146
Figure 5.13 — PCA of the first metacarpal of several Iberian brown and cave bears. 147
Figure 5.14 — a) Extremely worn canine FO.I-81 in occlusal view. b) Unworn canine FO.I-88 with black venation of the enamel in lingual view. c) Relatively little worn m2 (FO.I-153) in occlusal view. d) Unworn M1 with black venation of the enamel in occlusal view (FO.I-154). e) Extremely worn M1 (FO.I-151) with part of the maxilla still attached in occlusal view. f) Relatively little worn P4 (FO.I-157) in occlusal view. g) Relatively little worn m1 (FO.I.-156) in occlusal view. h)

Unworn m3 with black venation of the enamel (FO.i-152) in occlusal view. i) Juvenile mandible with deciduous tooth and erupting m1 (FO.I-162) in labial view. j) Partial mandible with an extremely worn m3 (FO.I-37) in occlusal view. Scale bars are 25 mm..... 148
Figure 5.15 — a) Biplot of length vs breadth of the P4 of several Iberian brown bears. b) Biplot of length vs breadth of the p4 of several Iberian brown bears. d) PCA of the m3 of several Iberian brown and cave bears..... 150
Figure 5.16 — Atlas from Fontainhas (FO.I-164) in anterior view. Scale bar is 25 mm..... 151
Figure 5.17 — a) Biplot of dorsal articular diameter vs ventral articular diameter of the atlas of several Iberian brown and cave bears. b) PCA of the atlas of several Iberian brown bears. .. 151
Figure 5.18 — FO.I-45 pathologically conjoined XI and XII vertebrae of a brown bear from Fontainhas Cave in a) dorsal, b) posterior, c) right lateral, d) anterior, e) ventral, and f) left lateral views. Scale bar is 50 mm..... 152
Figure 5.19 — a) Right humerus from Fontainhas (FO.I-34) in anterior view. b) Left ulna from Fontainhas (FO.I-56) in posterior view. c) Left radius from Fontainhas (FO.I-59) in anterior view. Scale bars are 50 mm..... 153
Figure 5.20 — a) Biplot of length vs transverse distal diameter of the humerus of several Iberian brown and cave bears. b) Biplot of transverse distal diameter vs transverse distal articular diameter of the humerus of several Iberian brown and cave bears. c) Biplot of length vs transverse distal diameter of the radius of several Iberian brown and cave bears. d) Biplot of interior proximal diameter vs transversal articular diameter of the ulna of several Iberian brown and cave bears..... 155
Figure 5.21 — a) Right pisiform from Fontainhas (FO.I-166) in lateral view. b) Left scapholunate bone from Fontainhas (FO.I-74) in distal view. Scale bars are 25 mm..... 155
Figure 5.22 — a) Biplot of length vs transverse diameter of the scapholunate of several Iberian brown and cave bears. b) Biplot of length vs transverse tubercular diameter of the pisiform of several Iberian brown and cave bears. c) PCA of the pisiform of several Iberian brown and cave bears..... 156
Figure 5.23 — a) Right acetabulum from Fontainhas (FO.I-46) in lateral view. Scale bar is 25 mm. b) Bar diagram showing the diameter of the acetabulum of several Iberian brown bears. 157
Figure 5.24 — a) Left femur from Fontainhas (FO.I-51) in anterior view. b) Patella from Fontainhas (FOI-72) in anterior view. Scale bar is 25 mm. e) Right tibia from Fontainhas (FO.I-50) in anterior view. f) Right fibula from Fontainhas (FO.I-62) in lateral view. Scale bars of long bones are 50 mm..... 158

Figure 5.25 — a) Biplot of length vs transverse proximal diameter of the femur of several Iberian brown and cave bears. b) Biplot of length vs transverse diameter of the patella of several Iberian brown and cave bears. c) Biplot of length vs transverse minimal diameter of the diaphysis of the tibia of several Iberian brown and cave bears. d) PCA of the of the tibia of several Iberian brown bears. e) PCA of the of the fibula of several Iberian brown and cave bears. 159
Figure 5.26 — a) Right calcaneus from Fontainhas (FO.I-?) in proximal view. b) Right astragalus from Fontainhas (FO.I-52) in proximal view. Scale bars are 25 mm. 161
Figure 5.27 — a) Biplot of transverse diameter vs length the calcaneus of several Iberian brown and cave bears. b) Biplot of length vs transverse diameter of the astragalus of several Iberian brown and cave bears. c) PCA of the astragalus of several Iberian brown and cave bears. ... 162
Figure 5.28 — Partial distal metapodial with vertical marks from Fontainhas (FO.I-56) in lateral view. 163
Figure 5.29 — Canine from Furninha Cave in lingual view. Scale bar is 25 mm. 164
Figure 5.30 — a) P4 from Furninha Cave in occlusal view. Scale bar is 25 mm. b) PCA of the P4 of several Iberian brown bears. 165
Figure 5.31 — Three M1s from Furninha Cave in occlusal view, note the different morphologies, wear stages, patina color and overall sizes. Scale bar is 25 mm. 166
Figure 5.32 — a) M2 from Furninha Cave in occlusal view. b) GFP-1422, M2 which has a label attached mis-classifying it as m2 of a cave bear. Scale bars are 25 mm. c) Biplot of length vs breadth of the M2 of several Iberian brown and cave bears. d) PCA of the M2 of several Iberian brown and cave bears. 167
Figure 5.33 — a) p4 from Furninha Cave in occlusal view. Scale bar is 25 mm. b) PCA of the p4 of several Iberian brown bears. 168
Figure 5.34 — a) m1 from Furninha cave in occlusal view. Scale bar is 25 mm. b) PCA of the m1 of several Iberian brown bears. 169
Figure 5.35 — Two m2s from Furninha Cave in occlusal view, note the different morphologies, wear stages, patina color and overall sizes. Scale bars are 25 mm. 170
Figure 5.36 — a) m3s from Furninha Cave in occlusal view. Scale bar is 25 mm. b) Biplot of length vs breadth of the m3 of several Iberian brown, black and cave bears. 171
Figure 5.37 — Deciduous tooth (d4) of brown bear from Furninha Cave in lingual view. Scale bar is 25 mm. 171
Figure 5.38 — a) Braincase of brown bear from Furninha Cave in left lateral view. Scale bar is 25 mm. b) PCA of the skull of several Iberian brown bears. 172

Figure 5.39 — a) Left hemimandible of brown bear from Furninha Cave in labial view. Scale bar is 25 mm. b) Biplot of the height and diameter of the mandibular condyle of Iberian brown and cave bears. c) Biplot of the height of the mandibular ramus and its diameter of several Iberian brown and cave bears. 174
Figure 5.40 — a) Left hemimandible of brown bear from Furninha Cave in labial view. Scale bar is 25 mm. b) Biplot of the height and diameter of the mandibular condyle of Iberian brown and cave bears. c) Biplot of the height of the mandibular ramus and its diameter of several Iberian brown and cave bears. 175
Figure 5.41 — a) Scapula of brown bear from Furninha Cave in distal view. Scale bar is 25 mm. b) Biplot of the height and diameter of the scapular articular surface in several Iberian brown and cave bears. c) PCA of the scapula of Iberian brown and cave bears. 176
Figure 5.42 — a) Distal left humerus from Furninha Cave in anterior view, with the label "U. spelaeus" on it. b) Proximal left ulna from Furninha Cave in medial view. c) Left radius from Furninha Cave in anterior view. Scale bars are 50 mm. 177
Figure 5.43 — a) Biplot of the minimum mediolateral and anteroposterior diameters of the diaphysis of the humerus of diverse Iberian brown bears. b) Biplot of the mediolateral articular diameter and diameter of the trochlea of the humerus of diverse Iberian brown and cave bears. 178
Figure 5.44 — a) Left pisiform of brown bear from Furninha Cave in dorsal view. Scale bar is 25 mm. 179
Figure 5.45 — a) Proximal left femur from Furninha Cave in anterior view. b) Right tibia from Furninha Cave in anterior view. c) Distal left fibula from Furninha Cave in lateral view. Scale bars are 50 mm. 179
Figure 5.46 — a) PCA of the femur of diverse Iberian brown bears. d) PCA of the fibula of diverse Iberian brown bears. 180
Figure 5.47 — Morphological comparison of long bones from bears from Fontainhas and Furninha caves: a) Humerus. b) Femur. c) Radius. Scale bars are 50 mm. 181
Figure 5.48 — a) Right astragalus of brown bear from Furninha Cave in dorsal view. Scale bar 25 mm. b) PCA of the calcaneus of several Iberian brown and cave bears. 182
Figure 5.49 — a) First metacarpal from Furninha Cave in ventral view. b) First metatarsal from Furninha Cave in ventral view. c) Second metacarpal from Furninha Cave in dorsal view. d) Third metatarsal from Furninha Cave in ventral view. e) Third metacarpal from Furninha Cave in ventral view. f) Fourth metatarsal from Furninha Cave in dorsal view. Scale bars are 25 mm. 183

Figure 5.50 — PCAs from the metapodial bones of a diverse set of Iberian brown and cave bears. *U. spelaeus* are black dots. *U. arctos* are squares of different colors; green for modern bears, blue for Holocene bears from NW Spain, orange, brown and light blue for bears from Furninha Cave and yellow for bears from Fontainhas Cave. Red ellipses are marked around the area occupied by the majority of the specimens from Furninha Cave. 184
Figure 5.51 — Robustness index (Length/Distal mediolateral diameter) for the metapodial bones of Iberian *U. spelaeus*, *U. arctos* (Modern bears, Holocene remains from NW Spain and Portuguese Pleistocene remains from other caves) compared with *U. arctos* from Furninha Cave. The whiskers on the graphs mark the standard deviation from the mean for each sample. 185
Figure 5.52 — a) Selection of some of the first phalanges from Furninha Cave in dorsal view. b) Selection of some of the second phalanges from Furninha Cave in dorsal view. c) Selection of some of the third phalanges from Furninha Cave in lateral view. Scale bars are 25 mm. 187
Figure 5.53 — a) Detail of the right acetabulum of a brown bear pelvis from Furninha Cave in lateral view showing pathological bone overgrowths. b) Comparison of the distal part of the first metacarpal of two brown bears from Furninha Cave in dorsal view. Note the pathological bone overgrowths on the right one. c) Comparison of the third metacarpal of two brown bears from Furninha Cave in ventral view. Note the pathological bone overgrowths on the bottom one. d) Second phalanges of brown bears from Furninha Cave with pathological bone surfaces in dorsal view. e) Fibula of brown bear from Furninha Cave in medial view, showing a diaphysis bone growth that might represent a healed fracture. f) Left pisiform of brown bear from Furninha Cave in dorsal view, showing pathological bone growth in the tubercle. g) Left calcaneus of brown bear from Furninha Cave in dorsal view, showing pathological bone overgrowth. h) Detail of the occiput, cranial condyles, and foramen magnum of a brown bear skull (GFP-1338) from Furninha Cave in posterior view. Note the asymmetry between the condyles and the overall shape of foramen magnum, tilted towards the right. Scale bars are 25 mm. 188
Figure 5.54 — a) Proximal humerus of brown bear from Furninha Cave in lateral view, presenting gnawing marks. b) Distal radius of brown bear from Furninha Cave in anterior view, bearing two deep pits on the bone. c) Detail of calcaneus of brown bear from Furninha Cave showing a deep cut on its ventral surface. d) Second phalanx of juvenile brown bear from Furninha Cave in dorsal view with surface bone texture and damage compatible with digestion. e) Partial mandible of brown bear from Furninha Cave in lateral view, showing two punctures on the lateral surface that collapsed the surface of the bone. f) Proximal ulna of brown bear

from Furninha Cave in posterior view, showing gnawing marks on the surface of bone. g) Distal femur of brown bear from Furninha Cave in posterior view, showing the almost completely gnawed out condyles. h) Gnawing marks in the parietal of the skull of brown bear GFP-1338 from Furninha Cave. Scale bars are 25 mm. 190
Figure 5.55 — a) Body masses of individual brown bears from Western Iberian Peninsula. Brown, Pleistocene of Portugal; dark blue, Pleistocene of NW Spain; light blue, Holocene NW Spain; green, modern Iberian bears. Red bar at 200 kg mark separate males from females of Early Holocene population from NW Spain. b) Average masses of male brown bears from different North American populations compared with the average weight of male brown bears from Early Holocene NW Spain. Whiskers indicate the standard deviation. c) Average masses of female brown bears from different North American populations compared with the average weight of female brown bears from Early Holocene NW Spain. Whiskers indicate the standard deviation. d) Percentage of weight difference among average male and female bears from different North American populations compared with brown bears from Early Holocene NW Spain and modern Iberian bears. 197
Figure 6.1 — Top; number of taxa per each of the 36 sites compiled in the list. Bottom; number of species appearing one, two, three, four, between five and ten times and more than 10 times. 212
Figure 6.2 — Top; number of taxa living in Portugal nowadays detected in the fossil record per group. Bottom; % of taxa living in Portugal nowadays detected in the fossil record per group. 216
Figure 6.3 — Top; number of taxa living in Portugal, detected in the Pleistocene fossil record, and detected in the fossil record (without caves) per group. Bottom; % of taxa living in Portugal, detected in the Pleistocene fossil record, and detected in the fossil record (without caves) per group..... 217
Figure 6.4 — Top; number of known extinct taxa, overall and without caves, per group. Bottom; % of known extinct taxa, overall and without caves, per group. 218
Figure 6.5 — a) Sample based rarefaction applied to the real number of species and sites from the Pleistocene of Portugal. b) Sample based rarefaction applied to hypothetical 124 sites. c) Sample based rarefaction applied to the real number of species and sites (no caves) from the Pleistocene of Portugal. d) Sample based rarefaction applied to hypothetical 90 sites (no caves). 220

Figure 6.6 — Non-parametric estimations calculated over the dataset without caves: a) Number of species estimated, b) Number of species estimated (bootstrapping), c) % of total species estimated, d) % of total species estimated (bootstrapping). 222
Figure 6.7 — Non-parametric estimations calculated over the dataset including caves: a) Number of species estimated, b) Number of species estimated (bootstrapping), c) % of total species estimated, d) % of total species estimated (bootstrapping). 223
Figure 7.1 — Selected vertebrate species known from the Pleistocene of Portugal. Paleoart by José Pedro Ferreira. *Homo sapiens* for scale (190 cm). 1. *Panthera uncia lusitana*, 2. *Palaeoloxodon antiquus*, 3. cf. *Mammuthus primigenius*, 4. *Eucladoceros* sp., 5. *Stephanorhinus hemitoechus*, 6. *Equus ferus antunesi*, 7. *Panthera pardus*, 8. *Capreolus capreolus*, 9. *Cuon alpinus europaeus*, 10. *Bos primigenius*, 11. *Homotherium latidens*, 12. *Crocuta crocuta spelaea*, 13. *Panthera spelaea*, 14. *"Hyaena" prisca*, 15. *Pinguinus impennis*, 16. *Hippopotamus antiquus*, 17. *Hippopotamus amphibius*, 18. *Sus scrofa*, 19. *Castor fiber*, 20. *Dama sp.*, 21. *Canis lupus*, 22. *Cervus elaphus*, 23. *Ursus arctos*, 24. *Rupicapra* sp., 25. *Capra pyrenaica*, 26. *Macaca sylvanus*. 235

List of Tables

Table 6.1 — Taxa found in the Portuguese Pleistocene fossil record. The table includes their group, ELMAs in which they appear, number of localities where they have been detected, and current status (L.P, living in Portugal; L.P N.N, living in Portugal but not nesting for birds; L.E, locally extinct; EX, totally extinct). 205
Table 6.2 — Resume table of number and % of taxa for diverse categories. Green background, modern species. No background, Pleistocene fossil record. Grey background, Pleistocene record minus caves. 215

ACRONYMS & ABBREVIATIONS

aDNA	Ancient DNA analyses
B.P.	Before present
ca.	Circa
cal B.P.	Calibrated before present (for molecular datings)
CBL	Collection Borsatti-Lowenstein, University of Florence
DCT	Departamento de Ciências da Terra, NOVA School of Science and Technology
DNA	Deoxyribonucleic acid
ESR dating	Electron spin resonance dating
FCT-NOVA	Facultade de Ciência e Tecnologia, Universidade NOVA de Lisboa
FMHN	Field Museum of Natural History (Zoology) Mammal Collection
GCs	Geo-archeological complexes
Ka	*Kilo annum* (1000 years)
LACM	Natural History Museum of Los Ángeles
LGM	Last Glacial Maximum
Loc.	Loci of a site
Ma	*Mega annum* (1000000 years)
masl	Meters above sea level
MG	Museu Geológico (Geological Museum of Lisbon)
MIS	Marine Isotopic Stage
MMMH	Bell Museum mammals
MN	Mammal Neogene Zones
MZUF	Museum of Zoology, University of Florence
PCA	Principal component analysis
SDM	Species distribution modelling
YBP	Years before present

1

INTRODUCTION

1.1 History of Pleistocene vertebrate paleontology in Portugal

Published as: Estraviz-López, D., Ríos, M., & Grandal-d'Anglade, A. (2024). The dawn of Pleistocene vertebrate paleontology in Portugal. *Zubía*, (42), 305-310.

A version of this section was presented as an oral communication at the XXII EJIP (Encuentro de Jóvenes Investigadores en Paleontología), held at Igea, La Rioja, Spain in April of 2024. It was later published in volume of the journal *Zubía* (Estraviz-López et al., 2024).

1.1.1 Context

Most of the works on the History of Quaternary paleontology in Portugal are strongly focused on one scientist's career and the most general ones are several decades old (Cardoso, 1997). The study of Pleistocene fossil faunal assemblages, particularly in their early years, was closely linked to archeological research. The discovery of tools, first, and then human remains (nowadays we know that they were in fact younger) in the terraces of the Somme River in France associated with the remains of extinct fauna like rhinoceroses and elephants at the beginning of the second half of the XIX century, sparked the interest of the scientific community about the antiquity of humanity and the search of new bone material and artifacts in Pleistocene deposits (Cardoso, 2015a). From the mid-19th century, two significant factors further drove the interest in Pleistocene paleontology: Charles Darwin's publication of "The Origin of Species" and the rise of nationalist sentiment, which prompted European scientists to compete

with each other. As we will see, Portugal was not exempt from this European trend (Cardoso, 2015a).

1.1.2 Methodology

Through bibliographical review, we will provide a summary of the History of Pleistocene vertebrate paleontology in Portugal. We will discuss key events, scientists and categorize different time periods with the aid of said bibliographical revision. Some final remarks will be drawn from the presented historical revision. This chronological overview on itself will assist researchers in understanding its development and integrating the evolution of this discipline with the broader History of paleontology at Iberian and European levels.

1.1.3 Chronology

1.1.3.1 The first studies (1857-1885)

In Portugal, the scientific study of the Quaternary started in 1857 with the 2nd Geological Commission of Portugal, notably led by Carlos Ribeiro (Cardoso, 2015b) whose work proved that it was possible to know about the distant past (well before the written texts, oral traditions and collective memory), just thanks to the study of material remains (being them bones or tools) coming from alluvial and cave deposits.

Carlos Ribeiro (1813-1884) was a military engineer who pioneered prehistoric archeology and Pleistocene paleontology in Portugal (Daveau, 2000). He led the Geological Commission alongside Pereira da Costa from 1857 until his death (Daveau, 2000). Ribeiro provided an accurate description of Quaternary deposits and he raised the question about how old the humanity could be and pointed towards the possibility that some tools that he collected could be from "Tertiary" (Cardoso, 2000a, 2015a). He also carried numerous fieldwork campaigns in the late 1870s, possibly to discover new materials to present at the IX International Congress of Anthropology and Prehistoric Archeology, held in Lisbon in September 1880. This event marked the culmination of 25 years of his work and is a hallmark for the study of Pleistocene vertebrates from Portugal (Cardoso, 2013).

Joaquim Felipe Nery Delgado (1835-1908) was also a significant figure in the genesis of the study of the Quaternary in Portugal. In 1857, he became an adjunct to the Director of the Geological Commission of Portugal. Later, he led the commission since the death of Carlos Ribeiro in 1884 until his own death in 1908 with more than 51 years of study and research in the areas of geologic cartography and prehistoric archeology on his back. During the 1880s he

excavated Furninha cave, which was a crucial excavation in the History of the Portuguese Pleistocene paleontology (Delgado, 1884). The excavation methodology employed was advanced for its time: Each item was identified at the layer level and coordinated in a grid system; making Nery Delgado a pioneer in the 3D location of archeological artifacts (Cardoso, 2021). As geologist his major interest was the study of the Paleozoic rocks in Portugal, mostly from Alentejo, as well as the nature (animal or vegetal) of the then enigmatic marks of "bilobites" now known as *Cruziana* (Delgado, 1886).

Both Nery Delgado and Carlos Ribeiro were respected scholars who corresponded with other foreign scientists (Cardoso & Avila de Melo, 2001). At the time, the quality of their work put Portugal in the frontline of this type of research in Europe (Cardoso, 2015a).

1.1.3.2 The turn of the century (1885-1911)

During the turn of the century Paul Choffat, a swiss geologist, who inherited the lead of the Geological Services after Nery Delgado, uncovered some hippopotamus and proboscidean remains in the calcareous tuffs of Condeixa in 1893 (Choffat, 1895). Years later, he also promoted the diggings in the Pleistocene sites of Algar de João Ramos and Serra de Molianos. Around the same time, Edouard Harlé, one of the top experts in the Pleistocene research at that time, studied Portuguese material from sites like Furninha. His work would become a major reference of Pleistocene paleontology in Portugal for the next 80 years (Harlé, 1910; Cardoso, 1996a).

1.1.3.3 The stagnation period (1911-1950)

Following the outburst of the early 20th century, the study of the Pleistocene fauna in Portugal entered a phase of stagnation. Paul Choffat noted that: "*By reasons that we should not comment, although that our faculties are filled with professors of great erudition, there are few of them that are dedicated to the progress of observation sciences*" (Daveau, 2000).

1.1.3.4 The Renaissance of Pleistocene paleontology in Portugal (1950-1985)

Octávio da Veiga Ferreira (1917-1997) was a mine engineer who joined the Geological Services in 1950. He became a prominent figure in Iberian archeology and within paleontology, he authored 32 papers, four of them focusing on Pleistocene vertebrates. One of his most notable contributions is his study of Pleistocene rhinoceroses from Portugal (Cardoso, 2008).

Georges Zbyszewski (1909-1999) was the direct superior of Octávio da Veiga Ferreira. He was born in the Russian Empire, later becoming a French national. He visited Portugal for the first time in 1935 for his PhD thesis. In 1940 he joined the Geological Services and spent 40

years researching a wide array of topics. He wrote approximately 300 scientific publications, including over 100 publications on Quaternary lithic industries and fauna. Through the years "Zby" as he was affectionally known by friends and family (Cardoso, 2000b) compiled information about the Quaternary of Portugal, which in 1990, together with Veiga Ferreira synthesized with the new works of the next generation (Zbyszewski & Veiga Ferreira, 1990).

1.1.3.5 The modern era (1985-2025)

Miguel Telles Antunes (1937) is a highly prolific figure in the History of the Portuguese paleontology. He began his career at the University of Lisbon in 1960 after earning his PhD in Geology. In 1974 he relocated to the Universidade NOVA de Lisboa. He has authored more than 450 scientific articles and supervised 9 doctoral theses, on various topics. In the 1980s, he produced several works on Pleistocene faunas from Portugal, which are crucial for our understanding of several important sites. Antunes' contribution to the study of Pleistocene faunas remains significant to this day (FCT/UNL, 2016).

During the 1990s, João Luis Cardoso (1956), one of Antunes' students, emerged as a key researcher in the History of Pleistocene vertebrate paleontology in Portugal during the 1990s. He documented the occurrence of over seven Pleistocene mammal taxa for the first time, and named a new subspecies of Pleistocene horse, *Equus ferus antunesi*. His doctoral thesis published in 1993 "Contribuição para o conhecimento dos grandes mamíferos do Plistocénico Superior de Portugal" is a book of more than 500 pages. To this date, it remains the most comprehensive publication on Portugal's Pleistocene megafauna, encompassing remains of 26 taxa across 28 localities nationwide (Cardoso, 1993). During the next decades João Luis Cardoso continued to develop this research line, reviewing material from his thesis.

Other researchers have also made significant contributions to the advance of the field in the last decades: For example, Silvério Figueiredo focused on avifauna (Figueiredo, 2010), while archeologist João Zilhão uncovered numerous faunal remains with paleontological importance, focusing on an archeological perspective (Zilhão, 1987).

1.1.4 Remarks about the History of Pleistocene paleontology in Portugal.

As demonstrated by the excavations of Nery Delgado in the XIX century to the more recent work at the Almonda karstic system, the Pleistocene vertebrate paleontology in Portugal has developed in tandem with prehistoric archeology. Future discoveries are expected to result from the continued collaboration between archeologists and paleontologists, emphasizing the

study of faunal remains, not just in an archeozoological perspective but also delving into the paleobiology of Pleistocene fossil vertebrates. Emphasis should be placed on areas with significant development potential in Portugal, particularly in in the fields of molecular paleontology or microvertebrates. However, it is important not to neglect remains in geological contexts.

1.2 Main Pleistocene sites with fossil fauna from Portugal

This subsection provides a concise overview of each Pleistocene locality with fossil vertebrates in Portugal. It should be noted that this list is not exhaustive, as other sites with remains of Pleistocene vertebrates have been discovered (although these may not have been thoroughly studied in a paleontological or archeozoological context, or only one species has been discovered). For their locations on a map, see Figure 1.1. Localities are ordered from North to South. These locations are extremely influenced by lithology; being all of them but four situated in the Carbonated Mesozoic basins of Portugal: the Lusitanian Basin, in the West (Kullberg et al., 2013), and the Algarve basin in the South (Pais et al., 2000). From the other sites, two are in the caves of the carbonated rocks of the Hesperic massif (Cardoso, 1995a) and other two are open-air sites near rivers (Gabriel & Béarez, 2009; Cunha et al., 2019).

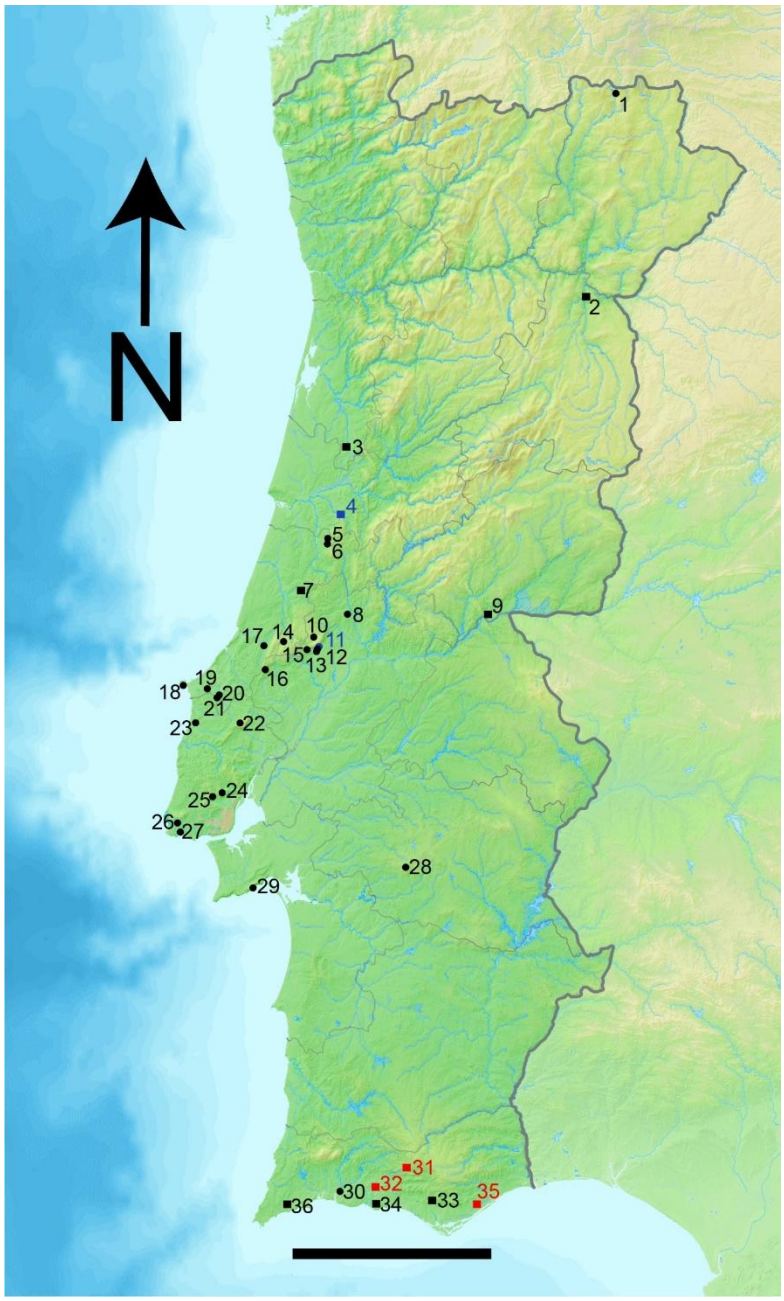


Figure 1.1 — Map of main paleontological Pleistocene sites in Portugal. Dots are cave localities, squares are open-air sites. Sites are numbered roughly from North to South. Red, Early Pleistocene; blue, Middle Pleistocene; black, Late Pleistocene. 1) Lorga de Dine; 2) Fariseu; 3) Mealhada; 4) Condeixa; 5) Buraca Grande; 6) Buraca Escura; 7) Lagar Velho; 8) Caldeirão; 9) Foz do Enxarrique; 10) Lapa do Picareiro; 11) Aroeira; 12) Oliveira; 13) Lapa dos Coelhos; 14) Algar da Manga Larga; 15) Casais Robustos; 16) Algar de João Ramos; 17) Serra de Molianos; 18) Furninha; 19) Casa da Moura; 20) Gruta Nova da Columbeira; 21) Lapa do Suão; 22) Fontainhas; 23) Lapa da Rainha; 24) Pedreira e Gruta das Salemas; 25) Pego do Diabo; 26) Porto Covo; 27) Algar de Cascais; 28) Escoural; 29) Figueira Brava; 30) Gruta de Ibn Amar; 31) Santa Margarida; 32) Algoz; 33) Goldra; 34) Guia; 35) Morgadinho; 36) Vale Boi. Modified from map by Wikipedia commons user Waldyrious (2020). Scale is 100 km.

1.2.1 Lorga de Dine

The cave of Lorga de Dine is located in Vinhais, Bragança, in northern Portugal, at a distance of 4 km from the Spanish border (Cardoso, 1995a). It is formed within Silurian limestones, making it one of the only two caves in Portugal with significant Pleistocene fauna from the Iberian Hesperic massif (Cardoso, 1995a). The latter is characterized by rocks that are usually too acidic for the preservation of Pleistocene fossils (Cardoso, 1995a).

The site contains the remains of chalcolithic humans and artifacts from the upper layers of the site which have been dated using radiocarbon dating and subjected to DNA analysis (Pereira et al., 2018; González-Fortes et al., 2019). However, the absolute dating of the Pleistocene layers below them has been not possible due to the low collagen content of the bones (Cardoso, 1995a).

No evidence of human presence has been found from the Pleistocene layers, leading to the assumption that the remains of herbivores correspond to prey of the carnivores that used the cave as a refuge. The most prevalent species are *Cervus elaphus*, *Bos primigenius*, and *Equus ferus*, with the presence of the rhinoceros *Stephanorhinus hemitoechus* being notable among herbivores (Cardoso, 1993). Among carnivores, it is noteworthy the presence of two subspecies of cave hyaenas: *Crocuta crocuta spelaea* and *Crocuta crocuta intermedia*. This observation suggests the potential for either the cave to contain some of the oldest Pleistocene levels in Portugal, or for this subspecies of hyaena to have survived later in the Iberian Peninsula, in a manner analogous to that of the *'Hyaena' prisca* from Furninha (Cardoso, 1994a).

1.2.2 Fariseu

The Fariseu site is located on the left bank of the Côa River, approximately 5 km from its confluence with the Douro. It is an open-air site that presents paleolithic art engravings (as many sites within the Côa valley) but it is the only open-air Upper Paleolithic site in the region with preserved faunal remains (Aubry et al., 2012). The site provides evidence for human presence dating back between 31.000 and 12.000 YBP, with the great majority of the skeletal remains originating from layer 4, dated to the Younger Dryas between 11.000 and 12.000 YBP by radiocarbon (Aubry et al., 2014).

The presence of burn and cutting marks on some of the faunal remains indicates potential human activities. The species present include *Cervus elaphus*, *Sus scrofa*, *Rupicapra* sp., *Oryctolagus cuniculus*, and *Sciurus vulgaris*, although fish remains are also present, indicating that human populations exploited a variety of resources. However, the fragmented state of the remains (Figure 1.2) prevented the recording of many measurements from them (Gabriel & Béarez, 2009).



Figure 1.2 — Left astragalus of *Cervus elaphus* used as reference (top). Left astragalus of *Cervus elaphus* from Fariseu (bottom). Image modified from Gabriel & Béarez (2009). Scale bar equals 3 cm.

1.2.3 Mealhada

The site of Mealhada is located approximately 14 km north of Coimbra, Portugal, on the banks of the Cértima River (Harlé, 1910; Zbyszewski, 1977; Cunha-Ribeiro, 1997). It is regarded as a notable open-air site for the study of the Paleolithic in Portugal since 1878, when it was presented it to the scientific community by Carlos Ribeiro (Harlé, 1910; Zbyszewski, 1977; Cunha-Ribeiro, 1997).

The chronology of this site has been the subject of much debate, but the archeological evidence (Acheulean tools), palynological analyses (including species typical of temperate conditions), and the faunal assemblage, indicate that this deposit can be ascribed to the end of the Riss glaciation (0.2–0.13 Ma). The most recent studies have suggested two main possibilities for the timing of this deposit: either it was formed during an interglacial episode, or it was deposited at the very beginning of the Late Pleistocene (Antunes et al., 1988; Cunha-Ribeiro, 1997).

The site's remarkable faunal assemblage is noteworthy among the Pleistocene Portuguese sites, with the presence of three species of chelonians (making it the oldest site in Iberian Peninsula with this level of species diversity), including *Mauremys leprosa, Emys orbicularis,* and an indeterminate testudine, whose remains exhibit potential cut marks produced by humans (Boneta Jiménez, Pérez-García, et al., 2023). The site is also one of the only three sites in Portugal to have yielded remains of hippopotamus, specifically a cuboid and a phalanx that are attributed to *Hippopotamus* cf. *amphibius* (Antunes et al., 1988; Martino et al., 2023). Finally, Mealhada is the site of discovery of the only sabretooth felid remain within the Portuguese Pleistocene fossil record, an astragalus ascribed to *Homotherium* (Antunes, 1986).

1.2.4 Condeixa

The calcareous tuffs of Condeixa are located between the villages of Condeixa-a-Velha and Condeixa-a-Nova, in the vicinity of the Roman city of Conimbriga, which is situated on the border of the plateau (Choffat, 1895). These calcareous tuffs have been found to contain numerous fossils of invertebrates (snails) and plant remains, including both as roots and leaves fossils (Azenha, 2020). The age of this deposit is not yet fully established, but it has been attributed to a Middle Pleistocene interglacial, with an estimated age of around 0.4 Ma, in base of the fauna appearing in the calcareous tuffs (Marques, 1997).

The site provided the first documented evidence of fossil hippopotamuses in Portugal (Choffat, 1895), as well as a molar of *Palaeoloxodon antiquus* (Cardoso, 1993). The hippopotamus remains include a relatively complete mandible (Figure 1.3) that has been attributed based on metrical and morphological characteristics to *H. antiquus*. The estimated age of approximately 0.4 Ma would place this specimen as the final documented occurrence of the species on the European continent (Martino et al., 2023).



Figure 1.3 — *Hippopotamus* remains collected from Condeixa. MG3665, right mandible fragment (A, dorsal view; B, m3 occlusal view; C, left lateral view; D, anterior view; E, right lateral view); MG3677, left canine (F, lateral view; G, mesial view); MG25172, left I2 (H, lateral view; I, ventral view); MG25170, right M1/M2 (J, occlusal view; K, labial view); MG25175, left m3 (L, labial view; M, occlusal view; N, lingual view); MG25171 thoracic vertebra (O, anterior view). Image modified from Martino et al. (2023). All scale bars equal 3 cm.

1.2.5 Buraca Grande

Buraca Grande is a karstic cavity located in the Vale do Poio Novo, Redinha, Portugal approximately 20 km southeast of Coimbra (Aubry et al., 1992). It is situated in the western part of the Serra do Sicó, in the Dogger limestone at 256 m above sea level, facing towards the south. The cave is about 13 m long and 3-4 m wide. The entrance is situated at a height of over 5 m (Aubry et al., 1992).

The cave's stratigraphy, influenced by the karstic nature of the site, exhibits three distinct zones with variable stratigraphic arrangements. The second area, specifically, has fourteen layers, separated by three unconformities, which delineate four distinct sediment packages (Aubry et al., 1997). The uppermost layer is entirely Holocene in age, while the second layer corresponds to the transition from the Pleistocene to the Holocene, with an estimated age ranging from 7.500 to 20.000 YBP dated with radiocarbon. The majority of the faunal remains were

recovered from this second layer. The third stratum is estimated to span from 24.000 to 29.000 YBP while the lower stratum corresponds to the Middle Paleolithic (Aubry et al., 2011).

The faunal elements include numerous rabbit bones, as well as *Cervus elaphus*, *Capra pyrenaica*, *Equus ferus*, *Sus scrofa,* and *Crocuta* sp. (Aubry et al., 1992). Significantly, this cave has provided paleobotanical evidence that this region acted as a refugium for Mediterranean species such as the olive tree *Olea europaea* (Figueiral & Terral, 2002).

1.2.6 Buraca Escura

The site of Buraca Escura is located on the opposite side of the Vale do Poio Novo to Buraca Grande; being it on the southern side of the valley and facing north at an altitude of 223 masl (Aubry et al., 2001).

The deposit of the cave is primarily comprised of two distinct packages of sediments. The first, lower package is of Middle Paleolithic origin, with an estimated thickness of approximately 80 cm and an age range of 50 ka and 80 ka. The second package corresponds to the Upper Paleolithic period, with an estimated thickness of around 40 cm and a stratigraphic division into six layers, dating from approximately between 25 ka and 32 ka when dated with radiocarbon (Aubry et al., 2011).

The faunal material from Buraca Escura includes 1440 identified elements from US 2 (Upper Paleolithic) and 1247 from US 3 (Middle Paleolithic). The cave is characterized by a relatively high biodiversity, including five herbivore species, six carnivore species, and nine taxa of mesofauna (seven birds, one leporid, and one turtle), although the Middle Paleolithic levels are more diverse, especially for carnivores. The most prevalent herbivorous species at the site is *Capra pyrenaica*, with numerous juvenile remains present. The most abundant carnivore species is *Lynx pardinus*, which is particularly prevalent in the Upper Paleolithic levels (accounting for over 90% of the carnivore remains). Among the mesofauna, at least seven species of birds have been identified (Arceredillo et al., 2018).

1.2.7 Lagar Velho

The rock shelter of Lagar Velho is located in the Lapedo Valley, on the left bank of the Caranguejeira stream, in close proximity to the city of Leiria (Zilhão & Trinkaus, 2002). The shelter is an elongated platform with an area of approximately 125 m^2, situated at an altitude of 85 m. It is notable for the discovery of a child from the Gravettian period, estimated to be approximately five years old at the time of his death (Zilhão & Trinkaus, 2002).

The excavated stratigraphic succession has been subdivided into a series of geoarcheological complexes (GCs) based on relative positioning, pedosedimentary characteristics, and anthropic features. The original succession was partially destroyed by terracing activities that exposed the burial of the child. The succession is complex and there is a lack of lateral continuity record across all sectors, leading to uncertainties in correlations between the east and central-west areas (Arnold et al., 2024).

The deposits span a time period of between 35.000 to 23.000 YBP. The site records three periods of human activity: Late Gravettian 31.6–26.0 ka, Terminal Gravettian 26.5–24.5 ka, and Middle Solutrean 25.2–23.4 ka (Arnold et al., 2024). The child burial site turned out to be slightly younger than previously reported. A direct radiocarbon dating of the collagen from the bones provided and age of 27780 to 28550 YBP, while taking into consideration the entire formation of the site and other radiocarbon, U-Th and ESR datings, it would be of 29.410 to 28.280 YBP; with the burial taking place at around the start of the second half of the 29th millennium B.P (Linscott et al., 2025).

A total of 135 skeletal remains from 11 taxa of small mammals (*Erinaceus* sp., *Talpa occidentalis*, *Crocidura* cf. *suaveolens*, *Sorex* cf. *granarius*, *Arvicola sapidus*, *Microtus agrestis*, *Microtus arvalis*, *Microtus arvalis-agrestis*, *Iberomys cabrerae*, *Terricola lusitanicus*, and *Apodemus sylvaticus*) have been recovered at the site, indicating relatively cold conditions near the LGM, with an open forest in the vicinity (López-García et al., 2021). Nevertheless, some Mediterranean plant species still survived these colder conditions in nearby areas, alongside riparian taxa (Ochando et al., 2022). Notably, the site has been identified as a nesting area for bearded vultures (Figure 1.4), (*Gypaetus barbatus*), with coprolites characteristic of the species being found (Sanz et al., 2023). Additionally, the presence of large ungulates, such as *Cervus elaphus*, *Equus* sp. , and *Bos primigenius*, has been documented, suggesting human activities in the shelter, at least for some time periods (Zilhão & Trinkaus, 2002).



Figure 1.4 — Lagar Velho rock shelter as observed from a northerly perspective, illustrating a bearded vulture pair nesting in a recess situated above the area of occupation, 29 Ka cal B.P. (A)—location of the infant burial; (B)—layer 143 from where the studied coprolites were recovered; (C)—the Hanging Remnant, a recess preserving sediments with Upper Palaeolithic remains dated from 26 to 24 Ka cal B.P. Image modified from Sanz et al. (2023).

1.2.8 Caldeirão

The cave of Caldeirão is situated 140 km northeast of Lisbon, Portugal, near the town of Tomar, in the right bank of the River Nabão. The cave opens in the northern slope of the valley of the River Nabão, facing south (Davis, 2002).

The majority of the works were conducted during the 1980s, although further archeological work is currently underway. The site comprises three distinct excavation zones: the entrance, the corridor, and the so-called "Black Chamber", which is situated at a considerable depth within the cave (Zilhão et al., 2021).

The layers are designated from A to P, and extend to a depth of nine meters. The layers A-Ea are of Holocene age, whereas the lower units are of Late Pleistocene age. The aforementioned layers are divided into three distinct groups on the basis of the presence of

discontinuities, dated by radiocarbon and single-grain optically stimulated luminescence. The layers designated Fa to Ja are between 22 and 28 ka old; the layers Jb to K are between 29 and 35 ka and the layers L to N are between 37 to 42 ka old. The layer O is estimated to be approximately about 55 ka old (Zilhão et al., 2021). A comprehensive study of the cave's fauna (see Chapter 6 and Appendix E for the complete list), including micromammals, was conducted, revealing evidence of a cold climate (Povoas et al., 1992; López-García et al., 2020) and the presence of animals that are relatively rare in the Portuguese fossil record, such as the beaver (Antunes, 1989). From a taphonomic perspective, the deposition of bones in the lower levels appears to have been driven by big carnivores, particularly hyaenas. It has been hypothesized that the cave might have also served as an hibernation den for bears (Davis, 2002). The observed pattern suggests that the more modern the level is, the more bones of anthropic origin it contains (Davis et al., 2007; Lloveras et al., 2011).

1.2.9 Foz do Enxarrique

The site of Foz do Enxarrique is an open air site located at the confluence of the Enxarrique stream with the Tagus River, at Vila Velha de Ródão, about 10 km from the border between Portugal and Spain, mainly dug during the 1990s (Brugal & Raposo, 1999).

The site is part of the terrace T6 of the Tagus River and is characterized by a single archeological level containing fossil bones and Mousterian tools, within a stratigraphic sequence approximately 6 m thick, situated at the base of the T6 terrace. Utilizing post-infrared infrared stimulated luminescence (pIRIR) it was possible to ascertain that this T6 terrace is between 60 ka at the base to 35 ka at the top, with the archeological unit being dated to nearly 44 ka (Cunha et al., 2019).

The faunal remains are predominantly comprised of *Cervus elaphus* and *Equus ferus*, accounting for over 75% of the total. The presence of *Bos primigenius* is minimal, with only a few remains identified. The only carnivores found are *Crocuta* sp. and *Vulpes* sp., accounting for less than 5% of the total remains. Of particular interest is the presence of rhinoceros (likely *Stephanorhinus hemitoechus*) and *Palaeoloxodon antiquus*, representing one of the final occurrences, if not the final occurrence, of straight-tusked elephants globally (Figueiredo et al., 2021).

1.2.10 Lapa do Picareiro

Lapa do Picareiro is located in the Serra de Aire, at an altitude of 570 m. The cave's entrance faces in a west-north-easterly direction, and its triangular form extends to a depth of approximately 10 m and a width of 8 m. The interior chamber of the cave is substantial in size, measuring approximately 11 x 14 m, and features a wide opening at the entrance (Bicho et al., 2003).

The sedimentary infilling of Lapa do Picareiro is approximately 10 m deep, having begun accumulating during the Marine Isotope Stage (MIS) 4 and continuing until the Holocene. The cave's stratigraphy comprises approximately 40 strata, with 36 being of Pleistocene age (Levels E to NN). The site possesses a continuous sedimentary sequence, which is considered to be the most extensive and complete cave sequence in Portugal, exhibiting no significant erosional unconformities or substantial diagenetic alterations (Haws, Benedetti, Carvalho, et al., 2021). The age range has been studied with radiocarbon dating and extends from approximately 10 ka on layer E, to 45 ka in the lowest dated layer, with the lowest layer estimated to be between 65 to 77.8 ka (Benedetti et al., 2019).

The site appears to be predominantly the consequence of anthropogenic activities (Bicho et al., 2003; Carvalho et al., 2022). Rabbits were brought to the site whole, cooked over fires, and consumed. Over 10.000 rabbit bones have been found (Bicho et al., 2003). Carnivores are generally scarce, with the most prevalent species being *Lynx pardinus*. Amongst herbivores, *Cervus elaphus* and *Capra pyrenaica* are the most abundant, and their paleoecology has been reconstructed in this cave via isotopic analysis (Carvalho et al., 2022). In addition to the aforementioned taxa, the cave has produced hundreds of remains of at least 25 taxa of birds, seven taxa of herpetofauna, and varied microvertebrates, which are yet to be studied alongside at least four taxa of fish likely brought to the cave by humans. However, there is still discussion regarding the precise interpretation of this site (Zilhão, 2021; Haws, Benedetti, Bicho, et al., 2021; Zilhão, 2022)

1.2.11 Aroeira

Aroeira Cave represents a seminal site in our understanding of the Middle Pleistocene fauna of Portugal, renowned for its significant paleontological discoveries, including the recovery of a relatively complete human cranium (Daura et al., 2017). Situated in Torres Novas, close to the modern source of the Almonda river, the cave is positioned at an altitude of 144 m. It is part of the Almonda karst system, a network of passages that were former outlets of the

Almonda river and which contain Pleistocene sedimentary infills (Daura et al., 2018). The cave has been dug several times since the last century (Marks, Monigal, et al., 2002; Marks, Brugal, et al., 2002).

The stratigraphy of the site consists of three major units: Unit 1 is the uppermost, a brecciated infill capped by flowstone. Unit 2 is a 2.2-m thick mud-supported breccia, rich in angular and sub-rounded clasts, which corresponds to the Acheulean layer X. This layer is divided into sub-layers X and Xb/c. Unit 3 is a basal endokarst fluvial deposit comprising two layers: layer XI is a silty sand, and layer XII is a slightly gravelly sand. The site's age is determined to be approximately 400 ka, specifically Marine Isotope Stage (MIS) 11. Layer X concretely is dated to between 389 and 436 ka by U-Th (Daura et al., 2018; Croitor et al., 2019; Daura et al., 2020; Sanz et al., 2024).

The small vertebrates are present, including anurans, squamates, insectivores, bats, and rodents, indicating an open-woodland landscape with relatively mild, humid conditions (to see the species found see Appendix E). These species reflect the climate conditions of the end of MIS 11 and biostratigraphically coincide with the absolute dating (López-García et al., 2018). Notably, the site has yielded the oldest beaver remains from Western Iberia (Cuenca-Bescós et al., 2021). The site also yielded numerous bird remains, constituting the only avifauna from the Middle Pleistocene known in Portugal (Marks, Brugal, et al., 2002). The most prevalent large mammals are the deer, from which there are four taxa have been identified: *Cervus elaphus*, *Praedama savini*, *Dama vallonnetensis,* and *Haploidoceros mediterraneus*, representing the only occurrence in Portugal for the last three species, which coexisted in the area (Croitor et al., 2019; Sanz et al., 2024). The site also yielded remains of non-human primates, like *Macaca sylvanus* cf. *pliocena* (Figure 1.5) (Marks, Brugal, et al., 2002; Marks, Monigal, et al., 2002; Alba et al., 2019). In summary, the Aroreira Cave is the most significant Middle Pleistocene site in Western Iberia for understanding the faunas of this time period, having provided evidence of human presence and human remains associated with all of this fauna (Trinkaus et al., 2003; Daura et al., 2017; Sanz et al., 2024).

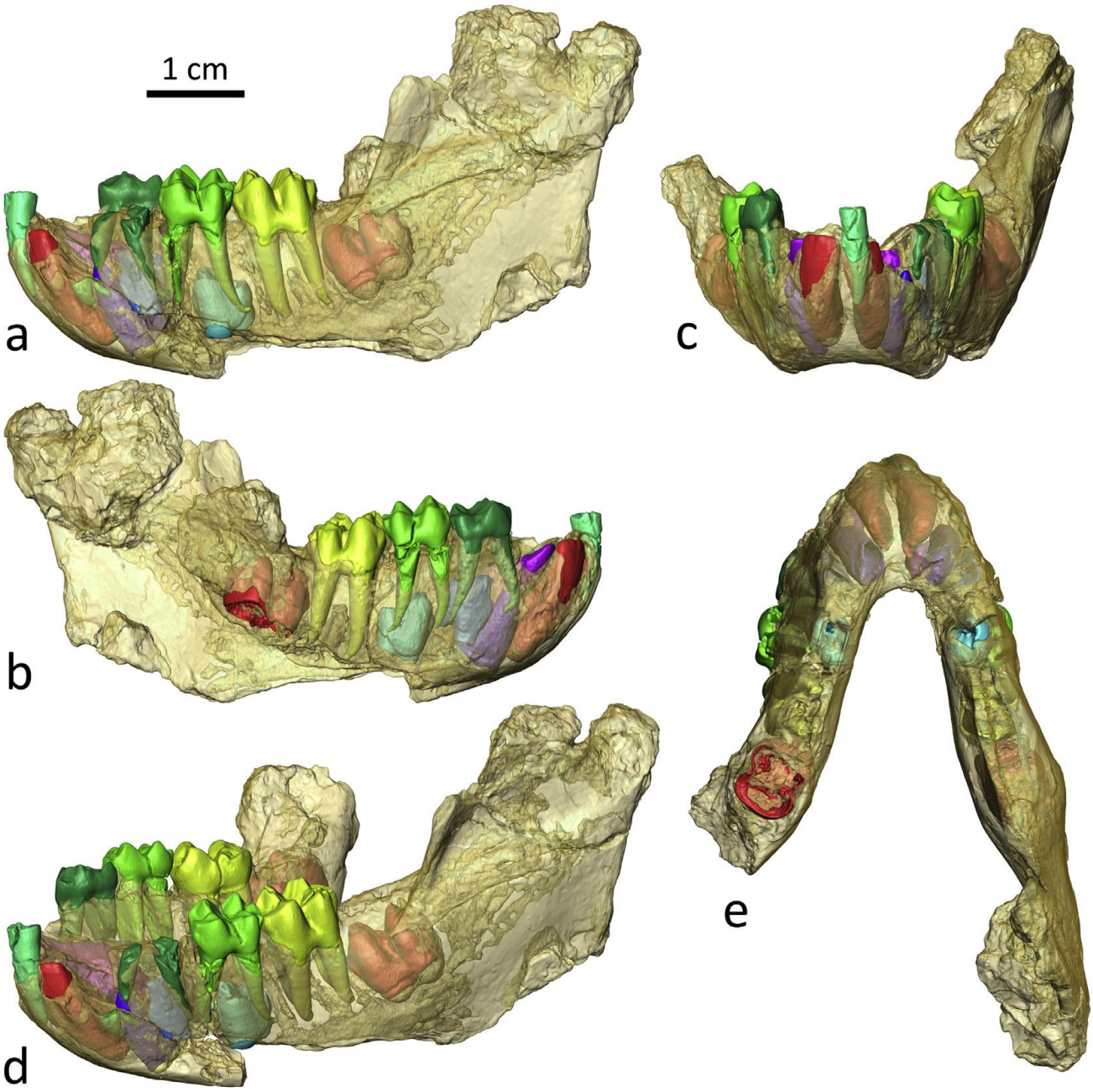


Figure 1.5 — Digital renderings of the juvenile macaque mandible ARO 934 from Gruta da Aroeira, in left lateral (a), right lateral (b), frontal (c), oblique (d), and basal (e) views. The mandibular bone is shown in semitransparent ocher, whereas tooth loci are denoted with different colors. Image modified from Alba et al. (2019). Scale bar equals 1 cm.

1.2.12 Oliveira

Oliveira Cave is situated at a lower level on the same escarp as Aroreira Cave, forming part of the same karstic system. The cave's entrance is located at an altitude of 114 m, 40 m above the spring of the Almonda river. From 1989 to 2012, it was the focus of extensive excavations (Zilhão et al., 2013).

Despite its complex topography and the collapse of the entrance, the stratigraphy has been the subject of extensive study. The dating of this cave has been achieved through the utilization of multiple radiometric methods, including the use of C^{14} and U-Th techniques, as well as direct speleothem and OSL dating (Angelucci & Zilhão, 2009; Zilhão, Angelucci, Arnold, Demuro, et al., 2021). The archeological succession, which spans approximately 6 m, encompasses a period of approximately 30 ka. This includes including the final phase of the MIS 5c at its lower levels (layers 23-25 are older than 92 ka ago) and the entirety of MIS 5b and MIS 5a, with the exception of a hiatus between the layers 14 and 15. This hiatus corresponds to the interstadial GI 21. The upper layers (8-14) are estimated to be between 72.3 to 77.8 92 ka old (Zilhão, Angelucci, Arnold, Demuro, et al., 2021).

A diverse vertebrate fauna was recovered from the cave; including 12272 remains of 4686 individuals from 22 micromammal taxa. This allowed the reconstruction of the climate and environment of the surrounding area of the cave as an open woodland (López-García et al., 2022). Another noteworthy faunal discovery is the presence of tortoises, which were identified at all levels of the site. A total of 5701 remains from at least 79 tortoises were discovered, indicating that they were likely accumulated by Neanderthals (Nabais & Zilhão, 2019). The megafauna has been less extensively studied but is seems probable that periods of occupancy of the cave by carnivores and humans alternated. The most common carnivores are the lion and wolf in the older layers (25-15), which date from the MIS 5b, while the bear and the lynx dominate in the younger layers (14-7), which date from the MIS 5a. The presence of over 300 remains from rhinocerontids is especially noteworthy given that few remains of this group are known from other Portuguese caves (Angelucci et al., 2023).

1.2.13 Lapa dos Coelhos

Lapa dos Coelhos is another former spring of the Almonda river situated slightly at a lower level in the escarpment (known as Arrife) than Aroeira and Oliveira (Gameiro et al., 2017). The archeological excavation of the site took place between 1997 and 2010. The cavity had a sub-triangular shape at the beginning of the works, with an area of about 8 m^2. Subsequent

excavations revealed a corridor morphology, exhibiting an east-west orientation (Gameiro et al., 2017).

Ten strata of varying ages have been identified, being dated by radiocarbon, with strata 3 and 4 estimated to date from 13 to 14 ka, while the oldest layers of the sequence reach Mousterian times (indicating an age greater than 40 ka) (Gameiro et al., 2017).

A wide variety of mammalian species have been identified, albeit in comparatively low numbers, including *Capreolus capreolus*, *Cervus elaphus*, *Sus scrofa*, *Bos primigenius*, *Capra pyrenaica*, *Rupicapra* sp., *Lepus* sp., and *Oryctolagus cuniculus*, as well as carnivores such as *Ursus arctos*, *Crocuta crocuta*, *Canis lupus*, and *Vulpes vulpes* (Gameiro et al., 2017).

Iberian ibex from layer 4 of Lapa dos Coelhos exhibited a comparable pattern of seasonal altitudinal mobility (as evidenced by strontium isotope analysis) to that observed in Mousterian ibexes from the nearby Oliveira cave. These specimens demonstrated a tendency to migrate moving between higher altitudes on the Serra de Aire during winter months and lower altitudes in in the vicinity of the Almonda karst system during summer. Evidence of mobility between two distinct areas is also exhibited by the coeval red deer. The least radiogenic values are consistent with the Tagus River banks, corresponding to the warmer months, while the most radiogenic values are consistent with the Neogene sediments of the Tagus Basin (Linscott et al., 2023).

1.2.14 Algar da Manga Larga

The Algar da Manga Larga is a cave located at the periphery of the Planalto de Santo António, in the municipality of Porto de Mós. The its entrance directed to the west at 460 masl (Regala & Cardoso, 2007). It consists in a series of deep vertical wells, reaching a depth of 186 m. During the beginning of the 2000s a series of skeletal remains were located in the cave: the skeleton of a juvenile wildcat (*Felis silvestris*), bird bones and a partial skeleton of a big felid including the skull (Figure 1.6), as well as some scattered wildcat bones in other galleries (Regala & Cardoso, 2007). These remains lacked more associated fauna or sedimentological context. Some years later the partial skeleton was published as belonging to a Pleistocene leopard (*Panthera pardus*) (Cardoso & Regala, 2006). But this ascription has recently being reviewed in Chapter 3 of this thesis (Jiangzuo et al., 2025), with more work about it to be done in the future (Chapter 4).

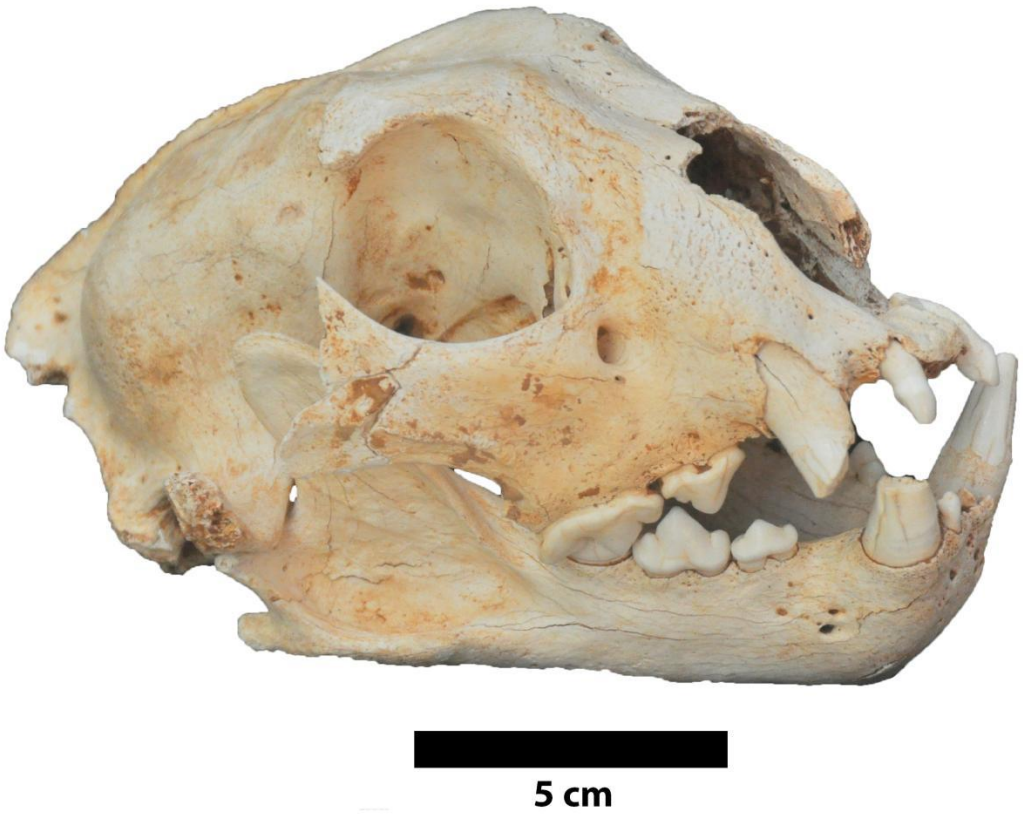


Figure 1.6 — *Panthera uncia lusitana.* Skull from Algar da Manga Larga (MG1355.0001-0002) in anterolateral view. Geological Museum, Lisbon. Image from Estraviz-López (2019). Scale equals 5 cm.

1.2.15 Casais Robustos & Cabeço de Morto

The two localities of Casais Robustos and Cabeço de Morto are situated in close proximity to each other within the municipality of Alcanena, in the vicinity of Minde. These sites were first documented by Cardoso (1993) in his doctoral thesis. The sites are located within a limestone quarry, and the discovery of these remains was serendipitous rather than the result of an excavation campaign. Consequently, no information is available regarding their stratigraphy; however, their age may be approximately the "Late Würm" (Cardoso, 1993). The remains comprise predominantly specimens of *Cervus elaphus, Equus ferus* and *Capra pyrenaica*, along with a distal right humerus of *Lynx pardinus*, which was also recovered from the site (Estraviz-López & Mateus, 2018a).

1.2.16 Algar de João Ramos

The Algar de João Ramos, also known as Gruta das Redondas, is a karstic cave located in the Jurassic limestones of the western foothills of the Serra dos Candeeiros, near the village of Redondas, in the municipality of Alcobaça (Cardoso & Carreira, 1991). The Neolithic layers of the cave were first explored by M. Vieira Natividade, and then the lower Pleistocene layers were excavated by Romão de Sousa (Cardoso & Carreira, 1991).

The stratigraphy of the cave consists of four layers from top to bottom: Layer 1 is up to 50 cm thick and contains Neolithic remains; Layer 2 is composed of red clays without bones, one meter thick; Layer 3 is also composed of red clay, but contains Pleistocene bones; and Layer 4 is composed of sands and clays, without bones. A bone from layer 4 gave a radiocarbon date of ~14 Ka (Antunes, Cabral, et al., 1989).

The Pleistocene fauna of the site is mainly characterized by large ungulates, with *Dama* deer, *Cervus elaphus*, *Bos primigenius,* and rare *Capra pyrenaica*; although there are at least some *Canis lupus* remains from the cave (Cardoso, 1993). The cave is also one of the few localities where remains of the horse subspecies *Equus ferus antunesi* have been found (Cardoso & Eisenmann, 1989). However, the most significant discovery from the cave is a bone of considerable size, which is most likely a proboscidean femur. This bone, which was discovered in layer 3, is estimated to be approximately 14 Ka making it one of the few remains of *Mammuthus primigenius* discovered in Portugal to date (Antunes & Cardoso, 1992).

1.2.17 Serra de Molianos

The cave of Serra de Molianos is among the most enigmatic localities from the Pleistocene of Portugal. The precise location of the site remains unknown, although it is known to be situated within the Molianos range, at the municipality of Alcobaça (Cardoso, 1993). The stratigraphy of the site remains poorly understood according to Harlé, (1910). However, Cardoso (1993) documented the presence of 21 remains of different species like *Cervus elaphus*, *Sus scrofa*, and, one ulna, two radii, and one first metacarpal of *Ursus arctos*. In a work concerning the bear remains from this site, Torres (1979) proposed that the site's age aligns with the Early Würm period, which is roughly contemporaneous with Furninha. The presence of *Stephanorhinus hemitoechus* remains in the cave has also been documented (Cardoso, 1990).

1.2.18 Furninha

Furninha Cave is located on the southern edge of the Peniche Peninsula, in the Leiria district, nowadays in close proximity to the sea (Delgado, 1884). A classical Portuguese Pleistocene locality, its excavation during the late 19th century constituted a pivotal moment in the advancement of Portuguese prehistoric archeology (Delgado, 1884) and was an extraordinarily well recorded for the time (Cardoso, 2021). The fauna was subjected to extensive study at the beginning of the 20th century and it was the best studied collection of Pleistocene fauna in Portugal for decades (Harlé, 1910).

The cave comprises an upper layer of Holocene sediments (with Neolithic human remains), which overlay the Pleistocene layers. The latter exhibit a rhythmic succession of sterile aeolian sands and four highly fossiliferous groups of levels, situated at 4-4.5, 6-6.5, 7-7.5 and 8.8-9.3 m of depth (Brugal et al., 2012). The cave has provided a single absolute date, derived from a bone recovered at a depth of 7.5 m using the Uranium/Thorium method (U/Th). However, the resulting standard deviation (80.886 +42.423/-31.265 YBP) is considerable (Raposo, 1995). A marine conglomerate within the cave, at the base of the excavation pit is attributed to MIS 5e, around 125 ka. According to the paleoenvironmental context, most of the deposit is believed to originate from a period between the MIS 5d to MIS 5a, extending to an upper limit around the beginning of MIS 4 (Cardoso, 1993; Brugal et al., 2012).

The fauna of Furninha is among the most diverse in the Pleistocene of Portugal, with even marine mammals being present (Figueiredo et al., 2022). The microvertebrates and herpetofauna are not as well studied, and not that many of them have been recovered, but the general good condition of the bone remains is evidenced by the rich avifauna of Furninha (with at least 436 remains from 33 species), as these specimens are particularly fragile (Figueiredo et al., 2017). Among these birds it is of special interest the occurrence of the great auk, *Pinguinus impennis* (Pimenta et al., 2008). But the main feature about the fauna of Furninha cave is the number of carnivores remains: over 3000 remains from 9 species. This assemblage is dominated by *'Hyaena' prisca* and *Ursus arctos* with over 500 identified remains in both cases (Brugal et al., 2012). The *'Hyaena' prisca* (Figure 1.7) collection is the largest of the world (Cardoso, 2021) and the brown bear the largest collection from a single site on Iberian Peninsula (see Chapter 5). This cave therefore would have acted as hyaena den (probably during the summer) and a hibernation den for brown bears during winter, with sporadic human visits to the site.

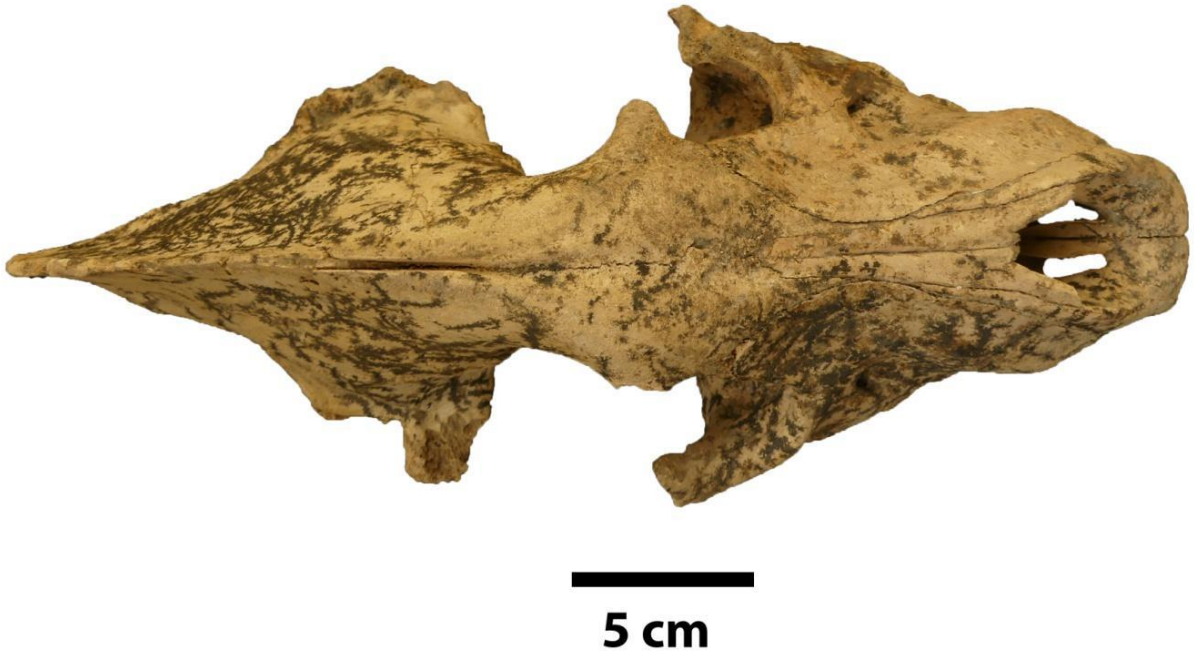


Figure 1.7 — Skull of *'Hyaena' prisca* from Furninha cave in dorsal view. Geological Museum, Lisbon. Image from Estraviz-López (2019). Scale bar equals 5 cm.

1.2.19 Casa da Moura

The Casa da Moura Cave is located in the municipality of Óbidos, on the northern edge of the Cesaredas plateau (Cardoso & Bicho, 2021). The cave entrance is a sinkhole, situated at an elevation of approximately 160 m, overlooking a vast landscape to the north. The Casa da Moura excavation marked a significant milestone in the annals of prehistoric archeology in the Iberian Peninsula, being the first excavation of a prehistoric cave in the region. This groundbreaking endeavor was initiated by Nery Delgado in the years 1865-1866 (Cardoso & Bicho, 2021).

The cave is composed of two clearly distinguishable layers. The upper layer is characterized by a poorly consolidated, blackish-brown sediment that contains human remains, and artifacts from the Neolithic and Chalcolithic periods. In contrast, the Pleistocene layer is described as a succession of sterile sands, more or less cemented, suggesting that Nery Delgado had removed all the paleontologically significant Pleistocene filling. There is one radiocarbon date for the deposit of around 25000 YBP (Antunes, Cabral, et al., 1989).

The Pleistocene fauna is dominated by *Canis lupus* and *Lynx pardinus*, although numerous remains of avifauna have been located on this cave too (Cardoso, 1993; Figueiredo, 2010).

1.2.20 Gruta Nova da Columbeira

Gruta Nova da Columbeira is a Middle Paleolithic site situated in Bombarral Municipality, within the Rôto Valley, near the edge of the Cesaredas plateau. It was discovered in 1962 during mining activities. The cave is notable for providing Neanderthal remains (Cardoso & Raposo, 2002).

Nine archeological levels were originally discovered within the cave, with the majority of human presence located within layers 6 and 9. Level 8 is of particular interest, as it contains the majority of the turtle and human remains. The age of the deposit, which was originally thought to be more recent and to contain proof of the late survival of the Neanderthals, is now thought to be between the MIS 5 and 3, so between 130 ka and 57 ka, based on the rhinoceros bone from level 8 which was dated by U-Thseries in 87.1 ± 6.3 ka BP (Zilhão et al., 2011).

The fauna of Gruta Nova da Columbeira is characterized by a high level of biodiversity, including two species of turtles, 19 species of microvertebrates, 28 species of birds and 17 species of megafauna. The turtles were brought by humans to the cave primarily as a food source, given their abundance (Jiménez Fuentes et al., 1998; Boneta Jiménez, Cardoso, et al., 2023). The presence of birds in the cave suggests a relatively open, mountainous and cold environment (Figueiredo et al., 2018). The most prevalent large mammals are deer and horse, with also some rhinoceroses. The most common carnivore was *Crocuta crocuta spelaea* (Fernández-Laso et al., 2015).

1.2.21 Lapa do Suão

Lapa do Suão is a cave situated in the Rôto Valley, in close proximity to Gruta Nova da Columbeira. Its entrance faces the northeast and is formed by a long passage with a southwest inclination and a 25 m^2 room at the end (Furtado et al., 1969).

A total of 12 layers have been described from the site, including Neolithic, Magdalenian, and Late Solutrean levels, which, according to radiocarbon dates, extend back to approximately 15000 YBP (Valente & Haws, 2006).

The most prevalent animal species in this locality is the rabbit, *Oryctolagus cuniculus*, with over 5000 bones belonging to at least 234 individuals. The microfauna includes species such as *Eliomys quercinus* or *Arvicola amphibius*, while the most common bird species are

Alectoris rufa and *Anas platyrhynchos*. The most prevalent species of carnivore is *Lynx pardinus*, while deer and wild boar dominate among the large herbivores (Valente & Haws, 2006).

1.2.22 Fontainhas

Fontainhas Cave is situated in the Montejunto range, in the municipality of Cadaval, about 400 masl. The excavation of this cave was not conducted with due consideration for the stratigraphy, as it was not undertaken by professional researchers around 1880 (Cardoso, 2020).

Despite this relative lack of stratigraphic context, there were at least two faunal assemblages identified, one of older age (Pleistocene) and one of younger origin (Holocene) (Cardoso, 2020). A single C^{14} date obtained for a bone from the older assemblage yielded an age of 22 ka (Antunes, Cabral, et al., 1989).

The bone material from this locality is in relatively good condition, and some cranial remains were identified, including the type specimen of a horse subspecies endemic to Portugal (Figure 1.8) named *Equus ferus antunesi* (Cardoso & Eisenmann, 1989). The fauna has been the subject of previous studies since the beginning of the 20th century (Cardoso, 1993). The second largest sample of bear remains (*Ursus arctos*) from Portugal was identified from this cave, dominated by a very complete large skeleton of brown bear (see Chapter 5 for more details).



Figure 1.8 — Type specimen of *Equus ferus antunesi* (FO.I-1) in lateral view. Geological Museum, Lisbon. Image from Estraviz-López (2019).

1.2.23 Lapa da Rainha

Lapa da Rainha is located on the left bank of the Alcabrichel river valley, opposite the village of Maceira, in the municipality of Torres Vedras (Cardoso & Santos, 1999). It is a cavity excavated within Jurassic limestone, forming a scarp at the summit of the hillside (Cardoso, 1993).

During the initial excavations conducted between 1968 and 1969, seven layers were described within the cave designated from C.1 (top) to C.7 (bottom). Layer C.5 was distinguished by the presence of numerous hyaena coprolites, while layers C.4 and C.3 revealed indications of human presence, dated to approximately 25 to 20 ka by two radiocarbon datings (Cardoso, 1993).

The avifauna consists on at least 16 species, with corvids being the most common elements, although the presence of *Lagopus* and *Tetrao urogallus* is noteworthy (Figueiredo, 2010). Among the big mammals *Cervus elaphus* dominates, with also an interesting amount of remains from *Capreolus capreolus*, as well as a deciduous tooth from a rhinoceros remains. Among carnivores, remains of *Felis silvestris*, *Lynx*, *Canis lupus* and *Crocuta crocuta spelaea* have been located, as well as numerous coprolites from the former (Cardoso, 1993, 1996a).

1.2.24 Pedreira e Gruta das Salemas

The two sites of Pedreira e Gruta das Salemas are located on the east side of the Lousa River valley, on top of a scarp formed by Cenomanian limestone (Upper Cretaceous). These two independent sites are extremely close together and share a relatively similar chronology and depositional history (Cardoso, 2017).

Pedreira das Salemas comprises a series of deep karstic fissures, which were identified during the course of limestone quarrying operations. The stratigraphic succession of the site is comprised of at least four distinct layers, delineated from the uppermost to the lowest. The uppermost layer, designated C.5, is dated to the Neolithic period, while the second layer, C.4, is assigned to the Upper Paleolithic. This layer has been identified as a source of human remains and has been linked to the presence of fauna. The third layer, C.3, is characterized by a substantial thickness, reaching up to 5 meters, and is composed of a sterile terra rossa. The fourth and final layer, C.2, is believed to be a Middle Paleolithic layer, distinguished by the presence of greenish clays and a notable abundance of fauna. It should be noted that while one radiocarbon dating has been performed on the site, this gave a wide age range of between 30,000 and 15,000 years BP (Cardoso, 1993, 1996a, 2017).

The fauna of Pedreira das Salemas is of considerable interest, as it includes the first remains of *Panthera spelaea* identified in Portugal (Antunes & Cardoso, 1986), an astragalus of rhinoceros (Cardoso, 1993, 2017), remains from *Dama* deer (Cardoso, 1989), and the presence of both the endemic horse *Equus ferus antunesi* and the rare *Equus hydruntinus* (Cardoso & Eisenmann, 1989; Cardoso, 1995b).

Gruta das Salemas constitutes a cave which is part of the same karstic system as Pedreira das Salemas. The cave was excavated during 1959 and 1960. The stratigraphy of the cave comprises eight distinct layers, ranging from the superficial to the deepest points. Notably, layer 8 contained a human decidual tooth, attributed to a Neanderthal, although the estimated age by radiocarbon of approximately 25000 YBP, most likely is not correct. The majority of the Pleistocene sequence is likely to be younger than that of Pedreira das Salemas (Cardoso, 1993, 2017).

Among the fauna, the occurrence of *Capreolus capreolus* (Cardoso, 1993) and *Rupicapra* (Cardoso & Antunes, 1989) on this site is of particular interest, given their divergent habitat requirements. Furthermore, a javelin tip composed of the penis bone of a bear from this site has been documented (Cardoso, 2017).

1.2.25 Pego do Diabo

The location of Pego do Diabo is within the municipal boundaries of Loures (Valente, 2004). This site is characterized by a cave formation oriented towards the north, situated at an elevation of approximately 250 m above sea level. It is positioned on a Turonian limestone ridge (Valente, 2004).

The cave is divided into six stratigraphic units: Layer A, is constituted by historical sediments; Layer 1 is formed by recent sediments mixed with some reworked Pleistocene elements; Layer 2 is the layer from which the majority of fauna is sourced and is dated by AMS to approximately 28000 YBP; Layer 3 also presents faunal elements, but with a different color due to the presence of manganese oxide; Layer 4 presents almost no archeological material, and Layer 5 has no archeological material whatsoever. It was inferred that layers 3 and 4 were Middle Paleolithic, though there is a paucity of material or dating evidence to substantiate this. However, the color of the bones suggests that some material from Layer 1 may be attributable to Pleistocene sediments found in Layer 2 (Valente, 2004; Zilhão et al., 2010).

Among the avifauna, the occurrence of a humerus of a pheasant (Figure 1.9) might be of particular interest, should it be determined to be actually a Pleistocene specimen, as this species is considered to be from Asian origin, being its presence in Europe unexpected (Figueiredo,

2010). Amongst herbivores, the most prevalent species is *Cervus elaphus*, whilst *Rupicapra* is present, as in the neighboring Gruta das Salemas (Cardoso, 2017). Among carnivores, the most common species is *Lynx pardinus*, while *Vulpes vulpes*, *Canis lupus*, *Crocuta,* and *Ursus arctos* are also present in very limited numbers (Valente, 2004; Zilhão et al., 2010).

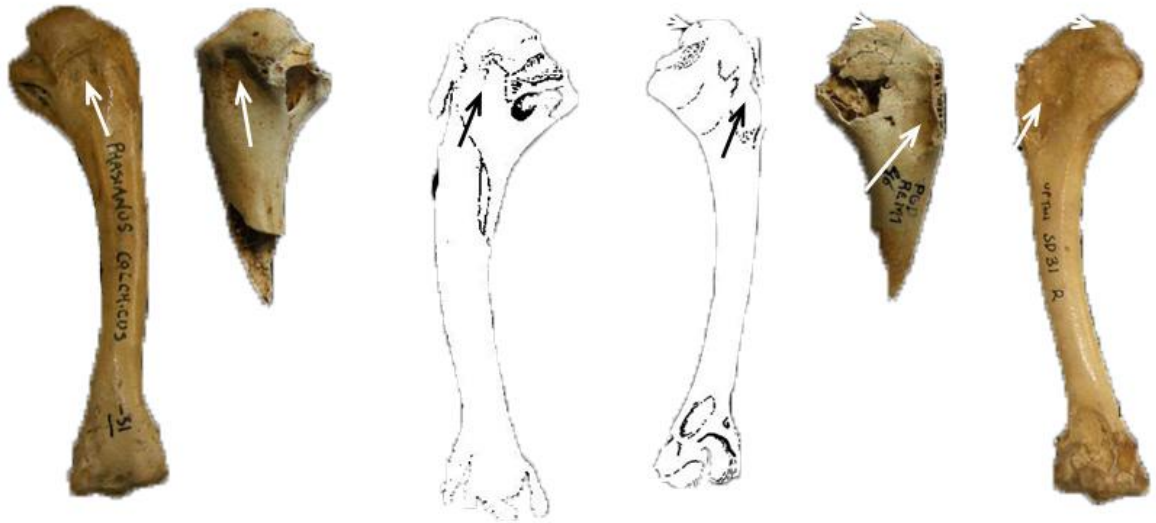


Figure 1.9 — Comparison of the proximal humerus fragment assigned to *Phaisanus colchicus* from Pego do Diabo compared with the specimen from the CIPA collection, and the 1:1 scale drawing by Cohen & Serjeantson, 1996. Cranial view (left) and caudal view (right). The arrows indicate the similarities considered for taxonomic classification. Image modified from Figueiredo (2010). Scale not provided in the original.

1.2.26 Porto Covo

Porto Covo is a cave situated on the municipality of Cascais, which was excavated under the supervision of Carlos Ribeiro in the 19th Century (Cardoso, 1994b; Gonçalves, 2008). The stratigraphy of the site and its precise chronology remain the subject of ongoing research. However, it is known that the cave was used as a burial site during the Neolithic. The presence of Pleistocene fauna is only attested thanks to the presence of *Crocuta*, with *Capreolus capreolus* and *Cervus elaphus* also appearing. The presence of turtle remains in the sediments may also be indicative of a Pleistocene origin, while a proximal femur of a wolf has been suggested as a more recent specimen (Cardoso, 1994b; Gonçalves, 2008).

1.2.27 Algar de Cascais

The Algar de Cascais is a karstic cavity situated within the urban area of Cascais, in compact Cretaceous limestone (Figure 1.1). It is located in the same escarpment where the well-known Poço Velho caves are found (Cardoso, 1993, 1994b).

The cavity is a small, vertical shaft with an approximate depth of 4 m. The exploratory findings in 1967 revealed a 1.20 m thick stratum of sediments at the base, comprising five distinct layers. Notably, only the layer C.2 contained fauna within a brownish-yellowish clay sediment. A bone from this layer was dated by radiocarbon to approximately 18000 YBP, although this date must be treated with a margin of error of more than 2000 years (Cardoso, 1993, 1994b).

The fauna is dominated by *Equus* remains, aurochs (*Bos primigenius*) and *Cervus elaphus*, including well-preserved metapodials from the latter species. Among the carnivores the most prevalent elements are *Vulpes vulpes* and *Lynx*, with few remains belonging to *Canis lupus*, *Ursus arctos* and *Crocuta crocuta spelaea* (Cardoso, 1993, 1994b).

1.2.28 Escoural

The Escoural Cave is located approximately 15 km from Montemor-o-Novo, near the village of Santiago do Escoural, in the Alentejo region of Portugal (Cardoso, 1995a). It is the sole cave in the Alentejo region with a significant known Pleistocene fauna, and the second within the Hesperian massif in Portugal, situated on Cambrian crystalline limestones (Cardoso, 1995a). The cave was discovered in 1963 during quarry operations and subsequently underwent extensive excavation throughout the 1960s. A second excavation effort was conducted between 1989 and 1992. A third phase of excavation is currently underway (Cobo-Sánchez et al., 2024). The cave is characterized by a labyrinthic shape (Figure 1.10) and a complex network of interconnected levels, with a main gallery (approximately 12 x 15 m) connected to about 17 karstic channels. The primary focus of research conducted at the site is the exceptional parietal cave art (Otte & Silva, 1996; Mauran et al., 2017), as well as the Neolithic necropolis (Otte & Silva, 1996; Peyroteo Stjerna et al., 2018).



Figure 1.10 — Escoural Cave and location of the test profiles excavated in 2020. Image modified from Cobo-Sánchez et al., 2024.

Nevertheless, below the Holocene Neolithic necropolis there are Pleistocene levels with Middle Paleolithic industries. One U-Th dating of a horse tooth provided an age of around 48 Ka (Cobo-Sánchez et al., 2024). From a taphonomic perspective, the cave was considered to have been predominantly utilized by carnivores, concretely hyaenas, during the Pleistocene (Cardoso, 1993). New works have found that the Iberian lynx likely played a crucial role in the deposition of the rabbit remains of this cave, although the sporadic presence of Neanderthals in the cave is likely (Cobo-Sánchez et al., 2024).

Among the fauna, Escoural has yielded intriguing findings, including the remains of rhinoceroses (Cardoso, 1990), and the occurrence of the dhole (*Cuon alpinus*) (Figure 1.11) (Cardoso, 1992). Additionally, the site has yielded the largest collection of leopard fossils from Portugal (Cardoso, 1995a).

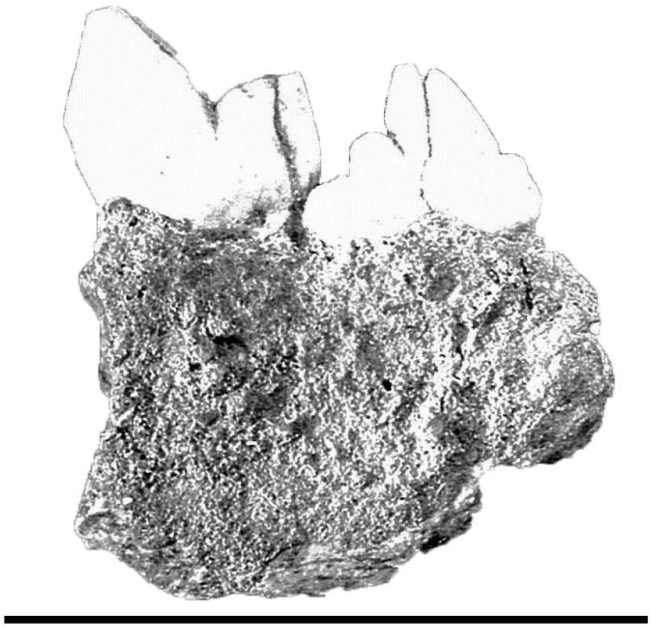


Figure 1.11 — Fragment of left hemimandible of *Cuon alpinus* with P4 and fragment of M1 from Escoural cave in lingual view. Scale bar is 35 mm. Image modified from Cardoso (1992).

1.2.29 Figueira Brava

Figueira Brava is a site of significant global importance in the study of Neanderthal behavior, being among the most studied Late Pleistocene localities in Portugal and the world. Excavations at the site were conducted in two phases, from 1986 to 1989, and from 2010 to 2013. Located in the southern coast of the Setubal Peninsula, at the foot of the Arrábida range, the site is situated at a height of 5 m above modern sea level, with a relatively open morphology (Figure 1.12) (Antunes, 2000b; Zilhão et al., 2020).

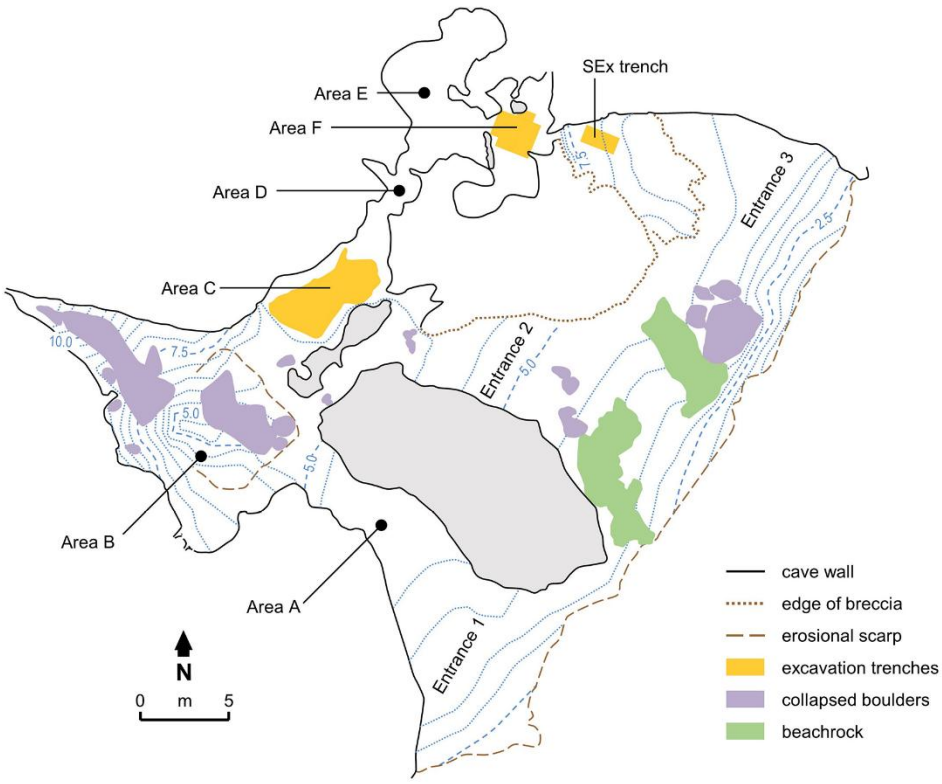


Figure 1.12 — Plan of Figueira Brava with position of excavation trenches (Area C, 1986 to 1989 paleontological work; Areas F and SEx, 2010 to 2013 archeological excavation) and indication of main features. Image modified from Zilhão et al. (2021).

The cave's bedrock is constituted by Lower Miocene Azeitão marine lutites and marls, which are overthrusted by Jurassic limestone. The cave formation was the result of coastal action by waves, as the Pleistocene sediment sequence is located over a Marine abrasion terrace from MIS 6 to MIS 5e (Eemian). The deposit underwent four phases of formation (FB-1 to FB-4) happened between 106 to 86 thousand years ago (MIS 5b and 5c), with hiatuses and/or flowstones capping the sediment in some cases, which allowed the U-Th and OSL dating of the. The deposit dates entirely to the end of the Last Interglacial, around 80-110 ka B.P, with some reworked younger sediment on top (Zilhão et al., 2020).

The faunal assemblage found at Figueira Brava Cave is extraordinarily diverse, given that it contains at least 86 taxa of terrestrial vertebrates, thus establishing this cave as the most diverse locality in the Portuguese Pleistocene (See Chapter 6 for more information). some of the levels of the cave have been found to contain a high abundance of remains indicating that Neanderthals had used the cave as a dwelling, with evidence of significant consumption of

marine vertebrates (e.g. sharks or dolphins) (Antunes, 2000a; Zilhão et al., 2020), and marine invertebrates (e.g. crabs) (Nabais et al., 2023).

Among the herpetofauna, three species of amphibians and seven of reptiles are present on the cave (E. G. Crespo et al., 2000), although the most notable elements are the 91 remains of chelonians, result of the exploitation of tortoises as a food source by Neanderthals (Nabais & Zilhão, 2019; Zilhão et al., 2020).

Birds are represented by at least 37 taxa, including some extinct species such as *Grus primigenia* or *Puffinus holeae* (Mourer-Chauviré & Antunes, 2000; Pimenta et al., 2015; Zilhão et al., 2020). However, the most interesting occurrence is that of the great auk, *Pinguinus impennis*, one of the only three in Portugal (Mourer-Chauviré & Antunes, 1991).

Among the micromammals, four insectivores, seven bats, nine rodents and two lagomorphs have been identified (Mein & Antunes, 2000; Jeannet, 2000), but the most remarkable among them is the only known occurrence so far of the porcupine (*Hystrix*) in the Pleistocene of Portugal (Figure 1.13) (Cardoso et al., 2021).

The assemblage of macromammals, is dominated by *Cervus elaphus* and *Capra pyrenaica* although there is a molar lamella from a *Palaeoloxodon antiquus*. The most common large carnivore is the bear *Ursus arctos*, although the remains from this cave are very poorly preserved. *Canis lupus* and *Crocuta* are also present, as well as *Panthera pardus*, but only some *Felis silvestris* mandibles are relatively well preserved (Cardoso, 1996a; Zilhão et al., 2020).



Figure 1.13 — *Hystrix* mandible from Figueira Brava. Lingual (top), occlusal (center) and labial (bottom) views. Image modified from Cardoso et al. (2021). Scale bar is 10 mm.

1.2.30 Gruta de Ibn Amar

Gruta de Ibn Amar is located in the Arade River estuary, near Portimão (Bicho, 2004). The cave is part of a karstic system in a limestone outcrop, from which several springs emerge. It is the only definitive Middle Paleolithic cave in the Algarve region of Portugal with Pleistocene fauna that has studied and published to date (Bicho, 2004).

Preliminary analysis indicates that the deposition of these faunal remains and lithic artifacts was the result of a very low energy depositional process. The faunal remains show slight abrasion damage resulting from contact with fine particles during slope washing. There is also no evidence of sorting, as the chipped remains (pieces smaller than 5 mm) make up more than half of the lithic assemblage (Bicho, 2004).

The fauna is dominated by rabbits and tortoise (Bicho, 2004), as we have seen these species might have been easily eaten by Neanderthals (Nabais & Zilhão, 2019). The cave also yielded remains of *Cervus elaphus* and a likely a small-sized *Equus* which could be *Equus hydruntinus* (Bicho, 2004).

1.2.31 Santa Margarida

The Santa Margarida site is located in the municipality of Loulé, in Algarve (Estraviz-López, 2019). It is situated on the slope of a hill, at an altitude of 300 m. It overlooks a small valley covered with vegetation between the villages of Alte and Santa Margarida (Estraviz-López, 2019). The site is part of the karst of the Picavessa Formation (Early Jurassic) and is one of the three Early Pleistocene sites known in Portugal.

The presence of extremely brecciated *terra rossa* and speleothems in the immediate vicinity suggests an eroded cave deposit. However, the exact stratigraphy of the site remains a mystery due to the lack of extensive systematic excavations (Estraviz-López, 2019). Nevertheless, the presence of the Early Pleistocene arvicolids *Victoriamys chalinei* and *Iberomys huescarensis* (as this is their only known occurrence in Portugal) as well as the appearance of *Iberomys brecciensis*, indicates the presence on the site of older layers of Early Pleistocene age (0.9 Ma) and younger layers of Middle Pleistocene age (0.6 Ma) (Estraviz-López et al., 2025).

In addition to the species mentioned above, seven other species of microvertebrates are known from this site, which has no known megafauna: Lacertidae indet., *Crocidura* sp., *Sorex* sp., *Oryctolagus* cf. *cuniculus*, *Eliomys* cf. *quercinus, Apodemus* cf. *sylvaticus*, and *Allocricetus bursae* (for more information see Chapter 2).

1.2.32 Algoz

The site of Algoz is located in the Silves municipality, Algarve. It is remarkable for being the oldest site known to date from the Pleistocene of Portugal (Estraviz-López et al., 2025).

It was first reported by Zbyszewski, (1950), and its discovery was made by construction workers while digging a well, at a depth of 18 to 20 m. The site is composed of yellowish sandy clays containing gravels and limestone blocks. This deposit lies on top of grayish clays with remnants of vegetation, bivalves, and gastropods, but devoid of vertebrate remains. Taphonomically, it was likely formed by a torrential stream deposit over a lacustrine environment (Estraviz-López et al., 2025). The chronological framework of the deposit was ascertained to be broadly ''Biharian mammal fauna, MN17 to MN20", dating back to ca. 1 Ma (Antunes, Azzaroli, et al., 1986; Pais et al., 2000). More recent works, given the strong metric similarity of the hippopotamus remains from Algoz (Figure 1.14) to *H. antiquus* specimens from around the Jaramillo reversal period (1 Ma) than to those from the post-Jaramillo period (Martino et al., 2023) and the presence of typical Villafranchian elements (Estraviz-López et al., 2025) ascribe the age of the site to the earliest Epivillafranchian, 1.2 Ma.

The well provided ten remains of hippopotamus, 15 remains of a relatively large cervid, two remains of a medium-sized cervid, and two remains of a lagomorph. The remains of the hippopotamus from Algoz recently underwent a reexamination by Martino et al., (2023). They concurred with Antunes, Azzaroli et al., (1986) in attributing these remains to *H. antiquus*. Restudying of the rest of the material from Algoz was carried out on the Chapter 2 of this thesis (Estraviz-López et al., 2025); identifying two individuals of the deer *Metacervocerus rhenanus* and other two of *Eucladoceros* sp. as well as two metapodial bones from an indeterminate leporid.



Figure 1.14 — *Hippopotamus* remains collected from Algoz. A, MG25769.1, femur head (A, proximal view). MG25769.2, right tibia (B, distal view; C, lateral view); MG25769.3, right calcaneus (D, posterior view; E, distal view; F, articular surface for the astragalus; G, medial view); MG25769.4, right astragalus (H, anterior view; I, lateral view; J, distal view; K, posterior view; L, medial view; M, proximal view); MG25769.10, right cuboid (N, anterior view; O, proximal view); MG25769.5, right navicular (P, proximal view; Q, anterior view; R, lateral view; S, distal view); MG25769.6, right MTIII (T, anterior view; U, lateral view; V, posterior view; W, medial view); right phalanxes in anterior view (X, MG25769.9, third proximal phalanx; Y, MG25769.8, third middle phalanx; Z, MG25769.7, second middle phalanx). Image modified from Martino et al. (2023). Scale bars equal 3 cm.

1.2.33 Goldra

The Goldra site is located in the Algarve region of Portugal, in close proximity to the small city of Loulé, specifically in Cerro de Nexe. The site is characterized by the infilling of a karst depression within the "Calcários bioérmicos de Cerro da Cabeça" (Antunes, Manuppella, et al., 1986).

The infilling of the karst depression consists of dolomite pebbles at the base, indicating potential transportation processes. Above this, a breccia is present, characterized by a ferruginous terra rossa matrix, calcitic cement, and rare quartz grains. The breccia contains bone fragments, teeth, and stone artifacts crafted from flint, quartz, quartzite, and graywacke. A significant proportion of the mammal remains exhibit indications of burning. The lithological composition and granulometry of the deposit vary rapidly, with some parts being coarser and richer in clasts while others are finer and richer in bones and teeth of micromammals (Antunes, Manuppella, et al., 1986).

The age of the deposit is determined by two factors: the stone industries and fauna. The former point to the "Early Würm" (Antunes, Manuppella, et al., 1986), with the presence of *Iberomys brecciensis* indicating the final part of the Middle Pleistocene.

The fauna of microvertebrates includes *Sorex araneus*, *Crocidura russula*, *Talpa europaea*, *Oryctolagus cuniculus*, *Apodemus sylvaticus*, *Microtus brecciensis*, *Pitymys duodecimcostatus*, and *Eliomys quercinus lusitanicus*, while the megafauna includes remains of *Cervus elaphus*, *Equus* sp., and *Sus scrofa* (Antunes, Manuppella, et al., 1986).

1.2.34 Guia

The seasonal Quaternary site of Guia is located in the vicinity of Cova da Areia, within the municipality of Albufeira in the Algarve region (Antunes, Crespo, et al., 1989).

The site is unique within the "Faro-Quarteira Sands". The outcropping levels correspond to white, fine, and incoherent sands, with rubefaction spots. The vertebrate remains are dispersed throughout the area, with no discernible layers are present. The stratigraphic succession of the deposit is designated as Upper Pleistocene, or potentially more recent, as it overlays the levels with Mousterian and Languedocian industries from the same sand unit (Antunes, Crespo, et al., 1989).

The fauna is comprised of microvertebrates, with the exception of a bovid tooth that has been tentatively identified as *Bos primigenius*. Five species of amphibians, four species of reptiles, and six species of micromammals are known from the site (Antunes, Crespo, et al., 1989).

Of particular interest among these species is the presence of *Mus musculus*. This species is either a modern contamination or indicates that the deposit is actually Holocene in age, as this species only reached the Iberian Peninsula during the last 7000-6000 years (Domínguez García et al., 2019; Cuenca-Bescós & Morcillo-Amo, 2022)

1.2.35 Morgadinho

The Morgadinho site is located within a well in the Tavira municipality (Antunes, Mein, et al., 1986). The site's discovery was the result of geological prospections conducted in this region of the Algarve. It is situated in a valley delimited by two faults and surrounded by Miocene marine sediments (Antunes, Mein, et al., 1986).

The well displays a Pleistocene succession with a thickness of approximately 150 m, comprising the following strata, listed from the uppermost to the lowermost: dark yellow superficial calichification silts, limestones with gastropods, clays with vertebrates and lignite, and finally marls with charophytes, gastropods and ostracods on top of several hundred meters of different sands of Neogene origin (Antunes, Mein, et al., 1986). Vertebrate fossils were discovered exclusively in the third clay layer that contained lignite. Palynological studies indicated the presence of a flora characteristic of humid and warm conditions, including *Keteleeria* and *Erodium* (Pais et al., 2000). Additionally, several invertebrates were identified, including nine species of aquatic gastropods suggesting a damp environment, and four ostracod species. The fauna was interpreted as correlative with that from Algoz, dating roughly from ''MN17 to MN20", ca. 1 Ma (Antunes, Mein, et al., 1986; Pais et al., 2000).

The vertebrate fossils recovered at Morgadinho include Cyprinidae (teeth), amphibians (indeterminate bone remains) and four species of small mammals, with minimal material assigned to each of them: a small-sized murid (represented by the antero-labial angle of a left M3 belonging to *Apodemus* or *Castillomys*), a large arvicoline (*Mimomys* sp.) with the size of *M. ostramosensis* or *M. savini* (represented by incomplete, very hypsodont teeth with cementum), the lagomorph *Prolagus* cf. *calpensis* (represented by tooth fragments), and the desman *Galemys kormosi* (represented by a well-preserved left P3) (Antunes, Mein, et al., 1986). The current location of this material is not known (see Chapter 2 for more information) (Estraviz-López et al., 2025).

1.2.36 Vale Boi

The site of Vale Boi is located in the municipality of Lagos, Algarve, in proximity to the southwestern most point of the Iberian Peninsula and 2.5 km from the modern coastline, situated along the incline of a hill. The site comprises three distinct loci: The Rockshelter, situated in proximity of the cliff face, The Slope, and The Terrace, located in the lower section above the alluvial plain (Tátá et al., 2014).

The site's stratigraphic sequence encompasses most of the Upper Paleolithic of Western Iberia featuring Gravettian, Proto-Solutrean, Solutrean, and Magdalenian occupations, plus Neolithic layers dated by numerous radiocarbon analyses. The Rockshelter comprises a sequence of five layers, designated from top (A) to bottom (E) and dated between 22 and 18 ka old. The Slope is divided into two subareas, with four layers: 1, 2a, 2b, and 3, dated between 25 and 17 ka. Finally, The Terrace is the most complete sequence of the site, with seven layers including a hiatus with Neolithic sediments on the uppermost part. The Pleistocene layers are estimated to date from approximately 30 to 20 ka (Manne et al., 2012; Cascalheira et al., 2013; Tátá et al., 2014; Paleček et al., 2024).

The site has gained notoriety in the archeological community due to the significant presence of rabbits used for grease extraction, as evidenced by the discovery of nearly 10000 bones from these animals across all layers of the site (Stiner, 2003; Manne et al., 2006, 2012). A further 3000 remains of fauna have been found, of which approximately 2500 belong to *Cervus elaphus* (Figure 1.15). Among the carnivores the most prevalent species is *Vulpes vulpes*, followed by *Lynx pardinus*. Of particular interest from a paleontological perspective is the appearance of the cave lion *Panthera spelaea* (Manne et al., 2012).



Figure 1.15 — Quartzite artifact embedded in first phalanx of red deer (*Cervus elaphus*) from Vale Boi. Image modified from Manne et al., (2012). Scale bar is 20 mm.

1.3 Pleistocene fauna of Portugal: A synthetic overview

This section offers a concise synopsis of the most salient fossil elements from the Pleistocene of Portugal, emphasizing prevailing trends and their ecological ramifications. It is not intended to be a comprehensive review of all discovered species. For a more comprehensive analysis, including extensive quantitative data, readers are referred to Chapter 6 of this thesis.

1.3.1 Herpetofauna

The fossil herpetofauna (amphibians and reptiles) of the Pleistocene of Portugal exhibits analogous patterns to those observed in other Southern European herpetofauna communities. The number of homeothermic taxa that have survived the last 2.5 Ma. of the Pleistocene is relatively low and consists of highly resilient taxa that could recover from low populations caused by glacial stages (Bisbal-Chinesta & Blain, 2018). The scarcity of fossils from the Early Pleistocene of Portugal precludes the presence of remains from the most vulnerable species to cold, which were the first to become extinct. Examples include the giant tortoises that inhabited Europe since the Miocene (Pérez-García et al., 2017), and the monitor lizards that

survived until the Middle Pleistocene in the Balkans (Georgalis et al., 2017). It is noteworthy that only a limited number of elements of the thermophilic Neogene herpetofauna have survived to the present day in Portugal, including the salamander *Chioglossa lusitanica* (Alexandrino et al., 2001).

Amongst the amphibian species, the olm (*Proteus anguinus*) is of particular interest. This species was identified at the site of Lapa do Picareiro, approximately 27000 YBP (U level). This species is not present nowadays in the Iberian Peninsula (Sánchez-Vialas et al., 2024) and is restricted to the Western Balkan Peninsula (Vörös et al., 2017). The presence of a troglobiont chordate so distant from its typical geographical distribution is an extremely interesting occurrence and warrants further detailed study in the future.

Amongst the reptilians, one group that is being recognized as important for the economy of humans is the turtles, which are the most common fossil reptiles in the Pleistocene of Portugal. Their significance as a food for Neanderthals is substantiated by the hundreds of remains found in Middle Paleolithic sites: over 350 remains from Oliveira (Nabais & Zilhão, 2019), over 90 from Figueira Brava (Zilhão et al., 2020), over 270 from Gruta Nova da Columbeira (Boneta Jiménez, Cardoso, et al., 2023), and over 120 remains from Mealhada (Boneta Jiménez, Pérez-García, et al., 2023). The most prevalent species among them is (by a wide margin) the testudine tortoise *Testudo hermanni*, a species which is currently locally extinct in Portugal, but still present in the east of the Iberian Peninsula (Sánchez-Vialas et al., 2024). The extant testudine species in Portugal, *Emys orbicularis* and *Mauremys leprosa,* were likely also targeted by Neanderthals, albeit in smaller numbers (Nabais & Zilhão, 2019; Boneta Jiménez, Cardoso, et al., 2023; Boneta Jiménez, Pérez-García, et al., 2023).

1.3.2 Avifauna

The avifauna (birds) of the Pleistocene of Portugal has received comparatively less attention than that of other areas of the Iberian Peninsula, but there has been an improvement in our knowledge over the last decade (Figueiredo, 2010; Pimenta et al., 2015). It is evident that numerous species formerly present in the Pleistocene of Portugal have become extinct in the southern regions of Europe, particularly outside of mountainous areas, including species such as the western capercaillie *Tetrao urogallus*, the rock ptarmigan *Lagopus muta*, and the gyrfalcon *Falco rusticolus*, which require colder climates for their survival (Poole & Boag, 1988). Of particular interest are also the occurrences of a handful of extinct bird species and subspecies.

One such example is *Corvus corax antecorax*, a Middle Pleistocene extinct subspecies of the common raven (Stewart, 2007) which is among the few Middle Pleistocene bird species

known in Portugal, having been discovered at Aroeira Cave (Marks, Brugal, et al., 2002). This raven is the most common bird species recovered in similar contexts in the Iberian Peninsula (e.g. Galeria, Atapuerca), so its appearance is not a surprise in the Middle Pleistocene of Portugal (Núñez-Lahuerta et al., 2022).

Another example is the crane *Grus primigenia*, a larger species than the modern *Grus grus*, comparable in size to the Asiatic sarus crane, *Grus antigone*. A single large scapula from Figueira Brava has been assigned to this species (Mourer-Chauviré & Antunes, 2000). These large cranes have been classified under several different species over the years (Stewart, 2007). These cranes survived throughout the Pleistocene and into the Holocene, as evidenced by fossil records found in France, Germany, Mallorca, Ibiza, and England, where they persisted until the Iron Age (Harrison & Cowles, 1977; Northcote & Mourer-Chauviré, 1985, 1988). This species is distinguished by its robust physique when compared with the sarus crane, it is hypothesized that it also exhibited a distinct lifestyle (Northcote & Mourer-Chauviré, 1988). The precise cause and timing of its extinction remains uncertain; however, the fact that other cranes narrowly avoided the same fate suggests that the reason may be related to the biology of the entire genus (Fontsere et al., 2024). The presence of tracks in Pleistocene sandstone, attributed to cranes, have also been documented in Portugal (Neto de Carvalho et al., 2023).

Puffinus holeae, the Canary dune shearwater, is another species whose remains—including coracoids, humerus, ulnas, and other—have been discovered in various layers of the Figueira Brava cave, including some Holocene layers (Pimenta et al., 2015). This marked the first recorded occurrence of the species outside its nesting grounds in the Canary Islands. Its presence in the Holocene sediments of Figueira Brava suggests that its extinction was likely caused by human colonization of the Canary islands, which resulted in the destruction of its colonies, rather than by climate change at the end of the Pleistocene, as it was later confirmed (Mourer-Chauviré & Antunes, 2000; Rando & Alcover, 2010).

Pinguinus impennis, commonly known as the great auk, has been identified on three separate locations in Portugal: One instance was from a geological context in Porto Santo Island (marking this as the southernmost occurrence of this species in the East Atlantic), and by two humeri at Figueira Brava, plus one humerus from Furninha, which was identified over a century after being collected (Mourer-Chauviré & Antunes, 1991; Pimenta et al., 2008).

Finally, a recent venue of investigation on the fossil avifauna of Portugal is the study of the coprolites left behind by the bearded vulture, *Gypaetus barbatus*. These coprolites have been first characterized at Lagar Velho, despite the fact that no body remains of this species

are known to be present in Portugal. However, their diagnostic characters have allowed their assignment to this highly specialized bird (Sanz et al., 2023).

A plethora of other aspects of the study of the Pleistocene avifauna in Portugal have yet to be explored, including the eggshells (Núñez-Lahuerta et al., 2021) and molecular studies of ancient DNA. These can facilitate the resolution of questions regarding like the precise identity of big cranes and the history of the populations of the great auk (Grealy et al., 2023).

1.3.3 Proboscidea

Among the mammals one of the most significant elements of the Pleistocene megafauna of Portugal are the proboscideans. The presence of one species, *Palaeoloxodon antiquus*, has been definitively confirmed, while the possibility of other species, *Mammuthus primigenius*, is also plausible. Fossils from the straight-tusked elephant, *Palaeoloxodon antiquus* include molars, tusks (Antunes & Cardoso, 1992; Cardoso, 1993), isolated lamellas (Cardoso, 1996b) and even a partial skeleton including the femur, tibia, phalanx, and vertebral apophysis (Estraviz-López & Mateus, 2018b; Estraviz-López, 2019). Tracks likely left by this species have been recorded along the southern coast of Portugal (Neto de Carvalho, 2010), in a similar manner to those found further south of Spain (Neto de Carvalho et al., 2021). The final occurrence of *Palaeoloxodon antiquus* on a global scale is documented at the Portuguese site of Foz do Enxarrique with an estimated age of 44 ka (Cunha et al., 2019; Figueiredo et al., 2021).

The presence of the woolly mammoth, *Mammuthus primigenius*, is much less well-stablished. Given the attribution of the material from Figueira Brava to *Palaeoloxodon antiquus* (Zilhão et al., 2020), two fossil remains that could belong to this species are left in Portugal. The first of these is a bone fragment from Algar de João Ramos, which, due to its size and radiocarbon dating (~15000 YBP), is tentatively assigned to the species, despite the absence of diagnostic traits, thus rendering this occurrence merely circumstantial (Antunes & Cardoso, 1992). The most compelling evidence to date for the presence of this species in Portugal is a dental lamella recovered from the Oeiras sea floor (Cruz Quebrada), which, through morphometric analysis, is found to fall within the expected parameters for this species (Cardoso & Regala, 2002). The presence of woolly mammoths as far south as Padul (Granada, Spain), suggests that these occurrences in Portugal, around the period of the LGM are plausible (Álvarez-Lao et al., 2009), but definitive evidence beyond doubt remains elusive.

1.3.4 Euarchontoglires

Euarchontoglires is a superorder of placental mammals that includes two major groups: Glires (rodents and lagomorphs) and Euarchonta (tree shrews, colugos, and primates).

The rodents of the Pleistocene of Portugal have experienced a surge in their study during the last seven years, with more information being published about them every year, and providing new data about the biostratigraphy and paleoclimate of the Pleistocene of Portugal (López-García et al., 2018, 2020; Haws, Benedetti, Carvalho, et al., 2021; López-García et al., 2022; Estraviz-López et al., 2025). Rodents of a particularly large size are represented by the beavers, which first appeared during the Middle Pleistocene (Antunes, 1989; Cuenca-Bescós et al., 2021), as well as the porcupine (Cardoso et al., 2021). However, to date, no fossils of marmots have been recovered. Lagomorphs are predominantly represented by the rabbit *Oryctolagus cuniculus*. This species is the most abundant mammal at Portuguese Pleistocene sites, despite that it is not recorded at all sites, with dozens of thousands of bones being recovered from at least 20 sites. This substantial collection of material has already enabled studies that would not have been feasible with other vertebrates. For instance, the surface temperature of Portugal during the LGM (6 to 7 Cº lower than today on average) has been calculated using the morphometry of the rabbit´s long bones (Davis, 2019). The presence of other species of lagomorphs that are now extinct (*Oryctolagus lacosti* and *Prolagus calpensis*) has been cited in the Early Pleistocene sites in Portugal, but this has not been confirmed yet (see chapter 2 for further information) (Antunes, Azzaroli, et al., 1986; Antunes, Mein, et al., 1986; Estraviz-López et al., 2025).

The non-human primates are represented by Middle Pleistocene barbary macaques, *Macaca sylvanus*, with all of their remains thus far being limited to the Aroeira Cave (Alba et al., 2019; Marks, Brugal, et al., 2002).

1.3.5 Chiroptera & Eulipotyphla

To date, no dedicated study has been conducted at the Portuguese level on either the Chiroptera (bats) or the Eulipotyphla (hedgehogs, gymnures, solenodons, moles, shrew-like moles, desmans, and true shrews). However, some localities, such as Figueira Brava (Mein & Antunes, 2000) have been the focus of research. The most prevalent species of chiropterans are the greater horseshoe bat *Rhinolophus ferrumequinum* and the greater mouse-eared bat *Myotis myotis* (see Chapter 6), although these species have not been described in numerous sites where their presence is probable (Galán et al., 2024). Among the Eulipotyphla, it is

noteworthy to mention the occurrence in Portugal of *Galemys kormosi*, an Early Pleistocene desman represented by one upper third premolar that could not be reviewed during this thesis (see Chapter 2) from the Morgadinho site (Antunes, Mein, et al., 1986). Its modern relative, *Galemys pyrenaicus*, which still exists today in the north of Portugal, has been discovered in the Middle Pleistocene of Aroeira (López-García et al., 2018) and in the Late Pleistocene of Lapa do Picareiro (Bicho et al., 2003)

1.3.6 Artiodactyla

The Artiodactyla (even-toed ungulates) is represented by numerous fossils, and is likely the most common megafaunal clade in the Pleistocene of Portugal (see chapter 6 for further information). Notably, even some scarce cetacean fossils have been found, suggesting that these may have been brought into caves (Figueira Brava and Furninha) by human activities (Antunes, 2000a; Zilhão et al., 2020; Figueiredo et al., 2022).

A recent re-evaluation of the three occurrences of hippopotamoids (hippopotamuses) in Portugal has yielded intriguing results. The Early Pleistocene material (predominantly distal limb elements) from Algoz has been ascribed to *Hippopotamus antiquus*, exhibiting metrical characteristics analogous to those observed on the Pre-Jaramillo reversal specimens of this species. The Middle Pleistocene material from Condeixa (mandible and teeth) has been ascribed too to *H. antiquus*, which would be one of the last occurrences (if not the last) of this taxon worldwide. The earliest Late Pleistocene material from Mealhada (cuboid and phalanx) has been assigned *to H. amphibious* thereby helping to clarify their biochronology at the Iberian level (Martino et al., 2023; Fidalgo et al., 2024).

In contrast, the suids (pigs and hogs) have not been subject to a dedicated study at the Portuguese level. However, given their absence from the scarce Early Pleistocene fossil record (see chapter 2), it can be assumed that all the Late Pleistocene material belongs to the modern wild boar species, *Sus scrofa*. This species is associated with forested areas and warm conditions, therefore, it is probable that it was relatively scarce in Portugal during the Pleistocene, given its limited occurrences (Cardoso, 1993).

Cervids (deer) represent the most prevalent group of fossilized megafauna in Portugal, with numerous species documented from the Early, Middle and Late Pleistocene. However, some remarkable elements found at the Iberian level (predominantly in the Cantabrian mountains) have not yet been discovered in Portugal, including the giant deer *Megaloceros* (van der Made, 2015, 2019; Uzunidis et al., 2023) and the reindeer *Rangifer tarandus* (Gómez-Olivencia et al., 2014). From the Early Pleistocene *Metacervocerus rhenanus* and *Eucladoceros* sp. are

known from the site of Algoz (see chapter 2) (Estraviz-López et al., 2025). The Middle Pleistocene deer diversity from Aroeira Cave merits particular attention, as evidenced by the co-occurrence of species such as *Praedama savini*, *Dama vallonnetensis*, *Haploidoceros mediterraneus*, and *Cervus elaphus,* which exhibited niche partitioning at this locality (Croitor et al., 2019; Sanz et al., 2024). The species *Cervus elaphus* is by far the most prevalent megamammal identified in the Late Pleistocene localities across Portugal, with thousands of remains having been recovered from most of the sites of this age in the country. However, the potential for comprehensive isotopic and microwear studies, encompassing a broad geographical and temporal scope, remains untapped, despite certain studies on the paleoecology and mobility of the red deer from the Almonda system (Linscott et al., 2023) or Lapa do Picareiro (Carvalho et al., 2022). The roe deer, *Capreolus capreolus*, is also present in several localities of Portugal, albeit at considerably lower numbers than the red deer (Cardoso, 1993). A similar phenomenon has been observed in the fallow deer, *Dama dama*. A more in-depth study of this species would be necessary, given the complex taxonomy of the *Dama*-like deer (Mecozzi et al., 2023), and the fact that there are no known remains of this species from the Pre-Roman Holocene, coming the oldest of this period from the Roman sites of São Pedro da Fronteira and Torre de Palma, so it is possible that the Pleistocene remains belong to another species of the genus *Dama* (Davis & MacKinnon, 2009).

As for the bovids (cattle, bison, buffalo, antelopes, sheep, and goats), the caprini (sheep and goats) Pleistocene fossils found in Portugal belong to two species: The Iberian wild goat (*Capra pyrenaica*) and the chamois (*Rupicapra* sp.). Although the alpine ibex (*Capra ibex*) is cited in the Reguerillo Cave in Madrid (Torres Pérez-Hidalgo, 1996), it is safe to assume that the Late Pleistocene *Capra* remains from Portugal belong to *Capra pyrenaica* (Cardoso, 1993). Remains from this species coming from Oliveira and Lapa dos Coelhos have been molecularly studied revealing their mobility patterns, as they spent the time during winter in the Serra de Aire and in summer near the source of Almonda River (Linscott et al., 2023). It is less clear which of the two species of chamois is present in Portugal (Cardoso & Antunes, 1989), and the matter would probably need further revision, as the difference between the species could be subtle, probably with the usage of advanced molecular techniques required (Pérez et al., 2002; Corlatti et al., 2011). As for large-size bovids currently there is only one known with certainty from the Pleistocene of Portugal: the aurochs, *Bos primigenius* (Cardoso, 1993). It is relatively common, but as it is the case with most other large mammals, molecular studies on Portuguese material are lacking, although they could help to clarify its position among other Iberian aurochs (Gurke et al., 2021). The absence of bison is also notable, as this species is relatively common in the

Pleistocene of other areas of the Iberian Peninsula. A detailed study of the large bovids from Portugal would be necessary, as the lack of cranial material makes the specific recognition of these challenging (Cardoso, 1993; van der Made et al., 2017).

1.3.7 Perissodactyla

The fossil Perissodactyla of the Pleistocene of Portugal is represented by equids (horses and asses) and rhinocerontids (rhinoceroses) (Cardoso, 1993).

Horses are among the most prevalent large mammals in Portuguese sites, second only to red deer (see Chapter 6). Notably, an extinct subspecies of horse, *Equus ferus antunesi*, has been described from the Late Pleistocene of Portugal (Figure 1.8) (Cardoso & Eisenmann, 1989). It is noteworthy that molecular phylogenies have identified a highly divergent clade of Iberian horses that emerged during the subsequent Holocene epoch, suggesting a potential relationship between this clade and the extinct *Equus ferus antunesi* from the Late Pleistocene of Portugal (Orlando, 2020). The European wild ass, *Equus hydruntinus*, has been identified in a number of Portuguese sites, though it is significantly less prevalent than the horse (Cardoso, 1995b) in a manner analogous to the relationship observed between the fallow deer and the red deer. This species has been shown by recent publications (Özkan et al., 2024) to be closely related to present-day onagers (*Equus hemionus*). It has been associated with the mysterious *zebro* (Nores et al., 2015), an equine mentioned in the medieval chronicles around Iberia, which became extinct in Portugal by the end of the 15th Century (Antunes, 2006). However, there are currently no known remains of *Equus hydruntinus* from historical archaeological contexts in Iberia that could support this relationship. But in Anatolia, this species reached the mid-first millennium BCE and may have inspired later accounts of Anatolian *onagri* by Strabo, Varro and Pliny the Elder (Özkan et al., 2024).

The oldest rhinoceros material of the Pleistocene in Portugal comprises a proximal femur, a third metatarsal, part of ulna, and two indeterminate metapodials from the Middle Pleistocene of Aroeira, tentatively classified as *Stephanorhinus etruscus* (Sanz et al., 2024). The Late Pleistocene fossils include approximately 30 isolated dental and tarsal elements from a minimum of eight localities, which are assigned to *Stephanorhinus hemitoechus* (Veiga Ferreira, 1975; Cardoso, 1990, 1993). The most extensive collection of rhinoceroses from Portugal, comprising over 300 specimens, originates from Oliveira Cave and awaits a dedicated study (Angelucci et al., 2023).

1.3.8 Carnivora

The order Carnivora (Feliformia and Caniformia) is represented in Portugal by a minimum of 18 species (see chapter 6 for further information).

The lynx has been identified as the most prevalent species of felid in Portugal (see Chapter 6). The question of whether one or two species are represented remains unresolved: There is ample evidence for the presence of the European lynx (*Lynx lynx*) in the Iberian Peninsula (Clavero & Delibes, 2013), as well as the Iberian lynx (*Lynx pardinus*) in Italy (Mecozzi et al., 2021), meaning that the modern distribution of these species varied quite a lot during the Pleistocene. Furthermore, the two species have been observed to hybridize during the last 2000 years (Lucena-Perez et al., 2024). It is hypothesized that both lynxes were present in Portugal during the Pleistocene epoch. However, this remains unconfirmed.

Pantherine cats are represented by three species in the Portuguese Pleistocene. the leopard, *Panthera pardus*, is the most prevalent (Villaluenga, 2016), especially in the Escoural Cave. The cave lion, *Panthera spelaea,* is rarer, but new and relatively complete material has been discovered and is awaiting a detailed study (Angelucci et al., 2023). Recently, a third pantherine cat, unique among the European felids has been described: chapters 3 and 4 of this thesis deal in detail with a new subspecies of snow leopard, *Panthera uncia lusitana*, discovered in the Algar da Manga Larga (Jiangzuo et al., 2025).

Two species of hyaena are present in Portugal: the spotted hyaena, *Crocuta crocuta*, and the European striped hyena, *Hyaena prisca*. The first species is represented by two subspecies (Cardoso, 1995a), *Crocuta crocuta intermedia* and *Crocuta crocuta spelaea* although the second is by far the most common, being the most abundant large carnivore after the wolf and the lynx (see chapter 6). The most extensive collection of *'Hyaena' prisca* (Figure 1.7) known worldwide today is from Furninha (Cardoso, 2021). This species may in fact represent a member of the *Pachycrocuta* lineage, as evidenced by the modern brown hyaena, *Parahyaena brunnea* (Pérez-Claros, 2024). The Portuguese collection (comprising nearly a thousand specimens) has the potential to greatly resolve the taxonomic position of this species, as it includes several well-preserved, near-complete cranial remains (Brugal et al., 2012).

The canids extant in Portugal during the Pleistocene are represented by four species. The most prevalent species is the wolf, *Canis lupus*, which continues to be present in Portugal, akin to the red fox, *Vulpes vulpes*. The third and fourth species, are the much more enigmatic dholes (genus *Cuon*). Despite their relative scarcity as fossils in the Iberian Peninsula, with only 35 documented occurrences, two of these species have been recorded in Portugal (Sanchis et al.,

2025). The first of these is *Cuon alpinus* (Cardoso, 1992) from the Late Pleistocene of Escoural (Figure 1.11). The second occurrence, which comprises significantly more complete remains, and is still awaiting a detailed publication, is *Cuon priscus* from the Middle Pleistocene of Aroreira Cave (Trinkaus et al., 2003; Zilhão, 2023).

The subject of the ursids from the Pleistocene of Portugal is comprehensively addressed in Chapter 5 of this thesis. However, only two species are currently recognized: the brown bear (*Ursus arctos*) and a Middle Pleistocene speleoid bear known by one premolar from Aroreira cave, likely *Ursus deningeri* (Sanz et al., 2024).

The only species of phocid mentioned in the literature is the ringed seal, *Pusa hispida,* including a right ulna from Figueira Brava that is attributed to this species that currently inhabits the High Arctic (Antunes, 2000a).

Finally, the fossil mustelids have not been the subject of detailed study, but at least three taxa are known, being the badger, *Meles meles*, the most common of these (see Chapter 6). All occurrences of mustelids are from the Late Pleistocene, but it appears that the wolverine, *Gulo gulo*, never reached Portugal, even during the LGM. This is not unexpected, as no evidence of cold-adapted land mammals (with the possible exception of the mammoth) has been unearthed in Portugal (Álvarez-Lao & García, 2011), although as previously mentioned Arctic birds and marine mammals appeared sometimes.

1.4 Objectives of this thesis

The present thesis seeks to address three principal objectives deemed relevant to our understanding of the Pleistocene fossil faunas of Portugal and general past life. These objectives are outlined below, alongside the hypotheses associated to them and a brief explanation:

Objective 1: To utilize the Pleistocene vertebrate record as a proxy to facilitate comprehension of the biodiversity of other time periods. (Chapters 3, 4 and 6).

Hypothesis H1: The fossil record of the Pleistocene is representative of contemporary fauna.

Hypothesis H2: It is possible to accurately infer the true number of species that existed within a particular ecosystem in the past, solely based on the analysis of fossil records.

The fossil record bias and the estimation of paleobiodiversity are central questions in the field of paleontology. The utilization of past biodiversity has the potential to shed light on this important topic by identifying and quantifying the bias in the fossil record. This can be achieved

by comparing the modern communities used as a template with the Late Pleistocene paleobiodiversity. Furthermore, insights derived from this analysis can inform ecological restoration initiatives, thereby impacting the conservation of extant species.

Objective 2: To provide a comprehensive analysis of the paleoecology and paleobiology of the fossil specimens of Ursidae and Ruminantia from the Pleistocene of Portugal. (Chapters 2 and 5).

Hypothesis H3: The only species of Ursidae to have been identified in the Late Pleistocene of Portugal is *Ursus arctos*.

Hypothesis H4: The absence of *Ursus spelaeus* during the Pleistocene had a certain impact on the paleoecology and paleobiology of the Portuguese brown bears.

Hypothesis H5: Portugal harbors a hitherto undiscovered biodiversity of Pleistocene ruminants.

The extensive availability of a plethora of specimens (unpublished and in collections, predominantly of bears) will facilitate the extensive utilization of novel methodologies for linear morphometric analyses. This will enable the exploration of numerous inquiries pertaining to their paleobiology and the establishment of a framework for further studies employing alternative methods, such as geometric morphometrics and molecular studies.

Objective 3: To shed light on the enigmatic nature of the Early Pleistocene epoch in Portugal. (Chapter 2).

Hypothesis H6: The Early Pleistocene of Portugal is better represented than is commonly perceived.

A critical examination of the existing faunal collections has been undertaken, with the Santa Margarida localities being investigated for the first time. These findings have the potential to provide new insights into the Early Pleistocene of Portugal.

Overall, the findings of this thesis will contribute significantly to our understanding of the Pleistocene fossil faunas of Portugal, offering new perspectives on biodiversity patterns, paleoecological dynamics, and the impact of taphonomic biases on the fossil record. The study will integrate multiple analytical approaches, including traditional morphometric techniques and emerging methodologies, with the aim of bridging existing knowledge gaps and providing a foundation for future research in paleontology and conservation science. The overarching

objectives of this study are aligned with broader efforts to reconstruct past ecosystems and enhance our comprehension of long-term ecological and evolutionary processes.

2

EARLY PLEISTOCENE (EPIVILLAFRANCHIAN) VERTEBRATES FROM PORTUGAL: AN UPDATED REVIEW

Published as: Estraviz-López, D., Grandal-d'Anglade, A., & Ríos, M. (2025). Early Pleistocene (Epivillafranchian) vertebrates from Portugal: An updated review. Geobios, 88–89, 77–89. https://doi.org/10.1016/j.geobios.2024.08.013

This chapter was published first as an abstract of the 4th PVC (Paleontological Virtual Congress) and in the special volume of the journal *Geobios* from said congress. We address the state of the art of the knowledge of Pleistocene vertebrates from the Early Pleistocene of Portugal and review them, including a new locality of this elusive chronology in Western Iberia.

2.1 Introduction

The Early Pleistocene is a period of Earth History that spans from 2.58 to 0.78 Ma. During this period, the Earth entered a regular cycle of glacial-interglacial stages (Bellucci et al., 2015). Towards the end of the Early Pleistocene, important changes occurred in the duration of these phases as well as the degree of seasonality, the so-called Early-Middle Pleistocene transition (Head & Gibbard, 2015). During the Early Pleistocene, the Villafranchian faunal assemblages were dominant, spanning from the Pliocene up until the latter part of the Early Pleistocene (Bellucci et al., 2015). The Villafranchian is divided into three parts: The early, middle, and late Villafranchian (Madurell-Malapeira et al., 2014). In addition, a biochronological unit called the Epivillafranchian has been identified, which separates the Villafranchian and Galerian faunas.

The Epivillafranchian ranges from 1.2 to 0.8 Ma and is marked by the first occurrences of *Praemegaceros verticornis* and *Bison menneri*, as well as the first occurrence of *Crocuta crocuta* (Bellucci et al., 2015). This unit is considered significant in terms of understanding the evolutionary history of many mammal species, as the Epivillafranchian represents the most relevant Pleistocene dispersal event concerning terrestrial large mammal communities (Rook & Martínez-Navarro, 2010; Bellucci et al., 2015). This biochron corresponds to the upper part of the Biharian mammal age. The Iberian Peninsula boasts an extraordinary record of Epivillafranchian and late Villafranchian localities, widely recognized as some of the most prominent in the world. Examples include those belonging to the groups of sites at Atapuerca or Orce, like Sima del Elefante (Huguet et al., 2017) and Fuente Nueva-3 (Sánchez-Bandera et al., 2020), both of them preserving proof of human presence. A number of Iberian localities also present an outstanding record of mammals, like Quibas (Piñero et al., 2022) and Cueva Victoria (Ferrández-Cañadell & Gibert, 2012) in the Murcia Region (southern Spain), as well as the localities of Barranc de la Boella (Vallverdú et al., 2014; Fidalgo et al., 2023) and the Vallparadís section (Madurell-Malapeira et al., 2010) in Catalonia (northeastern Spain), to name only some of them.

The western half of Iberia, in contrast, is nearly devoid of sites with faunas from this period (and the entire Early Pleistocene). This is related with the geology of the area, dominated by acidic Hercynian rocks that generate soils unfavorable for the preservation of vertebrate bone remains (Cardoso, 1995a). Nevertheless, three localities of approximate Epivillafranchian chronology were found in Portugal: Algoz, Morgadinho, and Santa Margarida (Antunes, Azzaroli, et al., 1986; Antunes, Mein, et al., 1986; Estraviz-López, 2019), all located in the Algarve region in the South of the country (Figure 2.1).



Figure 2.1 — Location of Early Pleistocene (Epivillafranchian) localities from Portugal, Iberian Peninsula (credit: LNEG). Scale bar: 25 km (regional level).

The main objective of this work is a revision of the fauna of microvertebrates and megamammals from these previously mentioned Early Pleistocene Portuguese localities, with the collection of biometrical and graphical data of all the vertebrate faunal elements, except from the hippopotamoids and the fauna of the site of Morgadinho (due to reasons explained in following sections). Concretely, an assessment of the taxonomic identity and ontogenetic stage of the Cervidae from Algoz will be carried out, as well as a confirmation and refinement of the identification of the most biochronologically significant taxa from Santa Margarida. Overall, we will carry out a comprehensive review of this fauna from Portugal in the context of the Epivillafranchian Iberian localities.

2.2 The Epivillafranchian localities of Portugal

2.2.1 Algoz

The site of Algoz is located in the Silves municipality (Figure 2.1). It was first reported by Zbyszewski, (1950), and its discovery was made by construction workers while digging a well, at a depth of 18 to 20 m. The site is composed of yellowish sandy clays containing gravels and limestone blocks. This deposit lies on top of grayish clays carrying remnants of vegetation, bivalves, and gastropods, but devoid of vertebrate remains. The well provided ten remains of hippopotamus, 15 remains of a relatively large cervid, two remains of a medium-sized cervid, and two remains of a lagomorph (see section ''Material" below for further information). According to Zbyszewski, (1950), this assemblage was initially considered to be from the Eemian interglacial, which dates back to ca. 125 ka.

Antunes, Azzaroli et al., (1986) conducted the initial faunal review, identifying four vertebrate species at Algoz: the hippopotamus remains were ascribed to *Hippopotamus antiquus*, the large-sized cervid was identified as *Eucladoceros* sp., the medium sized deer was classified as *Cervus* sp. (cf. *rhenanus-perolensis*), and the lagomorph remains assigned to *Oryctolagus lacosti*. The chronological framework of the deposit was ascertained to be broadly ''Biharian mammal fauna, MN17 to MN20", dating back to ca. 1 Ma (Antunes, Azzaroli, et al., 1986; Pais et al., 2000).

The remains of the hippopotamus from Algoz recently underwent a reexamination by Martino et al., (2023). They concurred with Antunes, Azzaroli et al., (1986) in attributing these remains to *H. antiquus*. This attribution was based of the morphology of the calcaneus, navicular and third metatarsal. Additionally, the morphometric analysis of the three aforementioned

bones, as well as the cuboid and astragalus, revealed a stronger metric similarity to *H. antiquus* specimens from around the Jaramillo reversal period (1 Ma) than to those from the post-Jaramillo period (or *H. amphibius*), thus supporting the proposed chronology for Algoz (Martino et al., 2023).

2.2.2 Morgadinho

The Morgadinho site is located within a well in the Tavira municipality (Figure 2.1). Its discovery was the result of geological prospections carried out in this region of Algarve. It is situated in a valley delimited by two faults and surrounded by Miocene marine sediments. The well presents a Pleistocene succession ca. 150 m thick, comprising the following strata listed from top to bottom: dark yellow superficial calichification silts, limestones with gastropods, clays with vertebrates and lignite, and finally marls with charophytes, gastropods and ostracods over several hundred meters of different sands of Neogene origin (Antunes, Mein, et al., 1986).

Vertebrate fossils were discovered exclusively in the third clay layer that contained lignite. Palynological studies indicated the presence of a flora characteristic of humid and warm conditions, including *Keteleeria* and *Erodium* (Pais et al., 2000). Additionally, several invertebrates, including nine species of aquatic gastropods suggesting a damp environment, and four ostracod species were identified.

The vertebrate fossils recovered at Morgadinho include Cyprinidae (teeth), amphibians (indeterminate bone remains) and four species of small mammals, with little material assigned to each of them: a small-sized murid (represented by the antero-labial angle of a left M3 belonging to *Apodemus* or *Castillomys*), a large arvicoline (*Mimomys* sp.) with the size of *M. ostramosensis* or *M. savini* (represented by incomplete, very hypsodont teeth with cementum), the lagomorph *Prolagus* cf. *calpensis* (represented by tooth fragments), and the desman *Galemys kormosi* (represented by a well preserved left P3). The fauna was interpreted as correlative with that from Algoz, dating roughly from ''MN17 to MN20", ca. 1 Ma (Antunes, Mein, et al., 1986; Pais et al., 2000).

2.2.3 Santa Margarida

The Santa Margarida site is located in the municipality of Loulé (Figure 2.1). It is nestled on the slope of a hill, at an elevation of 300 masl. It overviews a small valley covered with vegetation between the villages of Alte and Santa Margarida (Estraviz-López, 2019). In 2016, Jorge Graça, a local photographer, discovered a traditional Algarvian wall made of blocks filled

with hundreds of microvertebrate bones. The discovery was reported to a team from FCT-NOVA who were conducting fieldwork on the Triassic of Algarve. These blocks of bone breccia composing the wall were sourced in the immediate vicinity of the construction. The presence of extremely breccified terra rossa and speleothems in the immediate surroundings pointed towards an eroded cave deposit, making the site part of the karst of the Picavessa Fm. (Early Jurassic). The precise stratigraphy of the site is still an enigma due to the lack of an extensive systematic excavation (Estraviz-López, 2019).

Despite the difficult preparation of the blocks of bone breccia (the use of water softener was the only way to dislodge the pieces, what caused damages to several elements), the site resulted to be extraordinarily productive. From 0.5 kg of disaggregated sediment a total of 308 fossil remains were recovered (Estraviz-López, 2019). The remains discovered consisted of gastropods, lacertids, soricids, lagomorphs, and predominantly rodents (90% of remains; for further details, refer to the ''Material" section below).

The presence of vole molars, one identified as *Victoriamys chalinei* and another as *Iberomys huescarensis*, points towards an Early Pleistocene (late Biharian/Epivillafranchian) age for at least part of the deposit. Nevertheless, the occurrence of other vole molars morphologically congruent with *Iberomys brecciensis* might indicate a long hiatus in the deposit or a long period of time represented (Estraviz-López, 2019).

2.3 Material and methods

2.3.1 Material

For this study, all the material considered comes from the sites of Algoz and Santa Margarida. Regarding the material from Morgadinho, despite our diligent search in the Earth Sciences department of FCT-NOVA and other collections, the current whereabouts of the material recovered from this site remain elusive. The lack of published images of the fossils identified by Antunes, Azzaroli et al., (1986) impedes us to conduct a review of this collection.

The material from Algoz is stored at the Museu Geológico de Lisboa (Lisbon, Portugal). This study will not cover the hippopotamoid fossils reviewed recently (Martino et al., 2023). Here, we will focus on the cervid material, which includes 15 elements from a relatively large sized deer (MG-25768), and two elements from a medium-sized deer (MG-25770, MG-25771). The two lagomorph metapodials (MG-25772) will also be discussed. The complete measurements of the deer material are available in Appendix A.

The Santa Margarida material is curated the Earth Sciences Department at FCT-NOVA (Caparica, Portugal). Despite the large number of fossils recovered, most of them have limited taxonomic value due to them being damaged during the extraction process with water softener. This study will deal with the rodents (although other groups will be mentioned), especially arvicoline m1s and M3 due to their biostratigraphical relevance. See Appendix A for the complete list of material and measurements.

2.3.2 Methods

In the case of both the medium-sized and large-sized deer from Algoz, we first address the ontogenetic stage of the individuals and the minimal number of them. The remains were described and morphologically compared with a host of similar-sized deer with equivalent chronology in Eurasia. We follow the anatomical terminology proposed by Lister, (1996) in the case of medium-sized deer, and Breda, (2005) and van der Made, (2015) for the large-sized deer. We metrically compare them following measurements by van der Made, (2015). For the species usually classified within the genus *Metacervocerus*, we have decided to keep them in said genus for taxonomic stability, following Croitor and Robinson, (2020). Nevertheless, we have kept most of the rest of the *Dama*-like deer mentioned on this work within the genus *'Pseudodama'*, following Mecozzi et al., (2023) and for similar reasons – not taking a stance about the relationship of those species, a point far from the scope of this work. For the large-sized deer, we are following the classification used by van der Made (van der Made, 2015; van der Made & Dimitrijević, 2015; van der Made et al., 2017; van der Made, 2019) although we acknowledge that the relationship of some species and their systematics remain open to discussion (Croitor, 2021) a precise review on the issue is, again, well beyond the scope of this work.

For the microvertebrates from Santa Margarida, we first do a quick overview of the several groups recovered, including a brief description of a lizard mandible. For their relevance on the systematics of Pleistocene voles, m1s and M3s are often the only elements described and metrically studied (Cuenca-Bescós & Morcillo-Amo, 2022). To achieve this, we follow the terminology by López-García et al., (2015) and Martin, (2012). Finally, the arvicoline first lower molars are metrically compared (through scatter plots and principal component analysis) with an assortment of Southern European sites relevant for their specific determination (López-García, 2008; López-García et al., 2012, 2015, 2020).

2.4 Systematic paleontology

The vertebrate association from Algoz and Santa Margarida is diversified, comprising lizards, insectivores, rodents, lagomorphs, and artiodactyls (see Appendix A).

2.4.1 Algoz Cervidae: The medium-sized deer

Class Mammalia Linnaeus, 1758
Order Artiodactyla Owen, 1848
Family Cervidae Goldfuss, 1820
Genus *Metacervocerus* Dietrich, 1938
Metacervocerus rhenanus (Dubois, 1904) (Figure 2.2)

Description and remarks: The left hemimandible (MG-25770) has a d4 and belongs to a less than 20 months old individual, given that the last deciduous molar is still present and is not considerably worn. Meanwhile the distal right radius (MG-25771) has a completely fused distal portion, which only fuses after the two years of age in modern fallow deer (Bowen et al., 2016; Pfeiffer-Deml, 2020). This indicates that it is highly likely that the two fossils belong to different individuals.

The d4 of MG-25770 is not a particularly informative tooth, as its measurements are not commonly found in the literature. A portion of the mandible remains intact. The distal portion of the tooth, characterized by an enlarged hypoconulid, has been fractured, and the socket of the d3 is visible. The tooth displays minor wear. Little can be deduced metrically from this tooth, except that it shares a similar size with *'Pseudodama' vallonetensis* from Untermassfeld (Kahlke, 1997) and *'Pseudodama' nestii* from Pantalla (Cherin et al., 2022), while falling outside the variability of both taxa (for details see Appendix A).

The distal radius (MG-25771) belongs to a medium-sized deer in a relatively mature stage of life. It is broken irregularly around the midline of the shaft, with 174 mm of the distal portion still preserved. As seen in Figure 2.2, it bears a mosaic of characters typical of the distal radius of fallow deer and red deer, according to Lister, (1996). MG-25771 possesses – like the fallow deer – a convex dorsal edge of the articular surface of the medial carpal element, a ridge on the dorsal surface of the epiphysis and a shallow facet in anterior view. It also has some characters typical of the red deer, like the smooth ventral surface of the articular surface of the medial carpal element and a wider angle in the lateral most facet. A similar mosaic of characters appears in *Dama roberti*, an early representative of the genus *Dama*, so some of these elaphine

traits can be considered plesiomorphic traits typical of more archaic forms of the fallow deer lineage (Breda, 2015).

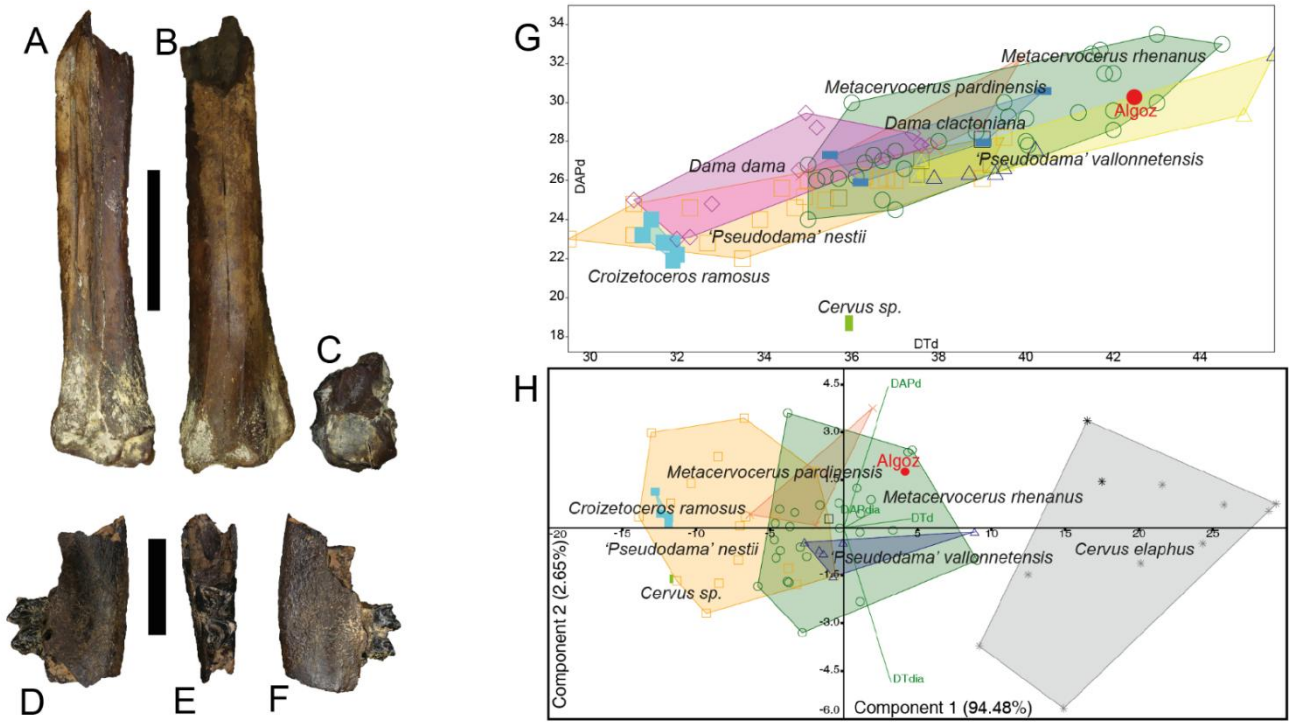


Figure 2.2 — A-C. Distal fragment of radius of *Metacervocerus rhenanus* from Algoz (MG-25771) in palmar or posterior (A), dorsal or anterior (B), and distal (C) views. D-F. Fragment of mandible with d4 of *Metacervocerus rhenanus* from Algoz (MG-25770) in labial (D), occlusal (E), and lingual (F) views. G. Scatter plot of the distal radius mediolateral and anteroposterior diameters of the Algoz specimen compared with other European *Dama*-like deer. H. Principal component analysis showing the position of the Algoz specimen compared with the radius of other European *Dama*-like deer. Scale bars: 50 mm (A-C), 25 mm (D-F).

The d4 of MG-25770 is not a particularly informative tooth, as its measurements are not commonly found in the literature. A portion of the mandible remains intact. The distal portion of the tooth, characterized by an enlarged hypoconulid, has been fractured, and the socket of the d3 is visible. The tooth displays minor wear. Little can be deduced metrically from this tooth, except that it shares a similar size with *'Pseudodama' vallonetensis* from Untermassfeld (Kahlke, 1997) and *'Pseudodama' nestii* from Pantalla (Cherin et al., 2022), while falling outside the variability of both taxa (for details see Appendix A).

The distal radius (MG-25771) belongs to a medium-sized deer in a relatively mature stage of life. It is broken irregularly around the midline of the shaft, with 174 mm of the distal portion still preserved. As seen in Figure 2.2, it bears a mosaic of characters typical of the distal radius of fallow deer and red deer, according to Lister, (1996). MG-25771 possesses – like the fallow

deer – a convex dorsal edge of the articular surface of the medial carpal element, a ridge on the dorsal surface of the epiphysis and a shallow facet in anterior view. It also has some characters typical of the red deer, like the smooth ventral surface of the articular surface of the medial carpal element and a wider angle in the lateral most facet. A similar mosaic of characters appears in *Dama roberti*, an early representative of the genus *Dama*, so some of these elaphine traits can be considered plesiomorphic traits typical of more archaic forms of the fallow deer lineage (Breda, 2015).

Metric analyses of the distal radius MG-25771 are inconclusive due to the significant overlap between various taxa (Figure 2.2). However, it can be ascertained that the Algoz specimen belongs to the group of relatively large *Dama*-like deer, surpassing in size modern *Dama dama, 'Pseudodama' nestii*, *Croizetoceros ramosus*, and an unnamed *Cervus* from the Early Pleistocene of Greece; as well as being smaller than *Cervus elaphus*. The principal component analyses reveal that the taxa most metrically similar to MG-25771 are *Metacervocerus rhenanus* from Senèze and *Metacervocerus pardinensis* from Saint-Vallier. Furthermore, the discriminant analysis conducted using the same dataset classifies the Algoz specimen as *Metacervocerus rhenanus* and correctly identifies 58% of the specimens when the Jackknife cross-validation method is employed. Simpler scatter plots demonstrate that the Algoz specimen falls within the range of variation of *Dama clactoniana* or outside that of any taxa. However, it consistently remains located relatively near the measurements from large *Metacervocerus rhenanus* (Figure 2.2).

In summary, the medium-sized Algoz deer (MG-25770 and MG-25771) is a relatively large-sized *Dama*-like deer with a radius size similar to those of some Middle Pleistocene species like *Dama clactoniana* or *'Pseudodama' vallonetensis*. Yet, it also metrically shows marked similarities with *Metacervocerus rhenanus* (Fig. 2). Combining the presence of *H. antiquus* with Pre-Jaramillo size in Algoz (Martino et al., 2023) and considering that the last occurrences of *Metacervocerus rhenanus* likely took place during the earliest Epivillafranchian, as evidenced by its presence in sites of almost this age such as Fuente-Nueva 3 (Rodríguez-Gómez et al., 2016), Durfort (Bellucci et al., 2015) and Mygdonia Basin (Konidaris et al., 2015), we ascribe the remains of the medium-sized deer from Algoz to *Metacervocerus rhenanus*.

2.4.2 Algoz Cervidae: The large-sized deer

Class Mammalia Linnaeus, 1758

Order Artiodactyla Owen, 1848

Family Cervidae Goldfuss, 1820

Genus *Eucladoceros* Falconer, 1868

Eucladoceros sp. (Figure 2.3)

Description and remarks: The large-sized cervid from Algoz (MG-25768) is a juvenile individual, considering the amount of unfused limb elements and deciduous teeth present on its skeleton (Figure 2.3). An antler (MG-25768.4), which is completely straight, has been documented as belonging to the same specimen of a large-sized cervid (MG-25768). Fallow deer tend to develop their first antlers around 8 months in age (Kierdorf & Bartoš, 1999), whereas in red deer this process begins around 9–10 months in age (Gaspar-López et al., 2008). This does not align with the age suggested by the dentition and postcranial skeleton, indicating that this antler either belongs to a different individual or that the Algoz cervid had a distinct developmental pattern compared to extant European deer.

The partial right hemimandible (MG-25768.1) bears both the slightly worn d3 and d4, with the m1 erupting and not showing any wear. All this evidence is congruent with a cervid individual 6 months in age, the first molar erupting around the same time in the red deer (Azorit et al., 2002) as in fallow deer (Bowen et al., 2016). Morphologically, the mandible MG-25768.1 has a straight ventral edge and slight pachyostosis. The d3 shows a large trigonid basin, with the entoconid and metaconid well separated, while the metaconid and the protoconid are united by a crest. This condition is comparable to that found in *Eucladoceros boulei* (Tong & Zhang, 2019) and *Eucladoceros montenegrensis* (van der Made & Dimitrijević, 2015), and unlike that seen in Megacerini like *Megaloceros novocarthaginiensis* (van der Made, 2015). The d4 features acute angles at the buccal side, mostly in the hypoconid and protoconid as seen in *Eucladoceros* (van der Made & Dimitrijević, 2015; Tong & Zhang, 2019), but not in megacerine deer like *Megaloceros novocarthaginiensis* (van der Made, 2015). It also features a slightly tilted entoconid, as *Eucladoceros* and unlike Megacerini. The m1 does not present a marked metaconid and metastylid clearly individualizing the posterior wing of the metaconid, the condition usually observed in Megacerini. Finally, the mesial lobe of the m1 is slightly arched over the distal part, which further enhance its similarity to *Eucladoceros* (Figure 2.4).

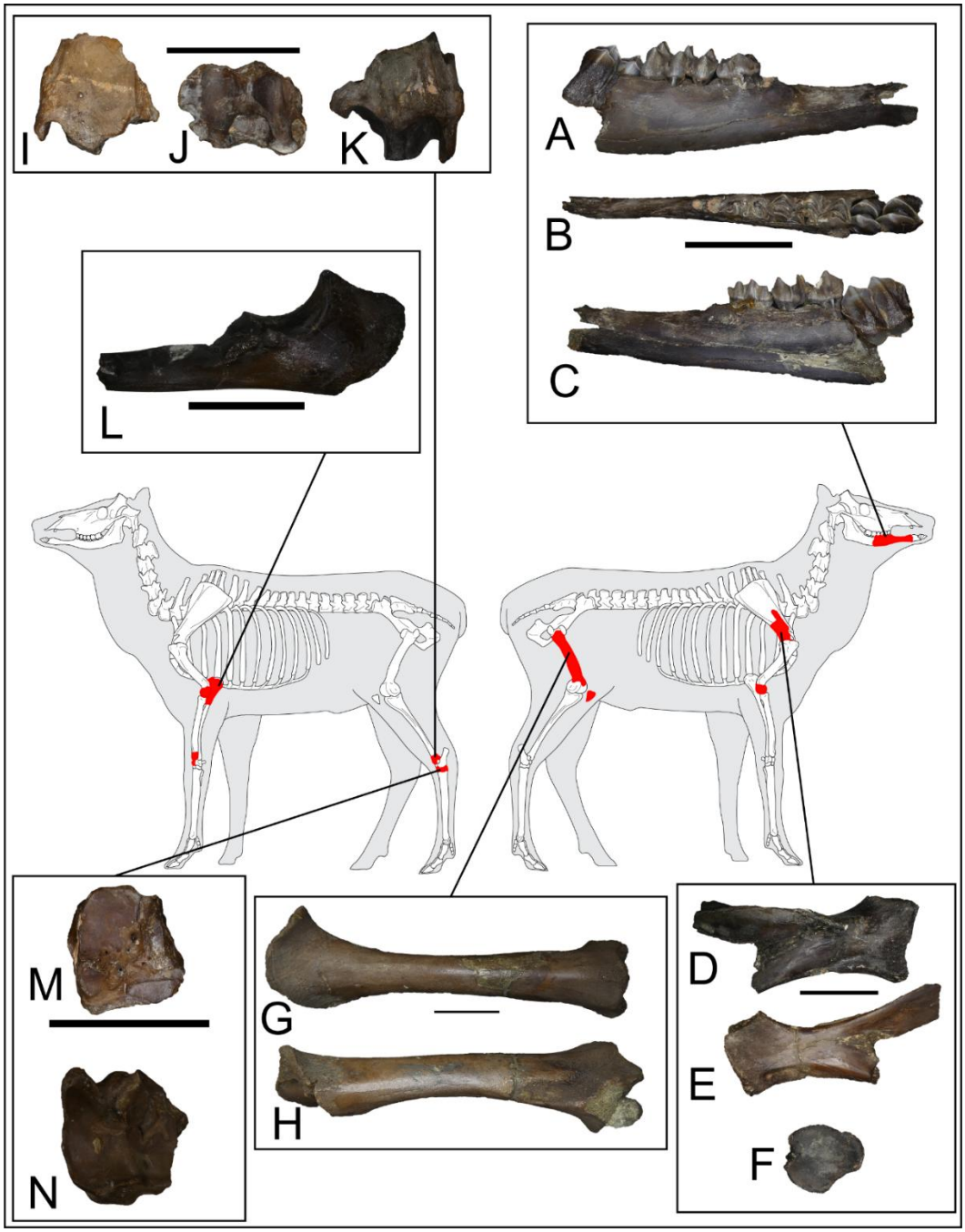


Figure 2.3 — Recovered material from the large-sized deer from Algoz, including 15 remains with different degrees of preservation from the same juvenile individual (MG-25768). A-C. Partial right hemimandible (MG-25768.1) in buccal (A), occlusal (B), and lingual (C) views. D-F. Partial right scapula (MG-25768.7) in dorsal (D) ventral (E), and distal (F) views. G, H. Right femur without epiphyses (MG-25768.8) in anterior (G) and lateral (H) views. I-K. Distal epiphysis of left tibia (MG-25768.16) in anterior or dorsal (I), distal (J), and posterior or palmar (K) views. L. Proximal epiphysis of left ulna (MG-25768.5) in lateral view. M, N. Left navico-cuboid in distal (M) and proximal (N) views. Skeletal diagram modified from ArcheoZoo.org (2003). Scale bars: 50 mm.

The proximal left ulna (MG-25768.5), distal right and left humeri (MG-25768.9, MG-25768.10), coracoid process of the right scapula (MG-25768.7), and both proximal and distal epiphysis of the right femur (MG-25768.8) remain unfused. The extremely damaged distal left radius (MG-25768.11) presents a distal epiphysis that is also not fused, although it was glued in an attempt to reconstruct this piece. Meanwhile, the distal left tibia (MG-25768.16) was fusing at the time of the death, with the line of the epiphyseal closure visible within the bone. This is again congruent with the age estimated for the teeth of 6 months, because the distal tibia is the first epiphysis to be fused on *Cervus elaphus* (Calderón et al., 2019).

The partial navico-cuboid (MG-25768.6) bears a large contact of the articular surface of the ''tenon lateralis" with the main articular surface of the trochlea for the astragalus, unlike in capreoline and megacerine deer (Breda, 2005) and similarly to what is seen in *E. boulei* (Tong & Zhang, 2019). The distal tibia (MG- 25768.16) presents an articular surface at the cochlea tibiae which in distal view is divided into medial and lateral articular facets, well separated as in megacerine deer. However, in plantar or posterior view, the shape of the cochlea tibiae from MG-25768.16 resembles that of *E. boulei* and not that of megacerini deer (Figure 2.4). The latero-plantar edge of the distal epiphysis is distally elongated, as in Megacerini, in which it rises as a wedge between the main articular surface for the astragalus and the plantar side of the articular surface for the malleolus. Yet, the shape of this area in MG-25768.16 differs from the giant deer (Figure 2.4), and is similar to that of *Eucladoceros* (Breda, 2005; Tong & Zhang, 2019).

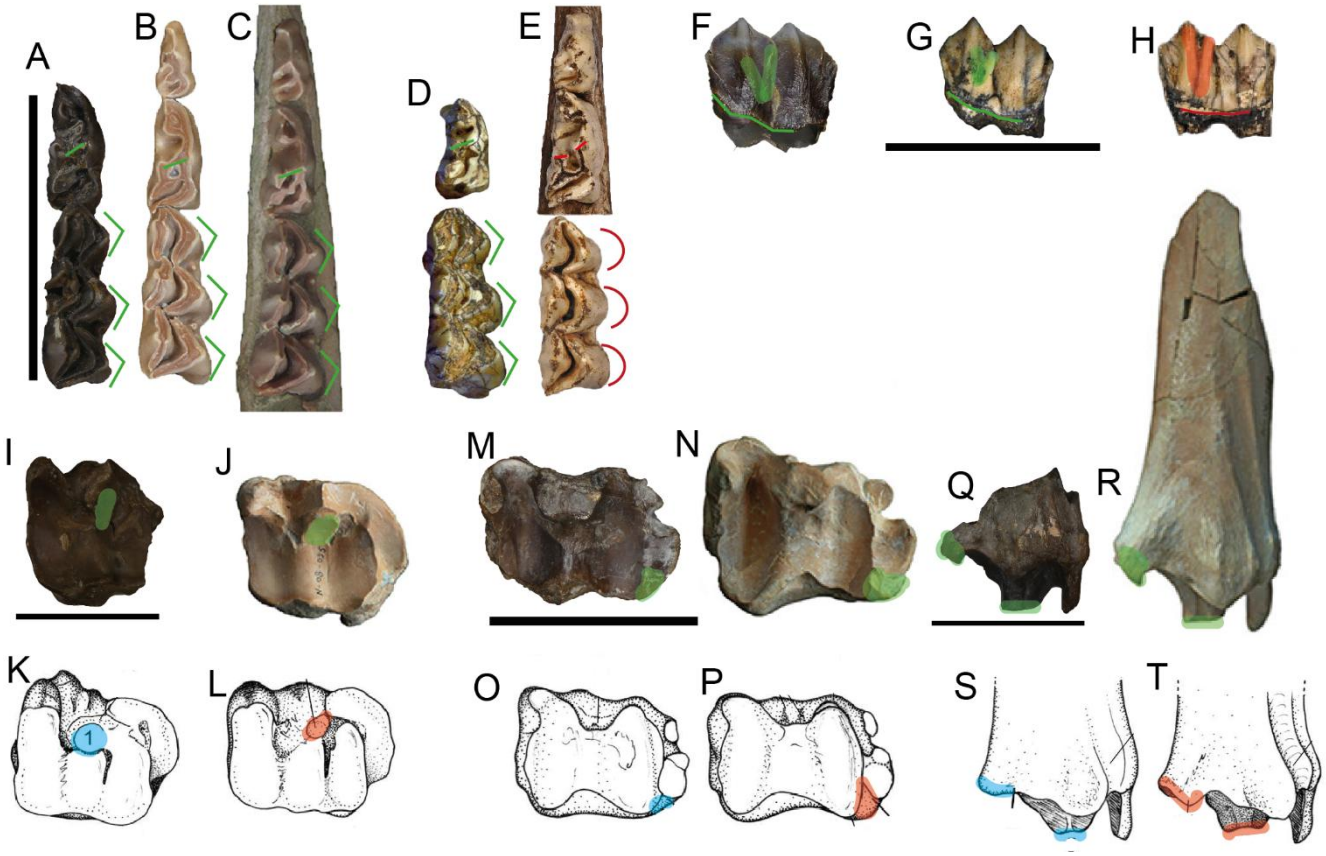


Figure 2.4 — Morphological comparison of the material from the large-sized deer from Algoz (MG-25768) with *Eucladoceros* and large Megacerini and Capreolini. A. Mandible from MG-25768 with d3 and d4 in occlusal view. B. Mandible from *E. boulei* with d3 and d4 in occlusal view. C. Mandible from *E. boulei* with d3 and d4 in occlusal view. D. Mandible from *E. montenegrensis* with d3 and d4 in occlusal view. E. Mandible from *M. novocarthaginiensis* with d3 and d4 in occlusal view. F. m1 in lingual view from MG-25768. G. m1 in lingual view from *E. montenegrensis*. H. m1 from *M. novocarthaginiensis* in lingual view. I. Navico-cuboid from MG25768 in proximal view. J. Navico-cuboid from *E. boulei* in proximal view. K. Navico-cuboid from *A. alces* in proximal view. L. Navico-cuboid from *M. giganteus* in proximal view. M. Tibia from MG25768 in distal view. N. Tibia from *E. boulei* in distal view. O. Tibia from *A. alces* in distal view. P. Tibia from *M. giganteus* in distal view. Q. Tibia from MG25768 in posterior or palmar view. R. Tibia from *E. boulei* in posterior or palmar view. S. Tibia from *A. alces* in posterior or palmar view. T. Tibia from *M. giganteus* in posterior or palmar view. Images from: *Eucladoceros boulei*, adapted from Tong and Zhang, (2019); *Eucladoceros montenegrensis* adapted from van der Made and Dimitrijevic´, (2015); *Megaloceros novocarthaginiensis* adapted from van der Made, (2015); *Alces alces* and *Megaloceros giganteus*, adapted from Breda, (2005). Green lines: condition of the character in *Eucladoceros*; red lines: condition in *Megaloceros*; blue lines: condition in *Alces alces*. Scale bars: 50 mm

The results of the metric analyses of the dental elements are not coherent with their morphology nor with those of the postcranial skeleton. All three teeth present in the mandible fall within the morphospace of *Megaloceros novocarthaginensis* and are classified as such by the discriminant analysis (Figure 2.5). The length of the deciduous tooth row of MG-25768 is

larger than that of *Eucladoceros* and similar in size to that of *Megaloceros giganteus* (Appendix A). Metric analyses of the postcranial skeleton (distal tibia, partial scapula, scaphoid, partial distal radius, distal humeri and femur diaphysis) of the large-sized Algoz deer (MG-25768) consistently place it within (or close to) the morphospace of either *Eucladoceros giulii* or *Eucladoceros boulei*. Upon conducting discriminant analysis on the scapula, it was categorized as belonging to *Eucladoceros giulii* (for the complete list of graphics, see Appendix A).

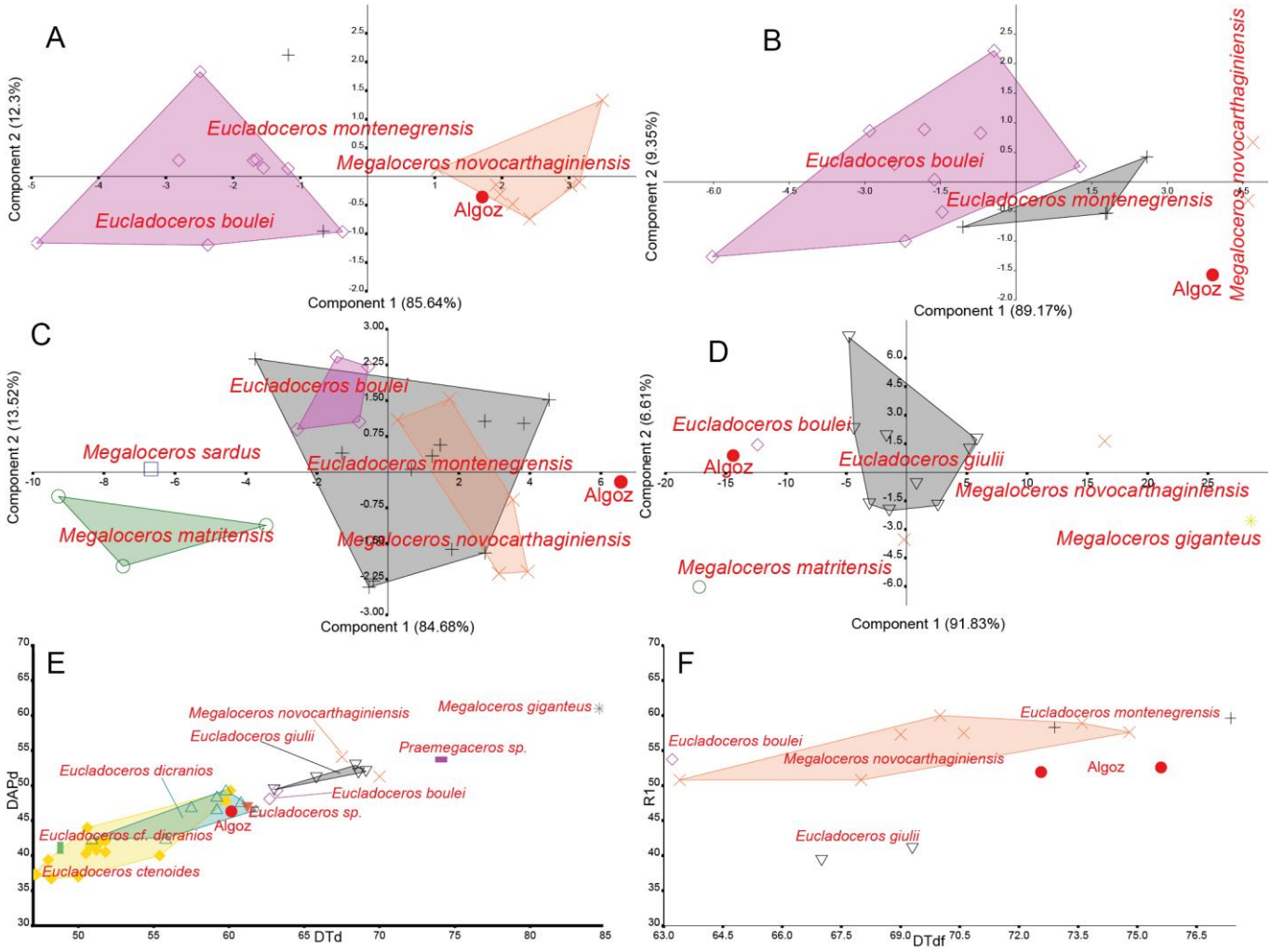


Figure 2.5 — Morphometric analyses of skeletal elements of the cranial and postcranial anatomy from the large-sized deer of Algoz (MG-25768) compared with several species of *Eucladoceros* and Megacerini deer. Check Appendix A for additional information. A. Principal component analysis (PCA) of d3. B. PCA of d4. C. PCA of m1. D. PCA of scapula. E. Scatter plot of transversal vs. anteroposterior diameters of the distal tibia. F. Scatter plot of the transverse diameter of the distal humerus vs. anteroposterior diameter.

The morphological characteristics (Figure 2.4) clearly point towards the genus *Eucladoceros*, although the described distinguishing features among the large-sized Megacerini deer and *Eucladoceros* are totally based on cranial elements that we lack (Vislobokova, 2013). Metrically, the postcranial skeleton also follows the same trend regarding measurements closer to those of diverse species of *Eucladoceros* than to Megacerini deer (Figure 2.5). Metrically, the postcranial skeleton also follows the same trend regarding measurements closer to those of *Eucladoceros* than to Megacerini (Figure 2.5). However, despite MG-25768 teeth closely morphologically resembling those of *Eucladoceros*, the measurements of the tooth row, as well as those of the individual teeth are of extremely large size, closer to those of Megacerini and in particular to *Megaloceros novocarthaginiensis*. Despite of these unusual proportions from the dentition, due to the overall morphology and the dimensions of postcranial elements, we are still confident to assign MG-25768 to the genus *Eucladoceros*.

2.4.3 Algoz Leporidae

Class Mammalia Linnaeus, 1758
Order Lagomorpha Brandt, 1855
Family Leporidae Fischer, 1817
Leporidae indet. (Figure 2.6)

Description and remarks: Antunes, Azzaroli et al., (1986) attributed to *Oryctolagus lacosti* a complete third metatarsal and distal fourth metatarsal (MG-25772) of a leporid from Algoz: '' *The size itself seems a little smaller than that of the Mt III of* Oryctolagus lacosti *from the Saint-Vallier site. Compared to the modern rabbit, the bone is clearly wider for the same length, it appears more massive, and the muscular insertions are more developed there. The foramen on the upper surface is located in a more distal position than in* O. cuniculus*.[…] Among the many names proposed for rabbits in Lower Pleistocene only the species* O. lacosti *is considered by the authors as valid*'' (Antunes, Azzaroli, et al., 1986). However, neither the postcranial anatomy of lagomorphs is extremely diagnostic, nor the taxonomy of the Early Pleistocene leporids is fully understood to provide a specific determination for this specimen with any certainty without an extensive metric study, MG-25772 being therefore only diagnosable at family level at the present moment (Angelone et al., 2020).

In summary, the two metapodial bones originally ascribed to *Oryctolagus lacosti* by Antunes, Azzaroli et al., (1986) are not diagnostic for this group at the specific level (Angelone et al., 2020), so we ascribe them to Leporidae indet.

2.4.4 The microvertebrates from Santa Margarida

As previously stated, the brecciated blocks of Santa Margarida yielded abundant remains of microvertebrates (Estraviz-López, 2019) from several groups (Figure 2.6), including Lacertidae indet., Soricidae (*Crocidura* sp., *Sorex* sp.), Lagomorpha (*Oryctolagus* cf. *cuniculus*), and primarily rodents including Gliridae (*Eliomys* cf. *quercinus*), Muridae (*Apodemus* cf. *sylvaticus*), Cricetinae (*Allocricetus bursae*) and Arvicolinae (three species). For a description and discussion of the taxa not presented in the main text of this chapter see Appendix A.

2.4.4.1 Lacertids

Class Reptilia Linnaeus, 1758

Order Squamata Oppel, 1811

Family Lacertidae Oppel, 1811

Lacertidae indet. (Figure 2.6)

Description and remarks: NOVA-FCT-DCT-5377 is a left dentary of a lacertid and the most complete remain of a non-mammalian vertebrate recovered from Santa Margarida (Figure 2.6). This specimen exhibits typical lacertid traits, including the pleurodont arrangement of cylindrical, single-cusped teeth, along with a Meckelian groove extending along its entire length (Blain et al., 2007). The fragility of the mandible prevented the usage of ultra-sounds for cleaning it; therefore, it was not possible to take reliable measurements of the piece that could have allowed further identification. Three more mandibular fragments of smaller size sharing these lacertid characters were retrieved from the disaggregated sediments.

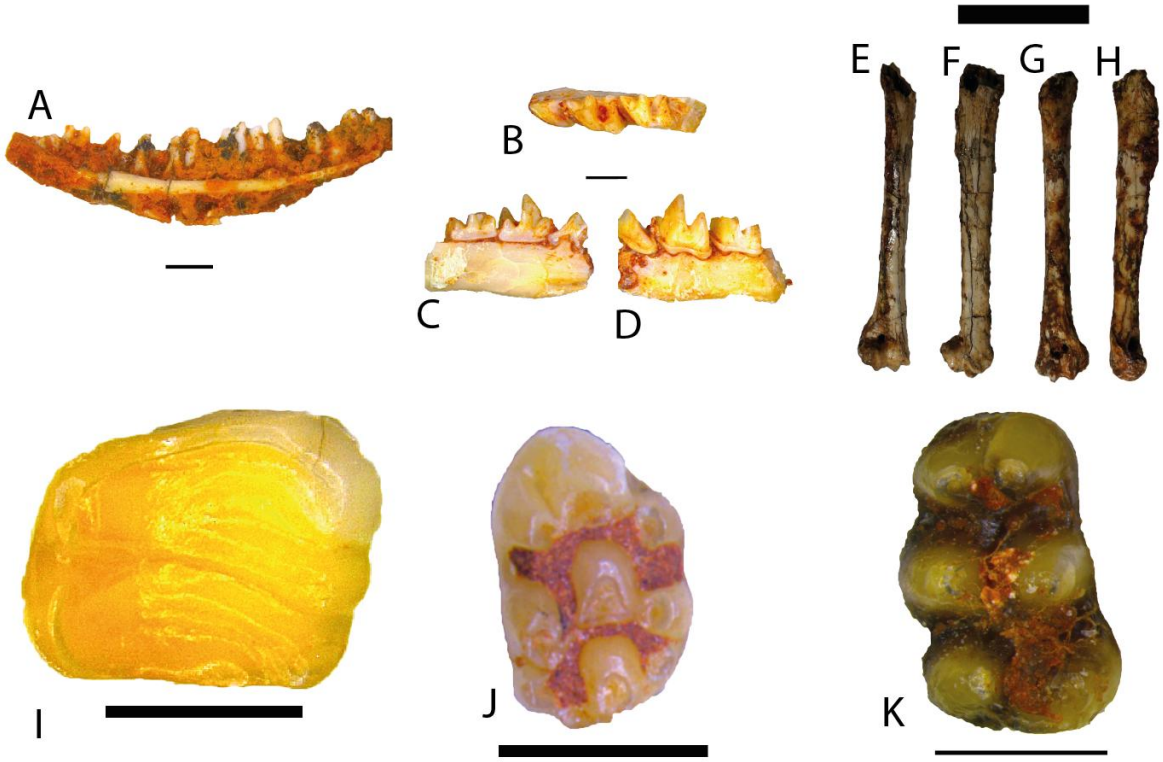


Figure 2.6 — Microvertebrate remains from Santa Margarida, modified from Estraviz-López, (2019). A. Lacertidae, left dentary (NOVA-FCT-DCT-5377) in lingual view. B-D. Soricidae, fragment of left mandible (NOVA-FCT-DCT-5378) in occlusal (B), lingual (C), and labial (D) views. E-H. Lagomorpha, distal left humerus (NOVA-FCT-DCT-5376) in anterior (E), exterior (F), posterior (G), and medial (H) views. I. Gliridae, upper molar (NOVA-FCT-DCT-5382 (2.8)) in occlusal view. J. Muridae, first upper molar (NOVA-FCT-DCT-5381 (1.6)) in occlusal view. K. *Allocricetus bursae*, first left upper molar (NOVA-FCT-DCT-5380 (1.17)) in occlusal view. Scale bars: 1 mm (A-D, I-K), 25 mm (E-H).

2.4.4.2 Rodents

Among the rodents found at Santa Margarida, the arvicolines hold significant importance as biostratigraphical markers. The m1 of the arvicolines serves as the most diagnostic part of their skeleton. Five complete or nearly complete m1s (Figure 2.7) were recovered from Santa Margarida (Cuenca-Bescós and Morcillo-Amo, 2022).

Class Mammalia Linnaeus, 1758

Order Rodentia Bowdich, 1821

Family Cricetidae Fischer, 1817

Genus *Victoriamys* Martin, 2012.

Victoriamys chalinei (Alcalde et al., 1981) (Figure 2.7A)

Description and remarks: NOVA-FCT-DCT-5383 is a right m1 with a slight wear on its mesial part. It has three closed triangles (T1-T3), while T4-T5 are very confluent, with a wide connection to the anterior cap. This results in broad angles for BRA3 and LRA4. Despite the anterior cap being wide, it is short, although the ACC as a whole is relatively long, lacking LRA5 entirely. The buccal and lingual triangles are comparable in size. These characteristics are diagnostic features of *Victoriamys chalinei* (Martin, 2012; Cuenca-Bescós & Morcillo-Amo, 2022). Meanwhile, NOVA-FCT-DCT-5383 metrically falls within the variability of the specimens of *Victoriamys chalinei* from Cueva Victoria and El Chaparral (Figure 2.8). Therefore, NOVA-FCT-DCT-5383 is ascribed both on morphological and metrical grounds to *Victoriamys chalinei*, being the first known occurrence of this species in Portugal.

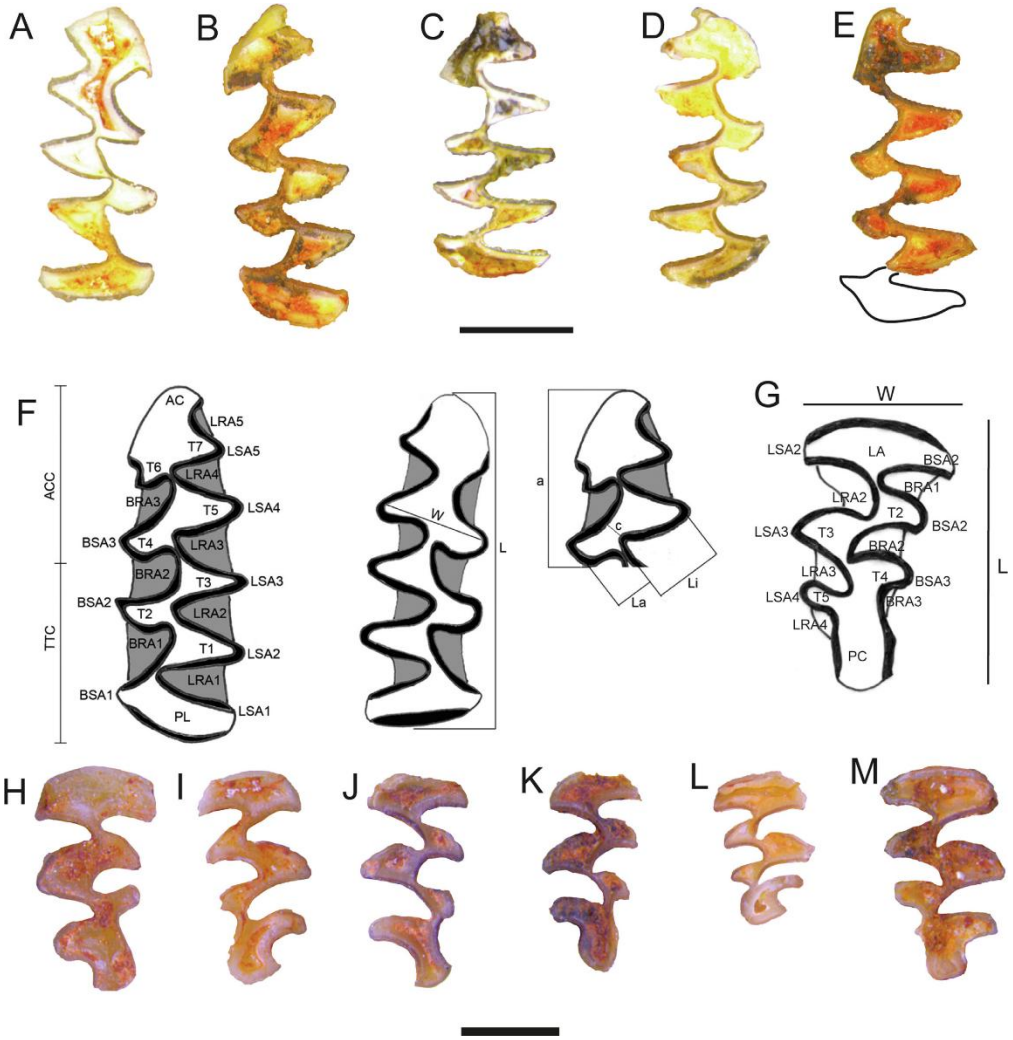


Figure 2.7 — Arvicolinae m1s and M3s from Santa Margarida. A-E. m1s in occlusal view, modified from Estraviz-López, (2019). A: NOVA-FCT-DCT-5383; B: NOVA-FCT-DCT-5384; C: NOVA-FCT-DCT-5385 (1); D: NOVA-FCT-DCT-5385 (2); E: NOVA-FCT-DCT-5386. F. Measurements and nomenclature of arvicoline m1s (from López-García et al., 2015): a, length of the anteroconid complex; ACC, anteroconid complex; AC, anterior cap; BRA, buccal reentrant angle; BSA, buccal salient angle; c, width of the opening of triangles T4-T5; L, length; La, mean width of T4; Li, mean width of T5; LRA, lingual re-entrant angle; LSA, lingual salient angle; PL, posterior lobe; TTC, trigonid-talonid complex, T1-T7, triangles 1–7; W, width. G. Measurements and nomenclature of arvicoline M3s (adapted from Martin, 2012): LA, anterior lobe; BRA, buccal reentrant angle; BSA, buccal salient angle; L, length; LRA, lingual re-entrant angle; LSA, lingual salient angle; PC, posterior cap; T1-T5, triangles 1–5; W, width. H-M. M3s in occlusal view. H: NOVA-FCT-DCT-5387 (1.3); I: NOVA-FCT-DCT-5388 (1.5); J: NOVA-FCT-DCT-5389 (1.6); K: NOVA-FCT-DCT-5390 (2.1); L: NOVA-FCT-DCT-5391 (2.2); M: NOVA-FCT-DCT-5392 (2.6). Scale bars: 1 mm.

Genus *Iberomys* Chaline, 1972

Iberomys huescarensis (Ruiz-Bustos, 1988) (Figure 2.7 B)

Description and remarks: NOVA-FCT-DCT-5384 presents a left m1 situated on the hemi-mandible, which also bears the m2. This specimen was mechanically extracted from the brecciated block, unlike other teeth from Santa Margarida that underwent chemical preparation. It features slightly larger lingual triangles compared to the labial ones. The connection between T4 and T5 is wide and conspicuous, although it shows a narrow link (neck) to the anterior cap. BRA4 and T6 are both absent, while LRA5 appears small, causing the T7 to almost blend with the anterior cap, despite both being identifiable. The anterior cap itself is short and triangular in shape. Metrically, NOVA-FCT-DCT-5384 measurements are congruent with *I. huescarensis* from El Chaparral and other localities (Figure 2.8). The studied specimen was diagnosed as *Iberomys huescarensis* on the basis of these features, being the first known occurrence of *I. huescarensis* from Portugal (López-García et al., 2012; Cuenca-Bescós & Morcillo-Amo, 2022).

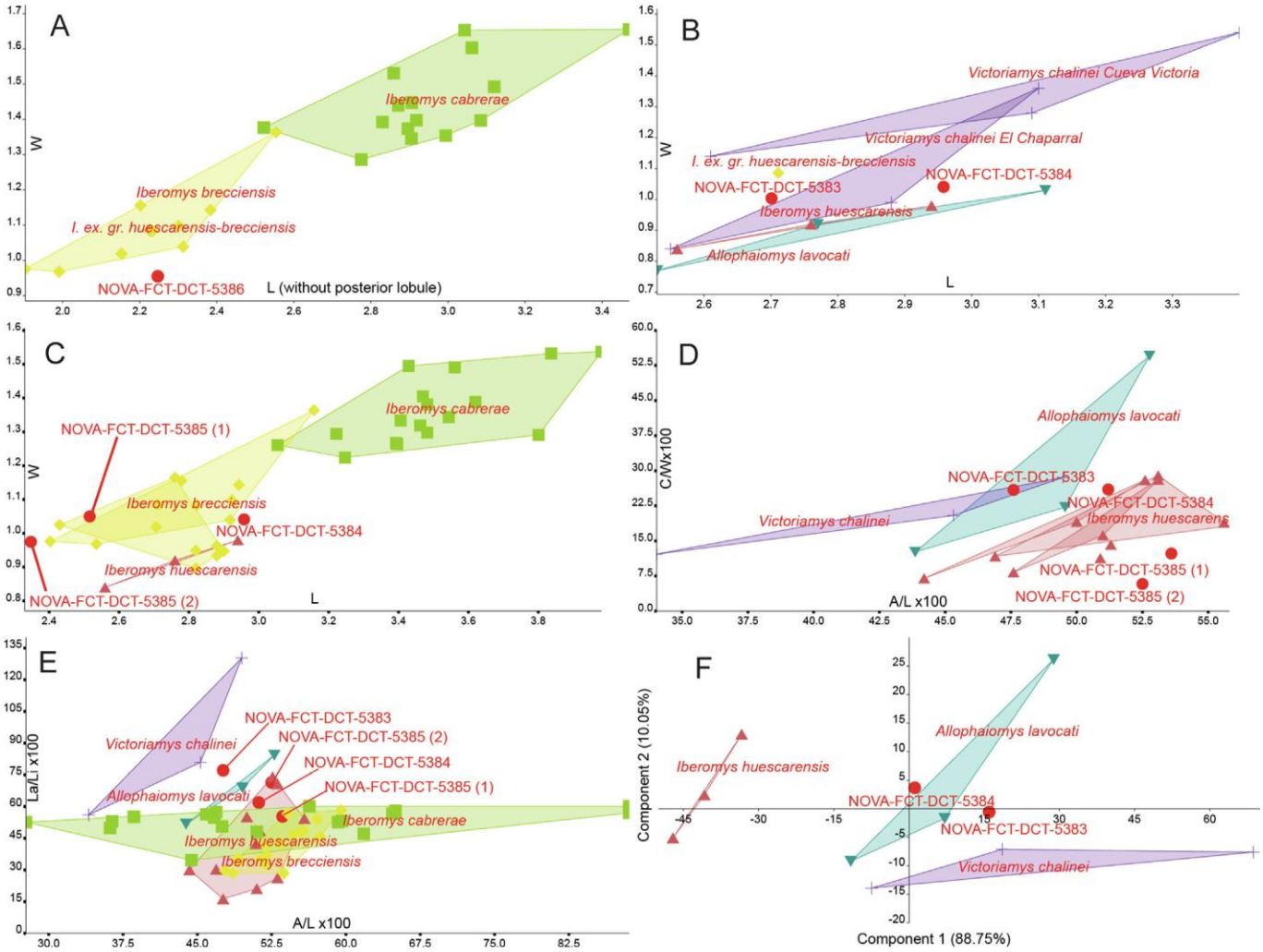


Figure 2.8 — Morphometric analysis of the Arvicolinae m1s from Santa Margarida. A. Scatter plot of length (without posterior lobe) vs. width of the specimen NOVA-FCT-DCT-5386 compared with *Iberomys brecciensis* and *Iberomys cabrerae*. B. Scatter plot of length vs. width of the specimens NOVA-FCT-DCT-5383 and NOVA-FCT-DCT-5384 compared with specimens of *Iberomys huescarensis*, *Victoriamys chalinei*, and *Allophaiomys lavocati*. C. Scatter plot of length vs. width of the specimens NOVA-FCT-DCT-5384, NOVA-FCT-DCT-5385 (1) and NOVA-FCT-DCT-5385 (2) compared with *Iberomys huescarensis*, *Iberomys brecciensis*, and *Iberomys cabrerae*. D. Scatter plot of A/L ratio vs. C/W ratio of specimens NOVA-FCT-DCT-5383, NOVA-FCT-DCT-5384, NOVA-FCT-DCT-5385 (1) and NOVA-FCT-DCT-5385 (2) compared with *Allophaiomys lavocati*, *Victoriamys chalinei*, and *Iberomys huescarensis*. E. Scatter plot of A/L ratio vs. La/Li ratio of specimens NOVA-FCT-DCT-5383, NOVA-FCT-DCT-5384, NOVA-FCT-DCT-5385 (1) and NOVA-FCT-DCT-5385 (2) compared with *Allophaiomys lavocati*, *Victoriamys chalinei*, *Iberomys huescarensis*, *Iberomys brecciensis*, and *Iberomys cabrerae*. F. Principal component analysis comparing specimens NOVA-FCT-DCT-5383 and NOVA-FCT-DCT-5384 with *Allophaiomys lavocati*, *Victoriamys chalinei*, and *Iberomys huescarensis*. See Appendix A for more details.

Besides the mentioned m1, three M3s have also been recovered from the sediments of Santa Margarida (Figure 2.7). They have a ''complex" morphology with four lingual angles. The T4 is not very developed and usually points slightly distally. The triangle of PC (posterior cap) or T5 can vary slightly, as this part of the tooth curves more or less lingually in different specimens. These characters are typical from M3s of *Iberomys*; however, there is insufficient research on this tooth morphology at the species level within this genus to make an accurate identification (Cuenca-Bescós & Morcillo-Amo, 2022). Nevertheless, the three M3s NOVA-FCT-DCT-5387 (1.3), NOVA-FCT-DCT-5388 (1.5), and NOVA-FCT-DCT-5392 (2.6) are characterized by open T2 and T3 with a broad connection between both triangles. They are also, on average, of slightly larger size both in length and width than other M3s recovered at Santa Margarida. The wide connection between the triangles seems analogous to that of the m1 of *Iberomys huescarensis*, so we tentatively ascribe them to this species.

Iberomys brecciensis (Giebel, 1847) (Figure 2.7 C, D, E)

Description and remarks: NOVA-FCT-DCT-5385 (1) and NOVA-FCT-DCT-5385 (2) are morphologically very similar teeth (Figure 2.7); the former is a left m1 and the later a right m1, with NOVA-FCT-DCT-5385 (1) still attached to part of its hemimandible. Their features resemble NOVA-FCT-DCT-5384, albeit with better developed lingual triangles and smaller labial ones. The connection between T4 and T5 is narrow, as well as the neck of the anterior cap. The LRA5 is noticeably defined in NOVA-FCT-DCT-5385 (2), creating separation between T7 and the anterior cap; while the T6 is visible in NOVA-FCT-DCT-5385 (1). These features are consistent with those of *Iberomys brecciensis* (López-García et al., 2015; Cuenca-Bescós & Morcillo-Amo, 2022). Both NOVA-FCT-DCT-5385 (1) and NOVA-FCT-DCT-5385 (2) fall conclusively within the metrical variability of *I. brecciensis* (Figure 2.8).

NOVA-FCT-DCT-5386 (Figure 2.7) represents a left m1 that is missing its posterior lobe. Nonetheless, the rest of the tooth is well preserved and it is possible to distinguish the elongated lingual triangles with acute angles at their tips. Each of the T1-T5 triangles is well individualized. Notably, the T7 exhibits significant development, matching the size of the lingual triangles, meanwhile the T6 is almost non-existent. The LRA5 is well defined. These characters are similar to those of *Iberomys cabrerae*, although some *I. brecciensis* can show extremely similar morphologies due to intraspecific variability (López-García & Cuenca-Bescós, 2012; Cuenca-Bescós & Morcillo-Amo, 2022).

In summary, NOVA-FCT-DCT-5385 (1) and NOVA-FCT-DCT-5385 (2) present morphological and metrical clear affinities with *Iberomys brecciensis*. NOVA-FCT-DCT-5386 originally recognized as *Iberomys cabrerae* due to its relatively advanced morphology (Estraviz-López, 2019) is herein recognized as an *I. brecciensis* with advanced morphology (Figure 2.7), thanks to measurements (Figure 2.8) that clearly differentiate between the two species (López-García et al., 2020).

Three M3s recovered from Santa Margarida sediments – NOVA-FCT-DCT-5389 (1.6), NOVA-FCT-DCT-5390 (2.1), and NOVA-FCT-DCT-5391 (2.2) – present characteristics compatible with the M3s of *Iberomys*, including a ''complex" morphology and a T4 underdeveloped and pointing distally. They differ from previously presented M3s as they have closed T2 and T3 with a narrow connection between them (Figure 2.7). This is a character analogous to that seen on the m1s of *Iberomys brecciensis*, so they are assigned to this species until further research is developed on this tooth at specific level within *Iberomys*.

2.5 Discussion

2.5.1 Chronology of the Epivillafranchian localities of Portugal

Concerning the age of the site of Algoz, given the likely presence of a typical Villafranchian element as *Metacervocerus rhenanus* and the measurements of *H. antiquus* from the site, it is likely that the deposit is 1.2 Ma and belongs to the earliest Epivillafranchian. The absence of a substantial amount of microvertebrates preclude us from reaching a more solid dating.

Considering the rodent species present at Santa Margarida, the levels from which the blocks were sourced in the locality are most likely representing: (i) at least one older, late Epivillafranchian level 0.9 Ma in age, with the presence of *V. chalinei* and *I. huescarensis*, and (ii) at least one younger, Middle Pleistocene level 0.6 Ma in age, with the presence of *I. brecciensis* (López-García et al., 2015). This means that the Early-Middle Pleistocene transition might be represented by the site.

2.5.2 Paleoenvironment of Epivillafranchian localities from Portugal

At Algoz, the presence of fine silts with aquatic plants and invertebrates overlaid by a sandy deposit with rocks and vertebrate bones might point towards a lacustrine environment that received a high energy stream which carried the animal remains. This will also partially

explain the damaged and disarticulated condition of the bones. Unfortunately, the depth from which the remains of Algoz were recovered – ca. 20 m – renders unlikely the possibility of further systematic interventions on the site in order to better understand its paleoecology (Zbyszewski, 1950; Antunes, Azzaroli, et al., 1986).

The paleoenvironment of Santa Margarida cannot be ascertain at the moment with the use of quantitative data due to the lack of a precise stratigraphy of the site, since a long time period (or long hiatus between fossiliferous layers) is likely represented on the site, having the paleoenvironment likely changed between layers. Nevertheless, it is safe to assume that the deposit formed in a cave part of the karst of the Picavessa Fm., given the breccified nature of the sediments and the eroded speleothems in the vicinity. The species presented in Appendix A will serve as basis for future studies in this direction, although not much more than their identification can be provided in the present work.

2.6 Conclusions

The site of Algoz is 1.2 Ma, and is the oldest Pleistocene site from Portugal known to date. It was likely formed by a torrential stream deposit over a lacustrine environment. Four species of vertebrates are present at Algoz: *Hippopotamus antiquus*, *Eucladoceros* sp., *Metacervocerus rhenanus* and an indeterminate leporid. Also, at least two individuals from each deer species are identified. All the remains of *Eucladoceros* from Algoz, except an isolated antler fragment, come from an individual about 6 months old.

The site of Santa Margarida is a cave deposit which presents older layers, Early Pleistocene in age (0.9 Ma) and younger layers, Middle Pleistocene in age (0,6 Ma). At least 10 species of microvertebrates are present at Santa Margarida: Lacertidae indet., *Crocidura* sp., *Sorex* sp., *Oryctolagus* cf. *cuniculus*, *Eliomys* cf. *quercinus*, *Apodemus* cf. *sylvaticus*, *Allocricetus bursae*, *Victoriamys chalinei*, *Iberomys huescarensis*, and *Iberomys brecciensis*. Santa Margarida represents the first known occurrence of the voles *Victoriamys chalinei* and *Iberomys huescarensis* in Portugal. The possible presence of the Early-Middle Pleistocene transition at Santa Margarida justifies a more detailed intervention on this site.

Given the extremely rare Early Pleistocene material from the Westernmost Iberian Peninsula in general, and from Portugal in particular, effort should be also focused in the future in relocating the material from Morgadinho or in the collection of new material at this locality (Antunes, Mein, et al., 1986).

3

INSIGHTS ON THE EVOLUTION AND ADAPTATION TOWARD HIGH-ALTITUDE AND COLD ENVIRONMENTS IN THE SNOW LEOPARD LINEAGE

Published as: Jiangzuo, Q., Madurell-Malapeira, J., Li, X., Estraviz-López, D., Mateus, O., Testu, A., Li, S., Wang, S., & Deng, T. (2025). Insights on the evolution and adaptation toward high-altitude and cold environments in the snow leopard lineage. *Science Advances*, 11(3), eadp5243. https://doi.org/10.1126/sciadv.adp5243

This chapter is the result of an international collaboration that happened during the development of this thesis and resulted in an important contribution for the paleobiodiversity of Portugal, as well as Europe: A subspecies of snow leopard from the Pleistocene of Portugal, *Panthera uncia lusitana*.

3.1 Introduction

The snow leopard (*Panthera uncia*) is one of the iconic animals of the Tibetan Plateau and distributes also in the ranged mountainous regions of central Asia as the Mongolian Plateau (Hemmer, 1972; Jianzhang et al., 2002; Shehzad et al., 2012; Kalashnikova et al., 2019; Lukarevskiy et al., 2019; McCarthy et al., 2016). It has distinctive morphological features, e.g., long and dense pelage, long tail, short face, steep and wide forehead, enlarged anterior chamber (ectotympanic) of the auditory bulla, high and steep mandibular symphysis, and relatively large cheek teeth (Hemmer, 1972; Gao, 1987; Hemmer, 2023; Jiangzuo & Liu, 2020; Kitchener et al., 2016), that clearly distinguish it from the other members of genus *Panthera*. Although

historically classified in its own genus, *Uncia* (Hemmer, 1972; Haltenorth, 1937; Pocock, 1917), modern phylogenetic analyses based on genetic and genomic data have conclusively placed it within the *Panthera* genus, particularly as the sister species of the tiger (*Panthera tigris*) (Mattern & McLennan, 2000; Johnson et al., 2006; Figueiró et al., 2017; G. Li et al., 2016).

The snow leopard typically inhabits within high alpine regions, above 3000 m, or above the tree line (McCarthy et al., 2017) but may also occur at much lower elevations below 1000 m in some areas of Russia (Mahmood et al., 2019). The status of the snow leopard in the International Union for Conservation of Nature Red List is vulnerable, with ~4000 individuals (McCarthy et al., 2017). However, under global warming, its distribution is expected to be substantially affected, as moving northward (Farrington & Li, 2024, p. 8) or upward to a higher altitude (X. Li et al., 2022) based on species distribution modeling (SDM) methods on current known distribution.

While the distinctive characteristics of the snow leopard have long been acknowledged, the correlation between these traits and its adaptation to the Tibetan Plateau environment, as well as their evolutionary history, remains largely unexplored. This gap in understanding is primarily due to the scarcity of snow leopard fossils in the Tibetan Plateau and its surrounding regions. Nevertheless, several potential records from northern China and Europe (Hemmer, 2023; Cardoso & Regala, 2006; Kurtén & Vasari, 1960; Testu et al., 2011) provided insight into the evolution and adaptation of this species. However, these records have yet to be rigorously tested using phylogenetic or statistical approaches, leaving their validation and phylogenetic positions uncertain.

In this study, we provide in-depth analyses of potential snow leopard records (Figure 3.1, A to D; see a review in the Supplementary Materials, Appendix B), especially the best-preserved skull from Manga Larga (Portugal) and a mandible from Longdan (China) with the implementation of phylogenetic and geometric morphometric analyses. We explored the ecological adaptation of the modern and fossil snow leopards, focusing on the function of their unique traits using anatomical study, finite element analysis, and morphometric approaches, and investigated how these traits evolved through the Quaternary. Then, we used species distribution models to predict the past distribution under the last glacial maximum (LGM) condition, which represents the potential largest distribution of the snow leopard, and this predicted distribution was compared with the fossil records to see whether the past adaptation of the snow leopard lineage is equivalent to that of the modern one. These analyses were then combined to infer the evolution and ecological adaptation/ requirements of the snow leopard.

3.2 Materials and methods

3.2.1 Phylogenetic analyses

To elucidate the evolutionary position of the analyzed specimens, a comprehensive phylogenetic analysis was performed, using a matrix modified from Salles (1992), Werdelin and Flink (2018), and Jiangzuo et al. (2022). A total of 160 craniodental and postcranial characters are present in the matrix, which is initially designed for whole members of the family Felidae (including Machairodontinae), so the matrix has some characters not necessarily informative within the species included in this analysis. As we focus on the evolutionary history and trait evolutionary rates of the subfamily Pantherinae, most irrelevant taxa were not added, only leaving *Catopuma temminckii* as the outgroup. Genetic data were adopted from Johnson et al. (2006), and four blocks (autosome DNA, X chromosome DNA, Y chromosome DNA, and Mitochondrial DNA) were set, together with the morphology block.

Bayes inferences with tip-dating under the fossilized birth-death model (Ronquist, Klopfstein, et al., 2012; Zhang et al., 2016) using the mkv model (Lewis, 2001, p. 200) for morphology block, and GTR + gamma for four DNA blocks were performed. MrBayes3.2.7 (Huelsenbeck & Ronquist, 2001; Ronquist, Teslenko, et al., 2012) was used in inference. Two independent runs, each with four chains, were used in analyses. Ten million generations were performed in each run. See the detailed settings in the Supplementary Materials file.

3.2.2 Metric and geometric morphometric analyses

To clarify the morphology and the taxonomical position of the studied specimens, we performed biometric, as well as, geometric morphometric analyses. Only species that has the potential to be misidentified as *P. uncia* was included in metric and geometric morphometric analyses to clarify their differences, i.e., extant *P. uncia*, extant *P. pardus* from Africa and Asia, *Panthera onca*, and *Puma concolor*. Dentognathic specimens from mammalian collection of American Museum of Natural History (AMNH M), New York, USA; Smithsonian National Museum of Natural History (USNM), Washington DC, USA; Museum of Comparative Zoology (MCZ), Boston, USA; Institute of Zoology, Chinese Academy of Sciences, Beijing, China (IOZ); and Kunming Institute of Zoology, Chinese Academy of Sciences, Kunming, China (KIZ), Northwest Institute of Plateau Biology, Chinese Academy of Sciences, Xining (NWIPB) were used in analyses. The landmarks and semilandmarks were obtained using software tpsDig2.32. The measurements of lower dentition and mandible follow the study of Jiangzuo and Liu (2020).

Geometric morphometric analyses were performed using Geomorph 4.0.1 package (Adams & Otárola-Castillo, 2013) of R 4.0.5 (R Core Team, 2016), and plots were made using the package ggplot2 (Wickham, 2016). PCA analyses were performed in software Past 4.0.3 (Hammer et al., 2001).

3.2.3 Anatomical study and fossil records

We reviewed the literature and the available fossil collections in Eurasian Museums and Research Centers to find potential snow leopard fossil records, which are tested and analyzed in this study. The details on the comments on fossil records are provided in the Supplementary Materials, Appendix B. Two of them, Niuyan Cave and Loc. 3 of Zhoukoudian, are both from Fangshan, Beijing, China (Pei, 1936; Tao et al., 1999), one from Arago cave, Tautavel, France (Hemmer, 2023; Testu et al., 2011), and one from Manga Larga Cave, Santo António Plateau, Portugal (Cardoso & Regala, 2006). None of these four records were identified as the snow leopard when they were first published but as *P. pardus* or *Panthera* sp. (or *Felis* sp.), but the similarity with the snow leopard was mostly recognized. The anatomic, morphometric, and geometric morphometric analyses of the mandible and lower dentition were carried out to study the phylogenetic and taxonomic features of these four records. The faunal composition of the four records was analyzed to infer the paleoenvironment.

3.2.4 Finite element analyses

Finite element analyses were performed in the Abaqus computer-aided engineering (CAE) (v. 6.14) software. For simplicity, two-dimensional (2D) finite element modeling for hemimandibles was used (Fletcher et al., 2010; Piras et al., 2013). First, photos of the mandibles of *P. uncia* AMNH M166952 and *P. pardus* AMNH M89009 were taken in the right lateral view. The outlines were plotted in the AutoCAD 2018 software, scaled to the same size, and exported .dxf files. The exported outline files were loaded into Abaqus CAE and generated 3D planar shell models with a uniform thickness of 2 mm. The models were assigned the homogeneous material property approximating mammalian cortical bone, with a Young's modulus of 15 GPa and a Poisson's ratio of 0.28, following the study of Drake et al. (2016). As our goal is to compare the mandibular mechanical behavior, we set the same bite force of temporal and masseteric muscles as 3000 and 1000 N, respectively, for all taxa used. The direction of muscle (temporal and masseteric) of the modern species is measured in the case seen in Figure 3.1, and the exact angle and bite force are given in table S1 of appendix B. The fossil species related to

modern *P. uncia* were set as the same angle. The following boundary conditions were set: 1, one point at the posterior border of the condyle, only allowing vertical movement; 2, one point at the dorsal border of the condyle, only allowing horizontal movement; and 3, the tip point of the canine, all the six movements were constrained.

3.2.5 Species distribution modeling

3.2.5.1 Data

The snow leopard occurrence data used in this study were from field surveys, literature, and the Global Biodiversity Information Facility database (table S4, appendix B). Most of the occurrences were derived from camera trap records, and others were from feces or footprints marked during line transect surveys (X. Li et al., 2022; Liu et al., 2019; Xiao et al., 2019). All occurrences used for SDMs were from recent surveys conducted after 2010, and more than 60% of the records were based on the surveys in the past 5 years. The minimum distance between occurrences is 5 km. All occurrences were recorded using GPS handsets.

We used the 19 bioclimate variables (30 arc sec) from the World-Clim 2.0 dataset (https://worldclim.org/) for current (1960–1990) climate conditions; and we used the World-Clim 1.4 downscaled data for climate conditions at the LGM (about 22,000 years ago) (Fick & Hijmans, 2017). For the LGM data, we selected the global climate model CCSM4, because it is a moderate model with temperature and precipitation neither too high nor too low (Flato et al., 2014).

3.2.5.2 Models

We used environmental variables to explain the presence or absence of the snow leopard using the model logit(p) = f(x1, x2, … xk), where p is the probability of the presence of snow leopard at a location, and x are environmental variables.

We applied random forest (Breiman, 2001) for SDMs. Random forest is a machine learning algorithm and is one of the frequently used SDM approaches (Kampichler et al., 2010; Rather et al., 2020; Iverson et al., 2008; Valavi et al., 2021). It is especially good for handling high-dimensional data (multiple correlated explanatory variables) and complex relationships such as interaction and high-order effects (Winham et al., 2012; Y. Kim et al., 2009; X. Li & Wang, 2013). We used the R package randomForest (Breiman, 2018, p. 20) for the analysis. We set the argument ntree (number of trees) to be 1000 and left others undefined (default settings, including no weights, were used).

For the current distribution of snow leopards, we used the occurrences and evenly distributed 50 × 50 = 2500 pseudo absence points as the dependent variables, with the 19 climate variables in the WorldClim dataset as explanatory variables, and build a model to quantify the association between snow leopard occurrences and climate variables. Then, we projected the historical distribution of the snow leopard using the model and the climate data at the LGM. The partial effects of the 12 most important elements and the basic evaluation parameter of the SDM model are provided in the Supplementary Materials, Appendix B.

3.3 Results and discussion

3.3.1 Systematics

Order Carnivora Bowdich, 1821
Family Felidae Batsch, 1788
Subfamily Felinae Batsch, 1788
Genus *Panthera* Oken, 1816
Panthera uncia (Schreber, 1775)
Panthera uncia lusitana subsp. nov.

Diagnosis— Small-sized pantherine cat (extant snow leopard-sized). Cranium broad and high, with short rostrum. Forehead slightly concave (in lateral view) and wide; orbit large; bony choana not widened; bulla relatively flat, with enlarged ectotympanic. Deep corpus, with vertical symphysis and low coronoid process; ventral margin of masseteric fossa not laterally expanded. P4 with straight buccal border; m1 slender with antero-buccal corner. Cheek teeth enlarged relative to skull overall size (large ratio of m1 length/mandible length).

Differential diagnosis—differs from modern *P. uncia* by having slightly narrower frontal and less inflated auditory bulla, P4 with straight buccal border; differs from *P. pyrenaica* by having slightly smaller size, shorter c-p3 diastema, larger cheek teeth, lower coronoid process; differs from all other *Panthera* species by having smaller size, wider frontal, concave forehead in lateral view, more inflated auditory bulla, more enlarged ectotympanic chamber, shorter rostrum, lower coronoid process.

Etymology—referred to Lusitania, the ancient region of the western Iberian Peninsula which became a Roman province and corresponds to most of the present-day Portugal and Spanish provinces of Salamanca and Cáceres.

Holotype—MG1355.0001-9, mostly complete skull with broken zygomatic arches and missing both upper second premolars and a few associated postcranial bones (partial humerus, one complete and two incomplete metacarpals, and cervical vertebrae).

Type locality and age—Manga Larga (39.51972°N, 8.83114°W), Porto de Mós Municipality, central Portugal, Late Pleistocene.

Description and comparisons—See the Supplementary Materials at Appendix B.

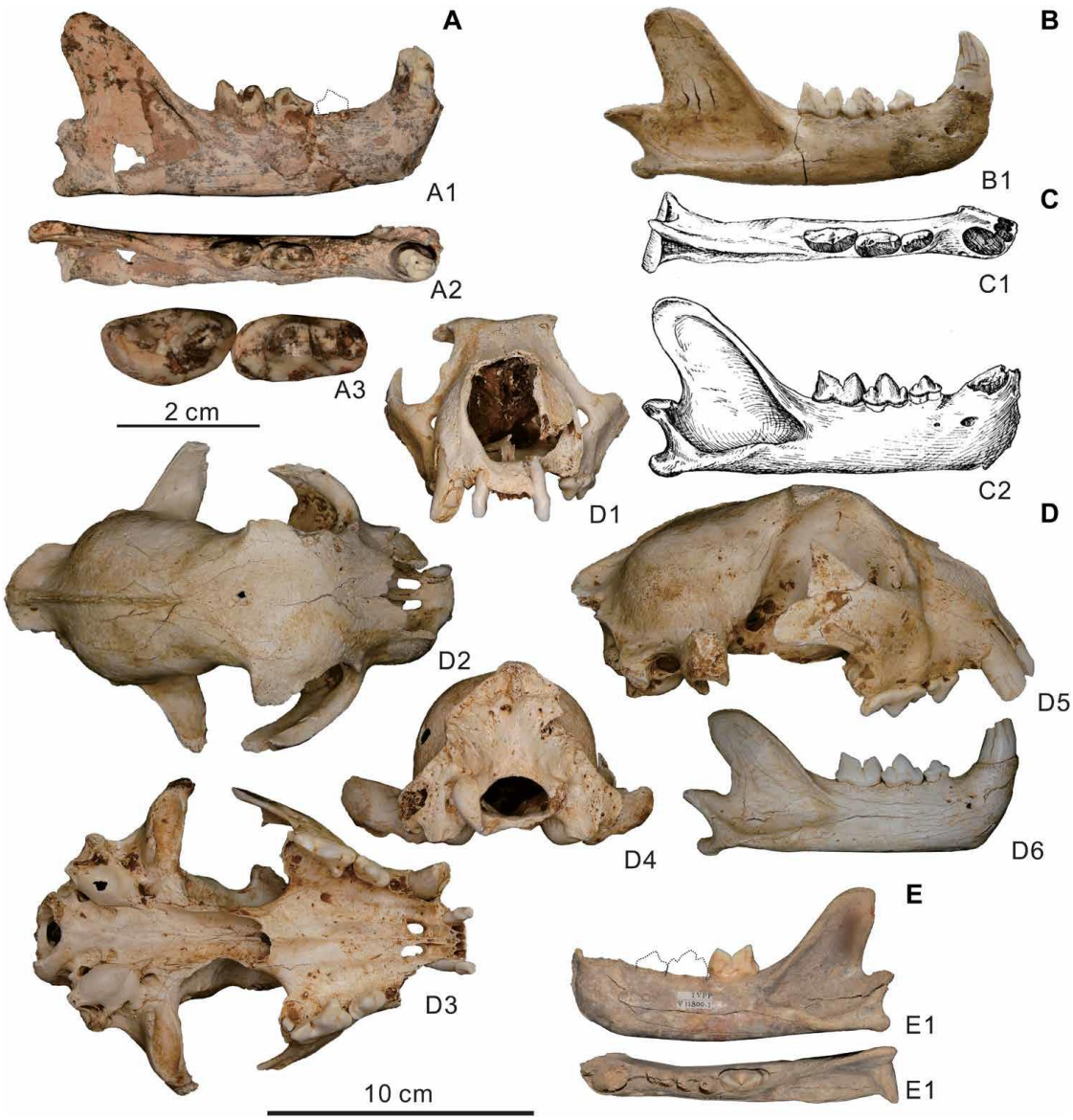


Figure 3.1 — Fossil snow leopards from Eurasia. (A) *Panthera* aff. *pyrenaica*, IVPP V31895, Longdan, Linxia Basin, northeastern Tibet, China. (B) *Panthera pyrenaica*, E14-EFNI-1001, Aragó Cave, Southeastern France. (C) *Panthera* aff. *uncia*, Zhoukoudian Loc. 3, Beijing, China. (D) *Panthera uncia lusitana* subsp. nov., MG1355.0001-0002, Manga Larga, Portugal. (E) *Panthera uncia*, IVPP V11800.1, Niuyan Cave, Beijing, China.

Panthera aff. *pyrenaica*

Diagnosis— Small-sized pantherine cat (extant leopard-sized). Symphysis relatively vertical (relative to horizontal plane) in orientation; ventral margin of masseteric fossa not laterally expanded. m1 buccolingually robust.

Differential diagnosis— Differs from *P. pyrenaica* by having less elevated symphysis, buccolingually wider m1; differs from modern *P. uncia* and *P. u. lusitana* by having less elevated symphysis, longer c-p3 diastema, higher coronoid process, smaller cheek teeth; differs from *P. palaeosinensis* by having smaller size, lower symphysis, less ventrally extended angular process and non-expanded ventral border of the masseteric fossa; differs from all other *Panthera* species by having smaller size, non-expanded ventral border of the masseteric fossa.

Material— Right hemimandible missing the p3, IVPP V31895. Institute of Vertebrate Paleontology and Paleoanthropology (IVPP), Chinese Academy of Sciences, Beijing, China.

Locality and age— Longdan, Linxia Basin, China, Early Pleistocene, 2.5 to 2.2 Ma.

Description and comparison— See the Supplementary Materials at Appendix B.

3.3.2 Ecomorphological adaptation of fossil snow leopard

The peculiar cranial morphology of the modern snow leopard has been noticed by many previous works (Hemmer, 2023; Haltenorth, 1937; Pocock, 1917; Salles, 1992; Sims, 2012). In the present study, we mainly compared its cranial anatomy with other pantherine cats, especially the similar-sized leopard *Panthera pardus* to elucidate the function of these traits.

The overall cranium morphology of the snow leopard is characterized by the wide and high skull, with an expanded and domed forehead and frontal sinus (Salles, 1992). An enlarged frontal sinus (often posteriorly extended) is quite common in Carnivora, especially Ailuropoda and bone-cracking hyaenids, as well as other fossil groups (Figueirido et al., 2013, 2011; Dong, 2008; Curtis & Van Valkenburgh, 2014; Vinuesa et al., 2016, 2015) and is suggested to be related to resisting high stresses during biting on hard substances (Tseng, 2013). This is unlikely to be the case for the snow leopard, whose frontal sinuses are not posteriorly expanded and the cheek teeth are not robust. The overall cranial morphology of the snow leopard is very similar to that of cheetah *Acinonyx jubatus*. A greatly laterally expanded frontal sinus was observed in both *P. uncia* and *A. jubatus* (Salles, 1992). Anatomical studies suggest that the frontal sinus is connected with nasal passages through small ostia and is normally in continual

communication with the nasal air (Reznik, 1990). An expanded frontal sinus in *P. uncia* and *A. jubatus* can serve as warming the cold air, or heat dissipation during running, and help in promoting the respiratory efficiency of the animals (Vinuesa et al., 2015; Joeckel, 1998; Reidenberg & Laitman, 2008; Negus, 1957). *P. uncia* lives at high altitudes with low-oxygen concentration, and *A. jubatus* has a chasing hunting behavior with vigorous locomotion (Hemmer, 1972; Kitchener et al., 2016; Torregrosa et al., 2010; O´Regan, 2002). Therefore, although the adaptations of *P. uncia* and *A. jubatus* are different, the enlarged frontal sinus can help in both cases in respiratory efficiency during hunting. We interpret this anatomical feature in the snow leopard, as an adaptation to high-altitude and cold environments. The enlarged cheek teeth are often correlated with slicing meat, and resisting forces of tendons and skin often seen in saber-toothed cats (Turner & Antón, 1997; Werdelin et al., 2010). In the Tibetan Plateau, food sources and competitors are relatively rare, and snow leopards stay near its kills for longer periods than do other large cats to consume its prey (Schaller, 1977; Fox et al., 1988, 2024). In high-altitude and cold environments, the kills will soon freeze, and the large cheek teeth of the snow leopard are also helpful in chewing hard frozen meat.

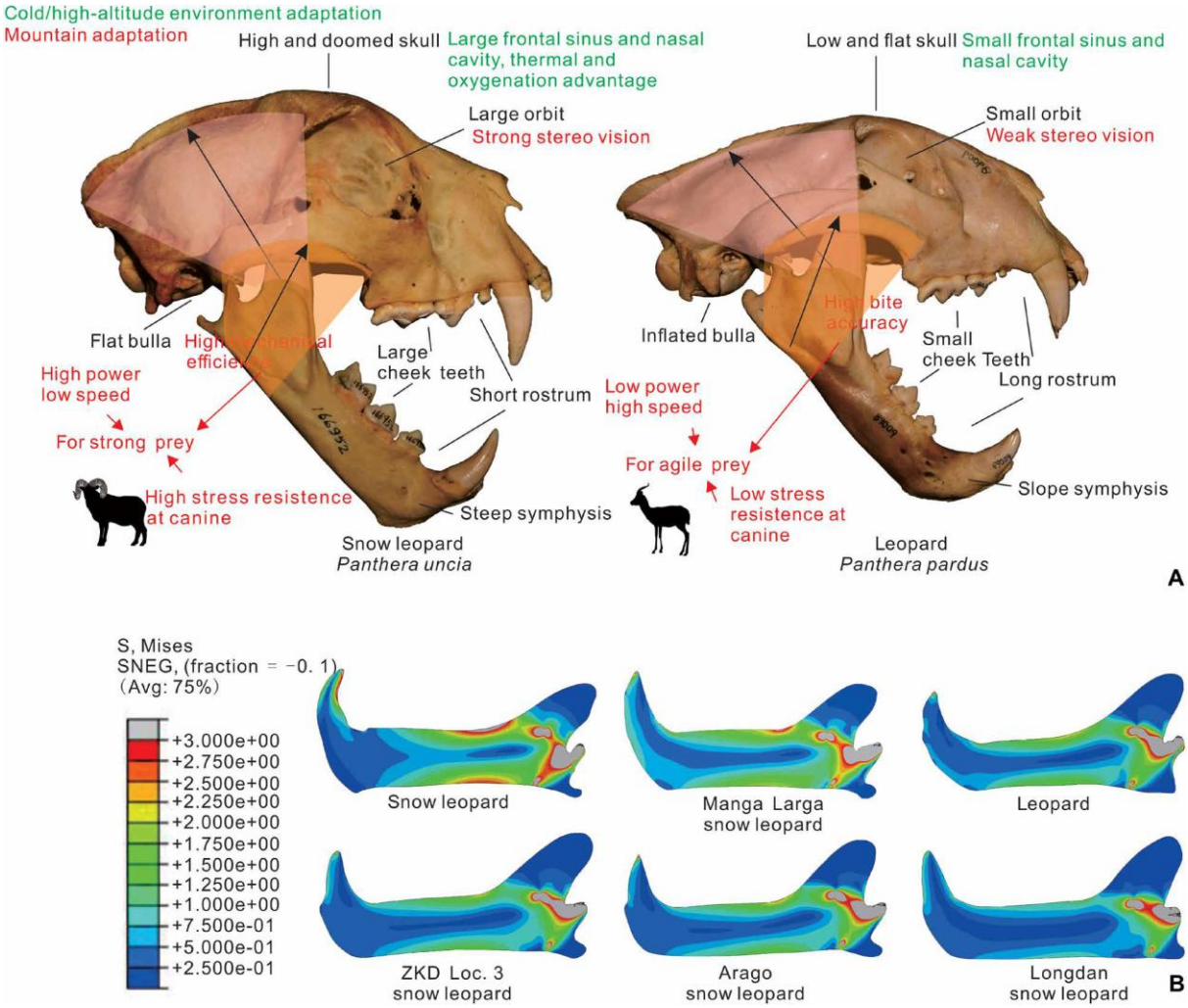


Figure 3.2 — Craniodental ecomorphology of the snow leopard and related taxa. (A) Cranial comparison of *P. uncia* AMNH M166952 and *P. pardus* AMNH M89009, highlighting functional traits related to high/cold adaptation (green) and (prey type related) mountain life (red). (B) Finite element analyses of mandibles of modern and fossil *P. uncia*, modern *P. pardus*, and several fossil snow leopards.

Other craniodental and postcranial traits are, however, not directly adapted to cold environments themselves. The short rostrum brings (Figure 3.1) a high mechanical advantage to the anterior part of the jaw. The high and steep symphysis suggests a strong resistance to stresses induced by the canine bite (Therrien, 2005). Our finite element analyses on the mandibular profile also show averaged low Von Mises stress (reflected by the stress contour diagram) at the symphysis part in modern *P. uncia* given by the same bite force (Figure 3.2). These findings suggest that the anterior portion of the jaw has better mechanical performance, enabling the snow leopard to withstand high bite forces in this region more effectively. The

relatively short braincase and absence of a posteriorly extended lambdoidal crest imply that the temporal muscle has a more vertical component and a small posterior component. Such muscle direction benefits a strong upward force during occlusion and a lower force to track the coronoid backward and resulted in low speed of occlusion. All these traits, as well as the rounded canine cross section (Hemmer, 1972; Tseng et al., 2014), support a strong canine bite of the snow leopard compared with *P. pardus* (Figure 3.2). The short rostrum and low speed of occlusion lead to a relatively slow bite. This is in accordance with the fact that *P. uncia* predates mainly on Caprini bovids (Shehzad et al., 2012; Lyngdoh et al., 2014; Oli et al., 1993; Mallon et al., 2024), which have short metapodial bones. The short distal limbs in mammals are correlated with a low speed but higher strength (Gutarra & Rahman, 2022; Biewener, 1990). Another important cranial trait of the snow leopard is the large and more anteriorly oriented orbit. The orbit diameter/condylobasal length ratio of *P. uncia* reaches 0.278 (0.264 to 0.296, n = 13), much larger than that of other species of *Panthera* (mean 0.226, 0.189 to 0.254, n = 48), suggesting a larger eye, and R square of lineal model (n = 90) of orbit diameter/condylobasal ratio and condylobasal of *Panthera* is very low at 0.24, suggesting that there is no significant allometry. The angle between the long axis of the orbit and the sagittal plane (in dorsal view) is significantly larger than other species of *Panthera* and *Puma* but comparable to *A. jubatus* (Figure 3.3 A2). A large angle suggests that the orbit is oriented more anteriorly, therefore with a large overlap of eyesight range of both eyes. This, together with the short rostrum, leads to a better stereo vision of *P. uncia* compared with the other species of *Panthera*, which is needed in prey discovery and focusing on the open mountainous region, as Caprini bovids generally have protective coloration in rock cover. Similar adaptation with a short rostrum and a more anteriorly oriented orbit can be seen in many open environment felid species, e.g., *Otocolobus manul*, *Felis margarita*, or *Felis nigripes* (fig. S12 of appendix B). The enlarged ectotympanic chamber (Figure 3.3A3) is also similar to that of *Acinonyx* but unlike that of other *Panthera* being adapted to hearing ability in the open environment (Huang et al., 2002). These cranial traits of the snow leopard are adapted to hunting Caprini bovids in the open mountainous region.

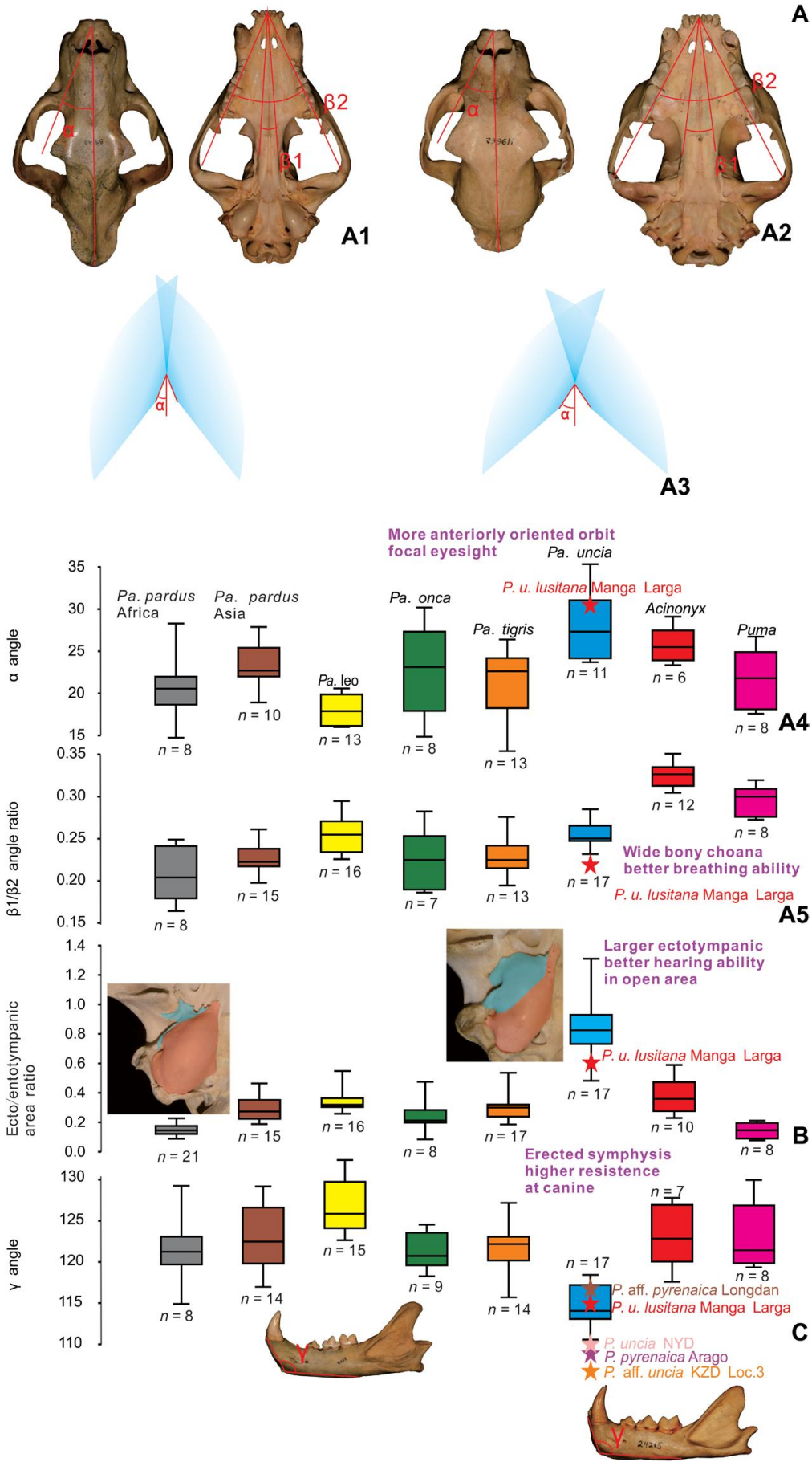

A
α
β2
β1
A1
A2
A3
More anteriorly oriented orbit
focal eyesight
Pa. uncia
P. u. lusitana Manga Larga
Acinonyx
Puma
Pa. onca
Pa. tigris
Pa. pardus Africa
Pa. pardus Asia
Pa. leo
α angle
A4
β1/β2 angle ratio
Wide bony choana
better breathing ability
P. u. lusitana Manga Larga
A5
Ecto/entotympanic area ratio
Larger ectotympanic
better hearing ability
in open area
P. u. lusitana Manga Larga
B
Erected symphysis
higher resistence
at canine
γ angle
P. aff. pyrenaica Longdan
P. u. lusitana Manga Larga
P. uncia NYD
P. pyrenaica Arago
P. aff. uncia KZD Loc.3
C

Figure 3.3 — Functional statistical traits of *Panthera uncia* and its fossil relatives in comparison with other felids. (A) Cranial angles of felids; (A1) Angle in the lion *P. leo*; (A2) angle in the snow leopard *P. uncia*; (A3) angle α and its impact on eyesight; (A4) comparison of angle α in modern and fossil felids; (A5) comparison of angle β in modern and fossil felids; (B) comparison of the ratio of ectotympanic and ectotympanic area in modern and fossils felids; (C) comparison of angle γ in modern and fossil felids.

Our analyses of postcranial skeletal proportions (Figure 3.4) suggest that the snow leopard has relatively long distal limbs, a cursorial adaptation in congruence with previous results (Gonyea, 1976). In the principal components analyses (PCAs) of 16 proportions (see the Supplementary Materials in Appendix B for details of these proportions), the morphospace of *P. uncia* is remote from those of other felid species. The PC1 is positively correlated with humerus distal condyle height, femur medial side distal condyle height, scapular length, and pelvis length and negatively correlated with tibia length. The species with positive scores have large girdle bones allowing the powerful muscle attachment with high mechanic advantage. The PC2 is mainly positively correlated with radius length and, to a lesser extent, tibia length, and species having positive scores have cursorial adaptations. The postcranial morphology of *P. uncia* is therefore built for speed not strength. The long distal limb bones, especially the tibia, as well as the long lumbar vertebral column and the long tail (Gonyea, 1976) support a strong jumping ability and are adapted to mountain life on steeped slopes. On the other hand, the distal condyle heights of the humerus and femur (table S3 of Appendix B), which directly correlated with a cross-sectional area that sustains the stress of joint, are related to sustaining the force from body mass and locomotion. In this aspect, the relatively low condyle of the snow leopard reflects its relatively small body size within *Panthera*. Alternatively, low condyle height of humerus can be balanced to retain high flexibility of foreleg for hunting.

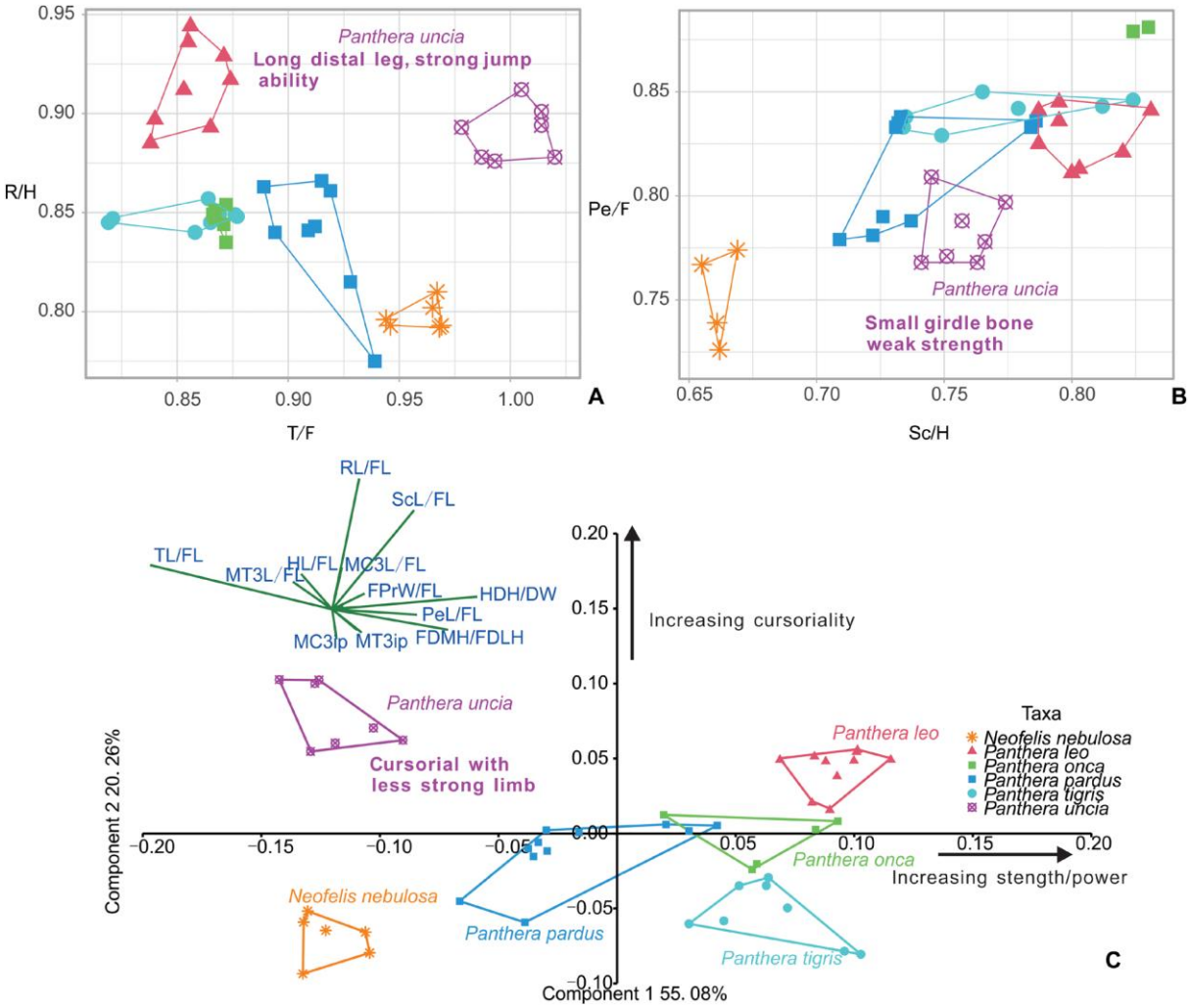


Figure 3.4 — Functional statistical postcranial traits of *Panthera uncia* in comparison with other felids. (A) Plot on tibia/femur length ratio and radius/humerus ratio. (B) Plot on pelvis/femur length ratio and scapular/humerus ratio. (C) PCA plot of 16 postcranial skeleton ratios; see the explanation in the appendix and raw data in table S3 of Appendix B. R, radius; H, humerus; T, tibia; DH, distal antero-posterior height (of long bone); DW, distal medio-lateral width (of long bone); Pe, pelvis; Sc, scapular; F, femur; L, length; MC, metacarpal; MT, metatarsal; P/p, upper/lower premolar.

In summary, the overall craniodental and postcranial morphology of the modern snow leopard shows the combination of adaptation to hunt in steeped slopes in open mountainous regions and adaptation to high altitude. The adaptations to mountainous regions exhibited in cranial and skeletal morphology (cranium mechanic design, skeleton proportions, and enlarged ectotympanic) seems to be more prominent than those to a high-altitude, cold, and low-oxygen environment (enlarged frontal sinuses and enlarged cheek teeth), suggesting that the local environment is probably more important concerning on the locomotion and hunting behavior

than the climate for snow leopards. On the other hand, the white coat, long hair, and some physiological traits in the snow leopard represented adaption to the cold environment (Kitchener et al., 2016).

3.3.3 Multiple out-of-Tibet dispersal and the rapid evolution of the snow leopard during the Middle and Late Pleistocene

As our results show, the unique craniodental and postcranial traits of the snow leopard are adapted to mountainous regions, prey type, and climate. The fossil record could help to explore how these traits evolved during the Quaternary.

We identified and analyzed five potential records in Europe and northern China (including the specimen from Longdan, northern China) that putatively belonging to the snow leopard lineage (see the detailed morphological comparison in the Supplementary Materials, Appendix B). Unexpectedly, most of these records are located far away from the Tibetan Plateau. Four of these records are of relatively recent age [i.e., <0.6 Ma]. To better study their evolutionary position, we perform total evidence phylogenetic analyses of the Pantherini, including both modern and fossil species (the poorly preserved Plio-Pleistocene species are not included).

The total evidence phylogenetic analyses using combined morphological and genetic data were performed to investigate the position of these putative fossil snow leopards. Our phylogenetic tree (Figure 3.5) supports the four potential records as a basal snow leopard and supports the oldest record *P.* aff. *pyrenaica* from Longdan as a very basal snow leopard (but with relatively low posterior probability at the latter, suggesting the presence of uncertainty). The phylogenetic tree using pure morphological data gives a similar result (fig. S13 of appendix B), with a different position of *P. uncia* lineage, but the same interspecies relationship within the *P. uncia* lineage. Both analyses support a successive sister group relationship of fossil records and modern species, which are fully consistent with their age (younger species are closer to living species). The topology supports a roughly rapid evolution of the snow leopard lineage since the Early Pleistocene.

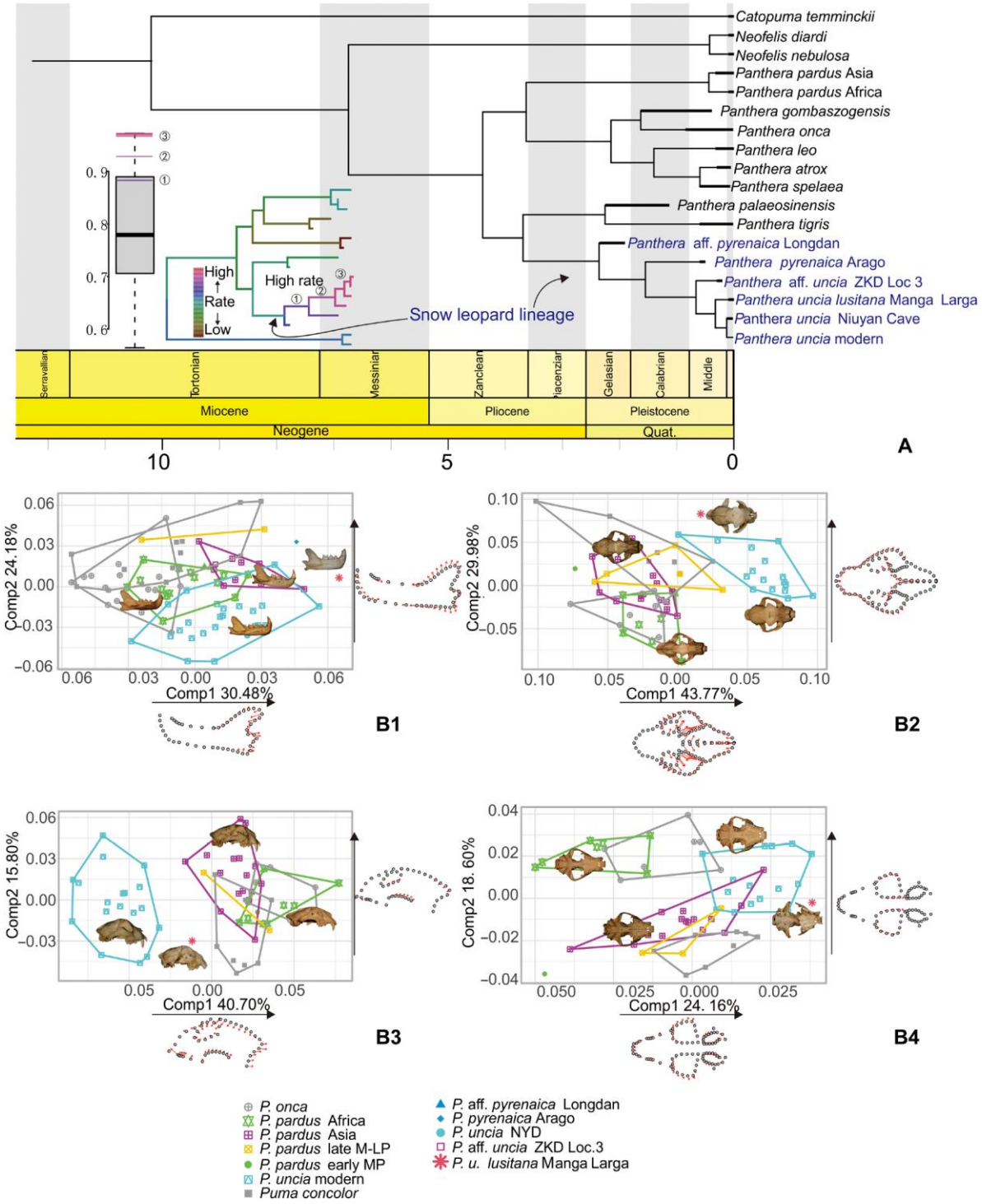


Figure 3.5 — Phylogenetic position and morphospace of modern and fossil snow leopards. (A) Time-calibrated total evidence phylogenetic tree of pantherine cats and the morphological evolutionary rate. (B) Geometric morphometric analyses on lateral views of the cranium and mandible of the fossil snow leopard in comparison with modern species. (B1) Mandible lateral profile, (B2) cranial dorsal view, (B3) cranial lateral view, and (B4) cranial ventral view.

Among these five records, only the latest Pleistocene Niuyan Cave one shows nearly the same traits as the modern snow leopard and should be assigned to the modern species *P. uncia*. The Late Pleistocene skull from Manga Larga shows partial discrepancy from the modern *P. uncia*, out of the range of modern species in some measurements, and is regarded as distinct subspecies. All other fossil records show significant differences from the modern species and should be regarded as distinct species. In general, the late Middle and Late Pleistocene (0.3 to 0.01 Ma) snow leopards already have basic adaptations similar to the modern species (wide forehead, short rostrum, elevated symphysis, enlarged cheek teeth, and enlarged ectotympanic) but still with certain differences. Specifically, *P. u. lusitana* from Manga Larga has a forehead (mainly frontal) with a less concave profile, and its bony choana is relatively narrower, whereas the mandibular corpus is much deeper than in modern *P. uncia*. Therefore, *P. u. lusitana* has less specialization of traits adapted to the cold environment compared with the modern species and also has a somewhat different feeding behavior from that of the modern species (deep mandibular corpus). The early Middle Pleistocene (0.6 to 0.5 Ma) snow leopard *P. pyrenaica*, however, does not have similar traits, as it has small cheek teeth similar to other pantherine cats, and the snout is also relatively longer, and these primitive traits are symplesiomorphic shared with *P. pardus* (Testu et al., 2011). The putative Early Pleistocene snow leopard *P.* aff. *pyrenaica* is basically similar to *P. pyrenaica*, although the symphysis is yet to be so verticalized, which is primitive in regard to modern *P. uncia*. The lack of large cheek teeth, short snout, and vertical symphysis (for *P.* aff. *pyrenaica*), as analyzed above, suggests less adaption to the cold environment and less reliance on Caprini prey type for *P. pyrenaica* and *P.* aff. *pyrenaica*. In the Longdan fauna, there is no Caprini recorded (Qiu et al., 2004).

As a species showing clear adaptation to the environment of the Tibetan Plateau, the majority of its evolutionary history is likely to occur there. The records outside the Tibetan Plateau are rare and incomplete. Longdan in the Linxia Basin is located at the northeastern border of Tibet, has a high altitude of ~2000 m (Qiu et al., 2004; Tao et al., 2013), and probably represents the general marginal distribution of the snow leopard at that time. The four other records are likely to represent the occasional spread of the snow leopard out of Tibet at (or shortly before) the age of the fossil records. These records can thus be used to trace the rapid specialization of the snow leopard during the Quaternary.

Although the overall shape inferred from geometric morphometric (GM) analysis in Figure 3.5 does not show a clear pattern, in regard to the most functional traits analyzed above and PCA plots (Figure 3.5 B), two periods can be distinguished. The first period is from the Early

Pleistocene and early Middle Pleistocene. The snow leopard in this period gradually developed verticalized symphysis suitable to prey on Caprini, but the rostrum is relatively long, so its adaption is initial. Its cheek teeth are small, implying that its adaptation to the cold environment is less developed than that of the modern snow leopard. The second period is from the late Middle Pleistocene to the present day. The snow leopard in this period already has basically the same functional traits as in modern species, with a short rostrum and enlarged cheek teeth, enlarged frontal sinus, enlarged ectotympanic chamber, large orbit, and better adapted to prey on Caprini-type species and cold environments than the snow leopard from the first period. This is supported by morphological evolutionary rates inferred from Bayesian analyses using the approach of Zhang and Wang (2019). The lineage leading to the modern *P. uncia* shows the highest morphological evolutionary rates among the branches in the tree (Figure 3.5 A). This is especially marked in the Middle-Late Pleistocene period. Such rapid evolution during the Early-Middle Pleistocene Transition is likely to be correlated with the onset of glaciation in the Tibetan Plateau in the Middle Pleistocene (Chen et al., 2018; Owen & Dortch, 2014), with the extensive period in marine isotope stages 18 to 16, 12, 6, and 4 to 2 (Ehlers et al., 2018). The climate and environmental change provided stronger selective pressure on the snow leopard adapted to living and catching unique prey in Tibet. The out-of-Tibet dispersal of the snow leopard is in accordance with its major prey, the Caprini bovids. The early evolution of Caprini is endemic to Tibet (S.-Q. Wang et al., 2019; X. Wang et al., 2016). Since the Plio-Pleistocene, some species already began to spread out of Tibet (Bibi et al., 2012; Bukhsianidze & Vekua, 2006; Chardin & Piveteau, 1930), but the large wave of such dispersals only occurred since the Middle Pleistocene, with the appearance of *Ovis* and *Hemitragus* in Europe (Moigne et al., 2006; Fosse et al., 2020) and *Pseudois* in lowland northern China (Beijing) (Tong et al., 2008; Tao et al., 1999). The increased amplitude of glaciation since the Early-Middle Pleistocene Transition brought a long period of the colder environment in Eurasia during several glacial stages (Head & Gibbard, 2015), providing both Caprini bovids and the snow leopard the opportunity to spread from Tibet to other mountainous regions in Eurasia. The functional trait PCA (Figure 3.6) also supports a gradually shift of the snow leopard lineage from a leopard-like space to a more specialized space.

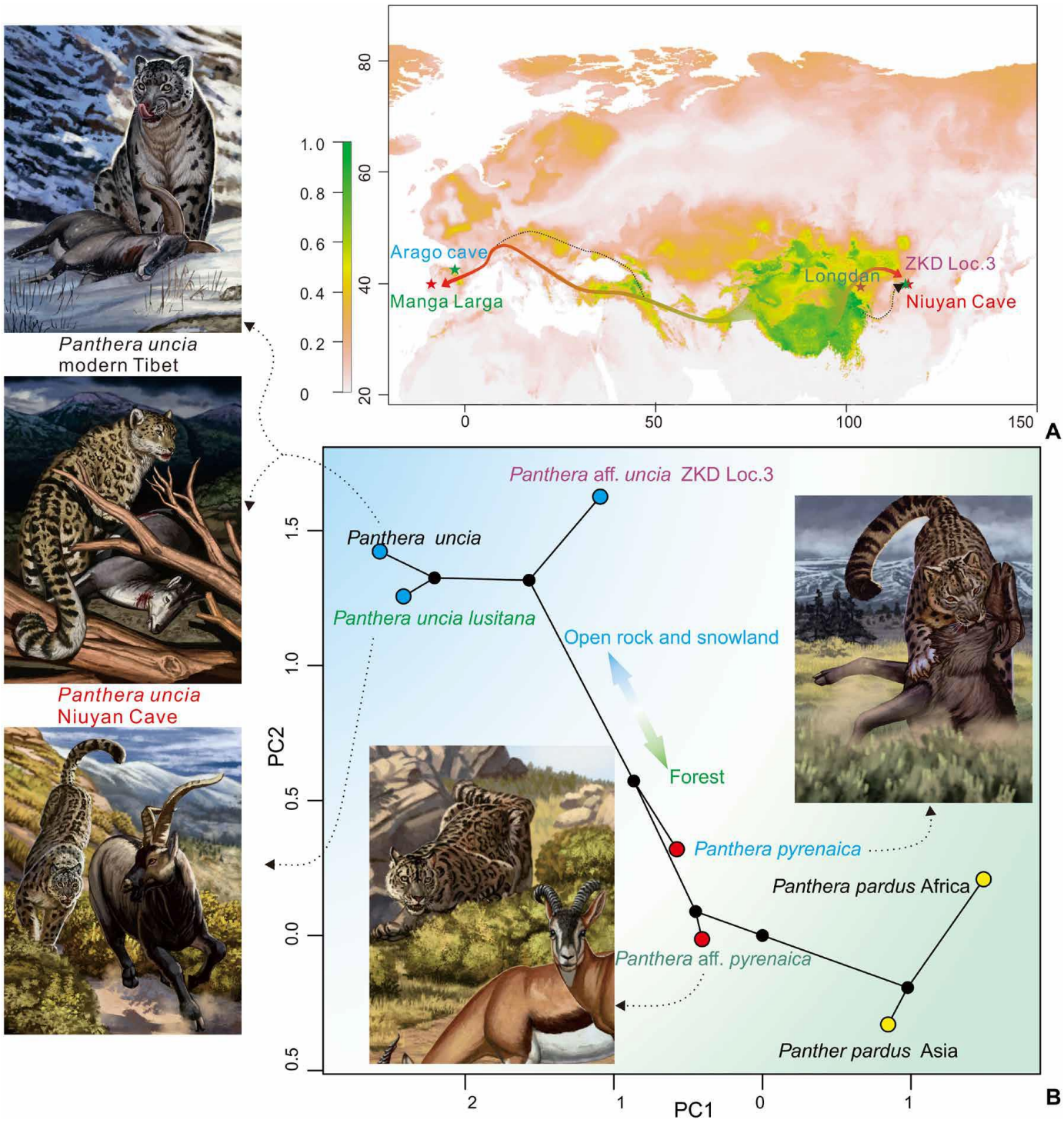


Figure 3.6 — SDM predicted suitable distribution and morphospace of the modern and fossil snow leopards. (A) The predicted probability of snow leopard presence under the LGM climate conditions. (B) Functional traits PCA morphospace, with reconstruction of fossil and modern snow leopards. Artwork by Jianhao Ye.

We find that during the late Middle and Late Pleistocene *P. pardus* also show certain adaptation toward Caprini prey (Ghezzo & Rook, 2015; Nagel, 1999; Spassov & Raychev, 1997), probably due to the harsh environment and abundance of Caprini during the different glacial stages (see the Supplementary Materials in Appendix B). Some characters of this leopard show some similarities to *P. uncia* (see details in the Supplementary Materials in Appendix B). However, our geometric morphometric analyses suggest that they are not much different from modern Asian *P. pardus*, and they lack some key traits seen in the snow leopard lineage (especially the auditory bulla). The lesser extent of cold/mountainous adaptations in *P. pardus* is likely due to the brief period during which leopards inhabited this environment and the unstable environmental conditions in Europe during the Middle and Late Pleistocene, which provided inconsistent selection pressures for cold/mountainous adaptations.

3.3.4 SDM analysis of potential LGM distribution and dispersal route of the snow leopard

To test whether the five fossil localities are within the area of suitable climate region of the snow leopard during the Pleistocene, we performed SDM to predict the probability of snow leopard presence under LGM climate conditions. Although none of the records can be precisely dated to LGM, the two Late Pleistocene ones are likely from this age. Nevertheless, during the LGM, the cold environment was predominant than at any other time of the Middle to Late Pleistocene (Hughes, 2022; Shackleton, 1967) and the snow leopard is likely to spread farthest from Tibet at the LGM. This condition, therefore, represents the largest potential distribution of the snow leopard. Note that the SDM cannot predict the presence or not of glaciation, which definitely present in the Tibetan Plateau during LGM, so the potential range of the snow leopard in the Tibetan Plateau must be much smaller during LGM.

The predicted suitable area (Figure 3.6) is much larger than the current condition (see fig. S14 of appendix B for the prediction under the current conditions for comparison). Except for the Longdan one, none of the other four putative records are located within the highly suitable area predicted by SDM, although they are all closer to the suitable area than they are found today. This makes sense considering the small number of snow leopard records discovered in these regions, and these records probably represent the occasional and marginal distribution of the Pleistocene snow leopard. All four Middle to Late Pleistocene localities are lower than

1000 m in altitude. This is especially true for the Loc. 3 of Zhoukoudian (Pei, 1936), which is not in a typical cold environment as in the LGM conditions.

The SDM results suggest that the fossil snow leopards probably have different climate adaptations as the modern snow leopards do. This is in accordance with our morphological analyses that most of these fossil snow leopards have less strong adaptation to cold and high altitudes. On the other hand, the snow leopard from Niuyan Cave, which we identified as modern snow leopard, is also located outside the predicted suitable area under the LGM conditions. Notably, the microenvironments are steeped slopes in mountainous regions in all four cases. We argue that for the snow leopard, climate and altitude only partially influence their distribution, but mountainous steeped slopes are necessary habitat. Most anatomical traits of the snow leopard analyzed above are adapted to preying focusing, catching, and killing in the mountainous region. In lowlands with heavy cover (warm and humid conditions), the advantage of the snow leopard (over the leopard) loses. This explains their rarity or absence in most of the faunae of the lowlands far away from Tibet.

Overall, our analyses suggest that the mountainous region with steeped slopes and heavy rock cover are probably more important factors that influence the snow leopard distribution during its evolutionary history than the temperature and altitude themselves. This information would benefit further protection.

The predicted suitable area may also infer the dispersal routes of the snow leopard during glacial stages, as this provides potential connectivity. However, topography, prey type, etc., which is not included in the SDM analyses, are also important for real dispersal, so the exact dispersal routes are still waiting for more fossil records.

In summary, our analyses support five fossil records putatively corresponding to the Pleistocene snow leopard lineage. According to the obtained results, the former lineage suffered a rapid evolution during the Quaternary, especially since the Middle Pleistocene. The earliest putative record of the lineage is located at Longdan (Linxia Basin) near the border of Tibet with an estimated chronology of 2.2 to 2.5 Ma. The other four records are far from Tibet and not located in the suitable area predicted by SDM under the LGM conditions. In consequence, snow leopards could disperse out of Tibet to lowland eastern Asia and Europe through different routes. These later four fossil records are still out of the suitable area, representing the marginal distribution at that time. All three aspects (morphology, paleoenvironment of fossil occurrence, and SDM under the LGM conditions) support that the temperature and altitude are less important than the local microscale landscape, and steeped slope and heavy rock are more important factors for snow leopard survival.

Our study suggests climate, prey type, and especially landscape (mountainous region) are important for snow leopard, probably more than altitude itself. This information will be beneficial for the future protection of this iconic animal. We highlight the importance that the combination of morphology, fossil records, and ecological methods (SDM) can have for providing more comprehensive and testable data on the ecology and adaption of modern species and provide information that might be helpful to develop protection strategies for the animal.

4

3D DIGITAL AND BIOGEOCHEMICAL ANALYSIS OF THE ALGAR DA MANGA LARGA PANTHERINE (*PANTHERA UNCIA LUSITANA*)

Abstract from a section of this chapter: Estraviz-López, D., Jiangzuo, Q., Madurell-Malapeira, J., Cardoso, J. L., Rios, M. & Grandal-d'Anglade, A. (2024). On the identity of the elusive pantherine from the Algar da Manga Larga, Portugal: A computed tomographic study of inner cranial cavities. XXXIX Jornadas de La Sociedad Española de Paleontología. Libro de Resúmenes. 5. p70.

This chapter presents the preliminary results of the follow up study of the Manga Larga pantherine, the type specimen of the Portuguese snow leopard, *Panthera uncia lusitana* (MG1355.0001-9). Part of the findings, concretely those related to the segmentation of the endocast, were presented at the XXXIX meeting of the Spanish Society of Paleontology, held in A Coruña (Spain) in 2024. In addition to these, the results of the molecular analyses conducted are also reported, and preliminary conclusions are discussed, along with potential venues for future research.

4.1 Introduction

4.1.1 The Manga Larga Pantherine: Discovery and Reassessment

The Algar da Manga Larga was discovered in 1975 by the Sociedade Portuguesa de Espeleologia (SPE) on the Planalto de Santo António within the Natural Park of the Serras d´Aire e

Candeeiros. Bone remains within the cave were initially observed by speleologists and later mentioned by Thomas (1985), who tentatively attributed them to a dog. In January 2003, a team from AESDA (Associação de Estudos Subterrâneos e Defesa do Ambiente) conducted a photographic survey of the cave. Analysis of these photographs led to the preliminary identification of the remains as belonging to a large felid. A subsequent visit to the cave allowed the collection of the bones; nevertheless, almost no other faunal remains were found in the vicinity and no clear stratigraphic context was present. The specimen was found lying over calcareous crusts, suggesting it was likely transported from another area of the cave system (Regala & Cardoso, 2007).

A comprehensive paleontological study was conducted under the scientific supervision of Professor João Luis Cardoso. The study aimed to compare morphologically and morphometrically the Manga Larga leopard to other *Panthera pardus* specimens. The remains belonged to a single adult pantherine felid. The cranial dimensions generally fall within the lower range recorded for *Panthera pardus*. However, the Manga Larga skull exhibits a proportionally short and wide cranium, with a wide and short snout and a broad and high forehead with spaced orbits. The transverse dimensions of the cranium are notably large relative to its longitudinal length, resulting in a convex cranial profile. These features are unique among both fossil and extant leopard specimens. Ultimately, the remains were donated by AESDA to the Geological museum of Lisbon for exhibition and further research (Cardoso & Regala, 2006).

Almost two decades later, in the context of an investigation about the origins and dispersion of the snow leopards (*Panthera uncia*), the specimen from Algar da Manga Larga (MG1355.0001-9) was re-evaluated and classified as the type specimen of a new fossil subspecies of snow leopard, *Panthera uncia lusitana*. This study was centered on qualitative characters, 2D Geometric Morphometrics (GM), Finite Element Analysis (FEA), and traditional morphometrics of the skull, which allowed its classification as a member of the snow leopard lineage. See Chapter 3 for further information (Jiangzuo et al., 2025).

4.1.2 Non-destructive 3D imaging in fossil analysis

Computed tomography (CT) scanning and other 3D digital techniques have revolutionized paleontology by providing powerful new ways to study fossils. These methods use technologies like X-rays (in CT scans), lasers, and structured light to create high-fidelity, three-dimensional (3D) digital representations of physical specimens without damaging the fossils. This non-destructive nature is particularly beneficial for studying rare and fragile fossils (Blackburn et al., 2024).

CT scans in particular reveal internal structures hidden within the fossilized matrix or the bone itself (Puértolas-Pascual & Mateus, 2020), such as endocasts (Puértolas-Pascual et al., 2023), vascular foramina (Mateus & Estraviz-López, 2022), sinuses (Frosali et al., 2023), dental growth layers (Baier-Stegmaier et al., 2023), and even histological studies, without the need of damaging the specimens (A. H. Lee et al., 2025).

The resulting 3D datasets enable a wide range of studies that were previously limited or impossible using traditional morphometrics, which have historically relied on qualitative descriptions or two-dimensional measurements. For example, they facilitate the application of geometric morphometrics, which analyzes the overall shape of structures independently of their size. This approach allows for more sophisticated studies into ontogeny, evolutionary relationships, functional morphology, and taxonomic differences (Chatar et al., 2024).

The generated 3D models can be easily shared and analyzed by researchers globally, fostering collaboration and helping science (Lambrides et al., 2024). The 3D models can also be used for education and public outreach, making paleontology more accessible for everyone (Depraetere et al., 2025).

4.1.3 Geochemical approaches for chronological and paleoecological reconstruction

4.1.3.1 Uranium-Thorium series dating

The Uranium-Thorium (U-Th) dating is a high-precision radiometric technique utilized for determining the chronological framework of calcium carbonate ($CaCO_3$). Materials that can be dated include speleothems (Spötl & Boch, 2019), corals (Andersen et al., 2009), molluscan shells (Cheong et al., 2006), and, in specific cases, lake carbonates (Placzek et al., 2006), bones, and teeth (Raposo, 1995; Zilhão et al., 2011). The efficacy of this method varies among substrates due to differential uranium incorporation and the exclusion of initial thorium (^{230}Th) within their crystalline structure, which is critical for minimizing contamination and ensuring robust age determinations (Spötl & Boch, 2019).

U-Th dating quantifies the ratios between the parent isotope (^{234}U) and its decay product (^{230}Th). This isotopic ratio serves as a proxy for evaluating the temporal progression of uranium decay, providing an age estimation for the sample (Spötl & Boch, 2019). High-precision mass spectrometry is utilized to detect the relative abundances of these isotopes. Using this method is possible to date samples up to 500.000 YBP or almost 10 times older than the limit for ^{14}C,

not relaying in the presence of organic matter in the sample for the dating (Hoffmann et al., 2018; Spötl & Boch, 2019).

U-Th dating relies on the assumption that the U-Th system remains undisturbed, meaning there is no loss of U or Th to the environment (leaching) or addition of external U or Th (uptake). If such changes can occur, the sample is considered an "open system," potentially affecting the accuracy of the dating process (Spötl & Boch, 2019). Corals, and speleothems are ideal for this technique, as their structure behaves like a closed system. In contrast, lacustrine carbonates, teeth, and bones may act as open systems, depending of the environment in which they were deposited, due to their porous nature (Hoffmann et al., 2013; Placzek et al., 2006).

4.1.3.2 Nitrogen quantification for trophic reconstruction and biomolecular preservation assessment

Nitrogen isotopes, particularly ^{15}N and ^{14}N, are widely used in ecological and molecular paleontological studies to understand trophic dynamics and ecological niches (Ben-David & Flaherty, 2012). The primary rationale for using Nitrogen (N) isotopes lies in the predictable fractionation that occurs as N moves through the food web. During metabolic processes, organisms tend to preferentially excrete the lighter isotope (^{14}N), leading to an enrichment of the heavier isotope (^{15}N) in their tissues. This enrichment, known as trophic discrimination, typically results in an increase of approximately 3–4‰ in ^{15}N per trophic level (Ben-David & Flaherty, 2012). This makes Nitrogen isotopes particularly useful for determining the trophic position of organisms within an ecosystem (Ben-David & Flaherty, 2012).

Nevertheless, any work using these isotopes must be conducted in bones that still retain sufficient N from organic matter (meaning they still preserve enough protein in the bone, specifically collagen). The quantity of N in the fossils is also a proxy for the feasibility of the use of ancient DNA and proteomic studies, as well as for radiometric dating of collagen (Orlando et al., 2021).

4.1.3.3 Stable isotope analysis of bioapatite ($\delta^{18}O$ and $\delta^{13}C$) as a proxy for paleoenvironmental and paleodietary reconstruction

Bioapatite ($Ca_{10}(P_{O4}, C_{O3})_6(OH, F)$) is the primary constituent of the teeth and bones of land vertebrates and records short-term environmental fluctuations in ecosystems while being deposited. Its exceptional strength and fossilization potential make it an ideal material for paleoclimatic and paleoenvironmental studies (Lee-Thorp & Sponheimer, 2003).

The oxygen isotope composition of bioapatite ($\delta^{18}O$) directly reflects the environmental conditions and climate experienced by an animal during its lifespan (Fricke & O'Neil, 1996). In terrestrial vertebrates, $\delta^{18}O$ values mirror the $\delta^{18}O$ content of ingested drinking water, making it a valuable proxy for reconstructing past temperatures. Higher proportions of $\delta^{18}O$ relative to the lighter isotope $\delta^{16}O$ in osseous tissues of terrestrial vertebrates typically indicate warmer environmental conditions, although they could also indicate different water sources or mobility of the animals (Ayliffe et al., 1992).

The carbon isotope composition of bioapatite ($\delta^{13}C$) is influenced by the carbon included by all the diet of the animal (lipids, proteins, carbohydrates…), and usually reflect the photosynthetic pathway of the plants consumed by an animal (or by its prey), enabling differentiation between C3, C4, and CAM plants. $\delta^{13}C$ values provide insights into the dietary habits of animals and, by extension, assist in reconstructing their habitats (open vs forested), particularly for herbivores. The $\delta^{13}C$ values of carnivores generally reflect the values of their prey. Typically, higher $\delta^{13}C$ values relative to the lighter isotope $\delta^{12}C$ in the osseous tissues of terrestrial vertebrates are indicative of more open environments (Koch, 2007).

The standard methodology for this type of analysis involves extracting small quantities of bioapatite from the bones or teeth -particularly teeth enamel due to its exceptional preservation and resistance to diagenesis- followed by purification of the carbonate fraction and analysis using a Isotope-Ratio Mass Spectrometer (IRMS), which measures the relative abundance of lighter versus heavier isotopes (Ben-David & Flaherty, 2012).

Used in conjunction $\delta^{18}O$ and $\delta^{13}C$ can help to understand the ecological niche of fossil animals (Sponheimer & Lee-Thorp, 1999; Robu et al., 2019).

4.1.4 Objectives

This chapter aims to provide the foundations for a detailed investigation of the type specimen of *Panthera uncia lusitana*, expanding upon the broader evolutionary context presented in the previous study (see Chapter 3). Two complementary lines of evidence are explored:

- First, a non-invasive analysis of the endocast through CT-scan data and segmentation of the inner cranial cavities, accompanied by a preliminary qualitative comparison with related species.

- Second, the application of a suite of molecular techniques to the specimen including: U-Th series dating to estimate the specimen's age; quantification of N content in the bone, as

a proxy for the presence of organic matter (including proteins and DNA); and, isotopic analysis of $\delta^{18}O$ and $\delta^{13}C$ in bioapatite to infer paleoenvironment and paleotemperature.

The results will be interpreted in the context of previous research and potential directions for future studies will be identified.

4.2 Material and methods

4.2.1 Material

The material includes the skull and mandible of the Algar da Manga Larga leopard (MG1355.0001-0002), which were subjected to CT-scanning. Samples were taken (Figure 4.1) from the lingual side of the left upper canine teeth of the skull of the type specimen of *Panthera uncia lusitana* (MG1355.0001), as well as from the ventro-proximal part of the diaphysis of the humerus (MG1355.0003). A total of 150 mg of enamel and dentine powder were extracted from the canine, as well as 200 mg of bone powder from the humerus for posterior biogeo-chemical analyses with the help of a diamond drill.



Figure 4.1 — Location of the sampled areas in the canine (MG1355.0001) (top), and in the humerus (MG1355.0003) (bottom) of the type specimen of *Panthera uncia lusitana*. Scale bars are 30 mm.

4.2.2 Methods

4.2.2.1 CT-Scan segmentation

The CT-Scans were obtained using the CT-scanner Siemens SOMATOM Definition AS+ located at the Affidea clinic at Avenida da República, Lisbon (Figure 4.2).

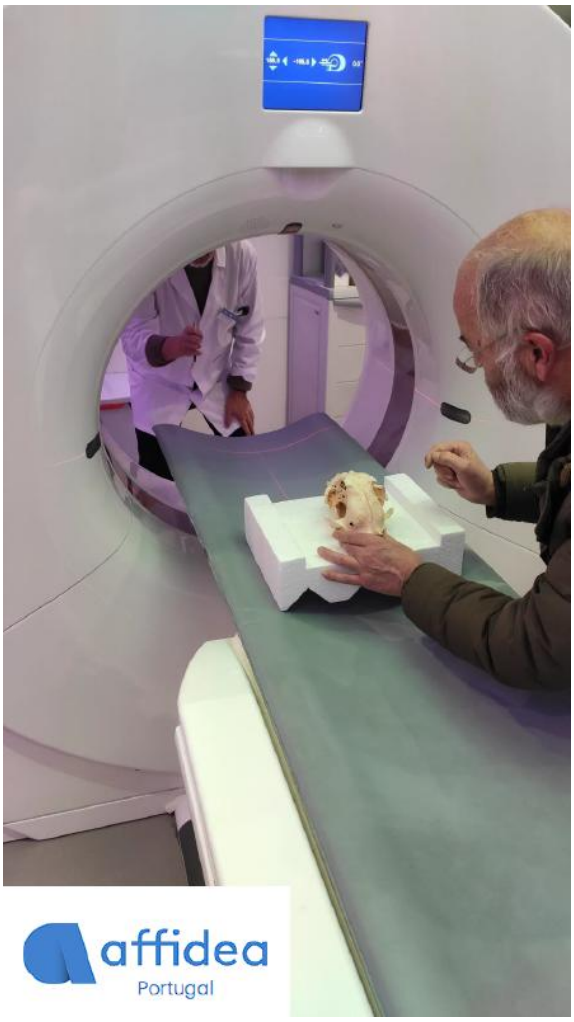


Figure 4.2 — Skull and mandible of *Panthera uncia lusitana* (MG1355.0001-2) undertaking CT-scanning at the Affidea clinic of Avenida da República, Lisbon.

The scan provided a total of 1588 slides, which were segmented preliminary with the usage of the software 3D Slicer v. 5.6.1 (Pieper et al., 2004). The volume of the endocast was extracted automatically with the function "Wrap solidify". Nevertheless, there was still clay adhered to the interior part of the skull, requiring manual editing of the endocast using the software 3D Slicer, which took approximately 100 hours to complete (Figure 4.3).

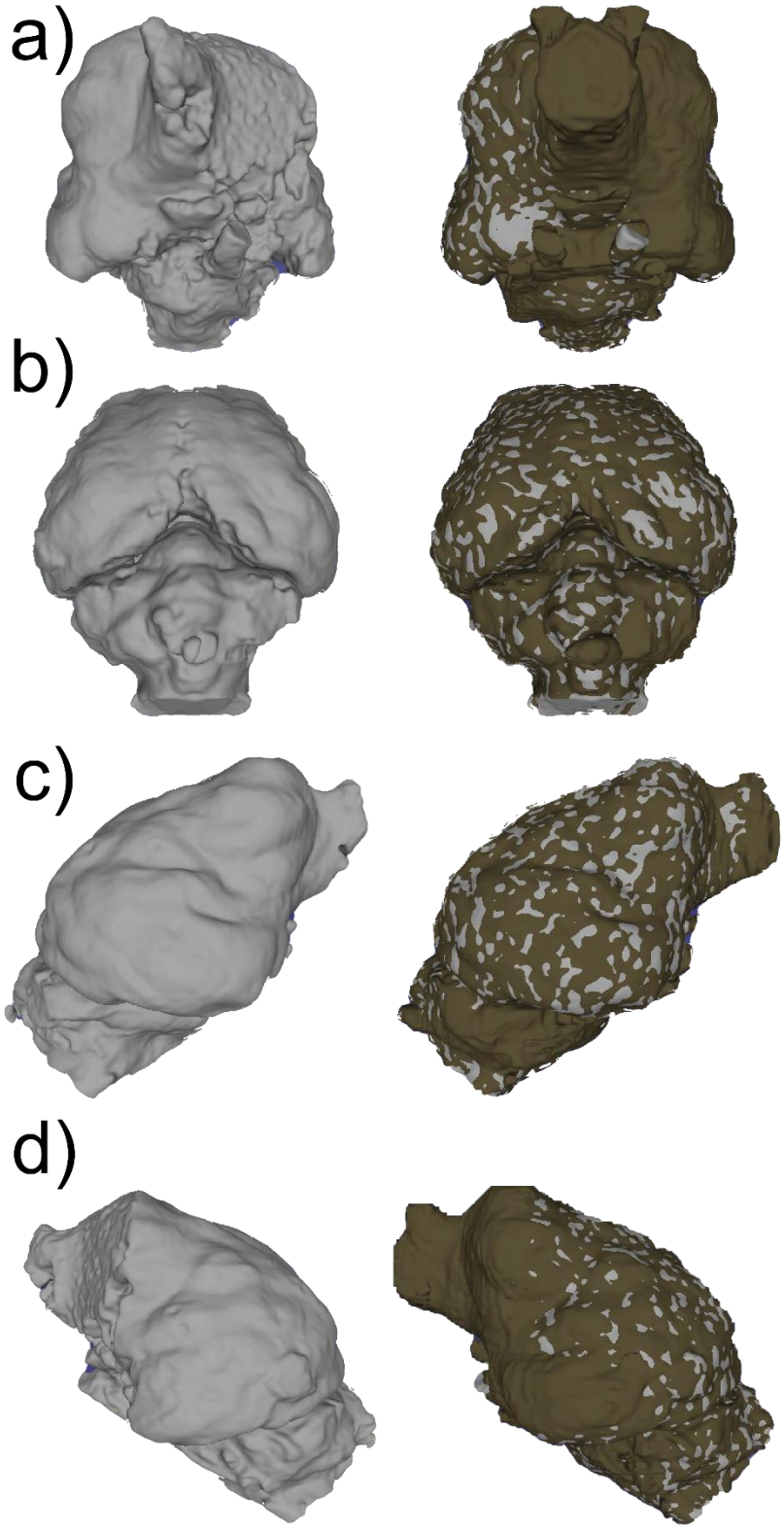


Figure 4.3 — Endocast of *Panthera uncia lusitana* (MG1355.0001) before (left) and after (right) undertaking 100 hours of manual editing in a) anterior, b) posterior, c) right lateral, and, d) left lateral views. The brown areas have been more manually reconstructed than the white ones.

4.2.2.2 U-Th series dating

Isobar Science co. laboratory was responsible for treating of the samples. Around 20 mg of homogenized sample (bone powder and enamel powder respectively) were dissolved in 0.45 M HNO3 to minimize leaching of U and Th from detrital materials.

Isolation of U and Th from each sample was achieved by extraction chromatography using Eichrom UTEVA resin following the methods of Pourmand et al. (2014) and Pourmand and Dauphas (2010). High precision U and Th isotope analysis was performed with a Thermo Fisher Neptune PlusTM MC-ICP-MS with an Apex-Q desolvation nebulizer, at the Isobar Science Co, lab from United States. Each sample measurement was bracketed with measurements of two wash solutions and two certified reference materials (CRM-112A and IRMM-035 for uranium and thorium respectively)

Uncertainties on the U-Th ages are reported at the 95% confidence interval (CI) and include propagation of systematic and random uncertainties by Monte Carlo simulation of measured analytical uncertainties on isotope ratios, and those associated with U and Th isotope decay constants.

Age calculation and propagation of the uncertainties were performed by using Monte Carlo simulation (Pourmand et al., 2014) and by taking into account the measured isotopic ratios of U and Th derived along with other variables such as the spike mass and concentration, sample mass, the decay constants of U and Th isotopes along with their associated uncertainties. The average initial $^{230}Th/^{232}Th$ activity ratio of 0.6±0.2 is used to correct for contribution of the detrital fraction to ^{230}Th.

4.2.2.3 Nitrogen quantification

The laboratory of SAI ("Servizos de apoio a Investigación") from university of A Coruña carried out these analyses. Following the protocol by Bocherens et al. (1997), 0.5 mg of bone powder from the humerus were successively washed for an elemental analysis. The sample was weighed precisely in a tin capsule on an MX-5 balance (Mettler Toledo). The analysis was performed using a FlashEA112 elemental analyzer (ThermoFinnigan). Then it was analyzed by flash combustion in a quartz tube filled with WO3 and copper, maintained at 1020º C. % of N in the sample is expressed as result.

4.2.2.4 $\delta^{18}O$ and $\delta^{13}C$ analysis

The laboratory of SAI ("Servizos de apoio a Investigación") from university of A Coruña carried out these samples. The carbonate from the osseous tissues (enamel powder) was

extracted using the method by de Winter et al., (2016): Approximately 11 mg of sample were pre-weighed for pretreatment and subsequently treated with a 1M calcium acetate-buffered acetic acid (CH_3COOH) solution in excess for 30 minutes. After treatment, samples were rinsed three times with milli-Q water and dried overnight at 50 ºC. Extracted carbonate samples were reacted with 100 μ L of 99% orthophosphoric acid (H_3PO_4) for each sample, and kept at 26ºC for 24 hours until the analysis was conducted. The analysis was performed in a carbonate preparation device (GasBench II analyzer), coupled to a MAT253 stable Isotope Ratio Mass Spectrometer (ThermoFinnigan). 2 mg of the sample were weighed into 12 ml vials which were subsequently evacuated with Helium. The generated CO_2 was separated from other gases on a PoraplotQ column (25m, 0.32 mm, Varian) maintained at 70ºC. The system was calibrated using NBS19, NBS18, CO-8, and LSVEC standards last (IAEA, Vienna, Austria). The results were expressed as $\delta\,^{13}C_c$ (‰)VPDB (Vienna Pee Dee Belemnite) and $\delta\,^{18}O_c$ (‰)VPDB.

To reconstruct an approximate temperature from bioapatite, first, it is necessary to change the reference scale of the isotopic values by converting the VPDB standard values to VSMOW (Vienna Standard Mean Ocean Water) using the equation by Kim et al. (2015):

$$\delta^{18}O_{VSMOW} = 1.03091 \times \delta^{18}O_{VPDB} + 30.91$$

Next, the values of the carbonate (c), which is the analyzed fraction, are transformed to the values of the phosphates (p), in order to calculate the $\delta\,^{18}O$ of drinking water, by using the equation from Iacumin et al. (1996):

$$\delta\,^{18}O_p = 0.98 \times \delta\,^{18}O_c - 8.5$$

This value of $\delta\,^{18}O$ on the phosphate of enamel can be correlated with the $\delta\,^{18}O$ of the drinking water ($\delta\,^{18}O_{dw}$) with a clade specific equation (for the entire Felidae), calculated on this case from the North American felids *Puma concolor* and *Lynx rufus* (Pietsch & Tütken, 2016):

$$\delta^{18}O_{dw} = (\delta^{18}O_p - 20.1) / 0.4$$

Finally, this value (that reflects the value of $\delta\,^{18}O$ from the water drank by the animal when its bone and teeth were being formed) can be used to estimate the temperature in which it lived. The equations for this last step are region, time and species-specific, so one developed

from the rodents of Cova dels Xaragalls, in the Pleistocene of Iberian Peninsula, was used (Fernández-García et al., 2019) as there was none developed from carnivores.

$$\text{Mean Annual Temperature (°C)} = 2.38\ (\pm 0.10) \times \delta\ ^{18}O_{dw} + 28.19\ (\pm 0.58)$$

The results of this final equation will be compared with the mean annual temperature experienced alongside the current distribution of the snow leopard as registered by IUCN Red List and worldclim.org, in order to compare the current climatic niche of *P. uncia* with that of the past.

4.3 Results

4.3.1 CT-scan segmentation

The CT-scan segmentation resulted in the retrieval of the virtual endocast of *Panthera uncia lusitana* (MG1355.0001), which was visualized using the software Blender 4.0. The endocast was compared at the same scale with those of other felids, including modern *Panthera uncia* (CBL 187), *Panthera pardus* (LACM 11704), *Panthera leo* (MMMH 17533), *Panthera onca* (CBL 142), *Panthera tigris* (MZUF8460), *Acinonyx jubatus* (FMHN29635) and *Puma concolor* (LACM 85440). See the comparisons at Figure 4.4, Figure 4.5, and, Figure 4.6.

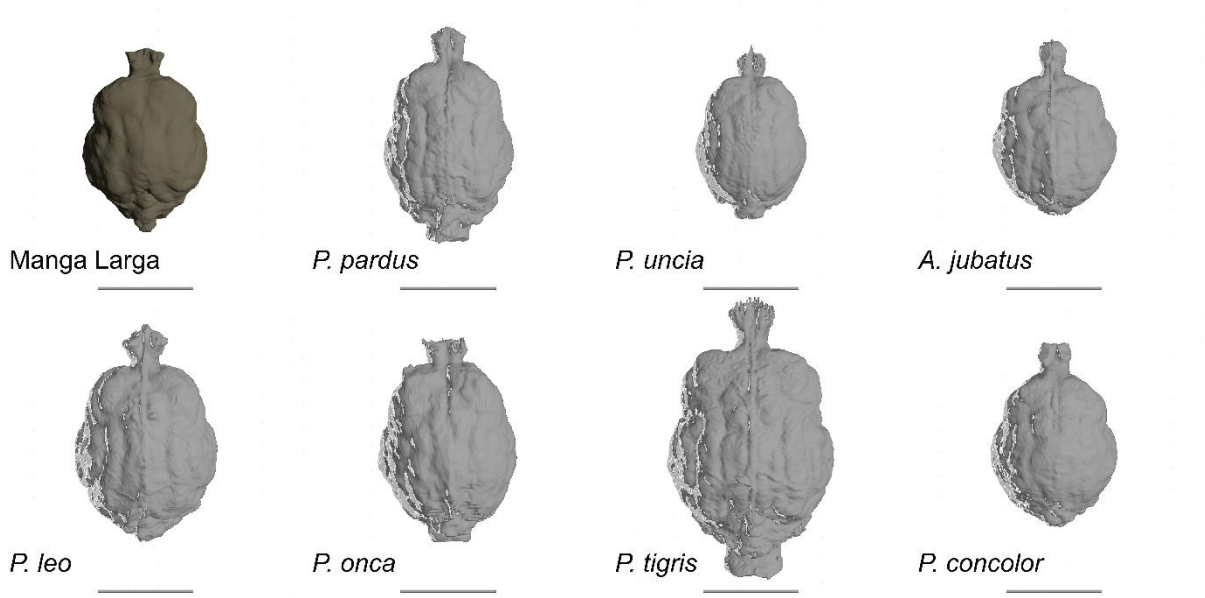


Figure 4.4 — Endocast of *Panthera uncia lusitana* (MG1355.0001) in dorsal view compared with the dorsal views of the endocast of related felids. Scale bars are 50 mm.

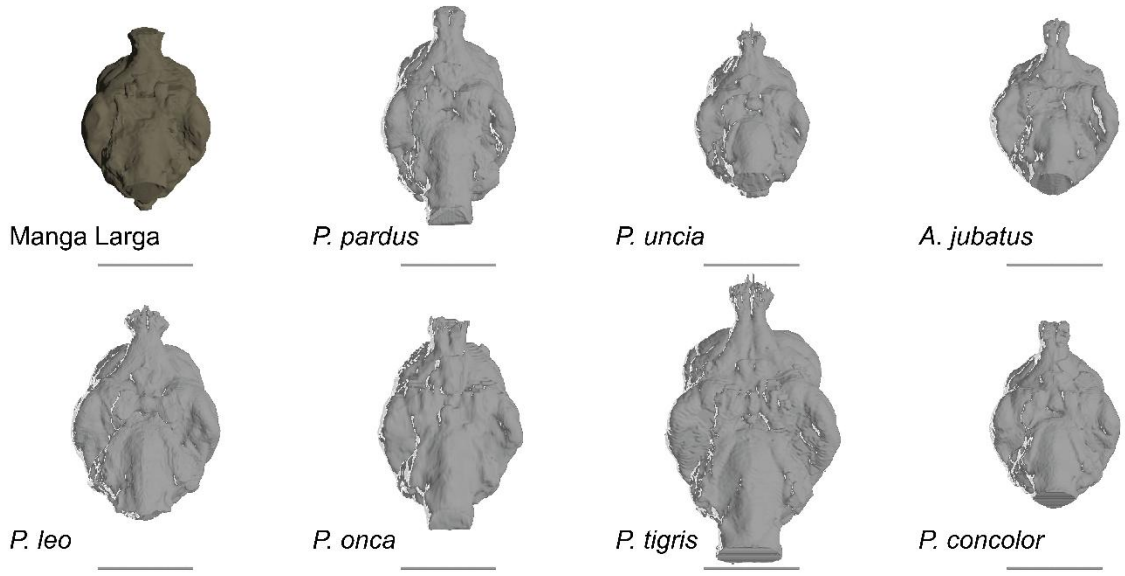


Figure 4.5 — Endocast of *Panthera uncia lusitana* (MG1355.0001) in ventral view compared with the ventral views of the endocast of modern related felids. Scale bars are 50 mm.

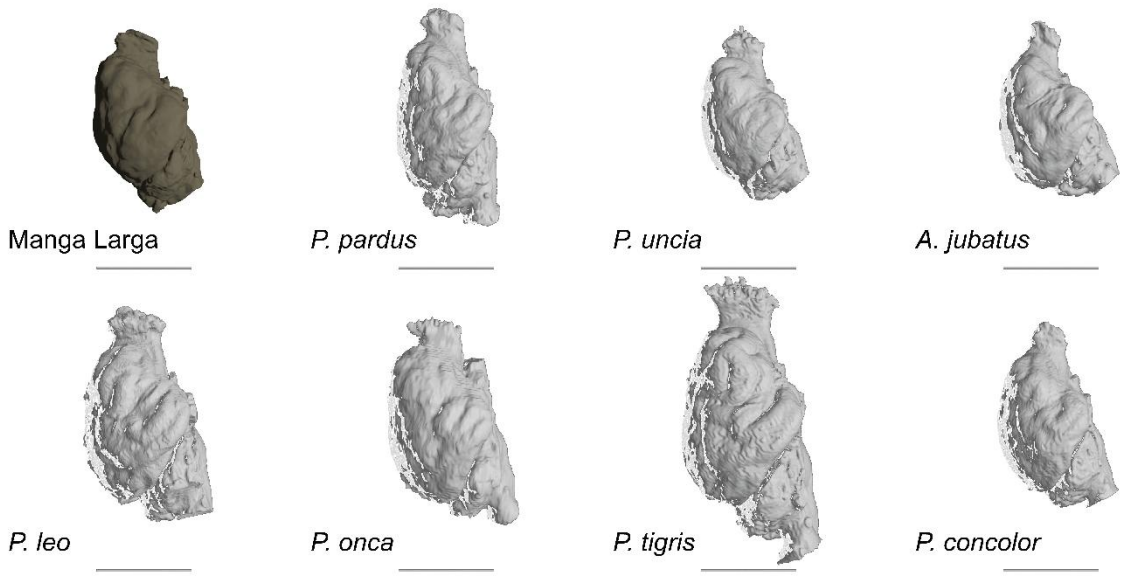


Figure 4.6 — Endocast of *Panthera uncia lusitana* (MG1355.0001) in right lateral view compared with the right lateral views of the endocast of modern related felids. Scale bars are 50 mm.

As shown in Figure 4.4, Figure 4.5, and Figure 4.6., the endocast of *Panthera uncia lusitana* (MG1355.0001) most closely resembles that of modern *Panthera uncia* in both general size and overall morphology. However, there are two notable differences: first, a greater constriction between the anterior and posterior parts of the cerebrum in *Panthera uncia lusitana* (Figure 4.4), and second, a more robust morphology, particularly evident in ventral view (Figure 4.5).

Compared to the modern african leopard (*Panthera pardus*), the Manga Larga specimen exhibits a dorso-ventral torsion of the telencephalon relative to the brainstem. In contrast, the modern African leopard shows a more antero-posteriorly straight brain cavity, with the Manga Larga specimen also presenting a relatively more ventral position of the foramen magnum (Figure 4.6). Additionally, the endocast of MG1355.0001 is also of smaller size than the endocast of the modern leopard.

MG1355.0001 endocast is also noticeably smaller in size compared to the endocast of *P. tigris*, *P. leo*, and *P. onca*. However, the *P. tigris* endocast also exhibits a comparable constriction between the anterior and posterior parts of the cerebrum (Figure 4.4), although it lacks the same degree of torsion of the telencephalon in lateral view (Figure 4.6).

Acinonyx jubatus displays an even greater degree of torsion of the telencephalon, with a round cerebrum and noticeably smaller olfactory bulb (Figure 4.6).

Finally, *Puma concolor* shows a similar overall morphology, but with a slightly smaller olfactory bulb (Figure 4.6) and more pronounced tapering of the anterior cerebrum in ventral view (Figure 4.5).

4.3.2 U-Th series dating

The results indicate that the calculated age exceeds the U-Th permissible clock. The samples exhibit an open system behavior, as shown in the graph in Figure 4.7, based on Osmond and Ivanovich (1992). A portion of the U and Th in the samples was lost to the environment, rendering further age estimation ineffective. For the full results, please refer to Appendix C.

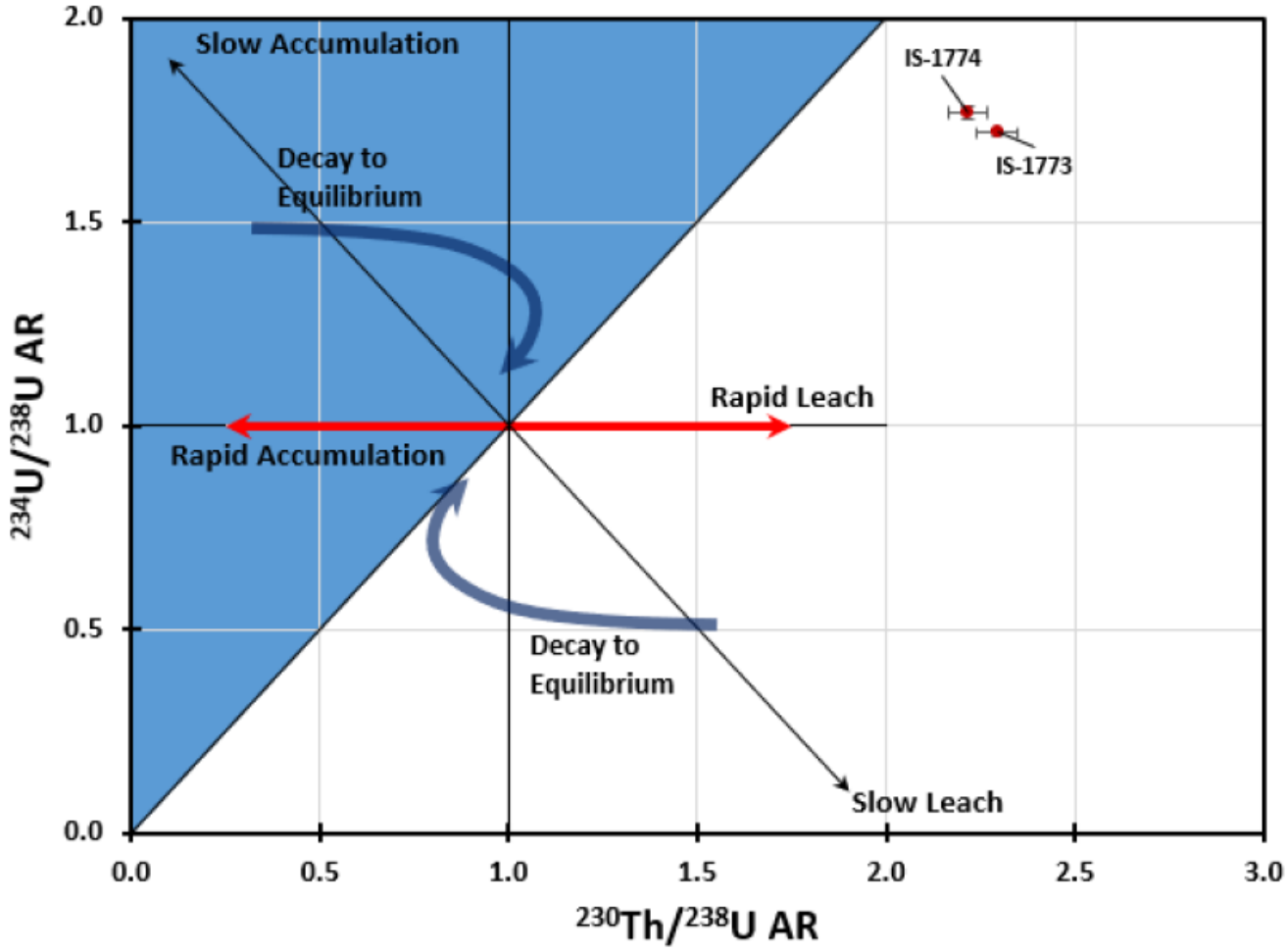


Figure 4.7 — Plot of $^{234}U/^{238}U$ activity ratios against $^{230}Th/^{238}U$ activity ratios for the samples of the leopard of Manga Larga (IS-1773 and IS-1773), modified after Osmond and Ivanovich (1992). This graphical representation is for reference only and should not be construed as an interpretation of these test results.

4.3.3 Nitrogen quantification

The results indicate that the percentage of N in the sample is <0,05%, rendering any further attempts of quantifying the N isotopes pointless, as there is not enough organic matter on the osseous tissues (Bocherens et al., 2005). This also means that the likelihood of proteins of ancient DNA being preserved on the fossils of Algar da Manga Larga is equally low. To see the full results, please refer to Appendix C.

4.3.4 $\delta^{18}O$ and $\delta^{13}C$ analysis

The uncorrected $\delta 13C_{VPDB}$‰ values of the samples from the tooth enamel were -10.79‰ and -10.81‰, with an average of -10.80‰. The $\delta^{18}O_{VPDB}$ ‰ values of the samples were -4.06‰ and -4.48‰, with an average of -4.27‰. For the complete laboratory results, see Appendix C.

The value of $\delta^{13}C_{VPDB}$ was corrected for carnivores with +1.3 ‰ for trophic discrimination (Domingo et al., 2017), which results in a corrected value of $\delta^{13}C_{VPDB}$ of -9,5‰ for *Panthera uncia lusitana*. These values can be compared to those from the Portuguese locality of Lapa do Picareiro (Carvalho et al., 2022). In this site, *Cervus elaphus* and *Capra pyrenaica* teeth with an age of 51.800 to 42.420 YBP have been subjected to the same analyses as the fossils from Algar da Manga Larga (Figure 4.8).

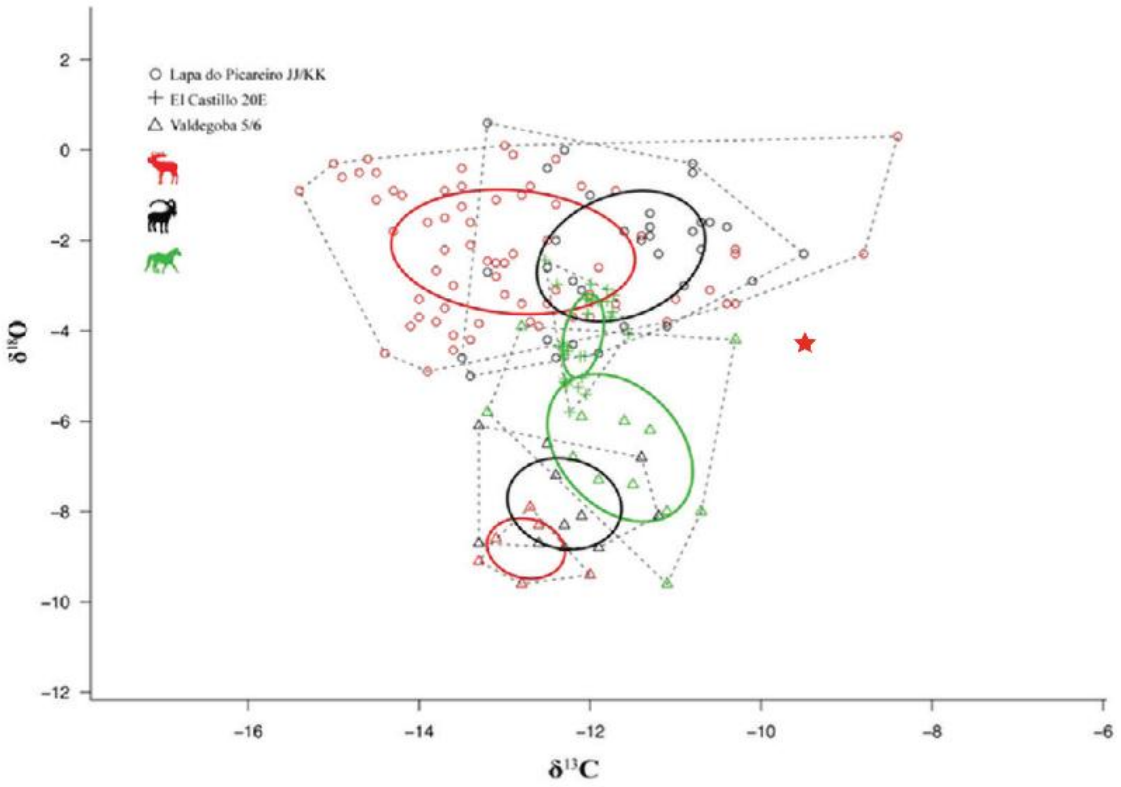


Figure 4.8 — Standard ellipse areas showing the isotopic niche space occupied by herbivores from Levels JJ and KK of Lapa do Picareiro, Level 5/6 of Valdegoba Cave and Level 20E of El Castillo Cave. The star represents the pantherine from Algar da Manga Larga. Image modified from Carvalho et al. 2022.

The conversion from $\delta^{18}O_{VPDB}$ to $\delta^{18}O_{VSMOW}$ yielded a value for the pantherine of Algar da Manga Larga of 26.5‰ and allows it to be compared with a larger sample of sites previously analyzed by Domingo et al. (2017) (Figure 4.9).

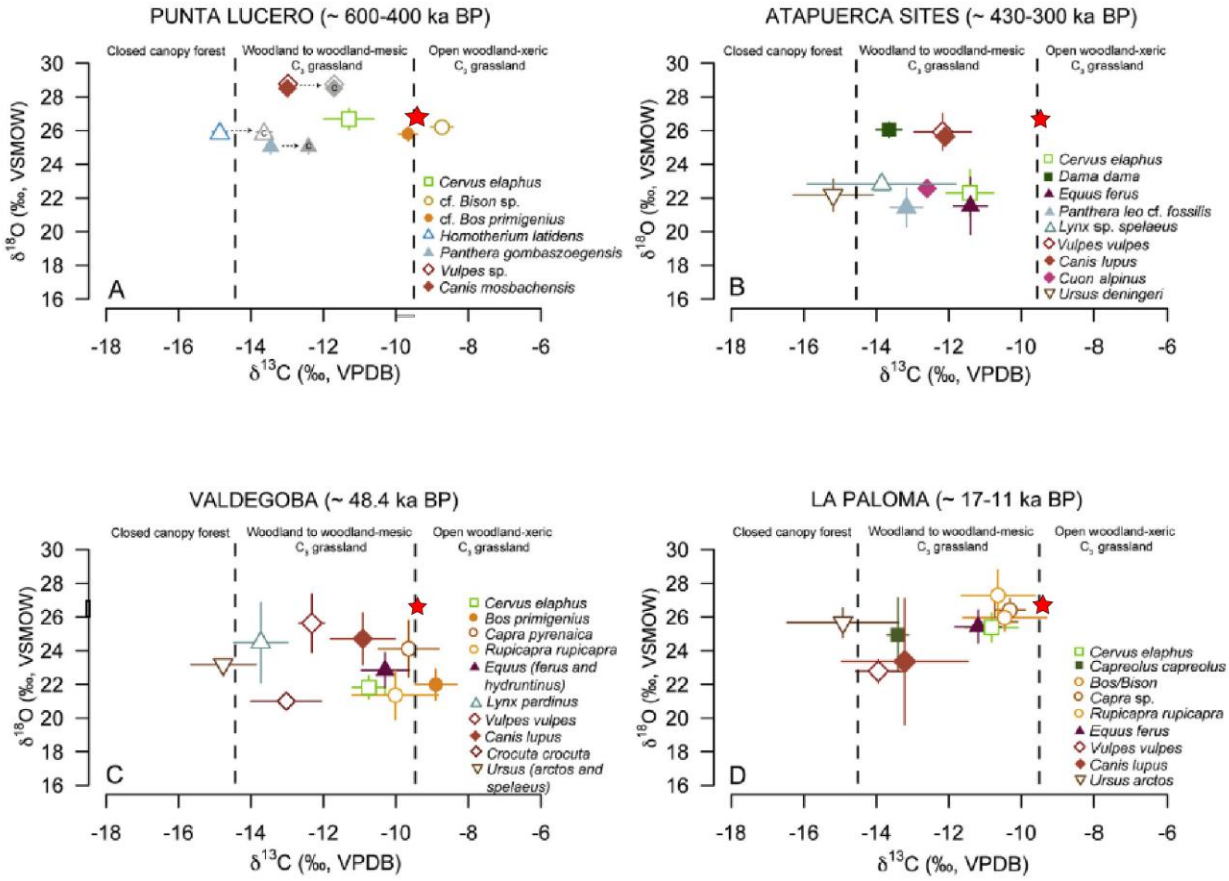


Figure 4.9 — Mean ± 1 standard deviation of $\delta^{13}C$ (‰, VPDB) and $\delta^{18}O$ (‰, VSMOW) values of mammalian tooth enamel from A) Punta Lucero, B) Atapuerca sites, C) Valdegoba, and D) La Paloma compared with the values of the pantherine from algar da Manga Larga (red star). Image modified from Domingo et al. (2017).

The conversion from $\delta^{18}O_{VSMOW}$ to $\delta^{18}Op$ provided a value of $\delta^{18}Op$ of 17.48‰ for the pantherine of Manga Larga, because other equations are calculated for the values on phosphate not, carbonate. The next step was the conversion from $\delta^{18}Op$ to $\delta^{18}Odw$ which provides a value of -6,55‰. The application of the final equation for calculating the temperature provides a MAT (ºC) value of between 12.53 °C to 12.68 °C, with an average of 12.6 ºC for Planalto of Santo António during the time where this specimen of *Panthera uncia lusitana* was alive.

4.4 Discussion

4.4.1 Endocast morphology

The greater constriction between the anterior and posterior parts of the cerebrum in *Panthera uncia lusitana* may indicate differences in brain organization, possibly reflecting adaptations in cognitive or sensory processing. The slightly more robust morphology of the brain might also reflect the even more robust mandibular morphology of *Panthera uncia lusitana* (Jiangzuo et al., 2025).

The differential location of the foramen magnum in a more ventral position and the torsion of the telencephalon compared with *Panthera pardus* reflect a more upright position of the head of *Panthera uncia lusitana* (maybe an adaptation to open habitat seen in cheetahs too) as well as an overall shorter braincase, reflecting the external morphology of the cranium typical of *Panthera uncia* when compared with *Panthera pardus* (Jiangzuo et al., 2025).

The smaller brain size of *P. uncia lusitana* relative to other large pantherines (*P. leo*, *P. onca* and *P. tigris*) is not surprising given its much smaller body size. The constriction between the anterior and posterior cerebrum in *P. tigris* is similar to that of *P. uncia lusitana*, which might reflect that *P. tigris* is the most closely related of the big pantherines to *P. uncia* and therefore would have a phylogenetic meaning and not an ecological one (Kitchener et al., 2016).

Acinonyx jubatus presents a greater torsion of the telencephalon and a round cerebrum, which might reflect even shorter skull of the cheetah, as well as its reliance of visual information (extremely small olfactory bulb, plus larger frontal lobe for processing visual stimuli) (Sims, 2012).

Puma concolor also presents similar morphology, with a smaller olfactory bulb and more pronounced tapering of the anterior cerebrum in ventral view, just not as extreme as with the cheetah, being a more generalist predator not as specialized in open habitats (Sims, 2012).

All these observations about the endocast will be better quantified in future analysis, with the usage of proven methodologies (Sakai et al., 2016). Other parts of the internal anatomy of the skull MG1355.0001 will also help to understand its affinities, like is the case of the frontal sinuses (Frosali et al., 2023). In addition, the digitalization of the skull and mandible of *Panthera uncia lusitana* for the extraction of the cranial cavities has also produced a reliable 3D model of the external anatomy of the skull, which (with some digital restoration) could be used for 3D geometric morphometries studies (Chatar et al., 2024).

Finally, as Jiangzuo et al. (2025) showed, the distal limb elements of *Panthera uncia* were some of the most differential among the pantherines, so the preserved metapodials of the Manga Larga pantherine (especially the complete one) could also be interesting objectives for traditional and geometric analyses by comparing them with those of living pantherines in future analysis

4.4.2 Isotopic analyses

The results of the U-Th dating were inconclusive, which is not surprising considering that the bones of MG1355.0001-9 were almost certainly transported by water (Cardoso & Regala, 2006). Additionally, the bones are open systems, meaning U and Th can be lost or gained from the environment (Hoffmann et al., 2013; Placzek et al., 2006). As a result, the precise chronology of the remains of Algar da Manga Larga remains uncertain for the time being.

The absence of N in the sample used for the analyses also means that no notable organic matter is left on the remains, so no ^{14}C dating, N isotopes, ancient DNA or paleoproteomic analyses could be performed on the samples. Nevertheless, organic matter might be hidden in other parts of the skull, and another attempt is possible in the future with more elaborated sampling techniques (Sirak et al., 2017). Also, after testing if the bioapatite of the bone has been subject to strong diagenetic alteration by the usage of Fourier transformed infrared spectroscopy (FTIR) (Larkin, 2017) it might be possible to perform a radiocarbon dating directly into the bioapatite, even if there is not enough organic matter on it (Cherkinsky, 2009; Zazzo & Saliège, 2011).

The isotopic analyses of the Carbon and Oxygen provided values comparable to those of other Iberian sites, which help in understanding the paleoecology of the *Panthera uncia lusitana*. When compared to the results presented by Carvalho et al. (2022), the pantherine from Algar da Manga Larga is isotopically closer to the *Capra pyrenaica* of the layers JJ and KK from Lapa do Picareiro (Figure 4.8). This is not surprising as Algar da Manga Larga is just 17 km to the west of Lapa do Picareiro, and considering the uncertainty surrounding the age of the felid, it may have been contemporaneous with them and possibly preying on the same population of Iberian ibex. Compared to the larger sample of Iberian sites presented by Domingo et al. (2017), it is apparent that the ecology of the Algar da Manga Larga pantherine was characterized by an extremely open and dry environment. This is not unexpected, considering that even today the Planalto of Santo António lacks surface running water, with most water being drained by the karstic system to which Algar da Manga Larga belongs. Its isotopic values were also similar to those of the *Bison* and *Bos primigenius* from Punta Lucero in the Middle

Pleistocene (Figure 4.9). Among Late Pleistocene sites, it shows closer isotopic values to the mountain ungulates (*Capra pyrenaica* and *Rupicapra rupicapra*) from La Paloma (~15 ka) and Valdegoba (~48 ka), suggesting that its ecology was likely similar to that of these mountain ungulates, although with a different trophic level (Figure 4.9).

Finally, thanks to the oxygen isotopes, it is possible to reconstruct the Mean Annual Temperature (MAT) that *Panthera uncia lusitana* experimented during its life, which is estimated to be 12.6 ºC trough an equation from rodents, but that was nevertheless developed from mammals of the Pleistocene of Iberian Peninsula, although caution is needed to interpret this being them animals with completely different metabolism to big carnivores. Today, the average temperature of Porto de Mós, located 8 km away from the Algar da Manga Larga, is 14.5 ºC (Instituto Português do Mar e da Atmosfera, 2023). For comparison, the MAT of Cova dels Xaragalls, the site where the equation used was calculated, was 12.12 ºC between 55 and 45 ka (Fernández-García et al., 2019), with a current MAT of 13.8 ºC for the nearest village. Using measurements from rabbit bones, Davis (2019) calculated that the average MAT of Portugal during the Last Glacial Maximum (LGM) would have been of around 7ºC lower than today, approximately 9 ºC. Considering the isotopic similarity to the Picareiro Iberian ibex, and the range of temperatures in which it lived (around 2ºC lower than today), *Panthera uncia lusitana* might have lived during the MIS 3, although without absolute dating, this remains a hypothesis.

Another paleoecological implication for *Panthera uncia lusitana* arises when comparing the reconstructed MAT of 12.6 ºC with the modern MAT across the current distribution of *Panthera uncia* (IUCN Red List, 2025). The modern snow leopard inhabits significantly colder environments, with a MAT of –3.43 ± 4.96 ºC (data from https://www.worldclim.org/) (Figure 4.10). This stark contrast suggests that *P. uncia lusitana* occupied a much milder climate than its extant relatives, which has important implications for understanding its ecological flexibility and potential niche during the Late Pleistocene.

Nevertheless it is important to note that the snow leopard likely experiment higher MAT's than those suggested just by their range, by avoiding the greatest peaks of the High Himalayas (Liu et al., 2019).

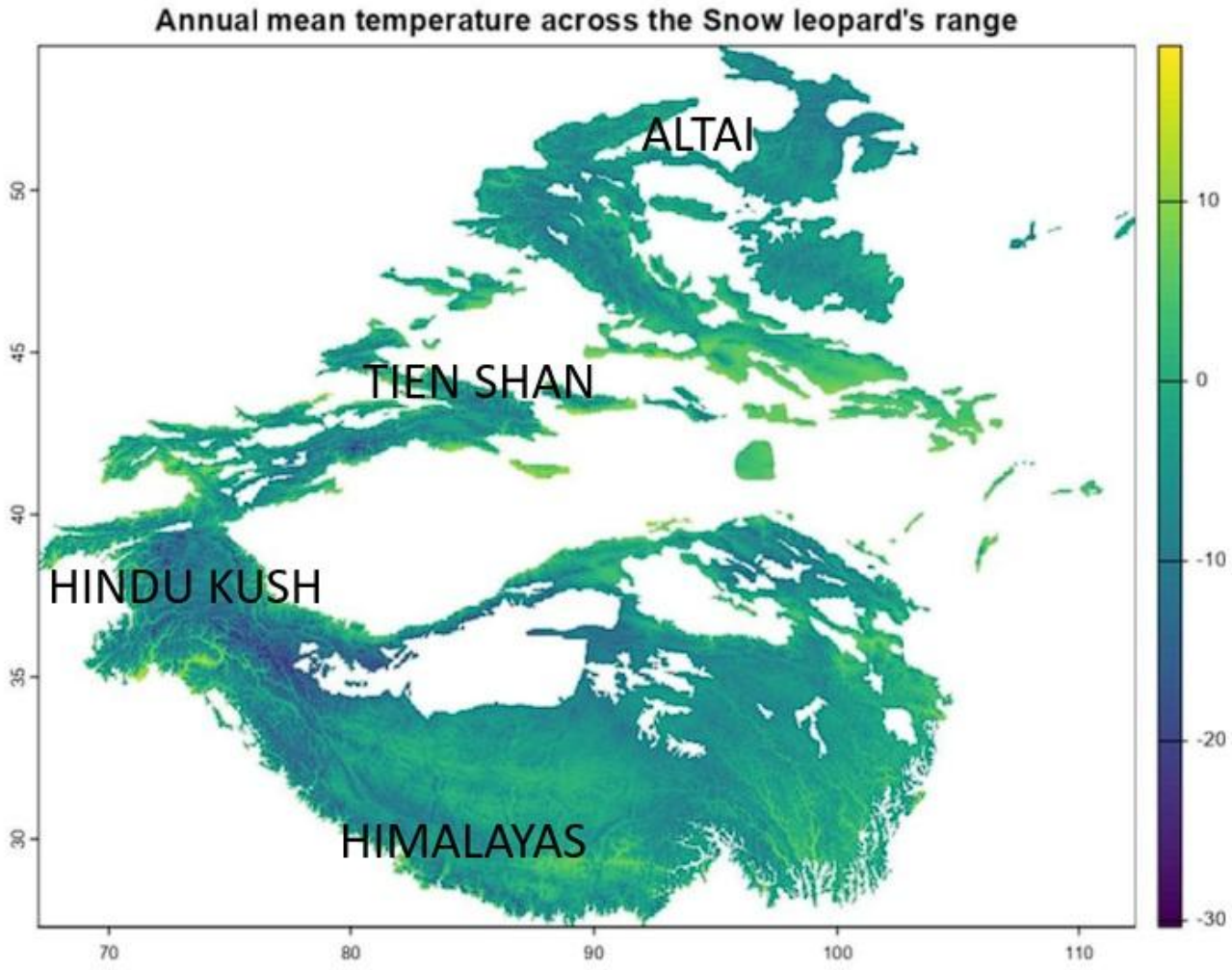


Figure 4.10 — Mean annual temperature (MAT) in ºC across snow leopard´s range. Data extracted from IUCN and worldclim.org .

4.5 Conclusions

The 3D digital analysis of the endocast of *Panthera uncia lusitana* (MG1355.0001) yields a substantial amount of significant morphological information. The endocast exhibits a greater similarity in size and morphology to the modern *Panthera uncia* (snow leopard), but with certain differences, namely, a greater constriction between the anterior and posterior parts of the cerebrum and a more robust overall morphology. In comparison to a modern African leopard (*Panthera pardus*), *P. uncia lusitana* exhibits a dorso-ventral torsion of the telencephalon and a foramen magnum in a more ventral position. The endocast is noticeably smaller than those of *P. tigris*, *P. leo*, and *P. onca*, but shares some similarities with *P. tigris*. *Acinonyx jubatus*

(cheetah) exhibits an even greater degree of telencephalon torsion and a more rounded cerebrum, while *Puma concolor* displays a similar morphology but with a smaller olfactory bulb and a more tapered anterior cerebrum.

Several biogeochemical techniques were also employed to conduct a more in-depth analysis of the remains. The U-Th dating results were inconclusive, due to possible water transport of the remains and the open-system behavior of the bones. Additionally, the absence of detectable organic matter excluded the possibility of applying radiocarbon dating (^{14}C), Nitrogen isotopic analysis, or ancient DNA/paleoproteomic investigations. Evidence from carbon and oxygen isotopic analysis indicates that *P. uncia lusitana* lived in an open, dry environment, and had a similar habitat to mountain ungulates like *Capra pyrenaica* from Lapa do Picareiro. The estimated Mean Annual Temperature during its lifetime was estimated to be 12.6 °C, suggesting it might have also lived during the MIS 3 period. *P. uncia lusitana* likely had a higher tolerance for warmer temperatures in comparison to the modern snow leopard, which inhabits much colder regions today.

Further research of the endocast morphology using quantitative methodologies is needed, as well as additional studies on the frontal sinuses and metapodials that could provide more insights into the paleobiology of *P. uncia lusitana*. Finally, an additional attempt to extract organic matter from the remains employing more sophisticated technology, has the potential to open numerous venues of investigation with the usage of molecular paleontology techniques like aDNA. Also, independently if organic matter is hidden in other areas of the specimen, paleoproteomic analyses could be tried on the enamel, and (after checking how much has the bone been altered by the environment through Fourier transformed infrared spectroscopy) there might be a possibility to perform radiocarbon dating on the bioapatite, even in the absence of said organic matter.

5

PLEISTOCENE FOSSIL URSIDAE FROM PORTUGAL: MORPHOMETRY AND PALEOBIOLOGICAL INFERENCES

Part of this chapter was presented as abstracts at the XXXVIII SEP meeting (Society of Spanish Paleontology) and XX EAVP Meeting held in Sabadell, both in 2023, as well as at the 5th Paleontological Virtual Congress and the XXIII EJIP (Encuentro de Jóvenes Investigadores en Paleontología) at Buñol, Spain both in 2025.

5.1 Introduction

5.1.1 Evolutionary history and adaptability of the brown bear (*Ursus arctos*)

The brown bear (*Ursus arctos* Linnaeus, 1758) belongs to the family Ursidae (Carnivora, Mammalia), a clade of caniform Carnivorans related with seals, mustelids and canids (Wesley-Hunt & Flynn, 2005). The family lacks formal definition but according to the phylogenies generated by Abella et al., (2012) and Jiangzuo & Flynn, (2020); Ursidae can be defined as the clade including "*Ursus arctos*, *Ailuropoda melanoleuca*, its common ancestor, and all its descendants". Ursidae as defined herein would not appear until the Burdigalian, about 20 million years ago (Ma) (Jiangzuo & Flynn, 2020). They can be diagnosed by three characters in the m1 (bunodont paraconid, protoconid equal or subequal in height compared to the paraconid, hypoconid as part of the lingual cristid in occlusal view) and one in the P4; a large protocone similar in size to the paracone and metastyle in occlusal view (Abella et al., 2012). Today they are represented by eight extant species widespread across the Americas and Eurasia, although as with many mammal groups, there were several more species in the Pleistocene that are now extinct; including the brown bear´s second closest relative after the polar bear, the extinct cave bear (*Ursus spelaeus*) (Krause et al., 2008). Molecular estimates suggest that the two taxa

diverged around 1.5 Ma; although there was some intermingling between the arctoid and speleoid lineages during the second half of the Middle Pleistocene, based on nuclear genomes (Barlow et al., 2018, 2021). *Ursus arctos* appears to have originated in Asia 0.62 Ma, with the oldest remains coming from the Zhoukoudian Cave in China (Kurtén, 1968), where it lived sympatrically with other ursid species such as *Ursus deningeri* (Jiangzuo et al., 2018). This hypothesis is also supported by a revision of ancient DNA studies (García-Vázquez, 2015). The oldest unequivocal remains of *Ursus arctos* in Europe are about 0.5 million years old and they appear at a similar time at Caune de l'Arago (French Pyrenees) and Fontana Ranuccio (central Italy) (Caloi & Palombo, 1997; Moigne et al., 2006). From then on, the brown bear became a relatively common component of Pleistocene European faunas (mostly during the Late Pleistocene), surviving the extinction of its relative the *Ursus spelaeus* (Grandal-d'Anglade et al., 2006; Baca et al., 2016).

The brown bear's adaptability to smaller caves for hibernation, even not needing them for wintering (Penteriani & Melletti, 2020), compared to the cave bear may have facilitated its extensive distribution and survival in the post-Pleistocene era. This adaptability is one of the possible factors explaining the ubiquity of the taxon (Fosse et al., 2004). It is also possible that other factors contributed to this phenomenon. These include the less recurrent use of the same sites by brown bears over extremely long periods of time, unlike cave bears (Fortes et al., 2016), and their (on average) more flexible diet which included both plant and animal items depending of the habitat and season (Fernández-Mosquera et al., 2001; Bocherens et al., 2011; Swenson et al., 2023). It is important to note, however, that recent microwear analysis indicate that the cave bear may have exhibited a dietary pattern similar to that of the brown bear for brief time periods (Ramírez-Pedraza et al., 2019). It seems probable that they would have consumed even greater quantities of protein than modern brown bears during periods of hyperphagia preceding hibernation (Duñó-Iglesias et al., 2024). The brown bear has a complex history of recolonizations and migrations after the Last Glacial Maximum (LGM) across Western Europe. Some mitochondrial lineages have been entirely removed from the gene pool (García-Vázquez et al., 2019), while in other areas their mitochondrial lineages have remained stable for thousands of years (Boulygina et al., 2022).

5.1.2 The evolution and distribution of *Ursus arctos* in the Iberian Peninsula

The first occurrence of *Ursus arctos* on the Iberian Peninsula is not totally clear. Nevertheless, multiple instances are nearly synchronous and they date from the final phase of the Middle Pleistocene, between 250 and 200 ka. These include the sites of Cova Negra, Valencia (Pérez-Ripoll, 1977; Fumanal & Villaverde, 2009; Richard et al., 2019); Molí de Mató, Alicante (Cuenca-Paya et al., 1986; Sarrion et al., 1987) and Mollet, Girona (Maroto et al., 1987, 2012, 2018). However, the most abundant (and likely the oldest) collection of Middle Pleistocene brown bears comes from Postes Cave (Badajoz), which has yielded 77 skeletal elements, including a mandible that is perfectly preserved. This mandible provides insight into the differences between Middle and Late Pleistocene brown bears, particularly in the height of the vertical mandibular ramus and the general length and size of the mandible (Villalba de Alvarado et al., 2022). It is also relevant to mention the occurrence of *Ursus arctos* at "Galeria Pesada" in the Almonda Karstic system (Torres Novas, Portugal), which exhibits a comparable chronology to the aforementioned examples. However, there is a paucity of information regarding this occurrence, aside from a mention in a faunal list (Trinkaus et al., 2003).

During the Late Pleistocene the brown bear became more common, although fewer remains are known in comparison with the hundreds of specimens of cave bears from several localities, such as Ekain (Torres Pérez-Hidalgo, 1984; García-Vázquez et al., 2015). The potential for competition between the two bear species is addressed by García-Vázquez et al. (2015) in the context of the observed discrepancy in the distribution of their respective remains. Specifically, only 16% of the localities where *Ursus arctos* is present also yield remains of *Ursus spelaeus*. Another aspect in which both species differ in the Iberian Peninsula is that no remains of *U. spelaeus* are known South of the Cave of Reguerillo (Madrid) (Torres Pérez-Hidalgo, 1984), except for an isolated metapodial fragment from Cueva del Ángel (Córdoba) (Ruiz et al., 2012). Meanwhile the majority of the oldest occurrences of *Ursus arctos* are located in the Southern half of the Iberian Peninsula (García-Vázquez et al., 2015; Villalba de Alvarado et al., 2022). The combination of this evidence, along with the genetic data indicating the North African clade of brown bears as the earlies branching known to date, might mean that brown bears might have migrated to the Iberian Peninsula from Africa (García-Vázquez, 2015).

In any case, several mitochondrial lineages of brown bears existed during the Late Pleistocene in the Iberian Peninsula, with some of them being endemic to the Peninsula. These Pleistocene lineages became extinct at the same time as the LGM, and by the advent of the

Holocene, only modern mitochondrial lineages remained. This evidence suggests that the Iberian Peninsula was not a glacial *refugium* for *U. arctos*, and that bears expanded from a cryptic refuge, potentially from the Atlantic coast of France (García-Vázquez et al., 2019).

A total of 16 sites in Portugal have yielded evidence of *Ursus arctos* (Figure 5.1). In addition to the previously mentioned Middle Pleistocene occurrence at Galeria Pesada (Trinkaus et al., 2003), there are some fragmentary and poorly preserved older remains, dating to nearly 400 ka, from a gallery of the same karstic system, the Aroeira Cave. These remains were originally ascribed to *Ursus* sp. (Daura et al., 2018), but they have recently been reclassified as *Ursus deningeri*. This is the first occurrence of an speleoid bear in the Pleistocene of Portugal (Sanz et al., 2024). The majority of the other sites in Portugal where *Ursus arctos* has been documented are Late Pleistocene in age. However, direct radiometric of *Ursus* fossils from the area has yet to be conducted (García-Vázquez et al., 2015). The Furninha collection is worthy of particular attention, as it comprises hundreds of cranial and postcranial remains of brown bears, the majority of which originate from the Pleistocene, with a very small number dating to the Holocene and being found among the Neolithic necropolis materials (Brugal et al., 2012). It is estimated that this collection contains approximately 700 remains, which makes it the most abundant collection of this species in a single location on the Iberian Peninsula. No other locations in Portugal have yielded such extensive quantities of remains.

It is also noteworthy to mention that the only bear tracks in the ichnological record that have been preserved in Pleistocene eolianites (open-air sandy deposits accumulated by wind) are located in Portugal. Specifically, they can be found in Praia do Cavalo, Odemira, dating from MIS 3-2 or about 30 ka BP (Neto de Carvalho & Belo, 2022). They are not the only recorded tracks attributed to bears in Portugal, as more than a hundred claw marks and tracks were recorded alongside the walls of the Algar do Vale da Pena, a locality were also skeletal remains of brown bear have been located (Estraviz López & Mateus, 2019).

The majority of direct radiometric data from Iberian brown bear remains originate from the Greenlandian stage of the Holocene (approximately spanning the first third of the period between ~12 and ~8 ka BP). However, none of these originate from Portugal (García-Vázquez et al., 2015). The record of prehistoric bears in Portugal from the second half of the Holocene (Meghalayan stage, last 4 ka BP) is limited and comprises isolated remains, including a single m3 from the Chalcolithic settlement of Leceia, Lisbon district (Pires et al., 2002) and a single fourth metacarpal from the also Chalcolithic settlement of Vila Nova de São Pedro, Santarem District (Detry et al., 2020). A scapula has been unearthed at the site of Monte Molião, in the Algarve region, which is dated to the Roman Imperial period (Detry & Arruda, 2013).

A substantial corpus of evidence from the Middle Ages attests to the presence of the brown bear within a considerable portion of Portugal until the 16th century. This species was particularly prevalent in areas north of the Tagus River, although it is probable that they extended their range at least as far south as the Guadiana River (Baeta Neves, 1967). Additionally, physical remnants from this period have been unearthed, including a left ulna that was processed for meat consumption and unearthed at the castle of Leiria (Cardoso, 2001). The gradual contraction of the bear range towards the northeast (Figure 5.1), was caused by human pressure, resulting in the species becoming locally extinct in Portugal during the second half of the 19th century, following the fate of the Spanish population at the other side of the border in Galicia (Nores & Naves, 1993).

5.1.3 Characterization of the Portuguese Pleistocene localities with presence of *Ursus arctos* considered on this work

As previously stated *Ursus arctos* is present in 16 Pleistocene Portuguese localities, in addition to four from the Holocene (Figure 5.1). The location of these deposits is significantly influenced by lithological factors, with only three localities observed outside the carbonated basement of the Lusitanian Basin. However, these occurrences are also associated with other carbonated sediments, including those from the Algarve Basin (Monte Molião, Lagos) and calcareous sediments from the Hesperic massif of Paleozoic age (Escoural and Lorga de Dine) (Cardoso, 1995a; Ribeiro & Bento dos Santos, 2010). This work will examine the characteristics of six Pleistocene localities (Figure 5.1) from which material has been studied. For further information about the localities in question (Oliveira, Escoural, Caldeirão, Serra de Molianos, Fontainhas, and Furninha) see their characteristics at Chapter 1 of this thesis.

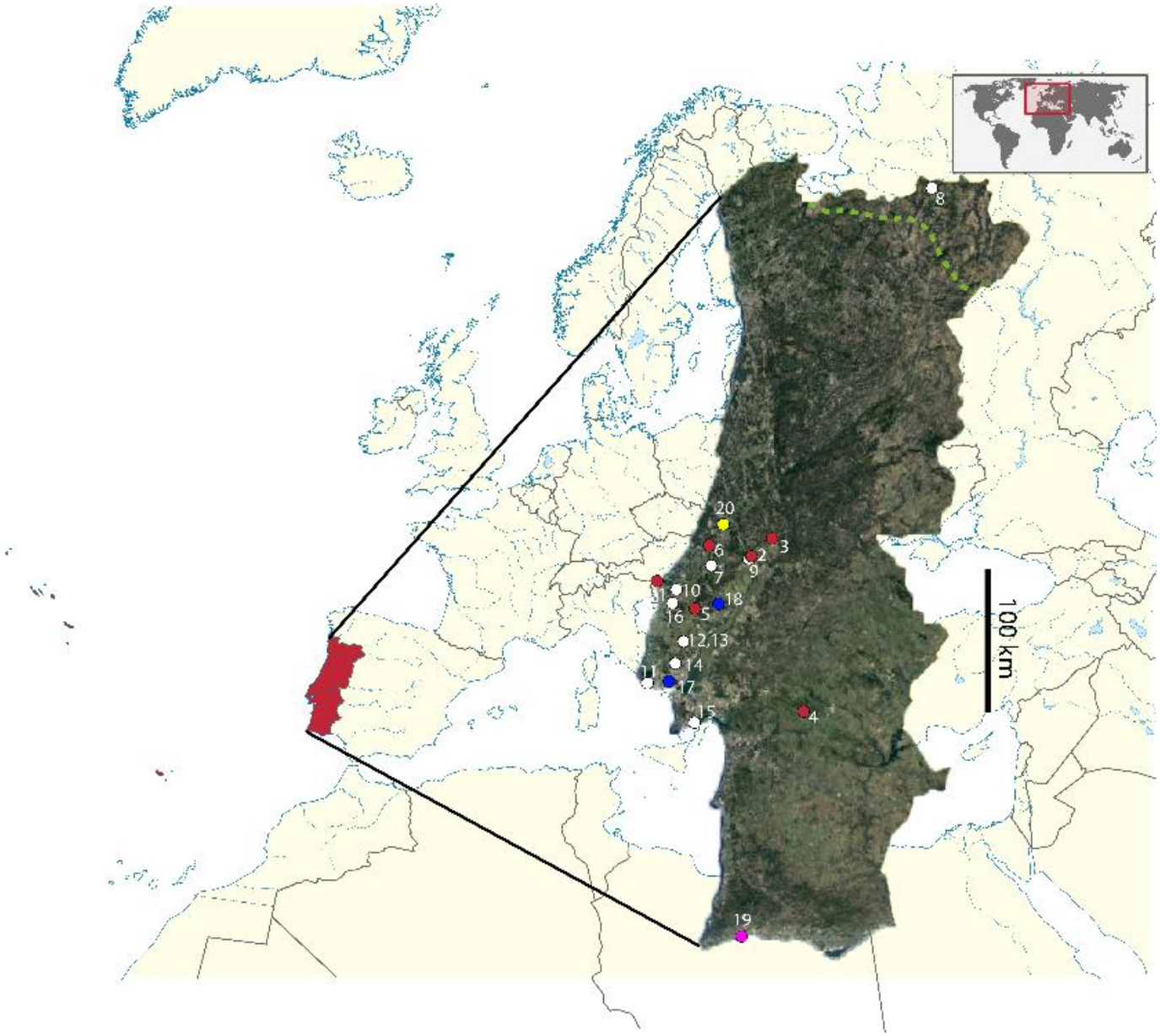


Figure 5.1 — Sites where Ursidae remains have been found in Portugal: Red, Pleistocene sites studied on this work; white, Pleistocene sites not studied on this work; blue, Holocene prehistoric sites; purple, Roman Imperial site; yellow, medieval site. North of green dotted line is the approximate distribution of *Ursus arctos* during the second half of the 19th century. 1, Furninha; 2, Oliveira; 3, Caldeirão; 4, Escoural; 5, Fontainhas; 6, Serra de Molianos; 7, Algar do Vale da Pena; 8, Lorga de Dine; 9, Aroeira; 10, Gruta Nova da Columbeira; 11, Algar de Cascais; 12, Pedreira das Salemas; 13, Gruta das Salemas; 14, Pego do Diabo; 15, Figueira Brava; 16, Pedreira São Bartolomeu dos Galegos; 17, Leceia; 18, Vila Nova de São Pedro; 19, Monte Molião; 20, Castle of Leiria.

5.2 Material and methods

5.2.1 Material

In the course of this study, the 535 remains of at least 35 individual bears were considered. The discrepancies between the number of remains studied and those cited from the bibliography from each locality, are due to two factors: firstly, the consideration of only those elements for which at least one reliable measurement could be taken; and secondly, the inability to locate all the material previously referenced (see the supplementary material in Appendix D and Figure 5.2 for further details).

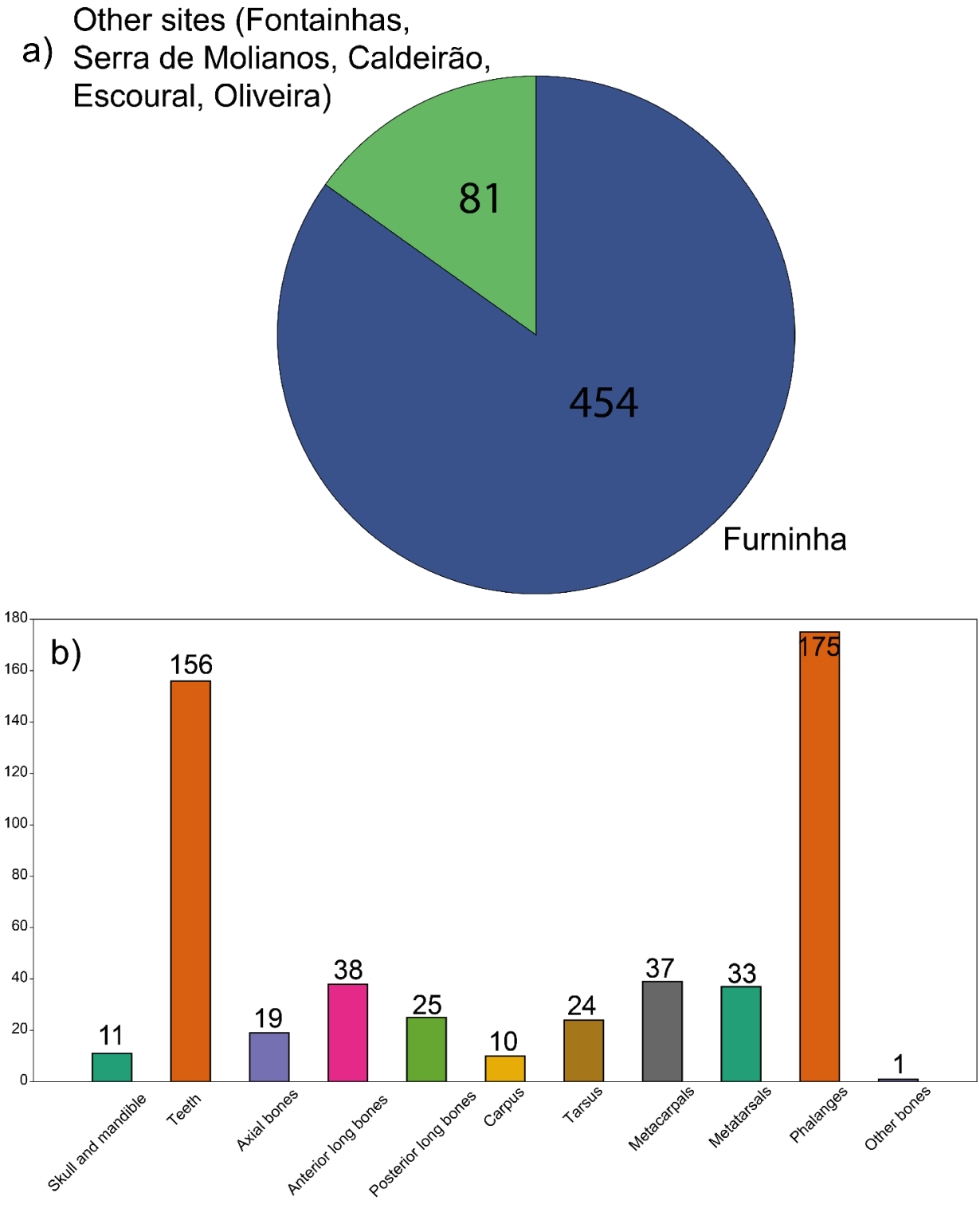


Figure 5.2 — a) Number of *Ursus arctos* remains by site. b) Number of brown bear remains in this work by body part, from all sites considered.

As illustrated in Figure 5.2, the majority of the bear remains examined on this study (454 remains representing 85% of the total sample) originate from Furninha Cave. A total of 63% of the remains from this locality, (or 286 elements), are comprised of phalanges and dental pieces. The remains are distributed across five layers; with the most prolific layer being that at 7-7,5 m of depth, which represents at least 12 individuals in base of the number of m3s. Notwithstanding the considerable quantity of material, the collections exhibit significant cataloguing deficiencies. In some instances, the numbers are provided for entire boxes of material, rather than for each individual bone marked with a catalog number on the bone itself, thus maintaining its unequivocal identity. Further information can be found in the supplementary material at Appendix D.

The second most abundant sample under consideration is that of Fontainhas Cave, which comprises 58 remains of at least two individuals, as determined by the number of canines and m3s. The most common remains are teeth (23), although the majority of the material originates from a single, exceptionally large, and aged individual, as evidenced by the wear on the teeth and the measurements of long bones.

The sample from Serra de Molianos yielded 12 measurable remains, attributable to at least two distinct individuals, as evidenced by the presence of two left radii.

A total of six bear remains were measured from Caldeirão Cave, originating from at least three distinct animals, with each specimen originating from a different layer.

From Escoural, three measurable remains were identified, which appear to originate from at least two different individuals. This is based on the observation of two distinct left m2s.

Finally, this study incorporates one tibia and one third phalanx from Oliveira Cave, which originate from two distinct individuals found on disparate stratigraphic layers. However, there are numerous other specimens currently undergoing preparation and analysis.

5.2.2 Methods

5.2.2.1 Morphological description

In order to characterize the sample from each locality a brief description is provided of the general qualitative morphological characters of the pieces, their preservation, and other noteworthy features, including pathologies, taphonomic processes, and the overall appearance. Due to the considerable number of specimens from specific localities, namely Furninha and Fontainhas, it is necessary to prioritize the description of those displaying exceptional characteristics or exhibiting particularly well-preserved qualities.

5.2.2.2 Terminology

We follow mainly the terminology proposed by Torres (1984) and Jiangzuo et al. (2019), although the characters mentioned by Villalba de Alvarado et al. (2024) are also useful and has been utilized. In the context of teeth, the uppercase letter "P" will be used to denote the upper premolars, the lowercase letter "p" will be used to denote the lower premolars; the uppercase letter "M" will be used to denote the upper molars, and the lowercase letter "m" will be used to denote the lower molars

5.2.2.3 Morphometric measurements

The measurements were taken with a digital caliper following the system of measurements for ursids from Tsoukala & Grandal-d´Anglade (2002). This widely used system allows the morphometric comparison of the pieces with a large sample of Iberian and European specimens.

In addition to comparisons between localities, the Portuguese specimens will be metrically compared with brown bears from NW Spain, mainly Holocene specimens from Galicia, but also including Holocene specimens from other areas of NW Spain, such as Asturias (García-Vázquez, 2015). Other older fossil brown bears are also included in the metrical analyses, such as those from the Middle Pleistocene of Iberia from Postes Cave, Extremadura, Spain (Villalba de Alvarado et al., 2022), in order to better frame the Portuguese Pleistocene brown bears geographically and temporally. Modern specimens from western Iberia (García-Vázquez, 2015) and newly measured specimens from Finland deposited in the LARC (Laboratório de Arqueociências) of Lisbon are also added to the comparison. Finally, specimens of cave bears (*Ursus spelaeus*) from Galician caves are added to the comparison. Specifically, those from the caves of Eirós (Grandal-d'Anglade, 1993), Liñares (López-González, 2003), and A Ceza (unpublished own data).

5.2.2.4 Morphometric analises

For each skeletal element, a minimum of one biplot was generated using the PAST software (version 4.16). In the case of skeletal elements for which several measurements were available and multiple specimens were well preserved, principal component analysis (PCA) and

discriminant analysis were conducted, allowing for the drawing of conclusions regarding size differences according to their spatial and temporal provenance.

5.2.2.5 Body mass estimation

The body masses of bears were calculated based on allometric equations, whenever suitable pieces available for analysis. Estimations based on teeth, either on the length of the m1 (Van Valkenburgh, 1990) or on the occlusal surface of the same tooth (Legendre & Roth, 1988), have been demonstrated previously to provide an overestimation of the mass of bears (García-Vázquez, 2015). Nevertheless, they have been calculated for bears of several Portuguese localities and can be seen in the supplementary material, Appendix D. The absence of a complete skull precluded the use of allometric equations based on skull length (Van Valkenburgh, 1990). Of greater interest are the mass estimations based on multiple measurements of long bones (Christiansen, 1999; Viranta, 1994). It is important to clarify that the objective of these equations is to calculate the most probable median mass of the bears with given measurements of long bones, not the minimum of maximum weights for said animals. The mean of the estimated values for each individual element (e.g., individual femur, tibia, humerus or radius) was calculated based on the average of the estimations derived from multiple measurements according to each available method. Some elements yielded only one measurement that was useful for estimation purposes. These were excluded in order to obtain more robust estimations based on multiple measurements for each bone. It should be noted that the equations in question have been known to provide unreliable mass estimations sometimes, with figures in the range of several tons (García-Vázquez, 2015). Therefore, masses over 500 kg and those below 50 kg (juveniles) have been excluded from the present study. Subsequently, for each element for which both estimation methods yielded available data (humerus and femurs), a final average was calculated based on the results of both equations. The aforementioned mass estimations were compared to those obtained by García-Vázquez (2015) following the same methods on Pleistocene and Holocene bears from NW Spain, as well as the real weights of modern bears hunted in the Cantabrian mountains between 1957 and 1965 (Notario, 1964) and in the Pyrenees between 1848 and 1951 (Couturier, 1954), as well as other modern North American an European brown bears.

5.3 Results

5.3.1 Oliveira

As previously stated in the section on materials, two specimens from this site are the focus of the present study, despite the fact that dozens more are currently under study and preparation. The third phalanx, O17-226 (Figure 5.3 b), although well preserved, is entirely encrusted in calcareous crust, which may potentially distort the measurements taken to some extent. This claw is straight and its dorsoventral diameter is relatively small in comparison to the overall length, resulting in a low profile in lateral view.

The left tibia O16-766 (Figure 5.3 d) was recovered from layer 20 and represents the oldest bear remain discovered at Oliveira Cave, with an estimated age range of between 90.1 to 92 ka. It is substantially crushed and encrusted along its length, with the exception of the proximal part. It bears a series taphonomic marks or pits along the medial surface, which may be attributed to carnivore activity, although no clear gnawing marks are evident. Morphologically, the proximal tibia is completely fused, although some porosity persists at few parts of the bone, giving it a texture akin some non-fused bones in some areas.

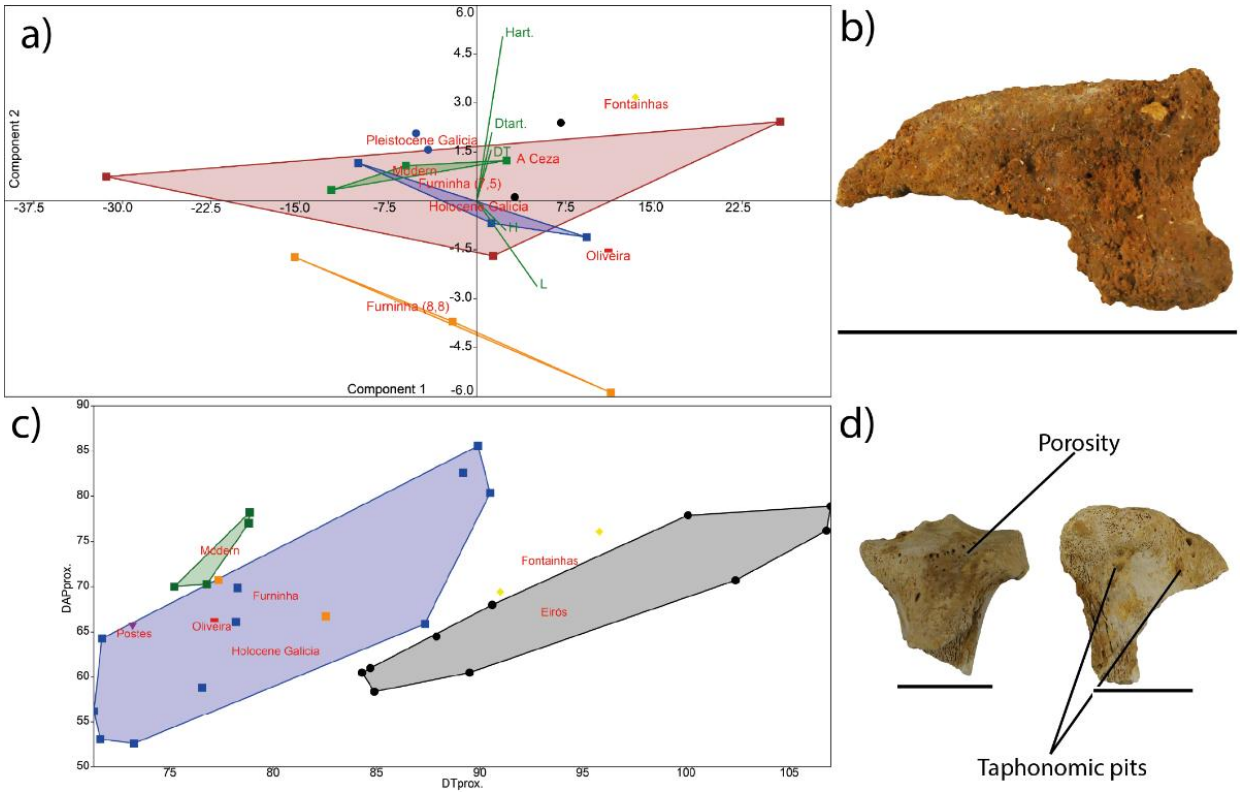


Figure 5.3 — a) Principal Component Analysis based on the measurements of third phalanges of bears, including several Portuguese specimens. b) Third phalanx from Oliveira Cave (O17-226) in lateral view. c) Biplot of antero-posterior and transverse diameters of the proximal tibia of Cave and brown bears, including Portuguese specimens. d) Proximal left tibia of brown bear from Oliveira Cave (O16-766) in anterior (left) and lateral (right) views. All scales are 50 mm.

Metrically, the third phalanx O17-226 is plotted in a PCA at a size that is slightly larger than the largest Holocene phalanges from NW Spain (Figure 5.3 a). Its measurements are larger than those of modern bears and of the majority of Furninha Cave specimens. It is relatively similar in size to the Fontainhas specimen (FO.I-165). It can therefore be concluded that this specimen represents and exceptionally large-sized bear.

The tibia O16-766 is, in contrast, situated within the morphospace of the modern Holocene Galician bears (Figure 5.3 c), being slightly wider mediolaterally than the Middle Pleistocene specimens from Postes Cave. It represents a moderately sized specimen.

5.3.2 Escoural

As previously stated, all specimens from this site are molars. The left lower first molar, Escral121966 (Figure 5.4 a) is well preserved and complete, including the root. It displays slight wear on all the cusps. Morphologically, when compared with other specimens figured by Torres, (1984) it features a labio-lingually enlarged distalmost area, meanwhile the mesial part is or similar size to other teeth, resulting in a slightly more triangular shape. The specimen is both longer and wider than modern specimens and brown bears from NW Spain, whether Pleistocene or Holocene. The dimensions of this specimen are comparable to those of the largest specimens from Furninha and those from Fontainhas and Caldeirão, although it is wider than both of them (Figure 5.4 d).

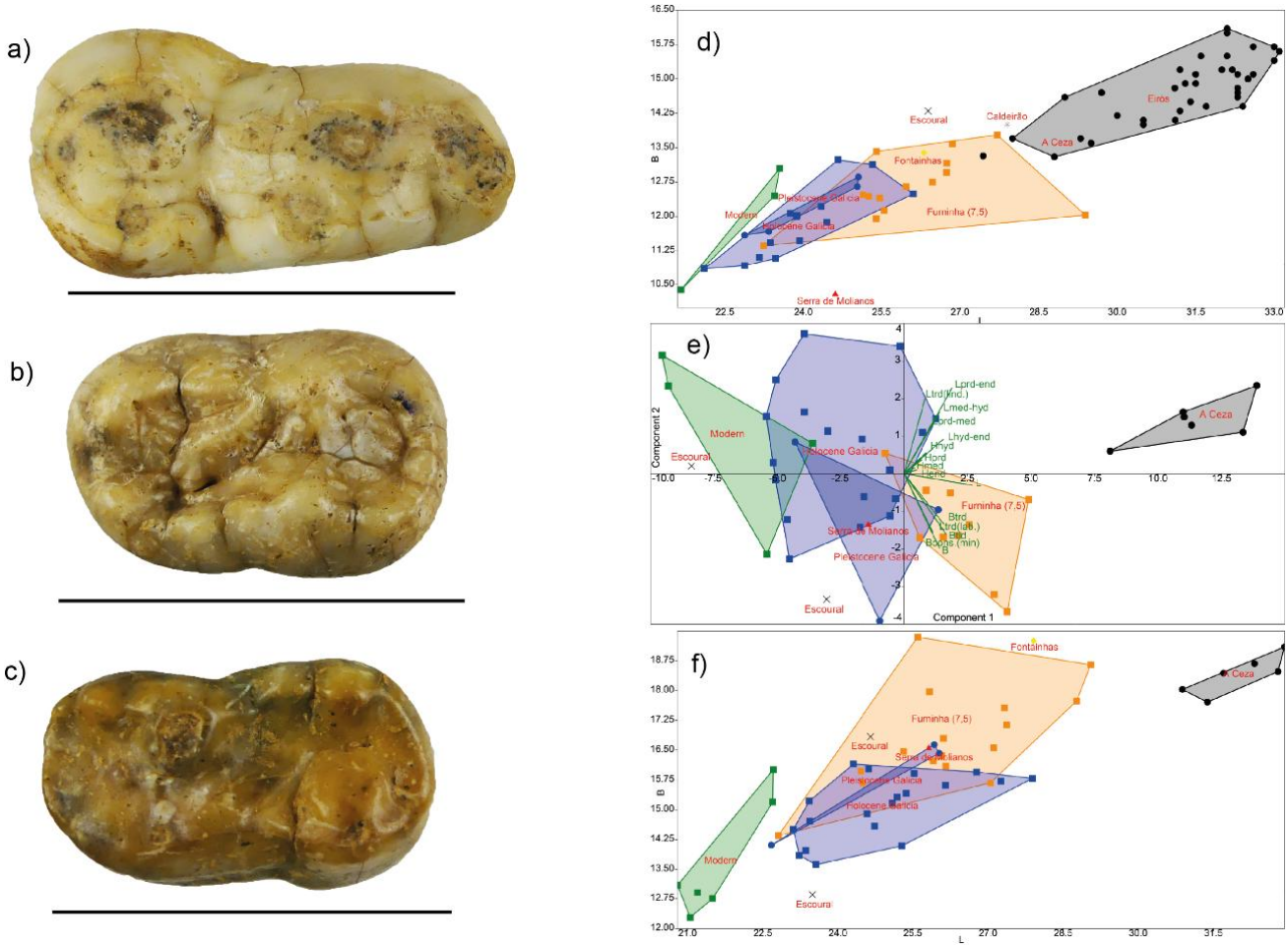


Figure 5.4 — a) Left lower first molar (Escral121966) from Escoural in occlusal view. b) Left m2 (EscGalEntrad1964) from Escoural in occlusal view. c) Right m2 (EscGal2Tal7C1) from Escoural in occlusal view. d) Biplot of length vs breadth of the m1. e) Principal component analysis of measurements of the m2. f) Biplot of length vs breadth of the m2. All scale bars are 25 mm.

The two m2s (Figure 5.4 b-c) exhibit a markedly disparate morphology, yet both conform to the typical 8-shaped molars observed in brown bears, characterized by a straight entproto-conid-entmetaconid. EscGalEntrad1964 is representative of the typical morphology observed in brown bears, characterized by wrinkled enamel and cusps, that are less separated than those observed in cave bears. In contrast EscGal2Tal7C1 exhibits a smooth enamel surface with markedly more separated cusps. Furthermore, both specimens exhibit considerable divergence from one another both the biplot and the PCA (Figure 5.4 e-f). EscGalEntrad1964 is comparable in size to the shortest m2s of Furninha, yet both exhibit a distinctive arrangement of cups appearing outside the variability of that observed in the broader bear sample.

5.3.3 Caldeirão

As previously stated, it was not feasible to quantify and document some of the specimens described and figured by Davis (2002). The three lower teeth (one incisor and two m1s) were too worn to be measured. They belonged to an individual of advanced age, described and figured by Davis, (2002). A M1 (P-11 886) that was not fully formed (lacking the root) was photographed and measured (Figure 5.5 d). Morphologically, it displays a well-isolated paracone and metacone, accompanied by a small sized parastyle and metastyle. On the lingual side, the cingulum is almost non-existent. These are typically *Ursus arctos* morphological features. Metrically, the tooth it is slightly more robust than modern specimens, yet falls within the lower end of the size range of Holocene and Pleistocene Galician bears (Figure 5.6).



Figure 5.5 — a) Three first phalanges from Caldeirão Cave in dorsal view, from left to right: P11 699; O14 sc 358 Jb J3 and P11 776. b) Left first metatarsal (P-11 666) from Caldeirão Cave in dorsal view. c) Second phalanx (N14-Sc341) from Caldeirão Cave in dorsal view. d) M1 (P-11 886) from Caldeirão Cave in occlusal view. All scale bars are 25 mm.

A left first metatarsal (P-11 666) is well preserved and is only missing part of the distal epiphysis (Figure 5.5 b). It falls within the variability of Pleistocene brown bears from Galicia (as is the case for the majority of specimens considered), and is of relatively small size, in both length and diameter (Figure 5.7 a).

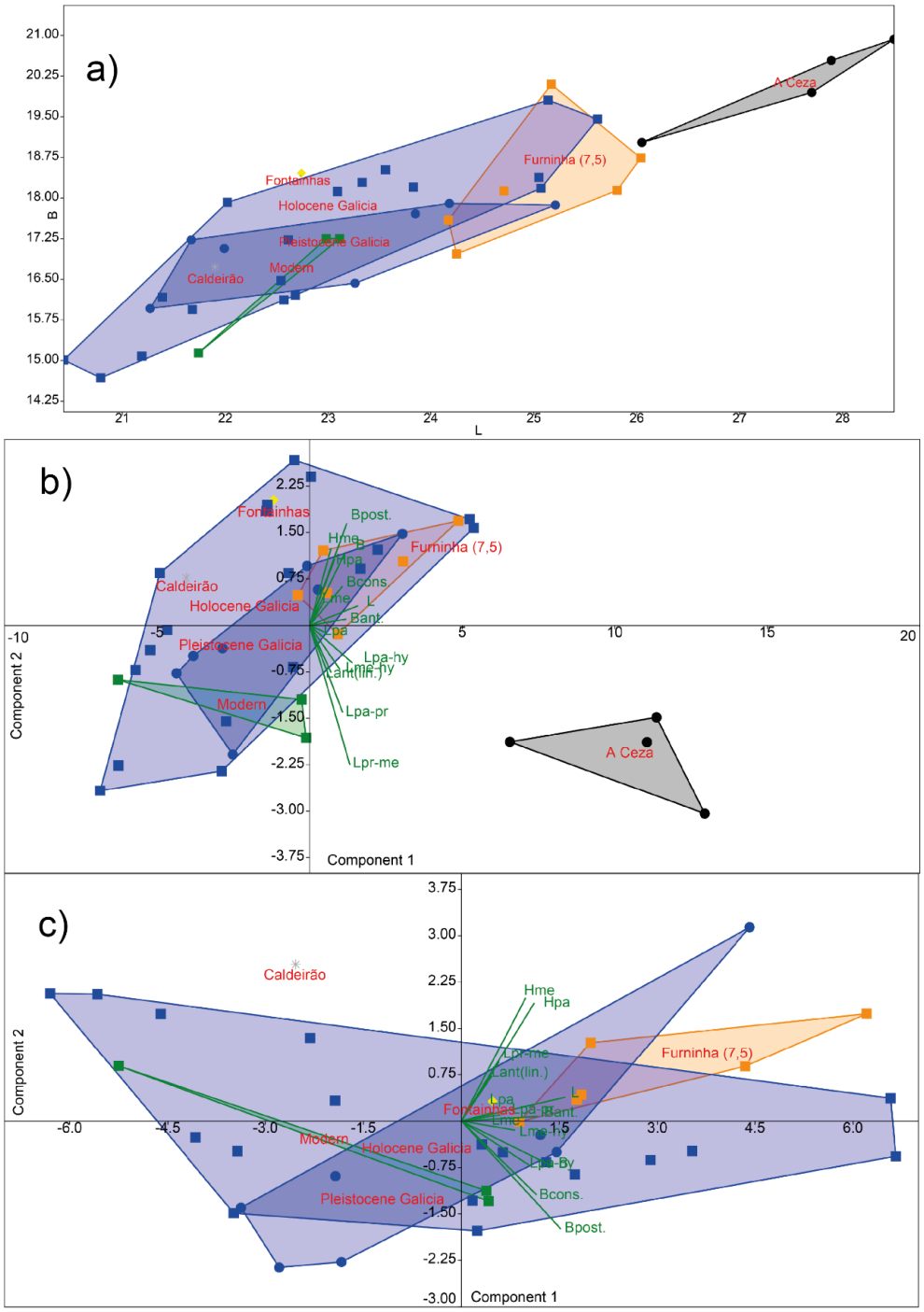


Figure 5.6 — a) Biplot of length vs breadth of the M1 of several Iberian brown and cave bears. b) PCA of the M1 of several Iberian brown and cave bears. c) PCA of the M1 of several Iberian brown bears.

It is also worth noting that one the first phalanges, P11-755, exhibits a pair of bulges along its diaphysis in ventral view, which may represent prominent muscular insertions. This suggests that it may not belong to a bear. The remaining three phalanges (Figure 5.5 a) are, however, of a small size, comparable to the smallest specimens from Furninha (Figure 5.7 b). Similarly, the second phalanx N14-Sc341 (Figure 5.5 c), exhibits a comparable trend, displaying slight robustness while maintaining a size comparable to that of the small-sized phalanges from Postes Cave (Figure 5.7 c).

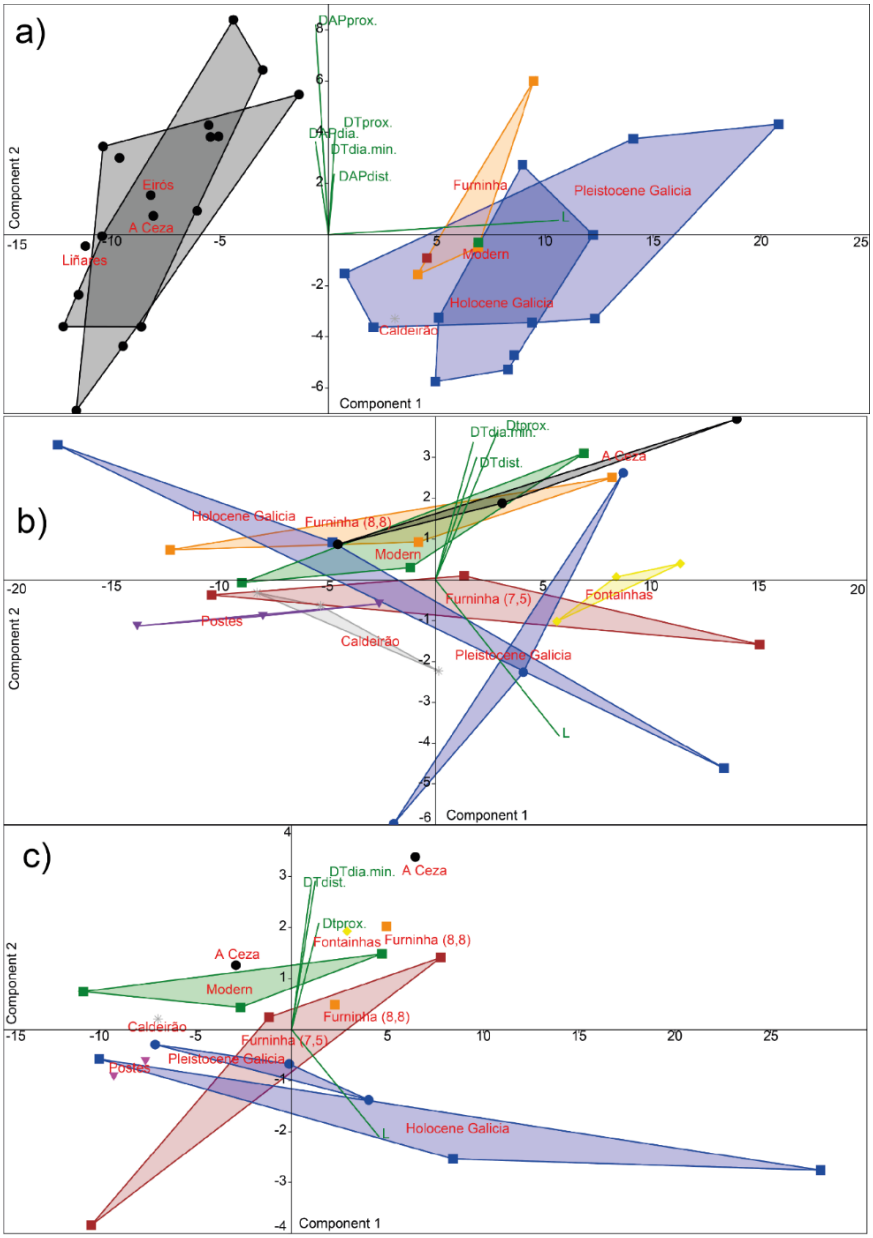


Figure 5.7 — a) PCA of the first metatarsal of several Iberian brown and cave bears modified to include the specimen from Caldeirão. b) PCA of the minimum, average and maximum measurements of first phalanges from diverse Iberian brown and cave bear localities. c) PCA of the minimum, average and maximum measurements of the second phalanges from diverse Iberian brown and cave bear localities.

5.3.4 Serra de Molianos

The sample from Serra de Molianos comprises predominantly teeth and anterior appendicular bones as measurable elements (Figure 5.8). However, several distal metapodials are also preserved (Figure 5.8). All of the elements exhibit slight wear, which may be of a chemical nature, manifesting as small, shallow depressions of varying dimensions and smooth edges on bones. Additionally, the majority of the remains are fragmented, with the most notable instance being the metapodials, whose proximal epiphysis (the most useful one for identification) is broken.

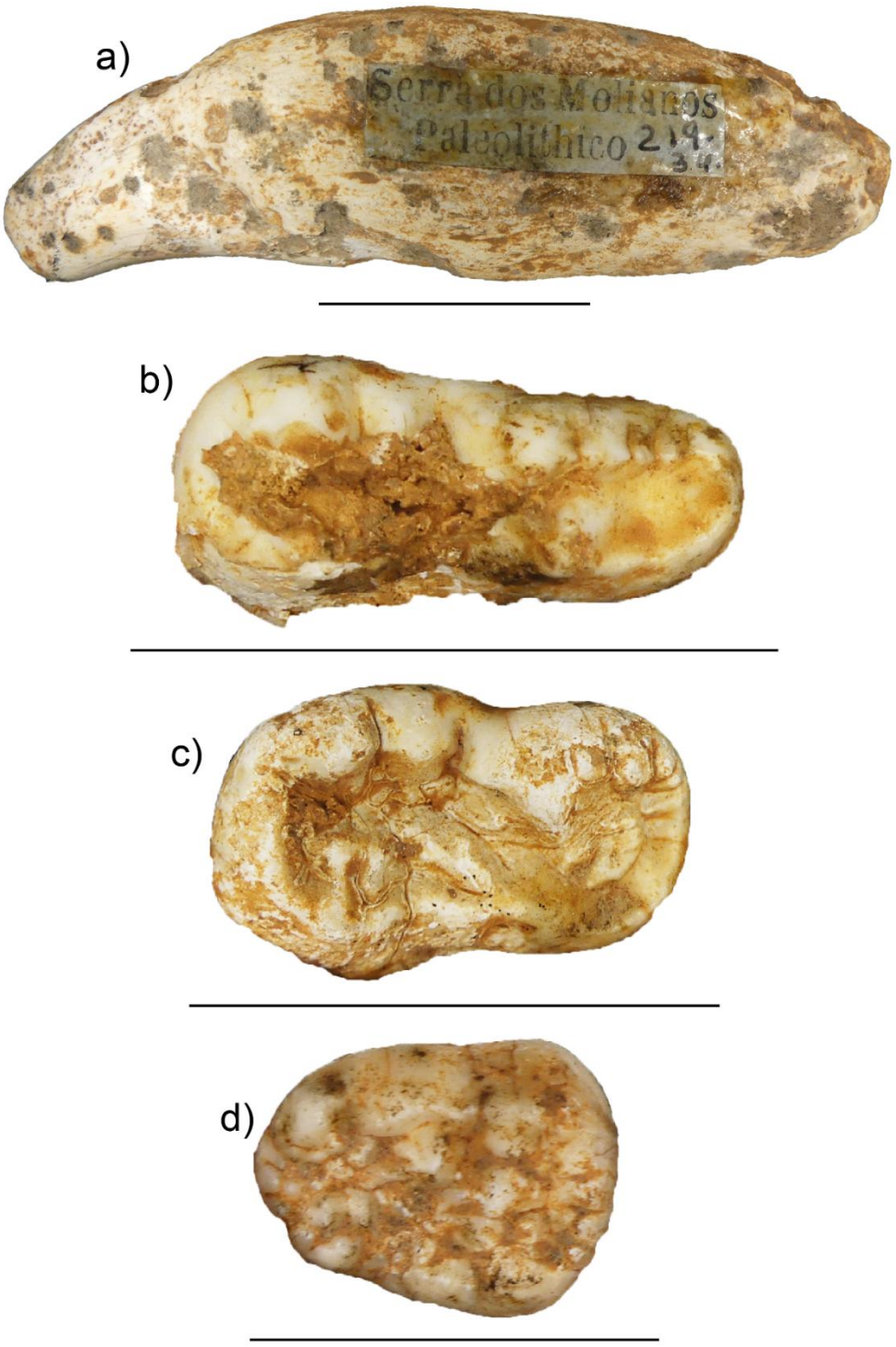


Figure 5.8 — Material from brown bears of Serra de Molianos. a) Canine SM219.34 in lateral view. b) m1 SM219.36 in occlusal view. c) m2 SM219.38 in occlusal view. d) m3 SM219.40 in occlusal view.

The canine SM219.34 (Figure 5.8 a) displays considerable wear on its occlusal surface, with a predominantly rounded appearance in lateral view. Metrically, its length and breadth are within the variability of modern-day samples, as well as Holocene Galician specimens. However, they are significantly larger than those of other Portuguese specimens, including the majority of those from Furninha and Fontainhas (Figure 5.9 a).

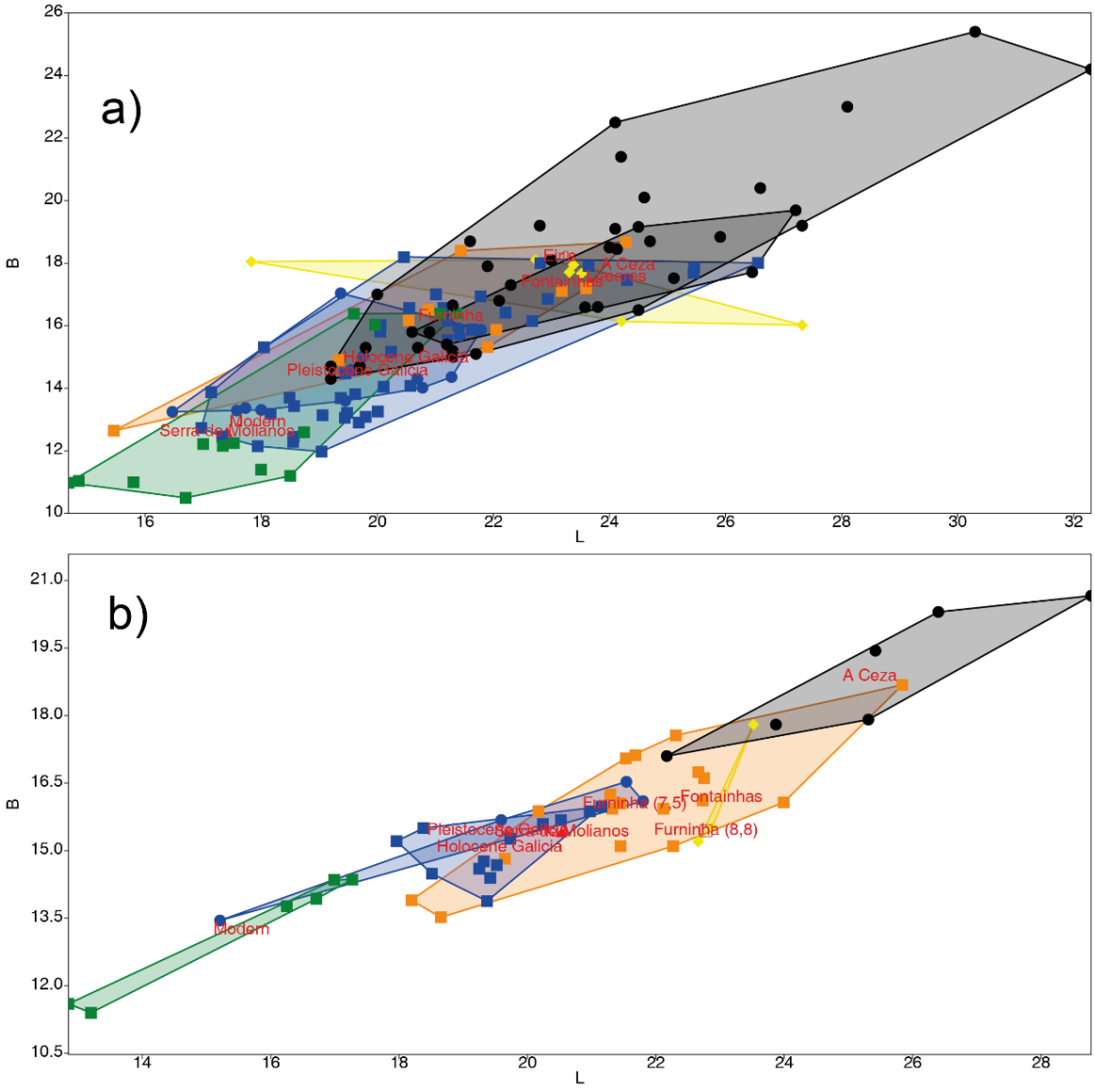


Figure 5.9 — a) Biplot of length vs breadth of the canine of several Iberian brown and cave bears. b) Biplot of length vs breadth of the m3 of several Iberian brown and cave bears.

The m1 SM219.36 (Figure 5.8 b) is still partially obscured by sediment, yet no evidence of wear is apparent. Morphologically, the paracone is notably wide, yet metrically the tooth overall is narrower (~20 mm less) in comparison to other teeth of similar length. It is metrically distinct from other specimens, with the most similar to those from Holocene Galicia (Figure 5.4).

The m2 SM219.38 is a remarkably well-preserved tooth (Figure 5.8 c), exhibiting the typical features of an m2 from a brown bear, including the 8 shape in occlusal view and a double entoconid (Villalba de Alvarado, Crégut-Bonnoure, et al., 2024). Metrically, the length and breadth of the tooth align with the morphospace observed in Pleistocene bears from both the Galicia and Furninha specimens (Figure 5.8). When considered within a PCA, SM219.38 is situated precisely within the range of variability observed in Pleistocene bears from NW Spain (Figure 5.4 e-f).

The m3 SM219.40 (Figure 5.8 d) exhibits the typical quadrangular morphology of these teeth, as well as a comparable number of enamel wrinkles to those observed in the teeth described by Torres (1984) from Cueva de la Corta or Lezetxiki. However, it displays a less "granular" occlusal surface than that seen in the specimens of Fontainhas, like FO.I-35 also illustrated by Torres (1984). Metrically SM219.40, falls within the range of variability observed in specimens from the Pleistocene and Holocene in Galicia, as well as among the smallest of the Furninha specimens (Figure 5.9 b).

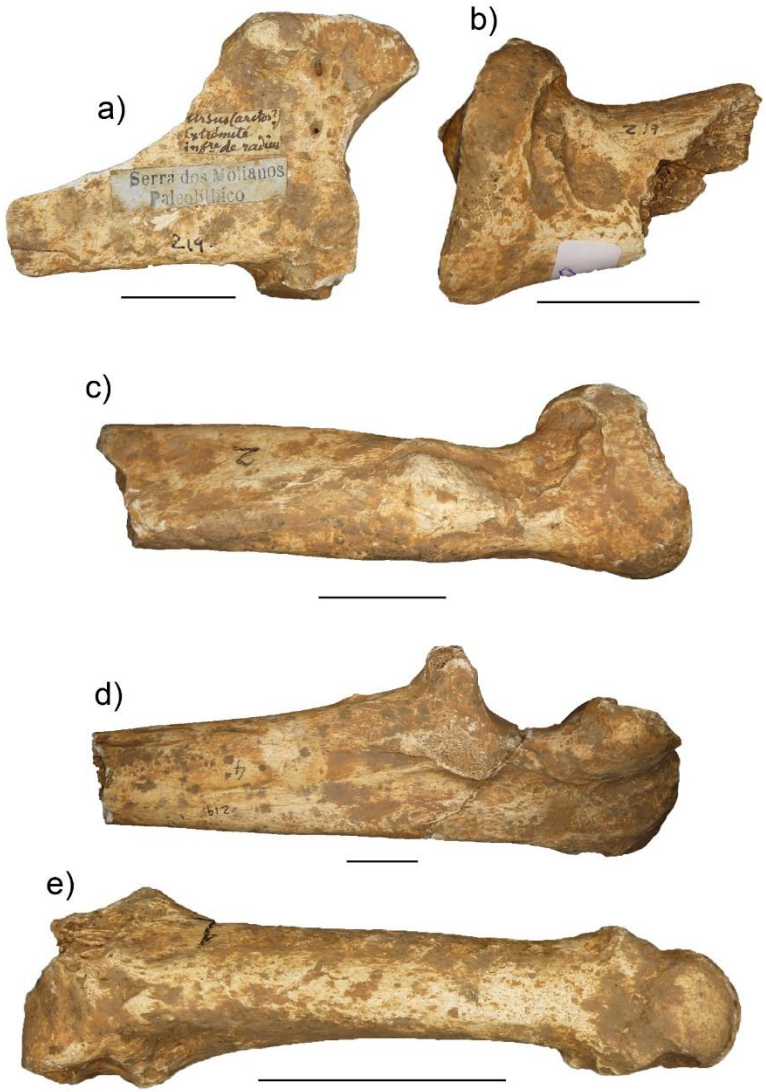


Figure 5.10 — a) Distal radius SM219.32.1 from Serra de Molianos in lateral view. b) Proximal radius SM219.32.2 from Serra de Molianos in lateral view. c) Proximal radius SM219.2 from Serra de Molianos in lateral view. d) Proximal ulna SM219.4 from Serra de Molianos in lateral view. e) First metacarpal SM219.33.1 from Serra de Molianos in dorsal view. All scale bars are 25 mm.

SM219.4 is a proximal epiphysis of a left ulna (Figure 5.10 d), that exhibits similar features to those documented by Torres, (1984) from the Saldarrañao Cave. Metrically, the anteroposterior and mediolateral diameters of the olecranon are consistent with the observed variability of Holocene bears from Galicia. However, they are smaller than those observed in other Portuguese localities (Figure 5.11).

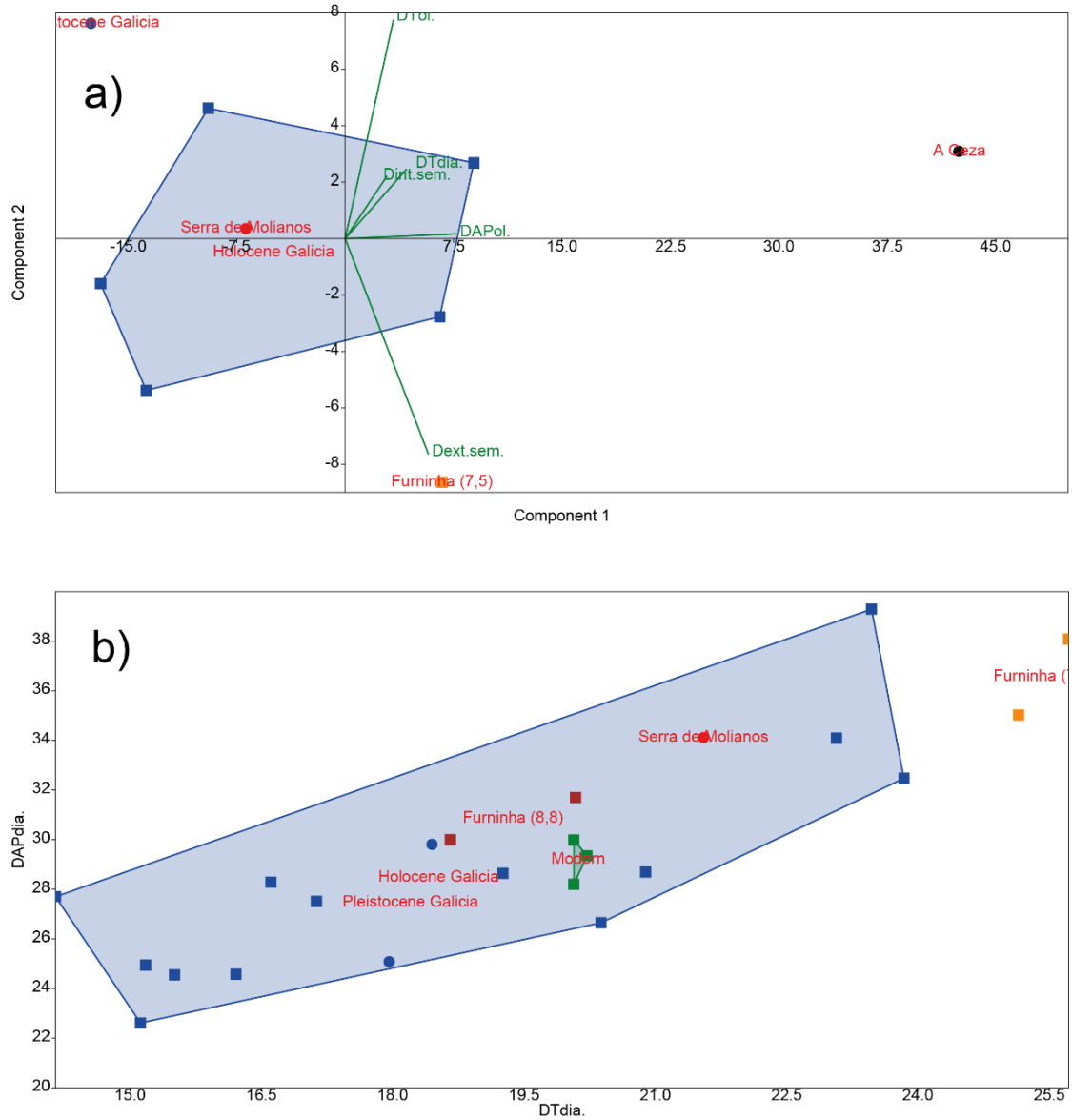


Figure 5.11 — a) PCA of the proximal ulna of several Iberian brown and cave bears. b) Biplot of transverse vs anteroposterior diameters of diaphysis of ulna of several Iberian brown bears.

The two proximal radii epiphysis SM219.32.2 and SM219.2 (Figure 5.10 b-c), are very similar in size. They appear within the range of variability observed in Holocene Galician bears, with an anteroposterior diameter that is smaller than that of the Furninha specimens (Figure 5.12 a). The proximal transverse diameters of the specimens are extremely similar, which lends support to the hypothesis that they come from the same individual. Upon application of the equation proposed by Viranta (1994) both specimens yielded an estimated mass of approximately 240 kg. SM219.32.1 (Figure 5.10 a) is a distal epiphysis of a left radius. Its morphology exhibits minimal muscular insertions, while metrically, its mediolateral and anteroposterior diameters range within the Holocene Galician bears variability (Figure 5.12 b). The distal transverse diameter, as calculated using the equation proposed by Viranta (1994), yielded an estimated mass of 222 kg. The mean mass of the bears from this site is estimated to be approximately 236 kg, which is consistent with the mean mass of males from the Holocene of Galicia (Supplementary material at Appendix D, discussion).

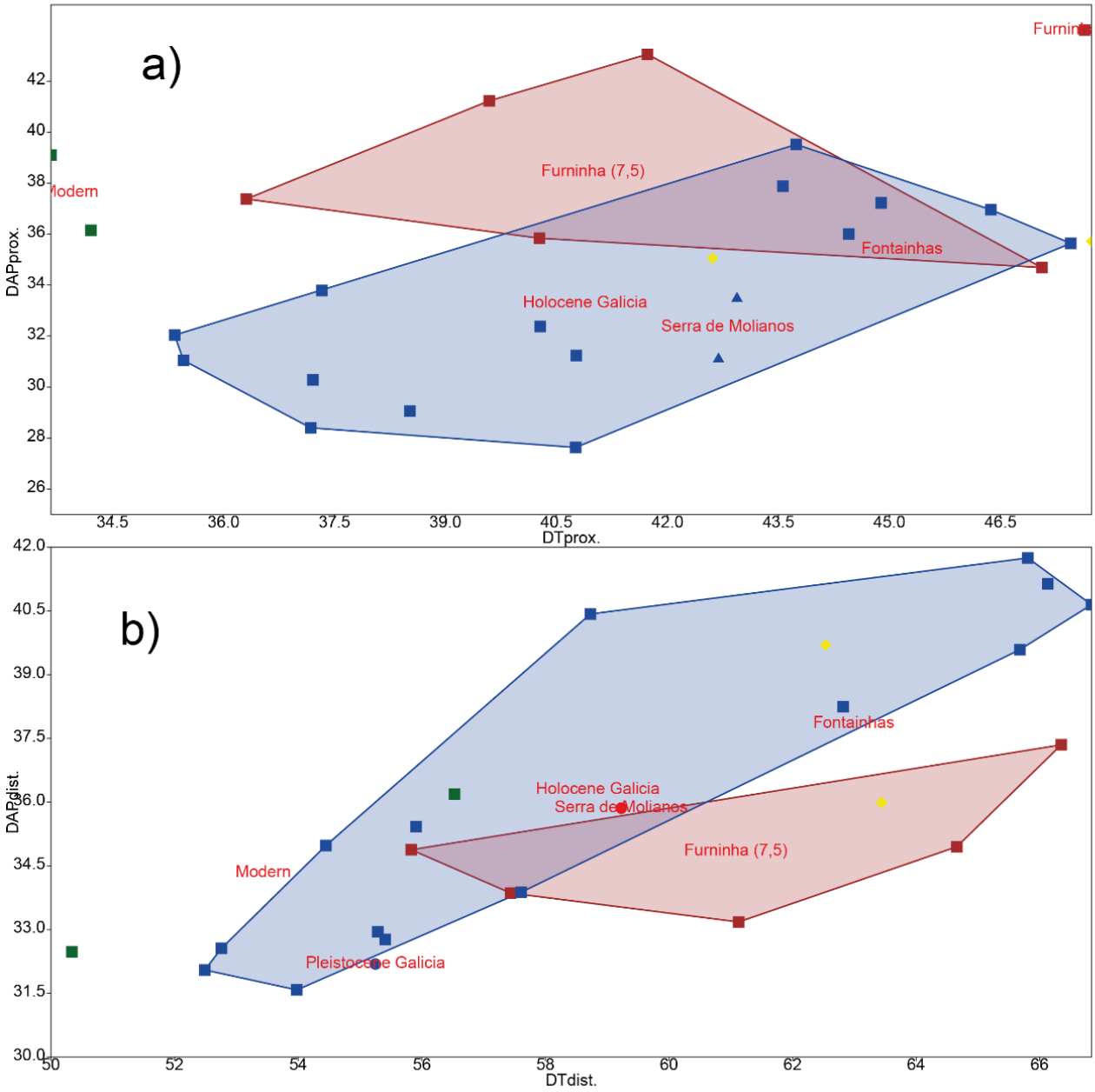


Figure 5.12 — a) Biplot of transverse vs anteroposterior diameters of the proximal radius of several Iberian brown bears. b) Biplot of transverse vs anteroposterior diameters of the distal radius of several Iberian brown bears.

SM219.33.1 is a right first metacarpal (Figure 5.10 e), which is the most well-preserved of the metapodials from this locality, yet it is not entirely undamaged. Metrically, within a PCA, it becomes evident that this specimen is within the range of variability observed in Holocene

Galician bears. It is more similar to the specimen from Tarelo displaying a greater degree of slenderness than those from Furninha (Figure 5.13).

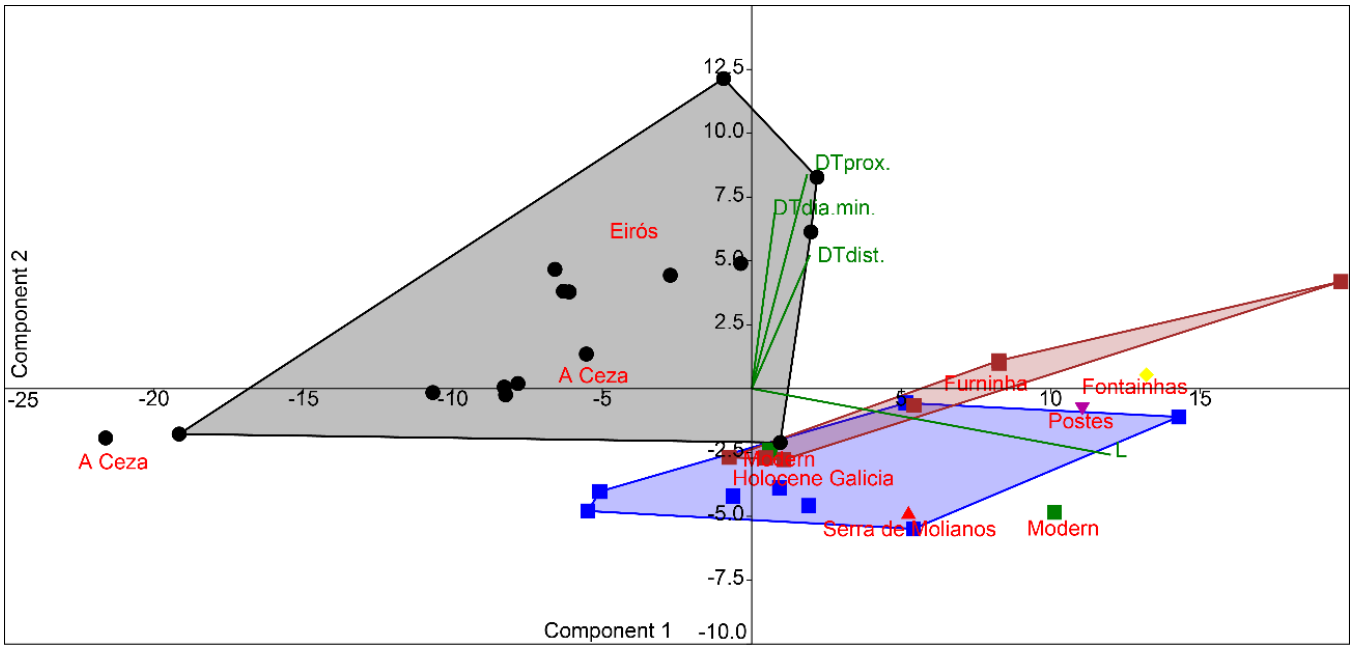


Figure 5.13 — PCA of the first metacarpal of several Iberian brown and cave bears.

5.3.5 Fontainhas

The sample from the Fontainhas site is the second largest considered in this work and, as mentioned, includes 23 teeth and several well-preserved long bones, from both forelimb and hindlimb. These remains belong to at least two individuals, but the presence of a juvenile mandible suggests that a third individual was present.

The dentognathic remains can be classified into three groups based on preservation, degree of crown wear, and ontogenetic state. The first would include, FO.I-162, a juvenile mandible (Figure 5.14 i) with the deciduous m1 still present, and with an erupting partial m1 still below it. This would suggest that this juvenile was about four months old at the time of death (Debeljak, 1996). The second group would include six teeth, which although completely formed, do not show a high degree of wear, and also have a peculiar coloration with black venation over folds and cracks in the enamel. They include a third upper incisor (FO.I-158), two canines (FO.I-87 and FO.I-88), an M1 (FO.I-154) and two m3s (FO.I-35 and FO.I-153) (Figure 5.14 b-h). The third and final group of teeth includes most of the dental specimens from the locality which are teeth with moderate to extreme wear. They may or may not belong to

different individuals, as the color of the sediment adhered to them is the same and none of them has black veining over the enamel. Some of the extremely worn ones are still attached to both parts of the mandible (FO.I-37) and maxilla (FO.I-151) (Figure 5.14 e-j).

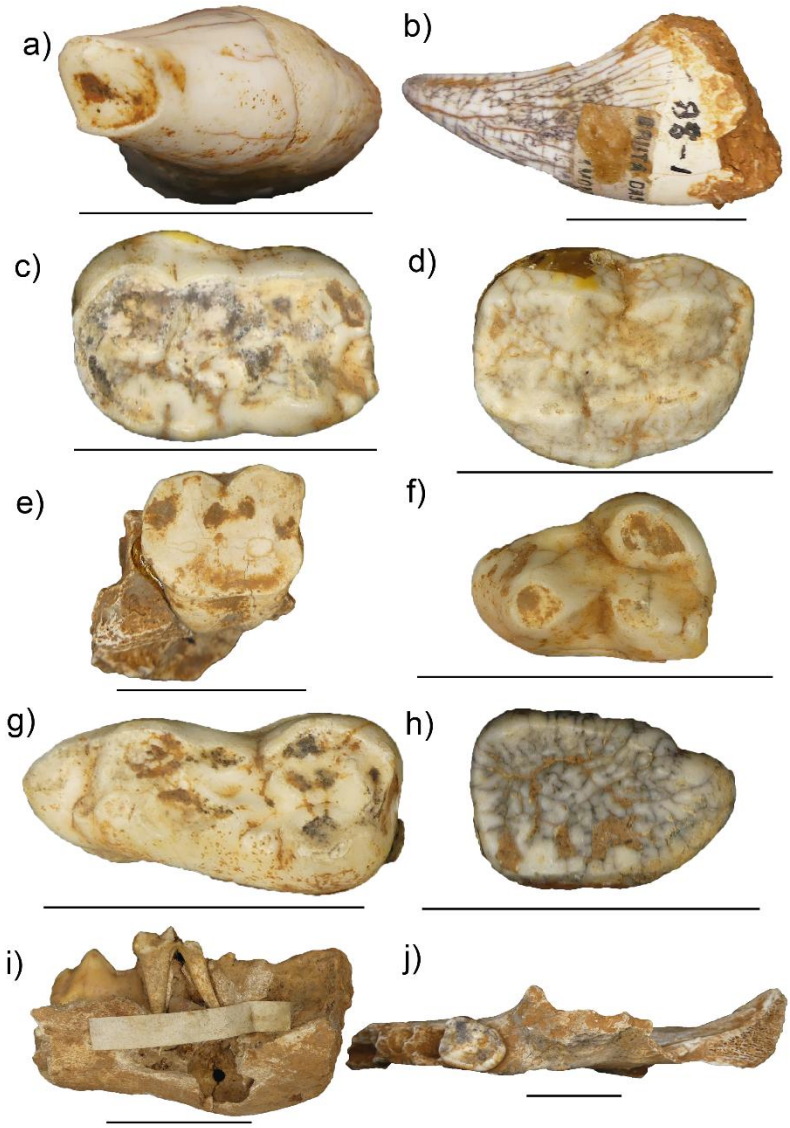


Figure 5.14 — a) Extremely worn canine FO.I-81 in occlusal view. b) Unworn canine FO.I-88 with black venation of the enamel in lingual view. c) Relatively little worn m2 (FO.I-153) in occlusal view. d) Unworn M1 with black venation of the enamel in occlusal view (FO.I-154). e) Extremely worn M1 (FO.I-151) with part of the maxilla still attached in occlusal view. f) Relatively little worn P4 (FO.I-157) in occlusal view. g) Relatively little worn m1 (FO.I.-156) in occlusal view. h) Unworn m3 with black venation of the enamel (FO.i-152) in occlusal view. i) Juvenile mandible with deciduous tooth and erupting m1 (FO.I-162) in labial view. j) Partial mandible with an extremely worn m3 (FO.I-37) in occlusal view. Scale bars are 25 mm.

Metrically, the teeth from Fontainhas Cave are generally among the largest recorded from brown bears in the entire Iberian Peninsula (Figure 5.15). The canines are of interest as some of them were either among the shortest or the longest relative to their size (Figure 5.9 a). Both the upper and lower fourth premolars are the longest recorded in this study, with the overall dimensions similar to the largest from Furninha Cave (Figure 5.15 a-b). The M1s, on the other hand, are much smaller, which can be attributed to the extreme wear of one of them (FO.I-151), while the unworn FO.I-154 falls within the morphospace of the Holocene brown bears from northern Spain in the PCA (Figure 5.6).

The m1 from Fontainhas (FO.I-156) is comparable in size to the largest teeth from of Furninha Cave, but is slightly narrower than the broadest teeth of this type recorded in this study, from both Caldeirão and Escoural (Figure 5.4 d). The m2 from Fontainhas, exhibiting moderate wear (FO.I-153), is comparable in width to cave bear teeth from A Ceza (Galicia) but slightly shorter, similar to some teeth from Furninha Cave (Figure 5.4 e-f). The two unworn m3s from Fontainhas (FO.I-35 and FO.I-153) are of a similar size to a m3 from the lower layer of Furninha Cave, which appears in the PCA within the morphospace of the Furninha bears (Figure 5.15 c). Meanwhile the extremely worn FO.I-37, which remains attached to the mandible, represents the second largest brown bear m3 in the study. Its width and length are comparable to those of small cave bears from A Ceza (Galicia) (Figure 5.9 b).

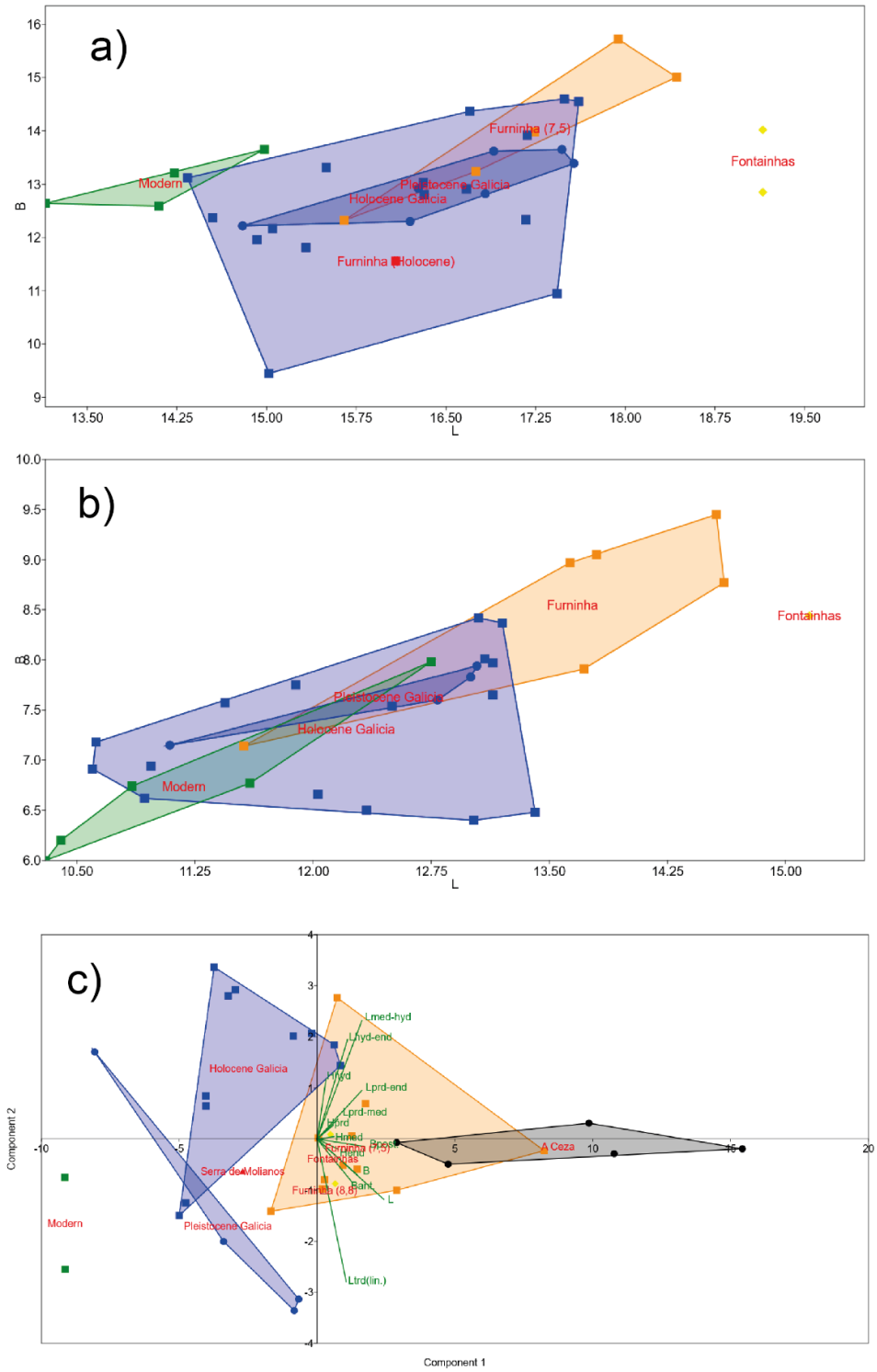


Figure 5.15 — a) Biplot of length vs breadth of the P4 of several Iberian brown bears. b) Biplot of length vs breadth of the p4 of several Iberian brown bears. d) PCA of the m3 of several Iberian brown and cave bears.

Regarding the postcranial remains, all of them exhibit a similar orangish patina and adhered clays as observed in some of the teeth (such as FO.I-151).



Figure 5.16 — Atlas from Fontainhas (FO.I-164) in anterior view. Scale bar is 25 mm.

The atlas FO.I-164 (Figure 5.16) is as robust as that of small cave bears from Eirós (Figure 5.17).

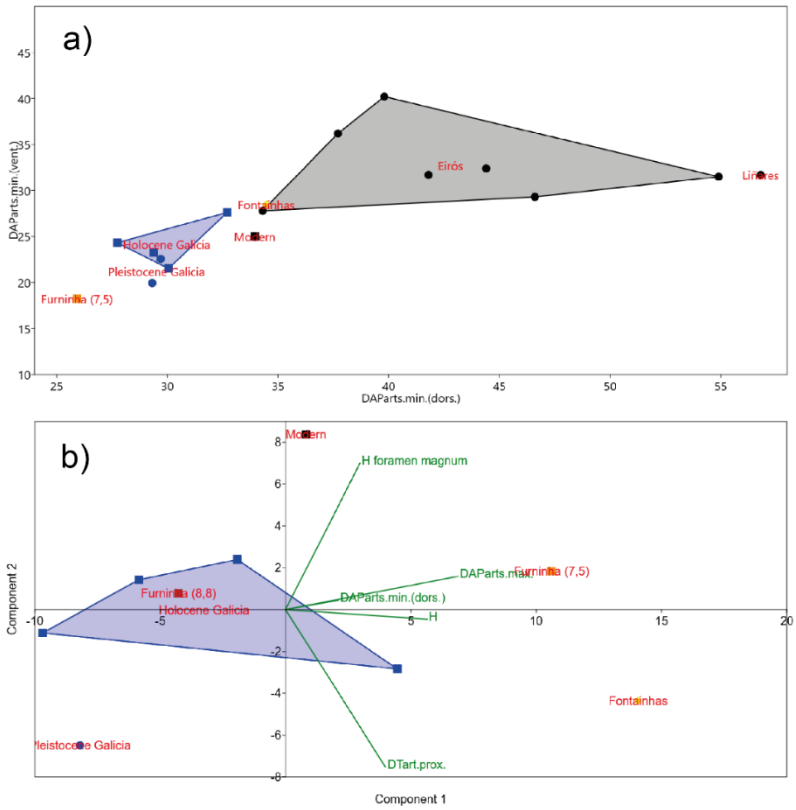


Figure 5.17 — a) Biplot of dorsal articular diameter vs ventral articular diameter of the atlas of several Iberian brown and cave bears. b) PCA of the atlas of several Iberian brown bears.

One of the most noteworthy specimens from the Fontainhas Cave is FO.I-45 (Figure 5.18) this specimen is constituted by two pathologically conjoined vertebrae, which are likely to be the XI and XII thoracic vertebrae. Such an assessment is feasible given the relatively anteroposteriorly thin and posteriorly inclined vertebral apophysis (more anterior vertebrae exhibit taller and less tilted apophyses, while more posterior ones present anteroposteriorly wider apophyses with less tilt). Additionally, the position and size of the articulation with the rib and the distal part of the transverse process are relatively distinctive within the thoracic sequence for the XI vertebra, which is transitional between the last three thoracic vertebrae with a shape analogous to those of lumbars and those of the anterior thoracics.

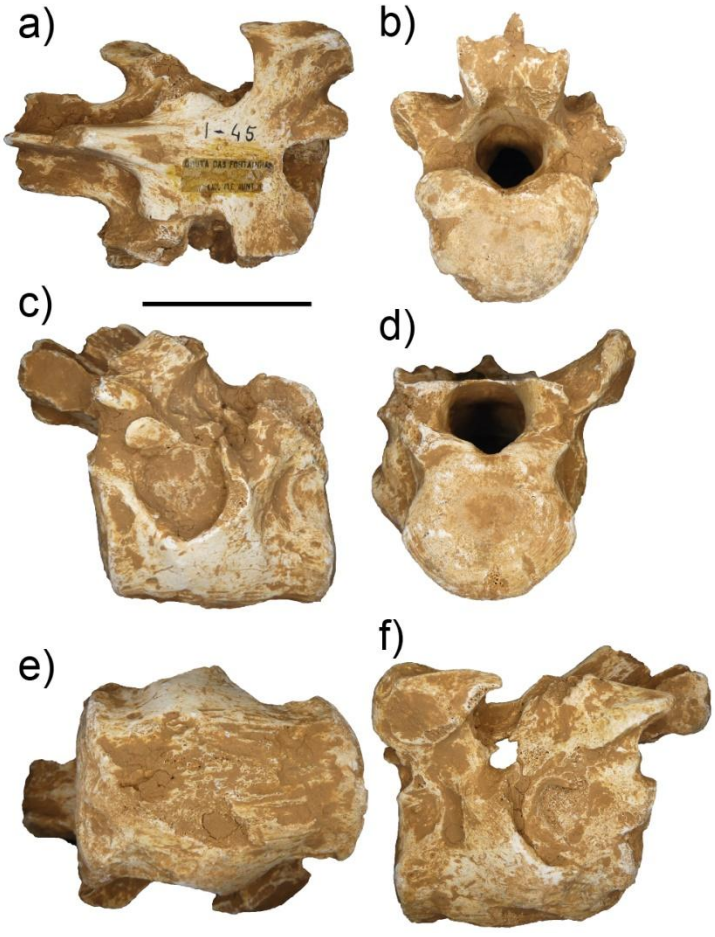


Figure 5.18 — FO.I-45 pathologically conjoined XI and XII vertebrae of a brown bear from Fontainhas Cave in a) dorsal, b) posterior, c) right lateral, d) anterior, e) ventral, and f) left lateral views. Scale bar is 50 mm.

The most significant bones from the postcranial remains are the long bones of the appendicular skeleton, as they are among the best preserved considered within this study (Figure 5.19). They include all the elements from stylopodium and zeugopodium, with pairs of left and right elements and with a similar patina to the other postcranial bones. It can be reasonably deduced that the aforementioned bones belong to a single individual.

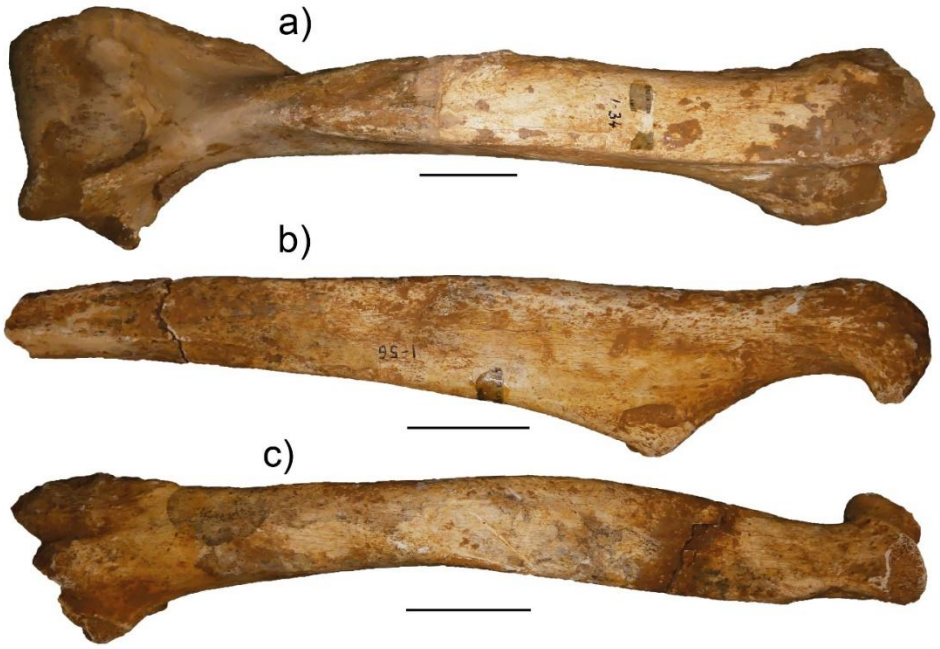


Figure 5.19 — a) Right humerus from Fontainhas (FO.I-34) in anterior view. b) Left ulna from Fontainhas (FO.I-56) in posterior view. c) Left radius from Fontainhas (FO.I-59) in anterior view. Scale bars are 50 mm.

The humeri from Fontainhas are even longer than those of cave bears, with a similarly sized transverse distal diameter (Figure 5.20 a). The distal articular diameter is comparable with that of the largest cave bears and one specimen from Furninha, although both of them present larger transverse distal diameters (Figure 5.20 b). The radii from Fontainhas are the longest for brown bears in the sample, although they follow the general trend for the species in possessing a smaller transverse distal diameter, for given lengths, than cave bears (Figure 5.20 c). As with other postcranial bones, the radius FO.I-59 exhibits two deep marks in the mid-diaphyseal region when observed in anterior view (Figure 5.19 c). The diameters of ulnae are also

comparable to those of small-sized cave bears (Figure 5.20 d). All the anterior appendicular bones present extremely elongated diaphyses.

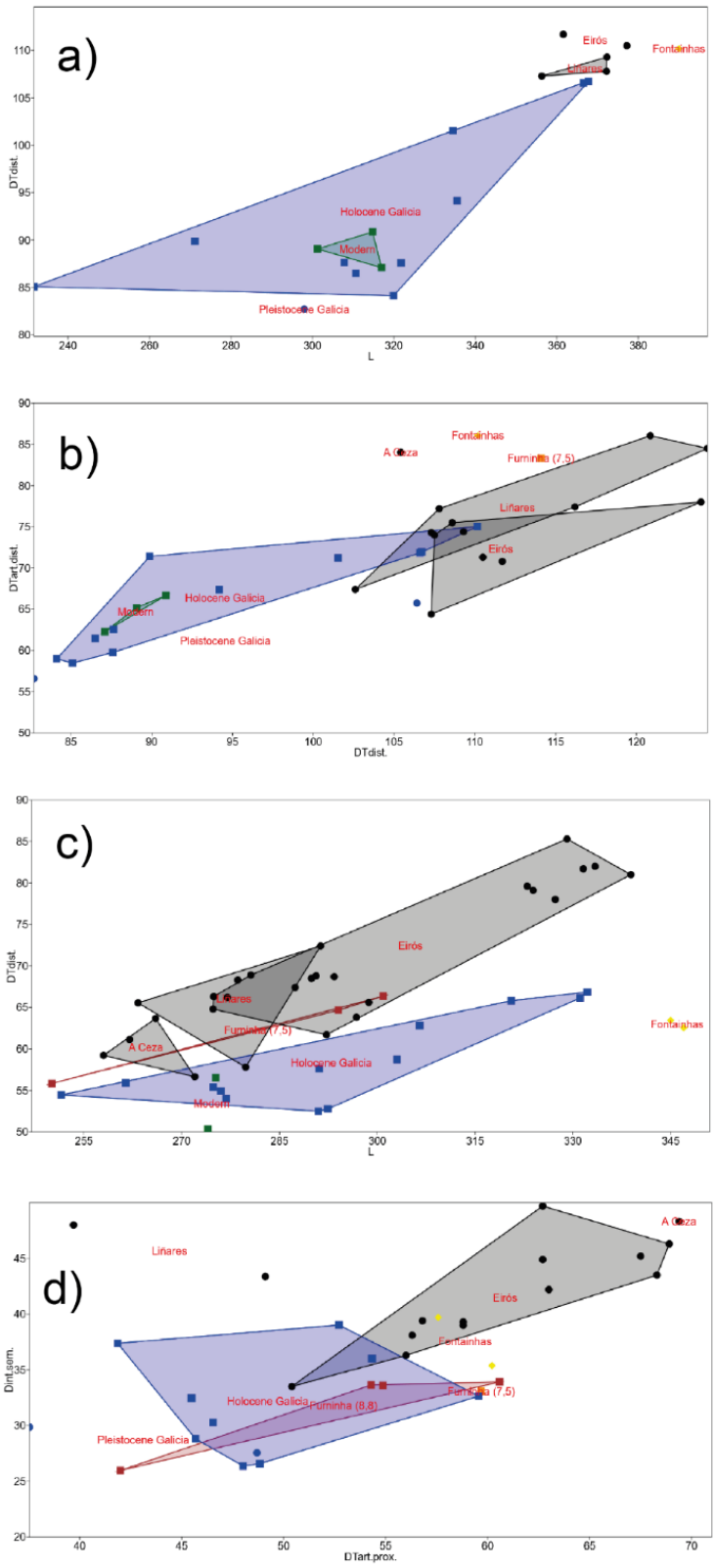


Figure 5.20 — a) Biplot of length vs transverse distal diameter of the humerus of several Iberian brown and cave bears. b) Biplot of transverse distal diameter vs transverse distal articular diameter of the humerus of several Iberian brown and cave bears. c) Biplot of length vs transverse distal diameter of the radius of several Iberian brown and cave bears. d) Biplot of interior proximal diameter vs transversal articular diameter of the ulna of several Iberian brown and cave bears.

A morphological comparison of other postcranial bones reveals a relatively slender and elongated morphology, a finding that is corroborated by the metric data presented (Figure 5.21). The pisiform FO.I-166 (Figure 5.21 a) exhibits measurements that align with those of small cave bears from A Ceza (Figure 5.22 b), yet, when considering several diameters in a PCA, it is observed to be significantly slenderer than the bones of cave bears (Figure 5.22 c). The scapholunate FO.I-74 (Figure 5.21 b) is the largest of the brown bear sample, yet with smaller diameters than those observed in cave bears from A Ceza (Figure 5.22 a).

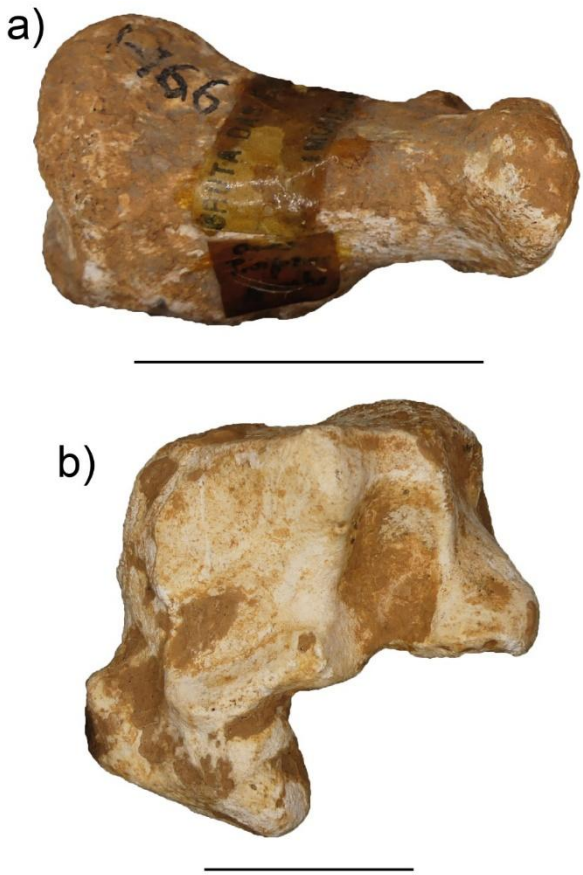


Figure 5.21 — a) Right pisiform from Fontainhas (FO.I-166) in lateral view. b) Left scapholunate bone from Fontainhas (FO.I-74) in distal view. Scale bars are 25 mm.

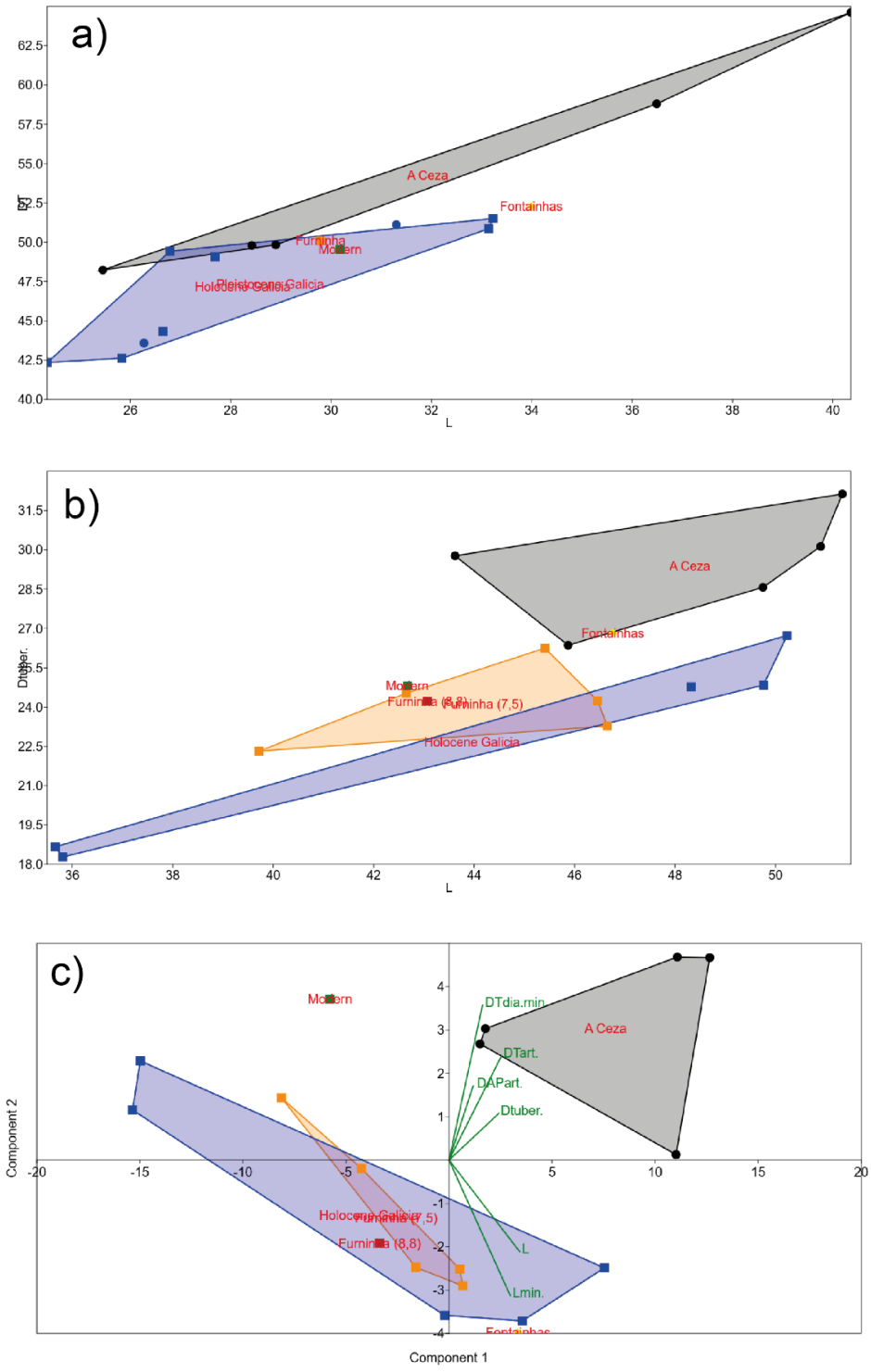


Figure 5.22 — a) Biplot of length vs transverse diameter of the scapholunate of several Iberian brown and cave bears. b) Biplot of length vs transverse tubercular diameter of the pisiform of several Iberian brown and cave bears. c) PCA of the pisiform of several Iberian brown and cave bears.

The acetabulum diameters of the right and left pelvises from Fontainhas, FO.I-46 and FO.I-47 are the largest observed in the sample of Iberian brown bears (Figure 23).

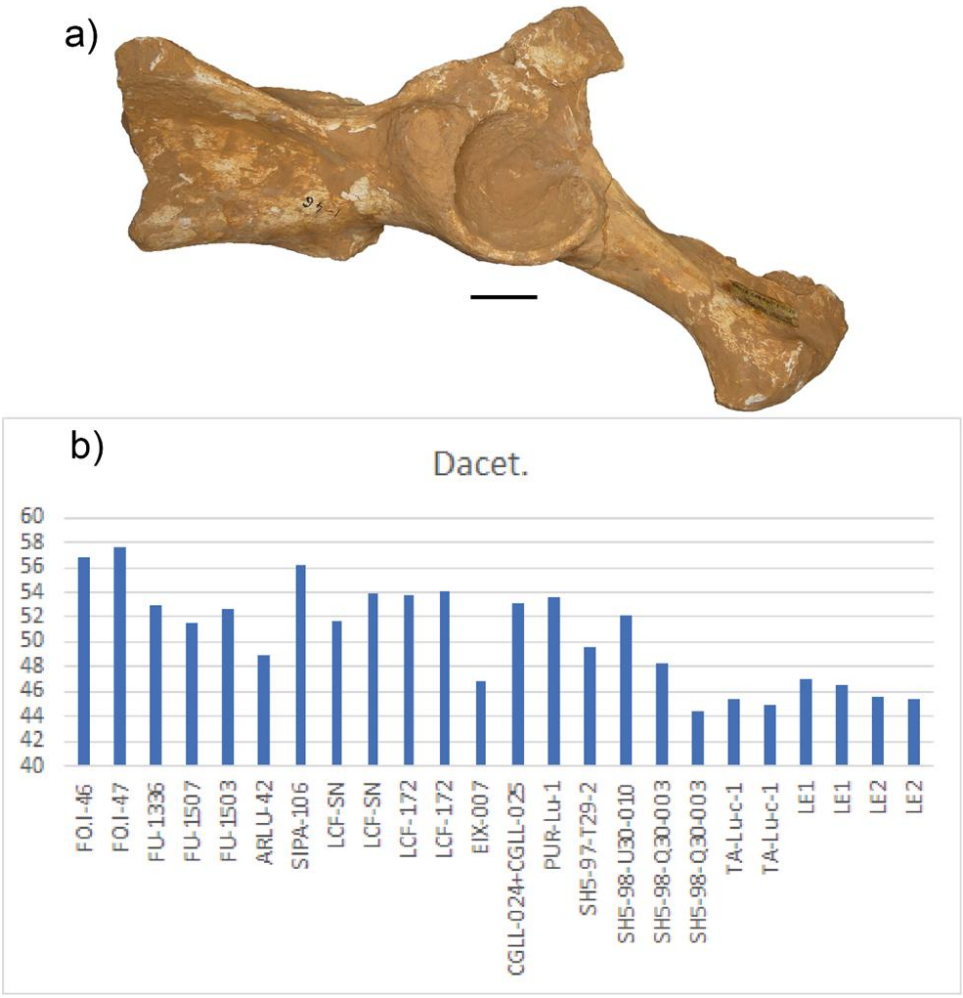


Figure 5.23 — a) Right acetabulum from Fontainhas (FO.I-46) in lateral view. Scale bar is 25 mm. b) Bar diagram showing the diameter of the acetabulum of several Iberian brown bears.

The femora (Figure 5.24 a) exhibit a comparable pattern to that observed in the humeri. Despite their slender morphology, they are notably longer and wider than any other brown bear in the sample, with measurements that closely resembles that of the large cave bears from Eirós (Figure 5.25 a). The patella FO.I-72 (Figure 5.24 b) is comparable in dimensions to those of female cave bears from Eirós Cave (Figure 5.25 b). The tibiae (Figure 5.24 c) lengths are similar to the largest Holocene Galician bears; this also appears to be the case for the diameters of the bone (Figure 5.25 c-d). It is not possible to make any meaningful observations about the fibula (Figure 5.24 d), other than to note that it does not fall within the morphospace of the Holocene Galician specimens (Figure 5.25 e).

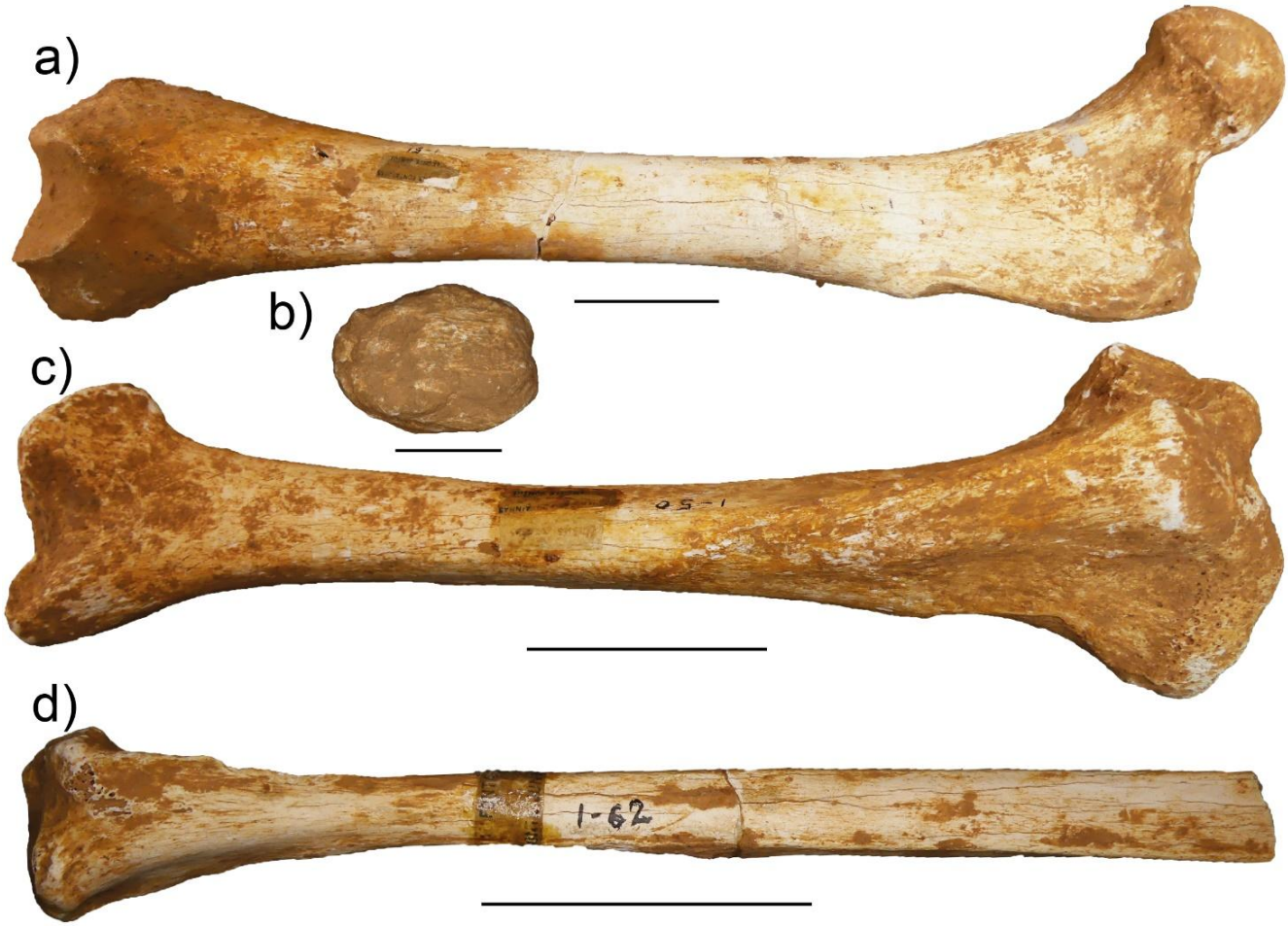


Figure 5.24 — a) Left femur from Fontainhas (FO.I-51) in anterior view. b) Patella from Fontainhas (FOI-72) in anterior view. Scale bar is 25 mm. e) Right tibia from Fontainhas (FO.I-50) in anterior view. f) Right fibula from Fontainhas (FO.I-62) in lateral view. Scale bars of long bones are 50 mm.

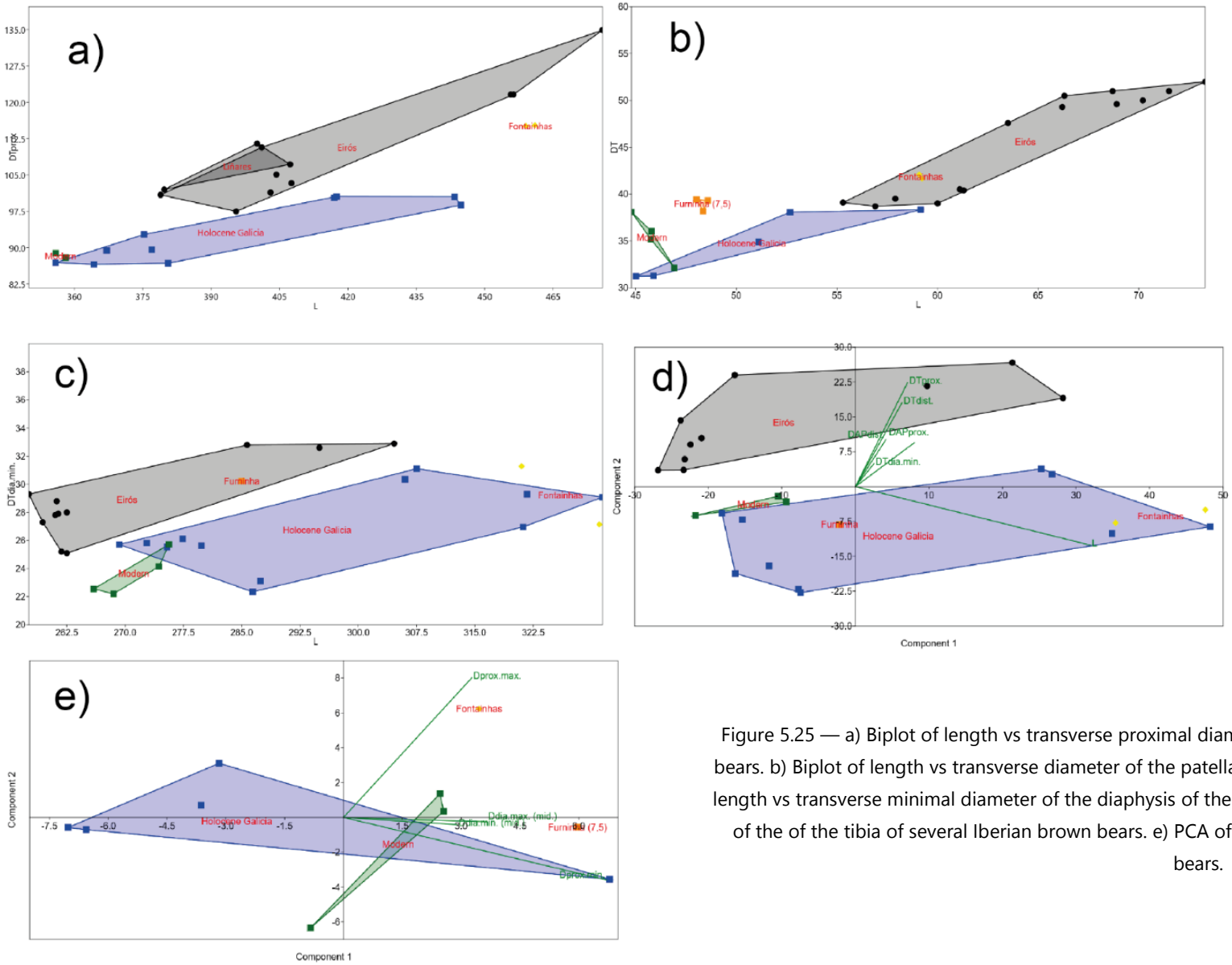


Figure 5.25 — a) Biplot of length vs transverse proximal diameter of the femur of several Iberian brown and cave bears. b) Biplot of length vs transverse diameter of the patella of several Iberian brown and cave bears. c) Biplot of length vs transverse minimal diameter of the diaphysis of the tibia of several Iberian brown and cave bears. d) PCA of the of the tibia of several Iberian brown bears. e) PCA of the of the fibula of several Iberian brown and cave bears.

The calcaneus (FO.I-?) displays several deep scratches on its dorsal surface (Figure 5.26 a). It is the longest from a brown bear in the sample (Figure 5.27 a). The astragalus from Fontainhas, FO.I-56 (Figure 5.26 b) is among the longest recorded in Iberia, yet it is not as robust as those of cave bears and few Galician Holocene brown bears (Figure 5.27 b-c).

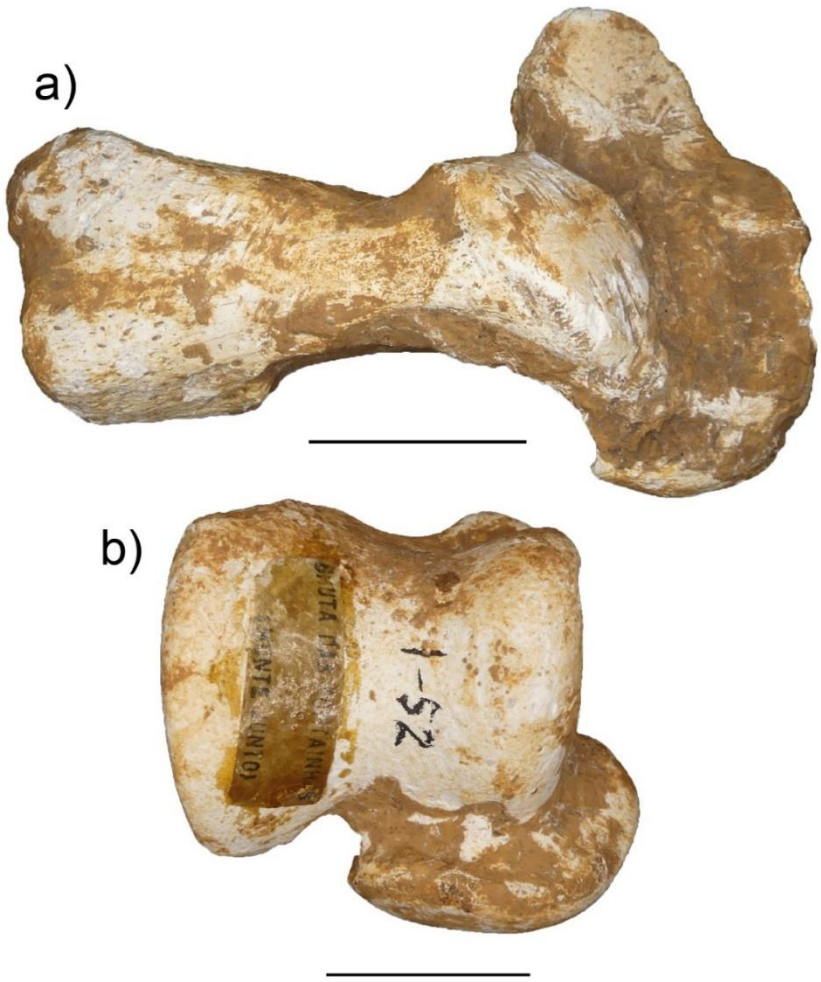


Figure 5.26 — a) Right calcaneus from Fontainhas (FO.I-?) in proximal view. b) Right astragalus from Fontainhas (FO.I-52) in proximal view. Scale bars are 25 mm.

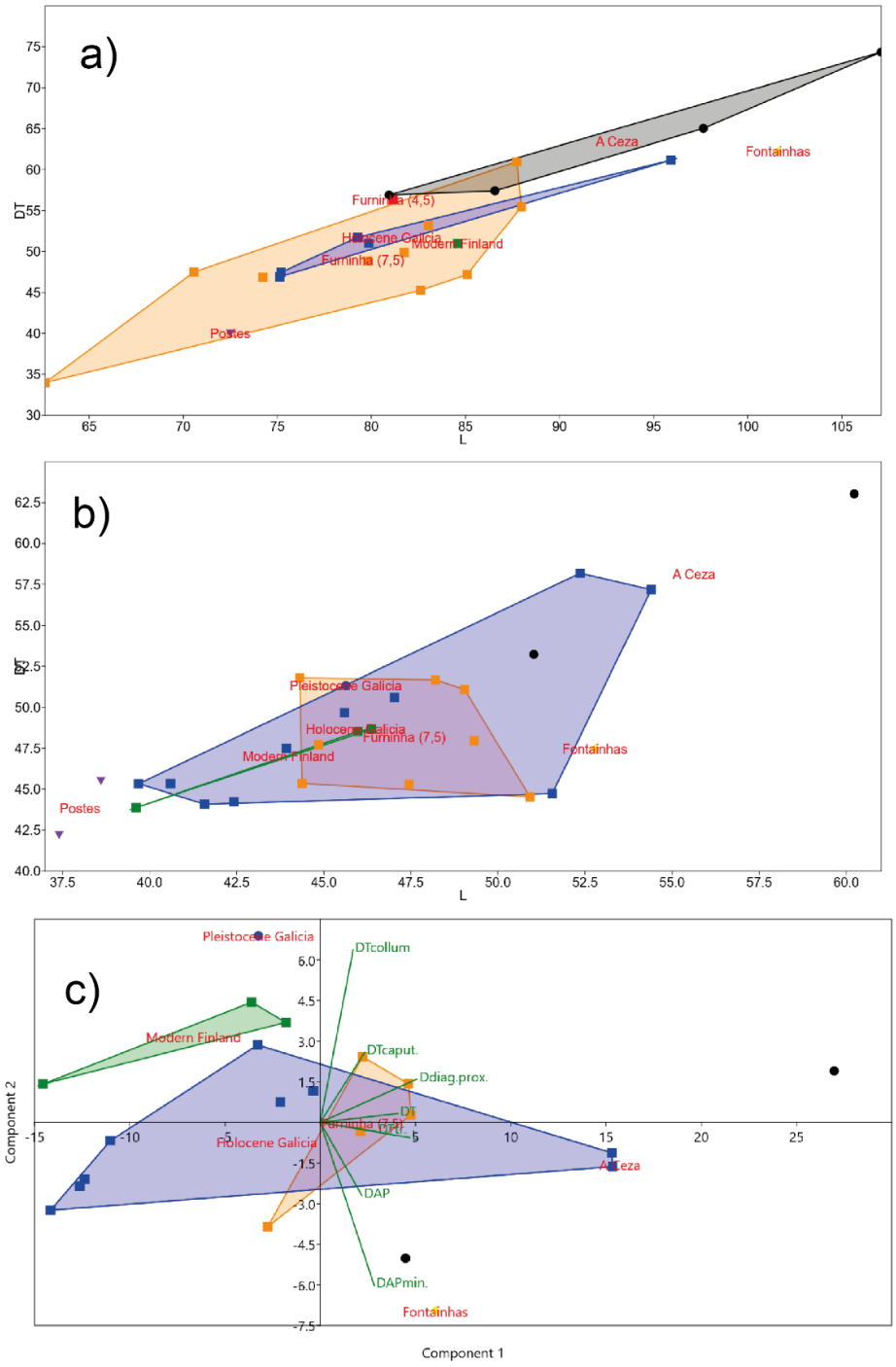


Figure 5.27 — a) Biplot of transverse diameter vs length the calcaneus of several Iberian brown and cave bears. b) Biplot of length vs transverse diameter of the astragalus of several Iberian brown and cave bears. c) PCA of the astragalus of several Iberian brown and cave bears.

The distal epiphysis of several metapodials are relatively well preserved, but their proximal epiphyses are slightly damaged, preventing the measurement of these bones. Some metapodials (Figure 5.28) exhibit relatively deep, parallel, and regularly spaced marks, many of which are located in the diaphysis. These marks differ from the gnawing marks typically left by carnivores in the epiphysis of bones, and are relatively similar to those seen in the calcaneus. They may have an anthropic origin, or could be the result of the trampling of the bones by other animals. One well preserved metacarpal from Fontainhas (FO.I-69) show that it is the longest among the brown bears of Pleistocene Iberian, while not being particularly robust (Figure 5.13). One third phalanx (FO.I-165) is of almost the same size as those of Cave bears from A Ceza (Figure 5.7 c).



Figure 5.28 — Partial distal metapodial with vertical marks from Fontainhas (FO.I-56) in lateral view.

The completeness of the long bones from Fontainhas Cave allows for the utilization of the both the equations for calculating the body mass proposed by Viranta (1996) and Christiansen (1999). While less precise, the first equation can be used for any appendicular long bones except the fibula. In contrast, the second equation is restricted to humeri and femora. The application of the Viranta (1996) equation to the appendicular bones from Fontainhas, in accordance with the previously outlined methodology, yielded the following results: an average of 358.02 kg for humeri, 239.74 kg for radii, 395.93 kg for femora, and 261.25 kg for tibiae; with an overall average weight of 313.73 kg. The Christiansen, (1999) equation yields an average of 406.63 kg for humeri and 387.28 kg for femora; resulting in an overall average weight of 396.95 kg. The combined average of both methods for individual humeri and femora is estimated to be 386.96 kg.

5.3.6 Furninha

As previously stated, the sample of bear remains from Furninha Cave comprises hundreds of remains, not all of which have been properly catalogued to this day, as it is the case with most remains from Furninha cave. Teeth are among the most common bear elements from the site after phalanges (Figure 5.2), with more than one hundred observed in all fossiliferous layers, including the Holocene sediments on top of the sequence. The teeth exhibit considerable variation in size, coloration, and morphology, as well as in the degree of wear. However, although none of them display the extreme wear observed in some teeth from Fontainhas.

The canines from Furninha Cave present occasional slight torsion of the root in comparison to the crown. However, their morphological characteristics appear to align with those typically observed in brown bear canines (Figure 5.29). Metrically they are typically larger than those from Serra de Molianos, modern specimens and Holocene and Pleistocene bears from Galicia. However, several Holocene specimens exhibit similarities in size. Furthermore, there is less variation in dimensions among them than is the case of those from Fontainhas Cave, despite them being more numerous (Figure 5.9 a).



Figure 5.29 — Canine from Furninha Cave in lingual view. Scale bar is 25 mm.

The P4s from Furninha (Figure 5.30) lack the additional cusplets that are typically present in cave bears. However, they exhibit more pronounced ridges compared to other brown bears, particularly between the hypocone and the other cusps. Metrically, some of the P4s from Furninha are among the largest in the sample (Figure 5.30). They differ from those from Fontainhas Cave in that they are more robust for a given size, although those of Fontainhas are longer (Figure 5.15 a).

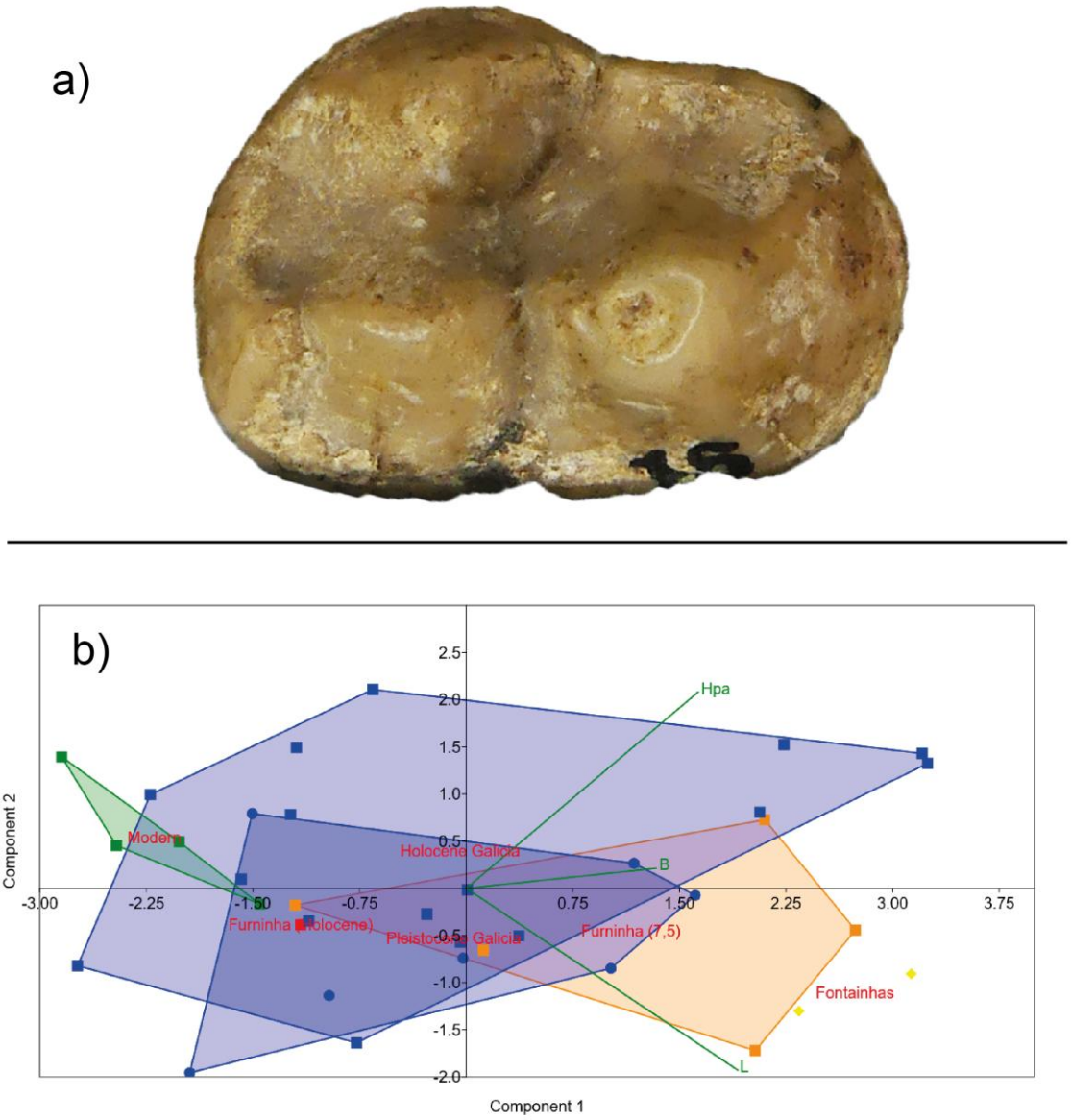


Figure 5.30 — a) P4 from Furninha Cave in occlusal view. Scale bar is 25 mm. b) PCA of the P4 of several Iberian brown bears.

The M1s from Furninha (Figure 5.31) lack the pronounced mesocone typical of speleoid bears, exhibiting instead the typical morphology of brown bears, with it having a size comparable to the other cusps. Metrically, they are situated within the upper range of the variability in size of the M1s from NW Spain, a similar pattern to that observed in the PCA. Metrically these teeth differ from those of cave bears, exhibiting overall shorter lengths (Figure 5.6).



Figure 5.31 — Three M1s from Furninha Cave in occlusal view, note the different morphologies, wear stages, patina color and overall sizes. Scale bar is 25 mm.

The M2s from Furninha Cave lack an individualized premetacone. Despite the relatively large talonid, the entmetaconule area is not as large as in the cave bears (Figure 5.32 a). Metrically they exhibit considerable variation in width, with some Holocene brown bears from Galicia displaying larger dimensions in both metrics (Figure 5.32 c-d). One of the M2s (GFP-1422) had a label attached to it, which classified it as a cave bear m2. However, an examination of its morphology (Figure 5.32 b) suggests an alternative attribution, namely that it is a M2 of a brown bear lacking the talonid and its distalmost part. The m2s of cave bears present a relative "8" shape, as well as numerous crenulations and conulids, featuring additional cusps. In contrast GFP-1422 displays relatively simple cusps, akin to those observed in other brown bear M2s from the site, whose measurements are fully documented. This evidence corroborates the classification of GFP-1422 as a brown bear M2 (Figure 5.32).

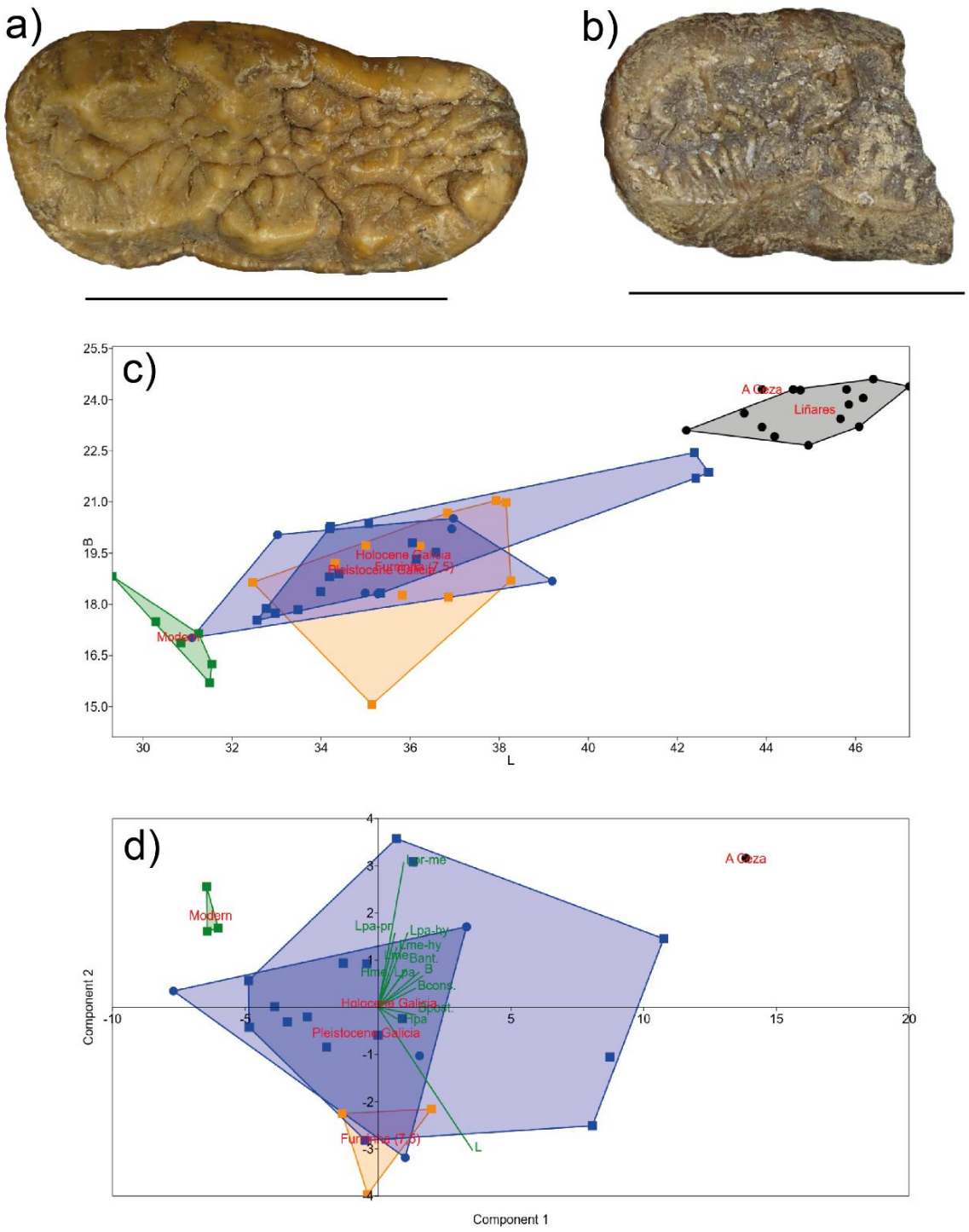


Figure 5.32 — a) M2 from Furninha Cave in occlusal view. b) GFP-1422, M2 which has a label attached mis-classifying it as m2 of a cave bear. Scale bars are 25 mm. c) Biplot of length vs breadth of the M2 of several Iberian brown and cave bears. d) PCA of the M2 of several Iberian brown and cave bears.

The p4s from Furninha (Figure 5.33 a) lack the distinct premetaconids observed in speleoid bears. Nevertheless, they represent the largest p4s in the sample of Iberian brown bears, with several specimens exhibiting a width that exceeds that of every other tooth considered (Figure 5.15 b). Furthermore, they do not occupy a position within the morphospace of modern, Holocene, and Pleistocene bears from NW Spain (Figure 5.33 b).

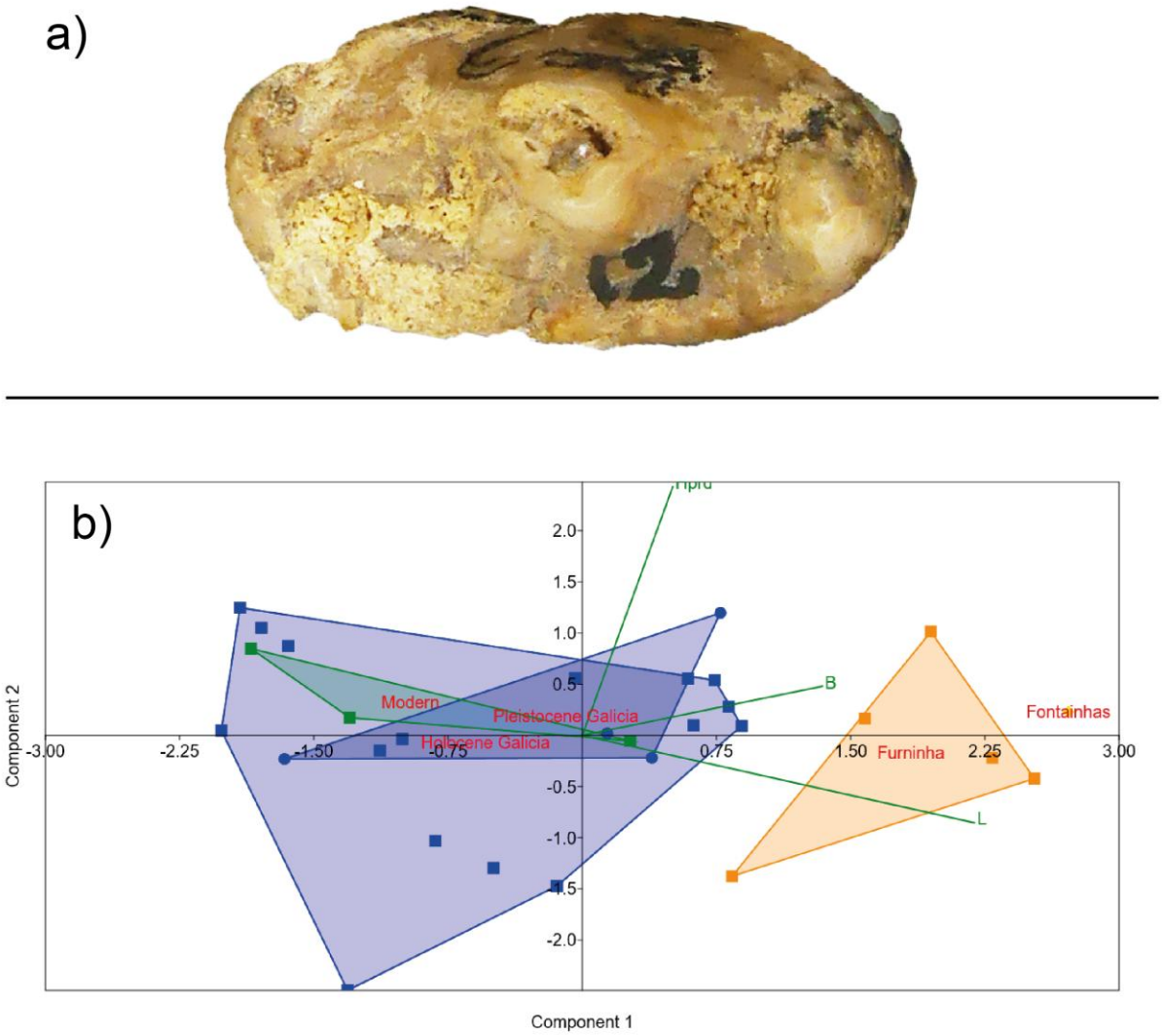


Figure 5.33 — a) p4 from Furninha Cave in occlusal view. Scale bar is 25 mm. b) PCA of the p4 of several Iberian brown bears.

The m1s from Furninha (Figure 5.34 a) lack the developed premetaconid and other mesial accessory cusplets that are typically present in cave bears. Metrically they are not significantly wider, but they do exhibit a greater average length than those from NW Spain (Figure 5.4 a). However, the remaining measurements are not markedly divergent from those of the bears from NW Spain, although most of them fall outside their morphospace (Figure 5.34 b).

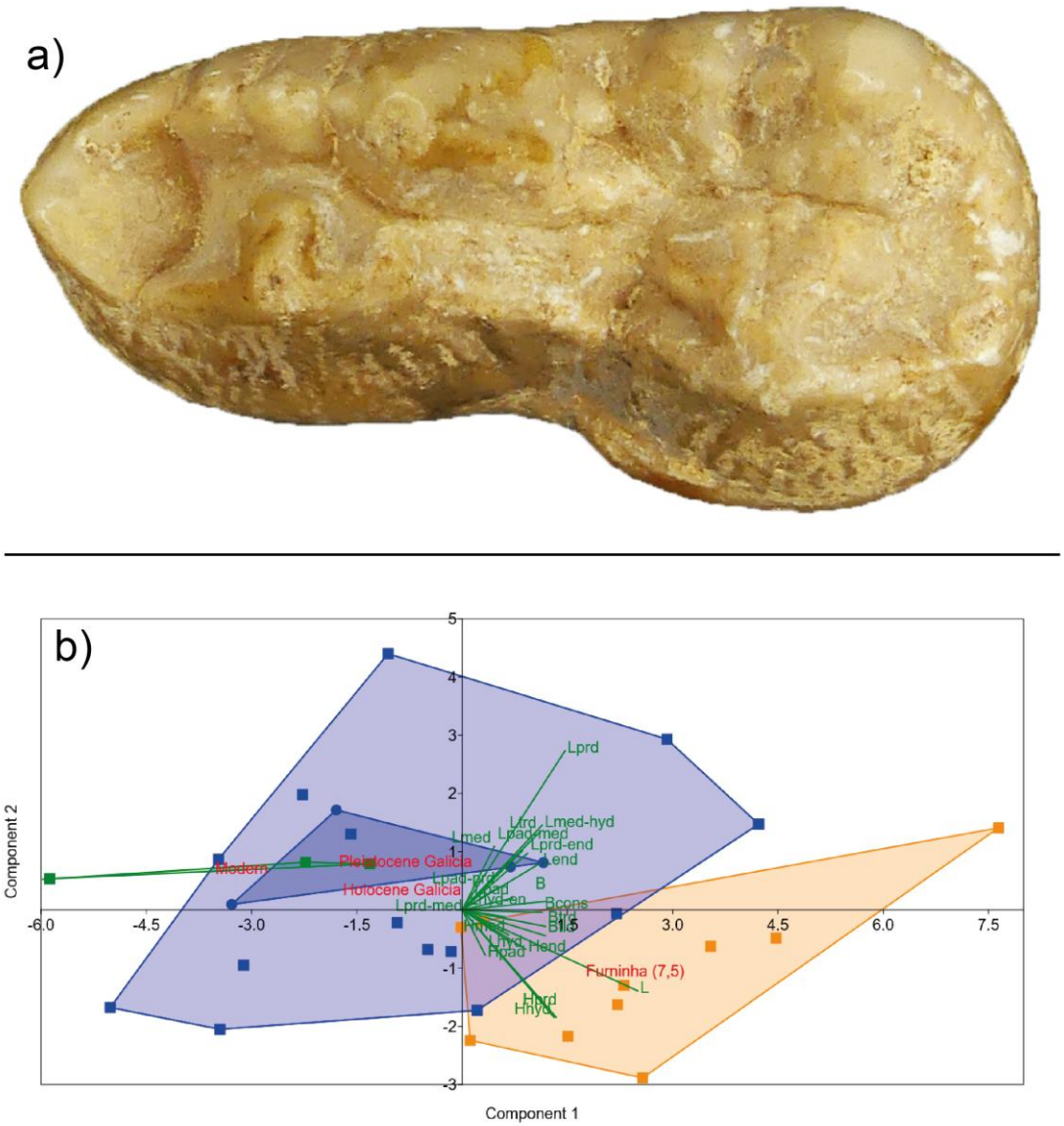


Figure 5.34 — a) m1 from Furninha cave in occlusal view. Scale bar is 25 mm. b) PCA of the m1 of several Iberian brown bears.

Some of the m2s from Furninha Cave exhibit considerable wear, yet none of them reach the same degree of wear as the Fontainhas specimens (Figure 5.35). Metrically these teeth are the widest brown bear teeth in the sample, exhibiting a width comparable to that of cave bear teeth, although they are shorter in length (Figure 5.4 e-f). The m2 in general demonstrates a discernible trend of broadening from modern specimens to those of the Holocene Galician period, then to those of Pleistocene Galician period, and ultimately those from Furninha Cave. The principal distinction between this specimen and the cave bear is the length of the latter's teeth, which are considerably longer (Figure 5.4 e).



Figure 5.35 — Two m2s from Furninha Cave in occlusal view, note the different morphologies, wear stages, patina color and overall sizes. Scale bars are 25 mm.

Cardoso, (1996a) states that two of the m3s from Furninha are comparable in size and morphology to the teeth of *U. thibetanus* Cuvier, 1823. Nevertheless, despite the globular shape of several m3s from Furninha, they are still more distally pointed than those of *U. thibetanus* and the vast majority of them are definitely quadrangular in shape and elongated as is typical of brown bears (Villalba de Alvarado, Crégut-Bonnoure, et al., 2024). However, none of the teeth exhibit the large lingual notch characteristic of cave bears (Figure 5.36 a). Metrically these teeth exhibit the greatest disparity in size, with some specimens exceeding the dimensions of those from NW Spain and others falling within the range of the smallest cave bears from A Ceza (Figure 5.9 b, Figure 5.15 c). The two smaller specimens from Furninha remain larger in both width and length than the largest *U. thibetanus*, both known as fossils from Europe or from modern-day Asiatic black bears (Figure 5.36 b).

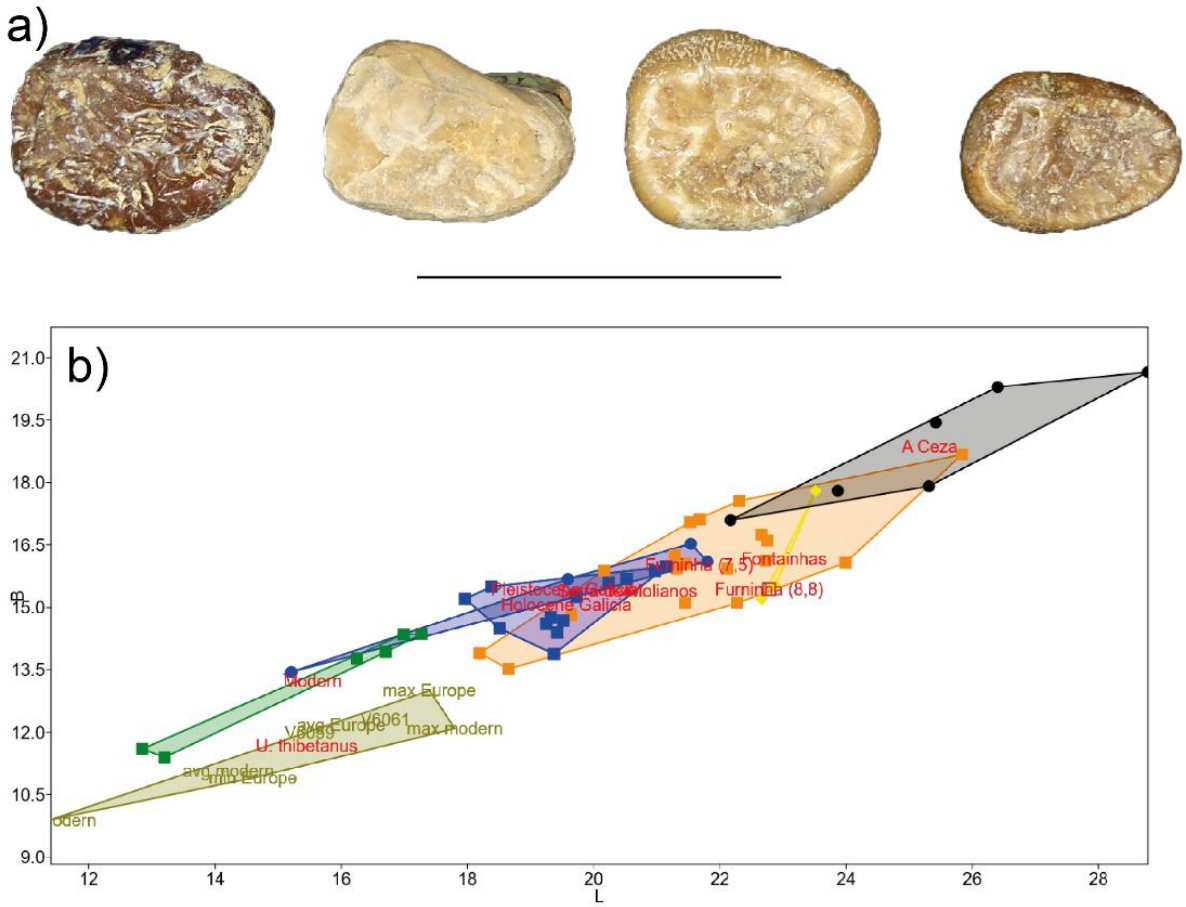


Figure 5.36 — a) m3s from Furninha Cave in occlusal view. Scale bar is 25 mm. b) Biplot of length vs breadth of the m3 of several Iberian brown, black and cave bears.

The record of Furninha Cave contains a limited number of juveniles remains, including deciduous molars without reabsorbed roots (Figure 5.37). It can therefore be surmised that some of the remains should belong to cubs less than three months old at the time of death (Debeljak, 1996).



Figure 5.37 — Deciduous tooth (d4) of brown bear from Furninha Cave in lingual view. Scale bar is 25 mm.

The assemblage from Furninha Cave also includes a large quantity of other cranial and postcranial bones. Of particular interest is the braincase GFP-1338 (Figure 5.38 a), which is notable not only for its pathological and diagenetic characteristics (which will be discussed subsequently), but also for being the most complete skull considered in this study. Metrically (Figure 5.38 b), it falls slightly beyond the morphospace of the Holocene bears from NW Spain and is markedly morphologically distinct from both modern and Pleistocene skulls from the same region.

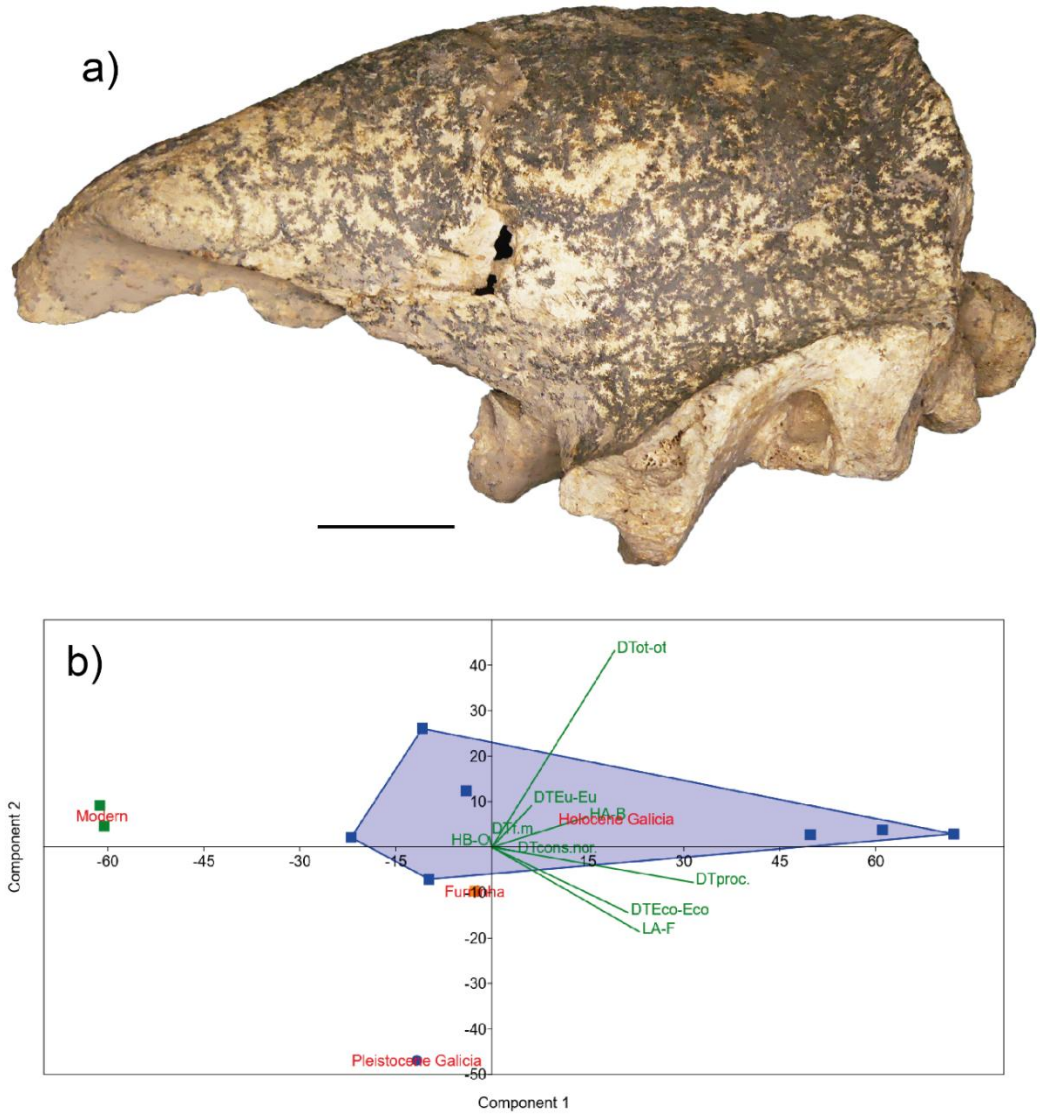


Figure 5.38 — a) Braincase of brown bear from Furninha Cave in left lateral view. Scale bar is 25 mm. b) PCA of the skull of several Iberian brown bears.

The left hemimandible GFP-1328 is the most well-preserved specimen of mandible considered in this study, exhibiting only minimal loss of the coronoid process and the symphysis (Figure 5.39 a). The specimen displays characteristics consistent with those observed in *U. arctos*, as evidenced by both dental and skeletal features. The mandibular corpus is relatively straight (albeit exhibiting a slight sigmoidal curvature) and lacks the dorsoventral curvature observed in *U. spelaeus*. The diastema is of moderate length and contains the alveoli of the p1 and p3. The m2 lacks a pronounced constriction at its midpoint, while the m3 also lacks the characteristic lingual notch, both of which are features typical of the morphology observed in cave bears. The pterygoid muscle insertion is well-defined and pointed, as observed in brown bears, in contrast to the rounded appearance seen in cave bears (Villalba de Alvarado, Prat-Vericat, et al., 2024). Metrically, this mandible (and others from Furninha) are distinctive due to the relatively modest dimensions of the mandibular condyles, which contrast with the augmented width and height of the mandibular corpus in comparison to any Holocene or modern brown bears considered (Figure 5.39 b-c).

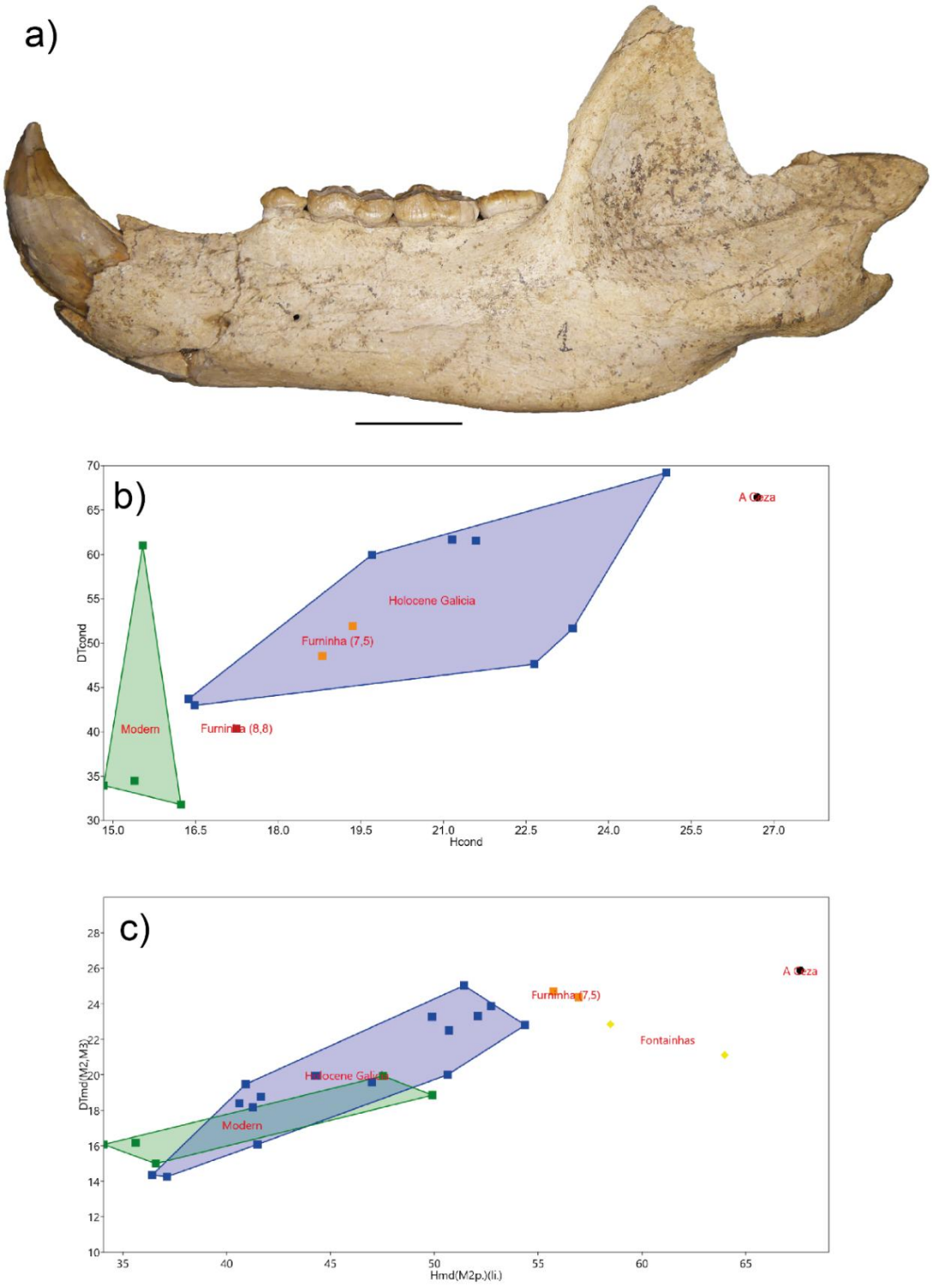


Figure 5.39 — a) Left hemimandible of brown bear from Furninha Cave in labial view. Scale bar is 25 mm. b) Biplot of the height and diameter of the mandibular condyle of Iberian brown and cave bears. c) Biplot of the height of the mandibular ramus and its diameter of several Iberian brown and cave bears.

As for axial postcranial remains, several atlases and axes have been discovered, the majority of which are too damaged to undergo a thorough measurement analysis. However, one axis (Figure 5.40) exhibits relatively large overall dimensions, comparable to those of female cave bears from Galicia.



Figure 5.40 — a) Left hemimandible of brown bear from Furninha Cave in labial view. Scale bar is 25 mm. b) Biplot of the height and diameter of the mandibular condyle of Iberian brown and cave bears. c) Biplot of the height of the mandibular ramus and its diameter of several Iberian brown and cave bears.

From the forelimb, the scapulae (Figure 5.41 a) are in a similar situation to the axes, with few specimens complete enough to take measurements. Nevertheless, those that are complete enough are larger than modern and most of the Holocene brown bears from Galicia, with a similar size to the smallest cave bears from Eirós (Figure 5.41 b-c).

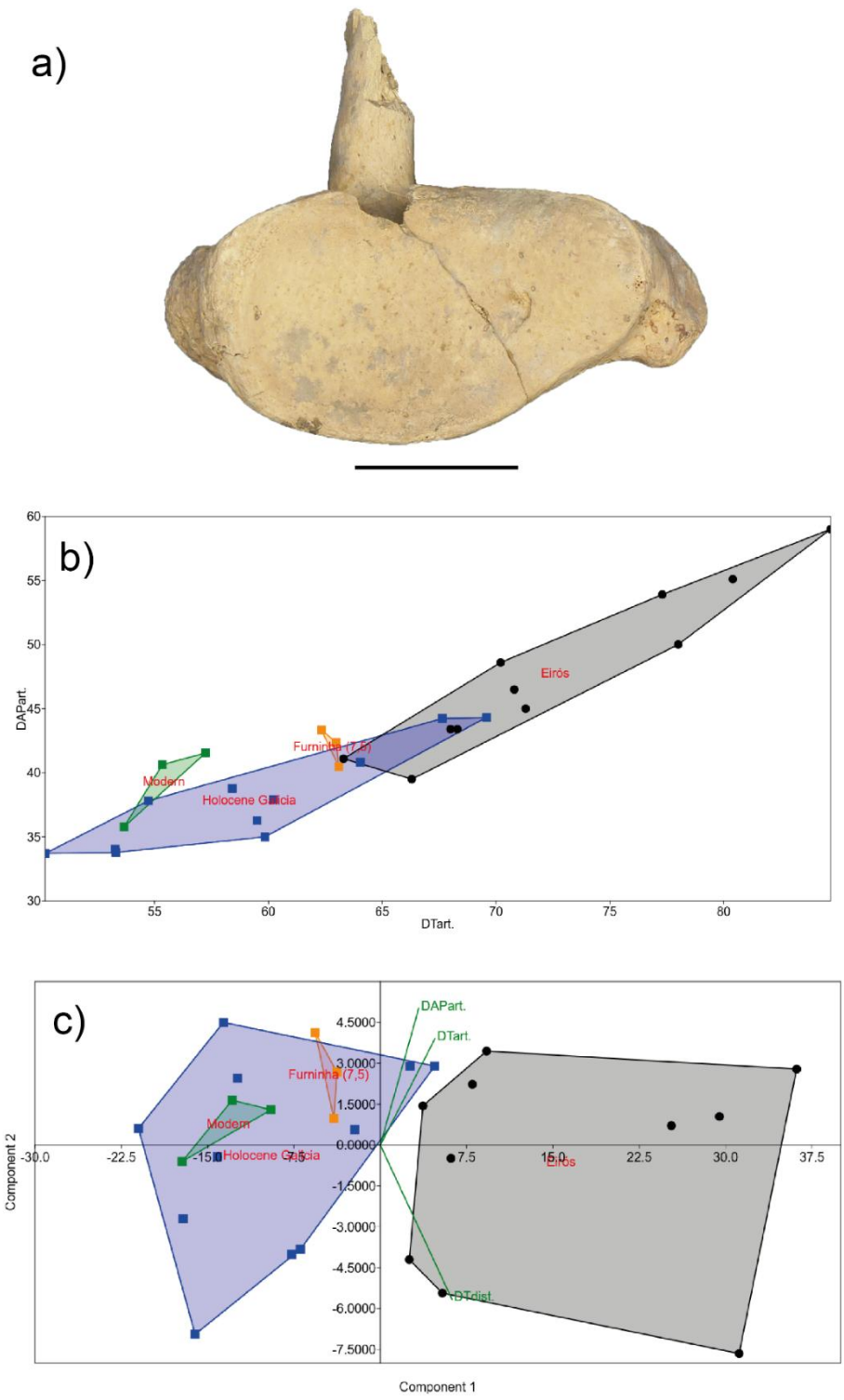


Figure 5.41 — a) Scapula of brown bear from Furninha Cave in distal view. Scale bar is 25 mm. b) Biplot of the height and diameter of the scapular articular surface in several Iberian brown and cave bears. c) PCA of the scapula of Iberian brown and cave bears.

The anterior long bones from Furninha Cave are not as complete as those from Fontainhas Cave; however, but they are still among the most complete in the sample (Figure 5.42). The specimens originate from individuals at different stages of development and are likely to represent both sexes. Some of the bones are severely damaged, which is likely the result of feeding behaviors by hyenas, the most common carnivore at Furninha Cave (Brugal et al., 2012). Of particular interest is the distal humerus GFP-1379 (Figure 5.42 a) which has been labeled as *U. spelaeus*. The supracondilar lateral crest is damaged, but it is possible to discern that it is relatively thin in comparison to the round and thick crest observed in cave bears. Morphologically it is more closely aligned with brown bears (Torres Pérez-Hidalgo, 1984).

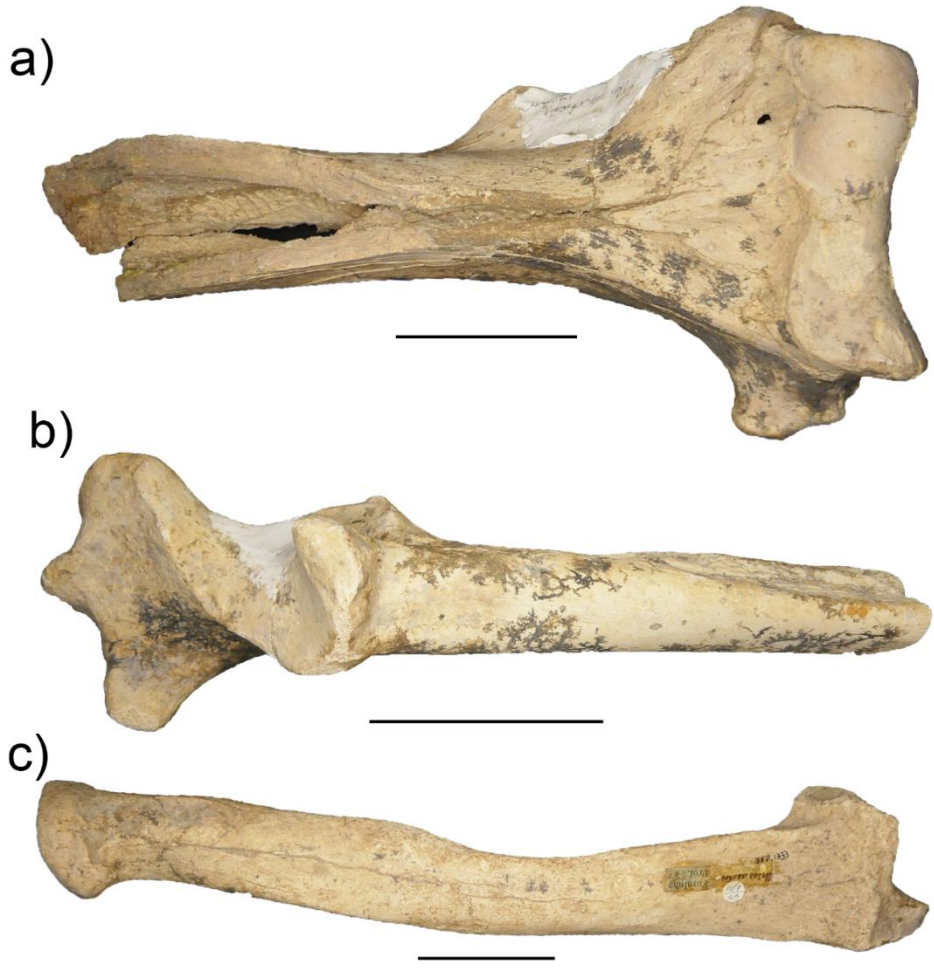


Figure 5.42 — a) Distal left humerus from Furninha Cave in anterior view, with the label "U. spelaeus" on it. b) Proximal left ulna from Furninha Cave in medial view. c) Left radius from Furninha Cave in anterior view. Scale bars are 50 mm.

Metrically (Figure 5.43), the observed characteristics of long bones are analogous to those observed in metapodials. The absolute dimensions of the specimens from Furninha and Fontainhas are larger than those of the bears from NW Spain. It is noteworthy that they also appear to exhibit ontogenetic trajectories comparable to those of cave bears, at least for certain bones (Figure 5.20 c). However, when additional measurements are incorporated they do not occupy the same morphospace as cave bears (Figure 5.43 b).

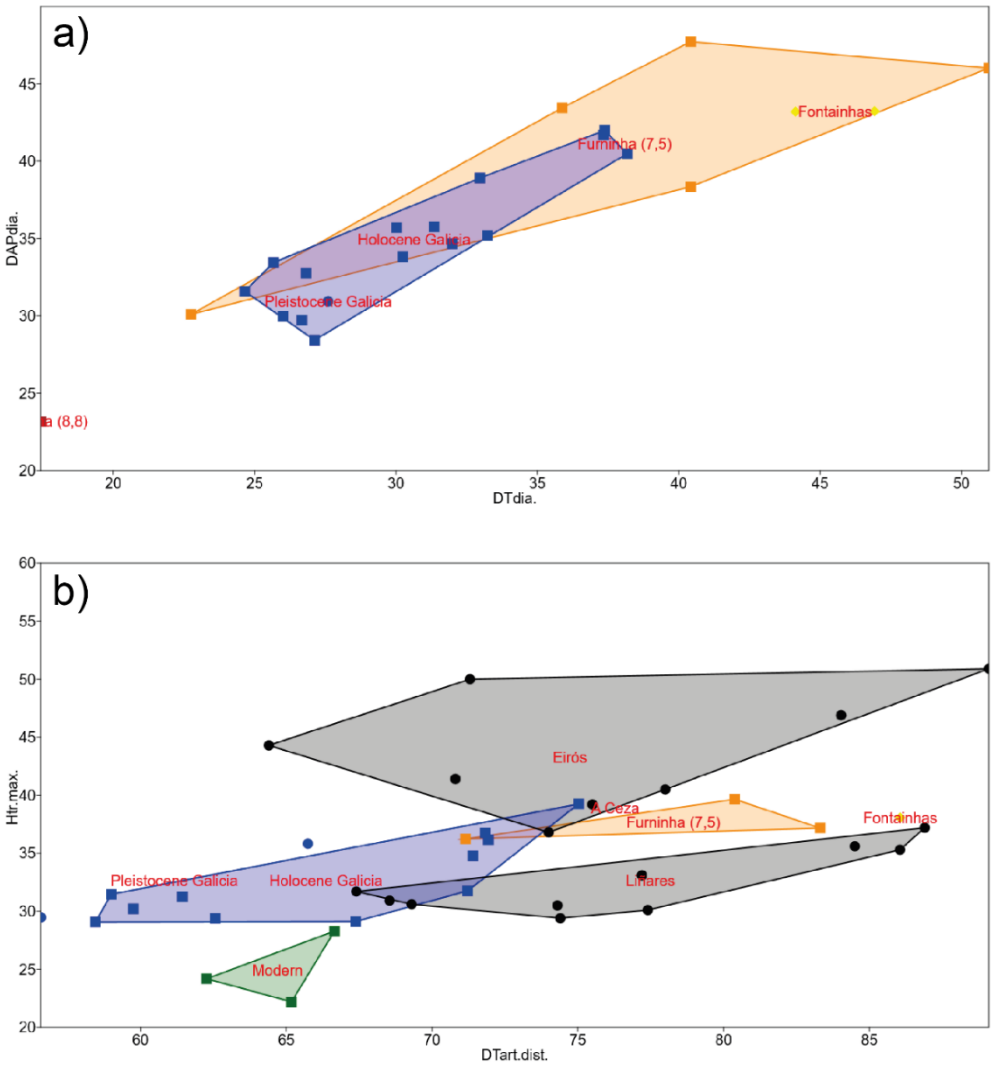


Figure 5.43 — a) Biplot of the minimum mediolateral and anteroposterior diameters of the diaphysis of the humerus of diverse Iberian brown bears. b) Biplot of the mediolateral articular diameter and diameter of the trochlea of the humerus of diverse Iberian brown and cave bears.

Metrically bones from the carpus (Figure 5.44) exhibit similarities with those of Holocene bears from NW Spain (Figure 5.22 b-c).



Figure 5.44 — a) Left pisiform of brown bear from Furninha Cave in dorsal view. Scale bar is 25 mm.

Both morphologically (Figure 5.45) and metrically (Figure 5.46) the posterior long bones of Furninha follow the same pattern as the anterior long bones: presence of specimens of different ontogenetic stages and possible sexes, being not as complete as those from Fontainhas, but still relatively complete, even when they present taphonomic marks that will be further discussed later.



Figure 5.45 — a) Proximal left femur from Furninha Cave in anterior view. b) Right tibia from Furninha Cave in anterior view. c) Distal left fibula from Furninha Cave in lateral view. Scale bars are 50 mm.

Despite all the considerable heterogeneity of the posterior appendicular remains from Furninha, a common feature can be identified even without taking into consideration the morphometric data: in comparison to the remains from other Portuguese and Galician caves, they are shorter or the same length but noticeably more robust (Figure 5.47). Additionally, while not reaching the extreme levels observed in cave bears, the muscular insertions on the epiphyses are notably well-defined, even in instances where said epiphyses have been partially gnawed (Figure 5.47).

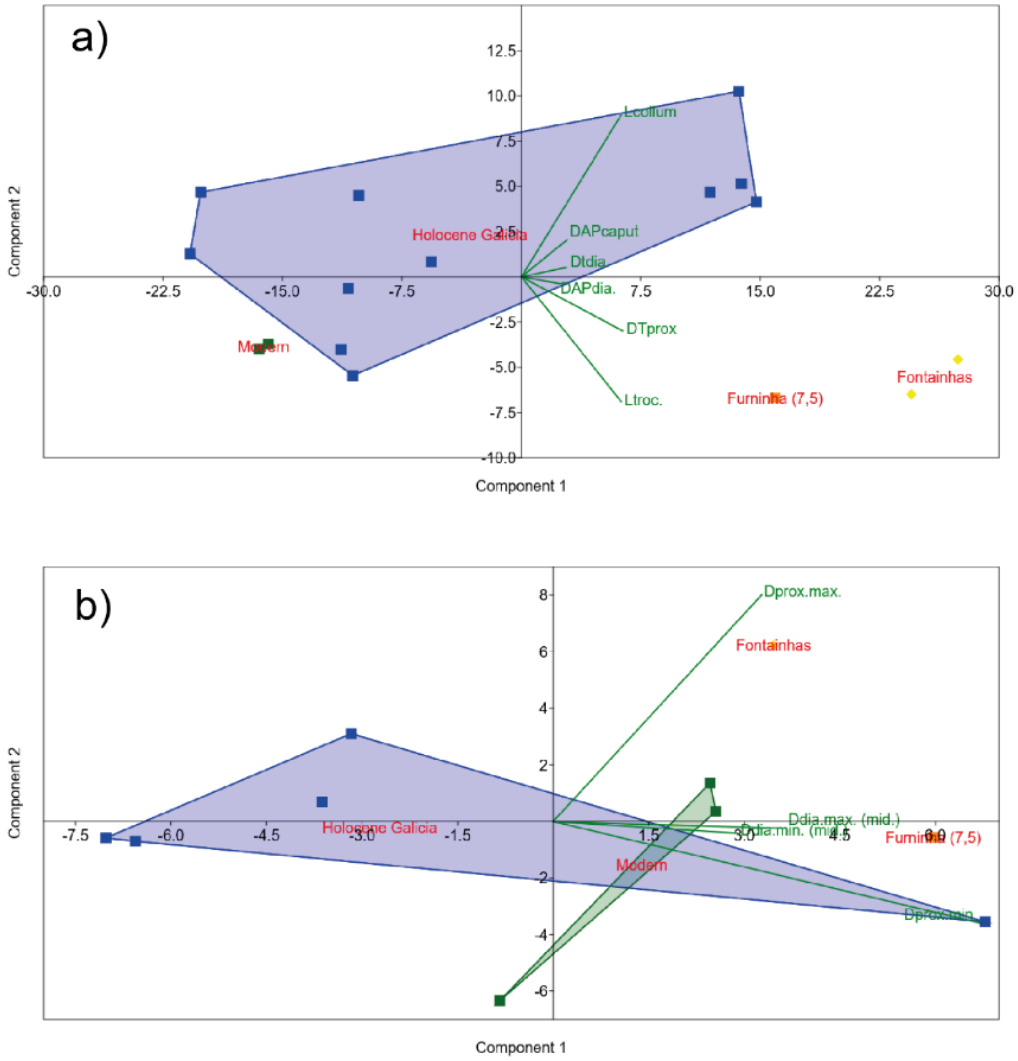


Figure 5.46 — a) PCA of the femur of diverse Iberian brown bears. d) PCA of the fibula of diverse Iberian brown bears.

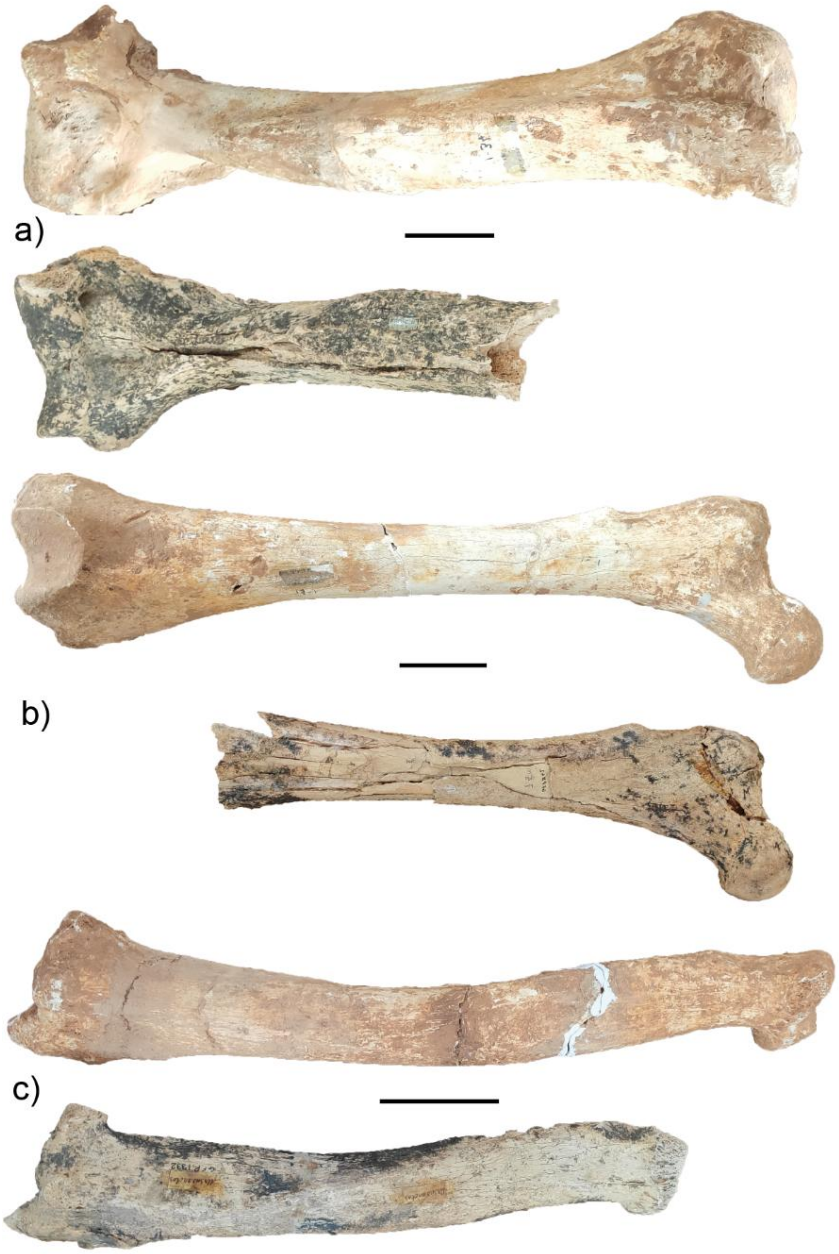


Figure 5.47 — Morphological comparison of long bones from bears from Fontainhas and Furninha caves: a) Humerus. b) Femur. c) Radius. Scale bars are 50 mm.

Despite the large quantity of long bones available for study, few of them are complete enough to apply most of the equations for inferring the body mass. Utilizing the equation proposed by Viranta (1996), it was feasible to ascertain the body mass of 16 specimens of Furninha, with recorded values ranging from 163.11 kg to 493.38 kg and an average of approximately 240 kg. The equation proposed by Christiansen (1999) was employed to calculate the masses of five specimens, with a minimum of 175.49 kg and a maximum of 451.73 kg, resulting in an average weight of 358.42 kg. Two of the specimens enabled a direct comparison of the

estimates obtained by the two methods: femur GFP-1142 yielded an average weight of 338.96 kg, while humerus GFP-1130.7 provided an average weight of 336.06 kg. It can therefore be surmised that the average measurement for the site of Furninha would be 337.51 kg.

The measurements of the tarsus of the bears from Furninha cave follow a very similar pattern to that of the carpus, with similar measurements of the Pleistocene Furninha bears to those of Holocene NW Spain (Figure 5.48).

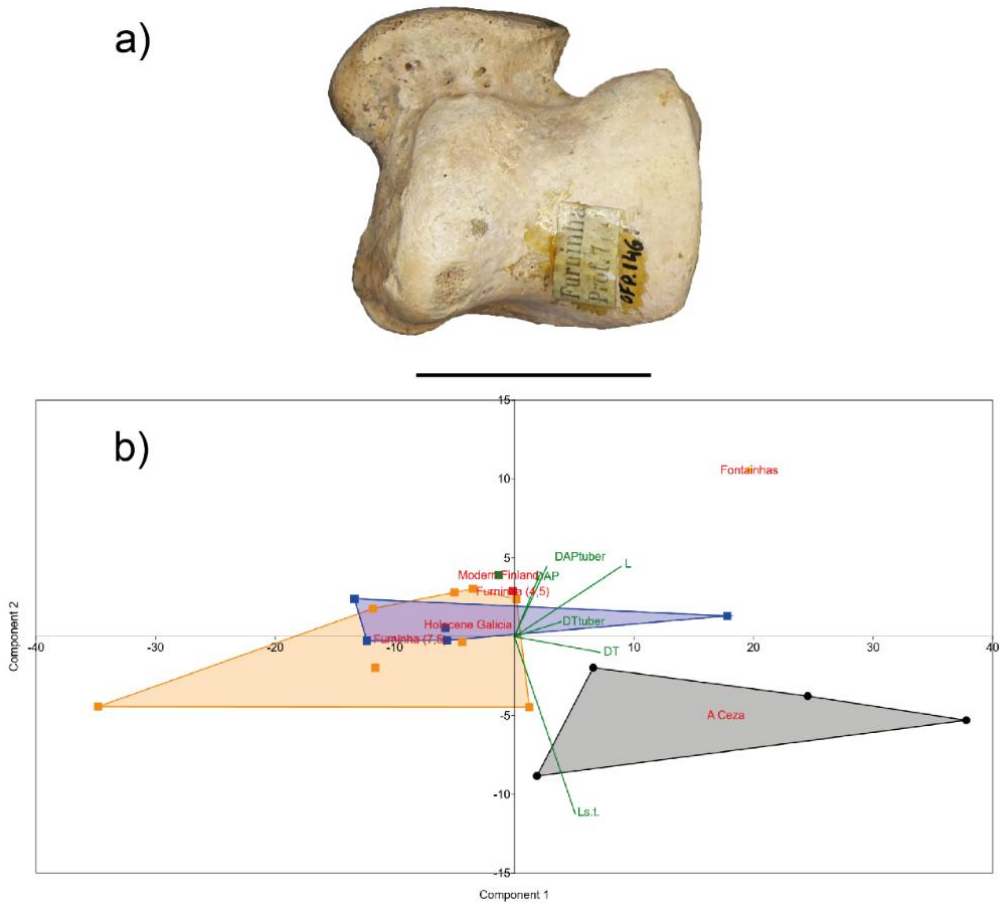


Figure 5.48 — a) Right astragalus of brown bear from Furninha Cave in dorsal view. Scale bar 25 mm. b) PCA of the calcaneus of several Iberian brown and cave bears.

The metapodials (Figure 5.49) have been demonstrated to reflect the taxonomy of bears and they are a straightforward way to metrically differentiate among different species of the family (Baryshnikov & Puzachenko, 2017; Estraviz-López et al., 2021). The Furninha Cave site contains measurable specimens from all the metapodial bones. Some specimens display severe pathological conditions, the specifics of which will be discussed in greater detail later. The majority of the specimens exhibit a distinctive yellowish-chestnut patina, with black venations and the typical morphology of brown bears.

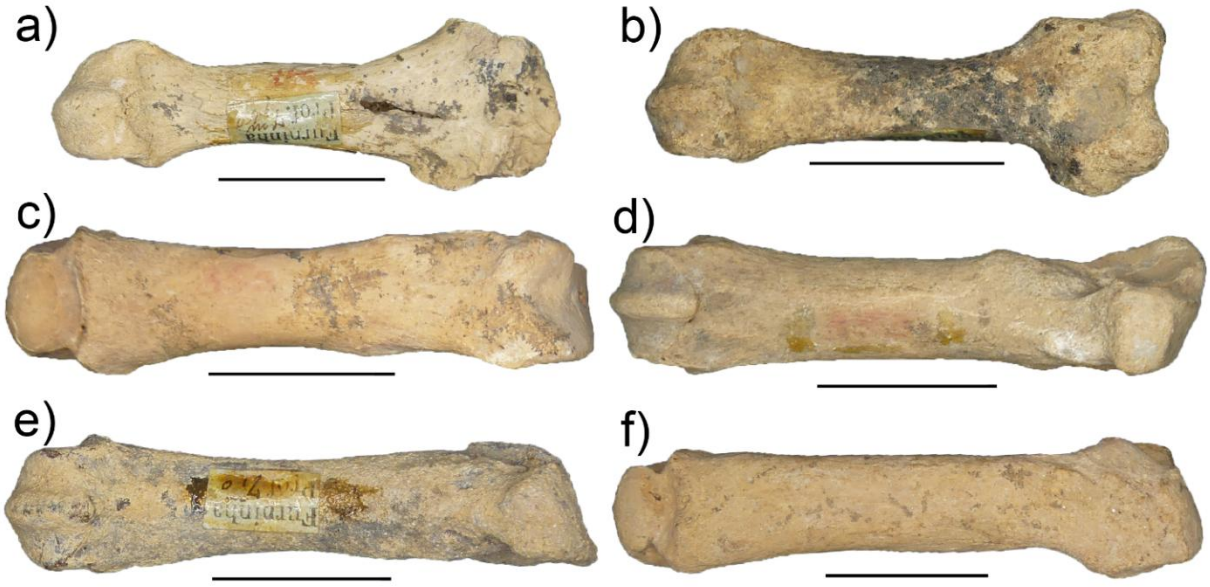


Figure 5.49 — a) First metacarpal from Furninha Cave in ventral view. b) First metatarsal from Furninha Cave in ventral view. c) Second metacarpal from Furninha Cave in dorsal view. d) Third metatarsal from Furninha Cave in ventral view. e) Third metacarpal from Furninha Cave in ventral view. f) Fourth metatarsal from Furninha Cave in dorsal view. Scale bars are 25 mm.

Metrically, the metapodials from Furninha align with those of the brown bears, yet, exhibit a closer affinity with the morphospace of cave bears than other brown bear specimens. Thus, they present larger transverse and anteroposterior diameters of epiphyses and diaphysis than the other brown bears, either from different Portuguese localities, Holocene NW Spain, and modern specimens (Figure 5.50).

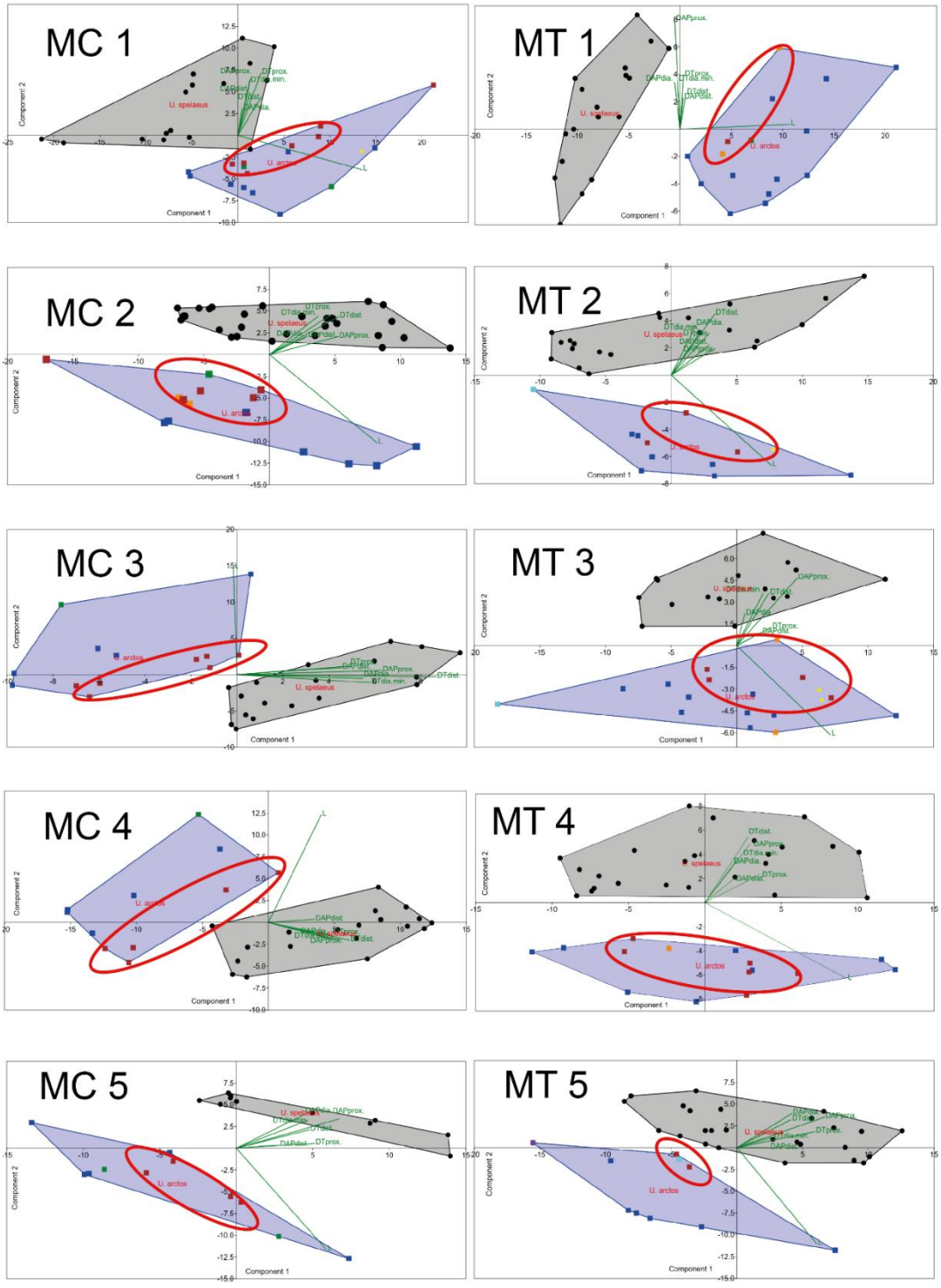


Figure 5.50 — PCAs from the metapodial bones of a diverse set of Iberian brown and cave bears. *U. spelaeus* are black dots. *U. arctos* are squares of different colors; green for modern bears, blue for Holocene bears from NW Spain, orange, brown and light blue for bears from Furninha Cave and yellow for bears from Fontainhas Cave. Red ellipses are marked around the area occupied by the majority of the specimens from Furninha Cave.

These characters of the metapodials are clearly represented by the robustness index. This index compares the mediolateral distal diameter of the metapodial with the total length of the bone. The metapodials of cave bears are markedly more robust than those of brown bears. However, it is noteworthy that this index is higher (on average) for the Furninha bears than in other brown bears on seven of the 10 metapodials (Figure 5.51).

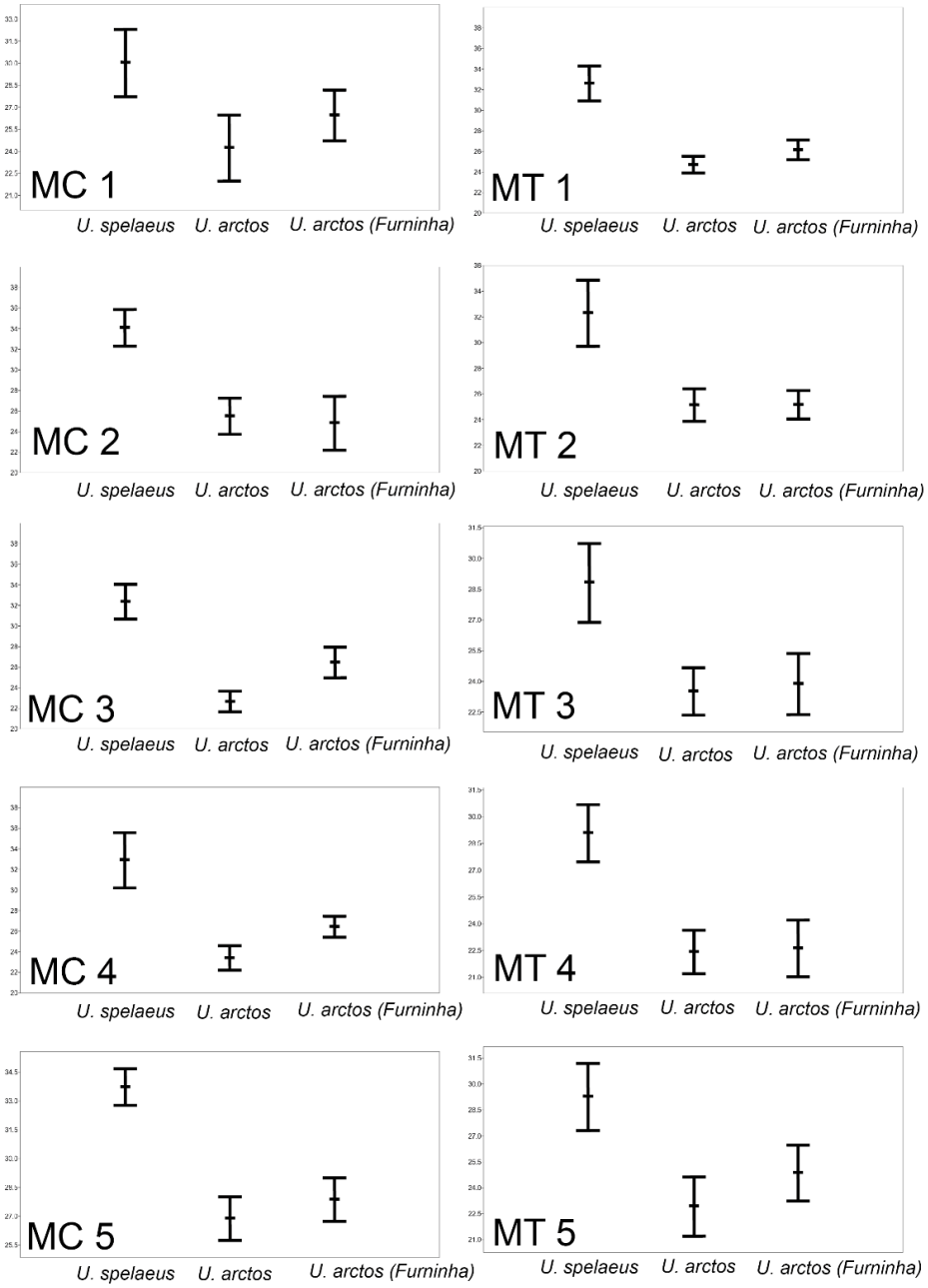


Figure 5.51 — Robustness index (Length/Distal mediolateral diameter) for the metapodial bones of Iberian *U. spelaeus*, *U. arctos* (Modern bears, Holocene remains from NW Spain and Portuguese Pleistocene remains from other caves) compared with *U. arctos* from Furninha Cave. The whiskers on the graphs mark the standard deviation from the mean for each sample.

The most frequently occurring body parts in the assemblage of Furninha after the dentognathic remains are the phalanges (Figure 5.52). The first phalanges exhibit the full range of sizes and morphologies typically observed in brown bears (ex. relatively slender diaphyses compared with the epiphyses), including a few pathological specimens (Figure 5.52 a). Metrically, it is noteworthy that the specimens from the deeper layer of 8.8 m exhibit greater robustness than those from the 7.5 m layer. There is no morphometric overlap between the two groups (Figure 5.7 b), although both of them are situated on the side with relatively robust phalanges, exhibiting a degree of overlap with the variability observed both in cave bears and modern bears. The specimens in question are shorter than those from Fontainhas Cave and longer than numerous others from NW Spain, Caldeirão, and the Middle Pleistocene specimens from Postes Cave.

The second phalanges (Figure 5.52 b) exhibit a comparable pattern to the first ones, although the Holocene specimens from NW Spain are markedly larger than any others in the sample (Figure 5.7 c). It is noteworthy that, despite this, both the Holocene and Pleistocene bears from NW Spain are still more slender than the average bears from Furninha.

The third phalanges (also called claws) typically exhibit a relatively straight ventral profile, with a moderate dorso-ventral height (Figure 5.52 c). These are typical characters of the brown bear's claws, which differ from those of cave bears in that they are much more curved and dorso-ventrally tall. Some of the claws from Furninha Cave belong to juveniles, while others exhibit evidence of having been digested by carnivores. Metrically (Figure 5.3 a), the third phalanges exhibit further differentiation between the specimens from the two layers of Furninha, with the observed pattern now differing from that seen in the first phalanges. The specimens from a depth of 7.5 m are of a greater thickness than those from 8.8 m.

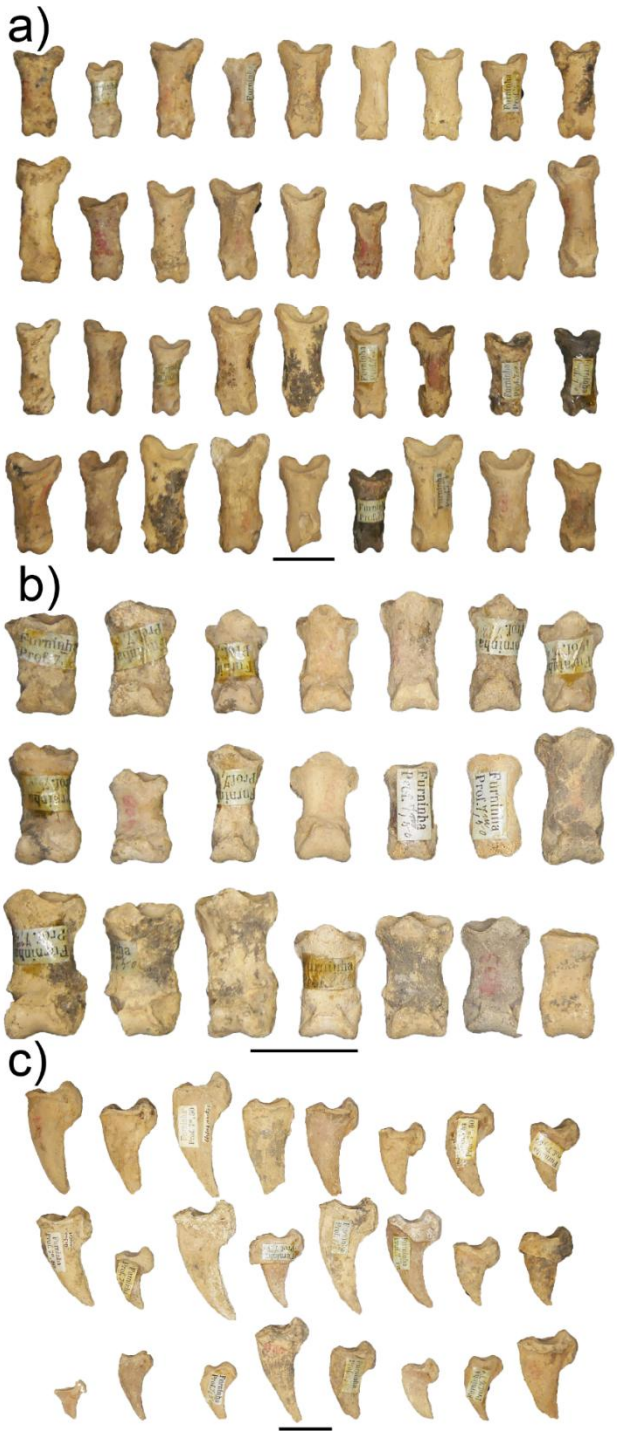


Figure 5.52 — a) Selection of some of the first phalanges from Furninha Cave in dorsal view. b) Selection of some of the second phalanges from Furninha Cave in dorsal view. c) Selection of some of the third phalanges from Furninha Cave in lateral view. Scale bars are 25 mm.

5.3.6.1 Prevalence of pathological conditions in the bear remains from Furninha

Another noteworthy feature of the bear remains from Furninha is the prevalence of pathological conditions (Figure 5.53).

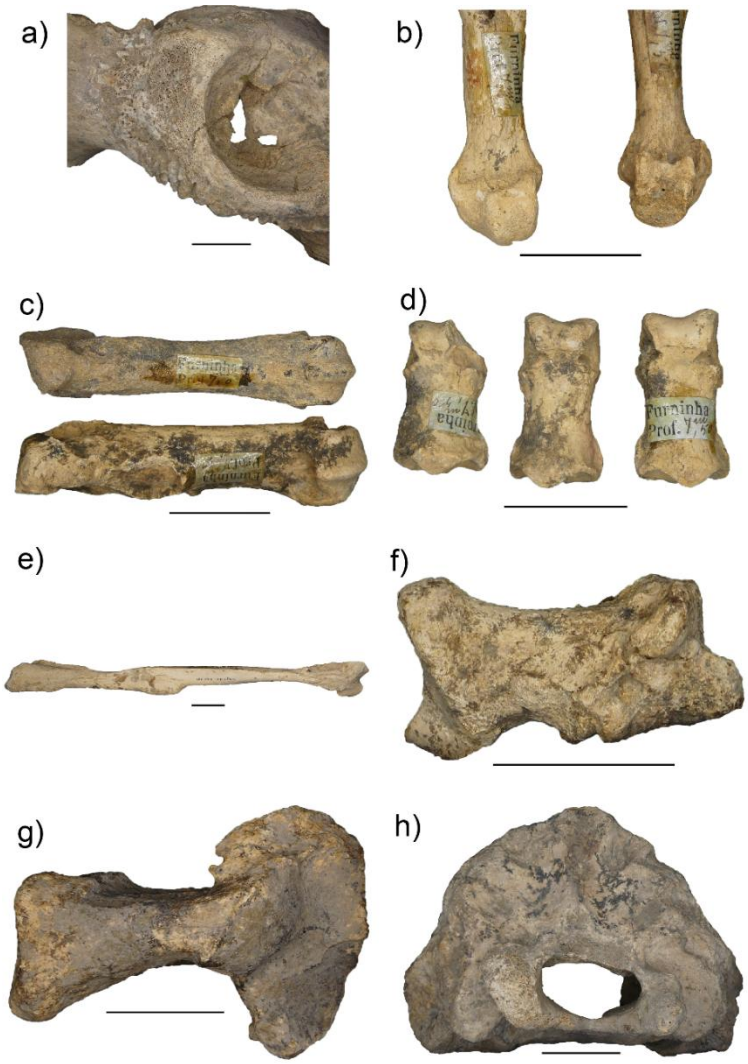


Figure 5.53 — a) Detail of the right acetabulum of a brown bear pelvis from Furninha Cave in lateral view showing pathological bone overgrowths. b) Comparison of the distal part of the first metacarpal of two brown bears from Furninha Cave in dorsal view. Note the pathological bone overgrowths on the right one. c) Comparison of the third metacarpal of two brown bears from Furninha Cave in ventral view. Note the pathological bone overgrowths on the bottom one. d) Second phalanges of brown bears from Furninha Cave with pathological bone surfaces in dorsal view. e) Fibula of brown bear from Furninha Cave in medial view, showing a diaphysis bone growth that might represent a healed fracture. f) Left pisiform of brown bear from Furninha Cave in dorsal view, showing pathological bone growth in the tubercle. g) Left calcaneus of brown bear from Furninha Cave in dorsal view, showing pathological bone overgrowth. h) Detail of the occiput, cranial condyles, and foramen magnum of a brown bear skull (GFP-1338) from Furninha Cave in posterior view. Note the asymmetry between the condyles and the overall shape of foramen magnum, tilted towards the right. Scale bars are 25 mm.

The majority of the pathological bones originate from the 7.5 m deep layer and exhibit a comparable patina of black venation on the surface, as well as the same type of bone overgrowths (exostosis) and rugose bone surfaces (Figure 5.53). These features of the bones are consistent with the hypothesis that they originated from the same individual who was severely affected by a disease and whose bones later suffered the same diagenetic processes. The skull GFP-1338 (Figure 5.53 h) displays a comparable patina to the aforementioned bones, suggesting that it might belong to the same bear too. However, it does not exhibit the pathological overgrowths observed in the other bones. The condyles and foramen magnum exhibit a deformed and tilted asymmetry, directed towards the right ventral aspect. Finally, a fibula (Figure 5.53 e) is observed to present a lump or relatively regular bone callus or growth in the middle of its diaphysis. The entire dorsoventral midline along the bone appears to be displaced from its centerline, both proximally and distally from the aforementioned lump (Figure 5.53 e).

5.3.6.2 Notable taphonomic features of the Furninha Cave collection

The final noteworthy features of the Furninha Cave collection, are those bones that present features that can provide further insight into the taphonomy of the site (Figure 5.54).

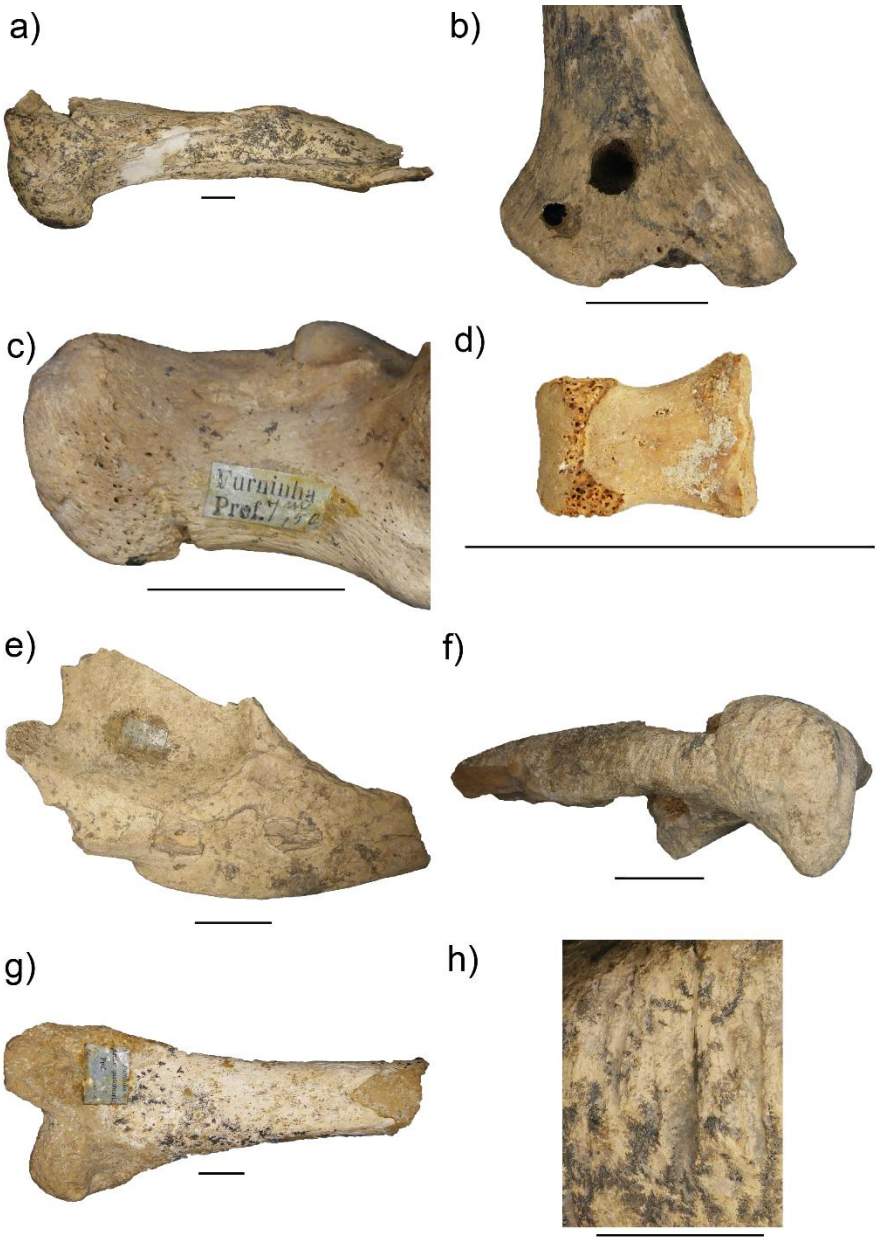


Figure 5.54 — a) Proximal humerus of brown bear from Furninha Cave in lateral view, presenting gnawing marks. b) Distal radius of brown bear from Furninha Cave in anterior view, bearing two deep pits on the bone. c) Detail of calcaneus of brown bear from Furninha Cave showing a deep cut on its ventral surface. d) Second phalanx of juvenile brown bear from Furninha Cave in dorsal view with surface bone texture and damage compatible with digestion. e) Partial mandible of brown bear from Furninha Cave in lateral view, showing two punctures on the lateral surface that collapsed the surface of the bone. f) Proximal ulna of brown bear from Furninha Cave in posterior view, showing gnawing marks on the surface of bone. g) Distal femur of brown bear from Furninha Cave in posterior view, showing the almost completely gnawed out condyles. h) Gnawing marks in the parietal of the skull of brown bear GFP-1338 from Furninha Cave. Scale bars are 25 mm.

A number of bones display deep pits, which appear to be isolated or in pairs, as observed in a distal radius and in a mandible (Figure 5.54 e). Furthermore, the skull GFP-1338, along with several distal femora epiphyses, proximal ulnae, and proximal radii epiphyses also exhibit the gnawing marks that were previously identified by Brugal et al. (2012). A small number of phalanges exhibit bone surface textures that are compatible with partial digestion. Additionally, the least common taphonomic feature observed in the brown bear bones from Furninha is the presence of several deep scratches, which resemble those seen in the same bone from Fontainhas. These scratches are particularly evident in the calcanea bones (Figure 5.54 c).

5.4 Discussion

5.4.1 Contextualizing Pleistocene Portuguese brown bears: observations from their sites

5.4.1.1 Oliveira Cave

The specimens from Oliveira Cave are well dated and exhibit either average (tibia O16-766) or large (third phalanx O17-226) dimensions in comparison to the remaining specimens under consideration. It is not possible to derive much information from them alone, although a number of other specimens are currently under study, which will contribute to a greater understanding of the paleobiology of the bears from this locality and contextualize the broadly coeval bears from Furninha (Angelucci et al., 2023). Given their age, it is anticipated that they will exhibit a comparable tendency in size to that observed in Furninha Cave.

5.4.1.2 Escoural Cave

The specimens from the Escoural Cave lack a precise chronological attribution, although they are of interest from both a metric and a morphological perspective. The m1 Escral121966 is among the largest brown bear molars found in the Iberian Peninsula, and also exhibits a particularly broad and triangular shape. The two m2s EscGalEntrad1964 and EscGal2Tal7C1 exhibit notable differences from one another, with EscGal2Tal7C1 being morphologically and metrically different from most other brown bear molars due to its smooth surface. They may originate from very different time periods, but due to the lack of a clear stratigraphic position within the cave is not possible to verify this hypothesis. These particularities, when considered in conjunction with the geographical location of the cave of Escoural in the heart of Alentejo, distant from other localities previously investigated in this study, present an intriguing avenue

for future research into bears from this site. This is particularly pertinent given the recent excavation campaigns at the site (Cobo-Sánchez et al., 2024).

5.4.1.3 Caldeirão Cave

The material from Caldeirão Cave is well contextualized, with the majority of it estimated to date from approximately 27.000 YBP. It was not possible to review some of the material mentioned by Davis (2002). The measured specimens are of relatively small size in comparison to others presented in this study. They are comparable in size to the average of those observed in both the Pleistocene and Holocene periods in NW Spain. This may be associated with the challenging circumstances during the MIS 2, nearing the LGM (López-García et al., 2020). Alternatively, it may be linked to a closer genetic affinity with the Holocene bears of the NW Iberian Peninsula than with contemporaneous Portuguese bears. It is not possible to provide definitive proof or disproof of the hypothesis put forward by Davis (2002) that Caldeirão acted as a hibernation den for these bears. Despite the observation of senile teeth in the cave, these could not be subjected to analysis in the present study. Furthermore, no specimens displaying clear juvenile characteristics (e.g. unfused epiphyses, deciduous teeth, extreme small size) could be located.

5.4.1.4 Serra de Molianos

The precise age of the specimens from Serra de Molianos remains unknown, as does the precise location of the cave itself. The material is morphologically and morphometrically consistent with the morphospace of the Holocene and Pleistocene material from NW Spain, suggesting that the age of the site is not "Early Würm" or roughly coeval to Furninha as proposed by Torres Pérez-Hidalgo, (1979). Instead, it may be of a similar age to MIS 2 layers Fa to Ja from Caldeirão. Additionally, the occurrence of *Stephanorhinus hemitoechus* Falconer, 1859 a species which appears to be confined to the interval between 30.000 and 20.000 YBP in Portugal, may provide further corroboration for this hypothesis for the age of the site (Cardoso, 1993).

5.4.1.5 Fontainhas

It seems probable that the Fontainhas specimens originate from three different individuals. In addition to the juvenile specimens, the dentognathic remains are consistent with those of exceptionally large individuals. The most complete individual is likely to be the largest individual of *U. arctos* known from the Iberian Peninsula. It also exhibits two pathologically fused thoracic vertebrae, which may represent a case of congenital block vertebra. This is similar to

that observed in an Iberian cave bear (Fuentes-Sánchez et al., 2019). The only absolute dating of the site is of 22.700 YBP (Cardoso, 1993). It is noteworthy that nor the age nor the distance to the Caldeirão site are significantly different, yet the metrical analysis reveals striking differences between the two sets of bones: The remains from Fontainhas Cave are notably larger. The taphonomic analysis of the remains indicates that they have not been subjected to the gnawing marks of other bears that have been studied on this work. However, the calcaneus exhibits some deep scratches that are similar to those observed in other calcanea from Furninha Cave (Figure 5.54 c). These scratches could be interpreted as either anthropic cut marks or effects of trampling.

5.4.1.6 Furninha cave

The Furninha Cave Collection as a Hibernation Den

The Furninha Cave collection represents the most extensive assemblage of brown bear fossils known from the Iberian Peninsula. It includes a significant number of juvenile and senile specimens, which collectively reinforce the argument that Furninha functioned as an hibernation den (Stiner, 1998).

Taphonomic Complexity and Carnivore Marks in the Furninha Assemblage

Taphonomically, the assemblage is quite complex. In their study, Brugal et al., (2012) noted that the gnawing marks on the skull GFP-1338 were of a size that could not be attributed to hyenas, as they were too large. Instead, they proposed that the deep marks in the partial mandible from box 1325 (Figure 5.54 e) were caused by two molars of a bear. It is possible that the space between the two pits on the mandible may have been caused by the canines of a carnivore, rather than gnawing with the carnassial as is evident in other bones. The canines may have broken the surface of the bone and then withdrawn. This may provide an explanation for the presence of deeper marks on some other bones from Furninha. Slightly similar marks have been produced by hyaena canines on juvenile bones that did not break (Diedrich, 2012). As with the Fontainhas assemblage, the presence of deep scratches may indicate the impact of trampling and/or anthropogenic cut marks (Figure 5.54 c) in a few specimens.

Pathological Features in the Furninha Cave Fossils

It is imperative to highlight the pathological bones from Furninha Cave. A minimum of 12 bones (including the skull, pelvis, fibula, calcaneum, pisiform, first and third metacarpals, two first phalanges, and three second phalanges) exhibit pathological characteristics. This number is still below the percentage of those detected in cave bear populations (Marciszak et al., 2024). The more common pathologies (present in all pathological bones except skull and

fibula) are exostoses, which are distributed throughout the whole surface of the bone. They are distinct from the usual localized exostoses that are produced by trauma (Rothschild & Diedrich, 2012). The fibula GFP-1624 presents a lump that is compatible with a traumatic bone fracture and with the bone subsequently undergoing healing. It is of interest to note that this kind of traumatic injury in cave bears typically occurs on the forelimbs, rather than the hindlimbs (Marciszak et al., 2024).

In addition to the perimortem gnawing marks, the skull GFP-1338 displays a congenital or developmental pathology in its occipital region, exhibiting marked asymmetry. The asymmetry affecting the chondrocranium is distinct from that observed in modern sea otters, with a tendency to occur centered in the orientation of the sagittal crest (Roest, 1993). The closest parallel in the Iberian fossil record are the developmental anomalies present on the *Canis (Xenocyon) lycaenoides* Kretzoï, 1938 skull VM-7000 from the Early Pleistocene of Venta Micena (Palmqvist et al., 1999; Bartolini-Lucenti et al., 2021).However, the anomalies of GFP-1338 are far less extreme, and it is currently unknown how much they affected the not-preserved anterior part of the cranium and dentition. One of the closest examples to the observed pathologies (asymmetric foramen magnum and condyles tilted to the right) would be those present not in a carnivore, but in a domestic four-horned lamb affected by occipital condylar dysplasia that did not survive long after birth (A. M. Lee et al., 2017). The available data indicate that the affected individual reached adulthood and was able to survive independently. However, the specific pathological process that resulted in the observed cranial features remains uncertain, and further investigation is necessary to elucidate this.

Morphological Traits of Furninha Bears

The specimens from Furninha exhibit not only larger specimens in absolute dimensions than those of Holocene and Pleistocene NW Iberia, but also remarkably robust bones, even when their measurements are surpassed in some parameters by the considerably slenderer Fontainhas bears. This characteristic general robustness and large size contrast to those specimens from Caldeirão and Serra de Molianos, which are of a younger age. This makes them somewhat convergent in shape with cave bears. This suggests that this robust morphotype of brown bears might have been occupying the ecological niche of the cave bear in the southwestern Iberian Peninsula during the initial half of the Late Pleistocene, a period during which this other species is almost entirely absent from the area (Ruiz et al., 2012). The characteristics exhibited by this population are almost more consistent with those of slender cave bears than brown bears. A relatively small population size may have resulted in significant homozygosity, which could have contributed to the pathological condition observed in GFP-1338 (Edwards et

al., 2013). Additionally, the fidelity to the same caves (as observed in cave bears) may have resulted in the extensive accumulation of bones from Furninha Cave (Fortes et al., 2016).

5.4.2 Body size evolution of brown bears in western Iberia.

The general trend of size reduction, observed not only in bears, but in numerous European Pleistocene mammals, is a well-documented phenomenon (Kurtén, 1965). However, the precise timing and intensity of this phenomenon vary between different clades. For example, while the bison reached its maximum size during the latter part of the Middle Pleistocene (Sorbelli et al., 2021), the reduction in size of bears appears to have been more gradual, with a precipitous decline over the past 2000 years (García-Vázquez, 2015). It is noteworthy that in the Western Iberian Peninsula, the specimens from Postes Cave, which are Middle Pleistocene in age, are consistently comparable in size to modern bears. However, they are discernibly smaller in overall dimensions than the next older specimens in the sample, which are more than 100.000 years younger from Furninha Cave (Villalba de Alvarado et al., 2022). It has been possible to apply the body mass equations to these subjects, considering that such estimates are inherently susceptible to both intrinsic error and fluctuations in the weight of bears over time. Indeed, studies have demonstrated that the weight of bears can vary significantly from year to year (Stringham, 1990), with some individuals exhibiting a 50-kilogram difference even during the same season (Clevenger & Iraizoz, 1991). Height to the shoulder of bears could be a better approximation to the size of the animals, but studies about its inference from skeletal remains are lacking.

Utilizing the data provided by García-Vázquez, (2015) (see Methods section), it was possible to calculate the average mass of 22 femora and humeri from Holocene NW Spain, originating from eight different localities. It was also possible to add one Pleistocene specimen from NW Spain and two recent ones. Furthermore, the average measured weights of both female and male modern bears hunted in the Cantabrian mountains between 1957 and 1965 (Notario,

1964) and in the Pyrenees between 1848 and 1951 were incorporated (Couturier, 1954). The Portuguese bears were compared to this data (Figure 5.55).

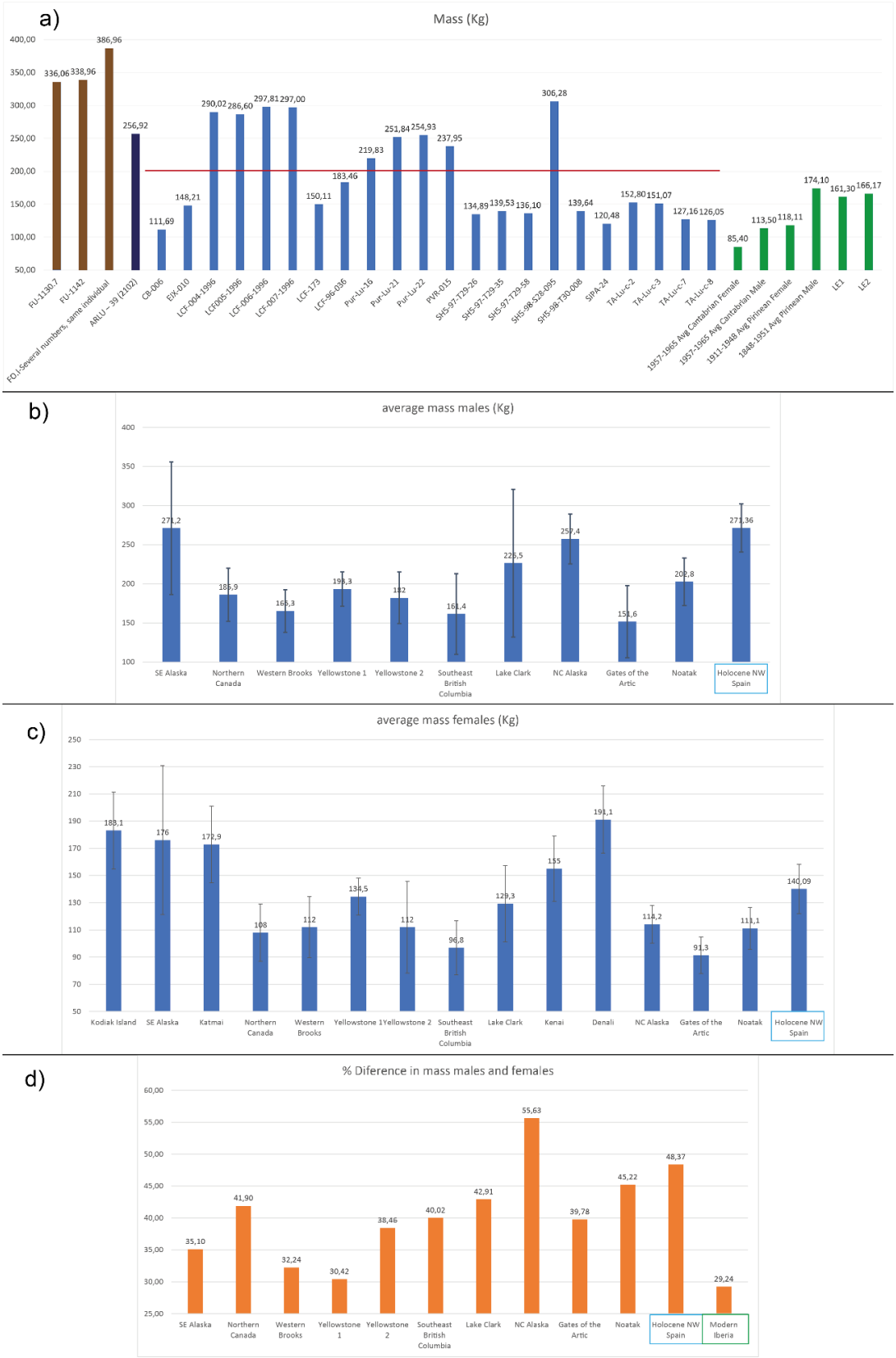


Figure 5.55 — a) Body masses of individual brown bears from Western Iberian Peninsula. Brown, Pleistocene of Portugal; dark blue, Pleistocene of NW Spain; light blue, Holocene NW Spain; green, modern Iberian bears. Red bar at 200 kg mark separate males from females of Early Holocene population from NW Spain. b) Average masses of male brown bears from different North American populations compared with the average weight of male brown bears from Early Holocene NW Spain. Whiskers indicate the standard deviation. c) Average masses of female brown bears from different North American populations compared with the average weight of female brown bears from Early Holocene NW Spain. Whiskers indicate the standard deviation. d) Percentage of weight difference among average male and female bears from different North American populations compared with brown bears from Early Holocene NW Spain and modern Iberian bears.

The average weight of the modern Iberian bears, is 143.8 kg for males and 101.75 kg for females, when the values of the Pyrenean and Cantabrian populations are averaged. Considering the extensive dataset pertaining to the early Holocene bears of NW Spain, it is feasible to put forth a weight distribution for both female and male bears. The female bears of this population appear to have a mean body mass of less than 200 kg, with a minimum of 111.69 kg and a maximum of 183.46 kg, resulting in an average of 140.09 kg for 13 females. The male bears appear to have a greater average weight than the females, with a minimum of 219.83 kg and a maximum of 306.28 kg, resulting in an average of 271.36 kg for the nine males. The mean between males and females is significantly different ($P < 0.001$, Kolmogorov–Smirnov).

This would entail a reduction in mass during the last millennia of approximately 50% in the size in males and 25% in females, which would also result in a reduction of sexual dimorphism, with females going from being approximately 50% smaller than males to just 30% smaller.

The modern-day Balkan bears from Slovenia and Croatia weight an average of 128 kg for females (115 kg in spring and 141 kg in autumn) and 245 kg for males. Those from Scandinavia (Norway and Sweden) also reach a size on average of 127 kg for females (96 to 158 kg) and 237 kg for males (201 to 273 kg) with a size dimorphism of around 50% (Swenson et al., 2023).

The modern-day North American grizzlies (depending of the population) exhibits a significant sexual dimorphism in body size, with males being on average 40% larger than females (Cameron et al., 2020). This dimorphism ranges from 55% to 30% of the mass depending of the population (Cameron et al., 2020). It can be inferred that the NW Iberian Early Holocene bears would have exhibited comparable dimensions and population structure to that of the large modern-day North American grizzly, as previously documented (García-Vázquez, 2015).

In the context of these data, the scattered Pleistocene specimens are notable for their exceptional size. The three Portuguese bears whose size could be reliably estimated all exceeded the 300 kg threshold, which represents the maximum estimated mass for the early Holocene bears of NW Iberia. The specimens whose size could not be calculated using of both equations for long bones (the less reliable data from Serra de Molianos), as well as the isolated Pleistocene specimen from Pleistocene NW Spain are estimated to weigh approximately 250 kg.

A timeline of the general evolution of brown bears in Western Iberia could be presented as follows: It is estimated that during the late Middle Pleistocene (~200.000 YBP), the first brown bears arrived on the Iberian Peninsula, either via the Pyrenees or Africa (García-Vázquez, 2015). These bears, represented by the Postes population (Villalba de Alvarado et al., 2022), were of a smaller size than the later Pleistocene brown bears. Following a lengthy interval without recorded fossils, we arrive at the initial half of the Late Pleistocene. During the MIS 5, we observe the emergence of a distinctive robust morphotype of bears from the Furninha Cave, which also exhibited particularly large dimensions (Cardoso, 1993). It is also possible that the specimens from Oliveira Cave (Angelucci et al., 2023) and, potentially, Escoural originate from bears belonging to the same population. However, a more extensive sample of specimens from these localities is required to substantiate this hypothesis and ascertain their degree of robustness. Subsequently, during the latter half of the Late Pleistocene, at the advent of MIS 2, we arrive to the bears from Caldeirão (Davis, 2002), Fontainhas Cave (Cardoso, 1993) and likely Serra de Molianos. Some of these bears exhibit significant divergence from those of Holocene NW Spain, though they are less robust than those from Furninha Cave. Nevertheless, some of these populations yielded specimens of considerable size, exemplified by those from Fontainhas Cave. These are among the largest specimens of brown bear in the fossil record, with sizes comparable to those of Siberian bears (F-2296, Indigirka River) and bears from the Urals (2079/244, Severnaya Cave) (Kosintsev et al., 2022). Notably, these bear specimens inhabited regions thousands of kilometers apart, yet exhibit similarities in morphology and size. This observation challenges the traditional view of the evolutionary history of the brown bear (Kosintsev et al., 2022). Following the advent of the Holocene, there were minor alterations in the size of bears during the initial phase of this period. However, some Pleistocene haplotypes were entirely extinct by the middle of the Holocene (García-Vázquez, 2015). This trend of initial relative stability in size at the start of the Holocene and abrupt decline from the Middle Holocene onwards has been verified in bears from slightly Eastern populations too, affecting with different degrees of intensity other mammals living with bears like the horse or the chamois

(Fidalgo et al., 2025). The range, population size, and overall size of the brown bear shrank markedly during the last few thousand years, with human pressure likely playing a significant role in this decline (Baeta Neves, 1967).

It would be beneficial for future research to contextualize these results at the molecular level, utilizing isotopic, genetic, and radiocarbon studies. This would enable an investigation in order to see how these bear populations have utilized resources and/or undergone genetic changes over time. A further line of research should concentrate on the paleopathologies identified in a number of bears remains. This will provide insights into their paleobiology and facilitate comparison with the remains of other brown bears. Finally, it would be beneficial to include additional data from other relevant localities including (but not limited to) Oliveira (Angelucci et al., 2023), Escoural (Cobo-Sánchez et al., 2024), Gruta Nova da Columbeira (Fernández-Laso et al., 2015), Lorga de Dine (Cardoso, 1995a), and Algar do Vale da Pena (Estraviz López & Mateus, 2019).

5.5 Conclusions

The present study encompasses the analysis of over 500 bear remains from six Portuguese Late Pleistocene localities. This extensive sample has yielded a plethora of biometrical and graphical data, which has led to the confirmation of the absence of *Ursus spelaeus* (cave bear) and *U. thibetanus* (Asian black bear) within the sample. Furthermore, this enabled us to update the inventory of specimens from these sites, as well as to contextualize the Portuguese Pleistocene brown bears within their geographical and temporal context. Additionally, we were able to morphometrically characterize their populations and propose a reconstruction of their evolution in western Iberia.

The relatively small sized, Middle Pleistocene bears from Postes Cave (SW Spain), may or may not be genetically linked to the subsequent Late Pleistocene bears, given the considerable divergence observed between them and the later Portuguese bears. The population of brown bears from Furninha Cave, MIS 5 in age (~80.000 YBP), is distinguished by the considerable number of remains of juveniles and mature specimens spanning a considerable time period, in a manner analogous to that observed in cave bear hibernation dens. Their overall large size (over 300 kg in some cases) and their notable robustness, seem convergent features with the cave bears, from which it has been hypothesized that they could be taking over their ecological niche in SW Iberia. The collection from this site is also relevant for the pathological features of several specimens, as well as gnawing marks and other features that allows the taphonomic

history of some remains to be reconstructed. It is possible that the specimens from the sites of Oliveira and Escoural might represent bears from this robust and large population too, although further fossils and research are required to substantiate this hypothesis.

Subsequently, during the Late Pleistocene, specifically the initial half of MIS 2, the fossil record reveals the presence of bears from Caldeirão, Fontainhas and potentially Serra de Molianos. They represent a population of relatively similar in size to those of coeval NW Spain, as evidenced by specimens from Serra de Molianos weighing approximately 250 kg, as those from NW Spain (Arcoia). These Pleistocene bears appear to exhibit a similar metric range to that observed in later Holocene bears. Nevertheless, some specimens attained a mass of over 385 kg, representing this specimen from Fontainhas one of the largest brown bears documented in the fossil record. However, they exhibited a slenderer physique than those from Furninha Cave.

During the Greenlandian stage of the Holocene the "Pleistocene giants" that were present on Fontainhas are no longer found. Additionally, several Pleistocene haplotypes have disappeared. NW Iberian bears reached sizes comparable to modern-day large North American grizzly, with males averaging approximately 270 kg and females around 140 kg. They presented a more marked sexual dimorphism than that observed in the contemporary Iberian bear, with males being approximately 50% larger than females. Finally, over the course of the last few thousand years, the size of the Iberian brown bear has undergone a significant reduction, with contemporary populations exhibiting an average mass of approximately 140 kg for males and 100 kg for females, as observed across the Pyrenees and the Cantabrian Mountains.

Further research will enable a more detailed examination of these conclusions, utilizing molecular and paleopathological data, as well as a larger sample.

6

PALEOBIODIVERSITY OF PLEISTOCENE VERTEBRATES FROM PORTUGAL

This chapter has not yet been presented in any congresses or published in scientific journals. It addresses some of the core objectives of the thesis, specifically the compilation of a census of Pleistocene paleobiodiversity in Portugal and the application of statistical analyses to characterize it. The resulting paleobiodiversity data are then compared to the current number of species within the major tetrapod groups inhabiting Portugal today, in order to assess how representative is the fossil record of the region's actual biodiversity.

6.1 Introduction

The bias inherent in the vertebrate fossil record—and, more broadly, the challenge of reconstructing true past biodiversity—has been a central question for paleontology for decades (Sepkoski, 2005; Close et al., 2020), rooted in a recognition of the fossil's record patchiness and incompleteness that dates back centuries (Battista & Schultz, 2024). Gaining an accurate understanding of past biodiversity requires accounting for its multiple dimensions, including measures such as alpha and beta diversity:

-Alpha diversity (α) refers to the local diversity or the number of species found within a designated area or habitat. Observed alpha diversity is often dependent of the size of the designated area (Koleff et al., 2003).

-Beta diversity (β) is a measure of the differentiation or spatial turnover in species between two or more local assemblages. This might actually be useful as comparison in order to understand which localities are more or less similar. As beta diversity increases, individual localities differ more markedly from one another in their species composition (Koleff et al., 2003).

Understanding both alpha and beta diversity is crucial for a comprehensive assessment of biodiversity at different spatial and temporal scales. However, the role that Pleistocene fossil faunas can play in our understanding of the paleobiodiversity of older time periods is mostly

understudied. The majority of works on this subject usually revolve around the changes of diversity caused by the extinction of species (Blois et al., 2010) and not quantifying which modern species are not present in the Pleistocene record of an area, in order to understand how good non-parametric estimations of diversity are when applied to them (Alroy, 2020).

Furthermore, the preponderance of research in the field of paleobiodiversity is contingent on data from online repositories, such as the Paleobiodiversity database (Varela et al., 2015; Uhen et al., 2023) and the NOW database (Žliobaitė et al., 2023). Many other points of information might still outside these massive repositories and even only partially on regional ones (Fialho et al., 2023), while even more important might be the data stored at museums, not at any online repository at all (Dean & Thompson, 2025). The most effective method of overcoming these challenges and avoiding excessive reliance on extensive online repositories is to undertake a systematic and meticulous bibliographic revision.

6.2 Methods

6.2.1 Census of paleobiodiversity of the Pleistocene of Portugal

A carefully curated and extensively reviewed dataset was compiled from the most up to date literature on the known Pleistocene paleobiodiversity of Portugal. This represents the first, most time-consuming and arguably most critical step of the process, as all subsequent comparisons and analyses rely on the data contained within this foundational list.

Each taxon documented in the Portugal Pleistocene fossil record is associated with:

1 - **The major group to which it belongs**: Lissamphibia, Reptilia (minus Aves), Aves, and Mammalia.

2 - **The European Land Mammal Age (ELMA) where it appears in Portugal**: We use as ELMAs the Villafranchian, from 3.5 to 1.2 Ma (Rook & Martínez-Navarro, 2010); the Epivillafranchian, from 1.2 to 0.8 Ma (Bellucci et al., 2015); the Galerian, from 0.8 to 0.4 Ma; and the Aurelian, from 0.4 Ma to today (Palombo, 2018).

3 - **The name of the localities where it appears:** Regardless of how many other species appear on said localities.

4- **The total number of localities where it appears**.

5- **The current status of the species in Portugal**: L.P (Living in Portugal), L.E (Locally extinct), and EX (completely extinct). Some birds appear as L.P (N.N), "not nesting". We use the Atlas of herpetofauna of Portugal for amphibians and reptiles (Loureiro et al., 2008), the IUCN red list

for birds (Almeida et al., 2023), and the IUCN red list for mammals (Mathias et al., 2023) in order to assess which of the previous categories better suits each species.

6- **References used**.

6.2.2 Comparison with online databases

Before proceeding with further analyses, the compiled list was compared against two major online databases to assess their completeness and determine whether they alone could have supported the subsequent analyses. The selected databases are: the NOW database (New and Old Worlds Database of Fossil Mammals), which focuses on Cenozoic mammal occurrences and is therefore well-suited for this comparison in theory (Žliobaitė et al., 2023); and the Paleobiology Database, a more generalist resource that includes data from all life forms throughout the Phanerozoic (Uhen et al., 2023).

6.2.3 Descriptive statistics of the main matrix.

The compiled list was transformed into a presence-absence data matrix. In this data matrix the columns represent the localities and the rows represent the species. To maintain a manageable number of localities, sites where only one species has been recorded -such as several proboscidean localities- were excluded from the analysis. Basic descriptive statistics about the diversity of the matrix were presented: the average number of species per site, the average number of sites per species, the most common species overall and within each major group, and the sites with the highest species richness overall and per group. Then, given the presence-absence nature of the data, beta diversity statistics will be presented in order to describe the dataset (Koleff et al., 2003). All statistical analyses were be conducted using PAST 5.2 software (Hammer et al., 2001).

6.2.4 Comparison of the Pleistocene fossil record with modern biodiversity: How representative is the fossil record? How important are caves?

To make a meaningful and fair comparison between the species in the fossil record and those currently living in Portugal, it is necessary to exclude certain species from both the fossil species list and the modern-day databases. From the fossil species list, species that only appeared in Portugal during the Epivillafranchian (1.2 to 0.8 Ma) must be excluded, as this period is characterized by a significantly different faunal composition from that of the present day

(Bellucci et al., 2015). Only species that are present starting from the Aurelian ELMA to the end of Pleistocene (0.4 Ma to 11.7 ka), which are more comparable to modern-day faunas, were considered in the analysis.

From the modern-day species lists, non-native species must be excluded, as they could not have been present in the Pleistocene fossil record. Additionally, species listed as regionally extinct, and therefore no longer found in Portugal, must also be excluded.

After comparing the total number of Aurelian species with modern species, the next step was to assess how cave deposits influence our understanding of the Pleistocene. This involved excluding karstic infillings and fossil species that are only known from these sites. Since karstic infillings are relatively short-lived in the context of the Phanerozoic (Schubert & Mead, 2019, p. 96) this exercise will serve to approximate how much we can know about other time periods from which this kind of deposits are not usually preserved until today.

6.2.5 Validation of non-parametric estimations for species number: How they perform with the Pleistocene fossil record?

Thanks to the Aurelian fauna being relatively comparable to modern day fauna, it was possible to quantify how the paleobiodiversity estimations employed in PAST 5.2 (Hammer et al., 2001) -including sample-based rarefaction, Chao 2, Jackknife 1, Jackknife 2, and Bootstrap- worked in estimating overall biodiversity and per group. It was also possible to assess how the absence or presence of caves affect these estimations.

6.3 Results

6.3.1 Paleobiodiversity census of the Pleistocene of Portugal

The resulting table (Table 6.1) was compiled using over 130 references that documented 680 occurrences of 200 taxa of terrestrial vertebrates found in the Pleistocene fossil record of Portugal, spanning more than 40 sites. This dataset encompassed a total of nine amphibians, 13 reptiles, 92 birds, and 86 mammals. For a complete list of the individual localities and references used on Table 6.1, please refer to Appendix E.

Table 6.1 — Taxa found in the Portuguese Pleistocene fossil record. The table includes their group, ELMAs in which they appear, number of localities where they have been detected, and current status (L.P, living in Portugal; L.P N.N, living in Portugal but not nesting for birds; L.E, locally extinct; EX, totally extinct).

TAXA	GROUP	ELMA	NUMBER OF LOCALITIES	STATUS
Salamandra salamandra (Linnaeus, 1758)	Lissamphibia	Aurelian	2	L.P
Triturus marmoratus (Latreille, 1800)	Lissamphibia	Aurelian	1	L.P
Pelodytes sp. Daudin, 1802	Lissamphibia	Aurelian	1	L.P
Bufo spinosus (Daudin, 1803)	Lissamphibia	Aurelian	4	L.P
Pelobates cultripes Cuvier, 1829	Lissamphibia	Aurelian	4	L.P
Pleurodeles waltl (Michahelles, 1830)	Lissamphibia	Aurelian	1	L.P
Epidalea calamita (Laurenti, 1768)	Lissamphibia	Aurelian	1	L.P
Pelophylax perezi (Seoane, 1885)	Lissamphibia	Aurelian	2	L.P
Rana iberica Boulenger, 1979	Lissamphibia	Aurelian	1	L.P
Timon lepidus (Daudin, 1802)	Reptilia	Aurelian	3	L.P
Psammodromus manuelae Busack *et al.*, 2006	Reptilia	Aurelian	1	L.P
*Podarcis*sp. Wagler, 1830	Reptilia	Aurelian	1	L.P
Acanthodactylus erythrurus (Schinz, 1833)	Reptilia	Aurelian	1	L.P
Rhinechis scalaris (Schinz, 1822)	Reptilia	Aurelian	1	L.P
Hemorrhois hippocrepis (Linnaeus, 1758)	Reptilia	Aurelian	1	L.P
Coronella girondica Daudin, 1803	Reptilia	Aurelian	2	L.P
Vipera lastei Bosca, 1878	Reptilia	Aurelian	1	L.P
Natrix maura (Linnaeus, 1758)	Reptilia	Aurelian	1	L.P
Blanus cinereus (Vandelli, 1797)	Reptilia	Aurelian	1	L.P
Testudo hermanni Gmelin, 1789	Reptilia	Aurelian	7	L.E
Mauremys leprosa (Schweiger, 1812)	Reptilia	Aurelian	4	L.P
Emys orbicularis (Linnaeus, 1758)	Reptilia	Aurelian	3	L.P
Tetrao urogallus Linnaeus, 1758	Aves	Aurelian	1	L.E
Alectoris rufa (Linnaeus, 1758)	Aves	Aurelian	6	L.P
Perdix perdix (Linnaeus, 1758)	Aves	Aurelian	4	L.E
Coturnix coturnix (Linnaeus, 1758)	Aves	Aurelian	2	L.P
Phaisanus colchicus Linnaeus, 1758	Aves	Aurelian	1	L.P
Lagopus (Linnaeus, 1758)	Aves	Aurelian	1	L.E
Lagopus muta (Montin, 1781)	Aves	Aurelian	1	L.E
Anas platyrhynchos Linnaeus, 1758	Aves	Aurelian	4	L.P
Anas crecca Linnaeus, 1758	Aves	Aurelian	1	L.P
Melanitta nigra (Linnaeus, 1758)	Aves	Aurelian	3	L.P (N. N.)
Melanitta fusca (Linnaeus, 1758)	Aves	Aurelian	1	L.E
Aythya sp. Boie, 1822	Aves	Aurelian	1	L.P
Clangula hyemalis (Linnaeus, 1758)	Aves	Aurelian	1	L.E
Tadorna tadorna (Linnaeus, 1758)	Aves	Aurelian	1	L.P
Tadorna ferruginea (Pallas, 1761)	Aves	Aurelian	1	L.E
Somateria mollisima (Linnaeus, 1758)	Aves	Aurelian	1	L.E
Mergus merganser (Linnaeus, 1758)	Aves	Aurelian	1	L.E
Mergellus albellus (Linnaeus, 1758)	Aves	Aurelian	1	L.E

Anser albifrons (Scopoli, 1769)	Aves	Aurelian	1	L.P (N. N.)
Cygnus olor (Gmelin, 1789)	Aves	Aurelian	2	L.P
Scolopax rusticola Linnaeus, 1758	Aves	Aurelian	3	L.P (N. N.)
Gallinago sp.	Aves	Aurelian	1	L.P
Numenius phaeopus (Linnaeus, 1758)	Aves	Aurelian	2	L.P (N. N.)
Tringa totanus (Linnaeus, 1758)	Aves	Aurelian	1	L.P
Calidris canutus (Linnaeus, 1758)	Aves	Aurelian	2	L.P (N. N.)
Calidris pugnax (Linnaeus, 1758)	Aves	Aurelian	1	L.P (N. N.)
Sterna hirundo Linnaeus, 1758	Aves	Aurelian	1	L.P (N. N.)
Larus fuscus Linnaeus, 1759	Aves	Aurelian	1	L.P
Pinguinus impennis (Linnaeus, 1758)	Aves	Aurelian	2	EX
Fratercula arctica (Linnaeus, 1758)	Aves	Aurelian	1	L.P (N. N.)
Alca torda Linnaeus, 1758	Aves	Aurelian	1	L.P (N. N.)
Vanellus vanellus (Linnaeus, 1758)	Aves	Aurelian	1	L.P
Pluvialis squatarola (Linnaeus, 1758)	Aves	Aurelian	1	L.P (N. N.)
Pluvialis apricaria (Linnaeus, 1758)	Aves	Aurelian	1	L.P (N. N.)
Podiceps nigricollis Brehm, 1831	Aves	Aurelian	1	L.P (N. N.)
Otis tarda Linnaeus, 1758	Aves	Aurelian	1	L.P
Grus grus (Linnaeus, 1758)	Aves	Aurelian	1	L.P (N. N.)
Grus primigenia (Milne-Edwards, 1869)	Aves	Aurelian	1	EX
Puffinus puffinus (Brünnich, 1764)	Aves	Aurelian	2	L.P (N. N.)
Puffinus holeae Walker *et al.*, 1990	Aves	Aurelian	1	EX
Phalacrocorax aristotelis (Linnaeus, 1761)	Aves	Aurelian	2	L.P
Phalacrocorax carbo (Linnaeus, 1758)	Aves	Aurelian	1	L.P (N. N.)
Morus bassanus (Linnaeus, 1758)	Aves	Aurelian	1	L.P (N. N.)
Phoenicopterus roseus Pallas, 1811	Aves	Aurelian	1	L.P (N. N.)
Gavia stellata (Pontoppidan, 1763)	Aves	Aurelian	1	L.P (N. N.)
Accipiter nisus (Linnaeus, 1758)	Aves	Aurelian	1	L.P
Aquila chrysaetos (Linnaeus, 1758)	Aves	Aurelian	5	L.P
Aquila adalberti (Brehm, 1861)	Aves	Aurelian	2	L.P
Aquila fasciata (Viellot, 1822)	Aves	Aurelian	1	L.P
Milvus migrans (Boddaert, 1783)	Aves	Aurelian	1	L.P
Buteo buteo (Linnaeus, 1758)	Aves	Aurelian	1	L.P
Haliaeetus albicilla (Linnaeus, 1758)	Aves	Aurelian	1	L.E
Gypaetus barbatus (Linnaeus, 1758)	Aves	Aurelian	2	L.E
Aegypius monachus (Linnaeus, 1766)	Aves	Aurelian	1	L.P
Gyps fulvus (Hablizl, 1783)	Aves	Aurelian	3	L.P
Falco tinnunculus Linnaeus, 1758	Aves	Aurelian	4	L.P
Falco rusticolus Linnaeus, 1758	Aves	Aurelian	1	L.E
Bubo bubo (Linnaeus, 1758)	Aves	Aurelian	6	L.P
Athene noctua (Scopoli, 1769)	Aves	Aurelian	7	L.P
Strix aluco Linnaeus, 1758	Aves	Aurelian	2	L.P
Tyto alba (Scopoli, 1769)	Aves	Aurelian	1	L.P
Asio flammeus (Potoppidan, 1763)	Aves	Aurelian	2	L.P (N. N.)
Pterocles orientalis (Linnaeus, 1758)	Aves	Aurelian	1	L.P

Streptopelia turtur (Linnaeus, 1758)	Aves	Aurelian	1	L.P
Columba livia Gmelin, 1789	Aves	Aurelian	7	L.P
Columba palumbus Linnaeus, 1758	Aves	Aurelian	5	L.P
Ciconia sp. Linnaeus, 1758	Aves	Aurelian	1	L.P
Egretta garzetta (Linnaeus, 1766)	Aves	Aurelian	1	L.P
Ardea alba Linnaeus, 1758	Aves	Aurelian	1	L.P (N. N.)
Pyrrhocorax pyrrhocorax (Linnaeus, 1758)	Aves	Aurelian	9	L.P
Pyrrhocorax graculus (Linnaeus, 1766)	Aves	Aurelian	8	L.E
Coloeus monedula (Linnaeus, 1758)	Aves	Aurelian	9	L.P
Corvus corax (Linnaeus, 1758)	Aves	Aurelian	6	L.P
Corvus corone Linnaeus, 1758	Aves	Aurelian	5	L.P
Corvus frugilegus Linnaeus, 1758	Aves	Aurelian	3	L.E
Corvus antecorax Mourer-Chauviré, 1975	Aves	Aurelian	1	EX
Pica pica (Linnaeus, 1758)	Aves	Aurelian	6	L.P
Garrulus glandarius (Linnaeus, 1758)	Aves	Aurelian	3	L.P
Turdus iliacus Linnaeus, 1766	Aves	Aurelian	2	L.P (N. N.)
Turdus pilaris Linnaeus, 1758	Aves	Aurelian	3	L.P (N. N.)
Turdus philomelos Brehm, 1831	Aves	Aurelian	2	L.P
Turdus merula Linnaeus, 1758	Aves	Aurelian	3	L.P
Picus sharpei (Saunders, 1872)	Aves	Aurelian	2	L.P
Cyanopica cooki Bonaparte, 1850	Aves	Aurelian	1	L.P
Sturnus unicolor Temminck, 1820	Aves	Aurelian	1	L.P
Sturnus vulgaris Linnaeus, 1758	Aves	Aurelian	2	L.P (N. N.)
Carduelis carduelis (Linnaeus, 1758)	Aves	Aurelian	1	L.P
Passer sp.	Aves	Aurelian	1	L.P
Ptyonoprogne rupestris (Scopoli, 1769)	Aves	Aurelian	1	L.P
Motacilla alba Linnaeus, 1758	Aves	Aurelian	1	L.P
Caprimulgus europaeus Linnaeus, 1758	Aves	Aurelian	2	L.P
Cuculus canorus Linnaeus, 1758	Aves	Aurelian	3	L.P
Erinaceus europaeus Linnaeus, 1758	Mammalia	Aurelian	6	L.P
Crocidura russula Hermann, 1780	Mammalia	Aurelian	7	L.P
Crocidura suaveolens Pallas, 1811	Mammalia	Aurelian	3	L.P
Sorex sp.	Mammalia	Aurelian	1	L.P
Sorex granarius Miller, 1910	Mammalia	Aurelian	1	L.P
Sorex araneus Linnaeus, 1758	Mammalia	Aurelian	1	L.E
Talpa occidentalis Cabrera, 1907	Mammalia	Aurelian	6	L.P
Galemys kormosi (Shereuder, 1940)	Mammalia	Epivillafranchian	1	EX
Galemys pyrenaicus Geoffroy, 1811	Mammalia	Aurelian	2	L.P
Rinolophus ferrumequinun (Shereber, 1774)	Mammalia	Aurelian	4	L.P
Rinolophus hipposideros (Bechstein, 1800)	Mammalia	Aurelian	2	L.P
Rinolophus meheleyi Matschie, 1901	Mammalia	Aurelian	1	L.P
Rinolophus euryale Blasius, 1853	Mammalia	Aurelian	2	L.P
Myotis myotis (Borkhausen, 1797)	Mammalia	Aurelian	4	L.P
Myotis blythi (Tomes, 1857)	Mammalia	Aurelian	1	L.P
Myotis nattereri (Khul, 1818)	Mammalia	Aurelian	1	L.E

Myotis mystacinus Khul, 1817	Mammalia	Aurelian	1	L.P
Nyctalus sp. Bowdich, 1825	Mammalia	Aurelian	1	L.P
Plecotus sp. Geoffroy, 1818	Mammalia	Aurelian	1	L.P
Miniopterus schreibersi (Khul, 1819)	Mammalia	Aurelian	3	L.P
Vespertilio murinus Linnaeus, 1758	Mammalia	Aurelian	1	L.E
Pipistrellus sp. Kaup, 1829	Mammalia	Aurelian	2	L.P
Apodemus sylvaticus (Linnaeus, 1758)	Mammalia	Epivillafranchian-Aurelian	7	L.P
Apodemus flavicollis (Melchior, 1834)	Mammalia	Aurelian	2	L.E
Sciurus vulgaris Linnaeus, 1758	Mammalia	Aurelian	3	L.P
Eliomys quercinus Linnaeus, 1766	Mammalia	Epivillafranchian-Aurelian	9	L.P
Glis glis (Linnaeus, 1766)	Mammalia	Aurelian	2	L.E
Allocricetus bursae Schaub., 1930	Mammalia	Aurelian	4	EX
Mimomys sp. Forsyth-Major, 1902	Mammalia	Aurelian	1	EX
Pliomys sp. Méhely, 1914	Mammalia	Aurelian	1	EX
Pliomys episcopalis Méhely, 1914	Mammalia	Aurelian	1	EX
Chionomys nivalis Martins, 1842	Mammalia	Aurelian	2	L.P
Arvicola sapidus Miller, 1908	Mammalia	Aurelian	4	L.P
Arvicola amphibious (Linnaeus, 1758)	Mammalia	Aurelian	2	L.E
Arvicola cantiana Hinton, 1910	Mammalia	Aurelian	1	EX
Victoriamys chalinei (Alcalde et al., 1981)	Mammalia	Epivillafranchian	1	EX
Microtus lusitanicus (Gerbe, 1879)	Mammalia	Aurelian	6	L.P
Microtus duodecimcostatus (de Selys-Longchamps, 1839)	Mammalia	Aurelian	4	L.P
Microtus arvalis (Pallas, 1778)	Mammalia	Aurelian	3	L.P
Microtus agrestis (Linnaeus, 1761)	Mammalia	Aurelian	4	L.P
Iberomys huescarensis Ruiz-Bustos, 1988	Mammalia	Epivillafranchian	1	EX
Iberomys brecciensis Forsyth Major, 1905	Mammalia	Aurelian	4	EX
Iberomys cabrerae (Thomas, 1906)	Mammalia	Aurelian	3	L.P
Hystrix cristata Linnaeus, 1758	Mammalia	Aurelian	1	L.E
Castor fiber Linnaeus, 1758	Mammalia	Aurelian	3	L.E
Prolagus calpensis Major, 1905	Mammalia	Epivillafranchian	1	EX
Lepus granatensis Rosenhauer, 1856	Mammalia	Aurelian	6	L.P
Oryctolagus cuniculus (Linnaeus, 1758)	Mammalia	Aurelian	20	L.P
Macaca sylvanus (Linnaeus, 1758)	Mammalia	Aurelian	1	L.E
Paleoloxodon antiquus (Falconer & Cautley, 1847)	Mammalia	Aurelian	11	EX
Mammuthus primigenius Blumebach, 1799	Mammalia	Aurelian	2	EX
Stephanorhinus hemitoechus (Falconer, 1859)	Mammalia	Aurelian	11	EX
Equus hydruntinus Regalia, 1905	Mammalia	Aurelian	3	EX
Equus ferus (Linnaeus, 1758)	Mammalia	Aurelian	26	L.E
Hippopotamus amphibious Linnaeus, 1758	Mammalia	Aurelian	1	L.E
Hippopotamus antiquus Desmaret, 1822	Mammalia	Epivillafranchian-Aurelian	2	EX
Sus scrofa Linnaeus, 1758	Mammalia	Aurelian	16	L.P
Cervus elaphus Linnaeus, 1758	Mammalia	Aurelian	31	L.P

Capreolus capreolus Linnaeus, 1758	Mammalia	Aurelian	9	L.P
Dama dama Linnaeus, 1758	Mammalia	Aurelian	4	L.P
Dama vallonnetensis De Lumley *et al.*, 1988	Mammalia	Aurelian	1	EX
Haploidoceros mediterraneus (Bonifay, 1967)	Mammalia	Aurelian	1	EX
Praedama savini (Dawkins, 1887)	Mammalia	Aurelian	1	EX
Metacervocerus rhenanus (Dubois, 1904)	Mammalia	Epivillafranchian	1	EX
Eucladoceros sp. Falconer, 1868	Mammalia	Epivillafranchian	1	EX
Bos primigenius Bojanus, 1827	Mammalia	Aurelian	15	L.E
Capra pyrenaica Schinz, 1838	Mammalia	Aurelian	16	L.P
Rupicapra pyrenaica Bonaparte, 1845	Mammalia	Aurelian	5	L.E
Canis lupus Linnaeus, 1758	Mammalia	Aurelian	17	L.P
Cuon priscus Thenius, 1954	Mammalia	Aurelian	1	EX
Cuon alpinus Pallas, 1811	Mammalia	Aurelian	1	L.E
Vulpes vulpes (Linnaeus, 1758)	Mammalia	Aurelian	15	L.P
Ursus deningeri Von Reichenau, 1904	Mammalia	Aurelian	1	EX
Ursus arctos Linnaeus, 1758	Mammalia	Aurelian	18	L.E
Mustela sp. Linnaeus, 1758	Mammalia	Aurelian	2	L.P
Martes foina (Erxeleben, 1777)	Mammalia	Aurelian	1	L.P
Martes sp. Pinel, 1792	Mammalia	Aurelian	3	L.P
Meles meles Linnaeus, 1758	Mammalia	Aurelian	4	L.P
"Hyaena" prisca de Serres, 1828	Mammalia	Aurelian	1	EX
Crocuta crocuta (Erxleben, 1777)	Mammalia	Aurelian	14	L.E
Felis silvestris Schreber, 1777	Mammalia	Aurelian	16	L.P
Lynx sp. Kerr, 1792	Mammalia	Aurelian	18	L.P
Panthera pardus Linnaeus, 1758	Mammalia	Aurelian	10	L.E
Panthera spelaea Goldfuss, 1810	Mammalia	Aurelian	6	EX
Panthera uncia Goldfuss, 1811	Mammalia	Aurelian	1	L.E
Homotherium latidens Owen, 1846	Mammalia	Aurelian	1	EX

Of these 200 species, 137 still live in Portugal, while around one third are only known as fossils; 34 are locally extinct and 29 are completely extinct.

6.3.2 Evaluation of online databases

Before proceeding, the list was compared with those available in online databases - namely, the NOW database (Žliobaitė et al., 2023) and the Paleobiology Database (Uhen et al., 2023)- to determine whether the manual search represented a significative improvement, despite being more time-consuming, or if the databases could offer additional references.

6.3.2.1 NOW database

Despite being focused on Cenozoic mammals, the NOW database's performance for Pleistocene fossils of Portugal was extremely underwhelming. It provided only three localities -Algar de João Ramos, Cruz Quebrada, and Figueira Brava- with a single species reported for each of them: *Mammuthus primigenius* (The NOW Community, 2025). As discussed in Chapter 1, the occurrence of Figueira Brava is outdated and most likely pertains to *Palaeoloxodon antiquus* (Zilhão et al., 2020) while the evidence for the one of Algar de João Ramos is circumstantial, being the one of Cruz Quebrada the most likely one to represent a woolly mammoth. These kind of shortcomings from NOW database have been already noted previously in the literature (V. D. Crespo & Castillo, 2025).

6.3.2.2 Paleobiology database

The Paleobiology database provided 100 records representing 73 taxa from 12 Portuguese sites, extracted from 12 references. For a simplified table of the PDB output, see Appendix E. The taxa include 37 mammals (compared to 86 in the manual search), 34 birds (compared to 92), two reptiles (compared to 13), and no amphibians (compared to 9). This indicates that only about one-third of the species identified through the manual bibliographic search were uploaded to the database, even though it represents roughly one-quarter of the sites and 10% of the references.

Additionally, among the references used, three are from publications that do not focus specifically on Portuguese localities but rather mention them in a broader context (Tyrberg, 1999; Torres et al., 2014; Serangeli et al., 2015). Other references, even when they address Portuguese material, do not focus primarily on compiling comprehensive paleobiodiversity lists; instead, their faunal lists served as contextual information within the framework of more targeted studies. For instance, the terrestrial mammals from Furninha Cave, were drawn from a study centered on cetaceans (Figueiredo et al., 2022), and the mammals from Gruta Nova da Columbeira were extracted from research focused on turtles (Boneta Jiménez, Cardoso, et al., 2023).

Finally, the references used for the birds of Furninha (Figueiredo et al., 2017); the faunas of Algoz, Goldra, and Morgadinho (Antunes, Azzaroli, et al., 1986; Antunes, Mein, et al., 1986; Antunes, Manuppella, et al., 1986); the isolated occurrences of the dhole in Escoural (Cardoso, 1992) and the Great Auk at Figueira Brava (Mourer-Chauviré & Antunes, 1991); as well as various localities associated with fossil proboscideans (Antunes & Cardoso, 1992) were relatively consistent.

6.3.3 Descriptive statistics of the presence-absence matrix

In Figure 6.1 several key statistics from the presence-absence matrix are displayed. Among the 36 localities where more than one species was recorded, the average number of species is 18.39, with ten sites exceeding this average. The three localities with the highest species richness were Figueira Brava (86 species), Lapa do Picareiro (58 species), and Furninha (56 species).

Among the 200-tetrapod species, there was an average of 3.31 occurrences per species. The three most common species -each a mammal- were *Cervus elaphus* (30 occurrences), *Equus ferus* (26 occurrences), and *Oryctolagus cuniculus* (20 occurrences). Notably, all the 14 species with more than 10 occurrences were mammals. Among birds, the most frequently recorded species were *Pyrrhocorax pyrrhocorax* and *Coloeus monedula* (each with nine occurrences), and *Pyrrhocorax graculus* (eight occurrences). For reptiles, the most common were *Testudo hermanni* (seven occurrences), *Mauremys leprosa* (four occurrences), *Emys orbicularis* (three occurrences), and *Timon lepidus* (three occurrences). Regarding amphibians, *Bufo spinosus* and *Pelobates cultripes* were the most prevalent, each with four occurrences, while *Pelophylax perezi* and *Salamandra salamandra* were each recorded twice.

Among the species considered locally extinct in Portugal (at least in the wild) the three most frequent were *Equus ferus* (26 occurrences), *Bos primigenius* (14 occurrences), and *Ursus arctos* (14 occurrences). In contrast, among species that are completely extinct, the three most common were *Stephanorhinus hemitoechus* (10 occurrences), *Panthera spelaea* (six occurrences), and *Palaeoloxodon antiquus* (five occurrences). Notably, apart from the great auk (*Pinguinus impennis*), which appears twice, all extinct species recorded more than once are mammals.

Overall, as shown in Figure 6.1, 50% of the species occur in only a single locality (*singletons* in ecology), whereas less than 20% (or one fifth) are represented by more than five occurrences.

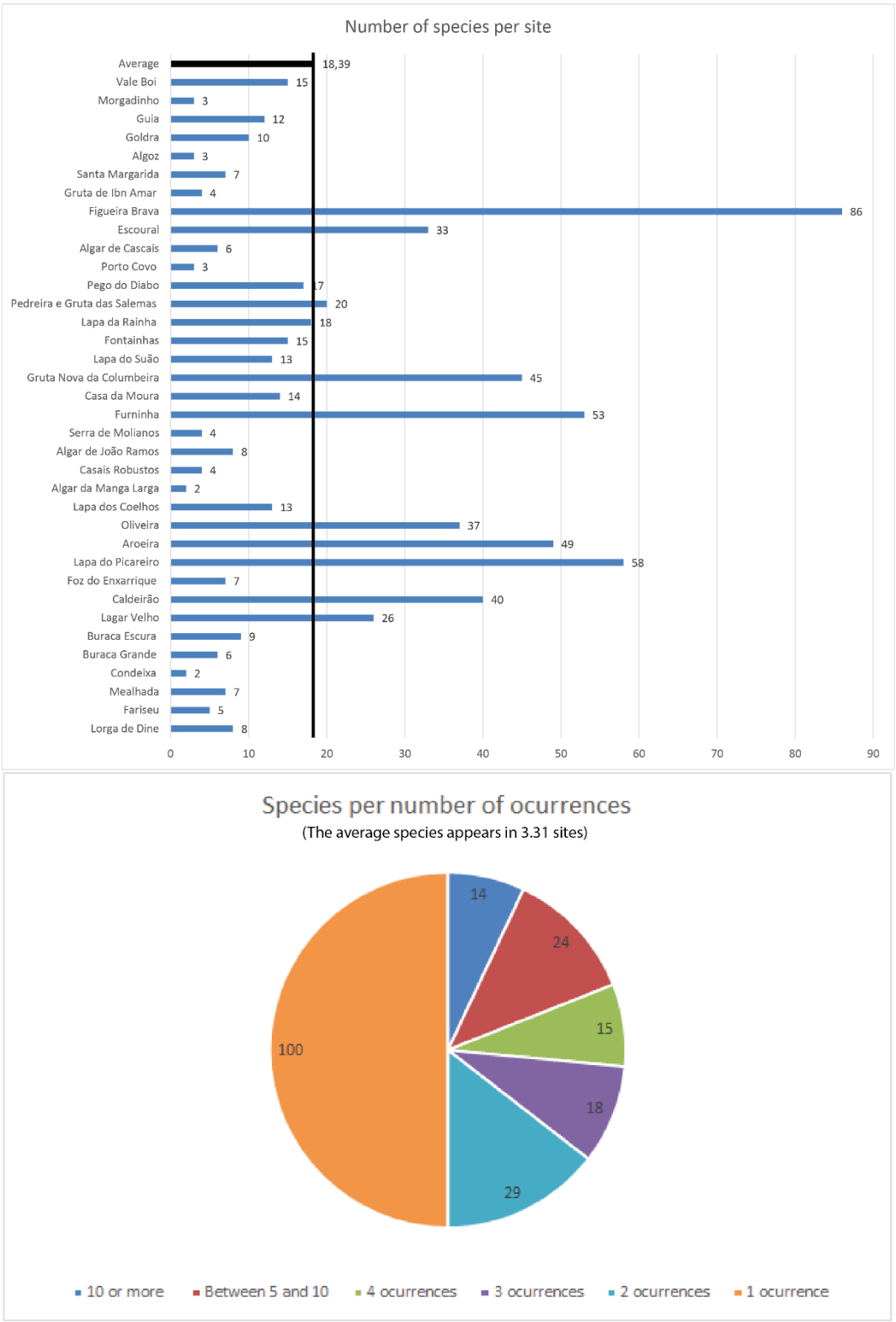


Figure 6.1 — Top; number of taxa per each of the 36 sites compiled in the list. Bottom; number of species appearing one, two, three, four, between five and ten times and more than 10 times.

The following beta diversity metrics are derived from the presence-absence data of taxa across sites. These statistics emphasize the differences **between sampled sites,** in contrast to alpha diversity which focuses on variations within **individual sites** based on the number of individuals (Koleff et al., 2003).

Whittaker (β w): 9.8761. This statistic quantifies the extent of ecological differentiation in species composition between the sites of an area. It does so by comparing the total species richness with the average species richness of each site. Low values (close to 0 or to 1) would indicate that the total species richness is similar to the average richness per site, suggesting low differentiation between sites (Koleff et al., 2003). The high value obtained, close to 10, demonstrates that the total richness (200 species) is roughly 10 times higher than the average site richness (18.39), thereby indicating a high degree of heterogeneity.

Harrison (β -1): 0.28218. This statistic accounts for the number of sites being compared within a given area. By normalizing the ratio of regional diversity by the number of samples, it provides a more standardized and comparable measure of beta diversity across sites with varying sampling efforts. Values close to one indicate extremely high heterogeneity, even after the correction (Koleff et al., 2003). The obtained value of approximately 0.28 suggests that, while heterogeneity is indeed high, it is not extreme.

Cody (β c): 464.5. Cody's beta diversity quantifies beta differentiation by averaging the number of species unique to each of the sites being compared. A higher β c value indicates a greater degree of species turnover and, therefore, higher differentiation. Unlike other metrics, it emphasizes the shared absence of species rather than their shared presence. In this case, the measure is applied cumulatively rather than pairwise (Koleff et al., 2003). The obtained value of 464.5 is exceptionally high, which is consistent with the fact that half of the species occur in only a single site.

Harrison 2 (β -2): 0.037874. This statistic assesses nestedness by evaluating how species diversity at different sites compares to the maximum diversity observed in the most species-rich site. A high value, close to 1, would indicate that most sites are very different even to the most diverse site considered (Koleff et al., 2003). The obtained value of around 0.038 indicates that most of the less rich sites present basically a subsample of the same species of the richest site which is Figueira Brava, with 86 taxa.

Williams (β -3): 0.57. This test estimates the degree of taxonomic overlap between sites. Values near 0 indicate that communities are largely similar, whereas values approaching 1 suggest that most species are unique to each site (Koleff et al., 2003). The obtained value of 0.57

suggests a moderate-to-high degree of differentiation, with over half of the species not shared across sites, indicating notable but not extreme variation in community composition.

The values of the Whittaker, Cody, and Williams indexes indicate a high degree of species uniqueness per site, consistent with the observation that 50% of species are singletons. Most compositional differences arise from species turnover rather than nestedness, suggesting that species in poorer sites tend to be subsets of those in richer ones. As indicated by the Harrison-2 value, there is a core set of shared specie across sites: however, this is accompanied by substantial site-specific uniqueness—unsurprising again given the high proportion of singleton taxa. Nevertheless, as reflected in the Harrison index, , the degree of turnover appears less extreme when considering all 36 sites collectively.

6.3.4 Comparison of the Pleistocene fossil record with modern biodiversity: How representative is the fossil record? How important are caves?

To enable a meaningful and fair comparison between the species represented in the fossil record and those currently inhabiting Portugal it was necessary to exclude certain taxa. Species exclusive to the Epivillafranchian in Portugal (*Metacervocerus rhenanus*, *Eucladoceros* sp., *Iberomys huescarensis*, *Victoriamys chalinei*, *Galemys kormosi,* and *Prolagus calpensis*), along with the sites of Algoz, Santa Margarida, and Morgadinho were omitted from the comparison, retaining only those species that belonged to the Aurelian faunas (Palombo, 2018; Estraviz-López et al., 2025). Regarding the number of modern species, those that arrived to Portugal during the Holocene, like *Ovis aries* or *Genetta genetta* (Mathias et al., 2023), were not considered, as they could not have been detected in the Pleistocene fossil record. A summary of the main statistics for this section is presented in Table 6.2.

Table 6.2 — Resume table of number and % of taxa for diverse categories. Green background, modern species. No background, Pleistocene fossil record. Grey background, Pleistocene record minus caves.

	Amphibians	Reptiles	Birds	Mammals	Total
Detected in the fossil record (% extant species)	9 (52.94%)	12 (42.86%)	73 (28.52%)	43 (81.13%)	**137 (38.7%)**
Detected in the fossil record (% extant species)	7 (41.18 %)	4 (14.29%)	4 (1.56%)	24 (45.28%)	**39 (11.02%)**
Undetected in the fossil record (% extant species)	8 (47.06%)	16 (57.14%)	183 (71,48 %)	10 (18.87%)	217 (61.30%)
Undetected in the fossil record (% extant species)	10 (58.82%)	24 (85.71%)	252 (98.44%)	29 (54.72%)	315 (88.98%)
Extant (Excluding introduced species, % extant species)	17 (4.8%)	28 (7.91%)	256 (72.32%)	53 (14.97%)	354 (100%)
Fossil (Excluding Epivillafranchian-only taxa, % fossil species)	9 (4.64%)	13 (6.70 %)	92 (47.42%)	80 (41,24%)	194 (100%)
Fossil (Excluding Epivillafranchian-only taxa, % fossil species)	7 (14%)	4 (8%)	5 (10%)	34 (68%)	50 (100%)
Extinct (% fossil species)	0 (0 %)	0 (0%)	4 (4.35%)	19 (23.75%)	23 (11.86%)
Extinct (% fossil species)	0 (0%)	0 (0%)	0 (0%)	5 (14.71%)	5 (10%)
Locally extinct (% fossil species)	0 (0%)	1 (7.69%)	15 (16,36%)	18 (22.50%)	34 (17.53%)
Locally extinct (% fossil species)	0 (0%)	0 (0%)	1 (20%)	5 (14.71%)	6 (12%)
Fossil only in Portugal (Extinct and locally extinct, % fossil species)	0 (0%)	1 (7.69%)	19 (20.65%)	37 (46.25%)	57 (29.38%)
Fossil only in Portugal (Extinct and locally extinct, % fossil species)	0 (0%)	0 (0%)	1 (20%)	10 (29.41%)	11 (22%)

In total, the Pleistocene fossil record captures **38.7%** of the current tetrapod biodiversity of Portugal. When cave deposits are excluded, this figure drops significantly to **11.02%**. However, the percentage of species detected varies greatly among different groups (Figure 6.2). Over 81% of extant mammals have been identified in the fossil record, whereas only about 28% of the bird species are represented. The disparity becomes even more pronounced when caves are excluded: approximately 45% of mammal species are still detected, but only a mere 1.56% of bird species are. Nearly half the herpetofauna is represented in the fossil record when cave deposits are included (52.94% of amphibians and 42.86% of reptiles). Without the cave sites, however, the percentage of detected reptiles falls to 14.29%, while amphibians are still relatively well represented, with 41.18% of species present.

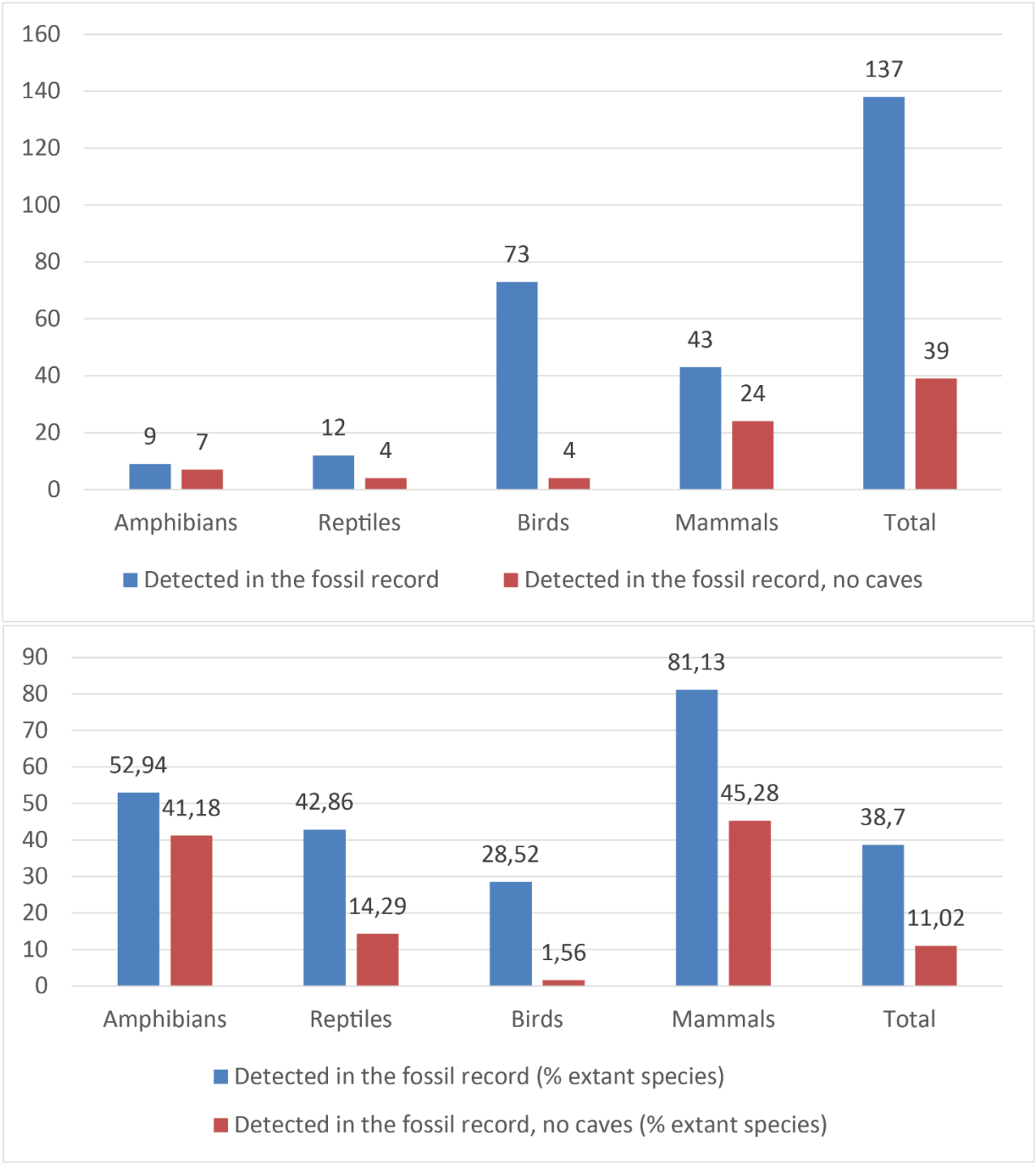


Figure 6.2 — Top; number of taxa living in Portugal nowadays detected in the fossil record per group. Bottom; % of taxa living in Portugal nowadays detected in the fossil record per group.

These varying detection rates, along with the presence of species known only from the fossil record, result in notable differences between the relative composition of the Portuguese fossil tetrapod fauna and that of the modern fauna (Figure 6.3). Mammals, which constitute only 14.97% of the modern tetrapod species are 41.24% of the fossil species, and become dominant when cave deposits are excluded, comprising approximately 68% (or two-thirds) of the total. In contrast, birds show the opposite trend: while they account for over 72% of modern tetrapod species, they represent only 47.42% of the fossil species when cave sites are included, and are nearly absent without them, making up just 1.56% of the recorded species.

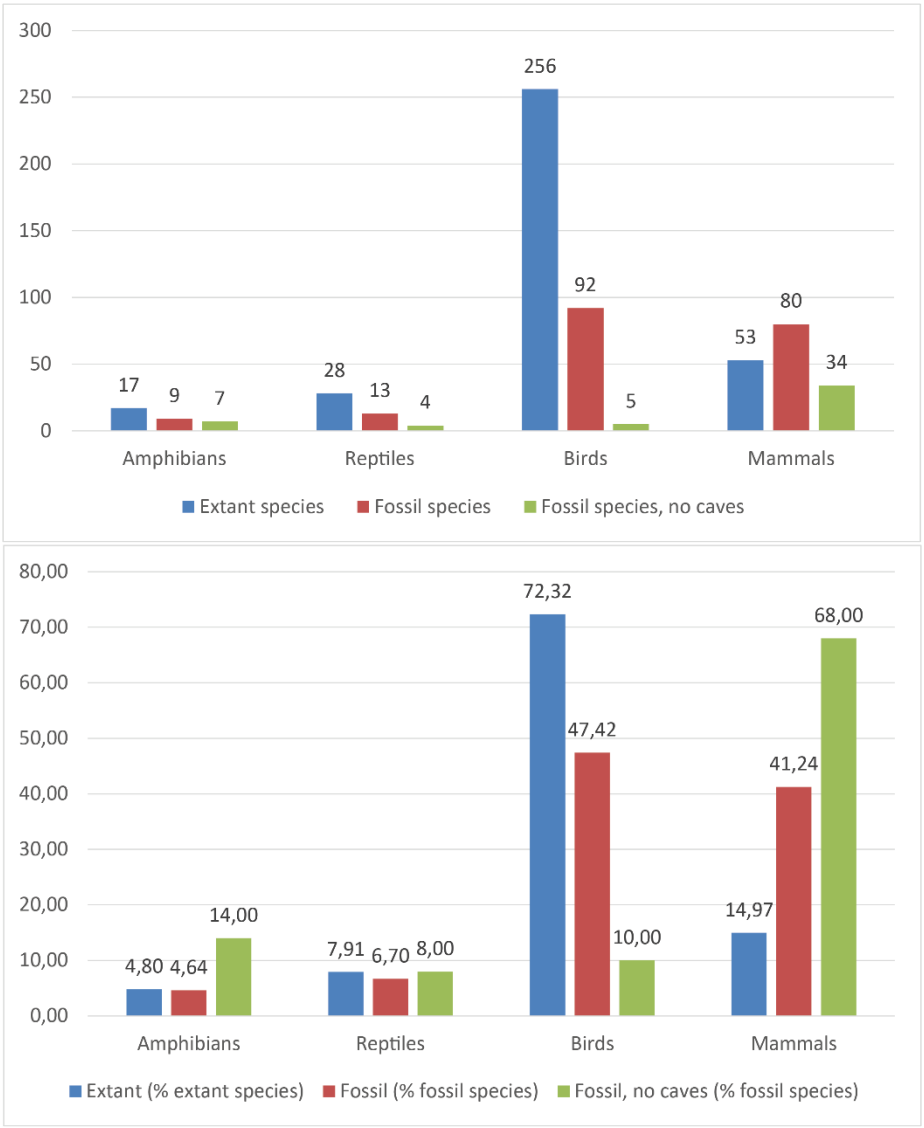


Figure 6.3 — Top; number of taxa living in Portugal, detected in the Pleistocene fossil record, and detected in the fossil record (without caves) per group. Bottom; % of taxa living in Portugal, detected in the Pleistocene fossil record, and detected in the fossil record (without caves) per group

For some species (those that are locally or entirely extinct), their presence in Portugal is only known thanks to the Pleistocene fossil record. These species represent 29.38% of the taxa identified when caves deposits are included, and 22% when they are excluded. Notably, nearly half of the mammal species documented as fossils (46.29%) are no longer present in Portugal due to total or local extinction (Figure 6.4).

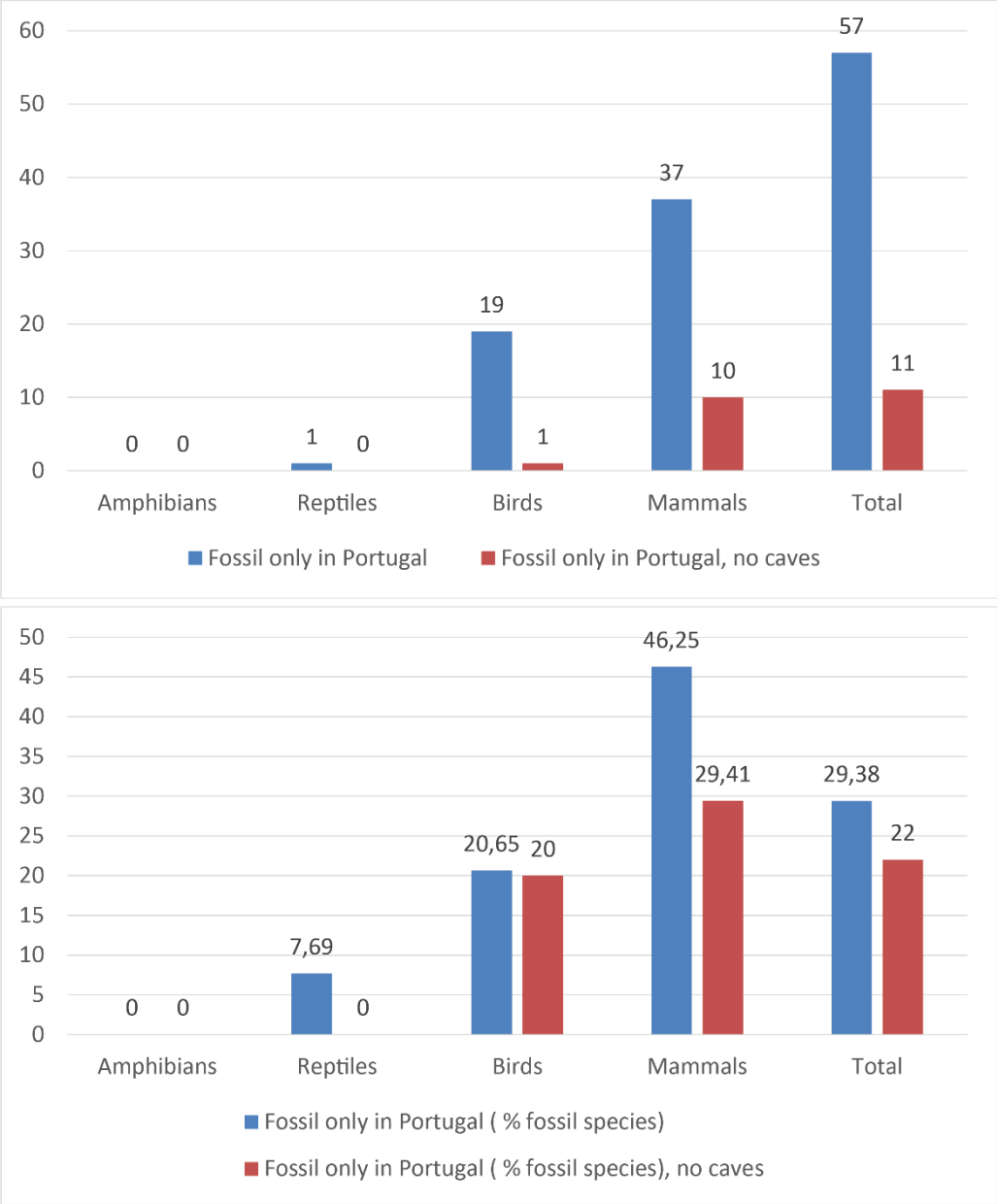


Figure 6.4 — Top; number of known extinct taxa, overall and without caves, per group. Bottom; % of known extinct taxa, overall and without caves, per group.

6.3.5 Validation of non-parametric estimations for species richness: How do they perform with the Pleistocene fossil record?

Modern-day biodiversity was used as a reference point-or "goalpost"-to evaluate how each method for estimating biodiversity performs, based on data from the Pleistocene fossil record (specifically Aurelian species that are also present in Portugal today, with and without the inclusion of cave sites).

The first method used is sample based rarefaction, using the "Mao´s Tau" implementation in the Software PAST. This approach estimates the expected species richness for a standardized sample size for a given dataset, thereby correcting for unequal sampling effort. It operates by subsampling the known sites without duplication of the taxa they contain, enabling comparisons of species richness between sites with varying number of taxa (Gotelli & Colwell, 2001; Gotelli et al., 2023). In PAST it is also possible to interpolate the expected number of taxa through sample-based rarefaction for a greater number of sites than those currently available. Figure 6.5 shows the method applied to the actual data for the Aurelian faunas, both including and excluding cave sites, as well as the interpolated results for 128 sites (including caves) and 90 sites (without caves). By approximately quadrupling the number of known Pleistocene sites in Portugal, the method predicts the presence of 205 taxa or around 57% of the total modern species richness. Similarly, by multiplying the number of non-cave sites by four (24), the model predicts the detection of 90 species, or approximately 25% of the total.

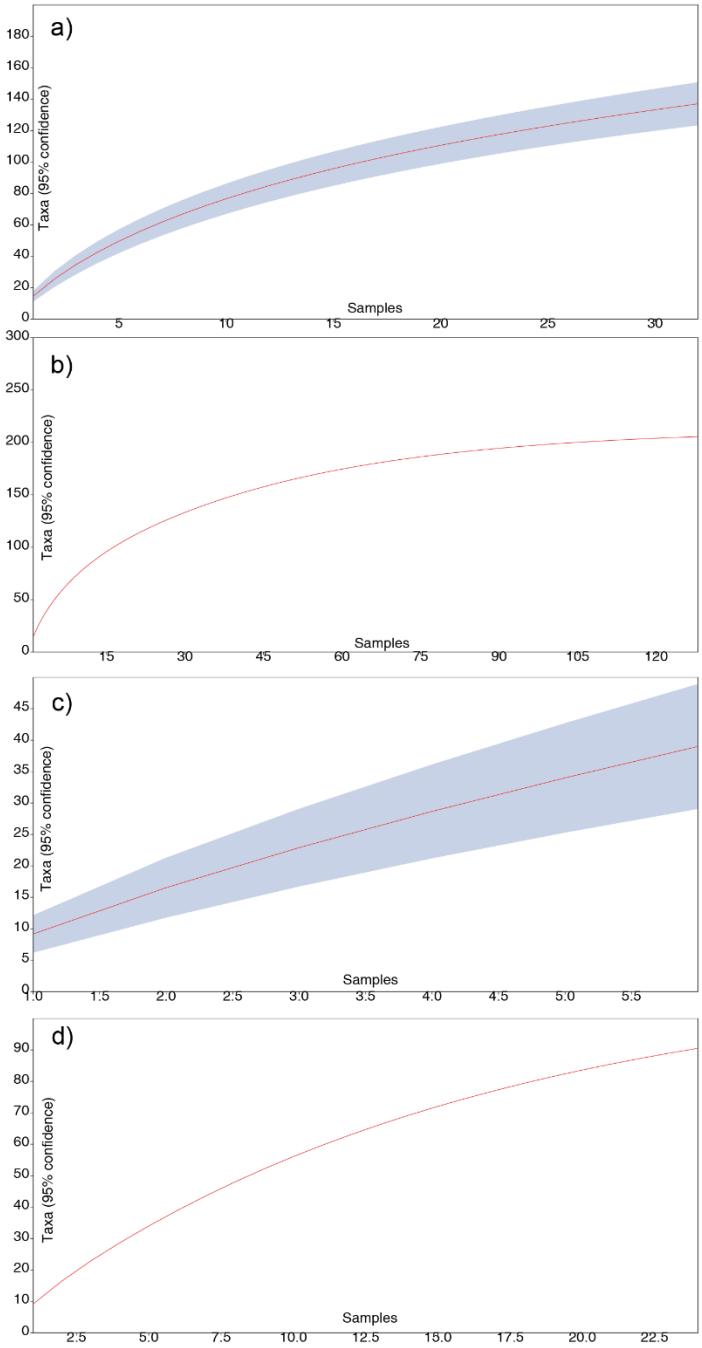


Figure 6.5 — a) Sample based rarefaction applied to the real number of species and sites from the Pleistocene of Portugal. b) Sample based rarefaction applied to hypothetical 124 sites. c) Sample based rarefaction applied to the real number of species and sites (no caves) from the Pleistocene of Portugal. d) Sample based rarefaction applied to hypothetical 90 sites (no caves).

The following biodiversity estimation methods are all non-parametric estimators. For further information, check Gotelli & Colwell (2001) and references herein:

Chao 2: This method estimates total species richness based on the number of *singletons* (species found in only one site) and *doubletons* (species found on two sites). It is very sensitive to the presence of rare species.

Jackknife 1: This method is primarily based on the number of singletons in the presence-absence data. It attempts to correct for the underestimation of observed richness by considering these rare species, assuming unobserved species are as frequent as singletons.

Jackknife 2: The rationale is the same as the previous method, but it reduces bias by accounting for both singletons and doubletons. Chao 2 also incorporates these, but its structure focuses on the proportion of rare species, while Jackknife 2 incorporates factors that mimic the "leave one out" (or subset) technique method to reduce bias. Chao 2 therefore tends to perform better in highly heterogeneous communities, while Jackknife 2 is generally less conservative than Chao 2 and better suited when rare species are not extremely sparse.

Bootstrap: The bootstrap estimates total species richness by simulating repeated sampling (with replacement) from the original dataset. Unlike Chao 2 and Jackknife 2 (which focus on rare species), it resamples the dataset to estimate total richness. Therefore, its effectiveness can be reduced in a very heterogeneous community with many rare species, if the sampling has been insufficient.

The bootstrap method is applied to each of the previously mentioned non-parametric estimators to improve the robusticity of the results. After calculating the estimators for the given dataset, PAST performs 1000 random resamples with replacement of the original dataset. This means that in each resampling, a number of samples equal to the original number is selected, but some original datapoints may be selected multiple times, while others may not be selected. For each of these 1000 generated datasets, PAST recalculates the same non-parametric method applied to the original data. Finally, the mean and standard deviation of these 1000 bootstrapped estimators is presented, what gives a very solid estimation (Hammer et al., 2001).

Since we have the actual number of species that could have been detected (354) we can present the results as percentages of the species predicted by each method, for both the original dataset and the bootstrapped samples. Figure 6.6 shows the results for the dataset without caves, while Figure 6.7 presents the results of the complete dataset.

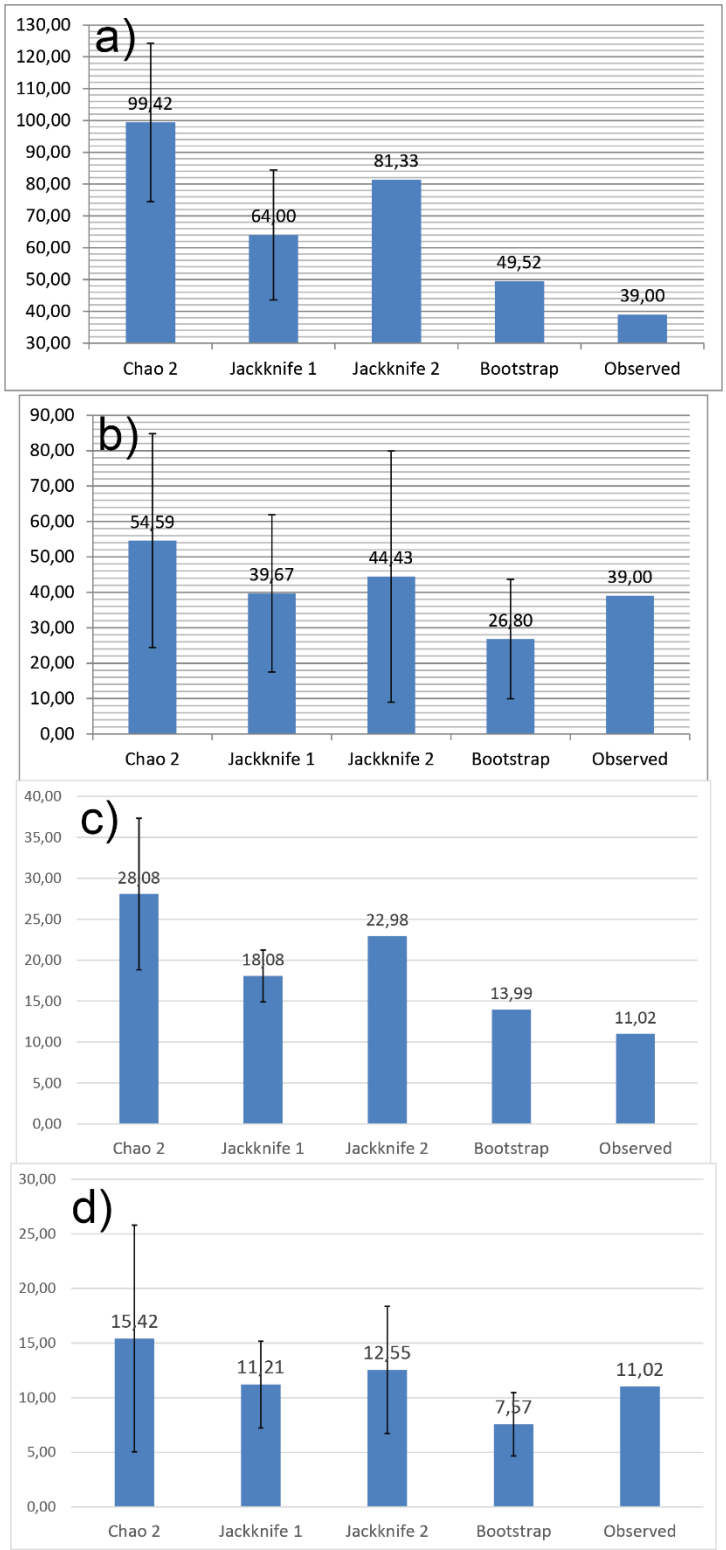


Figure 6.6 — Non-parametric estimations calculated over the dataset without caves: a) Number of species estimated, b) Number of species estimated (bootstrapping), c) % of total species estimated, d) % of total species estimated (bootstrapping).

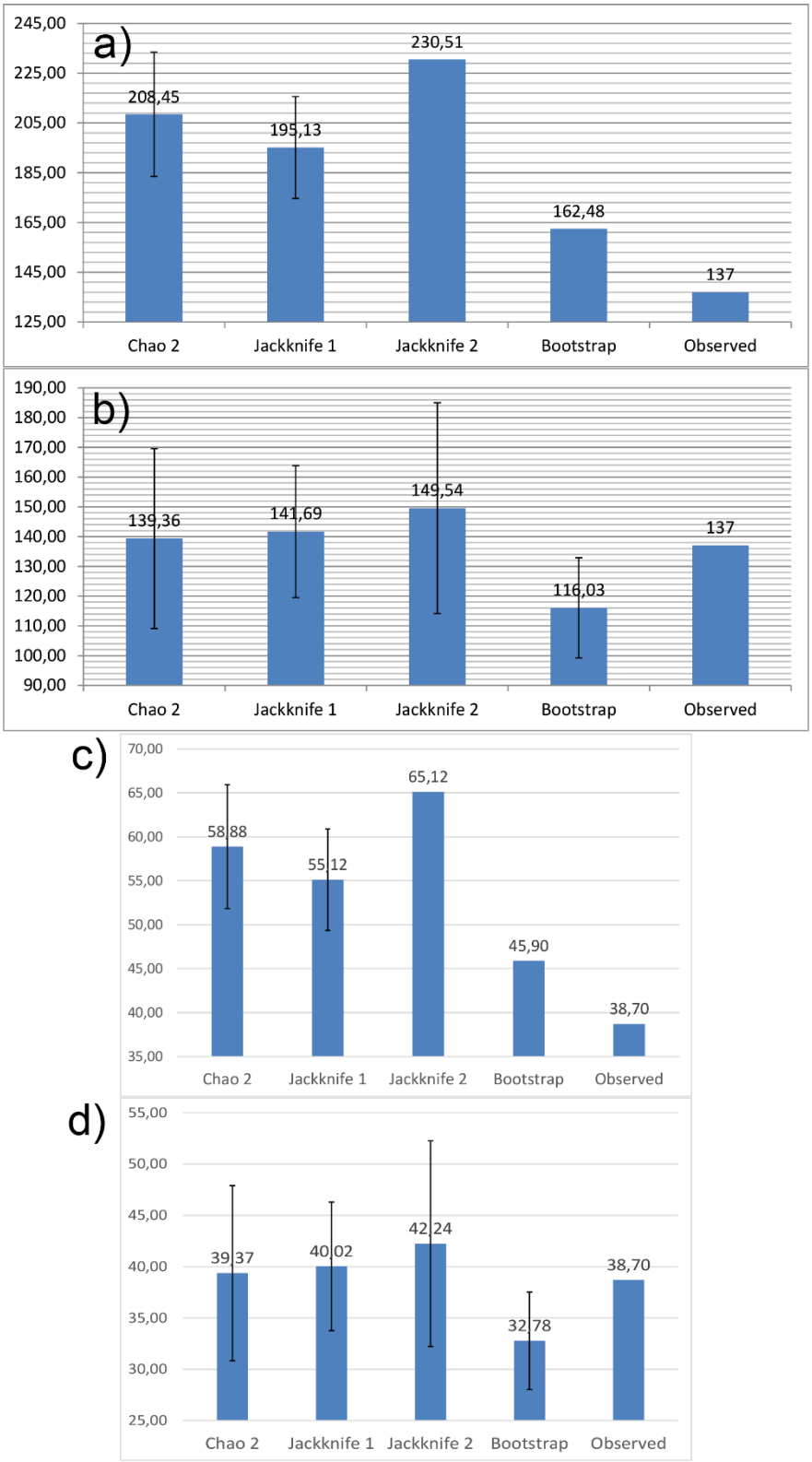


Figure 6.7 — Non-parametric estimations calculated over the dataset including caves: a) Number of species estimated, b) Number of species estimated (bootstrapping), c) % of total species estimated, d) % of total species estimated (bootstrapping).

In both cases (without caves and with the complete dataset), the non-parametric estimation methods that most closely approximated the real number of species were Chao 2 and Jackknife 2.

Chao 2 performed better on the dataset without caves, estimating around 28% of the species for the provided dataset and around 15% with bootstrapping.

Jackknife 2 performed better on the complete dataset, estimating nearly 66% of the species for the provided dataset and 42% with the bootstrapping.

Jackknife 1 generally performed worse than the two previous estimators but scored slightly better than Chao 2 (39.37% vs 40.02%) with bootstrapping on the complete dataset.

Bootstrap consistently underperformed compared to the previous estimators.

6.4 Discussion

The compiled list presented in this thesis constitutes the first-ever census of all known fossil terrestrial tetrapod paleobiodiversity in Portugal. It includes over 680 occurrences of 200 taxa across more than 40 localities, documented in over 130 scientific publications. This resource will be valuable not only for the aims of this thesis, but also for researchers in related fields such as archeology, ecology, and Pleistocene paleontology in general.

This list significantly surpasses those available from large online paleontological databases, such as the NOW database (Žliobaitė et al., 2023) and the Palaeobiology database (Uhen et al., 2023). The NOW database appears to be limited, for the Pleistocene of Portugal, to a single inconclusive record of *Mammuthus* remains (The NOW Community, 2025). Meanwhile the Palaeobiology database includes fewer than half of taxa documented here, covering only about one-third of the sites, and draws from less than 10% of the available references. The limitations of these databases are partly due to their broader focus: the NOW database emphasizes Neogene mammals, while the Palaeobiology database is structured around large-scale studies spanning multiple continents and wider geological time frames beyond just the Pleistocene (Uhen et al., 2023; Žliobaitė et al., 2023).

The application of various descriptive statistics for beta diversity - including Whittaker (β w), Harrison (β -1), Cody (β c), Harrison 2 (β -2), and Williams (β -3) - reveals a clear pattern of high species turnover, with more than half of the taxa occurring only once, with minor nestedness—a common pattern commonly observed in fragmented or patchy ecosystems (Koleff et al., 2003). Most of the least diverse sites appear to represent subsets of the most diverse sites, with a few taxa being nearly (or totally) exclusive for the site. Further investigation is

needed to determine whether this pattern is consistent across all groups (mammals, birds, reptiles, and amphibians), or if it is primarily driven by one or two taxonomic groups.

The number of taxa detected in the fossil record is less than half of the total known from modern biodiversity in Portugal when considering the complete dataset. Nevertheless, this percentage varies greatly among groups. Mammals are the best represented, with over 80% of modern species detected in the fossil record, missing mainly a few bats and shrews. In contrast, only about 28% of bird species are recorded, with most passerines notably absent. This, combined with differential extinction rates among groups -where no amphibians and only one reptile are extinct, but nearly half of Pleistocene mammals are- results in a distorted perception of the relative composition of the biota. For instance, while birds currently make up nearly 75% of the terrestrial tetrapod fauna in Portugal, they account for less than 10% of the species in the open-air fossil sites. The opposite trend is seen with mammals, which represent under 20% of the modern fauna but constitute about two-thirds of the species in open-air fossil assemblages. Meanwhile, the relative representation of herpetofauna in the fossil record is generally accurate, although the picture becomes somewhat skewed again when cave deposits are excluded.

If we exclude the cave deposits, which are notably rarely preserved to modern time across most of the Phanerozoic (Schubert & Mead, 2019), only about 10% of modern taxa are represented in the fossil record. As discussed in Chapter 1, Portugal has a long-standing tradition of prehistoric archeology that has yielded abundant remains of Pleistocene animals, far surpassing the number of remains and sites known from other time periods. For example, the Eocene is represented in Portugal by only a handful of sites, namely Silveirinha, Côja, Naia, Vale Furado, and Feligueira Grande (Antunes et al., 1997). If, despite this extensive archeological and paleontological effort, less than half of Pleistocene species are recorded—even with the contribution of the well-preserved and richly fossiliferous cave deposits—what level of species coverage can realistically be expected for older epochs like the Eocene? The challenge becomes even more pronounced when considering epochs even further back in time like the Late Jurassic. What percentage of the biota from that time period can we truly hope to document? Repeatedly, it has been shown that whenever focused work is conducted—whether on microvertebrates or megafauna—new elements of biodiversity are uncovered (Rotatori, 2024; Guillaume, 2024). Even exceptionally well-studied Late Jurassic sites such as Guimarota (Guillaume et al., 2025) continue to yield new discoveries. This underscores the extent to which our understanding of Jurassic biodiversity is still heavily reliant on a few exceptional lagerstätten, highlighting both the potential and the limitations of the fossil record.

Can we attempt to compensate for this substantial gap in information? By applying several non-parametric estimators, it is possible to partially infer part of the missing components of the biota. Given the high number of species that are only found once or twice in the dataset, it is not surprising that the best-performing estimators are those that take both singletons and doubletons into account, namely Chao 2 and Jackknife 2. Chao 2 performs better on the dataset excluding cave deposits, while Jackknife 2 weighs rare species less aggressively than Chao 2, making it more robust in the face of clustered rarity, such as that found among many cave-specific taxa (Gotelli & Colwell, 2001). In contrast, Jackknife 1, which only considers singletons and ignores the large number of doubletons, and the Bootstrap method, which does not specifically emphasize rare taxa, tend to be overly conservative and underperform relative to Chao 2 and Jackknife 2 (Gotelli & Colwell, 2001).

Even when applying the best-performing methods to the most complete dataset, only approximately 66% of the actual number of species can be predicted. It is therefore reasonable to assume that, for other time periods with less comprehensive fossil records than the Pleistocene, the predicted diversity would likely be even lower.

6.5 Conclusions

This chapter presents the first comprehensive census of fossil terrestrial tetrapods in Portugal, documenting over 680 occurrences of 200 taxa across more than 40 localities, as recorded by over 130 scientific works. The compiled dataset significantly surpasses any existing online paleontological databases and will greatly facilitate future research.

Beta diversity analyses and other relevant statistical methods were applied to the dataset, revealing a high species turnover, with over half of the species appearing only once. Further investigation is required to determine whether this trend is consistent across all tetrapod groups.

The Pleistocene fossil record of Portugal exhibits a biodiversity level that is less than 50% of the modern biodiversity, whilst demonstrating significant variation among the groups represented. Mammals are nearly fully represented (over 80%), while birds are severely underrepresented (28%). This discrepancy, along with the differential extinction affecting mammals to a greater extent, distorts the perceived composition of past ecosystems. At present, 75% of Portuguese terrestrial tetrapods are birds; however, an analysis of open-air fossil sites would suggest that mammals dominated, as they represent 66% of the total number of species.

In contrast, the percentage of herpetofauna in the Pleistocene fossil record is equivalent to the percentage that they represent in the current biodiversity.

In general, with the exception of caves, a mere 10% of extant taxa are detected, thereby emphasizing their paramount importance with regard to our understanding of the Pleistocene. Non-parametric estimators of biodiversity, such as Chao 2 and Jackknife 2, have been shown to partially compensate for missing data. It has been demonstrated that Jackknife 2 performs better on datasets including caves, while Chao 2 performs better on datasets excluding caves. However, even these estimators predict at best only 66% of the modern species, suggesting that the fossil record of earlier epochs with a lower number of fossils preserved in the rich fountain of fossils that are cave deposits (such as the Eocene or the Late Jurassic) will likely yield even lower coverage of the real number of species present. This work underscores the need for continued exploration, particularly of understudied groups and time periods, in order to faithfully reconstruct past paleobiodiversity.

7 CONCLUSIONS

First, the main conclusions drawn from each of the individual chapters will be presented here in sequence. Following these chapter-by-chapter conclusions, a set of overarching conclusions will be provided to synthesize the broader implications of the work as a whole.

7.1 Conclusions of previous chapters

7.1.1 Early Pleistocene (Epivillafranchian) vertebrates from Portugal: An updated review.

The site of Algoz is 1.2 Ma, and is the oldest Pleistocene site from Portugal known to date. It was likely formed by a torrential stream deposit over a lacustrine environment. The vertebrate fauna of Algoz comprises four species: *Hippopotamus antiquus*, *Eucladoceros* sp., *Metacervocerus rhenanus,* and an indeterminate leporid. Furthermore, the identification of at least two individuals from each deer species are identified. All the remains of *Eucladoceros* from Algoz (with the exception of an isolated antler fragment) originate from an individual estimated to be approximately six months of age.

The site of Santa Margarida is a cave deposit with older layers of Early Pleistocene age (0.9 Ma) and younger layers of Middle Pleistocene age (0,6 Ma). At least 10 species of microvertebrates are present at Santa Margarida: Lacertidae indet., *Crocidura* sp., *Sorex* sp., *Oryctolagus* cf. *cuniculus*, *Eliomys* cf. *quercinus*, *Apodemus* cf. *sylvaticus*, *Allocricetus bursae*, *Victoriamys chalinei*, *Iberomys huescarensis*, and *Iberomys brecciensis*. Santa Margarida represents the first known occurrence of the voles *Victoriamys chalinei* and *Iberomys huescarensis* in Portugal. The potential existence of the Early-Middle Pleistocene transition at Santa Margarida justifies a more detailed intervention on this site.

Given the extremely rare Early Pleistocene material from the Westernmost Iberian Peninsula in general, and from Portugal in particular, future research should concentrate on relocating the material from Morgadinho or on the collection of new material at this locality (Antunes, Mein, et al., 1986).

7.1.2 Insights on the evolution and adaptation toward high-altitude and cold environments in the snow leopard lineage.

This research identifies five valid fossil records of the snow leopard lineage outside the Tibetan Plateau, suggesting that the snow leopard dispersed from this region on multiple occasions during the Quaternary. Phylogenetic analysis of these fossils, combined with genetic and morphological data, supports a successive sister group relationship with the modern species, indicating rapid evolution of the snow leopard lineage, particularly since the Middle Pleistocene (~0.8 Ma). This rapid evolution likely correlates with the onset of glaciations on the Tibetan Plateau during the Middle Pleistocene, which exerted strong selective pressure on the lineage.

This study reveals that the osteological anatomy of the modern snow leopard exhibits significant adaptation to steep slopes and, to a lesser extent, to cold and high-altitude environments. Craniodental features such as the short rostrum, high mandibular symphysis, and large anteriorly oriented orbits, along with postcranial proportions favoring agility and leaping capacity, are adaptations for hunting caprine bovids in open mountainous regions. While the enlarged frontal sinuses and larger cheek teeth are interpreted as adaptations to cold and high-altitude conditions, the local landscape, characterized by steep slopes and rock cover, is a more influential factor in snow leopard distribution than temperature and altitude alone.

Species distribution models (SDMs) under Last Glacial Maximum (LGM) conditions indicate that most fossil sites are not within the predicted most suitable area for modern snow leopard populations, supporting the idea that these records represent occasional dispersals outside core habitat areas. Ultimately, this study underscores the importance of integrating morphological analyses, fossil records, and species distribution models to comprehensively understand the evolution and ecology of species as well as to inform conservation strategies for endangered species like the snow leopard. These findings suggest that conservation strategies must consider the critical importance of steep mountain habitats for the survival of the snow leopard.

7.1.3 3D digital and biogeochemical analysis of the Algar da Manga Larga pantherine (*Panthera uncia lusitana*)

The 3D digital analysis of the endocast of *Panthera uncia lusitana* (MG1355.0001) yields a substantial amount of significant morphological information. The endocast exhibits a greater similarity in size and morphology to the modern *Panthera uncia* (snow leopard), but with

certain differences, namely, a greater constriction between the anterior and posterior parts of the cerebrum and a more robust overall morphology. In comparison to a modern African leopard (*Panthera pardus*), *P. uncia lusitana* exhibits a dorso-ventral torsion of the telencephalon and a foramen magnum in a more ventral position. The endocast is noticeably smaller than those of *P. tigris*, *P. leo*, and *P. onca*, but shares some similarities with *P. tigris*. *Acinonyx jubatus* (cheetah) exhibits an even greater degree of telencephalon torsion and a more rounded cerebrum, while *Puma concolor* displays a similar morphology but with a smaller olfactory bulb and a more tapered anterior cerebrum.

Several biogeochemical techniques were also employed to conduct a more in-depth analysis of the remains. The U-Th dating results were inconclusive, likely due to possible water transport of the remains and the open-system behavior of the bones. Additionally, the absence of detectable organic matter excluded the possibility of applying radiocarbon dating (^{14}C), nitrogen isotopic analysis, or ancient DNA or paleoproteomic investigations. Evidence from carbon and oxygen isotopic analysis indicates that *P. uncia lusitana* lived in an open, dry environment, and had a similar habitat to mountain ungulates like *Capra pyrenaica* from Lapa do Picareiro. The estimated Mean Annual Temperature during its lifetime was estimated to be 12.6 °C, suggesting it might have also lived during the MIS 3 period. *P. uncia lusitana* likely had a higher tolerance for warmer temperatures in comparison to the modern snow leopard, which inhabits much colder regions today.

Further research of the endocast morphology using quantitative methodologies is needed, as well as additional studies on the frontal sinuses and metapodials that could provide more insights into the paleobiology of *P. uncia lusitana*. Finally, an additional attempt to extract organic matter from the remains employing more sophisticated technology, has the potential to open numerous venues of investigation with the usage of molecular paleontology techniques as ancient DNA or paleoproteomics.

7.1.4 Pleistocene fossil Ursidae from Portugal: Morphometry and paleobiological inferences

The present study encompasses the analysis of over 500 bear remains from six Portuguese Pleistocene localities. This extensive sample has yielded a plethora of biometrical and graphical data, which has led to the confirmation of the absence of *Ursus spelaeus* (cave bear) and *U. thibetanus* (Asian black bear) within the sample. Furthermore, this enabled us to update the inventory of specimens from these sites, as well as to contextualize the Portuguese

Pleistocene brown bears within their geographical and temporal context. Additionally, we were able to morphometrically characterize their populations and propose a reconstruction of their evolution in western Iberia.

The relatively small sized Middle Pleistocene bears from Postes Cave (SW Spain), may or may not be genetically linked to the subsequent Late Pleistocene bears, given the considerable divergence observed between them and the later Portuguese bears. The population of brown bears from Furninha Cave, MIS 5 in age (~80.000 YBP), is distinguished by the considerable number of remains of juveniles and mature specimens spanning a considerable time period, in a manner analogous to that observed in cave bear hibernation dens. The substantial size of the specimens (with some measuring over 300 kg) and their marked robustness appear to be convergent characteristics with those of cave bears. It has been hypothesized that these animals may be usurping the ecological niche of cave bears in south-western Iberia. The fossil collection from this site is also relevant for the pathological features of several specimens, as well as gnawing marks and other features that allows the taphonomic history of some remains to be reconstructed. It is possible that the specimens from the sites of Oliveira and Escoural represent bears from this robust and large population too, although further fossils and research are required to substantiate this hypothesis.

Subsequently, during the Late Pleistocene, specifically the initial half of MIS 2, the fossil record reveals the presence of bears from Caldeirão, Fontainhas, and potentially Serra de Molianos. They represent a population of relatively similar in size to those of coeval NW Spain, as evidenced by specimens from Serra de Molianos weighing approximately 250 kg, as those from NW Spain (Arcoia). These Pleistocene bears appear to exhibit a similar size range to that observed in later Holocene bears. Nevertheless, some specimens attained a mass of over 385 kg in the case of a specimen from Fontainhas, which represents one of the largest brown bears documented in the fossil record. However, these large specimens exhibited a slenderer physique than those from Furninha Cave.

During the Greenlandian stage of the Holocene the "Pleistocene giants" that that once inhabited Fontainhas were no longer present. Additionally, several Pleistocene haplotypes disappeared. NW Iberian bears reached sizes comparable to the modern-day large North American grizzly, with males averaging approximately 270 kg and females 140 kg. They presented a more marked sexual dimorphism than that observed in the contemporary Iberian bear, with males being approximately 50% larger than females. Finally, over the course of the last few thousand years, the size of the Iberian brown bear has undergone a significant reduction, with

contemporary populations exhibiting an average mass of approximately 140 kg for males and 100 kg for females, as observed across the Pyrenees and the Cantabrian Mountains.

Further research will enable a more detailed examination of these conclusions, utilizing molecular and paleopathological data, as well as a larger sample.

7.1.5 Paleobiodiversity of Pleistocene vertebrates from Portugal

This chapter presents the first comprehensive census of fossil terrestrial tetrapods in Portugal, documenting over 680 occurrences of 200 taxa across more than 40 localities, as recorded by over 130 scientific works. The compiled dataset significantly surpasses any existing online paleontological databases and will greatly facilitate future research.

Beta diversity analyses and other relevant statistical methods were applied to the dataset, revealing a high species turnover, with over half of the species appearing only once. Further investigation is required to determine whether this trend is consistent across all tetrapod groups.

The Pleistocene fossil record of Portugal exhibits a biodiversity level that is less than 50% of the modern biodiversity (38%), whilst demonstrating significant variation among the groups represented. Mammals are nearly fully represented (over 80%), while birds are severely underrepresented (28%). This discrepancy, along with the differential extinction affecting mammals to a greater extent, distorts the perceived composition of past ecosystems. At present, 75% of Portuguese terrestrial tetrapods are birds; however, an analysis of open-air fossil sites would suggest that mammals dominated, as they represent 66% of the total number of species. In contrast, the percentage of herpetofauna in the Pleistocene fossil record is equivalent to the percentage that they represent in the current biodiversity.

In general, without the caves, a mere 10% of extant taxa are detected, thereby emphasizing their paramount importance with regard to our understanding of the Pleistocene. Non-parametric estimators of biodiversity, such as Chao 2 and Jackknife 2, have been shown to partially compensate for missing data. It has been demonstrated that Jackknife 2 performs better on datasets including caves, while Chao 2 performs better on datasets excluding caves. However, even these estimators predict at best only 66% of the modern species, suggesting that the fossil record of earlier time periods with poorer fossil preservation (such as the Eocene or the Late Jurassic) will likely yield even lower coverage of the real species present. This work underscores the need for continued exploration, particularly of understudied groups and time periods, in order to faithfully reconstruct past paleobiodiversity.

7.2 General conclusions of the thesis

- The Algoz site (1.2 Ma) is the oldest Pleistocene locality in Portugal, with a fauna including *Hippopotamus antiquus*, *Eucladoceros* sp., *Metacervocerus rhenanus*, and an indeterminate leporid, indicating a torrential stream deposit over a lacustrine environment.
- Santa Margarida cave deposits (0.9–0.6 Ma), which might record the Early-Middle Pleistocene transition, reveals a rich microvertebrate assemblage with 10 species, including the first Portuguese records of the voles *Victoriamys chalinei*, and *Iberomys huescarensis*.
- The scarcity of Early Pleistocene fossils in western Iberia underscores the importance of revisiting sites.
- Phylogenetic analyses of new occurrences of fossils from the snow leopard lineage show that they dispersed multiple times outside the Tibetan Plateau during the Quaternary, with rapid evolution linked to Middle Pleistocene glaciations (~0.8 Ma).
- A new paleosubspecies of snow leopard from Portugal is described (*Panthera uncia lusitana*).
- Morphological adaptations of snow leopard lineage (like short rostrum and robust limbs) prioritize agility in steep terrain for hunting caprine bovids, emphasizing the importance of rugged landscapes for their survival.
- Species distribution models (SDMs) suggest that fossil records represent dispersal events outside core habitats, informing conservation strategies, as extreme cold and altitude are not as important as steep slope terrain for their survival.
- The endocast of *P. uncia lusitana* resembles the modern snow leopard but with distinct features (e.g., stronger cerebral constriction), indicating evolutionary divergence and differentiating it from other pantherines.
- Preliminary isotopic data suggest it inhabited open, dry environments (~12.6°C), with higher warmth tolerance than modern snow leopards.
- Future research on *Panthera uncia lusitana* should focus on quantitative endocast analyses, morphology of frontal sinuses, and advanced molecular techniques in order to better characterize the paleobiology of this elusive pantherine.

- Over 500 bear remains confirm that the brown bear (*Ursus arctos*) is the only ursid known so far in the Late Pleistocene of Portugal. There is an apparent absence of cave bears (*Ursus spelaeus*) and Asian black bears (*Ursus thibetanus*).
- Furninha Cave (MIS 5) housed large, robust brown bears (over 300 kg), maybe filling the ecological niche of cave bears in SW Iberia, while other later Late Pleistocene bears (Fontainhas, MIS 3) reached enormous sizes (~385 kg) but were slenderer.
- Modern brown bears show reduced size (males, ~140 kg) and sexual dimorphism, reflecting post-Pleistocene adaptations.
- The paleobiodiversity census documents 200 taxa from 40+ localities, revealing high species turnover (50% of species appearing only once).
- Caves are critical for fossil preservation, but even with them only 38% of the modern species are recorded and non-parametric estimators of biodiversity (like Chao 2) predict at best ≤66% of modern biodiversity.
- Discrepancies in fossil representation (mammal dominance and underrepresentation of birds) distort ecosystem reconstructions, necessitating targeted studies of these groups.

In summary, this thesis improves our knowledge of the Pleistocene fossil record of Portugal, underscores the importance of interdisciplinary collaboration, and demonstrates the enduring potential for new findings in the area. This work demonstrates that—even when considering the remarkable paleobiodiversity already documented in Portugal (Figure 7.1)—the Pleistocene fossil record continues to pose new questions and holds many more discoveries yet to be made.



Figure 7.1 — Selected vertebrate species known from the Pleistocene of Portugal. Paleoart by José Pedro Ferreira. *Homo sapiens* for scale (190 cm). 1. *Panthera uncia lusitana*, 2. *Palaeoloxodon antiquus*, 3. cf. *Mammuthus primigenius*, 4. *Eucladoceros* sp., 5. *Stephanorhinus hemitoechus*, 6. *Equus ferus antunesi*, 7. *Panthera pardus*, 8. *Capreolus capreolus*, 9. *Cuon alpinus europaeus*, 10. *Bos primigenius*, 11. *Homotherium latidens*, 12. *Crocuta crocuta spelaea*, 13. *Panthera spelaea*, 14. *"Hyaena" prisca*, 15. *Pinguinus impennis*, 16. *Hippopotamus antiquus*, 17. *Hippopotamus amphibius*, 18. *Sus scrofa*, 19. *Castor fiber*, 20. *Dama sp.*, 21. *Canis lupus*, 22. *Cervus elaphus*, 23. *Ursus arctos*, 24. *Rupicapra* sp., 25. *Capra pyrenaica*, 26. *Macaca sylvanus.*

BIBLIOGRAPHY

Abella, J., Alba, D. M., Robles, J. M., Valenciano, A., Rotgers, C., Carmona, R., Montoya, P., & Morales, J. (2012). Kretzoiarctos gen. Nov., the Oldest Member of the Giant Panda Clade. *PLOS ONE*, *7*(11), e48985. https://doi.org/10.1371/journal.pone.0048985

Adams, D. C., & Otárola-Castillo, E. (2013). geomorph: An r package for the collection and analysis of geometric morphometric shape data. *Methods in Ecology and Evolution*, *4*(4), 393–399. https://doi.org/10.1111/2041-210X.12035

Alba, D. M., Daura, J., Sanz, M., Santos, E., Yagüe, A. S., Delson, E., & Zilhão, J. (2019). New macaque remains from the Middle Pleistocene of Gruta da Aroeira (Almonda karst system, Portugal). *Journal of Human Evolution*, *131*, 40–47. https://doi.org/10.1016/j.jhevol.2019.02.003

Alexandrino, J., Froufe, E., Arntzen, J. W., & Ferrand, N. (2001). Genetic subdivision, glacial refugia and postglacial recolonization in the golden-striped salamander, Chioglossa lusitanica (Amphibia: Urodela). *Molecular Ecology*, *9*(6), 771–781. https://doi.org/10.1046/j.1365-294x.2000.00931.x

Almeida, J., Godinho, C., Leitão, D., & Lopes, R. (2023). *Lista Vermelha das Aves de Portugal Continental*. SPEA, ICNF, LabOR/UÉ, CIBIO/BIOPOLIS. https://dspace.uevora.pt/rdpc/handle/10174/36817

Alroy, J. (2020). On four measures of taxonomic richness. *Paleobiology*, *46*(2), 158–175. https://doi.org/10.1017/pab.2019.40

Álvarez-Lao, D. J., & García, N. (2011). Geographical distribution of Pleistocene cold-adapted large mammal faunas in the Iberian Peninsula. *Quaternary International*, *233*(2), 159–170. https://doi.org/10.1016/j.quaint.2010.04.017

Álvarez-Lao, D. J., Kahlke, R.-D., García, N., & Mol, D. (2009). The Padul mammoth finds—On the southernmost record of Mammuthus primigenius in Europe and its southern spread during the Late Pleistocene. *Palaeogeography, Palaeoclimatology, Palaeoecology*, *278*(1), 57–70. https://doi.org/10.1016/j.palaeo.2009.04.011

Andersen, M. B., Gallup, C. D., Scholz, D., Stirling, C. H., & Thompson, W. G. (2009). U-series dating of fossil coral reefs: Consensus and controversy. *PAGES News*, *17*, 54–56.

Angelone, C., Moncunill-Solé, B., & Kotsakis, T. (2020). Fossil Lagomorpha (Mammalia) of Italy: Systematics and Biochronology. *Rivista Italiana Di Paleontologia e Stratigrafia*, *126*(1), 157–187.

Angelucci, D. E., Nabais, M., & Zilhão, J. (2023). Formation processes, fire use, and patterns of human occupation across the Middle Palaeolithic (MIS 5a-5b) of Gruta da Oliveira (Almonda karst system, Torres Novas, Portugal). *PLOS ONE*, *18*(10), e0292075. https://doi.org/10.1371/journal.pone.0292075

Angelucci, D. E., & Zilhão, J. (2009). Stratigraphy and formation processes of the Upper Pleistocene deposit at Gruta da Oliveira, Almonda karstic system, Torres Novas, Portugal. *Geoarchaeology*, *24*(3), 277–310. https://doi.org/10.1002/gea.20267

Antunes, M. T. (1986). Acerca de um osso do Plistocénico da Mealhada: Presença de um «tigre dente de sabre», Homotherium latidens (OWEN, 1846). *Ciências Da Terra/Earth Sciences Journal*, *8*, 43–54.

Antunes, M. T. (1989). Castor fiber na gruta do Caldeirão: Existência, distribuição e extinção do castor em Portugal. *Ciências da Terra / Earth Sciences Journal*, *10*, 23–40.

Antunes, M. T. (2000a). Gruta da Figueira Brava: Pleistocene marine mammals. In *Últimos Neandertais em Portugal: Evidência, odontológica e outra.* (Vol. 38, pp. 245–558).

Antunes, M. T. (2000b). *Últimos Neandertais em Portugal: Evidência, odontológica e outra.* Academia das Ciências.

Antunes, M. T. (2006). The Zebro (Equidae) and its extinction in Portugal, with an appendix on the noun zebro and the modern zebra. *Equids in Time and Space*, 210–235.

Antunes, M. T., Azzaroli, A., Faure, M., Guérin, C., & Mein, P. (1986). Mammifères pleistocènes de Algoz, en Algarve: Une revision. *Ciências da terra*, *8*, 73–86.

Antunes, M. T., Cabral, J. M. P., Cardoso, J. L., Pais, J., & Soares, A. M. (1989). Paleolítico médio e superior em Portugal: Datas 14C, estado actual dos conhecimentos, síntese e discussão. *Ciências da Terra*, *10*, 127–138.

Antunes, M. T., & Cardoso, J. L. (1986). O leão das cavernas, Pantera (Leo) Spelaea (Goldfuss, 1810) em Portugal. In *Da Pré-história à história: Homenagem a Octávio da Veiga Ferreira* (pp. 73–80). Delta. https://repositorioaberto.uab.pt/handle/10400.2/3851

Antunes, M. T., & Cardoso, J. L. (1992). Quaternary elephants in Portugal: New data. *Ciências Da Terra*, *11*, 17–37.

Antunes, M. T., Cardoso, J. L., & Faure, M. (1988). Présence de Hippopotamus incognitus au Portugal et remarques sur les sites quaternaires de Mealhada. *Comunicações Geológicas*, *74*, 165–172.

Antunes, M. T., Casanovas, M. L., Cuesta, M. A., Checa, L., Santafé, J. V., & Agustí, J. (1997). Eocene mammals from Iberian peninsula. *Mémoires et Travaux de l'Institut de Montpellier*, *21*, 337–352.

Antunes, M. T., Crespo, E., Mein, P., Pais, J., & Teixeira, J. P. (1989). Guia (Algarve), gisement de vertébrés quaternaires à caractère saisonnier. *Ciências da Terra*, *10*(97–106). https://run.unl.pt/handle/10362/4427

Antunes, M. T., Manuppella, G., Mein, P., & Zbyszewski, G. (1986). Goldra: Premier gisement karstique en Algarve, faune et industries. *Ciências da terra*, *8*, 31–42.

Antunes, M. T., Mein, P., Nascimento, A., & Pais, J. (1986). Le gisement pleistocène de Morgadinho, en Algarve. *Ciências da Terra*, *8*, 9–22.

Arceredillo, D., Peyrouse, J.-B., & Aubry, T. (2018). Paléolithiques moyen et supérieur à Buraca Escura (Redinha, Pombal, Portugal): Comparaisons taphonomique et archéozoologique. *Quaternaire. Revue de l'Association française pour l'étude du Quaternaire*, *vol. 29/1*, Article 29/1. https://doi.org/10.4000/quaternaire.8615

Arnold, L. J., Demuro, M., Duval, M., Grün, R., Sanz, M., Costa, A. M., Araújo, A. C., & Daura, J. (2024). Single-grain luminescence and combined U-series/ESR dating of the early Upper Palaeolithic Lagar Velho Rock Shelter, Leiria, Portugal. *Quaternary Geochronology*, *83*, 101572. https://doi.org/10.1016/j.quageo.2024.101572

Aubry, T., Brugal, J.-P., Chauviere, F.-X., Figueiral, I., Moura Neves, M. H., & Plisson, H. (2001). Modalités d'occupations au Paléolithique supérieur dans la grotte de Buraca Escura (Redinha, Pombal, Portugal). *Revista Portuguesa de Arqueologia*, *4*(2), 19–46.

Aubry, T., Dimuccio, L. A., Almeida, M., Neves, M. J., Angelucci, D. E., & Cunha, L. (2011). Palaeoenvironmental forcing during the Middle–Upper Palaeolithic transition in central-

western Portugal. *Quaternary Research*, *75*(1), 66–79. https://doi.org/10.1016/j.yqres.2010.11.002

Aubry, T., Fontugne, M., & Moura, M.-H. (1997). Les Occupations De La Grotte De Buraca Grande Depuis Le Paléolithique Supérieur Et Les Apports De La Séquence Holocène À L'étude De La Transition Mésolithique/Néolithique Au Portugal. *Bulletin de La Société Préhistorique Française*, *94*(2), 182–190.

Aubry, T., Luís, L., Mangado Llach, J., & Matias, H. (2012). We will be known by the tracks we leave behind: Exotic lithic raw materials, mobility and social networking among the Côa Valley foragers (Portugal). *Journal of Anthropological Archaeology*, *31*(4), 528–550. https://doi.org/10.1016/j.jaa.2012.05.003

Aubry, T., Moura, M. H., & Zilhão, J. (1992). DADOS PRELIMINARES SOBRE A ORGANIZAÇÃO ESTRATIGRAFICA DA BURACA GRANDE DO VALE DO POIO NOVO (REDINHA). *Memórias e Notícias*, *114*, 119–132.

Aubry, T., Santos, A. T., & Luís, L. (2014). Stratigraphies du panneau 1 de Fariseu: Analyse structurelle d'un système graphique paléolithique à l'air libre de la vallée du Côa (Portugal). *P. Paillet (Ed.), Les Arts de La Préhistoire: Micro-Analyses, Mise En Contexte et Conservation: Actes Du Colloque "Micro-Analyses et Datations de l'art Préhistorique Dans Son Contexte Archéologique,"* 259–270. https://comum.rcaap.pt/bitstream/10400.26/23441/1/AubrySantos%26Luis2014.pdf

Ayliffe, L. K., Lister, A. M., & Chivas, A. R. (1992). The preservation of glacial-interglacial climatic signatures in the oxygen isotopes of elephant skeletal phosphate. *Palaeogeography, Palaeoclimatology, Palaeoecology*, *99*(3), 179–191. https://doi.org/10.1016/0031-0182(92)90014-V

Azenha, M. L. O. (2020). Os tufos calcários do Plistocénico superior e Holocénico de Condeixa e a sua pertinência para o ensino das Ciências da Terra. In *Uma visão holística da Terra e do Espaço nas suas vertentes naturais e humanas. Homenagem à Professora Celeste Romualdo Gomes.* (pp. 524–540). CITEUC. https://zenodo.org/records/4411931

Azorit, C., Analla, M., Carrasco, R., Calvo, J. A., & Muñoz-Cobo, J. (2002). Teeth eruption pattern in red deer (Cervus elaphus hispanicus) in southern Spain. *Anales de Biología*, *24*, 107–114.

Baca, M., Popović, D., Stefaniak, K., Marciszak, A., Urbanowski, M., Nadachowski, A., & Mackiewicz, P. (2016). Retreat and extinction of the Late Pleistocene cave bear (Ursus spelaeus sensu lato). *The Science of Nature*, *103*(11), 92. https://doi.org/10.1007/s00114-016-1414-8

Baeta Neves, C. M. (1967). Sobre a existência e extinção do urso em Portugal. *Gazeta Das Aldeias*, *2589*, 282–287.

Baier-Stegmaier, S., Gundlach, C., Chriél, M., Hansen, M. S., Vedel-Smith, C., Hansen, C. V., Johansson, D. K., Henriksen, L. B., Wahlberg, M., Thøstesen, C. B., Alstrup, A. K. O., Gregersen, K. M., Pertoldi, C., & Pagh, S. (2023). Computed Tomography as a Method for Age Determination of Carnivora and Odontocetes with Validation from Individuals with Known Age. *Animals*, *13*(11), Article 11. https://doi.org/10.3390/ani13111783

Barlow, A., Cahill, J. A., Hartmann, S., Theunert, C., Xenikoudakis, G., Fortes, G. G., Paijmans, J. L. A., Rabeder, G., Frischauf, C., Grandal-d'Anglade, A., García-Vázquez, A., Murtskhvaladze, M., Saarma, U., Anijalg, P., Skrbinšek, T., Bertorelle, G., Gasparian, B., Bar-Oz, G., Pinhasi, R., … Hofreiter, M. (2018). Partial genomic survival of cave bears in living brown

bears. *Nature Ecology & Evolution*, *2*(10), 1563–1570. https://doi.org/10.1038/s41559-018-0654-8

Barlow, A., Paijmans, J. L. A., Alberti, F., Gasparyan, B., Bar-Oz, G., Pinhasi, R., Foronova, I., Puzachenko, A. Y., Pacher, M., Dalén, L., Baryshnikov, G., & Hofreiter, M. (2021). Middle Pleistocene genome calibrates a revised evolutionary history of extinct cave bears. *Current Biology*, *31*(8), 1771-1779.e7. https://doi.org/10.1016/j.cub.2021.01.073

Bartolini-Lucenti, S., Madurell-Malapeira, J., Martínez-Navarro, B., Palmqvist, P., Lordkipanidze, D., & Rook, L. (2021). The early hunting dog from Dmanisi with comments on the social behaviour in Canidae and hominins. *Scientific Reports*, *11*(1), 13501. https://doi.org/10.1038/s41598-021-92818-4

Baryshnikov, G. F., & Puzachenko, A. Y. (2017). Morphometric analysis of metacarpal and metatarsal bones of cave bears (Carnivora, Ursidae). *Fossil Imprint*, *73*(1–2), 7–47. https://doi.org/10.1515/if-2017-0001

Battista, F., & Schultz, C. L. (2024). Sampling and collector biases as taphonomic filters: An overview. *Anais Da Academia Brasileira de Ciências*, *96*(4), e20231242.

Bellucci, L., Sardella, R., & Rook, L. (2015). Large mammal biochronology framework in Europe at Jaramillo: The Epivillafranchian as a formal biochron. *Quaternary International*, *389*, 84–89. https://doi.org/10.1016/j.quaint.2014.11.012

Ben-David, M., & Flaherty, E. A. (2012). Stable isotopes in mammalian research: A beginner's guide. *Journal of Mammalogy*, *93*(2), 312–328. https://doi.org/10.1644/11-MAMM-S-166.1

Benedetti, M. M., Haws, J., Bicho, N. F., Friedl, L., & Ellwood, B. B. (2019). Late Pleistocene site formation and paleoclimate at Lapa do Picareiro, Portugal. *Geoarchaeology*, *34*(6), 698–726. https://doi.org/10.1002/gea.21735

Bibi, F., Vrba, E., & Fack, F. (2012). A new african fossil caprin and a combined molecular and morphological bayesian phylogenetic analysis of caprini (Mammalia: Bovidae). *Journal of Evolutionary Biology*, *25*(9), 1843–1854. https://doi.org/10.1111/j.1420-9101.2012.02572.x

Bicho, N. (2004). The middle Paleolithic occupation of southern Portugal. In *Settlement Dynamics of the Middle Paleolithic and Middle Stone Age* (Vol. 2, pp. 513–531). Kerns Verlag Tübingen. https://www.academia.edu/download/5279663/bicho_2004.pdf

Bicho, N., Belcher, W., Haws, J., Markova, A., & Hockett, B. S. (2003). Paleoecologia e ocupação humana da Lapa do Picareiro: Resultados preliminares. *Revista portuguesa de arqueologia*, *6*(2), 49–82.

Biewener, A. A. (1990). Biomechanics of Mammalian Terrestrial Locomotion. *Science*, *250*(4984), 1097–1103. https://doi.org/10.1126/science.2251499

Bisbal-Chinesta, J. F., & Blain, H.-A. (2018). Long-term changes in composition and distribution patterns in the Iberian herpetofaunal communities since the latest Pleistocene. *Quaternary Science Reviews*, *184*, 143–166. https://doi.org/10.1016/j.quascirev.2017.06.010

Blackburn, D. C., Boyer, D. M., Gray, J. A., Winchester, J., Bates, J. M., Baumgart, S. L., Braker, E., Coldren, D., Conway, K. W., Rabosky, A. D., de la Sancha, N., Dillman, C. B., Dunnum, J. L., Early, C. M., Frable, B. W., Gage, M. W., Hanken, J., Maisano, J. A., Marks, B. D., … Stanley, E. L. (2024). Increasing the impact of vertebrate scientific collections through

3D imaging: The openVertebrate (oVert) Thematic Collections Network. *BioScience*, *74*(3), 169–186. https://doi.org/10.1093/biosci/biad120

Blois, J. L., McGuire, J. L., & Hadly, E. A. (2010). Small mammal diversity loss in response to late-Pleistocene climatic change. *Nature*, *465*(7299), Article 7299. https://doi.org/10.1038/nature09077

Bocherens, H., Billiou, D., Patou-Mathis, M., Bonjean, D., Otte, M., & Mariotti, A. (1997). Paleobiological Implications of the Isotopic Signatures (13C,15N) of Fossil Mammal Collagen in Scladina Cave (Sclayn, Belgium). *Quaternary Research*, *48*(3), 370–380. https://doi.org/10.1006/qres.1997.1927

Bocherens, H., Drucker, D., Billiou, D., & Moussa, I. (2005). Une nouvelle approche pour évaluer l'état de conservation de l'os et du collagène pour les mesures isotopiques (datation au radiocarbone, isotopes stables du carbone et de l'azote). *L'Anthropologie*, *109*(3), 557–567. https://doi.org/10.1016/j.anthro.2005.06.005

Bocherens, H., Stiller, M., Hobson, K. A., Pacher, M., Rabeder, G., Burns, J. A., Tütken, T., & Hofreiter, M. (2011). Niche partitioning between two sympatric genetically distinct cave bears (Ursus spelaeus and Ursus ingressus) and brown bear (Ursus arctos) from Austria: Isotopic evidence from fossil bones. *Quaternary International*, *245*(2), 238–248. https://doi.org/10.1016/j.quaint.2010.12.020

Boneta Jiménez, I., Cardoso, J. L., & Pérez-García, A. (2023). The turtles from the middle Paleolithic site of Gruta Nova da Columbeira (Bombarral, Portugal): Update through an archaeozoological perspective. *The Anatomical Record*, *n/a*(n/a). https://doi.org/10.1002/ar.25229

Boneta Jiménez, I., Pérez-García, A., & Liesau von Lettow-Vorbeck, C. (2023). Chelonians from the Middle Palaeolithic Site of Mealhada (Coimbra, Portugal): An Update. *Diversity*, *15*(2), Article 2. https://doi.org/10.3390/d15020243

Boulygina, E., Sharko, F., Cheprasov, M., Gladysheva-Azgari, M., Slobodova, N., Tsygankova, S., Rastorguev, S., Grigorieva, L., Kopp, M., Fernandes, J. M. O., Novgorodov, G., Boeskorov, G., Protopopov, A., Hwang, W.-S., Tikhonov, A., & Nedoluzhko, A. (2022). Ancient DNA Reveals Maternal Philopatry of the Northeast Eurasian Brown Bear (Ursus arctos) Population during the Holocene. *Genes*, *13*(11), Article 11. https://doi.org/10.3390/genes13111961

Bowen, F., Carden, R. F., Daujat, J., Grouard, S., Miller, H., Perdikaris, S., & Sykes, N. (2016). Dama Dentition: A New Tooth Eruption and Wear Method for Assessing the Age of Fallow Deer (Dama dama). *International Journal of Osteoarchaeology*, *26*(6), 1089–1098. https://doi.org/10.1002/oa.2523

Breda, M. (2005). The morphological distinction between the postcranial skeleton of Cervalces/Alces and Megaloceros giganteus and comparison between the two Alceini genera from the Upper Pliocene–Holocene of Western Europe. *Geobios*, *38*(2), 151–170. https://doi.org/10.1016/j.geobios.2003.09.008

Breda, M. (2015). The early Middle Pleistocene fallow deer Dama roberti: New insight on species morphology from a complete postcranial skeleton from Valdemino (northwestern Italy). *Geological Journal*, *50*(3), 257–270. https://doi.org/10.1002/gj.2624

Breiman, L. (2001). Random Forests. *Machine Learning*, *45*(1), 5–32. https://doi.org/10.1023/A:1010933404324

Breiman, L. (2018). Breiman and Cutler's random forests for classification and regression. *R Package Version*, *3*(3).

Brugal, J.-P., Argant, J., Crispim, J. A., Figueiredo, S. D., Serra, A. M., & Palmqvist, P. (2012). The complex carnivore-rich assemblages from Furninha (Peniche, Portugal): A multidisciplinary approach. *Journal of Taphonomy*, *10*(3–4), 417–438.

Brugal, J.-P., & Raposo, L. (1999). Foz do Enxarrique (Ródão—Portugal): Preliminary results of the analysis of a bone assemblage from A Midle Palaeolithic open site. In *The Role of Early Humans in the Accumulation of European Lower and Middle Palaeolithic Bone Assemblages* (pp. 367–379). Römisch Germanisches Zentralmuseum Mainz.

Bukhsianidze, M., & Vekua, A. (2006). Capra dalii nov. Sp.(Caprinae, Bovidae, Mammalia) at the limit of Plio-Pleistocene from Dmanisi (Georgia). *Courier-Forschungsinstitut Senckenberg*, *256*, 159.

Calderón, T., DeMiguel, D., Arnold, W., Stalder, G., & Köhler, M. (2019). Calibration of life history traits with epiphyseal closure, dental eruption and bone histology in captive and wild red deer. *Journal of Anatomy*, *235*(2), 205–216. https://doi.org/10.1111/joa.13016

Caloi, L., & Palombo, M. R. (1997). Biochronology of large mammals in the early and middle Pleistocene of the Italian peninsula. *Hystrix, the Italian Journal of Mammalogy*, *9*(1–2). https://doi.org/10.4404/hystrix-9.1-2-4103

Cameron, M. D., Hilderbrand, G. V., Joly, K., Schmidt, J. H., Gustine, D. D., Mangipane, L. S., Mangipane, B., & Sorum, M. S. (2020). Body size plasticity in North American black and brown bears. *Ecosphere*, *11*(8), e03235. https://doi.org/10.1002/ecs2.3235

Cardoso, J. L. (1989). Le daim dans le Pléistocène du Portugal. *Comunicações Geológicas*, *75*, 111–118.

Cardoso, J. L. (1990). Presença de Rinoceronte: Dicerorhinus hemitoechus (FALCONER, 1878) na gruta do Escoural. *Almansor*, *8*, 7–14.

Cardoso, J. L. (1992). Présence de Cuon alpinus europaeus BOURGUIGNAT, 1868 (Mammalia, Carnivora) dans le Pléistocène du Portugal. *Ciências da Terra*, *11*, 65–75.

Cardoso, J. L. (1993). *Contribuição para o conhecimento dos Grandes Mamíferos do Plistocénico superior de Portugal*. Cámara municipal de Oeiras.

Cardoso, J. L. (1994a). Crocuta crocuta intermedia (M. de Serres, 1828) (Mammalia, Carnivora) no Plistocénico de Portugal. *Comunicações Geológicas*, *80*, 89–97.

Cardoso, J. L. (1994b). Faunas plistocénicas do Concelho de Cascais. *Arquivo de Cascais. Boletim Cultural do Município*, *11*, 13–30.

Cardoso, J. L. (1995a). Grutas do Maciço Hespérico de Portugal com faunas de grandes mamíferos plistocénicos: Breve síntese. *Caderno do Laboratorio Xeolóxico de Laxe*, *20*, 213–229.

Cardoso, J. L. (1995b). Presença de Equus hydruntinus REGALIA, 1905 no Würm recente de Portugal. *Comunicações Geológicas*, *81*, 97–108.

Cardoso, J. L. (1996a). Les grands Mammifères du Pléistocène supérieur du Portugal. Essai de synthèse. *Geobios*, *29*(2), 235–250. https://doi.org/10.1016/S0016-6995(96)80047-7

Cardoso, J. L. (1996b). Nota sobre uma lamela de molar de elefante da gruta do Almonda (Torres Novas). *Comunicações Do Instituto Geológico e Mineiro*, *82*, 169–174.

Cardoso, J. L. (1997). As grutas, os grandes Mamíferos e o Homem Paleolítico: Uma aproximação integrada ao território português. *Estudos do Quaternário / Quaternary Studies*, *1*(1), 13–23.

Cardoso, J. L. (2000a). As investigações de Carlos Ribeiro e de Nery Delgado sobre o "Homem Terciário": Resultados e consequências na época e para além dela. *Estudos Arqueológicos de Oeiras*, *8*, 33–54.

Cardoso, J. L. (2000b). GEORGES ZBYSZEWSKI (1909-1999). *Estudos Arqueológicos de Oeiras*, *8*, 9–20.

Cardoso, J. L. (2001). *Sobre a presença do urso em Portugal: A propósito de uma peça do castelo de Leiria*. Núcleo Museológico da Torre de Menagem do Castelo de Leiria.

Cardoso, J. L. (2008). O. da Veiga Ferreira (1917-1997): Sua vida e obra científica. *Estudos Arqueológicos de Oeiras*, *16*, 13–123.

Cardoso, J. L. (2013). Carlos Ribeiro e Oeiras. Razões de uma homenagem. *Estudos Arqueológicos de Oeiras.*, *20*, 11–20.

Cardoso, J. L. (2015a). A investigação da antiguidade do Homem no Portugal de oitocentos: Um contributo para a história da ciência. *Estudos Arqueológicos de Oeiras*, *22*, 9–42.

Cardoso, J. L. (2015b). Carlos Ribeiro (1813-1882), as formações quaternárias portuguesas e a antiguidade do homem: Um manuscrito desconhecido. *Estudos Arqueológicos de Oeiras*, *22*, 43–92.

Cardoso, J. L. (2017). As faunas de grandes e médios mamíferos e a alimentação humana na região de Lisboa, do Paleolítico ao Bronze Final. In *Diz-me o que comes... Alimentação antes e depois da cidade* (pp. 8–23). Câmara Municipal de Lisboa.

Cardoso, J. L. (2020). Sobre a presença de Conus pulcher (Lightfoot), 1756 na gruta das Fontainhas (Cadaval) ou a ocorrência de objectos exóticos africanos em Portugal no decurso do século XVI. *Estudos Arqueológicos de Oeiras*, *27*, 387–396.

Cardoso, J. L. (2021). Among hyenas: Nery Delgado, Albert Gaudry, Edouard Harlé and the hyenas of Furninha cave (Portugal). In *Themes in Old World Zooarchaeology. From the Mediterranean to the Atlantic* (pp. 61–70). Oxbow Books. https://repositorio-aberto.uab.pt/handle/10400.2/10770

Cardoso, J. L., & Antunes, M. T. (1989). Rupicapra rupicapra (Mammalia) In the Late Pleistocene of Portugal. *Ciências Da Terra*, *10*, 81–96.

Cardoso, J. L., & Avila de Melo, A. (2001). Correspondência anotada de Carlos Ribeiro e de Nery Delgado: Contribuição para a história da Arqueologia em Portugal. *Comunicações Geo-lógicas*, *88*, 309–246.

Cardoso, J. L., & Bicho, N. (2021). Nery Delgado, Pioneer of Archaeological Excavation Methods at the Casa da Moura Cave (Portugal) in 1879–1880. *European Journal of Archaeology*, *24*(2), 249–265. https://doi.org/10.1017/eaa.2020.55

Cardoso, J. L., & Carreira, J. R. (1991). O espólio arqueológico do algar de João Ramos ou gruta das redondas, Turquel—Alcobaça. *Actas das IV Jornadas Arqueológlcas (Lisboa 1990)*. http://hdl.handle.net/10400.2/3852

Cardoso, J. L., Detry, C., & Zilhão, J. (2021). The first appearance of hystrix (rodentia,mammalia) in Portugal, last interglacial, gruta da Figueira Brava (Setúbal). *Quaternaire. Revue de l'Association Française Pour l'étude Du Quaternaire*, *vol. 32/3*, Article 32/3. https://doi.org/10.4000/quaternaire.18541

Cardoso, J. L., & Eisenmann, V. (1989). Equus Caballus Antunesi, nouvelle sous-espece quaternaire du Portugal. *Palaeovertebrata*, *19*, 48–72.

Cardoso, J. L., & Raposo, L. (2002). *A Gruta Nova da Columbeira (Bombarral)*. Câmara Municipal do Bombarral. http://hdl.handle.net/10400.2/6251

Cardoso, J. L., & Regala, F. T. (2002). Sobre a presença de Mamute, Mammuthus Primigenius (Blumembach, 1799) em Portugal: Descoberta de uma lamela dentária em depósitos Plistocénicos do fundo do estuário do Tejo (Cruz Quebrada, Oeiras). *Estudos Arqueológicos de Oeiras*, *10*, 39–47.

Cardoso, J. L., & Regala, F. T. (2006). O Leopardo, Panthera pardus (L., 1758), do Algar da Manga Larga (Planalto de Santo António, Porto de Mós). *Comunicações Geológicas*, *93*, 119–144.

Cardoso, J. L., & Santos, M. F. dos. (1999). Riqueza e diversidade do registo arqueológico: O caso do litoral a norte da praia de Santa Cruz (Torres Vedras). In *Fraternidade e Abnegação: Vol. II*. Academia Portuguesa da História. http://hdl.handle.net/10400.2/6053

Carvalho, M., Jones, E. L., Ellis, M. G., Cascalheira, J., Bicho, N., Meiggs, D., Benedetti, M., Friedl, L., & Haws, J. (2022). Neanderthal palaeoecology in the late Middle Palaeolithic of western Iberia: A stable isotope analysis of ungulate teeth from Lapa do Picareiro (Portugal). *Journal of Quaternary Science*, *37*(2), 300–319. https://doi.org/10.1002/jqs.3363

Cascalheira, J., Bicho, N., Marreiros, J., Pereira, T., Évora, M., Cortés Sánchez, M., Gibaja, J. F., Manne, T., Regala, F., & Gonçalves, C. (2013). Vale Boi (algarve, Portugal) and the solutrean in southwestern Iberia. *Espacio, Tiempo y Forma.*, *5*, 455–467.

Chardin, P. T. D., & Piveteau, J. (1930). Les mammifères fossiles de Nihowan (Chine). *Annales de Paléontologie*, *19*, 1–154.

Chatar, N., Michaud, M., Tamagnini, D., & Fischer, V. (2024). Evolutionary patterns of cat-like carnivorans unveil drivers of the sabertooth morphology. *Current Biology*, *34*(11), 2460-2473.e4. https://doi.org/10.1016/j.cub.2024.04.055

Chen, Y., Li, Y., Zhang, M., Cui, Z., & Liu, G. (2018). Much late onset of Quaternary glaciations on the Tibetan Plateau: Determining the age of the Shishapangma Glaciation using cosmogenic 26Al and 10Be dating. *Science Bulletin*, *63*(5), 306–313. https://doi.org/10.1016/j.scib.2018.01.020

Cheong, C.-S., Choi, M. S., Khim, B. K., Sohn, Y. K., & Kwon, S.-T. (2006). 230Th/234U dating of Holocene mollusk shells from Jeju Island, Korea, by multiple collectors inductively coupled plasma mass spectrometry. *Geosciences Journal*, *10*(1), 67–74. https://doi.org/10.1007/BF02910333

Cherin, M., Breda, M., Esattore, B., Hart, V., Turek, J., Porciello, F., Angeli, G., Holpin, S., & Iurino, D. A. (2022). A Pleistocene Fight Club revealed by the palaeobiological study of the Dama-like deer record from Pantalla (Italy). *Scientific Reports*, *12*(1), Article 1. https://doi.org/10.1038/s41598-022-18091-1

Cherkinsky, A. (2009). Can We Get a Good Radiocarbon Age from "Bad Bone"? Determining the Reliability of Radiocarbon Age from Bioapatite. *Radiocarbon*, *51*(2), 647–655. https://doi.org/10.1017/S0033822200055995

Choffat, P. (1895). Note sur les tufs de Condeixa et la découverte de l'hippopotame en Portugal. *Comunicações Geológicas*, *3*, 1–12.

Christiansen, P. (1999). What size were Arctodus simus and Ursus spelaeus (Carnivora: Ursidae)? *Annales Zoologici Fennici*, *36*(2), 93–102.

Clavero, M., & Delibes, M. (2013). Using historical accounts to set conservation baselines: The case of Lynx species in Spain. *Biodiversity and Conservation*, *22*(8), 1691–1702. https://doi.org/10.1007/s10531-013-0506-4

Clevenger, A. P., & Iraizoz, F. J. P. (1991). *Ecología del oso pardo en España* (Vol. 4). Museo Nacional de Ciencias Naturales.

Close, R. A., Benson, R. B. J., Alroy, J., Carrano, M. T., Cleary, T. J., Dunne, E. M., Mannion, P. D., Uhen, M. D., & Butler, R. J. (2020). The apparent exponential radiation of Phanerozoic land vertebrates is an artefact of spatial sampling biases. *Proceedings of the Royal Society B: Biological Sciences*, *287*(1924), 20200372. https://doi.org/10.1098/rspb.2020.0372

Cobo-Sánchez, L., Rufà, A., & Cascalheira, J. (2024). Alternating carnivore and Neanderthal activities at Escoural Cave: Insights from the taphonomic and machine learning analysis of leporid remains. *Frontiers in Environmental Archaeology*, *3*. https://doi.org/10.3389/fearc.2024.1473266

Corlatti, L., Lorenzini, R., & Lovari, S. (2011). The conservation of the chamois Rupicapra spp.: Biology and conservation of the chamois. *Mammal Review*, *41*(2), 163–174. https://doi.org/10.1111/j.1365-2907.2011.00187.x

Couturier, M. (1954). *L'ours brun: Ursus arctos L.*

Crespo, E. G., Patricio, G. A., & Antunes, M. T. (2000). Pleistocene Reptilia and Amphibia from Gruta da Figueira Brava (Arrábida, Portugal). In *Últimos Neandertais em Portugal: Evidência, odontológica e outra.* (Vol. 38, pp. 23–67).

Crespo, V. D., & Castillo, C. (2025). … and the devil is in the details: A response to Furió et al. (2024). *Palaeoworld*, *34*(4), 200932. https://doi.org/10.1016/j.palwor.2025.200932

Croitor, R. (2021). Taxonomy, Systematics and Evolution of Giant Deer Megaloceros Giganteus (Blumenbach, 1799) (Cervidae, Mammalia) from the Pleistocene of Eurasia. *Quaternary*, *4*(4), Article 4. https://doi.org/10.3390/quat4040036

Croitor, R., & Robinson, C. (2020). A revision of "Cervus" punjabiensis Brown, 1926 (Cervidae, Mammalia) from the Upper Siwaliks of Chandigarh, India. *Quaternary International*, *550*, 147–158. https://doi.org/10.1016/j.quaint.2020.04.020

Croitor, R., Sanz, M., & Daura, J. (2019). Deer remains from the Middle Pleistocene site of Gruta da Aroeira (Portugal): Iberian faunal endemism and implications for hominin paleobiogeography. *Quaternary Science Reviews*, *225*, 106022. https://doi.org/10.1016/j.quascirev.2019.106022

Cuenca-Bescós, G., & Morcillo-Amo, A. (2022). *Roedores, edades y paisajes en el Cuaternario de la Península Ibérica*. Prames.

Cuenca-Bescós, G., Sanz, M., Daura, J., & Zilhão, J. (2021). The fossils of castor fiber from the middle Pleistocene site of Gruta da Aroeira (Portugal) and human-beaver interaction. *Quaternaire. Revue de l'Association Française Pour l'étude Du Quaternaire*, *vol. 32/1*, Article 32/1. https://doi.org/10.4000/quaternaire.14975

Cuenca-Paya, A., Pomery, P. J., & Walker, M. J. (1986). *Chronological aspects of the middle Pleistocene in the coastal belt of southeastern Spain*. 353–363. http://pascal-francis.inist.fr/vibad/index.php?action=getRecordDetail&idt=8815954

Cunha, P. P., Martins, A. A., Buylaert, J.-P., Murray, A. S., Gouveia, M. P., Font, E., Pereira, T., Figueiredo, S. D., Ferreira, C., Bridgland, D. R., Yang, P., Stevaux, J. C., & Mota, R. (2019). The Lowermost Tejo River Terrace at Foz do Enxarrique, Portugal: A Palaeoenvironmental Archive from c. 60–35 ka and Its Implications for the Last Neanderthals in Westernmost Iberia. *Quaternary*, *2*(1), 3. https://doi.org/10.3390/quat2010003

Cunha-Ribeiro, J. P. (1997). A estação paleolítica da Mealhada nos 120 anos de estudo do Acheulense em Portugal. *O Arqueólogo Português*, *13/15*, 35–52.

Curtis, A. A., & Van Valkenburgh, B. (2014). Beyond the Sniffer: Frontal Sinuses in Carnivora. *The Anatomical Record*, *297*(11), 2047–2064. https://doi.org/10.1002/ar.23025

Daura, J., Sanz, M., Arsuaga, J. L., Hoffmann, D. L., Quam, R. M., Ortega, M. C., Santos, E., Gómez, S., Rubio, A., Villaescusa, L., Souto, P., Mauricio, J., Rodrigues, F., Ferreira, A., Godinho, P., Trinkaus, E., & Zilhão, J. (2017). New Middle Pleistocene hominin cranium from Gruta da Aroeira (Portugal). *Proceedings of the National Academy of Sciences*, *114*(13), 3397–3402. https://doi.org/10.1073/pnas.1619040114

Daura, J., Sanz, M., Deschamps, M., Matias, H., Igreja, M., Villaescusa, L., Gómez, S., Rubio, A., Souto, P., Rodrigues, F., & Zilhão, J. (2018). A 400,000-year-old Acheulean assemblage associated with the Aroeira-3 human cranium (Gruta da Aroeira, Almonda karst system, Portugal). *Comptes Rendus Palevol*, *17*(8), 594–615. https://doi.org/10.1016/j.crpv.2018.03.003

Daura, J., Sanz, M., Rodrigues, F., Souto, P., & Zilhão, J. (2020). O sítio acheulense do Plistocénico médio da Gruta da Aroeira. *Arqueologia em Portugal 2020 - Estado da Questão*, 693–702. https://doi.org/10.21747/978-989-8970-25-1/arqa51

Daveau, S. (2000). Fases históricas e perspectivas actuais do estudo do Quaternário em Portugal. *Estudos do Quaternário / Quaternary Studies*, *3*, 5–14.

Davis, S. (2002). The mammals and birds from the Gruta do Caldeirão, Portugal. *Revista portuguesa de arqueologia*, *5*(2), 29–98.

Davis, S. (2019). Rabbits and Bergmann's rule: How cold was Portugal during the last glaciation? *Biological Journal of the Linnean Society*, *128*(3), 526–549. https://doi.org/10.1093/biolinnean/blz098

Davis, S., & MacKinnon, M. (2009). Did the Romans bring fallow deer to Portugal? *Environmental Archaeology*, *14*(1), 15–26. https://doi.org/10.1179/174963109X400646

Davis, S., Robert, I., & Zilhão, J. (2007). Caldeirão cave (Central Portugal)-whose home? Hyaena, man, bearded vulture. *Courier-Forschungsinstitut Senckenberg*, *259*, 213–226.

Dean, C. D., & Thompson, J. R. (2025). Museum 'dark data' show variable impacts on deep-time biogeographic and evolutionary history. *Proceedings of the Royal Society B: Biological Sciences*, *292*(2041), 20242481. https://doi.org/10.1098/rspb.2024.2481

Debeljak, I. (1996). Ontogenetic development of dentition in the cave bear. *Geologija*, *39*(1), 13–77.

Delgado, J. F. N. (1884). La grotte de Furninha a Peniche. *Compte-Rend de La 9ème Session (Lisboa, 1880)*, 207–278.

Delgado, J. F. N. (1886). *Estudo sobre os Bilobites e outros fósseis das quartzites da base do systema Silurico de Portugal*. Typ. da Academia real das sciencias.

Depraetere, M., Akhlaq, S., Díaz, V. D., Heumann, I., & Schwarz, D. (2025). Virtual Access to Fossil & Archival Material from the German Tendaguru Expedition (1909–1913): More Than 100 years of Data-Meta-paradata Management for Improved Standardisation. In M. Ioannides, D. Baker, A. Agapiou, & P. Siegkas (Eds.), *3D Research Challenges in Cultural Heritage V: Paradata, Metadata and Data in Digitisation* (pp. 89–102). Springer Nature Switzerland. https://doi.org/10.1007/978-3-031-78590-0_8

Detry, C., & Arruda, A. M. (2013). A fauna da Idade do Ferro e da Época Romana de Monte Molião (Lagos, Algarve): Continuidades e rupturas na dieta alimentar. *Revista Portuguesa de Arqueologia*, 213–226.

Detry, C., Francisco, A. C., Diniz, M., Martins, A., Neves, C., & Arnaud, J. M. (2020). Estudo zooarqueológico das faunas do Calcolítico final de Vila Nova de São Pedro (Azambuja, Portugal): Campanhas de 2017 e 2018. *Arqueologia em Portugal 2020 - Estado da Questão*, 925–941. https://doi.org/10.21747/978-989-8970-25-1/arqa67

Diedrich, C. G. (2012). Cave bear killers and scavengers from the last ice age of central Europe: Feeding specializations in response to the absence of mammoth steppe fauna from mountainous regions. *Quaternary International*, *255*, 59–78. https://doi.org/10.1016/j.quaint.2011.06.048

Domingo, L., Rodríguez-Gómez, G., Libano, I., & Gómez-Olivencia, A. (2017). New insights into the Middle Pleistocene paleoecology and paleoenvironment of the Northern Iberian Peninsula (Punta Lucero Quarry site, Biscay): A combined approach using mammalian stable isotope analysis and trophic resource availability modeling. *Quaternary Science Reviews*, *169*, 243–262. https://doi.org/10.1016/j.quascirev.2017.06.008

Domínguez García, Á. C., Laplana, C., Sevilla, P., Blain, H.-A., Zumajo, N. P., & Benítez de Lugo Enrich, L. (2019). New data on the introduction and dispersal process of small mammals in southwestern Europe during the Holocene: Castillejo del Bonete site (southeastern Spain). *Quaternary Science Reviews*, *225*, 106008. https://doi.org/10.1016/j.quasci-rev.2019.106008

Dong, W. (2008). Virtual cranial endocast of the oldest giant panda (Ailuropoda microta) reveals great similarity to that of its extant relative. *Naturwissenschaften*, *95*(11), 1079–1083. https://doi.org/10.1007/s00114-008-0419-3

Drake, A., Haut Donahue, T. L., Stansloski, M., Fox, K., Wheatley, B. B., & Donahue, S. W. (2016). Horn and horn core trabecular bone of bighorn sheep rams absorbs impact energy and

reduces brain cavity accelerations during high impact ramming of the skull. *Acta Biomaterialia*, *44*, 41–50. https://doi.org/10.1016/j.actbio.2016.08.019

Duñó-Iglesias, P., Ramírez-Pedraza, I., Rivals, F., Prilepskaya, N. E., Belyaev, R. I., & Baryshnikov, G. F. (2024). Dental microwear analysis of Kudaro cave bears: Insights into dietary evolution from the Middle to Late Pleistocene. *Palaeogeography, Palaeoclimatology, Palaeoecology*, *653*, 112417. https://doi.org/10.1016/j.palaeo.2024.112417

Edwards, C. T. T., Rasmussen, G. S. A., Riordan, P., Courchamp, F., & Macdonald, D. W. (2013). Non-Adaptive Phenotypic Evolution of the Endangered Carnivore Lycaon pictus. *PLOS ONE*, *8*(9), e73856. https://doi.org/10.1371/journal.pone.0073856

Ehlers, J., Gibbard, P. L., & Hughes, P. D. (2018). Quaternary Glaciations and Chronology. In J. Menzies & J. J. M. van der Meer (Eds.), *Past Glacial Environments (Second Edition)* (pp. 77–101). Elsevier. https://doi.org/10.1016/B978-0-08-100524-8.00003-8

Estraviz López, D., & Mateus, O. (2019). Tracks and multiple skeletons of brown bear ("Ursus Arctos") in Algar do Vale da Pena, Portugal. *Zubía*, *31*, 77–82.

Estraviz-López, D. (2019). *Quaternary fossil vertebrates from continental Portugal: Paleobiodiversity, revision of specimens and new localities*. https://run.unl.pt/handle/10362/74150

Estraviz-López, D., García-Vázquez, A., & Grandal-d'Anglade, A. (2021). Quantitative classification of metapodial bones of Ursus spelaeus and Ursus arctos from Northwestern Iberia using multivariate analysis | Ciências da Terra Procedia. *Ciências Da Terra Procedia*, *1*, 92–95.

Estraviz-López, D., Grandal-d'Anglade, A., & Ríos, M. (2025). Early Pleistocene (Epivillafranchian) vertebrates from Portugal: An updated review. *Geobios*, *88–89*, 77–89. https://doi.org/10.1016/j.geobios.2024.08.013

Estraviz-López, D., & Mateus, O. (2018a). The Quaternary mammals from the caves of Casais Robustos and Cabeço de Morto, Alcanena (Portugal): The case of Lynx pardinus Temminck, 1827. *Life Finds a Way*, 159–162.

Estraviz-López, D., & Mateus, O. (2018b). The size and body mass estimations of the proboscidean Paleoloxodon antiquus (Falconer & Cautley, 1847) from the Quaternary of São Antão do Tojal, Portugal. *VIII Congresso de Jovens Investigadores Em Geociências*, 70–73. https://www.researchgate.net/publication/329483702_The_size_and_body_mass_estimations_of_the_proboscidean_Paleoloxodon_antiquus_Falconer_Cautley_1847_from_the_Quaternary_of_Sao_Antao_do_Tojal_Portugal

Estraviz-López, D., Ríos, M., & Grandal-d'Anglade, A. (2024). The dawn of Pleistocene vertebrate paleontology in Portugal. *Zubía*, *42*, 305–310.

Farrington, J. D., & Li, J. (2024). Chapter 8—Climate change impacts on snow leopard range. In D. Mallon & T. McCarthy (Eds.), *Snow Leopards (Second Edition)* (pp. 81–93). Academic Press. https://doi.org/10.1016/B978-0-323-85775-8.00037-6

FCT/UNL. (2016). *Sessão de Homenagem ao Professor Doutor Miguel Telles Antunes*. https://www.fct.unl.pt/noticias/2016/12/sessao-de-homenagem-ao-professor-doutor-miguel-telles-antunes

Fernández-García, M., Royer, A., López-García, J. M., Bennàsar, M., Goedert, J., Fourel, F., Julien, M.-A., Bañuls-Cardona, S., Rodríguez-Hidalgo, A., Vallverdú, J., & Lécuyer, C. (2019).

Unravelling the oxygen isotope signal (δ18O) of rodent teeth from northeastern Iberia, and implications for past climate reconstructions. *Quaternary Science Reviews*, *218*, 107–121. https://doi.org/10.1016/j.quascirev.2019.04.035

Fernández-Laso, M. C., Brugal, J.-P., & Raposo, L. (2015). Gruta Nova da Columbeira (Bombarral, Portugal): Un modelo de ocupación en cueva durante el Paleolítico Medio. Resultados del estudio del registro de macromamíferos. *Trabajos de Prehistoria*, *72*(2), 304–326.

Fernández-Mosquera, D., Vila-Taboada, M., & Grandal-d'Anglade, A. (2001). Stable isotopes data (δ13C, δ15N) from the cave bear (Ursus spelaeus): A new approach to its palaeo-environment and dormancy. *Proceedings of the Royal Society of London. Series B: Biological Sciences*, *268*(1472), 1159–1164. https://doi.org/10.1098/rspb.2001.1639

Ferrández-Cañadell, C., & Gibert, L. (2012). Introducción. Cueva Victoria, un yacimiento de vertebrados del Pleistoceno Inferior. *Mastia: Revista del Museo Arqueológico Municipal de Cartagena*, *11–13*, 17–45.

Fialho, P., Da Silva, R., Patrocínio, S., Costa, B., & Burigo, A. (2023). Portuguese Fossil Database: First phase report. *Comunicações Geológicas*, *110*(1), 25–29.

Fick, S. E., & Hijmans, R. J. (2017). WorldClim 2: New 1-km spatial resolution climate surfaces for global land areas. *International Journal of Climatology*, *37*(12), 4302–4315. https://doi.org/10.1002/joc.5086

Fidalgo, D., Fernández-Rodríguez, C., Ballesteros, D., Ordiz, A., Pérez de la Viuda, C., Cruz, J. A., García-Morato, S., & Fernández-Martínez, E. (2025). Highlighting the drastic body size decline in Cantabrian Brown Bear, Chamois and Wild Horse during the Holocene. *The Holocene*, 09596836251333290. https://doi.org/10.1177/09596836251333290

Fidalgo, D., Madurell-Malapeira, J., Martino, R., Pandolfi, L., & Rosas, A. (2024). An Updated Review of The Quaternary Hippopotamus Fossil Records from the Iberian Peninsula. *Quaternary*, *7*(1), Article 1. https://doi.org/10.3390/quat7010004

Fidalgo, D., Rosas, A., Madurell-Malapeira, J., Pineda, A., Huguet, R., García-Tabernero, A., Cáceres, I., Ollé, A., Vallverdú, J., & Saladie, P. (2023). A review on the Pleistocene occurrences and palaeobiology of *Hippopotamus antiquus* based on the record from the Barranc de la Boella Section (Francolí Basin, NE Iberia). *Quaternary Science Reviews*, *307*, 108034. https://doi.org/10.1016/j.quascirev.2023.108034

Figueiral, I., & Terral, J.-F. (2002). Late Quaternary refugia of Mediterranean taxa in the Portuguese Estremadura: Charcoal based palaeovegetation and climatic reconstruction. *Quaternary Science Reviews*, *21*(4), 549–558. https://doi.org/10.1016/S0277-3791(01)00022-1

Figueiredo, S. D. (2010). *A Avifauna Plistocénica de Portugal: Especificidades evolutivas, anatómicas e o seu contexto paleontológico, geológico e arqueológico* [PhD thesis, Universidad de Salamanca]. https://gredos.usal.es/jspui/handle/10366/76422

Figueiredo, S. D., Cunha, P., Martins, A., & Gouveia, M. (2017). *Aves plistocénicas da Gruta da Furninha (Peniche): Abordagem paleontológica e paleoecológica*. https://dspace.uevora.pt/rdpc/handle/10174/22688

Figueiredo, S. D., Cunha, P. P., & Carvalho, I. S. (2022). Marine mammals fossil remains and synthesis of the sedimentary and paleontological record of the Furninha Cave Pleistocene (Peniche, Portugal). *Cuaternario y Geomorfología: Revista de La Sociedad Española de Geomorfología y Asociación Española Para El Estudio Del Cuaternario*, *36*(1), 37–52.

Figueiredo, S. D., Raposo, L., & Sousa, M. F. (2021). Upper Pleistocene Fauna from the Middle Palaeolithic Site of Foz do Enxarrique (Vila Velha de Ródão, Naturtejo Unesco Global Geopark). *Geoconservation Research*, *4*(2). https://doi.org/10.30486/gcr.2021.1912483.1048

Figueiredo, S. D., Sousa, F., Silva, S., Raposo, L., Pereira, T., & Rosa, A. (2018). Pleistocene Birds of Gruta Nova da Columbeira (Bombarral-Portugal): A Paleontological and Paleoenvironmental Aproach. *Journal of Environmental Science and Engineering A*, *7*, 246–254.

Figueirido, B., Palmqvist, P., Pérez-Claros, J. A., & Dong, W. (2011). Cranial shape transformation in the evolution of the giant panda (Ailuropoda melanoleuca). *Naturwissenschaften*, *98*(2), 107–116. https://doi.org/10.1007/s00114-010-0748-x

Figueirido, B., Tseng, Z. J., & Martín-Serra, A. (2013). Skull shape evolution in durophagous carnivorans. *Evolution*, *67*(7), 1975–1993. https://doi.org/10.1111/evo.12059

Figueiró, H. V., Li, G., Trindade, F. J., Assis, J., Pais, F., Fernandes, G., Santos, S. H. D., Hughes, G. M., Komissarov, A., Antunes, A., Trinca, C. S., Rodrigues, M. R., Linderoth, T., Bi, K., Silveira, L., Azevedo, F. C. C., Kantek, D., Ramalho, E., Brassaloti, R. A., … Eizirik, E. (2017). Genome-wide signatures of complex introgression and adaptive evolution in the big cats. *Science Advances*, *3*(7), e1700299. https://doi.org/10.1126/sciadv.1700299

Flato, G., Marotzke, J., Abiodun, B., Braconnot, P., Chou, S. C., Collins, W., Cox, P., Driouech, F., Emori, S., Eyring, V., Forest, C., Gleckler, P., Guilyardi, E., Jakob, C., Kattsov, V., Reason, C., Rummukainen, M., & more. (2014). Evaluation of climate models. In *Climate Change 2013: The Physical Science Basis. Contribution of Working Group I to the Fifth Assessment Report of the Intergovernmental Panel on Climate Change* (pp. 741–866). Cambridge University Press. https://doi.org/10.1017/CBO9781107415324.020

Fletcher, T. M., Janis, C. M., & Rayfield, E. J. (2010). Finite element analysis of ungulate jaws: Can mode of digestive physiology be determined. *Palaeontologia Electronica*, *13*(3), 1–15.

Fontsere, C., Speak, S. A., Caven, A. J., Rodríguez, J. A., Wang, X., Pacheco, C., Cassatt-Johnstone, M., Femerling, G., Maloney, B., Balacco, J., Collins, J., Sims, Y., Abueg, L., Fedrigo, O., Jarvis, E. D., Hartup, B. K., Shapiro, B., Gilbert, M. T. P., Oosterhout, C. van, & Morales, H. E. (2024). *Persistent genomic erosion in whooping cranes despite demographic recovery* (p. 2024.12.12.628160). bioRxiv. https://doi.org/10.1101/2024.12.12.628160

Fortes, G. G., Grandal-d'Anglade, A., Kolbe, B., Fernandes, D., Meleg, I. N., García-Vázquez, A., Pinto-Llona, A. C., Constantin, S., Torres, T. J. de, Ortiz, J. E., Frischauf, C., Rabeder, G., Hofreiter, M., & Barlow, A. (2016). Ancient DNA reveals differences in behaviour and sociality between brown bears and extinct cave bears. *Molecular Ecology*, *25*(19), 4907–4918. https://doi.org/10.1111/mec.13800

Fosse, P., Besson, J.-P., Laborde, H., Thomas-Cantié, F., Cazenave, G., Delmasure, M.-C., Leveque, T., Laudet, F., & Quiles, J. (2004). Denning behaviour of «modern» brown bear (Ursus arctos, L.) in caves: Biological and paleontological considerations from French Pyrenean sites. *Publications Du Musée Des Confluences*, *2*(1), 171–182.

Fosse, P., Fourvel, J. B., & Madeleine, S. (2020). Quaternary cliff-dwelling bovids (Capra, Rubicapra, Hemitragus, Ovis): Site's typology and taphonomic remarks. *SAGVNTVM Extra*, *21*, 137–163.

Fox, J. L., Chundawat, R. S., Kachel, S., Tallian, A., & Johansson, Ö. (2024). Chapter 2 - What is a snow leopard? Behavior and ecology. In D. Mallon & T. McCarthy (Eds.), *Snow Leopards (Second Edition)* (pp. 15–29). Academic Press. https://doi.org/10.1016/B978-0-323-85775-8.00051-0

Fox, J. L., Sinha, S. P., Chundawat, R. S., & Das, P. K. (1988). A field survey of snow leopard presence and habitat use in northwestern India. *Proceedings of the Fifth International Snow Leopard Symposium. International Snow Leopard Trust and Wildlife Institute of India, Seattle, Washington*, 99–111.

Frosali, S., Bartolini-Lucenti, S., Madurell-Malapeira, J., Urciuoli, A., Costeur, L., & Rook, L. (2023). First digital study of the frontal sinus of stem-Canini (Canidae, Carnivora): Evolutionary and ecological insights throughout advanced diagnostic in paleobiology. *Frontiers in Ecology and Evolution*, *11*. https://doi.org/10.3389/fevo.2023.1173341

Fuentes-Sánchez, D., Mateos, A., Aldea, J., & Rodríguez, J. (2019). Evidence of congenital block vertebra in Pleistocene Cave Bear (*Ursus spelaeus*) from Cueva de Guantes (Palencia, Spain). *International Journal of Paleopathology*, *24*, 165–170. https://doi.org/10.1016/j.ijpp.2018.10.010

Fumanal, M. P., & Villaverde, V. (2009). Las excavaciones en la Cova Negra en los años ochenta, la estratigrafía y el marco cronológico. *Historia de Xàtiva. I. La Prehistoria. Los Primeros Pobladores de La Costera: La Cova Negra de Xàtiva*, 25–57.

Furtado, A., Maurício, A. S., Côrtes, V., & Monteiro, J. A. (1969). Lapa do suão (Bombarral). *O Arqueólogo Português*, *3*, 63–69.

Gabriel, S., & Béarez, P. (2009). Caçadores-pescadores do Vale do Côa: Os restos de fauna do sítio do Fariseu. In *200 séculos da história do Vale do Côa: Incursões na vida quotidiana dos caçadores artistas do Paleolítico [Trabalhos de Arqueologia, 52]* (Vol. 52, pp. 331–339). IGESPAR, Instituto de Gestão do Património Arquitectónico e Arqueológico. https://comum.rcaap.pt/bitstream/10400.26/23837/1/Gabriel%26B%C3%A9arez2009.pdf

Galán, J., López-García, J. M., Cuenca-Bescós, G., & Sevilla, P. (2024). The Quaternary record of fossil bats in the Iberian Peninsula and the Balearic Islands: Palaeobiogeographical changes and palaeoenvironmental implications. *Palaeogeography, Palaeoclimatology, Palaeoecology*, *646*, 112243. https://doi.org/10.1016/j.palaeo.2024.112243

Gameiro, C., Davis, S., & Almeida, F. (2017). A sequência estratigráfica da Lapa dos Coelhos: Funcionalidade e subsistência ao longo do Plistocénico Superior no sopé na Serra de Aire (Portugal). *Arqueologia em Portugal. 2017 – Estado da Questão*, 357–374.

Gao, Y. (1987). *Fauna Sinica. Mammalia, Vol. 8: Carnivora* (Vol. 8). Science Press.

García-Vázquez, A. (2015). *Caracterización del oso pardo (Ursus arctos L.) fósil en el NW de la Península Ibérica: Datos morfométricos y moleculares* [PhD thesis, Universidad de A Coruña]. http://ruc.udc.es/dspace/handle/2183/15810

García-Vázquez, A., Llona, A. C. P., González-Fortes, G. M., & Grandal-d'Anglade, A. (2015). Distribución y cronología del oso pardo (Ursus arctos L.) en la Península Ibérica durante el Pleistoceno Superior y Holoceno. *Spanish Journal of Palaeontology*, *30*(1), Article 1. https://doi.org/10.7203/sjp.30.1.17233

García-Vázquez, A., Pinto Llona, A. C., & Grandal-d'Anglade, A. (2019). Post-glacial colonization of Western Europe brown bears from a cryptic Atlantic refugium out of the Iberian Peninsula. *Historical Biology*, *31*(5), 618–630. https://doi.org/10.1080/08912963.2017.1384473

Gaspar-López, E., García, A. J., Landete-Castillejos, T., Carrión, D., Estevez, J. A., & Gallego, L. (2008). Growth of the first antler in Iberian red deer (Cervus elaphus hispanicus). *European Journal of Wildlife Research*, *54*(1), 1–5. https://doi.org/10.1007/s10344-007-0096-0

Georgalis, G. L., Villa, A., & Delfino, M. (2017). The last European varanid: Demise and extinction of monitor lizards (Squamata, Varanidae) from Europe. *Journal of Vertebrate Paleontology*, *37*(2), e1301946. https://doi.org/10.1080/02724634.2017.1301946

Ghezzo, E., & Rook, L. (2015). The remarkable Panthera pardus (Felidae, Mammalia) record from Equi (Massa, Italy): Taphonomy, morphology, and paleoecology. *Quaternary Science Reviews*, *110*, 131–151. https://doi.org/10.1016/j.quascirev.2014.12.020

Gómez-Olivencia, A., Arceredillo, D., Álvarez-Lao, D. J., Garate, D., San Pedro, Z., Castaños, P., & Rios-Garaizar, J. (2014). New evidence for the presence of reindeer (Rangifer tarandus) on the Iberian Peninsula in the Pleistocene: An archaeopalaeontological and chronological reassessment. *Boreas*, *43*(2), 286–308. https://doi.org/10.1111/bor.12037

Gonçalves, V. S. (2008). *A utilização pré-histórica da Gruta de Porto Covo (Cascais). Uma revisão e algumas novidades*. Câmara Municipal de Cascais. https://repositorio.ul.pt/bitstream/10451/9730/1/5.%20GON%C3%87ALVES_2008.A%20gruta%20de%20Porto%20Covo.pdf

Gonyea, W. J. (1976). Adaptive differences in the body proportions of large felids. *Acta Anatomica*, *96*(1), 81–96. https://doi.org/10.1159/000144663

González-Fortes, G., Tassi, F., Trucchi, E., Henneberger, K., Paijmans, J. L. A., Díez-del-Molino, D., Schroeder, H., Susca, R. R., Barroso-Ruíz, C., Bermudez, F. J., Barroso-Medina, C., Bettencourt, A. M. S., Sampaio, H. A., Grandal-d'Anglade, A., Salas, A., de Lombera-Hermida, A., Fabregas Valcarce, R., Vaquero, M., Alonso, S., … Barbujani, G. (2019). A western route of prehistoric human migration from Africa into the Iberian Peninsula. *Proceedings of the Royal Society B: Biological Sciences*, *286*(1895), 20182288. https://doi.org/10.1098/rspb.2018.2288

Gotelli, N. J., Booher, D. B., Urban, M. C., Ulrich, W., Suarez, A. V., Skelly, D. K., Russell, D. J., Rowe, R. J., Rothendler, M., Rios, N., Rehan, S. M., Ni, G., Moreau, C. S., Magurran, A. E., Jones, F. A. M., Graves, G. R., Fiera, C., Burkhardt, U., & Primack, R. B. (2023). Estimating species relative abundances from museum records. *Methods in Ecology and Evolution*, *14*(2), 431–443. https://doi.org/10.1111/2041-210X.13705

Gotelli, N. J., & Colwell, R. K. (2001). Quantifying biodiversity: Procedures and pitfalls in the measurement and comparison of species richness. *Ecology Letters*, *4*(4), 379–391. https://doi.org/10.1046/j.1461-0248.2001.00230.x

Grandal-d'Anglade, A. (1993). *El oso de las cavernas en Galicia: El yacimiento de Cova Eirós* (Vol. 8). O Castro. Laboratorio Xeolóxico de Laxe. Area de Xeoloxía e Minería.

Grandal-d'Anglade, A., Vidal-Romani, J. R., Vaqueiro-Gonzalez, M., & Mendez, E. (2006). O Re-bolal: A new cave in Galicia (NW Spain) with rencent cave bear remains: preliminary report. *Scientific Annals, School of Geology Aristotle University of Thessaloniki (AUTH)*, *98*, 173–178.

Grealy, A., Miller, G. H., Phillips, M. J., Clarke, S. J., Fogel, M., Patalwala, D., Rigby, P., Hubbard, A., Demarchi, B., Collins, M., Mackie, M., Sakalauskaite, J., Stiller, J., Clarke, J. A., Legendre, L. J., Douglass, K., Hansford, J., Haile, J., & Bunce, M. (2023). Molecular exploration of fossil eggshell uncovers hidden lineage of giant extinct bird. *Nature Communications*, *14*(1), 914. https://doi.org/10.1038/s41467-023-36405-3

Guillaume, A. R. D. (2024). *Albanerpetontidae (Lissamphibia) and other small herpetofauna (Crocodylomorpha, Lepidosauria, Choristodera) from the Iberian Mesozoic, with focus on the Upper Jurassic of Portugal* [doctoralThesis]. https://run.unl.pt/handle/10362/177874

Guillaume, A. R. D., Puértolas-Pascual, E., & Moreno-Azanza, M. (2025). Revisiting the choristodere and stem-lepidosaur specimens of the Guimarota Beds (Kimmeridgian, Portugal): Taxonomic implications. *ACTA PALAEONTOLOGICA POLONICA*, *70*(1), 77–96.

Gurke, M., Vidal-Gorosquieta, A., Pajimans, J. L. A., Węcek, K., Barlow, A., González-Fortes, G., Hartmann, S., Grandal-d'Anglade, A., & Hofreiter, M. (2021). Insight into the introduction of domestic cattle and the process of Neolithization to the Spanish region Galicia by genetic evidence. *PLOS ONE*, *16*(4), e0249537. https://doi.org/10.1371/journal.pone.0249537

Gutarra, S., & Rahman, I. A. (2022). The locomotion of extinct secondarily aquatic tetrapods. *Biological Reviews*, *97*(1), 67–98. https://doi.org/10.1111/brv.12790

Haltenorth, T. (1937). *Die verwandtschaftliche Stellung der Großkatzen zueinander* [PhD Thesis]. Berger.

Hammer, Ø., Harper, D. A. T., & Ryan, P. D. (2001). PAST: Paleontological statistics software package for education and data analysis. *Palaeontologia Electronica*, *4*(1), 9.

Harlé, E. (1910). Les mammifères et oiseaux quaternaires connus jusqu'ici en Portugal: Mémoire suivi d'une liste générale de ceux de la Péninsule Ibérique. *Comunicações Geológicas*, *8*, 22–85.

Harrison, C. J. O., & Cowles, G. S. (1977). The extinct large cranes of the North-West palaearctic. *Journal of Archaeological Science*, *4*(1), 25–27. https://doi.org/10.1016/0305-4403(77)90110-8

Haws, J., Benedetti, M., Carvalho, M., Ellis, G., Pereira, T., Cascalheira, J., Bicho, N., & Friedl, L. (2021). Human adaptive responses to climate and environmental change during the

Gravettian of Lapa do Picareiro (Portugal). *Quaternary International*, *587–588*, 4–18. https://doi.org/10.1016/j.quaint.2020.08.009

Haws, J., Benedetti, M. M., Bicho, N. F., Cascalheira, J., Ellis, M. G., Carvalho, M. M., Friedl, L., Pereira, T., & Talamo, S. (2021). The early Aurignacian at Lapa do Picareiro really is that old: A comment on 'The late persistence of the Middle Palaeolithic and Neandertals in Iberia: A review of the evidence for and against the "Ebro Frontier" model.' *Quaternary Science Reviews*, *274*, 107261. https://doi.org/10.1016/j.quascirev.2021.107261

Head, M. J., & Gibbard, P. L. (2015). Early–Middle Pleistocene transitions: Linking terrestrial and marine realms. *Quaternary International*, *389*, 7–46. https://doi.org/10.1016/j.quaint.2015.09.042

Hemmer, H. (1972). Uncia uncia. *Mammalian Species*, *20*, 1–5.

Hemmer, H. (2023). An intriguing find of an early Middle Pleistocene European snow leopard, Panthera uncia pyrenaica ssp. Nov. (Mammalia, Carnivora, Felidae), from the Arago cave (Tautavel, Pyrénées-Orientales, France). *Palaeobiodiversity and Palaeoenvironments*, *103*(1), 207–220. https://doi.org/10.1007/s12549-021-00514-y

Hoffmann, D. L., Pike, A. W. G., Wainer, K., & Zilhão, J. (2013). New U-series results for the speleogenesis and the Palaeolithic archaeology of the Almonda karstic system (Torres Novas, Portugal). *Quaternary International*, *294*, 168–182. https://doi.org/10.1016/j.quaint.2012.05.027

Hoffmann, D. L., Standish, C. D., García-Diez, M., Pettitt, P. B., Milton, J. A., Zilhão, J., Alcolea-González, J. J., Cantalejo-Duarte, P., Collado, H., de Balbín, R., Lorblanchet, M., Ramos-Muñoz, J., Weniger, G.-Ch., & Pike, A. W. G. (2018). U-Th dating of carbonate crusts

reveals Neandertal origin of Iberian cave art. *Science*, *359*(6378), 912–915. https://doi.org/10.1126/science.aap7778

Huang, G., Rosowski, J., Ravicz, M., & Peake, W. (2002). Mammalian ear specializations in arid habitats: Structural and functional evidence from sand cat (Felis margarita). *Journal of Comparative Physiology A*, *188*(9), 663–681. https://doi.org/10.1007/s00359-002-0332-8

Huelsenbeck, J. P., & Ronquist, F. (2001). MRBAYES: Bayesian inference of phylogenetic trees. *Bioinformatics*, *17*(8), 754–755.

Hughes, P. D. (2022). Chapter 46—Concept and global context of the glacial landforms from the Last Glacial Maximum. In D. Palacios, P. D. Hughes, J. M. García-Ruiz, & N. Andrés (Eds.), *European Glacial Landscapes* (pp. 355–358). Elsevier. https://doi.org/10.1016/B978-0-12-823498-3.00039-X

Huguet, R., Vallverdú, J., Rodríguez-Álvarez, X. P., Terradillos-Bernal, M., Bargalló, A., Lombera-Hermida, A., Menéndez, L., Modesto-Mata, M., Van der Made, J., Soto, M., Blain, H.-A., García, N., Cuenca-Bescós, G., Gómez-Merino, G., Pérez-Martínez, R., Expósito, I., Allué, E., Rofes, J., Burjachs, F., … Carbonell, E. (2017). Level TE9c of Sima del Elefante (Sierra de Atapuerca, Spain): A comprehensive approach. *Quaternary International*, *433*, 278–295. https://doi.org/10.1016/j.quaint.2015.11.030

Iacumin, P., Bocherens, H., Mariotti, A., & Longinelli, A. (1996). Oxygen isotope analyses of co-existing carbonate and phosphate in biogenic apatite: A way to monitor diagenetic alteration of bone phosphate? *Earth and Planetary Science Letters*, *142*(1), 1–6. https://doi.org/10.1016/0012-821X(96)00093-3

Instituto Português do Mar e da Atmosfera. (2023). *Boletim Anual 2023* (p. 36). Instituto Português do Mar e da Atmosfera. https://www.ipma.pt/resources.www/docs/im.publicacoes/edicoes.online/20240325/NJwiNVXlahTAV-KioLFka/cli_20231201_20231231_pcl_aa_co_pt.pdf

IUCN Red List. (2025). *The IUCN Red List of Threatened Species*. IUCN Red List of Threatened Species. https://www.iucnredlist.org/en

Iverson, L. R., Prasad, A. M., Matthews, S. N., & Peters, M. (2008). Estimating potential habitat for 134 eastern US tree species under six climate scenarios. *Forest Ecology and Management*, *254*(3), 390–406. https://doi.org/10.1016/j.foreco.2007.07.023

Jeannet, M. (2000). Gruta da Figueira Brava: Les rongeurs. In *Últimos Neandertais em Portugal: Evidência, odontológica e outra.* (Vol. 38, pp. 179–243).

Jiangzuo, Q., & Flynn, J. J. (2020). The Earliest Ursine Bear Demonstrates the Origin of Plant-Dominated Omnivory in Carnivora. *iScience*, *23*(6), 101235. https://doi.org/10.1016/j.isci.2020.101235

Jiangzuo, Q., & Liu, J. (2020). First record of the Eurasian jaguar in southern Asia and a review of dental differences between pantherine cats. *Journal of Quaternary Science*, *35*(6), 817–830. https://doi.org/10.1002/jqs.3222

Jiangzuo, Q., Liu, J., & Chen, J. (2019). Morphological homology, evolution and proposed nomenclature for bear dentition. *Acta Palaeontologica Polonica*, *64*. https://doi.org/10.4202/app.00629.2019

Jiangzuo, Q., Madurell-Malapeira, J., Li, X., Estraviz-López, D., Mateus, O., Testu, A., Li, S., Wang, S., & Deng, T. (2025). Insights on the evolution and adaptation toward high-altitude

and cold environments in the snow leopard lineage. *Science Advances*, *11*(3), eadp5243. https://doi.org/10.1126/sciadv.adp5243

Jiangzuo, Q., Wagner, J., Chen, J., Dong, C., Wei, J., Ning, J., & Liu, J. (2018). Presence of the Middle Pleistocene cave bears in China confirmed – Evidence from Zhoukoudian area. *Quaternary Science Reviews*, *199*, 1–17. https://doi.org/10.1016/j.quascirev.2018.09.012

Jiangzuo, Q., Werdelin, L., & Sun, Y. (2022). A dwarf sabertooth cat (Felidae: Machairodontinae) from Shanxi, China, and the phylogeny of the sabertooth tribe Machairodontini. *Quaternary Science Reviews*, *284*, 107517. https://doi.org/10.1016/j.quascirev.2022.107517

Jianzhang, M., Hongfei, Z., & Kun, C. (2002). The distribution status of Snow Leopard (Uncia uncia) in China. *Contributed Papers to the Snow Leopard Survival Strategy Summit*, 209.

Jiménez Fuentes, E., Cardoso, J. L., & Crespo, E. G. (1998). Presencia de Agrionemys (=Testudo) hermanni (Gmelin, 1789) en el Paleolítico Medio de la Gruta Nova da Columbeira (Bombarral, provincia de Estremadura, Portugal). *Studia geologica salmanticensia*, *34*, 123–139.

Joeckel, R. M. (1998). Unique frontal sinuses in fossil and living Hyaenidae (Mammalia, Carnivora): Description and interpretation. *Journal of Vertebrate Paleontology*, *18*(3), 627–639. https://doi.org/10.1080/02724634.1998.10011089

Johnson, W. E., Eizirik, E., Pecon-Slattery, J., Murphy, W. J., Antunes, A., Teeling, E., & O'Brien, S. J. (2006). The Late Miocene Radiation of Modern Felidae: A Genetic Assessment. *Science*, *311*(5757), 73–77. https://doi.org/10.1126/science.1122277

Kahlke, H. D. (1997). Die Cerviden-Reste aus dem unterpleistozän von untermassfeld. In *Das Pleistozän von Untermassfeld bei Meiningen (Thüringen)* (Vol. 1, pp. 181–276). Dr Rudolf Habelt GMBH Bonn.

Kalashnikova, Y. A., Karnaukhov, A. S., Dubinin, M. Y., Poyarkov, A. D., & Rozhnov, V. V. (2019). Potential habitat of snow leopard (Panthera uncia, Felinae) in South Siberia and adjacent territories based on the maximum entropy distribution model. *Зоологический Журнал*, *98*(3), 332–342.

Kampichler, C., Wieland, R., Calmé, S., Weissenberger, H., & Arriaga-Weiss, S. (2010). Classification in conservation biology: A comparison of five machine-learning methods. *Ecological Informatics*, *5*(6), 441–450. https://doi.org/10.1016/j.ecoinf.2010.06.003

Kierdorf, U., & Bartoš, L. (1999). Treatment of the growing pedicle with retinoic acid increased the size of first antlers in fallow deer (Dama dama L.). *Comparative Biochemistry and Physiology Part C: Pharmacology, Toxicology and Endocrinology*, *124*(1), 7–9. https://doi.org/10.1016/S0742-8413(99)00038-9

Kim, S.-T., Coplen, T. B., & Horita, J. (2015). Normalization of stable isotope data for carbonate minerals: Implementation of IUPAC guidelines. *Geochimica et Cosmochimica Acta*, *158*, 276–289. https://doi.org/10.1016/j.gca.2015.02.011

Kim, Y., Wojciechowski, R., Sung, H., Mathias, R. A., Wang, L., Klein, A. P., Lenroot, R. K., Malley, J., & Bailey-Wilson, J. E. (2009). Evaluation of random forests performance for genome-wide association studies in the presence of interaction effects. *BMC Proceedings*, *3*(7), S64. https://doi.org/10.1186/1753-6561-3-S7-S64

Kitchener, A. C., Driscoll, C. A., & Yamaguchi, N. (2016). Chapter 1 - What is a Snow Leopard? Taxonomy, Morphology, and Phylogeny. In T. McCarthy & D. Mallon (Eds.), *Snow Leopards* (pp. 3–11). Academic Press. https://doi.org/10.1016/B978-0-12-802213-9.00001-8

Koch, P. L. (2007). Isotopic Study of the Biology of Modern and Fossil Vertebrates. In *Stable Isotopes in Ecology and Environmental Science* (pp. 99–154). John Wiley & Sons, Ltd. https://doi.org/10.1002/9780470691854.ch5

Koleff, P., Gaston, K. J., & Lennon, J. J. (2003). Measuring beta diversity for presence–absence data. *Journal of Animal Ecology*, *72*(3), 367–382. https://doi.org/10.1046/j.1365-2656.2003.00710.x

Konidaris, G. E., Tourloukis, V., Kostopoulos, D. S., Thompson, N., Giusti, D., Michailidis, D., Koufos, G. D., & Harvati, K. (2015). Two new vertebrate localities from the Early Pleistocene of Mygdonia Basin (Macedonia, Greece): Preliminary results. *Comptes Rendus Palevol*, *14*(5), 353–362. https://doi.org/10.1016/j.crpv.2015.05.004

Kosintsev, P. A., Bocherens, H., Kirillova, I. V., Levchenko, V. A., Zazovskaya, E. P., Trofimova, S. S., Lan, T., & Lindqvist, C. (2022). Palaeoecological and genetic analyses of Late Pleistocene bears in Asiatic Russia. *Boreas*, *51*(2), 465–480. https://doi.org/10.1111/bor.12570

Krause, J., Unger, T., Noçon, A., Malaspinas, A.-S., Kolokotronis, S.-O., Stiller, M., Soibelzon, L., Spriggs, H., Dear, P. H., Briggs, A. W., Bray, S. C., O'Brien, S. J., Rabeder, G., Matheus, P., Cooper, A., Slatkin, M., Pääbo, S., & Hofreiter, M. (2008). Mitochondrial genomes reveal an explosive radiation of extinct and extant bears near the Miocene-Pliocene boundary. *BMC Evolutionary Biology*, *8*(1), 220. https://doi.org/10.1186/1471-2148-8-220

Kullberg, J. C., Rocha, R. B., Soares, A. F., Rey, J., Terrinha, P., Azerêdo, A. C., Callapez, P., Duarte, L. V., Kullberg, M. C., Martins, L., Miranda, R., Alves, C., Mata, J., Madeira, J., Mateus, O., Moreira, M., & Nogueira, C. R. (2013). A Bacia Lusitaniana: Estratigrafia, paleogeografia e tectónica. In *Geologia de Portugal: Vol. Volume II – Geologia Meso-cenozóica de Portugal.* Escolar editora. https://run.unl.pt/handle/10362/1487

Kurtén, B. (1965). The carnivore of the Palestine caves. *Acta Zool Fenn*, *107*, 1–74.

Kurtén, B. (1968). *Pleistocene Mammals of Europe*. Routledge. https://doi.org/10.4324/9781315126470

Kurtén, B., & Vasari, Y. (1960). *An attempted parallelization of the Quaternary mammalian faunas of China and Europe*. Societas scientiarum Fennica.

Lambrides, A. B. J., Ristevski ,Jorgo, Mein ,Erin, van Zoelen ,Jacob D., McNiven ,Ian J., Leavesley ,Matthew, David ,Bruno, Ulm ,Sean, & and Weisbecker, V. (2024). Fishboneviz: Enhancing the availability of zooarchaeological fish reference collections through an open access 3D database. *Australian Archaeology*, *90*(2), 236–248. https://doi.org/10.1080/03122417.2024.2350098

Larkin, P. (2017). *Infrared and Raman Spectroscopy: Principles and Spectral Interpretation*. Elsevier.

Lee, A. H., Moore, J. M., Covarrubias, B. V., & Lynch, L. M. (2025). Segmentation of cortical bone, trabecular bone, and medullary pores from micro-CT images using 2D and 3D deep learning models. *The Anatomical Record*, *n/a*(n/a). https://doi.org/10.1002/ar.25633

Lee, A. M., Fletcher, N. F., Rowan, C., & Jahns, H. (2017). Occipital condylar dysplasia in a Jacob lamb (Ovis aries). *Open Veterinary Journal*, *7*(2), Article 2. https://doi.org/10.4314/ovj.v7i2.8

Lee-Thorp, J., & Sponheimer, M. (2003). Three case studies used to reassess the reliability of fossil bone and enamel isotope signals for paleodietary studies. *Journal of Anthropological Archaeology*, *22*(3), 208–216. https://doi.org/10.1016/S0278-4165(03)00035-7

Legendre, S., & Roth, C. (1988). Correlation of carnassial tooth size and body weight in recent carnivores (mammalia). *Historical Biology*, *1*(1), 85–98. https://doi.org/10.1080/08912968809386468

Lewis, P. O. (2001). A likelihood approach to estimating phylogeny from discrete morphological character data. *Systematic Biology*, *50*(6), 913–925.

Li, G., Davis, B. W., Eizirik, E., & Murphy, W. J. (2016). Phylogenomic evidence for ancient hybridization in the genomes of living cats (Felidae). *Genome Research*, *26*(1), 1–11. https://doi.org/10.1101/gr.186668.114

Li, X., Ma, L., Hu, D., Ma, D., Li, R., Sun, Y., & Gao, E. (2022). Potential Range Shift of Snow Leopard in Future Climate Change Scenarios. *Sustainability*, *14*(3), Article 3. https://doi.org/10.3390/su14031115

Li, X., & Wang, Y. (2013). Applying various algorithms for species distribution modelling. *Integrative Zoology*, *8*(2), 124–135. https://doi.org/10.1111/1749-4877.12000

Linscott, B., Devièse, T., Duarte, C., Trinkaus, E., & Zilhão, J. (2025). Direct hydroxyproline radiocarbon dating of the Lapedo child (Abrigo do Lagar Velho, Leiria, Portugal). *Science Advances*, *11*(10), eadp5769. https://doi.org/10.1126/sciadv.adp5769

Linscott, B., Pike, A. W. G., Angelucci, D. E., Cooper, M. J., Milton, J. S., Matias, H., & Zilhão, J. (2023). Reconstructing Middle and Upper Paleolithic human mobility in Portuguese Estremadura through laser ablation strontium isotope analysis. *Proceedings of the National Academy of Sciences*, *120*(20), e2204501120. https://doi.org/10.1073/pnas.2204501120

Lister, A. M. (1996). The morphological distinction between bones and teeth of fallow deer (Dama dama) and red deer (Cervus elaphus). *International Journal of Osteoarchaeology*,

6(2), 119–143. https://doi.org/10.1002/(SICI)1099-1212(199603)6:2<119::AID-OA265>3.0.CO;2-8

Liu, Y., Li, X., Liang, X., Liu, Y., Cheng, C., Li, J., Tang, P., Qi, H., Bian, X., & He, B. (2019). Where and How many? The status of snow leopard (Panthera uncia) density surveys and knowledge gaps in China. *Biodiversity Science*, *27*(9), 919–931.

Lloveras, L., Moreno-García, M., Nadal, J., & Zilhão, J. (2011). Who brought in the rabbits? Taphonomical analysis of Mousterian and Solutrean leporid accumulations from Gruta do Caldeirão (Tomar, Portugal). *Journal of Archaeological Science*, *38*(9), 2434–2449. https://doi.org/10.1016/j.jas.2011.05.012

López-García, J. M. (2008). *Evolución de la diversidad taxonómica de los micromamíferos en la península ibérica y cambios paleoambientales durante el Pleistoceno Superior.* [PhD thesis, Universitat Rovira i Virgili]. https://dialnet.unirioja.es/servlet/tesis?codigo=80124

López-García, J. M., Berto, C., Luzi, E., Valle, C. D., Bañuls-Cardona, S., & Sala, B. (2015). The genus Iberomys (Rodentia, Arvicolinae, Mammalia) in the Pleistocene of Italy. *Italian Journal of Geosciences*, *134*(1), 162–169. https://doi.org/10.3301/IJG.2014.48

López-García, J. M., Blain, H.-A., Sanz, M., Daura, J., & Zilhão, J. (2018). Refining the environmental and climatic background of the Middle Pleistocene human cranium from Gruta da Aroeira (Torres Novas, Portugal). *Quaternary Science Reviews*, *200*, 367–375. https://doi.org/10.1016/j.quascirev.2018.10.003

López-García, J. M., & Cuenca-Bescós, G. (2012). Changes in the geographical distribution of Microtus (Iberomys) cabrerae (Thomas, 1906) from the Late Pleistocene to the Holocene. *Revista Española de Paleontología*, *27*(2), 117–124.

López-García, J. M., Cuenca-Bescós, G., Blain, H.-A., Cáceres, I., García, N., Made, J. V. D., Gutierrez, J. M., Santiago, A., & Pacheco, F. G. (2012). Biochronological data inferred from the early Pleistocene Arvicolinae (Mammalia, Rodentia) of the El Chaparral site (Sierra del Chaparral, Cádiz, southwestern Spain). *Journal of Vertebrate Paleontology*, *32*(5), 1149–1156. https://doi.org/10.1080/02724634.2012.676584

López-García, J. M., Fagoaga, A., Nabais, M., Póvoas, L., & Zilhão, J. (2022). Late Quaternary (MIS 5a-5b) climate and environments of western Iberia inferred from the small-mammal assemblage of Gruta da Oliveira, Torres Novas, Portugal. *Palaeogeography, Palaeoclimatology, Palaeoecology*, *603*, 111194. https://doi.org/10.1016/j.palaeo.2022.111194

López-García, J. M., Pimenta, C., Araújo, A. C., Costa, A. M., Sanz, M., & Daura, J. (2021). USING SMALL MAMMALS TO RECONSTRUCT THE CLIMATIC CONTEXT OF THE LATE PLEISTOCENE LAGAR VELHO ROCKSHELTER (LEIRIA, PORTUGAL). *Alpine and Mediterranean Quaternary*, *34*(2), Article 2. https://doi.org/10.26382/AMQ.2021.04

López-García, J. M., Póvoas, L., & Zilhão, J. (2020). Note on the taxonomy of the Microtus (Iberomys) (Arvicolinae, Rodentia) from the Late Pleistocene of Gruta do Caldeirão (Tomar, Portugal) and paleoclimatic interpretation of the rodent assemblage. *Estudios Geológicos*, *76*(1 (enero–junio)), 7.

López-González, F. (2003). *Paleontology and taphonomy of Pleistocene macromammals of Galicia (NW Iberian Peninsula)* (Vol. 22). O Castro. Laboratorio Xeolóxico de Laxe. Area de Xeoloxía e Minería.

Loureiro, A., Ferrand de Almeida, N., Carretero, M. A., & Paulo, O. S. (2008). *Atlas dos Anfíbios e Répteis de Portugal* (1º). Instituto da Conservação da Natureza e da Biodiversidade. http://www2.icnf.pt/portal/pn/biodiversidade/patrinatur/atlas-anfi-rept/inicio

Lucena-Perez, M., Paijmans, J. L. A., Nocete, F., Nadal, J., Detry, C., Dalén, L., Hofreiter, M., Barlow, A., & Godoy, J. A. (2024). Recent increase in species-wide diversity after interspecies introgression in the highly endangered Iberian lynx. *Nature Ecology & Evolution*, *8*(2), 282–292. https://doi.org/10.1038/s41559-023-02267-7

Lukarevskiy, V. S., Dalannast, M., Lukarevskiy, S., & Damdin, E. (2019). Factors determining the distribution and status of the snow leopard population (Panthera uncia) in Western Mongolia. *Animal and Veterinary Sciences*, *7*(6), 127–132.

Lyngdoh, S., Shrotriya, S., Goyal, S. P., Clements, H., Hayward, M. W., & Habib, B. (2014). Prey Preferences of the Snow Leopard (Panthera uncia): Regional Diet Specificity Holds Global Significance for Conservation. *PLOS ONE*, *9*(2), e88349. https://doi.org/10.1371/journal.pone.0088349

Madurell-Malapeira, J., Minwer-Barakat, R., Alba, D. M., Garcés, M., Gómez, M., Aurell-Garrido, J., Ros-Montoya, S., Moyà-Solà, S., & Berástegui, X. (2010). The Vallparadís section (Terrassa, Iberian Peninsula) and the latest Villafranchian faunas of Europe. *Quaternary Science Reviews*, *29*(27), 3972–3982. https://doi.org/10.1016/j.quascirev.2010.09.020

Madurell-Malapeira, J., Ros-Montoya, S., Espigares, M. P., Alba, D. M., & Aurell-Garrido, J. (2014). Villafranchian large mammals from the Iberian Peninsula: Paleobiogeography, paleoecology and dispersal events. *Journal of Iberian Geology*, *40*(1), 167–178. https://doi.org/10.5209/rev_JIGE.2014.v40.n1.44093ww

Mahmood, T., Younas, A., Akrim, F., Andleeb, S., Hamid, A., & Nadeem, M. S. (2019). Range contraction of snow leopard (Panthera uncia). *PLOS ONE*, *14*(8), e0218460. https://doi.org/10.1371/journal.pone.0218460

Mallon, D., Harris, R. B., & Wegge, P. (2024). Chapter 4—Snow leopard diet and prey. In D. Mallon & T. McCarthy (Eds.), *Snow Leopards (Second Edition)* (pp. 43–51). Academic Press. https://doi.org/10.1016/B978-0-323-85775-8.00010-8

Manne, T., Cascalheira, J., Évora, M., Marreiros, J., & Bicho, N. (2012). Intensive subsistence practices at Vale Boi, an Upper Paleolithic site in southwestern Portugal. *Quaternary International*, *264*, 83–99. https://doi.org/10.1016/j.quaint.2012.02.026

Manne, T., Stiner, M. C., & Bicho, N. (2006). Evidence for bone grease rendering during the Upper Paleolithic at Vale Boi (Algarve, Portugal). *Promontoria Monografica*, *3*, 145–158.

Marciszak, A., Mackiewicz, P., Borówka, R. K., Capalbo, C., Chibowski, P., Gąsiorowski, M., Hercman, H., Cedro, B., Kropczyk, A., Gornig, W., Moska, P., Nowakowski, D., Ratajczak-Skrzatek, U., Sobczyk, A., Sykut, M. T., Zarzecka-Szubińska, K., Kovalchuk, O., Barkaszi, Z., Stefaniak, K., & Mazza, P. P. A. (2024). Fate and preservation of the Late Pleistocene cave bears from Niedźwiedzia Cave in Poland, through taphonomy, pathology, and geochemistry. *Scientific Reports*, *14*(1), 9775. https://doi.org/10.1038/s41598-024-60222-3

Marks, A. E., Brugal, J.-P., Chabai, V. P., Monigal, K., Goldberg, P., Hockett, B., Peman, E., Elorza, M., & Mallol, C. (2002). Le gisement pléistocène moyen de Galeria Pesada (Estrémadure, Portugal): Premiers résultats. *PALEO. Revue d'archéologie préhistorique*, *14*, 77–100.

Marks, A. E., Monigal, K., Chabai, V. P., Brugal, J.-P., Goldberg, P., Hockett, B., Pemán, E., Elorza, M., & Mallol, C. (2002). Excavations at the Middle Pleistocene cave site of Galeria Pesada, Portuguese Estremadura: 1997–1999. *O Arqueólogo Português*, *20*, 7–38.

Maroto, J., i Masferrer, N. S., & Mir, A. (1987). La cueva de Mollet I (Serinyà, Gerona). *Cypsela: Revista de Prehistòria i Protohistòria*, 101–110.

Maroto, J., Julià, R., López-García, J. M., & Blain, H.-A. (2012). Chronological and environmental context of the Middle Pleistocene human tooth from Mollet Cave (Serinyà, NE Iberian Peninsula). *Journal of Human Evolution*, *62*(6), 655–663. https://doi.org/10.1016/j.jhevol.2012.01.009

Maroto, J., López-García, J. M., Blain, H. A., Millán, F., Álvarez Alcaine, M., & Julià Brugués, R. (2018). Les excavacions recents a la cova de Mollet (Serinyà, Pla de l'Estany): Hienes i humans fa 200.000 anys. *Maroto, Julià López-García, Juan Manuel Blain, Hugues Alexandre Millán, Ferran Álvarez Alcaine, Meritxell Julià Brugués, Ramón 2018 Les excavacions recents a la cova de Mollet (Serinyà, Pla de l'Estany): hienes i humans fa 200.000 anys Tribuna d'Arqueologia 2015-2016 104 120*. https://dugi-doc.udg.edu/handle/10256/20614

Marques, J. F. (1997). O significado dos depósitos quaternários do Baixo Mondego. In *Uma retrospectiva. Seminário O Baixo Mondego–Organização geossistémica e recursos naturais, Coimbra* (pp. 21–39).

Martin, R. A. (2012). Victoriamys, a new generic name for Chaline's vole from the Pleistocene of Western Europe. *Geobios*, *45*(5), 445–450. https://doi.org/10.1016/j.geobios.2012.01.001

Martino, R., Ríos, M. I., Mateus, O., & Pandolfi, L. (2023). Taxonomy, chronology, and dispersal patterns of Western European Quaternary hippopotamuses: New insight from Portuguese fossil material. *Quaternary International*, *674–675*, 121–137. https://doi.org/10.1016/j.quaint.2022.12.010

Mateus, O., & Estraviz-López, D. (2022). A new theropod dinosaur from the early cretaceous (Barremian) of Cabo Espichel, Portugal: Implications for spinosaurid evolution. *PLOS ONE*, *17*(2), e0262614. https://doi.org/10.1371/journal.pone.0262614

Mathias, M. da luz, Fonseca, C., Rodrigues, L., Grilo, C., Lopes-Fernandes, M., Palmeirim, J. M., Santos-Reis, M., Alves, P. C., Cabral, J. A., Ferreira, M., Mira, A., Eira, C., Negrões, N., Paupério, J., Pita, R., Rainho, A., Rosalino, L., Tapisso, J., & Vingada, J. (2023). *Livro Vermelho Dos Mamíferos de Portugal Continental*. FCiências.ID, ICNF. https://books.google.es/books?hl=es&lr=&id=TkfCE-AAAQBAJ&oi=fnd&pg=PP8&dq=Livro+vermelho+aves+Portugal&ots=0Atr-AeokR&sig=ODSeY_EpAo_MNYAIwqGq6uz-f8Y

Mattern, M. Y., & McLennan, D. A. (2000). Phylogeny and Speciation of Felids. *Cladistics*, *16*(2), 232–253. https://doi.org/10.1006/clad.2000.0132

Mauran, G., Rosado, T., Schiavon, N., Silva, A., Mirão, J., Caldeira, A. T., & Candeias, A. (2017, April). Redécouverte des représentations pariétales de la grotte d'Escoural (Alentejo, Portugal): Techniques picturales et matières colorantes noires du Paléolithique Supérieur. *GMPCA-2017*. https://hal.archives-ouvertes.fr/hal-02906084

McCarthy, T., Mallon, D., Jackson, R., Zahler, P., & McCarthy, K. (2017). *Panthera uncia.* Gland, Switzerland: The IUCN Red List of Threatened Species.

McCarthy, T., Mallon, D., Sanderson, E. W., Zahler, P., & Fisher, K. (2016). Chapter 3 - What is a Snow Leopard? Biogeography and Status Overview. In T. McCarthy & D. Mallon (Eds.), *Snow Leopards* (pp. 23–42). Academic Press. https://doi.org/10.1016/B978-0-12-802213-9.00003-1

Mecozzi, B., Sardella, R., Boscaini, A., Cherin, M., Costeur, L., Madurell-Malapeira, J., Pavia, M., Profico, A., & Iurino, D. A. (2021). The tale of a short-tailed cat: New outstanding Late Pleistocene fossils of *Lynx pardinus* from southern Italy. *Quaternary Science Reviews*, *262*, 106840. https://doi.org/10.1016/j.quascirev.2021.106840

Mecozzi, B., Sardella, R., & Breda, M. (2023). Late Early to late Middle Pleistocene medium-sized deer from the Italian Peninsula: Implications for taxonomy and biochronology. *Palaeobiodiversity and Palaeoenvironments*. https://doi.org/10.1007/s12549-023-00583-1

Mein, P., & Antunes, M. T. (2000). Gruta da Figueira Brava: Petits mammifères–Insectívora, Chiroptera, Lagomorpha. In *Últimos Neandertais em Portugal: Evidência, odontológica e outra.* (Vol. 38, pp. 163–177).

Moigne, A.-M., Palombo, M. R., Belda, V., Heriech-Briki, D., Kacimi, S., Lacombat, F., de Lumley, M.-A., Moutoussamy, J., Rivals, F., Quilès, J., & Testu, A. (2006). Les faunes de grands mammifères de la Caune de l'Arago (Tautavel) dans le cadre biochronologique des faunes du Pléistocène moyen italien. *L'Anthropologie*, *110*(5), 788–831. https://doi.org/10.1016/j.anthro.2006.10.011

Mourer-Chauviré, C., & Antunes, M. T. (1991). Présence du grand pingouin,Pinguinus impennis (aves, charadriiformes) dans le Pléistocène du Portugal. In *Geobios* (Vol. 24, pp. 201–205). https://www.sciencedirect.com/science/article/pii/S001669959180007M

Mourer-Chauviré, C., & Antunes, M. T. (2000). L'Avifaune Pléistocène et Holocene de Gruta da Figueira Brava. In *Últimos Neandertais em Portugal: Evidência, odontológica e outra.* (Vol. 38, pp. 129–162).

Nabais, M., Dupont, C., & Zilhão, J. (2023). The exploitation of crabs by Last Interglacial Iberian Neanderthals: The evidence from Gruta da Figueira Brava (Portugal). *Frontiers in Environmental Archaeology*, *2*. https://doi.org/10.3389/fearc.2023.1097815

Nabais, M., & Zilhão, J. (2019). The consumption of tortoise among Last Interglacial Iberian Neanderthals. *Quaternary Science Reviews*, *217*, 225–246. https://doi.org/10.1016/j.quascirev.2019.03.024

Nagel, D. (1999). Panthera pardus vraonensis n. Ssp., a new leopard from the Pleistocene of Vraona/Greece. *Neues Jahrbuch Für Geologie Und Paläontologie-Monatshefte*, 129–150.

Negus, V. (1957). The Function of the Paranasal Sinuses. *A.M.A. Archives of Otolaryngology*, *66*(4), 430–442. https://doi.org/10.1001/archotol.1957.03830280060007

Neto de Carvalho, C. (2010). Vertebrate tracksites from the Mid-Late Pleistocene eolianites of Portugal: The first record of elephant tracks in Europe. *Geological Quarterly*, *53*(4), 407–414.

Neto de Carvalho, C., Belaústegui, Z., Toscano, A., Muñiz, F., Belo, J., Galán, J. M., Gómez, P., Cáceres, L. M., Rodríguez-Vidal, J., Cunha, P. P., Cachão, M., Ruiz, F., Ramirez-Cruzado, S., Giles-Guzmán, F., Finlayson, G., Finlayson, S., & Finlayson, C. (2021). First tracks of newborn straight-tusked elephants (Palaeoloxodon antiquus). *Scientific Reports*, *11*(1), 17311. https://doi.org/10.1038/s41598-021-96754-1

Neto de Carvalho, C., & Belo, J. (2022). Bear-claw deep tracks in the Pleistocene at north of Praia do Cavalo, Odemira (Portugal). *Ciências Da Terra / Earth Sciences Journal*, *20*(1), 21–25. https://doi.org/10.21695/cterra/esj.v20i1.436

Neto de Carvalho, C., Belo, J., Figueiredo, S., Cunha, P. P., Muñiz, F., Belaústegui, Z., Cachão, M., Rodriguez-Vidal, J., Cáceres, L. M., Baucon, A., Murray, A. S., Buylaert, J.-P., Zhang, Y., Ferreira, C., Toscano, A., Gómez, P., Ramírez, S., Finlayson, G., Finlayson, S., & Finlayson, C. (2023). Coastal raptors and raiders: New bird tracks in the Pleistocene of SW iberian Peninsula. *Quaternary Science Reviews*, *313*, 108185. https://doi.org/10.1016/j.quascirev.2023.108185

Nores, C., Muñiz, A. M., Rodríguez, L. L., Bennett, E. A., & Geigl, E.-M. (2015). The Iberian zebro: What kind of a beast was it? *Anthropozoologica*, *50*(1), 21–32. https://doi.org/10.5252/az2015n1a2

Nores, C., & Naves, J. (1993). Distribución histórica del oso pardo en la Península Ibérica. In *El oso pardo (Ursus arctos) en España* (pp. 13–33). Instituto Nacional para la Conservación de la Naturaleza.

Northcote, E., & Mourer-Chauviré, C. (1985). The distinction between the extinct Pleistocene European Crane,Grus primigenia, and the extant Asian Sarus Crane, G. antigone. *Geobios*, *18*(6), 877–881. https://doi.org/10.1016/S0016-6995(85)80041-3

Northcote, E., & Mourer-Chauviré, C. (1988). The extinct crane Grus primigenia Milne-Edwards in Majorca (Spain). *Geobios*, *21*(2), 201–208. https://doi.org/10.1016/S0016-6995(88)80018-4

Notario, R. (1964). *El oso pardo en España.* Ministerio de Agricultura.

Núñez-Lahuerta, C., Galán, J., Cuenca-Bescós, G., García-Medrano, P., & Cáceres, I. (2022). A bird assemblage across the MIS 9/8 boundary: The Middle Pleistocene of Galería (Atapuerca). *Quaternary Science Reviews*, *293*, 107708. https://doi.org/10.1016/j.quascirev.2022.107708

Núñez-Lahuerta, C., Moreno Azanza, M., & Cuenca-Bescós, G. (2021). Avian eggshell remains in the human bearing level TD6 of the Gran Dolina site (Early Pleistocene, Atapuerca, Spain). *Historical Biology*, *33*(5), 660–671. https://doi.org/10.1080/08912963.2019.1655009

O´Regan, H. J. (2002). Defining Cheetahs, a multivariate analysis of skull shape in big cats. *Mammal Review*, *32*(1), 58–62. https://doi.org/10.1046/j.1365-2907.2002.00093.x

Ochando, J., Carrión, J. S., Daura, J., Sanz, M., Araújo, A. C., & Costa, A. M. (2022). Coprolite palynology from Abrigo do Lagar Velho (Portugal) and a revision of Gravettian vegetation in the Iberian Peninsula. *Review of Palaeobotany and Palynology*, *299*, 104609. https://doi.org/10.1016/j.revpalbo.2022.104609

Oli, M. K., Taylor, I. R., & Rogers, D. M. E. (1993). Diet of the snow leopard (Panthera uncia) in the Annapurna Conservation Area, Nepal. *Journal of Zoology*, *231*(3), 365–370. https://doi.org/10.1111/j.1469-7998.1993.tb01924.x

Orlando, L. (2020). Ancient Genomes Reveal Unexpected Horse Domestication and Management Dynamics. *BioEssays*, *42*(1), 1900164. https://doi.org/10.1002/bies.201900164

Orlando, L., Allaby, R., Skoglund, P., Der Sarkissian, C., Stockhammer, P. W., Ávila-Arcos, M. C., Fu, Q., Krause, J., Willerslev, E., Stone, A. C., & Warinner, C. (2021). Ancient DNA analysis. *Nature Reviews Methods Primers*, *1*(1), 1–26. https://doi.org/10.1038/s43586-020-00011-0

Osmond, J. K., & Ivanovich, M. (1992). Uranium-series mobilization and surface hydrology. In *Uranium-series disequilibrium: Applications to earth, marine, and environmental sciences.* (2nd ed., pp. 259–289). https://inis.iaea.org/search/search.aspx?orig_q=RN:25066325

Otte, M., & Silva, A. (1996). *Recherches préhistoriques à la grotte d'Escoural, Portugal*. Université de Liège, Service de Préhistoire.

Owen, L. A., & Dortch, J. M. (2014). Nature and timing of Quaternary glaciation in the Himalayan–Tibetan orogen. *Quaternary Science Reviews*, *88*, 14–54. https://doi.org/10.1016/j.quascirev.2013.11.016

Özkan, M., Gürün, K., Yüncü, E., Vural, K. B., Atağ, G., Akbaba, A., Fidan, F. R., Sağlıcan, E., Altınışık, E. N., Koptekin, D., Pawłowska, K., Hodder, I., Adcock, S. E., Arbuckle, B. S., Steadman, S. R., McMahon, G., Erdal, Y. S., Bilgin, C. C., Togan, İ., … Somel, M. (2024). The first complete genome of the extinct European wild ass (Equus hemionus hydruntinus). *Molecular Ecology*, *33*(14), e17440. https://doi.org/10.1111/mec.17440

Pais, J., Legoínha, P., Elderfield, H., Sousa, L., & Estevens, M. (2000). The Neogene of Algarve (Portugal). *Ciências Da Terra / Earth Sciences Journal*, *14*, 277–288.

Paleček, D., Falini, G., Wacker, L., Mannino, M. A., Bicho, N., Cascalheira, J., Rombolà, A. G., Fabbri, D., & Talamo, S. (2024). To date or not to date? A comparison of different 14C pretreatment methods applied to archeological marine shells from Vale Boi (Portugal). *Radiocarbon*, *66*(4), 699–720. https://doi.org/10.1017/RDC.2024.80

Palmqvist, P., Arribas, A., & Martínez-Navarro, B. (1999). Ecomorphological study of large canids from the lower Pleistocene of southeastern Spain. *Lethaia*, *32*(1), 75–88. https://doi.org/10.1111/j.1502-3931.1999.tb00583.x

Palombo, M. R. (2018). TWENTY YEARS LATER: REFLECTIONS ON THE AURELIAN EUROPEAN LAND MAMMAL AGE. *Alpine and Mediterranean Quaternary*, *31*, 177–180.

Pei, W. (1936). On the mammalian remains from Locality 3 at Choukoutien. *Paleont. Sinica*, *7*, 1–108.

Penteriani, V., & Melletti, M. (2020). *Bears of the World: Ecology, Conservation and Management*. Cambridge University Press.

Pereira, T., Sampaio, H. T. P. A. G., Bettencourt, A. M. S., Cunha-Ribeiro, J. P., & Brito, M. (2018). Chalcolithic and Bronze Age funerary practices in the cave of Lorga de Dine (Vinhais, North of Portugal): Anthropological study. *Férvedes: Revista de Investigación*, *9*, 59–66.

Pérez, T., Albornoz, J., & Domínguez, A. (2002). Phylogeography of chamois (Rupicapra spp.) inferred from microsatellites. *Molecular Phylogenetics and Evolution*, *25*(3), 524–534. https://doi.org/10.1016/S1055-7903(02)00296-8

Pérez-Claros, J. A. (2024). Unravelling the origin of the brown hyena (Parahyena brunnea) and its evolutionary and paleoecological implications for the Pachycrocuta lineage. *Palaeontologia Electronica*, *27*(1), 1–25.

Pérez-García, A., Vlachos, E., & Arribas, A. (2017). The last giant continental tortoise of Europe: A survivor in the Spanish Pleistocene site of Fonelas P-1. *Palaeogeography, Palaeoclimatology, Palaeoecology*, *470*, 30–39. https://doi.org/10.1016/j.palaeo.2017.01.011

Pérez-Ripoll, M. (1977). *Los mamíferos del yacimiento musteriense de Cova Negra (Játiva, Valencia)* (Vol. 53). Servicio de Investigación Prehistórica, Diputación Provincial.

Peyroteo Stjerna, R., Araújo, A. C., & Diniz, M. (2018). *The dead at Escoural Cave (Montemor-o-Novo, Portugal): Early farmer's interactions in south-western Iberian Peninsula*. 65–83. http://urn.kb.se/resolve?urn=urn:nbn:se:uu:diva-369972

Pfeiffer-Deml, T. (2020). What Does the Mass Accumulation of 100 Late Pleistocene Fallow Deer Skeletons (Dama geiselana) and Red Deer Skeletons (Cervus elaphus) from Neumark-Nord Reveal about the Cause of Death? In *Heritage*. IntechOpen. https://doi.org/10.5772/intechopen.91293

Pieper, S., Halle, M., & Kikinis, R. (2004). 3D Slicer. *2004 2nd IEEE International Symposium on Biomedical Imaging: Nano to Macro (IEEE Cat No. 04EX821)*, 632-635 Vol. 1. https://doi.org/10.1109/ISBI.2004.1398617

Pietsch, S. J., & Tütken, T. (2016). Oxygen isotope composition of North American bobcat (Lynx rufus) and puma (Puma concolor) bone phosphate: Implications for provenance and climate reconstruction. *Isotopes in Environmental and Health Studies*. https://www.tandfonline.com/doi/abs/10.1080/10256016.2015.1113957

Pimenta, C. M., Figueiredo, S. D., & García, M. M. (2008). Novo registo de Pinguim ("Pinguinus impennis") no Plistocénico de Portugal. *Revista portuguesa de arqueologia*, *11*(2), 361–370.

Pimenta, C. M., Moreno García, M., & Lourenço, A. (2015). O registo ornito-arqueológico em Portugal: Inventários, comentários e mapas. *Revista Portuguesa de Arqueologia*, *18*, 289–312.

Piñero, P., Agustí, J., Laborda, C., Duval, M., Zhao, J., Blain, H.-A., Furió, M., Laplana, C., Rosas, A., & Sevilla, P. (2022). Quibas-Sima: A unique 1 ma-old vertebrate succession in southern Iberian Peninsula. *Quaternary Science Reviews*, *283*, 107469. https://doi.org/10.1016/j.quascirev.2022.107469

Piras, P., Maiorino, L., Teresi, L., Meloro, C., Lucci, F., Kotsakis, T., & Raia, P. (2013). Bite of the cats: Relationships between functional integration and mechanical performance as revealed by mandible geometry. *Systematic Biology*, *62*(6), 878–900.

Pires, F., Cardoso, J. L., & Petrucci-Fonseca, F. (2002). Estudo arqueozoológico dos carnívoros do povoado pré-histórico de Leceia (Oeiras). *Estudos Arqueológicos de Oeiras*, *10*, 183–247.

Placzek, C., Patchett, P. J., Quade, J., & Wagner, J. D. M. (2006). Strategies for successful U-Th dating of paleolake carbonates: An example from the Bolivian Altiplano. *Geochemistry, Geophysics, Geosystems*, *7*(5). https://doi.org/10.1029/2005GC001157

Pocock, R. I. (1917). The classification of existing Felidae. *Annals and Magazine of Natural History.*, *20*, 329–350.

Poole, K. G., & Boag, D. A. (1988). Ecology of gyrfalcons, Falco rusticolus, in the central Canadian Arctic: Diet and feeding behaviour. *Canadian Journal of Zoology*, *66*(2), 334–344. https://doi.org/10.1139/z88-050

Pourmand, A., & Dauphas, N. (2010). Distribution coefficients of 60 elements on TODGA resin: Application to Ca, Lu, Hf, U and Th isotope geochemistry. *Talanta*, *81*(3), 741–753. https://doi.org/10.1016/j.talanta.2010.01.008

Pourmand, A., Tissot, F. L. H., Arienzo, M., & Sharifi, A. (2014). Introducing a Comprehensive Data Reduction and Uncertainty Propagation Algorithm for U-Th Geochronometry with Extraction Chromatography and Isotope Dilution MC-ICP-MS. *Geostandards and Geoanalytical Research*, *38*(2), 129–148. https://doi.org/10.1111/j.1751-908X.2013.00266.x

Povoas, L., Zilhão, J., Chaline, J., & Brunet-Lecomte, P. (1992). La faune de rongeurs du Pléistocene supérieur de la grotte de Caldeirao (Tomar, Portugal). *Quaternaire*, *3*(1), 40–47. https://doi.org/10.3406/quate.1992.1971

Puértolas-Pascual, E., Kuzmin, I. T., Serrano-Martínez, A., & Mateus, O. (2023). Neuroanatomy of the crocodylomorph Portugalosuchus azenhae from the late cretaceous of Portugal. *Journal of Anatomy*, *242*(6), 1146–1171. https://doi.org/10.1111/joa.13836

Puértolas-Pascual, E., & Mateus, O. (2020). A three-dimensional skeleton of Goniopholididae from the Late Jurassic of Portugal: Implications for the Crocodylomorpha bracing

system. *Zoological Journal of the Linnean Society*, *189*(2), 521–548. https://doi.org/10.1093/zoolinnean/zlz102

Qiu, Z. X., Deng, T., & Wang, B. Y. (2004). *Early pleistocene mammalian fauna from Longdan, Dongxiang, Gansu, China.* Palaeontologia Sinica Science Press.

R Core Team, R. (2016). *R: A language and environment for statistical computing* [Computer software]. R Foundation for Statistical Computing. https://apps.dtic.mil/sti/citations/AD1039033

Ramírez-Pedraza, I., Tornero, C., Pappa, S., Talamo, S., Salazar-García, D. C., Blasco, R., Rosell, J., & Rivals, F. (2019). Microwear and isotopic analyses on cave bear remains from Toll Cave reveal both short-term and long-term dietary habits. *Scientific Reports*, *9*(1), Article 1. https://doi.org/10.1038/s41598-019-42152-7

Rando, J. C., & Alcover, J. A. (2010). On the extinction of the Dune Shearwater (Puffinus holeae) from the Canary Islands. *Journal of Ornithology*, *151*(2), 365–369. https://doi.org/10.1007/s10336-009-0463-6

Raposo, L. (1995). Ambientes, territorios y subsistencia en el Paleolítico Medio de Portugal. *Complutum*, *6*, 57–77. https://doi.org/10.5209/CMPL.31071

Rather, T. A., Kumar, S., & Khan, J. A. (2020). Multi-scale habitat modelling and predicting change in the distribution of tiger and leopard using random forest algorithm. *Scientific Reports*, *10*(1), 11473. https://doi.org/10.1038/s41598-020-68167-z

Regala, F. T., & Cardoso, J. L. (2007). Vestígios paleontológicos do Algar da Manga Larga. *Trogle*, *5*. http://hdl.handle.net/10400.2/5701

Reidenberg, J. S., & Laitman, J. T. (2008). Sisters of the Sinuses: Cetacean Air Sacs. *The Anatomical Record*, *291*(11), 1389–1396. https://doi.org/10.1002/ar.20792

Reznik, G. K. (1990). Comparative anatomy, physiology, and function of the upper respiratory tract. *Environmental Health Perspectives*, *85*, 171–176. https://doi.org/10.1289/ehp.85-1568330

Ribeiro, M. L., & Bento dos Santos, T. (2010). A nova Carta Geológica de Portugal à escala 1: 1.000. 000 e a importância da cartografia geológica de base. *Portugal Tecnológico 2010*.

Richard, M., Falguères, C., Pons-Branchu, E., Foliot, L., Guillem, P. M., Martínez-Valle, R., Eixea, A., & Villaverde, V. (2019). ESR/U-series chronology of early Neanderthal occupations at Cova Negra (Valencia, Spain). *Quaternary Geochronology*, *49*, 283–290. https://doi.org/10.1016/j.quageo.2018.05.004

Robu, M., Wynn, J., Puşcaş, C. M., Meleg, I. N., Martin, J. E., & Constantin, S. (2019). Palaeoecology and palaeoclimatic context of Romanian Carpathian MIS 3 cave bears using stable isotopes (δ13C and δ18O). *Palaeogeography, Palaeoclimatology, Palaeoecology*, *534*, 109288. https://doi.org/10.1016/j.palaeo.2019.109288

Rodríguez-Gómez, G., Palmqvist, P., Rodríguez, J., Mateos, A., Martín-González, J. A., Espigares, M. P., Ros-Montoya, S., & Martínez-Navarro, B. (2016). On the ecological context of the earliest human settlements in Europe: Resource availability and competition intensity in the carnivore guild of Barranco León-D and Fuente Nueva-3 (Orce, Baza Basin, SE Spain). *Quaternary Science Reviews*, *143*, 69–83. https://doi.org/10.1016/j.quascirev.2016.05.018

Roest, A. I. (1993). Asymmetry in the Skulls of California Sea Otters (enhydra Lutris Nereis). *Marine Mammal Science*, *9*(2), 190–194. https://doi.org/10.1111/j.1748-7692.1993.tb00443.x

Ronquist, F., Klopfstein, S., Vilhelmsen, L., Schulmeister, S., Murray, D. L., & Rasnitsyn, A. P. (2012). A total-evidence approach to dating with fossils, applied to the early radiation of the Hymenoptera. *Systematic Biology*, *61*(6), 973–999.

Ronquist, F., Teslenko, M., Van Der Mark, P., Ayres, D. L., Darling, A., Höhna, S., Larget, B., Liu, L., Suchard, M. A., & Huelsenbeck, J. P. (2012). MrBayes 3.2: Efficient Bayesian phylogenetic inference and model choice across a large model space. *Systematic Biology*, *61*(3), 539–542.

Rook, L., & Martínez-Navarro, B. (2010). Villafranchian: The long story of a Plio-Pleistocene European large mammal biochronologic unit. *Quaternary International*, *219*(1), 134–144. https://doi.org/10.1016/j.quaint.2010.01.007

Rotatori, F. (2024). *Evolutionary Rates Of Basal Iguanodontians Around Jurassic-Cretaceous Transition In Europe* [doctoralThesis]. https://run.unl.pt/handle/10362/170256

Rothschild, B. M., & Diedrich, C. G. (2012). Pathologies in the extinct Pleistocene Eurasian steppe lion *Panthera leo spelaea* (Goldfuss, 1810)—Results of fights with hyenas, bears and lions and other ecological stresses. *International Journal of Paleopathology*, *2*(4), 187–198. https://doi.org/10.1016/j.ijpp.2012.09.004

Ruiz, C. B., Ortega, D. B., Caparrós, M., Moigne, A. M., Celiberti, V., Bohórquez, A. M., Cabello, L. P., Gómez, G. M., Testu, A., Barsky, D., Notter, O., Cantal, J. A. R., Rodríguez, M. P., León, M. I. C., Khatib, S., Saos, T., Gregoire, S., Bailon, S., Solano, J. A. G., … Lumley, H. de. (2012). La cueva del Ángel (Lucena, Córdoba): Un hábitat achelense de cazadores en Andalucía. *Menga: Revista de prehistoria de Andalucía*, *3*, 27–56.

Sakai, S. T., Arsznov, B. M., Hristova, A. E., Yoon, E. J., & Lundrigan, B. L. (2016). Big Cat Coalitions: A Comparative Analysis of Regional Brain Volumes in Felidae. *Frontiers in Neuroanatomy*, *10*. https://doi.org/10.3389/fnana.2016.00099

Salles, L. O. (1992). Felid phylogenetics: Extant taxa and skull morphology (Felidae, Aeluroidea). *American Museum Novitates*, *3047*, 1–67.

Sánchez-Bandera, C., Oms, O., Blain, H.-A., Lozano-Fernández, I., Bisbal-Chinesta, J. F., Agustí, J., Saarinen, J., Fortelius, M., Titton, S., Serrano-Ramos, A., Luzón, C., Solano-García, J., Barsky, D., & Jiménez-Arenas, J. M. (2020). New stratigraphically constrained palaeoenvironmental reconstructions for the first human settlement in Western Europe: The Early Pleistocene herpetofaunal assemblages from Barranco León and Fuente Nueva 3 (Granada, SE Spain). *Quaternary Science Reviews*, *243*, 106466. https://doi.org/10.1016/j.quascirev.2020.106466

Sánchez-Vialas, A., Buckley, D., Recuero, E., Martínez-Freiría, F., Velo-Antón, G., Bisbal-Chinesta, J., & Martínez-Solano, I. (2024). Species list of the Spanish herpetofauna: An update. *Basic and Applied Herpetology*, *38*, 5–23. https://doi.org/10.11160/bah.300

Sanchis, A., Duarte, E., Pérez, L., Real, C., Gómez-Olivencia, A., Pastor, F., & de la Rasilla, M. (2025). Morphometry of a partial Late Pleistocene dhole (Cuon alpinus europaeus; (Bourguignat, 1868); Carnivora, Canidae) skeleton from Llonin Cave (Asturias, Spain) and its taphonomic origin. *Geobios*, *88–89*, 227–240. https://doi.org/10.1016/j.geobios.2024.03.001

Sanz, M., Daura, J., Costa, A. M., & Araújo, A. C. (2023). The characterization of bearded vulture (Gypaetus barbatus) coprolites in the archaeological record. *Scientific Reports*, *13*(1), 57. https://doi.org/10.1038/s41598-022-25288-x

Sanz, M., Daura, J., Rivals, F., & Zilhão, J. (2024). The residential occupation of the Gruta da Aroeira (Almonda, Portugal) cave site: Shedding light on hunting and subsistence practices in the Middle Pleistocene of western Eurasia. *Archaeological and Anthropological Sciences*, *16*(8), 139. https://doi.org/10.1007/s12520-024-02026-0

Sarrion, I., Dupre, M., Fumanal, M. P., & Garay, P. (1987). *El yacimiento paleontológico de Moli de Mato, Agrès, Alicante*. 59–62. http://pascal-francis.inist.fr/vibad/index.php?action=getRecordDetail&idt=7702043

Schaller, G. B. (1977). *Mountain Monarchs: Wild Sheep and Goats of the Himalaya*. University of Chicago Press.

Schubert, B. W., & Mead, J. I. (2019). Paleontology of caves. In W. B. White, D. C. Culver, & T. Pipan (Eds.), *Encyclopedia of Caves (Third Edition)* (pp. 794–805). Academic Press. https://doi.org/10.1016/B978-0-12-814124-3.00096-0

Sepkoski, D. (2005). Stephen Jay Gould, Jack Sepkoski, and the 'Quantitative Revolution' in American Paleobiology. *Journal of the History of Biology*, *38*(2), 209–237. https://doi.org/10.1007/s10739-004-2084-5

Serangeli, J., Van Kolfschoten, T., Starkovich, B. M., & Verheijen, I. (2015). The European saber-toothed cat (Homotherium latidens) found in the "Spear Horizon" at Schöningen (Germany). *Journal of Human Evolution*, *89*, 172–180. https://doi.org/10.1016/j.jhevol.2015.08.005

Shackleton, N. (1967). Oxygen Isotope Analyses and Pleistocene Temperatures Re-assessed. *Nature*, *215*(5096), 15–17. https://doi.org/10.1038/215015a0

Shehzad, W., McCarthy, T. M., Pompanon, F., Purevjav, L., Coissac, E., Riaz, T., & Taberlet, P. (2012). Prey Preference of Snow Leopard (Panthera uncia) in South Gobi, Mongolia. *PLOS ONE*, *7*(2), e32104. https://doi.org/10.1371/journal.pone.0032104

Sims, M. E. (2012). Cranial morphology of five felids: Acinonyx jubatus, Panthera onca, Panthera pardus, Puma concolor, Uncia uncia. *Russian Journal of Theriology*, *11*(2), 157–170.

Sirak, K. A., Fernandes ,Daniel M., Cheronet ,Olivia, Novak ,Mario, Gamarra ,Beatriz, Balassa ,Tímea, Bernert ,Zsolt, Cséki ,Andrea, Dani ,János, Gallina ,József Zsolt, Kocsis-Buruzs ,Gábor, Kővári ,Ivett, László ,Orsolya, Pap ,Ildikó, Patay ,Róbert, Petkes ,Zsolt, Szenthe ,Gergely, Szeniczey ,Tamás, Hajdu ,Tamás, & and Pinhasi, R. (2017). A Minimally-Invasive Method for Sampling Human Petrous Bones from the Cranial Base for Ancient DNA Analysis. *BioTechniques*, *62*(6), 283–289. https://doi.org/10.2144/000114558

Sorbelli, L., Alba, D. M., Cherin, M., Moullé, P.-É., Brugal, J.-P., & Madurell-Malapeira, J. (2021). A review on *Bison schoetensacki* and its closest relatives through the early-Middle Pleistocene transition: Insights from the Vallparadís Section (NE Iberian Peninsula) and other European localities. *Quaternary Science Reviews*, *261*, 106933. https://doi.org/10.1016/j.quascirev.2021.106933

Spassov, N., & Raychev, D. (1997). Late Wurm Panthera pardus remains from Bulgaria: The European fossil leopards and the question of the probable species survival until the Holocene on the Balkans. *Historia Naturalis Bulgarica*, *7*, 71–96.

Sponheimer, M., & Lee-Thorp, J. A. (1999). Oxygen Isotopes in Enamel Carbonate and their Ecological Significance. *Journal of Archaeological Science*, *26*(6), 723–728. https://doi.org/10.1006/jasc.1998.0388

Spötl, C., & Boch, R. (2019). Chapter 128—Uranium series dating of speleothems. In W. B. White, D. C. Culver, & T. Pipan (Eds.), *Encyclopedia of Caves (Third Edition)* (pp. 1096–1102). Academic Press. https://doi.org/10.1016/B978-0-12-814124-3.00128-X

Stewart, J. R. (2007). *An Evolutionary Study of Some Archaeologically Significant Avian Taxa in the Quaternary of the Western Palaearctic*. BAR Publishing. https://doi.org/10.30861/9781407300894

Stiner, M. C. (1998). Mortality analysis of Pleistocene bears and its paleoanthropological relevance. *Journal of Human Evolution*, *34*(3), 303–326. https://doi.org/10.1006/jhev.1997.0198

Stiner, M. C. (2003). Zooarchaeological evidence for resource intensification in Algarve, southern Portugal. *Promontoria, Revista Do Departamento de Historia, Arqueologia e Patrimonio Da Universidade Do Algarve*, *1*, 23–58.

Stringham, S. F. (1990). Grizzly Bear Reproductive Rate Relative to Body Size. *Bears: Their Biology and Management*, *8*, 433–443. https://doi.org/10.2307/3872948

Swenson, J. E., Ciucci, P., Huber, Đ., Penteriani, V., & Zedrosser, A. (2023). Brown Bear Ursus arctos Linnaeus, 1758. In K. Hackländer & F. E. Zachos (Eds.), *Handbook of the Mammals of Europe* (pp. 1–36). Springer International Publishing. https://doi.org/10.1007/978-3-319-65038-8_147-1

Tao, D., Wanbo, H., & Hongjie, W. (1999). The Late Pleistocene mammalian fossils from Niuyan Cave in Mentougou, Beijing, China. *Vertebrata Palasiatica*, *37*, 156–164.

Tao, D., Zhanxiang, Q., & Banyue, W. (2013). Late Cenozoic Biostratigraphy of the Linxia Basin, Northwestern China. In *Fossil Mammals of Asia* (pp. 243–273). Columbia University Press.

Tátá, F., Cascalheira, J., Marreiros, J., Pereira, T., & Bicho, N. (2014). Shell bead production in the Upper Paleolithic of Vale Boi (SW Portugal): An experimental perspective. *Journal of Archaeological Science*, *42*, 29–41. https://doi.org/10.1016/j.jas.2013.10.029

Testu, A., Moigne, A.-M., & de Lumley, H. (2011). La panthère Panthera pardus des niveaux inférieurs de la Caune de l'Arago à Tautavel (Pyrénées-Orientales, France) dans le contexte des Felidae (Felinae, Pantherinae) de taille moyenne du Pléistocène européen. *Quaternaire*, *Hors-série*(4), 271–281.

The NOW Community. (2025). *New and Old Worlds Database of Fossil Mammals (NOW)*. https://nowdatabase.org/

Therrien, F. (2005). Mandibular force profiles of extant carnivorans and implications for the feeding behaviour of extinct predators. *Journal of Zoology*, *267*(3), 249–270. https://doi.org/10.1017/S0952836905007430

Thomas, C. (1985). *Grottes et Algares du Portugal*. Self Published.

Tong, H.-W., & Zhang, B. (2019). New fossils of Eucladoceros boulei (Artiodactyla, Mammalia) from Early Pleistocene Nihewan Beds, China. *Palaeoworld*, *28*(3), 403–424. https://doi.org/10.1016/j.palwor.2019.05.003

Tong, H.-W., Zhang, S., Li, Q., & Xu, J. (2008). Late Pleistocene mammalian fossils from Xitaiping Cave, Shidu, Beijing. *Vertebrata Palasiatica*, *46*(1), 51–70.

Torregrosa, V., Petrucci, M., Pérez-Claros, J. A., & Palmqvist, P. (2010). Nasal aperture area and body mass in felids: Ecophysiological implications and paleobiological inferences. *Geobios*, *43*(6), 653–661. https://doi.org/10.1016/j.geobios.2010.05.001

Torres, C. R., Ogawa, L. M., Gillingham, M. A., Ferrari, B., & van Tuinen, M. (2014). A multi-locus inference of the evolutionary diversification of extant flamingos (Phoenicopteridae). *BMC Evolutionary Biology*, *14*(1), 36. https://doi.org/10.1186/1471-2148-14-36

Torres Pérez-Hidalgo, T. (1979). Osos pardos fósiles encontrados en Portugal. *Cuadernos de Espeleologia, Santander*, *9–10*, 157–167.

Torres Pérez-Hidalgo, T. (1984). *Úrsidos del pleistoceno-holoceno de la península ibérica* [PhD thesis, Universidad Politécnica de Madrid]. https://dialnet.unirioja.es/servlet/tesis?codigo=2780

Torres Pérez-Hidalgo, T. (1996). El yacimiento paleontológico de la Cueva del Reguerillo. In *La cueva del Reguerillo y su entorno: Un estudio multidisciplinar* (pp. 7–18). E.T.S.I. Minas (UPM). https://oa.upm.es/4299/

Trinkaus, E., Marks, A. E., Brugal, J.-P., Bailey, S. E., Rink, W. J., & Richter, D. (2003). Later Middle Pleistocene human remains from the Almonda Karstic system, Torres Novas, Portugal. *Journal of Human Evolution*, *45*(3), 219–226. https://doi.org/10.1016/j.jhevol.2003.07.001

Tseng, Z. J. (2013). Testing Adaptive Hypotheses of Convergence with Functional Landscapes: A Case Study of Bone-Cracking Hypercarnivores. *PLOS ONE*, *8*(5), e65305. https://doi.org/10.1371/journal.pone.0065305

Tseng, Z. J., Wang, X., Slater, G. J., Takeuchi, G. T., Li, Q., Liu, J., & Xie, G. (2014). Himalayan fossils of the oldest known pantherine establish ancient origin of big cats. *Proceedings of the Royal Society B: Biological Sciences*, *281*(1774), 20132686. https://doi.org/10.1098/rspb.2013.2686

Tsoukala, E., & Grandal-d'Anglade, A. (2002). Système de mesures du squelette des Ursidés. *Études et Recherches Archéologiques de l'Université de Liège (ERAUL)*, *100*, 265–287.

Turner, A., & Antón, M. (1997). *The big cats and their fossil relatives: An illustrated guide to their evolution and natural history*. Columbia University Press.

Tyrberg, T. (1999). Seabirds and late Pleistocene marine environments in the northeast Atlantic and the Mediterranean. *Smithson. Contrib. Zool*, *89*, 139–157.

Uhen, M. D., Allen, B., Behboudi, N., Clapham, M. E., Dunne, E., Hendy, A., Holroyd, P. A., Hopkins, M., Mannion, P., & Novack-Gottshall, P. (2023). Paleobiology database user guide version 1.0. *PaleoBios*, *40*(11). https://escholarship.org/uc/item/6tm05630

Uzunidis, A., Rivals, F., Rufà, A., Blasco, R., & Rosell, J. (2023). The Exceptional Presence of Megaloceros giganteus in North-Eastern Iberia and Its Palaeoecological Implications: The Case of Teixoneres Cave (Moià, Barcelona, Spain). *Diversity*, *15*(2), Article 2. https://doi.org/10.3390/d15020299

Valavi, R., Elith, J., Lahoz-Monfort, J. J., & Guillera-Arroita, G. (2021). Modelling species presence-only data with random forests. *Ecography*, *44*(12), 1731–1742. https://doi.org/10.1111/ecog.05615

Valente, M. J. (2004). Humans and carnivores in the early upper Paleolithic in Portugal: Data from Pego do Diabo cave. *Revue de Paléobiologie*, *23*(2), 611–626.

Valente, M. J., & Haws, J. (2006). Animal carcass utilization during the Late Upper Paleolithic occupation of Lapa do Suão (Portugal). In *Paleolithic Zooarchaeology in Practice* (pp. 29–38). BAR INTERNATIONAL SERIES.

Vallverdú, J., Saladié, P., Rosas, A., Huguet, R., Cáceres, I., Mosquera, M., Garcia-Tabernero, A., Estalrrich, A., Lozano-Fernández, I., Pineda-Alcalá, A., Carrancho, Á., Villalaín, J. J.,

Bourlès, D., Braucher, R., Lebatard, A., Vilalta, J., Esteban-Nadal, M., Bennàsar, M. L., Bastir, M., … Carbonell, E. (2014). Age and Date for Early Arrival of the Acheulian in Europe (Barranc de la Boella, la Canonja, Spain). *PLOS ONE*, *9*(7), e103634. https://doi.org/10.1371/journal.pone.0103634

van der Made, J. (2015). The latest Early Pleistocene giant deer Megaloceros novocarthaginiensis n. Sp. And the fallow deer" Dama cf. Vallonnetensis" from Cueva Victoria (Murcia, Spain). *Mastia: Revista Del Museo Arqueológico Municipal de Cartagena "Enrique Escudero de Castro," Volumen temático: Palaeontología y geología de Cueva Victoria*(11-12–13), 269–323.

van der Made, J. (2019). The dwarfed "giant deer" Megaloceros matritensis n.sp. From the Middle Pleistocene of Madrid—A descendant of M. savini and contemporary to M. giganteus. *Quaternary International*, *520*, 110–139. https://doi.org/10.1016/j.quaint.2018.06.006

van der Made, J., & Dimitrijević, V. (2015). Eucladoceros montenegrensis n. Sp. And other Cervidae from the Lower Pleistocene of Trlica (Montenegro). *Quaternary International*, *389*, 90–118. https://doi.org/10.1016/j.quaint.2015.02.058

van der Made, J., Rosell, J., & Blasco, R. (2017). Faunas from Atapuerca at the Early–Middle Pleistocene limit: The ungulates from level TD8 in the context of climatic change. *Quaternary International*, *433*, 296–346. https://doi.org/10.1016/j.quaint.2015.09.009

Van Valkenburgh, B. (1990). Skeletal and dental predictors of body mass in carnivores. In *Body size in Mammalian Paleobiology Estimation and biological implications.: Vol. Body Size in Mammalian Paleobiology Estimation and Biological Implications* (pp. 181–205). Cambridge University Press. https://cir.nii.ac.jp/crid/1573950398851008640

Varela, S., González-Hernández, J., Sgarbi, L. F., Marshall, C., Uhen, M. D., Peters, S., & McClennen, M. (2015). paleobioDB: An R package for downloading, visualizing and processing data from the Paleobiology Database. *Ecography*, *38*(4), 419–425. https://doi.org/10.1111/ecog.01154

Veiga Ferreira, O. (1975). Os rinocerontes quaternarios encontrados em Portugal. *Comunicações Geológicas*, *59*, 15–25.

Villalba de Alvarado, M., Collado Giraldo, H., Arsuaga, J. L., Bello Rodrigo, J. R., van Heteren, A. H., & Gómez-Olivencia, A. (2022). Looking for the earliest evidence of Ursus arctos LINNAEUS, 1758 in the Iberian Peninsula: The Middle Pleistocene site of Postes cave. *Boreas*, *51*(1), 159–184. https://doi.org/10.1111/bor.12537

Villalba de Alvarado, M., Crégut-Bonnoure, E., Arsuaga, J. L., Collado Giraldo, H., van der Made, J., & Gómez-Olivencia, A. (2024). Pleistocene Asian black bear (Ursus thibetanus Cuvier, 1823) in the Iberian Peninsula: New evidence and a complete review. *Quaternary Science Reviews*, *325*, 108385. https://doi.org/10.1016/j.quascirev.2023.108385

Villalba de Alvarado, M., Prat-Vericat, M., Arriolabengoa, M., Madurell- Malapeira, J., & Gómez-Olivencia, A. (2024). The mandible of Salbatore II: A new Ursus deningeri site in the northern Iberian Peninsula. *Geobios*. https://doi.org/10.1016/j.geobios.2024.08.019

Villaluenga, A. (2016). Presencia de felinos (Felis, Lynx y Panthera) en el registro arqueológico de la Península Ibérica durante el Pleistoceno Superior. *Archaeofauna*, *25*, 185–204.

Vinuesa, V., Iurino, D. A., Madurell-Malapeira, J., Liu, J., Fortuny, J., Sardella, R., & Alba, D. M. (2016). Inferences of social behavior in bone-cracking hyaenids (Carnivora, Hyaenidae) based on digital paleoneurological techniques: Implications for human–carnivoran

interactions in the Pleistocene. *Quaternary International*, *413*, 7–14. https://doi.org/10.1016/j.quaint.2015.10.037

Vinuesa, V., Madurell-Malapeira, J., Fortuny, J., & Alba, D. M. (2015). The Endocranial Morphology of the Plio-Pleistocene Bone-Cracking Hyena Pliocrocuta perrieri: Behavioral Implications. *Journal of Mammalian Evolution*, *22*(3), 421–434. https://doi.org/10.1007/s10914-015-9287-8

Viranta, S. (1994). Limb bone proportions and body mass of the cave bear (Ursus spelaeus). *Historical Biology*, *7*(3), 239–250. https://doi.org/10.1080/10292389409380456

Vislobokova, I. A. (2013). Morphology, taxonomy, and phylogeny of megacerines (Megacerini, Cervidae, Artiodactyla). *Paleontological Journal*, *47*(8), 833–950. https://doi.org/10.1134/S0031030113080017

Vörös, J., Márton, O., Schmidt, B. R., Gál, J. T., & Jelić, D. (2017). Surveying Europe's Only Cave-Dwelling Chordate Species (Proteus anguinus) Using Environmental DNA. *PLOS ONE*, *12*(1), e0170945. https://doi.org/10.1371/journal.pone.0170945

Wang, S.-Q., Yang, Q., Zhao, Y., Li, C.-X., Shi, Q.-Q., Zong, L.-Y., & Ye, J. (2019). New Olonbulukia material and its related assemblage reveal an early radiation of stem Caprini along the north of the Tibetan Plateau. *Journal of Paleontology*, *93*(2), 385–397. https://doi.org/10.1017/jpa.2018.65

Wang, X., Li, Q., & Takeuchi, G. T. (2016). Out of Tibet: An early sheep from the Pliocene of Tibet, Protovis himalayensis, genus and species nov. (Bovidae, Caprini), and origin of Ice Age mountain sheep. *Journal of Vertebrate Paleontology*, *36*(5), e1169190. https://doi.org/10.1080/02724634.2016.1169190

Werdelin, L., & Flink, T. (2018). The phylogenetic context of Smilodon. In *Smilodon: The iconic sabertooth* (pp. 14–29). Johns Hopkins University Press Baltimore. https://books.google.es/books?hl=es&lr=&id=fmBVDwAAQBAJ&oi=fnd&pg=PA14&dq=The+phylogenetic+context+of+Smilodon&ots=B6gFCOsuaO&sig=o9e24mSDmvPdE6STltsvkQYOSa0

Werdelin, L., Yamaguchi, N., Johnson, W. E., & O'Brien, S. J. (2010). Phylogeny and evolution of cats (Felidae). In *Biology and conservation of wild felids* (pp. 59–82). Oxford University Press. https://www.researchgate.net/profile/Nobuyuki-Yamaguchi-2/publication/266755142_Phylogeny_and_evolution_of_cats_Felidae/links/543ba0710cf2d6698be30c5e/Phylogeny-and-evolution-of-cats-Felidae.pdf

Wesley-Hunt, G. D., & Flynn, J. J. (2005). Phylogeny of the carnivora: Basal relationships among the carnivoramorphans, and assessment of the position of 'miacoidea' relative to carnivora. *Journal of Systematic Palaeontology*, *3*(1), 1–28. https://doi.org/10.1017/S1477201904001518

Wickham, H. (2016). *ggplot2: Elegant graphics for data analysis* [Computer software]. Springer. https://www.jstatsoft.org/htaccess.php?volume=077&type=b&issue=02&filename=paper

Winham, S., Wang, X., de Andrade, M., Freimuth, R., Colby, C., Huebner, M., & Biernacka, J. (2012). Interaction detection with random forests in high-dimensional data. *Genetic Epidemiology*, *36*(2), 142–142.

Winter, N. J. de, Snoeck, C., & Claeys, P. (2016). Seasonal Cyclicity in Trace Elements and Stable Isotopes of Modern Horse Enamel. *PLOS ONE*, *11*(11), e0166678. https://doi.org/10.1371/journal.pone.0166678

Xiao, L., Cheng, C., Wan, H., Zhang, D., Wang, Y., Tsedan, Hou, P., Li, J., Yang, X., Lü, Z., & Liu, Y. (2019). Defining conservation priority areas of snow leopard habitat in the Sanjiangyuan Region. *Biodiversity Science*, *27*(9), 943–950. https://doi.org/10.17520/biods.2019014

Zazzo, A., & Saliège, J.-F. (2011). Radiocarbon dating of biological apatites: A review. *Palaeogeography, Palaeoclimatology, Palaeoecology*, *310*(1), 52–61. https://doi.org/10.1016/j.palaeo.2010.12.004

Zbyszewski, G. (1950). Les restes d'Hippopotame et de Cerfs d'Algoz. *Comunicações Dos Serviços Geológicos de Portugal*, *31*, 413–422.

Zbyszewski, G. (1977). Nova contribuição para o conhecimento da jazida Quaternária da Mealhada. *Memórias e Noticias*, *84*, 1–37.

Zbyszewski, G., & Veiga Ferreira, O. (1990). Les Vertébrés Quaternaires Portugais à la Lueur des Études Recentes. *Revista da Universidade Coimbra*, *35*, 155–162.

Zhang, C., Stadler, T., Klopfstein, S., Heath, T. A., & Ronquist, F. (2016). Total-evidence dating under the fossilized birth–death process. *Systematic Biology*, *65*(2), 228–249.

Zhang, C., & Wang, M. (2019). Bayesian tip dating reveals heterogeneous morphological clocks in Mesozoic birds. *Royal Society Open Science*, *6*(7), 182062. https://doi.org/10.1098/rsos.182062

Zilhão, J. (1987). A Gruta do Caldeirão (Pedreira, Tomar): Balanço de sete anos de escavações arqueológicas (1979-1985). *Algar (Bol. Soc. Portuguesa Espeleologia)*, *1*, 29–38.

Zilhão, J. (2021). The late persistence of the Middle Palaeolithic and Neandertals in Iberia: A review of the evidence for and against the "Ebro Frontier" model. *Quaternary Science Reviews*, *270*, 107098. https://doi.org/10.1016/j.quascirev.2021.107098

Zilhão, J. (2022). Everything you always wanted to ask about the Lapa do Picareiro Aurignacian and should not be afraid to know: A reply to 'The early Aurignacian at Lapa do Picareiro really is that old.' *Quaternary Science Reviews*, *277*, 107296. https://doi.org/10.1016/j.quascirev.2021.107296

Zilhão, J. (2023). *Portugal na idade do gelo: Território e habitantes*. Fundação Francisco Manuel dos Santos.

Zilhão, J., Angelucci, D. E., Arnold, L. J., d'Errico, F., Dayet, L., Demuro, M., Deschamps, M., Few-lass, H., Gomes, L., Linscott, B., Matias, H., Pike, A. W. G., Steier, P., Talamo, S., & Wild, E. M. (2021). Revisiting the Middle and Upper Palaeolithic archaeology of Gruta do Caldeirão (Tomar, Portugal). *PLOS ONE*, *16*(10), e0259089. https://doi.org/10.1371/journal.pone.0259089

Zilhão, J., Angelucci, D. E., Arnold, L. J., Demuro, M., Hoffmann, D. L., & Pike, A. W. G. (2021). A revised, Last Interglacial chronology for the Middle Palaeolithic sequence of Gruta da Oliveira (Almonda karst system, Torres Novas, Portugal). *Quaternary Science Reviews*, *258*, 106885. https://doi.org/10.1016/j.quascirev.2021.106885

Zilhão, J., Angelucci, D. E., Aubry, T., Badal, E., Brugal, J.-P., Carvalho, R., Gameiro, C., Hoffmann, D. L., Matias, H., Maurício, J., Nabais, M., Pike, A. W. G., Póvoas, L., Richter, D., Souto, P., Trinkaus, E., Wainer, K., & Willman, J. (2013). A Gruta da Oliveira (Torres Novas): Uma jazida de referência para o Paleolítico Médio da Península Ibérica. In *Arqueologia em Portugal – 150 Anos* (pp. 259–268). Associação dos Arqueólogos Portugueses. https://repositorio.ul.pt/handle/10451/31145

Zilhão, J., Angelucci, D. E., Igreja, M. A., Arnold, L. J., Badal, E., Callapez, P., Cardoso, J. L., d'Errico, F., Daura, J., Demuro, M., Deschamps, M., Dupont, C., Gabriel, S., Hoffmann, D. L.,

Legoinha, P., Matias, H., Soares, A. M. M., Nabais, M., Portela, P., … Souto, P. (2020). Last Interglacial Iberian Neandertals as fisher-hunter-gatherers. *Science*, *367*(6485). https://doi.org/10.1126/science.aaz7943

Zilhão, J., Cardoso, J., Pike, A., & Weninger, B. (2011). Gruta Nova da Columbeira (Bombarral, Portugal): Site stratigraphy, age of the Mousterian sequence, and implications for the timing of Neanderthal extinction in Iberia. *Quartär*, *58*, 93–112.

Zilhão, J., Davis, S. J. M., Duarte, C., Soares, A. M. M., Steier, P., & Wild, E. (2010). Pego do Diabo (Loures, Portugal): Dating the Emergence of Anatomical Modernity in Westernmost Eurasia. *PLOS ONE*, *5*(1), e8880. https://doi.org/10.1371/journal.pone.0008880

Zilhão, J., & Trinkaus, E. (2002). Portrait of the Artist as a Child: The Gravettian human skeleton from the Abrigo do Lagar Velho and its archaeological context. Trabalhos de Arqueologia. *Trabalhos de Arqueologia*, *22*, 609.

Žliobaitė, I., Fortelius, M., Bernor, R. L., van den Hoek Ostende, L. W., Janis, C. M., Lintulaakso, K., Säilä, L. K., Werdelin, L., Casanovas-Vilar, I., Croft, D. A., Flynn, L. J., Hopkins, S. S. B., Kaakinen, A., Kordos, L., Kostopoulos, D. S., Pandolfi, L., Rowan, J., Tesakov, A., Vislobokova, I., … Vepsäläinen, J. (2023). The NOW Database of Fossil Mammals. In I. Casanovas-Vilar, L. W. van den Hoek Ostende, C. M. Janis, & J. Saarinen (Eds.), *Evolution of Cenozoic Land Mammal Faunas and Ecosystems: 25 Years of the NOW Database of Fossil Mammals* (pp. 33–42). Springer International Publishing. https://doi.org/10.1007/978-3-031-17491-9_3

A

APPENDIX: "EARLY PLEISTOCENE (EPIVILLAFRANCHIAN) VERTEBRATES FROM PORTUGAL: AN UPDATED REVIEW"

A.1 List of vertebrate taxa from Algoz and Santa Margarida.

Taxa from Algoz:

Hippopotamus antiquus

Metacervocerus rhenanus

Eucladoceros sp.

Leporidae indet.

Taxa from Santa Margarida:

Lacertidae indet.

Crocidura sp.

Sorex sp.

Oryctolagus cf. *cuniculus*

Eliomys cf. *quercinus*

Apodemus cf. *sylvaticus*

Allocricetus bursae

Victoriamys chalinei

Iberomys huescarensis

Iberomys brecciensis

A.2 Measurements and dataset for metric comparisons of medium-sized deer from Algoz.

Complete measurements of the remains of medium-sized deer from Algoz.

MG-25770	**Left hemimandible with d4**					
DAPb	**Dta (est)**	**DTp**	**DTpp**			
18,28	7,11	8,45	9,34			
MG-25771	**Distal right radius**					
L frag	**DTd**	**DAPd**	**DAPdf**	**Dtdia**	**DAPdia**	**CIRCdia**
174,28	42,48	30,29	24,92	26,86	21,58	84

Measurements of the distal radius of *Dama*-like deer compared with Algoz deer.

Specimen	**Species**	**DTd**	**DAPd**	**DTdia**	**DAPdia**	**Site**	**Reference**
MG-25771	*Metacervocerus rhenanus*	42,48	30,29	26,86	21,58	Algoz	this work
IGF-2815V	*'Pseudodama'* cf. *lyra*	37				Montopoli	Azzaroli, 1992
IGF-397	*'Pseudodama' nestii*	39,5				Tasso	Azzaroli, 1992
IGF-394	*'Pseudodama' nestii*	43				Tasso	Azzaroli, 1992
IGF-453	*'Pseudodama' nestii*	38				Tasso	Azzaroli, 1992
IGF-454	*'Pseudodama' nestii*	36,5				Tasso	Azzaroli, 1992
IGF-455	*'Pseudodama' nestii*	36,5				Tasso	Azzaroli, 1992
IGF-466	*'Pseudodama' nestii*	40				Tasso	Azzaroli, 1992
Average	*'Pseudodama' nestii*	38,92				Tasso	Azzaroli, 1992
IGF-1250	*'Pseudodama' nestii*	40				Figline	Azzaroli, 1992
VA-2478	*'Pseudodama' nestii*		26,8	23,2	14	Valdarno	Catalano, 1984
VA-2479	*'Pseudodama' nestii*	39,5	28,2	24,2	15,6	Valdarno	Catalano, 1984
VA-2483	*'Pseudodama' nestii*	37	26	24	15,8	Valdarno	Catalano, 1984
VA-2482	*'Pseudodama' nestii*	35,4	25	23	15,8	Valdarno	Catalano, 1984
VA-849	*'Pseudodama' nestii*	32,3	24,6	20,9	14,6	Valdarno	Catalano, 1984
VA-880	*'Pseudodama' nestii*			25	13,6	Valdarno	Catalano, 1984
VA-1584	*'Pseudodama' nestii*	34,4	25,6	20,8	14,5	Valdarno	Catalano, 1984
VA-603	*'Pseudodama' nestii*			23,2	15,8	Valdarno	Catalano, 1984
VA-1786	*'Pseudodama' nestii*			25,7	14,7	Valdarno	Catalano, 1984
VA-983	*'Pseudodama' nestii*		27	24,3	16	Valdarno	Catalano, 1984

VA-1232	*'Pseudodama' nestii*	32,7	22,8	20	13,2	Valdarno	Catalano, 1984
VA-1231	*'Pseudodama' nestii*			20,4	13,5	Valdarno	Catalano, 1984
IGF-454	*'Pseudodama' nestii*	31	23,2	23,5	12,2	Valdarno	Catalano, 1984
IGF-456	*'Pseudodama' nestii*	34,7	24,6	24,3	14,3	Valdarno	Catalano, 1984
IGF-453	*'Pseudodama' nestii*	33,9	24	24,5	12,2	Valdarno	Catalano, 1984
IGF-455j	*'Pseudodama' nestii*	31	24,8	18,6	11,9	Valdarno	Catalano, 1984
IGF-397	*'Pseudodama' nestii*	39	26,1	27,1	19,6	Valdarno	Catalano, 1984
IGF-394	*'Pseudodama' nestii*	36,8	26,1	27	16,1	Valdarno	Catalano, 1984
IGF-1248	*'Pseudodama' nestii*	36,6	26	26,2	16	Valdarno	Catalano, 1984
IGF-1250	*'Pseudodama' nestii*	33,5	22	24,1	14	Valdarno	Catalano, 1984
IGF-1245	*'Pseudodama' nestii*	36,3	26,2	20	16,5	Valdarno	Catalano, 1984
IGF-1246	*'Pseudodama' nestii*			27,6	16,2	Valdarno	Catalano, 1984
IGF-1247	*'Pseudodama' nestii*	29,5	23	20,5	12,2	Valdarno	Catalano, 1984
IGF-1254	*'Pseudodama' nestii*	35	26			Valdarno	Catalano, 1984
Average	*'Pseudodama' nestii*	34,92	25,16	23,40	14,71	Valdarno	Catalano, 1984
IGF-2523	*'Pseudodama' nestii*	39,2	26,8			Olivola	Catalano, 1984
IGF-2524	*'Pseudodama' nestii*	35,7	25,1			Olivola	Catalano, 1984
IGF-1767	*'Pseudodama' nestii*	37,6	27			Olivola	Catalano, 1984
Average	*'Pseudodama' nestii*	37,50	26,30			Olivola	Catalano, 1984
IGF-G141	*'Pseudodama' nestii*	39	28,1	26,2	16,5	Gionella	Catalano, 1984
NHMB-527	*Croizetoceros ramosus*	31,2	23,2	21	14,1	Saint Vallier	Catalano, 1984
NHMB-178	*Croizetoceros ramosus*	31,9	22,8	19,4	12,5	Saint Vallier	Catalano, 1984
NHMB-177	*Croizetoceros ramosus*	32	22,2	19,9	13,6	Saint Vallier	Catalano, 1984
NHMB-179	*Croizetoceros ramosus*	31,9	21,9			Saint Vallier	Catalano, 1984
NHMB-530	*Croizetoceros ramosus*	31,4	24			Saint Vallier	Catalano, 1984
NHMB-928	*Croizetoceros ramosus*			20,9	13,2	Saint Vallier	Catalano, 1984
NHMB-532	*Croizetoceros ramosus*			23,2	14,8	Saint Vallier	Catalano, 1984
Average	*Croizetoceros ramosus*	31,68	22,82	20,88	13,64	Saint Vallier	Catalano, 1984
STV136	*Metacervocerus pardinensis*		23,3			Saint Vallier	Catalano, 1984
STV649	*Metacervocerus pardinensis*	39,9	32,3	25,6	19	Saint Vallier	Catalano, 1984
STV135	*Metacervocerus pardinensis*			29,8	17,7	Saint Vallier	Catalano, 1984
STV652	*Metacervocerus pardinensis*	39	28,8	24,9	16,8	Saint Vallier	Catalano, 1984
STV650	*Metacervocerus pardinensis*	34,9	26,4	24	14,1	Saint Vallier	Catalano, 1984

Average	*Metacervocerus pardinensis*	37,93	27,70	26,08	16,90	Saint Vallier	Catalano, 1984
NHMB-1845ds	*Metacervocerus rhenanus*	35	24	25,2	17,6	Séneze	Catalano, 1984
NHMB-1845sx	*Metacervocerus rhenanus*	35,2	26	25,8	17,2	Séneze	Catalano, 1984
NHMB-1090	*Metacervocerus rhenanus*	40,05	27,8	29,5	16,3	Séneze	Catalano, 1984
NHMB-1098	*Metacervocerus rhenanus*	36,7	25	26	17,5	Séneze	Catalano, 1984
NHMB-1096	*Metacervocerus rhenanus*	44,5	33	33	19	Séneze	Catalano, 1984
NHMB-1226	*Metacervocerus rhenanus*	39,5	30,02	27,5	20	Séneze	Catalano, 1984
NHMB-567	*Metacervocerus rhenanus*	37	24,5	27,8	18,1	Séneze	Catalano, 1984
NHMB-1231	*Metacervocerus rhenanus*	36	30	23,2	16	Séneze	Catalano, 1984
NHMB-586	*Metacervocerus rhenanus*			28,5	18,6	Séneze	Catalano, 1984
NHMB-214	*Metacervocerus rhenanus*	39,6	29,3	28	17,5	Séneze	Catalano, 1984
NHMB-1645	*Metacervocerus rhenanus*	43	30	31		Séneze	Catalano, 1984
NHMB-590	*Metacervocerus rhenanus*	38	28	25,6	18	Séneze	Catalano, 1984
NHMB-218	*Metacervocerus rhenanus*	43	33,5	28,5		Séneze	Catalano, 1984
NHMB-1844.1	*Metacervocerus rhenanus*	42	31,5	29		Séneze	Catalano, 1984
NHMB-1844.2	*Metacervocerus rhenanus*	42	28,6	29		Séneze	Catalano, 1984
NHMB-1843	*Metacervocerus rhenanus*	41,2	29,5	26,2	15,6	Séneze	Catalano, 1984
NHMB-1845.1	*Metacervocerus rhenanus*	35,7	26,1	25,6	17,2	Séneze	Catalano, 1984
NHMB-1845.2	*Metacervocerus rhenanus*	35,4	26,2	25,2	17	Séneze	Catalano, 1984
NHMB-1100	*Metacervocerus rhenanus*			25,6	16,8	Séneze	Catalano, 1984
NHMB-1101	*Metacervocerus rhenanus*			26	17,2	Séneze	Catalano, 1984
NHMB-1463a	*Metacervocerus rhenanus*	37	27,5	25,2	15,9	Séneze	Catalano, 1984
NHMB-1463b	*Metacervocerus rhenanus*	36,7	27	26,3	16,9	Séneze	Catalano, 1984
NHMB-583	*Metacervocerus rhenanus*	37,2	26,6	25	16	Séneze	Catalano, 1984
NHMB-1128	*Metacervocerus rhenanus*	40	29,2	27,2	18,2	Séneze	Catalano, 1984
NHMB-213a	*Metacervocerus rhenanus*	36,1	26,2	24,5	16,7	Séneze	Catalano, 1984
NHMB-213d	*Metacervocerus rhenanus*	36,3	26,9	24,5	16,2	Séneze	Catalano, 1984
NHMB-1464a	*Metacervocerus rhenanus*	42	29,6	28,4	18,3	Séneze	Catalano, 1984
NHMB-1464b	*Metacervocerus rhenanus*	41,8	31,5	28,8		Séneze	Catalano, 1984
NHMB-212a	*Metacervocerus rhenanus*	41,5	32,5	27,8	19,5	Séneze	Catalano, 1984
NHMB-212b	*Metacervocerus rhenanus*	41,7	32,7	27,9	19,5	Séneze	Catalano, 1984
NHMB-1922/5d	*Metacervocerus rhenanus*	36,5	27,3	27	17,2	Séneze	Catalano, 1984
NHMB-1922/5s	*Metacervocerus rhenanus*	35	26,8	27,5	16,5	Séneze	Catalano, 1984

NHMB-1922/1	*Metacervocerus rhenanus*	40	28	25,6	17,7	Séneze	Catalano, 1984
Average	*Metacervocerus rhenanus*	38,86	28,49	27,03	17,44	Séneze	Catalano, 1984
MZB 95-0602	*Dama dama*	34,95	29,48			Modern, Barcelona	Elpiniki Parparousi pers. communication
MZB 95-0602	*Dama dama*	35,2	28,72			Modern, Barcelona	Elpiniki Parparousi pers. communication
94-0993	*Dama dama*	37,6	27,8			Modern, Barcelona	Elpiniki Parparousi pers. communication
94-0993	*Dama dama*	36,8	27,2			Modern, Barcelona	Elpiniki Parparousi pers. communication
91-0219	*Dama dama*	32	23			Modern, Barcelona	Elpiniki Parparousi pers. communication
91-0219	*Dama dama*	32,3	23,1			Modern, Barcelona	Elpiniki Parparousi pers. communication
94-0730	*Dama dama*	37,4	28,4			Modern, Barcelona	Elpiniki Parparousi pers. communication
94-0730	*Dama dama*	37,8	27,8			Modern, Barcelona	Elpiniki Parparousi pers. communication
96-0134-B	*Dama dama*	32,8	24,8			Modern, Barcelona	Elpiniki Parparousi pers. communication
96-0134-B	*Dama dama*	31	25			Modern, Barcelona	Elpiniki Parparousi pers. communication
Average	*Dama dama*	34,79	26,53			Modern, Barcelona	Elpiniki Parparousi pers. communication
Ata2002, TD8b, G-12, 27	*'Pseudodama' vallonnetensis*	37,6	27			Atapuerca TD8	Van der Made et al., 2017
Ata2002, TD8b, G-7, 31	*'Pseudodama' vallonnetensis*					Atapuerca TD8	Van der Made et al., 2017
Ata2002, TD8b, G-8, 3	*'Pseudodama' vallonnetensis*	37,5	26,1			Atapuerca TD8	Van der Made et al., 2017
Ata2002, TD8b, G-8, 25	*'Pseudodama' vallonnetensis*	45	29,4			Atapuerca TD8	Van der Made et al., 2017
Ata2002, TD8b, G-12, 34	*'Pseudodama' vallonnetensis*					Atapuerca TD8	Van der Made et al., 2017
Ata04, TD8b, G-5, 20	*'Pseudodama' vallonnetensis*	38,1				Atapuerca TD8	Van der Made et al., 2017

Ata05, TD8b, E−13, 5	*'Pseudodama' vallonnetensis*		24,9			Atapuerca TD8	Van der Made et al., 2017
Average	*'Pseudodama' vallonnetensis*	39,55	26,85			Atapuerca TD8	Van der Made et al., 2017
IQW1980/15 429(Mei. 14 941)sin.	*'Pseudodama' vallonnetensis*			29,7		Untermaßfeld	Kahlke, 1997
IQW1980/15 745(Mei. 15 257)dex.	*'Pseudodama' vallonnetensis*			26,9	14,2	Untermaßfeld	Kahlke, 1997
IQW1980/15 903(Mei. 15 414)sin.	*'Pseudodama' vallonnetensis*			22,2	13,3	Untermaßfeld	Kahlke, 1997
IQW1980/16 087(Mei. 15 598)sin.	*'Pseudodama' vallonnetensis*			26	16,8	Untermaßfeld	Kahlke, 1997
IQW1980/16 804(Mei. 16 325)sin.	*'Pseudodama' vallonnetensis*	45,7	32,5	31,4	19	Untermaßfeld	Kahlke, 1997
IQW1980/17 470(Mei. 16 992)dex.	*'Pseudodama' vallonnetensis*	38,7	26,4	26,3	18,5	Untermaßfeld	Kahlke, 1997
IQW1981/17 646(Mei. 17 168)dex.	*'Pseudodama' vallonnetensis*			27,2	16,5	Untermaßfeld	Kahlke, 1997
IQW1982/18 317(Mei. 17 837)dex.	*'Pseudodama' vallonnetensis*	39,3	26,4	26	16,6	Untermaßfeld	Kahlke, 1997
IQW1982/18 334(Mei. 17 854)sin.	*'Pseudodama' vallonnetensis*	37,9	26,2	25,5	17,6	Untermaßfeld	Kahlke, 1997
IQW1984/20 002(Mei. 19 522)dex.	*'Pseudodama' vallonnetensis*	39,5	26,7	27,4	16,5	Untermaßfeld	Kahlke, 1997
Average	*'Pseudodama' vallonnetensis*	40,22	27,64	26,86	16,56	Untermaßfeld	Kahlke, 1997
Riano 6	*Dama clactoniana*	44		30,8		Riano	Mecozzi et al., 2023
MPUR9/8	*Dama clactoniana*	36,2	25,9	23,7		Vitinia - upper level	Mecozzi et al., 2023
MPUR9/49	*Dama clactoniana*	35,5	27,3	24,4		Vitinia - upper level	Mecozzi et al., 2023
MPUR9/51	*Dama clactoniana*	40,4	30,6			Vitinia - upper level	Mecozzi et al., 2023
Average	*Dama clactoniana*	39,03	27,93	26,30		Vitinia - upper level	Mecozzi et al., 2023
M.19993	*Dama clactoniana*	42		28		Clacton	Leonardi & Petronio, 1970
M.19999	*Dama clactoniana*	41		28		Clacton	Leonardi & Petronio, 1970
M.28012	*Dama clactoniana*	46		31		Clacton	Leonardi & Petronio, 1970
Average	*Dama clactoniana*	43,00		29,00		Clacton	Leonardi & Petronio, 1970
no nº	*Dama clactoniana*	47		27		Swanscombe	Leonardi & Petronio, 1970
no nº	*Dama clactoniana*	40		28		Swanscombe	Leonardi & Petronio, 1970

Average	*Dama clactoniana*	43,50		27,50		Swanscombe	Leonardi & Petronio, 1971
TSR H17-22d	*Cervus* sp.	35,94	18,7	19,63	12,74	Tsiotra Vryssi (Mygdonia Basin)	Kokotini, 2020
MM1949/61	*Cervus elaphus*	50	31	38	21	Mosbach	Di Stefano et al., 2015
MM1949/248	*Cervus elaphus*	48	33	34	21	Mosbach	Di Stefano et al., 2015
MM1956/358	*Cervus elaphus*	46	30	34	19	Mosbach	Di Stefano et al., 2015
MM1964/529	*Cervus elaphus*	56	39	39	25	Mosbach	Di Stefano et al., 2015
MM1955/1136	*Cervus elaphus*	54	40	37	22	Mosbach	Di Stefano et al., 2015
MM1958/42	*Cervus elaphus*	60	43	41	23	Mosbach	Di Stefano et al., 2015
MM1973/299	*Cervus elaphus*	51	32			Mosbach	Di Stefano et al., 2015
MM1961/69	*Cervus elaphus*			34	24	Mosbach	Di Stefano et al., 2015
MM1966/192	*Cervus elaphus*	58	41	39	22	Mosbach	Di Stefano et al., 2015
MM1959/217	*Cervus elaphus*			41	23	Mosbach	Di Stefano et al., 2015
MM1958/355	*Cervus elaphus*			32	18	Mosbach	Di Stefano et al., 2015
MM1962/1233	*Cervus elaphus*			39	25	Mosbach	Di Stefano et al., 2015
MM1961/292	*Cervus elaphus*	61	40	39	27	Mosbach	Di Stefano et al., 2015
Average	*Cervus elaphus*	53,78	36,56	37,25	22,50	Mosbach	Di Stefano et al., 2015
I1	*Cervus elaphus*	51	37,5	32	24	Ingarano	Di Stefano et al., 2015
I3	*Cervus elaphus*	56	34			Ingarano	Di Stefano et al., 2015
I4	*Cervus elaphus*			34	21	Ingarano	Di Stefano et al., 2015
Average	*Cervus elaphus*	53,50	35,75	33,00	22,50	Ingarano	Di Stefano et al., 2015
A1	*Cervus elaphus*			27,5	16	Avetrana	Di Stefano et al., 2015
A5	*Cervus elaphus*			30	20	Avetrana	Di Stefano et al., 2015
Average	*Cervus elaphus*			28,75	18,00	Avetrana	Di Stefano et al., 2015
P4217	*Cervus elaphus*	45,2	33			Sora - Valle Radice	Di Stefano et al., 2015
no nº	*Cervus elaphus*	42,5	31			Sora - Valle Radice	Di Stefano et al., 2015
no nº	*Cervus elaphus*	44,9	31,9			Sora - Valle Radice	Di Stefano et al., 2015
no nº	*Cervus elaphus*	45,3	31,3			Sora - Valle Radice	Di Stefano et al., 2015
no nº	*Cervus elaphus*	39,7	29,2			Sora - Valle Radice	Di Stefano et al., 2015
Average	*Cervus elaphus*	43,52	31,28			Sora - Valle Radice	Di Stefano et al., 2015
P1696	*Cervus elaphus*	45	32			Grotta Romanelli	Di Stefano et al., 2015
P1698	*Cervus elaphus*	45	33			Grotta Romanelli	Di Stefano et al., 2015
P1699	*Cervus elaphus*	46	32			Grotta Romanelli	Di Stefano et al., 2015

P1700	*Cervus elaphus*	46,5	31			Grotta Romanelli	Di Stefano et al., 2015
P1697	*Cervus elaphus*	46	30			Grotta Romanelli	Di Stefano et al., 2015
no nº	*Cervus elaphus*	45,5	31			Grotta Romanelli	Di Stefano et al., 2015
no nº	*Cervus elaphus*	44,4	30,9			Grotta Romanelli	Di Stefano et al., 2015
no nº	*Cervus elaphus*	45,9	32,4			Grotta Romanelli	Di Stefano et al., 2015
Average	*Cervus elaphus*	45,54	31,54			Grotta Romanelli	Di Stefano et al., 2015

Measurements of the d4 of *Dama*-like deer used as comparison with Algoz deer.

Specimen	**Species**	**L**	**B**	**Site**	**Reference**
MG-25770	*Metacervocerus rhenanus*	18,28	9,34	Algoz	This work
SABAP_UMB167339	*'Pseudodama' nestii*	18,4	9,6	Pantalla	Cherin et al., 2022
SABAP_UMB167356	*'Pseudodama' nestii*	20,3	8,2	Pantalla	Cherin et al., 2022
SABAP_UMB337632	*'Pseudodama' nestii*	19,5	9,4	Pantalla	Cherin et al., 2022
min	*'Pseudodama' vallonnetensis*	17,4	8,3	Untermaßfeld	Kahlke, 1997
mean	*'Pseudodama' vallonnetensis*	19,3	8,57	Untermaßfeld	Kahlke, 1998
max	*'Pseudodama' vallonnetensis*	20,4	8,9	Untermaßfeld	Kahlke, 1999

A.3 Measurements and dataset for metric comparisons of large-sized deer from Algoz.

Complete measurements of the large-sized deer from Algoz.

MG-25768.13	**Left scaphoid**							
H	**DT**	**DAP**						
35,15	22,59	42,6						
MG-25768.15	**Left magnotrapezoid**							
H	**DT**	**DAP**						
18,54	33,76	40,14						
MG-25768.14	**Left semilunate**							
H	**DTp**	**DTd**	**DAP**	**Fun**	**Fma**			
31,32	26,66	19,63	38,64	11,96	10,7			
MG-25768.9	**Right distal humerus**							
DTdf	**R1**	**R2**	**R3**	**R4**				
75,6	52,59	41,23	47,11	35,83				
MG-25768.10	**Left distal humerus**							
DTdf	**R1**	**R2**	**R3**	**R4**				

72,56	51,93	41,43	46,84	32,7				
MG-25768.11	**Partial left distal radius**							
DAPd								
51,33								
MG-25768.16	**Left distal tibia**							
DTd	**DAPd**	**Dtfast**						
60,16	46,32	39,99						
MG-25768.3	**Left astragalus fragment**							
R	**Lm**							
40,26	66,02							
MG-25768.17	**Patella**							
DT	**DAP**	**H**						
48,26	29,5	57,56						
MG-25768.6	**Left cubonavicular partial**							
DT	**DAP**	**Hcub**	**Hnav**	**Htot**	**Hant.tot**	**Dtfast**		
46,31	48,35	26,27	14,56	46,83	36,37	42,39		
MG-25768.8	**Right femur diaphysis (unfused)**							
DTdia	**DAPdia**	**Cdia**	**DTd**					
34,31	30,16	106	77					
MG-25768.5	**Left proximal ulna (Unfused)**							
DTmax	**DTn**	**(DAP)**	**DAPmax**	**DAPn**				
39,49	19,65	35,59	60,05	54				
MG-25768.7	**Right Partial scapula**							
DAPn	**DTn**	**DAPdf**	**DTdf**					
39,04	22,87	53,46	46,5					
MG-25768.4	**Partial antler**							
Circun								
103								
MG-25768.1	**Partial mandible**							
L d2-d4								
70,12								
from MG-25768.1	**d3**							
DAP	**DAPb**	**DTa**	**DTp**	**DTpp**	**Dd2**	**Wd2**		
20,89	20,91	9,6	10,28		30,03	13,22		

from MG-25768.1	**d4**							
DAP	**DAPb**	**DTa**	**DTp**	**DTpp**	**Dd3**	**Wd3**		
33,24	30,32	10,65	13,6	13,5	31,72	16,13		
from MG-25768.1	**Unerupted m1**							
DAP	**DAPb**	**DTa**	**DTp**	**DTpp**	**Dd4**	**Wd4**	**Ha**	**Hp**
30,94	26,66	19,29	17,36		35,11	19,32	26,06	26,22

Measurements and comparison of M1.

Specimen	**Species**	**DAP**	**DAPb**	**DTa**	**DTp**	**Ha**	**Hp**	**Site**	**Refer-ence**
from MG-25768.1	*Eucladoceros* sp.	30,94	26,66	19,29	17,36	26,06	26,22	Algoz	This work
TRL 90/42/1	*Eucladoceros montenegrensis*	24,1	22,2	15,3	16			Trlica	Van der Made & Dimitri-jevic, 2015
TRL 90/69/1	*Eucladoceros montenegrensis*				18,7			Trlica	Van der Made & Dimitri-jevic, 2015
TRL 88/56/1	*Eucladoceros montenegrensis*	20,9	20,9	16,1	15,9			Trlica	Van der Made & Dimitri-jevic, 2015
TRL 90/28/1	*Eucladoceros montenegrensis*	27,7	25,3	16,1	15,2	22,5		Trlica	Van der Made & Dimitri-jevic, 2015
TRL 90/82/3	*Eucladoceros montenegrensis*				18,7			Trlica	Van der Made & Dimitri-jevic, 2015
TRL 90/15/13	*Eucladoceros montenegrensis*	28,4	25,9	18,8	18,3			Trlica	Van der Made & Dimitri-jevic, 2015
TRL 90/42/2	*Eucladoceros montenegrensis*	25,9	23,1	16,2	16,2			Trlica	Van der Made & Dimitri-jevic, 2015
TRL 88/9/2	*Eucladoceros montenegrensis*	27,1	15,8	17,8	17,4	24,4		Trlica	Van der Made & Dimitri-jevic, 2015
TRL 90/53/1	*Eucladoceros montenegrensis*	28,1	26,6	17,9	18			Trlica	Van der Made & Dimitri-jevic, 2015

TRL 88/28/28	*Eucladoceros montenegrensis*	28,6	24,9	15,9	15,9			Trlica	Van der Made & Dimitri-jevic, 2015
TRL 90/36/4	*Eucladoceros montenegrensis*				17		22	Trlica	Van der Made & Dimitri-jevic, 2015
TRL 90/24/4	*Eucladoceros montenegrensis*				17,3			Trlica	Van der Made & Dimitri-jevic, 2015
TRL 90/93/4	*Eucladoceros montenegrensis*			14,8				Trlica	Van der Made & Dimitri-jevic, 2015
TRL 90/18/8	*Eucladoceros montenegrensis*	26,4		16,2	17,3			Trlica	Van der Made & Dimitri-jevic, 2015
TRL 88/23/28	*Eucladoceros montenegrensis*	26,2	23,3	14,6	14,2	20,6		Trlica	Van der Made & Dimitri-jevic, 2015
TRL 90/64/3	*Eucladoceros montenegrensis*	26,3	24,5	16,2	16,9			Trlica	Van der Made & Dimitri-jevic, 2015
TRL 01/21/15	*Eucladoceros montenegrensis*	27,7			17,4			Trlica	Van der Made & Dimitri-jevic, 2015
TRL 90/18/11	*Eucladoceros montenegrensis*	25		16,6				Trlica	Van der Made & Dimitri-jevic, 2015
TRL 88/23/27	*Eucladoceros montenegrensis*	26,2	23,2	14,2	14,3	20,5		Trlica	Van der Made & Dimitri-jevic, 2015
IVPP V 25966.15	*Eucladoceros boulei*	24,2		15,6	16,8			Shans-henmiaozui	Tong & Zhang, 2019
IVPP V 25966.11	*Eucladoceros boulei*	22,8		14,8	16,1			Shans-henmiaozui	Tong & Zhang, 2019
IVPP V 25966.16	*Eucladoceros boulei*	23		15,7	17,8			Shans-henmiaozui	Tong & Zhang, 2019
IVPP V 25966.24	*Eucladoceros boulei*	23,8		16,4	17,6			Shans-henmiaozui	Tong & Zhang, 2019
min	*Eucladoceros giulii*	20,2		13,6				Unter-massfeld	Kahlke, 1997
average	*Eucladoceros giulii*	23,74		16,08				Unter-massfeld	Kahlke, 1997

max	*Eucladoceros giulii*	26,9		17,42				Untermassfeld	Kahlke, 1997
Ty5370	*Megaloceros sardus*	19,7	19,7	13	13,9			Capo Figari	Van der Made & Palombo, 2005
Ata2002, TD8b, G-7, G-3	*Megaceroides solilhacus*	24,4						Atapuerca TD8	Van der Made et al., 2017
CV-MC-431	*Megaloceros novocarthaginiensis*	26,1	25,2	17	17,9			Cueva Victoria	Van der Made, 2015
CV-MC-423	*Megaloceros novocarthaginiensis*	25	25	16,8	16,6			Cueva Victoria	Van der Made, 2015
CV-P-257	*Megaloceros novocarthaginiensis*	28,7	26,5	16,7	17			Cueva Victoria	Van der Made, 2015
CV53	*Megaloceros novocarthaginiensis*	29,9	28	15,6	16,5			Cueva Victoria	Van der Made, 2015
CV72	*Megaloceros novocarthaginiensis*	29,2		15,5	16			Cueva Victoria	Van der Made, 2015
CEU-62/16982	*Megaloceros matritensis*	21,4						Fluvial terraces Madrid	Van der Made, 2019
AM/62-4772	*Megaloceros matritensis*	23	21,5	14,2	13,8			Fluvial terraces Madrid	Van der Made, 2019
AM/61-963	*Megaloceros matritensis*			12,2				Fluvial terraces Madrid	Van der Made, 2019
C-97 H-6	*Megaloceros matritensis*	20						Fluvial terraces Madrid	Van der Made, 2019
MNCN-5305	*Megaloceros matritensis*	17,5	17					Fluvial terraces Madrid	Van der Made, 2019
73/58/M2-1	*Megaloceros matritensis*	17,7	17,7	12,3	12,1			Fluvial terraces Madrid	Van der Made, 2019
96/79/XIII/1314/547	*Megaloceros matritensis*	20	20	12,3	11,7			Fluvial terraces Madrid	Van der Made, 2019
Bilhausen	*Megaloceros verticornis*	29		18,5				Bilhausen	Pfeiffer, 2002
Bilhausen	*Megaloceros verticornis*	29,5		19				Bilhausen	Pfeiffer, 2002
Krasnyi Yar	*Megaloceros giganteus*	28		20,5				Western Siberia	Shpansky, 2014
POIKM,no. KP 7191	*Megaloceros giganteus*	30						Western Siberia	Shpansky, 2014
MP PGPI,no. 721	*Megaloceros giganteus*	24		16,5				Western Siberia	Shpansky, 2014
Fladmosen, cat. no. 13.	*Megaloceros giganteus*	33,5		18,7				Fladmosen	Aaris-Sorensen & Liljegren, 2004

Measurements and comparison of d4.

Specimen	Species	DAP	DAPb	DTa	DTp	DTpp	Site	Reference
from MG-25768.1	*Eucladoceros* sp.	33,24	30,32	10,65	13,6	13,5	Algoz	This work

TRL 01/21/22	*Eucladoceros montenegrensis*	30,8	27,4	10,4	12,8	14,2	Trlica	Van der Made & Dimitrijevic, 2015
TRL 10/21/22	*Eucladoceros montenegrensis*	30,8	22,4	10,5	12,9	14	Trlica	Van der Made & Dimitrijevic, 2015
TRL 90/87/3	*Eucladoceros montenegrensis*	28,3	26,5	9,5	11,9	13,1	Trlica	Van der Made & Dimitrijevic, 2015
TRL 88/22/11	*Eucladoceros montenegrensis*					12,8	Trlica	Van der Made & Dimitrijevic, 2015
TRL 90/36/11	*Eucladoceros montenegrensis*	31,5		9,9	12,7		Trlica	Van der Made & Dimitrijevic, 2015
TRL 01/22/23	*Eucladoceros montenegrensis*	31,2	29,5	11,6	13,9	14,5	Trlica	Van der Made & Dimitrijevic, 2015
min	*Eucladoceros giulii*	28		12,3			Untermassfeld	Kahlke, 1997
average	*Eucladoceros giulii*	30,49		13,52			Untermassfeld	Kahlke, 1997
max	*Eucladoceros giulii*	33,4		15,1			Untermassfeld	Kahlke, 1997
IVPP V 25966.4	*Eucladoceros boulei*	27,4		9,2		12,3	Shanshenmiaozui	Tong & Zhang, 2019
IVPP V 25966.11	*Eucladoceros boulei*	27,8		12,5		13,9	Shanshenmiaozui	Tong & Zhang, 2019
IVPP V 25966.5	*Eucladoceros boulei*	28,1		11,3		13,2	Shanshenmiaozui	Tong & Zhang, 2019
IVPP V 25966.12	*Eucladoceros boulei*	27,5		10,1		13,1	Shanshenmiaozui	Tong & Zhang, 2019
IVPP V 25966.21	*Eucladoceros boulei*	30,1		11,3		13,7	Shanshenmiaozui	Tong & Zhang, 2019
IVPP V 25966.23	*Eucladoceros boulei*	26,7		10,2		12,8	Shanshenmiaozui	Tong & Zhang, 2019
IVPP V 25966.6	*Eucladoceros boulei*	27		10,8		13,3	Shanshenmiaozui	Tong & Zhang, 2019
IVPP V 25966.20	*Eucladoceros boulei*	27,9		9,9		12,57	Shanshenmiaozui	Tong & Zhang, 2019
IVPP V 25966.13	*Eucladoceros boulei*	26		10,4		13,1	Shanshenmiaozui	Tong & Zhang, 2019
IVPP V 25966.22	*Eucladoceros boulei*	24,1		8,3		10,4	Shanshenmiaozui	Tong & Zhang, 2019
CV-P-141 (P353)	*Megaloceros novocarthaginiensis*	33,4	29,5	11,9	13	14,2	Cueva Victoria	Van der Made, 2015
CV-U-13+25	*Megaloceros novocarthaginiensis*	33,1	29,4	12,7	13,1	14,7	Cueva Victoria	Van der Made, 2015

Measurements and comparison of d3.

Specimen	**Species**	**DAP**	**DAPb**	**DTa**	**DTp**	**Site**	**Reference**
from MG-25768.1	*Eucladoceros* sp.	20,89	20,91	9,6	10,28	Algoz	This work
TRL 01/22/8	*Eucladoceros montenegrensis*	17,3	16,1	8,4	10,9	Trlica	Van der Made &

							Dimitrijevic, 2015
TRL 88/61/1	*Eucladoceros montenegrensis*	19,7	17,9	7,7	9	Trlica	Van der Made & Dimitrijevic, 2015
min	*Eucladoceros giulii*	18,3		9,7		Untermassfeld	Kahlke, 1997
average	*Eucladoceros giulii*	19,73		10,58		Untermassfeld	Kahlke, 1997
max	*Eucladoceros giulii*	22,2		11,2		Untermassfeld	Kahlke, 1997
IVPP V 25966.4	*Eucladoceros boulei*	17,3		7,1	8,8	Shanshenmiaozui	Tong & Zhang, 2019
IVPP V 25966.11	*Eucladoceros boulei*	16,5		7,8	10	Shanshenmiaozui	Tong & Zhang, 2019
IVPP V 25966.5	*Eucladoceros boulei*	18,7		7,4	9,7	Shanshenmiaozui	Tong & Zhang, 2019
IVPP V 25966.12	*Eucladoceros boulei*	18,2		7,3	9,5	Shanshenmiaozui	Tong & Zhang, 2019
IVPP V 25966.21	*Eucladoceros boulei*	18,1		7,8	9,3	Shanshenmiaozui	Tong & Zhang, 2019
IVPP V 25966.23	*Eucladoceros boulei*	19,9		7,9	9,1	Shanshenmiaozui	Tong & Zhang, 2019
IVPP V 25966.20	*Eucladoceros boulei*	18,6		6,8	8	Shanshenmiaozui	Tong & Zhang, 2019
IVPP V 25966.13	*Eucladoceros boulei*	18,3		7,7	9,3	Shanshenmiaozui	Tong & Zhang, 2019
IVPP V 25966.22	*Eucladoceros boulei*	16,5		6,4	6,4	Shanshenmiaozui	Tong & Zhang, 2019
CV-P-141 (P353)	*Megaloceros novocarthaginiensis*	21,4	19,1	9,8	12,9	Cueva Victoria	Van der Made, 2015
CV-PR-198	*Megaloceros novocarthaginiensis*	20,3	19,9	8,6	10,7	Cueva Victoria	Van der Made, 2015
CV-U-16	*Megaloceros novocarthaginiensis*	21,4	20,7	9,4	10,6	Cueva Victoria	Van der Made, 2015
CV-D-59	*Megaloceros novocarthaginiensis*	21,8	21	10	11,2	Cueva Victoria	Van der Made, 2015
CV-I-158	*Megaloceros novocarthaginiensis*	21,8	20,9	10,3	11,2	Cueva Victoria	Van der Made, 2015
CV-MC-464	*Megaloceros novocarthaginiensis*	21,9	21,2	8,9	10,8	Cueva Victoria	Van der Made, 2015
P-29	*Megaloceros novocarthaginiensis*	21,1	20,3	9	10,9	Cueva Victoria	Van der Made, 2015
Sala Unión, 2008 teeth	*Megaloceros novocarthaginiensis*	21,3	19,6	8,8	10,9	Cueva Victoria	Van der Made, 2015

Measurements and comparison of mandible.

Specimen	**Species**	**L d2-d4**	**Site**	**Reference**
from MG-25768.1	*Eucladoceros* sp.	70,12	Algoz	This work
IQW1980/15507(Mei.15019)	*Eucladoceros giulii*	61,5	Untermassfeld	Kahlke, 1997
IQW1980/15517(Mei.15029)	*Eucladoceros giulii*	63,8	Untermassfeld	Kahlke, 1997

IQW1980/15723(Mei.15235)	*Eucladoceros giulii*	65	Untermassfeld	Kahlke, 1997
IQW1980/15724(Mei.15236)	*Eucladoceros giulii*	65,6	Untermassfeld	Kahlke, 1997
IQW1980/15822(Mei.15333)	*Eucladoceros giulii*	61,6	Untermassfeld	Kahlke, 1997
IQW1980/15853(Mei.15364)	*Eucladoceros giulii*	63,8	Untermassfeld	Kahlke, 1997
IQW1980/15989(Mei.15500)	*Eucladoceros giulii*	63,4	Untermassfeld	Kahlke, 1997
IQW1980/16298(Mei.15809)	*Eucladoceros giulii*	64,8	Untermassfeld	Kahlke, 1997
IQW1980/16545(Mei.16066)	*Eucladoceros giulii*	63,1	Untermassfeld	Kahlke, 1997
IQW1980/16891(Mei.16412)	*Eucladoceros giulii*	63	Untermassfeld	Kahlke, 1997
IQW1980/16977(Mei.16498)	*Eucladoceros giulii*	64	Untermassfeld	Kahlke, 1997
IQW1980/1755(Mei.16576)	*Eucladoceros giulii*	62,5	Untermassfeld	Kahlke, 1997
IQW1980/17149(Mei.16670)	*Eucladoceros giulii*	67,8	Untermassfeld	Kahlke, 1997
IQW1982/18332(Mei.17852)	*Eucladoceros giulii*	62,4	Untermassfeld	Kahlke, 1997
IQW1983/18947(Mei.18467)	*Eucladoceros giulii*	62,5	Untermassfeld	Kahlke, 1997
IQW1983/19208(Mei.18728)	*Eucladoceros giulii*	64,2	Untermassfeld	Kahlke, 1997
IQW1987/22111(Mei.21630)	*Eucladoceros giulii*	69,3	Untermassfeld	Kahlke, 1997
IQW1988/22453(Mei.21972)	*Eucladoceros giulii*	67,5	Untermassfeld	Kahlke, 1997
IVPP V 25966.4	*Eucladoceros boulei*	56,4	Shanshenmiaozui	Tong & Zhang, 2019
IVPP V 25966.11	*Eucladoceros boulei*	56,8	Shanshenmiaozui	Tong & Zhang, 2019
IVPP V 25966.5	*Eucladoceros boulei*	63,6	Shanshenmiaozui	Tong & Zhang, 2019
IVPP V 25966.12	*Eucladoceros boulei*	59,5	Shanshenmiaozui	Tong & Zhang, 2019
IVPP V 25966.21	*Eucladoceros boulei*	59,9	Shanshenmiaozui	Tong & Zhang, 2019
IVPP V 25966.23	*Eucladoceros boulei*	64,5	Shanshenmiaozui	Tong & Zhang, 2019
IVPP V 25966.22	*Eucladoceros boulei*	51,6	Shanshenmiaozui	Tong & Zhang, 2019
Fladmosen, cat. no. 13.	*Megaloceros giganteus*	71	Fladmosen	Aaris-Sorensen & Liljegren, 2004

Measurements and comparison of humerus.

Specimen	Species	DTdf	R1	R2	R3	R4	Site	Reference
MG-25768.9	*Eucladoceros* sp.	75,6	52,59	41,23	47,11	35,83	Algoz	This work
MG-25768.10	*Eucladoceros* sp.	72,56	51,93	41,43	46,84	32,7	Algoz	This work
TRL 88/52/1	*Eucladoceros monte-negrensis*	77,5	59,5	45,8	54,2	36,6	Trlica	Van der Made & Dimitrijevic, 2015
TRL 88/24/2	*Eucladoceros monte-negrensis*	72,9	58,3	42,1	48,5	34,9	Trlica	Van der Made & Dimitrijevic, 2015

IVPP V25966.26	*Eucladoceros boulei*	63	53,1			35,7	Shans-henmiaozui	Tong & Zhang, 2019
IQW 1980/15459 (Mei. 14971)	*Eucladoceros giulii*	69,3	41				Untermass-feld	Kahlke, 1997
IQW 1982/18267 (Mei. 17787)	*Eucladoceros giulii*	67	39,3				Untermass-feld	Kahlke, 1997
CV-BL1-212	*Megaloceros novocar-thaginiensis*	70,6	57,5	43,7	50,4	36,8	Cueva Victoria	Van der Made, 2015
CV-BL1-210	*Megaloceros novocar-thaginiensis*	70	60	42,8	44,2	36,4	Cueva Victoria	Van der Made, 2015
CV-P-265	*Megaloceros novocar-thaginiensis*	69	57,3	41	47,3	38,4	Cueva Victoria	Van der Made, 2015
CV-I-1689	*Megaloceros novocar-thaginiensis*	63,4	50,8	50,8	41,7	33,8	Cueva Victoria	Van der Made, 2015
CV-MC-437 (CV-2009, andamio sup. B)	*Megaloceros novocar-thaginiensis*	74,8	57,6	40,6	45,1		Cueva Victoria	Van der Made, 2015
CV-MC-442 (CV-2009, andamio sup. B)	*Megaloceros novocar-thaginiensis*	68	50,8	39,9	45,4		Cueva Victoria	Van der Made, 2015
CV-MC-463 (CV-2009, andamio sup. B)	*Megaloceros novocar-thaginiensis*	73,6	58,9	42,8	50,6	38,9	Cueva Victoria	Van der Made, 2015

Measurements and comparison of tibia.

Specimen	Species	DTd	DAPd	Site	Reference
MG-25768.16	*Eucladoceros* sp.	60,16	46,32	Algoz	This work
TRL 01/18/7	*Alces* cf. *carnutorum*	53,2		Trlica	Van der Made & Dimitri-jevic, 2015
MM1957/587	*Cervus elaphus*	48	35,5	Mosbach	Di Stefano et al., 2015
MM1954/68	*Cervus elaphus*	49	38	Mosbach	Di Stefano et al., 2015
MM1959/137	*Cervus elaphus*	48,5	38	Mosbach	Di Stefano et al., 2015
MM1961/1118	*Cervus elaphus*	60	42	Mosbach	Di Stefano et al., 2015
MM1962/1772	*Cervus elaphus*	50,5	37	Mosbach	Di Stefano et al., 2015
MM1961/201	*Cervus elaphus*	55	42,5	Mosbach	Di Stefano et al., 2015
MM1956/186	*Cervus elaphus*	50	35	Mosbach	Di Stefano et al., 2015
MM1957/357	*Cervus elaphus*	45	34	Mosbach	Di Stefano et al., 2015
MM1957/181	*Cervus elaphus*	61	47	Mosbach	Di Stefano et al., 2015
MM1954/519	*Cervus elaphus*	55	43	Mosbach	Di Stefano et al., 2015
MM1961/76	*Cervus elaphus*	55	43	Mosbach	Di Stefano et al., 2015
MM1955/377	*Cervus elaphus*	58	42	Mosbach	Di Stefano et al., 2015
I11	*Cervus elaphus*	50,5	40	Ingarano	Di Stefano et al., 2015

I12	*Cervus elaphus*	51	42	Ingarano	Di Stefano et al., 2015
I13	*Cervus elaphus*	57	42	Ingarano	Di Stefano et al., 2015
I14	*Cervus elaphus*	51	41	Ingarano	Di Stefano et al., 2015
A13	*Cervus elaphus*	51,5	41	Avetrana	Di Stefano et al., 2015
A14	*Cervus elaphus*	50	40	Avetrana	Di Stefano et al., 2015
P1065	*Cervus elaphus*	50	40	Grotta del Fossellone	Di Stefano et al., 2015
A10V75	*Cervus elaphus*	56	44,5	Riparo di Fumane	Di Stefano et al., 2015
P4235	*Cervus elaphus*	48	36	Sora - Valle Radice	Di Stefano et al., 2015
no n°	*Cervus elaphus*	41,7	34	Sora - Valle Radice	Di Stefano et al., 2015
no n°	*Cervus elaphus*	41,7	32,1	Sora - Valle Radice	Di Stefano et al., 2015
no n°	*Cervus elaphus*	40	32,6	Sora - Valle Radice	Di Stefano et al., 2015
no n°	*Cervus elaphus*	53,6	42,3	Sora - Valle Radice	Di Stefano et al., 2015
no n°	*Cervus elaphus*	42,4	35	Sora - Valle Radice	Di Stefano et al., 2015
no n°	*Cervus elaphus*	41,8	33,8	Sora - Valle Radice	Di Stefano et al., 2015
no n°	*Cervus elaphus*	43,1	33,5	Sora - Valle Radice	Di Stefano et al., 2015
no n°	*Cervus elaphus*	40,5	30,2	Sora - Valle Radice	Di Stefano et al., 2015
no n°	*Cervus elaphus*	42,6	33,5	Sora - Valle Radice	Di Stefano et al., 2015
P1765	*Cervus elaphus*	45	34	Grotta Romanelli	Di Stefano et al., 2015
P1759	*Cervus elaphus*	47	39	Grotta Romanelli	Di Stefano et al., 2015
P1766	*Cervus elaphus*	50	41	Grotta Romanelli	Di Stefano et al., 2015
P1760	*Cervus elaphus*	49	37	Grotta Romanelli	Di Stefano et al., 2015
P1764	*Cervus elaphus*	47	37	Grotta Romanelli	Di Stefano et al., 2015
P1758	*Cervus elaphus*	47	36	Grotta Romanelli	Di Stefano et al., 2015
P1762	*Cervus elaphus*	47,2	37,5	Grotta Romanelli	Di Stefano et al., 2015
no n°	*Cervus elaphus*	45,8	32,7	Grotta Romanelli	Di Stefano et al., 2015
no n°	*Cervus elaphus*	46,4	35,4	Grotta Romanelli	Di Stefano et al., 2015
no n°	*Cervus elaphus*	45,2	36,4	Grotta Romanelli	Di Stefano et al., 2015
FP1-2001-0158	*Eucladoceros* sp.	61,21	46,9	Fonelas P-1	Garrido, 2008
IQW1980/16 171(Mei. 15 682)	*Eucladoceros giulii*	63	49,4	Untermassfeld	Kahlke, 1997
IQW1980/16 204(Mei. 15 715)	*Eucladoceros giulii*	65,8	51,1	Untermassfeld	Kahlke, 1997
IQW1980/16 432(Mei. 15 943)	*Eucladoceros giulii*	69,1	52	Untermassfeld	Kahlke, 1997
IQW1986/21 690(Mei. 21 209)	*Eucladoceros giulii*	68,6	51,8	Untermassfeld	Kahlke, 1997
IQW1988/22 565(Mei. 22 084)	*Eucladoceros giulii*	65,7		Untermassfeld	Kahlke, 1997
IQW1988/22 760(Mei. 22 279)	*Eucladoceros giulii*	68,4	52,9	Untermassfeld	Kahlke, 1997
IVPPV 25966.36	*Eucladoceros boulei*	62,7	48,1	Shanshenmiaozui	Tong & Zhang, 2019
IVPP V 25966.31	*Eucladoceros boulei*	63,2	49,3	Shanshenmiaozui	Tong & Zhang, 2019
45336	*Eucladoceros cf. dicranios*	48,8	41,1	Leu	Croitor & Aurelian, 2011
21575	*Eucladoceros ctenoides*	47,2	37,3	Sénèze	Croitor & Aurelian, 2011

210660	*Eucladoceros ctenoides*	51,2	40,8	Sénèze	Croitor & Aurelian, 2011
211040	*Eucladoceros ctenoides*	50,8	41,3	Sénèze	Croitor & Aurelian, 2011
211099	*Eucladoceros ctenoides*	47	37,3	Sénèze	Croitor & Aurelian, 2011
1922-3	*Eucladoceros ctenoides*	55,4	40	Sénèze	Croitor & Aurelian, 2011
1903-4	*Eucladoceros ctenoides*	48,2	36,7	Sénèze	Croitor & Aurelian, 2011
1923-4	*Eucladoceros ctenoides*	50	37	Sénèze	Croitor & Aurelian, 2011
1922-5	*Eucladoceros ctenoides*	50,6	44	Sénèze	Croitor & Aurelian, 2011
1922-3	*Eucladoceros ctenoides*	48	39,4	Sénèze	Croitor & Aurelian, 2011
no nº	*Eucladoceros ctenoides*	51,8	40,5	Sénèze	Croitor & Aurelian, 2011
no nº	*Eucladoceros ctenoides*	51,8	42,1	Sénèze	Croitor & Aurelian, 2011
96128dx	*Eucladoceros ctenoides*	60,1	49,3	Sénèze	Croitor & Aurelian, 2011
96128sin	*Eucladoceros ctenoides*	59,8	47,8	Sénèze	Croitor & Aurelian, 2011
96131dx	*Eucladoceros ctenoides*	50,5	40,3	Sénèze	Croitor & Aurelian, 2011
96131sin	*Eucladoceros ctenoides*	51,4	41,8	Sénèze	Croitor & Aurelian, 2011
v9c2	*Eucladoceros ctenoides*	57,5	47	Upper Valdarno	Croitor & Aurelian, 2011
IGF1289	*Eucladoceros ctenoides*	61,8	46,5	Upper Valdarno	Croitor & Aurelian, 2011
IGF31V	*Eucladoceros ctenoides*	60,8	47,7	Upper Valdarno	Croitor & Aurelian, 2011
IGF395	*Eucladoceros ctenoides*	59,2	46,7	Upper Valdarno	Croitor & Aurelian, 2011
IGF3269	*Eucladoceros ctenoides*	59,2	48,5	Upper Valdarno	Croitor & Aurelian, 2011
IGF460	*Eucladoceros ctenoides*	59,8	49,4	Upper Valdarno	Croitor & Aurelian, 2011
IGF	*Eucladoceros ctenoides*	50,9	42,4	Upper Valdarno	Croitor & Aurelian, 2011
IGF462	*Eucladoceros ctenoides*	55,8	42,5	Upper Valdarno	Croitor & Aurelian, 2011
TSR H23-2	*Praemegaceros* sp.	74,09	53,73	Tsiotra Vryssi (Mygdonia Basin)	Kokotini, 2020
Bilshausen	*Megaloceros verticomis*	78,5		Bilshausen	Pfeiffer, 2002
Lysmosen, cat. no. 2.	*Megaloceros giganteus*	92		Lysmosen	Aaris-Sørensen & Liljegren, 2004
POIKM,no. KP 7191	*Megaloceros giganteus*	85	61	Western Siberia	Shpansky, 2014
CV-B1-64	*Megaloceros novocarthaginiensis*	67,5	54,1	Cueva Victoria	Van der Made, 2015
2006, no number	*Megaloceros novocarthaginiensis*	70	51,3	Cueva Victoria	Van der Made, 2015
Sárbogárd	*Eucladoceros tetraceros*	47,5		Sárbogárd	Vörös, 1993

Measurements and comparison of femur.

Specimen	Species	DTdia	Site	Reference
MG-25768.8	*Eucladoceros* sp.	34,31	Algoz	This work
Fladmosen, cat. no. 13.	*Megaloceros giganteus*	47	Fladmosen	Aaris-Sorensen & Liljegren, 2004
IQW1988/22 754(Mei. 22 273)	*Eucladoceros giulii*	38,8	Untermassfeld	Kahlke, 1997
Bilhausen	*Megaloceros verticornis*	42,5	Bilhausen	Pfeiffer, 2002

Measurements and comparison of radius.

Specimen	Species	DAPd	Site	Reference
MG-25768.8	*Eucladoceros* sp.	51,33	Algoz	This work
Sárbogárd	*Eucladoceros tetraceros*	36	Sárbogárd	Vörös, 1993
IQW1980/17 206(Mei. 16 728)	*Eucladoceros giulii*	53	Untermassfeld	Kahlke, 1997
IQW1982/18 020(Mei. 17 540)	*Eucladoceros giulii*	53	Untermassfeld	Kahlke, 1997
IQW 1982/18 268 1982/18 335(Mei. 17 788) (Mei. 17 855)	*Eucladoceros giulii*	47,3	Untermassfeld	Kahlke, 1997
IQW1985/20 560(Mei. 20 079)	*Eucladoceros giulii*	53	Untermassfeld	Kahlke, 1997
IQW 1985/20 835 (Mei. 20 354)	*Eucladoceros giulii*	48	Untermassfeld	Kahlke, 1997
IQW 1986/21 338 (Mei. 20 857)	*Eucladoceros giulii*	53,3	Untermassfeld	Kahlke, 1997
IQW 1986/21 340 (Mei. 20 859)	*Eucladoceros giulii*	55	Untermassfeld	Kahlke, 1997
IQW 1987/22 169 (Mei. 21 668)	*Eucladoceros giulii*	50	Untermassfeld	Kahlke, 1997
ZPALUWr/B/W/97/1703	*Megaloceros giganteus*	68,4	Bisnik Cave	Croitor et al., 2013
Schlutup, Germany	*Megaloceros giganteus*	96,2	Schlutup, Germany	Croitor et al., 2013
Ireland, NHMB, no number	*Megaloceros giganteus*	69	Ireland	Croitor et al., 2013
Ireland, NHMB, no number,	*Megaloceros giganteus*	71	Ireland	Croitor et al., 2013
NMNH, 1856-25	*Megaloceros giganteus*	83,5	Ireland	Croitor et al., 2013
NMNH, 8-VI-80	*Megaloceros giganteus*	68,8	Ireland	Croitor et al., 2013
MNHUW, no number	*Megaloceros giganteus*	82,6	Ireland	Croitor et al., 2013
MNHUW, no number	*Megaloceros giganteus*	81,9	Ireland	Croitor et al., 2013
MNHUW, no number	*Megaloceros giganteus*	93,8	Ireland	Croitor et al., 2013

Measurements and comparison of scapula.

Specimen	Species	DAPn (SLC)	DTn	DAPpf (LG)	DTpf (BG)	Site	Reference
MG-25768.7	*Eucladoceros* sp.	39,04	22,87	53,46	46,5	Algoz	This work
Fladmosen, cat. no. 13.	*Megaloceros giganteus*				69	Fladmosen	Aaris-Sorensen & Liljegren, 2004
IQW 1980/15 766 (Mei. 15 278)	*Eucladoceros giulii*	44,5		57,8	54,2	Untermassfeld	Kahlke, 1997
IQW 1980/15 767 (Mei. 15 279)	*Eucladoceros giulii*	50		61,5	53,5	Untermassfeld	Kahlke, 1997
IQW 1980/16 567 (Mei. 16 088)	*Eucladoceros giulii*	46,5		60,6	54	Untermassfeld	Kahlke, 1997

IQW 1980/17 071 (Mei. 16 592)	*Eucladoceros giulii*	49,6		60,1	51,2	Untermassfeld	Kahlke, 1997
IQW 1982/17 929 (Mei. 17 449)	*Eucladoceros giulii*	51,5		64	57,4	Untermassfeld	Kahlke, 1997
IQW 1983/19 139 (Mei. 18 659)	*Eucladoceros giulii*	48,3		58,3	51,5	Untermassfeld	Kahlke, 1997
IQW 1985/20 652 (Mei. 20 171)	*Eucladoceros giulii*	40,5		62	54	Untermassfeld	Kahlke, 1997
IQW 1985/20 836 (Mei. 20 355)	*Eucladoceros giulii*	52		62,6	53,3	Untermassfeld	Kahlke, 1997
IQW 1985/20 845 (Mei. 20 364)	*Eucladoceros giulii*	51,5		63,8	58,7	Untermassfeld	Kahlke, 1997
IVPP V25966.25	*Eucladoceros boulei*	40		51,9	50,7	Shans-henmiaozui	Tong & Zhang, 2019
Ata04, TD8b, G-5, 4	*Cervus elaphus*	43,8		47,4		Atapuerca TD8	Van der Made et al., 2017
U-22	*Megaloceros novocarthaginiensis*	51,6	29,2	58,6	52,6	Cueva Victoria	Van der Made, 2015
B1-13	*Megaloceros novocarthaginiensis*	58,4	30	70,6	63,3	Cueva Victoria	Van der Made, 2015
P-159	*Megaloceros novocarthaginiensis*	52,1	27,2	62		Cueva Victoria	Van der Made, 2015
C-75, V-5 (3-V-60)	*Megaloceros matritensis*	42,5	21,1	48,3	42,3	Fluvial terraces Madrid	Van der Made, 2019
Bilhausen	*Megaloceros verticornis*			72,5	61,5	Bilhausen	Pfeiffer, 2002
POIKM,no. KP 7191	*Megaloceros giganteus*	69,5		73,6	69,5	Western Siberia	Shpansky, 2014

Measurements and comparison of scaphoid.

Specimen	Species	H	DT	DAP	Site	Reference
MG-25768.13	*Eucladoceros* sp.	35,15	22,59	42,6	Algoz	This work
min	*Eucladoceros giulii*	32,7	21	40,8	Untermassfeld	Kahlke, 1997
mean	*Eucladoceros giulii*	35,36	24,89	44,3	Untermassfeld	Kahlke, 1997
max	*Eucladoceros giulii*	39,3	28	51,9	Untermassfeld	Kahlke, 1997
Ata03, TD8b, G-5, 58	*Megaceroides* or *Eucladoceros*	32	28,9	45,8	Atapuerca TD8	Van der Made et al., 2017
CEU-62/16982	*Megaloceros matritensis*	29,9	20,9	39,9	Fluvial terraces Madrid	Van der Made, 2019

A.4 Measurements and dataset for metric comparisons of arvicoline rodents from Santa Margarida.

Measurements of arvicoline m1s from Santa Margarida.

	NOVA-FCT-DCT-5383	NOVA-FCT-DCT-5384	NOVA-FCT-DCT-5385 (1)	NOVA-FCT-DCT-5385 (2)	NOVA-FCT-DCT-5386
	Victoriamys chalinei	*Iberomys huescarensis*	*Iberomys brecciensis*	*Iberomys brecciensis*	*Iberomys brecciensis*
L	2,70	2,96	2,52	2,33	
W	1,00	1,04	1,05	0,97	0,96
TTC	1,45	1,43	1,21	1,06	
ACC	1,29	1,51	1,35	1,22	1,42
a	1,29	1,51	1,35	1,22	1,42
c	0,26	0,27	0,13	0,06	0,04
La	0,38	0,41	0,38	0,42	0,30
Li	0,49	0,66	0,69	0,58	0,69
A/L	0,48	0,51	0,54	0,52	
C/W	0,26	0,26	0,12	0,06	0,05
La/Li	0,77	0,62	0,55	0,71	0,44
A/L x100	47,61	51,18	53,62	52,49	
C/Wx100	25,90	26,03	12,29	5,76	4,50
La/Lix100	77,08	61,95	55,33	71,40	44,19

Measurements of arvicoline M3s from Santa Margarida.

Specimen	Morph	L	W	Work
NOVA-FCT-DCT-5387 (1.3)	Santa Margarida Morph 2	2,46	1,31	This work
NOVA-FCT-DCT-5388 (1.5)	Santa Margarida Morph 2	2,16	1,04	This work
NOVA-FCT-DCT-5389 (1.6)	Santa Margarida Morph 1	2,28	1,06	This work
NOVA-FCT-DCT-5390 (2.1)	Santa Margarida Morph 1	2,05	0,92	This work
NOVA-FCT-DCT-5391 (2.2)	Santa Margarida Morph 1	1,55	0,93	This work
NOVA-FCT-DCT-5392 (2.6)	Santa Margarida Morph 2	2,08	1,09	This work

Comparison of L vs W of *Iberomys* incomplete m1 from Santa Margarida.

Specimen	Species	L (wihtout posterior lobe)	W	Work
NOVA-FCT-DCT-5386	*Iberomys brecciensis*	2,25	0,96	This work
CAL/P11/F1oeste/Fb	*Iberomys cabrerae*	2,52	1,38	López-García et al., 2020
CAL/P12/F13/Fc	*Iberomys cabrerae*	2,78	1,29	López-García et al., 2020
CAL/P12/H5/I	*Iberomys cabrerae*	2,86	1,53	López-García et al., 2020
CAL/P12/I4/I	*Iberomys cabrerae*	3,04	1,65	López-García et al., 2020

CAL/P13/F11/Fc	*Iberomys cabrerae*	3,12	1,49	López-García et al., 2020
CAL/P14/J14/Jb	*Iberomys cabrerae*	2,92	1,40	López-García et al., 2020
CAL/N3/F2(2)/Eb	*Iberomys cabrerae*	3,47	1,66	López-García et al., 2020
CAL/P12/H2/I	*Iberomys cabrerae*	2,91	1,45	López-García et al., 2020
CAL/P12/K1/K	*Iberomys cabrerae*	2,83	1,39	López-García et al., 2020
CAL/P13/F8/Fc	*Iberomys cabrerae*	2,90	1,37	López-García et al., 2020
CAL/P11/H3/Fc	*Iberomys cabrerae*	3,06	1,60	López-García et al., 2020
CAL/O15/E2/Eb	*Iberomys cabrerae*	2,91	1,35	López-García et al., 2020
CAL/P15/F12/Fc	*Iberomys cabrerae*	2,87	1,44	López-García et al., 2020
CAL/P12/J5/Ja	*Iberomys cabrerae*	2,99	1,35	López-García et al., 2020
CAL/P11/I8/I	*Iberomys cabrerae*	3,09	1,40	López-García et al., 2020
Spessa	*I.* ex. gr. *huescarensis-brecciensis*	2,23	1,09	López-García et al., 2015
Isernia	*Iberomys brecciensis*	1,90	0,98	López-García et al., 2015
Valdemino 1	*Iberomys brecciensis*	2,31	1,04	López-García et al., 2015
Valdemino 2	*Iberomys brecciensis*	2,15	1,02	López-García et al., 2015
Valdemino 3	*Iberomys brecciensis*	1,99	0,97	López-García et al., 2015
Montagnola Senese II 1	*Iberomys brecciensis*	2,38	1,14	López-García et al., 2015
Montagnola Senese II 2	*Iberomys brecciensis*	2,23	1,08	López-García et al., 2015
Montagnola Senese II 3	*Iberomys brecciensis*	2,30	1,10	López-García et al., 2015
Montagnola Senese II 4	*Iberomys brecciensis*	2,20	1,16	López-García et al., 2015
Paglicci	*Iberomys brecciensis*	2,55	1,36	López-García et al., 2015

Comparison of L vs W of *Iberomys* m1s from Santa Margarida.

Specimen	Species	L	W	Work
NOVA-FCT-DCT-5384	*Iberomys huescarensis*	2,96	1,04	This work
NOVA-FCT-DCT-5385 (1)	*Iberomys brecciensis*	2,52	1,05	This work
NOVA-FCT-DCT-5385 (2)	*Iberomys brecciensis*	2,33	0,97	This work
CAL_P11_F11oeste_Fb_1	*Iberomys cabrerae*	3,05	1,26	López-García et al., 2020
CAL_P11_H3_Fc_2	*Iberomys cabrerae*	3,84	1,53	López-García et al., 2020
CAL_P11_I8_I_3	*Iberomys cabrerae*	3,80	1,29	López-García et al., 2020
CAL_P12_F13_Fc_4	*Iberomys cabrerae*	3,40	1,26	López-García et al., 2020
CAL_P12_F15_Fc_5	*Iberomys cabrerae*	3,41	1,33	López-García et al., 2020
CAL_P12_H5_I_6	*Iberomys cabrerae*	3,43	1,50	López-García et al., 2020
CAL_P12_H2_I_7	*Iberomys cabrerae*	3,48	1,38	López-García et al., 2020
CAL_P12_I4_I_8	*Iberomys cabrerae*	3,56	1,49	López-García et al., 2020
CAL_P12_K1_K_9	*Iberomys cabrerae*	3,47	1,41	López-García et al., 2020
CAL_P12_J5_Ja_10	*Iberomys cabrerae*	3,62	1,39	López-García et al., 2020
CAL_P13_F8_Fc_11	*Iberomys cabrerae*	3,39	1,27	López-García et al., 2020
CAL_P13_F10_Fc_12	*Iberomys cabrerae*	3,46	1,32	López-García et al., 2020
CAL_P13_F11_Fc_13	*Iberomys cabrerae*	3,54	1,34	López-García et al., 2020
CAL_P14_J5_Jb_14	*Iberomys cabrerae*	3,48	1,30	López-García et al., 2020
CAL_O15_E2_Eb_15	*Iberomys cabrerae*	3,25	1,22	López-García et al., 2020
CAL_L15_E1(1)_Eb_16	*Iberomys cabrerae*	3,22	1,29	López-García et al., 2020

CAL_N3_E2(2)_Eb_17	*Iberomys cabrerae*	3,98	1,54	López-García et al., 2020
ARO_Xc_1	*Iberomys brecciensis* Aroeira	2,82	0,90	López-García et al., 2020
ARO_Xc_2	*Iberomys brecciensis* Aroeira	2,76	1,17	López-García et al., 2020
ARO_Xc_3	*Iberomys brecciensis* Aroeira	2,88	0,96	López-García et al., 2020
ARO_Xc_4	*Iberomys brecciensis* Aroeira	2,43	1,03	López-García et al., 2020
ARO_Xc_5	*Iberomys brecciensis* Aroeira	2,88	0,93	López-García et al., 2020
ARO_Xc_6	*Iberomys brecciensis* Aroeira	2,90	0,95	López-García et al., 2020
ARO_Xc_7	*Iberomys brecciensis* Aroeira	2,82	0,95	López-García et al., 2020
Spessa	*I.* ex. gr. *huescarensis-brecciensis*	2,71	1,09	López-García et al., 2015
Isernia	*Iberomys brecciensis* Italy	2,40	0,98	López-García et al., 2015
Valdemino 1	*Iberomys brecciensis* Italy	2,92	1,04	López-García et al., 2015
Valdemino 2	*Iberomys brecciensis* Italy	2,71	1,02	López-García et al., 2015
Valdemino 3	*Iberomys brecciensis* Italy	2,54	0,97	López-García et al., 2015
Montagnola Senese II 1	*Iberomys brecciensis* Italy	2,94	1,14	López-García et al., 2015
Montagnola Senese II 2	*Iberomys brecciensis* Italy	2,82	1,08	López-García et al., 2015
Montagnola Senese II 3	*Iberomys brecciensis* Italy	2,92	1,10	López-García et al., 2015
Montagnola Senese II 4	*Iberomys brecciensis* Italy	2,78	1,16	López-García et al., 2015
Paglicci	*Iberomys brecciensis* Italy	3,16	1,36	López-García et al., 2015
Iberomys huescarensis el Chaparral max	*Iberomys huescarensis*	2,94	0,98	López-García et al., 2012
Iberomys huescarensis el Chaparral average	*Iberomys huescarensis*	2,76	0,92	López-García et al., 2012
Iberomys huescarensis el Chaparral min	*Iberomys huescarensis*	2,56	0,84	López-García et al., 2012

Comparison of L vs W of *Victoriamys* m1 from Santa Margarida.

Specimen	**Species**	**L**	**W**	**Work**
NOVA-FCT-DCT-5383	*Victoriamys chalinei*	2,70	1,00	This work
NOVA-FCT-DCT-5384	*Iberomys huescarensis*	2,96	1,04	This work
Spessa	*I.* ex. gr. *huescarensis-brecciensis*	2,71	1,09	López-García et al., 2015
Iberomys huescarensis el Chaparral max	*Iberomys huescarensis*	2,94	0,98	López-García et al., 2012
Iberomys huescarensis el Chaparral average	*Iberomys huescarensis*	2,76	0,92	López-García et al., 2012
Iberomys huescarensis el Chaparral min	*Iberomys huescarensis*	2,56	0,84	López-García et al., 2012
El Chaparral *Allophaiomys lavocati*	*Allophaiomys lavocati*	2,77	0,92	López-García et al., 2012
El Chaparral *Allophaiomys lavocati* max	*Allophaiomys lavocati*	3,11	1,03	López-García et al., 2012
El Chaparral *Allophaiomys lavocati* min	*Allophaiomys lavocati*	2,53	0,77	López-García et al., 2012
El Chaparral *Victoriamys chalinei*	*Victoriamys chalinei* El Chaparral	2,88	0,99	López-García et al., 2012
El Chaparral *Victoriamys chalinei* max	*Victoriamys chalinei* El Chaparral	3,10	1,36	López-García et al., 2012

El Chaparral *Victoriamys chalinei* min	*Victoriamys chalinei* El Chaparral	2,55	0,84	López-García et al., 2012
Cueva Victoria *Victoriamys chalinei*	*Victoriamys chalinei* Cueva Victoria	3,09	1,28	Martin, 2012
Cueva Victoria *Victoriamys chalinei* max	*Victoriamys chalinei* Cueva Victoria	3,40	1,54	Martin, 2012
Cueva Victoria *Victoriamys chalinei* min	*Victoriamys chalinei* Cueva Victoria	2,61	1,14	Martin, 2012

Comparison of A/L vs C/W ratios of arvicoline m1s from Santa Margarida.

Specimen	Species	A/L x100	C/Wx100	Work
NOVA-FCT-DCT-5383	*Victoriamys chalinei*	47,61	25,90	This work
NOVA-FCT-DCT-5384	*Iberomys huescarensis*	51,18	26,03	This work
NOVA-FCT-DCT-5385 (1)	*Iberomys brecciensis*	53,62	12,29	This work
NOVA-FCT-DCT-5385 (2)	*Iberomys brecciensis*	52,49	5,76	This work
Vallparadis min	*Iberomys huescarensis* Vallparadis	44,20	7,00	López-García et al., 2015
Vallparadis	*Iberomys huescarensis* Vallparadis	50,00	19,10	López-García et al., 2015
Vallparadis max	*Iberomys huescarensis* Vallparadis	52,60	28,00	López-García et al., 2015
TD 3-4 min	*Iberomys huescarensis* TD 3-4	46,90	11,70	López-García et al., 2015
TD 3-4	*Iberomys huescarensis* TD 3-4	55,80	18,20	López-García et al., 2015
TD 3-4 max	*Iberomys huescarensis* TD 3-4	53,10	29,00	López-García et al., 2015
El Chaparral min	*Iberomys huescarensis* El Chaparral	47,60	8,30	López-García et al., 2012
El Chaparral	*Iberomys huescarensis* El Chaparral	51,00	16,20	López-García et al., 2012
El Chaparral max	*Iberomys huescarensis* El Chaparral	53,10	28,10	López-García et al., 2012
Riffredo	*Iberomys huescarensis* Riffredo	51,30	14,20	López-García et al., 2015
Spessa	*Iberomys huescarensis* Spessa	50,90	11,30	López-García et al., 2015
El Chaparral *Allophaiomys lavocati*	*Allophaiomys lavocati*	49,56	22,20	López-García et al., 2012
El Chaparral *Allophaiomys lavocati* max	*Allophaiomys lavocati*	52,77	54,56	López-García et al., 2012
El Chaparral *Allophaiomys lavocati* min	*Allophaiomys lavocati*	43,86	12,62	López-García et al., 2012
El Chaparral *Victoriamys chalinei*	*Victoriamys chalinei*	45,32	20,44	López-García et al., 2012
El Chaparral *Victoriamys chalinei* max	*Victoriamys chalinei*	49,48	28,57	López-García et al., 2012
El Chaparral *Victoriamys chalinei* min	*Victoriamys chalinei*	34,03	12,17	López-García et al., 2012

Comparison of A/L vs La/Li ratios of arvicoline m1s from Santa Margarida.

Specimen	Species	A/L x100	La/Li x100	Work
NOVA-FCT-DCT-5383	*Victoriamys chalinei*	47,61	77,08	This work
NOVA-FCT-DCT-5384	*Iberomys huescarensis*	51,18	61,95	This work
NOVA-FCT-DCT-5385 (1)	*Iberomys brecciensis*	53,62	55,33	This work
NOVA-FCT-DCT-5385 (2)	*Iberomys brecciensis*	52,49	71,40	This work
El Chaparral *Allophaiomys lavocati*	*Allophaiomys lavocati*	49,56	68,79	López-García et al., 2012

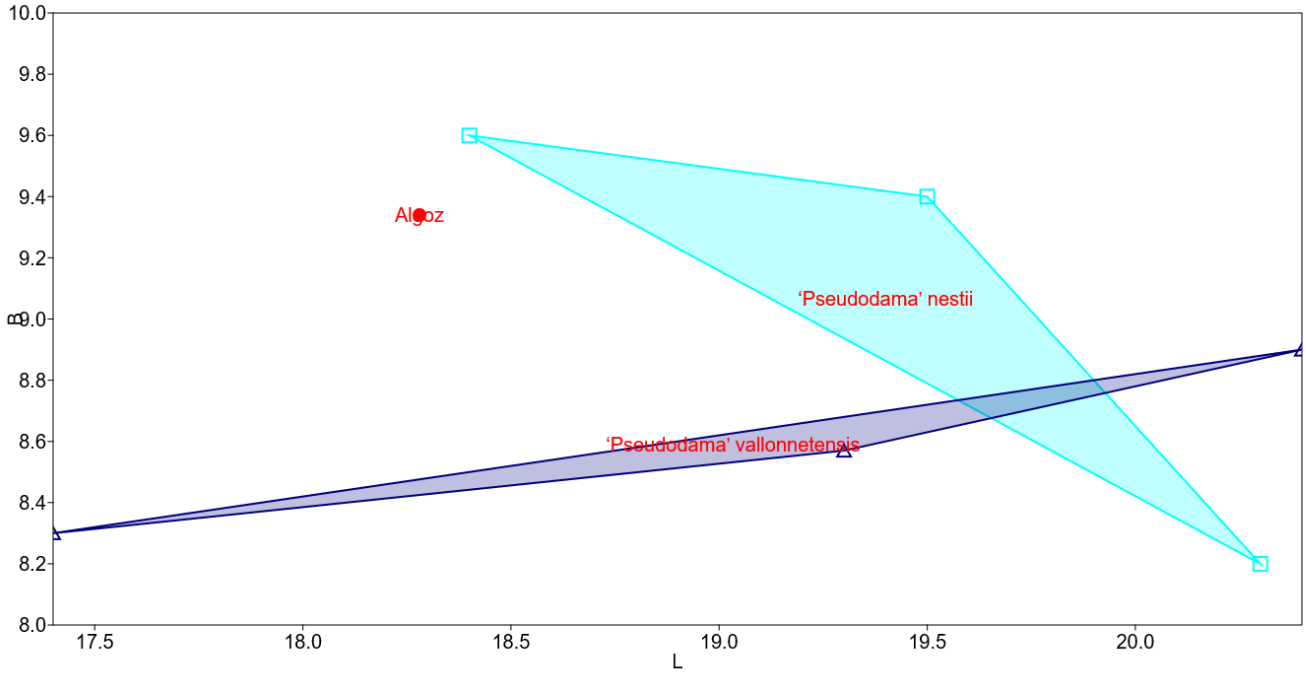
El Chaparral *Allophaiomys lavocati* max	*Allophaiomys lavocati*	52,77	84,31	López-García et al., 2012
El Chaparral *Allophaiomys lavocati* min	*Allophaiomys lavocati*	43,86	51,67	López-García et al., 2012
El Chaparral *Victoriamys chalinei*	*Victoriamys chalinei*	45,32	80,91	López-García et al., 2012
El Chaparral *Victoriamys chalinei* max	*Victoriamys chalinei*	49,48	130,30	López-García et al., 2012
El Chaparral *Victoriamys chalinei* min	*Victoriamys chalinei*	34,03	56,06	López-García et al., 2012
Vallparadis min	*Iberomys huescarensis*	44,20	30,00	López-García et al., 2015
Vallparadis	*Iberomys huescarensis*	50,00	55,10	López-García et al., 2015
Vallparadis max	*Iberomys huescarensis*	52,60	74,00	López-García et al., 2015
TD 3-4 min	*Iberomys huescarensis*	46,90	30,30	López-García et al., 2015
TD 3-4	*Iberomys huescarensis*	55,80	54,30	López-García et al., 2015
TD 3-4 max	*Iberomys huescarensis*	53,10	70,70	López-García et al., 2015
Chaparral min	*Iberomys huescarensis*	47,60	16,30	López-García et al., 2015
Chaparral	*Iberomys huescarensis*	51,00	21,10	López-García et al., 2015
Chaparral max	*Iberomys huescarensis*	53,10	26,20	López-García et al., 2015
Riffredo	*Iberomys huescarensis*	51,30	48,50	López-García et al., 2015
Spessa	*Iberomys huescarensis*	50,90	42,30	López-García et al., 2015
TEUU min	*Iberomys brecciensis*	51,90	32,50	López-García et al., 2015
TEUU	*Iberomys brecciensis*	54,10	56,70	López-García et al., 2015
TEUU max	*Iberomys brecciensis*	57,40	45,70	López-García et al., 2015
Paglicci	*Iberomys brecciensis*	51,40	35,00	López-García et al., 2015
M. Senese II min	*Iberomys brecciensis*	49,10	35,50	López-García et al., 2015
M. Senese II	*Iberomys brecciensis*	51,90	41,80	López-García et al., 2015
M. Senese II max	*Iberomys brecciensis*	54,70	46,70	López-García et al., 2015
Isernia	*Iberomys brecciensis*	49,20	34,30	López-García et al., 2015
Valdermino min	*Iberomys brecciensis*	47,80	29,70	López-García et al., 2015
Valdermino	*Iberomys brecciensis*	52,00	36,80	López-García et al., 2015
Valdermino max	*Iberomys brecciensis*	55,70	48,50	López-García et al., 2015
Galeria min	*Iberomys brecciensis*	53,70	28,40	López-García et al., 2015
Galeria	*Iberomys brecciensis*	55,50	48,20	López-García et al., 2015
Galeria max	*Iberomys brecciensis*	57,10	53,90	López-García et al., 2015
TD 10 min	*Iberomys brecciensis*	48,60	28,40	López-García et al., 2015
TD 10	*Iberomys brecciensis*	53,30	42,70	López-García et al., 2015
TD 10 max	*Iberomys brecciensis*	59,50	58,20	López-García et al., 2015
C. Gegant min	*Iberomys cabrerae*	36,20	49,90	López-García et al., 2015
C. Gegant	*Iberomys cabrerae*	46,70	54,80	López-García et al., 2015
C. Gegant max	*Iberomys cabrerae*	64,70	56,60	López-García et al., 2015
A. Romani min	*Iberomys cabrerae*	36,40	53,00	López-García et al., 2015
A. Romani	*Iberomys cabrerae*	45,90	56,30	López-García et al., 2015
A. Romani max	*Iberomys cabrerae*	56,30	60,10	López-García et al., 2015
Gorham´s min	*Iberomys cabrerae*	27,70	52,60	López-García et al., 2015
Gorham´s	*Iberomys cabrerae*	38,60	55,10	López-García et al., 2015
Gorham´s max	*Iberomys cabrerae*	46,90	57,40	López-García et al., 2015
El Portalón min	*Iberomys cabrerae*	51,00	48,00	López-García et al., 2015
El Portalón	*Iberomys cabrerae*	59,60	53,20	López-García et al., 2015
El Portalón max	*Iberomys cabrerae*	65,00	58,00	López-García et al., 2015

MTV-Chimeneas min	*Iberomys cabrerae*	44,40	34,60	López-García et al., 2015
MTV-Chimeneas	*Iberomys cabrerae*	61,80	47,10	López-García et al., 2015
MTV-Chimeneas max	*Iberomys cabrerae*	88,60	57,00	López-García et al., 2015
Current MNCNM min	*Iberomys cabrerae*	47,50	50,60	López-García et al., 2015
Current MNCNM	*Iberomys cabrerae*	59,20	52,60	López-García et al., 2015
Current MNCNM max	*Iberomys cabrerae*	88,60	60,10	López-García et al., 2015

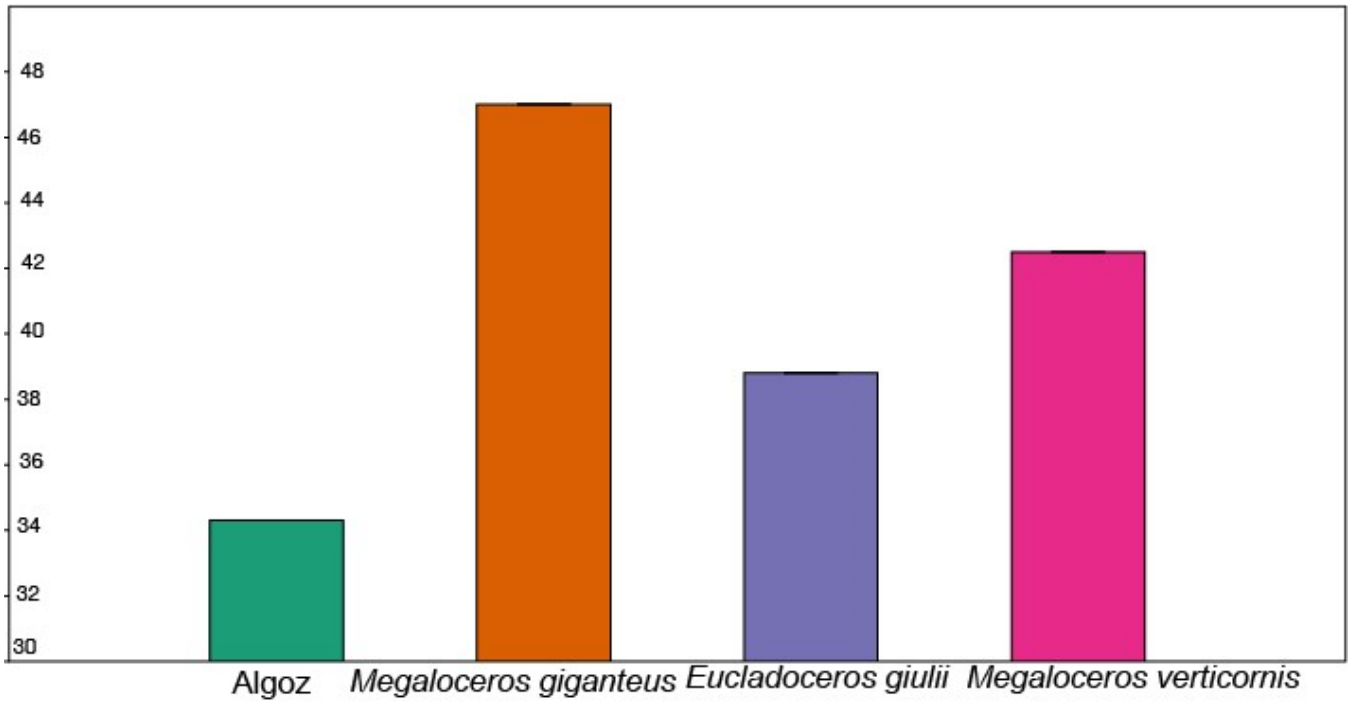
Comparison of A/L vs La/Li vs C/W ratios of arvicoline m1s from Santa Margarida.

Specimen	**Species**	**A/L x100**	**La/Li x100**	**C/Wx100**	**Work**
NOVA-FCT-DCT-5383	*Victoriamys chalinei*	47,61	77,08	25,90	This work
NOVA-FCT-DCT-5384	*Iberomys huescarensis*	51,18	61,95	26,03	This work
El Chaparral *Allophaiomys lavocati*	*Allophaiomys lavocati*	49,56	68,79	22,20	López-García et al., 2012
El Chaparral *Allophaiomys lavocati* max	*Allophaiomys lavocati*	52,77	84,31	54,56	López-García et al., 2012
El Chaparral *Allophaiomys lavocati* min	*Allophaiomys lavocati*	43,86	51,67	12,62	López-García et al., 2012
El Chaparral *Victoriamys chalinei*	*Victoriamys chalinei*	45,32	80,91	20,44	López-García et al., 2012
El Chaparral *Victoriamys chalinei* max	*Victoriamys chalinei*	49,48	130,30	28,57	López-García et al., 2012
El Chaparral *Victoriamys chalinei* min	*Victoriamys chalinei*	34,03	56,06	12,17	López-García et al., 2012
El Chaparral *Iberomys huescarensis*	*Iberomys huescarensis*	51,04	21,08	16,23	López-García et al., 2012
El Chaparral *Iberomys huescarensis* max	*Iberomys huescarensis*	53,10	26,22	28,09	López-García et al., 2012
El Chaparral *Iberomys huescarensis* min	*Iberomys huescarensis*	47,59	16,32	8,33	López-García et al., 2012

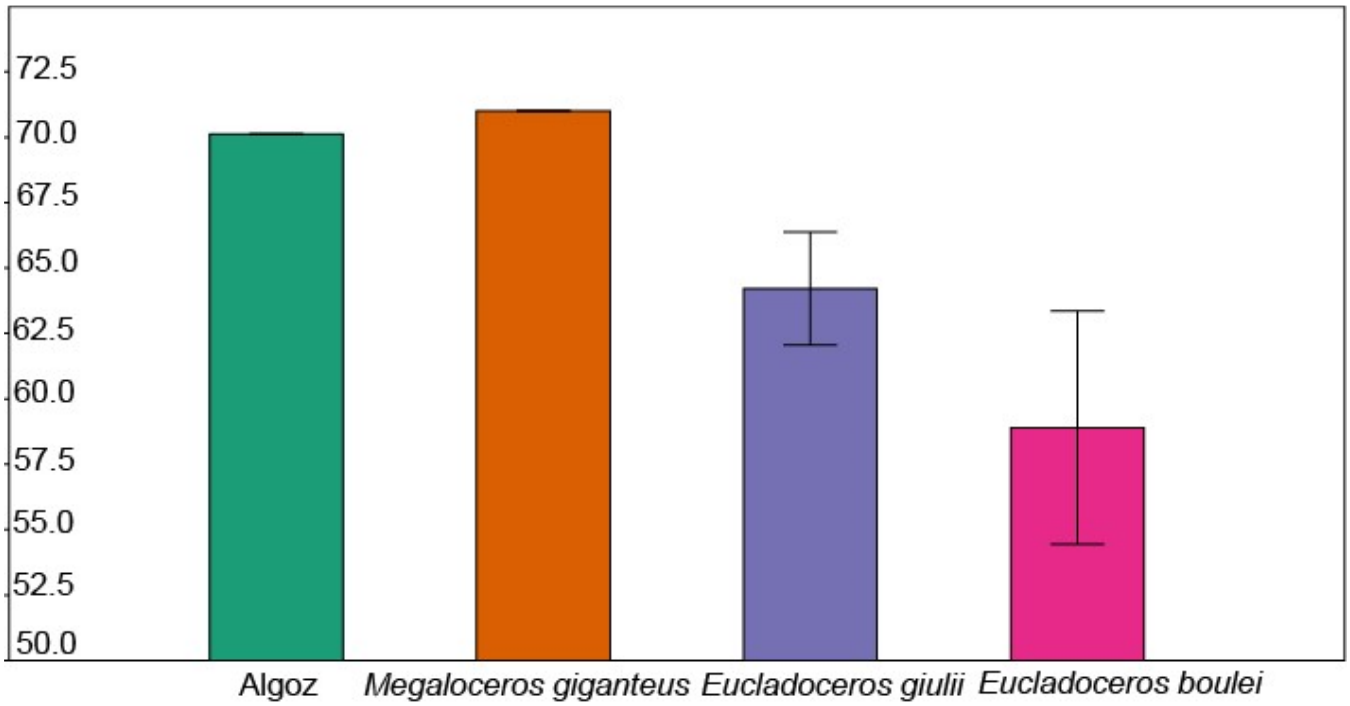
A.5 Supplementary figures about metric comparisons of Algoz cervids and image of leporid metatarsals from Algoz.



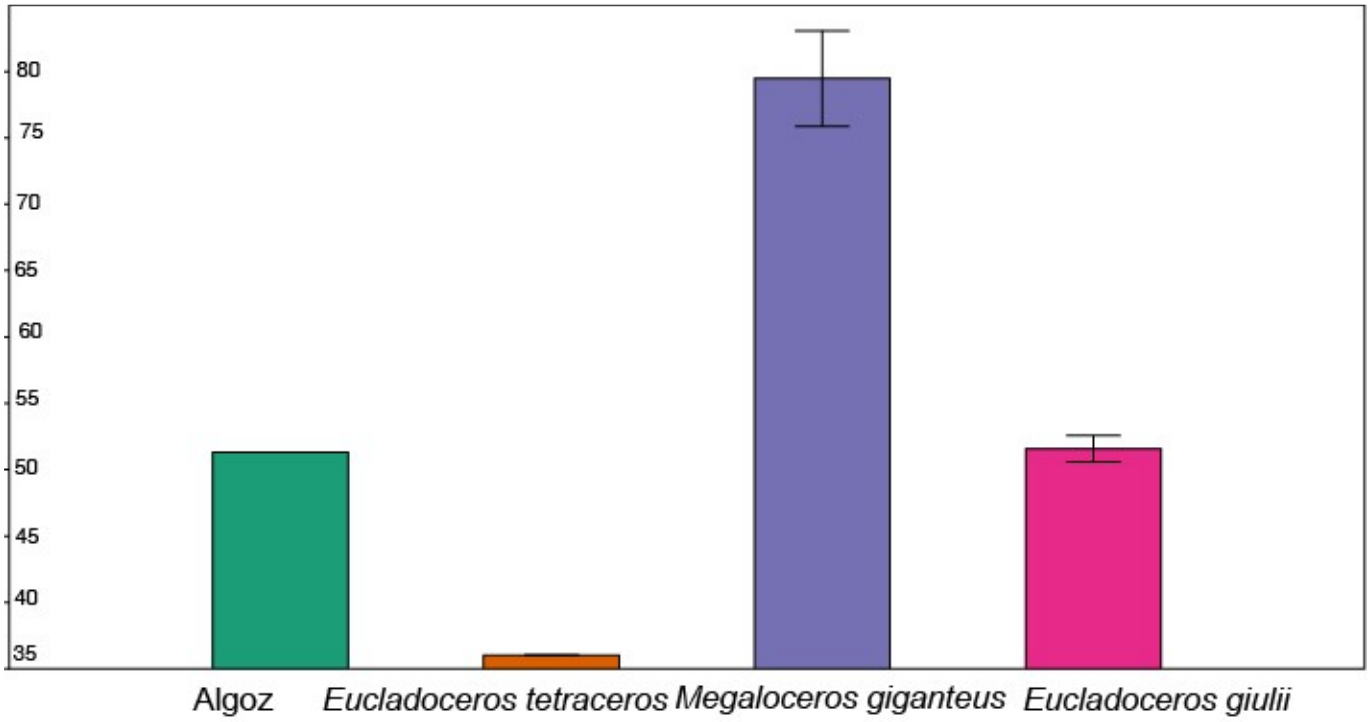
Breadth and length of the d4 from the Algoz medium sized deer (MG-25770) compared with other *Dama*-like deer.



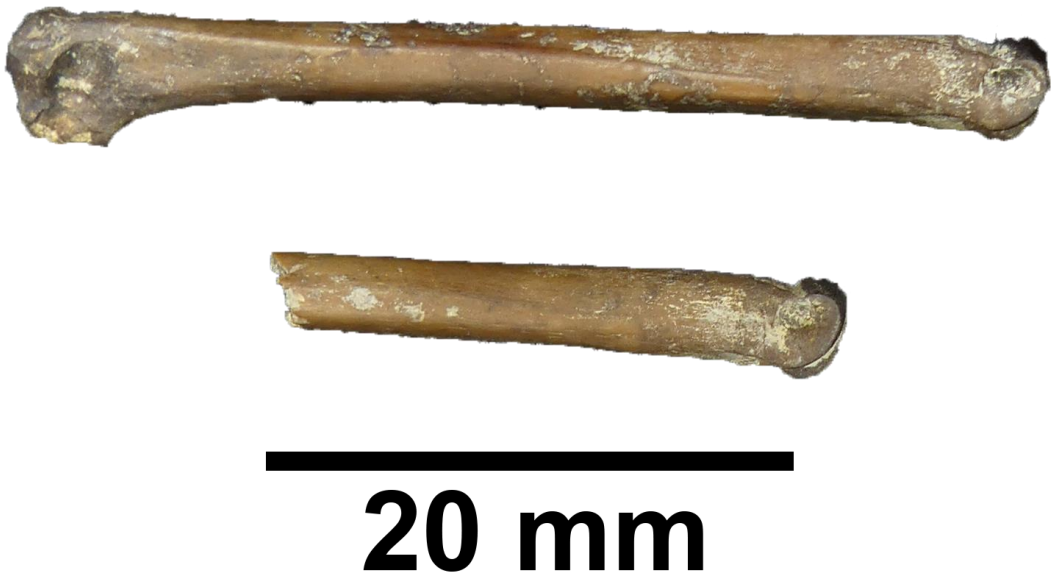
Boxplot of the femur width on the diaphysis of MG-25768 compared with other large-sized Pleistocene Eurasian deer.



Boxplot of the length of the deciduous teeth row (d2-d4) of MG-25768 compared with other large-sized Pleistocene Eurasian deer.



Boxplot of the distal anteroposterior diameter of the radius of MG-25768 compared with other large-sized Pleistocene Eurasian deer.



Leporid metatarsals from Algoz (MG-25772) in lateral view.

A.6 Description and figures of taxa from Santa Margarida without important biostratigraphic meaning.

Class Mammalia Linnaeus, 1758

Order Eulipotyphla Wadell et al., 1999

Family Soricidae Fischer, 1814

Genus *Sorex* Linnaeus, 1758

Sorex sp.

Fig. S1

Description and remarks: This taxon is represented at Santa Margarida by one fissident (with small medial cupule) upper incisor with red pigmented enamel, of relatively small size (Fig. S1), all of these are characters of the genus *Sorex* (Reumer, 1984).

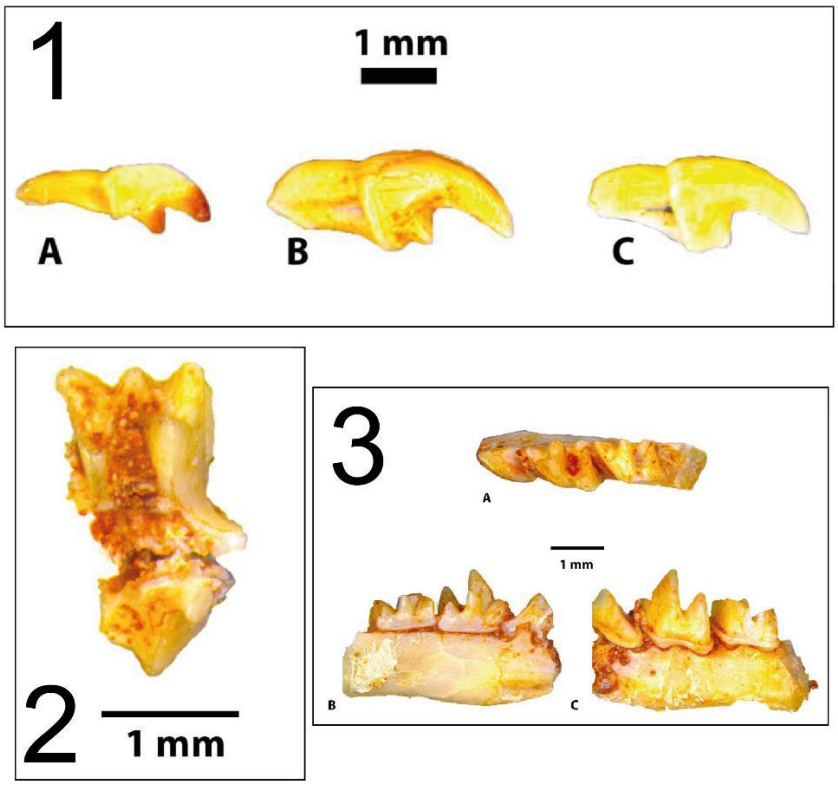


Fig. S1. 1. Soricidae upper incisors recovered from Santa Margarida (Portugal) in labial view. A: *Sorex*, B, C: *Crocidura*. **2.** Broken second upper molar of *Crocidura* recovered from Santa Margarida (Portugal) in occlusal view. Labial part to the right. **3.** Fragment of *Crocidura* mandible (bearing p4, m1 and m2) recovered from Santa Margarida (Portugal) in occlusal (A), lingual (B) and labial (C) views.

Genus Crocidura Linnaeus, 1758

Crocidura sp.

Fig. S1

Description and remarks: This taxon is represented at Santa Margarida by several incisors, molars, and a fragment of a mandible. The upper incisors (Fig. S1) present unpigmented enamel and a marked and slightly undulated cingulum in the posterior buccal part, as well as a larger size than *Sorex* (Reumer, 1984).

An M2 (Fig. S1) presents an hypocone situated in a postero-lingual position relative to the protocone and poorly individualized of it. There is also a deep valley between the protocone and the metacone and a crest connecting it with the paracone. Its trapezoidal shape is congruent with a second upper molar. Given the absence of enamel coloration, its size, and the previously mentioned characters it is assigned to the genus *Crocidura* (Reumer, 1984).

Some teeth recovered from the locality were still attached to parts of the mandible, but only one mandible part is conserved with more than one tooth (Fig. S1). It presents the p4, m1 and m2 (Moyá-Costa, Pers. comm. 2019). The p4 is tetrahedral shaped; the m1 and m2 have the valley openings well above the cingulum in labial view. The cingulum is well marked and undulated in the labial part and weak in the lingual. The mandible also poses a small mandibular foramen situated in labial view in the transition of the p4 to the m1. All these characteristics allow us to attribute this mandible fragment to the genus *Crocidura* (Reumer, 1984).

Order Rodentia Bowdich, 1821

Family Muridae Illiger, 1811

Genus Apodemus Kaup, 1829

Apodemus cf. *sylvaticus* (Linnaeus, 1758)

Fig. S2

Description and remarks: In the Santa Margarida sample there is a total of 51 teeth (six third lower molars, two second lower molars, 15 first lower molars, five third upper molars, nine second upper molars, five first upper molars and eight indeterminate teeth) whose morphology is congruent with *Apodemus* (Hillson, 2005). Moreover, in the first lower and upper molars we can see six low principal cusps, which is a characteristic of *Apodemus* (López-García, 2008). All the first upper molars have a developed tubercle 7 (t7) on them as well as a t7–t4 connection in almost all cases (Fig. S2) (Piñero et al., 2015). In all the lower first molars the anterocentral cusp is connected to the anterolabial and anterolingual cusps, meanwhile in the *Apodemus mystacinus* from the Quibas site (Spain) around 1/3 of them have this cusp totally isolated

(Piñero et al., 2015). All these characteristics allow us to classify the teeth as belonging to *Apodemus* cf. *sylvaticus*.

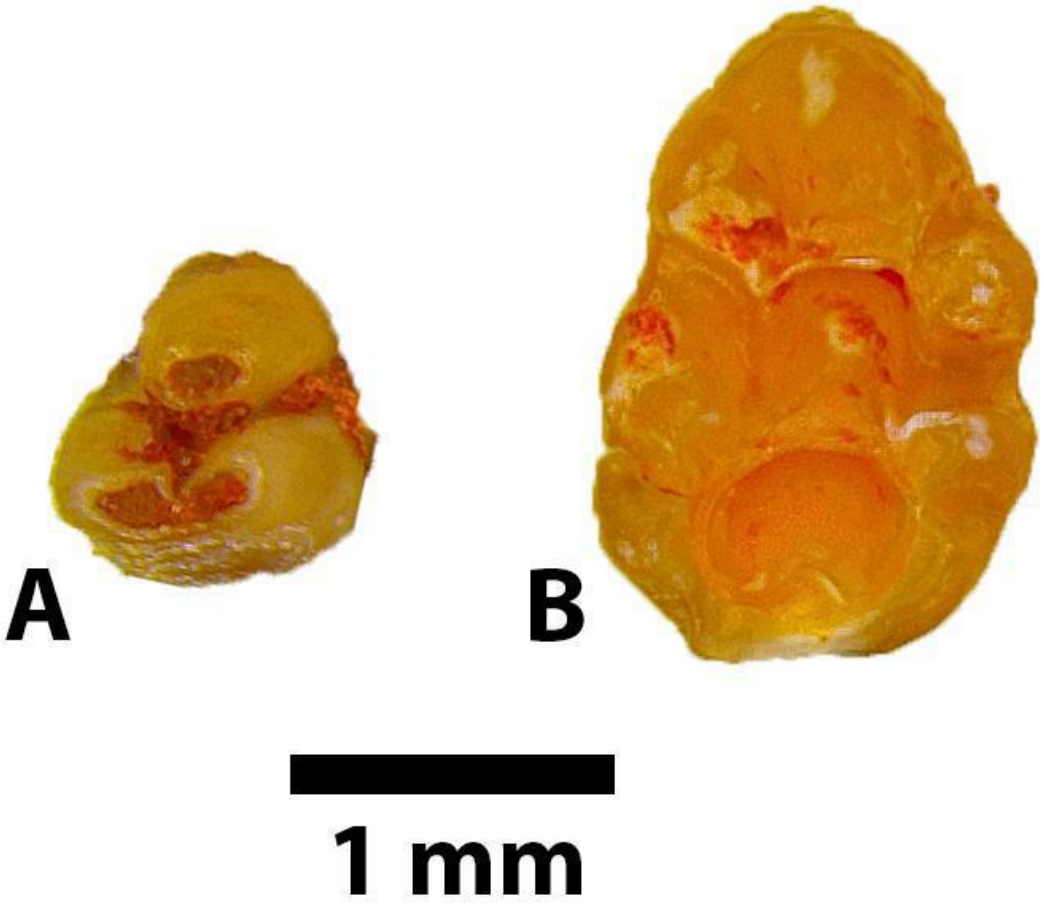


Fig. S2. m3 (**A**) and M1 (**B**) of *Apodemus* cf. *sylvaticus* from Santa Margarida (Portugal), in occlusal view.

Family Gliridae Muirhead in Brewster, 1819

Genus ***Eliomys*** Wagner, 1840

Eliomys cf. *quercinus* (Linnaeus, 1766)

Fig. S3

Description and remarks: Dormice are characterized by their cheek teeth: "brachydont, low and table-like in most genera, with multiple ridges running buccolingually across the occlusal surface" (Hillson, 2005). There is one lower premolar, one second lower molar, two second upper molars and one indeterminate molar present in the sample. The teeth of Santa Margarida (Fig. S3) present highly curved and continuous ridges without extra cusps besides the four main

ones and strongly triangular shaped premolars, which allow us to ascribe them (most likely) to *Eliomys quercinus* (Linnaeus, 1766) (Hillson, 2005; Piñero *et al.*, 2015).

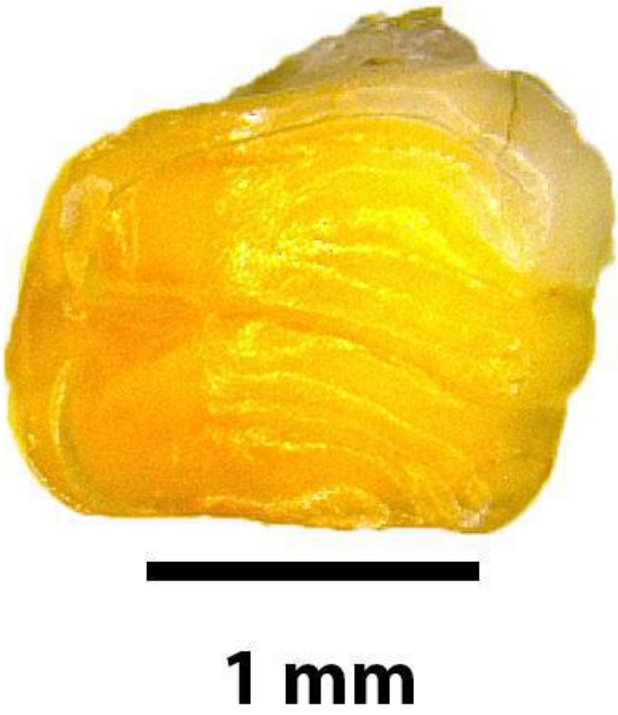


Fig. S3. Left upper first or second molar of *Eliomys* cf. *quercinus* from Santa Margarida (Portugal), in occlusal view.

Family Cricetidae Fischer, 1819
Genus ***Allocricetus*** Schaub, 1930
Allocricetus bursae Schaub, 1930
Fig. S4

Description and remarks: A cricetine rodent is represented at Santa Margarida by an upper first molar (Fig. S4) that bears the characteristic low crown with six cusps aligned in two rows (Hillson, 2005). It has not anterostyle, the anterolophule is clearly bifurcated and the lingual side (judging for the position of the anterolophule relative to the protocone) is longer than the labial one. These characteristics are typical of the species *Allocricetus bursae* Schaub, 1930 (Cuenca-Bescós, 2003). Unlike in *Cricetulus*, according to Cuenca-Bescós & Morcillo (2022), the M1s of *Allocricetus* usually present a posteroloph, as the it is the case for specimen from Santa Margarida. The question of *Allocricetus* reaching into the Late Pleistocene, or if the Late

Pleistocene specimens should be classified as *Cricetulus* is open to debate (Cuenca-Bescós & Morcillo-Amo, 2022). Yet considering the presence of a posteroloph in the specimen, we ascribe it to *Allocricetus bursae*.



Fig. S4. Left upper first molar of *Allocricetus bursae* from Santa Margarida (Portugal), in occlusal view.

Order Lagomorpha Brandt, 1855
Family Leporidae Linnaeus, 1755
Genus Oryctolagus Lilljeborg, 1873
Oryctolagus cf. *cuniculus* (Linnaeus, 1758)
Fig. S5

Description and remarks: One of the few relatively large sized bones recovered with an air-scribe from one of the blocks is a distal left humerus (Fig. S5). It has a narrow trochlea that is inclined towards the medial line of the body; the coronoid fossa and the olecranon fossa are connected by a distinctive supratrochleal foramen; the anterior half of the diaphysis is mostly

straight in lateral view meanwhile the posterior part is slightly curved caudally, making the proximal part of the diaphysis wider in lateral view. Compared with modern remains of rabbit (*Oryctolagus cuniculus*) it is easy to see the great similarity to this species, given the mentioned characteristics, nevertheless being it only postcranial material, not really diagnostic for lagomorphs (Angelone et al., 2020), the attribution cannot be certain. Regardless, this is the animal species of largest size identified at this moment in Santa Margarida.



Fig. S5. Left distal *Oryctolagus* cf. *cuniculus* humerus from Santa Margarida (Portugal), in anterior (**A**), lateral (**B**), posterior (**C**) and medial (**D**) views.

Supplementary references

Angelone, C., Moncunill-Solé, B., Kotsakis, T., 2020. Fossil Lagomorpha (Mammalia) of Italy: Systematics and Biochronology. Rivista Italiana Di Paleontologia e Stratigrafia 126, 157–187.

Cuenca-Bescós, G., 2003. Allocricetus (Cricetidae, Rodentia, Mammalia) from the Pleistocene. A phylogenetical approach. Coloquios de Paleontolgía 1, 95–113.

Cuenca-Bescós, G., Morcillo-Amo, A., 2022. Roedores, edades y paisajes en el Cuaternario de la Península Ibérica. Prames.

Hillson, S., 2005. Teeth (2nd ed.). Cambridge University Press. http://discovery.ucl.ac.uk/11267/

López-García, J.M., 2008. Evolución de la diversidad taxonómica de los micromamíferos en la península ibérica y cambios paleoambientales durante el Pleistoceno Superior. Ph.D. thesis, Universitat Rovira i Virgili, Roma, Italy (unpubl.). https://dialnet.unirioja.es/servlet/tesis? codigo=80124

Piñero, P., Furió, M., Agustí, J., Blain, H.-A., Laplana, C., 2015. Biochronological data for the Early Pleistocene site of Quibas (SE Spain) inferred from rodent assemblage. Geologica acta 13, 229–241.

Reumer, J., 1984. Ruscinian and early Pleistocene Soricidae (Insectivora, Mammalia) from Tegelen (The Netherlands) and Hungary. Scripta Geologica 73, 1–173.

B

APPENDIX: "INSIGHTS ON THE EVOLUTION AND ADAPTATION TOWARD HIGH-ALTITUDE AND COLD ENVIRONMENTS IN THE SNOW LEOPARD LINEAGE"

B.1 Addenda to Introduction

The potential record of cold-adapted large mammal species outside the Tibetan Plateau and the surrounding area, especially in Europe, has been long noticed by previous scholars. Since the establishment of *Leopardus irbisoides* from Turská Maštal (Czech Republic) by Woldřich (1893), the discussion on whether the presence of the snow leopard in the European Pleistocene has been an ongoing debate for nearly 130 years (Hemmer, 1971; Hemmer, 2023; Cardoso & Regala, 2006; Testu et al., 2011; Spassov & Raychev, 1997; Thenius, 1971; Hemmer & Schütt, 1973; Filoux et al., 2013; Bacon et al., 2008), without a clear conclusion. Different authors hold their views based on evidence from different anatomical structures and fossil materials, which often lead to different conclusions. The biggest problem lies in two aspects: (1) scarcity of well-preserved material and (2) incomplete sample and comparison of modern specimens. The present work tries to shed light and resolve several questions of this long-lasting and hot debate.

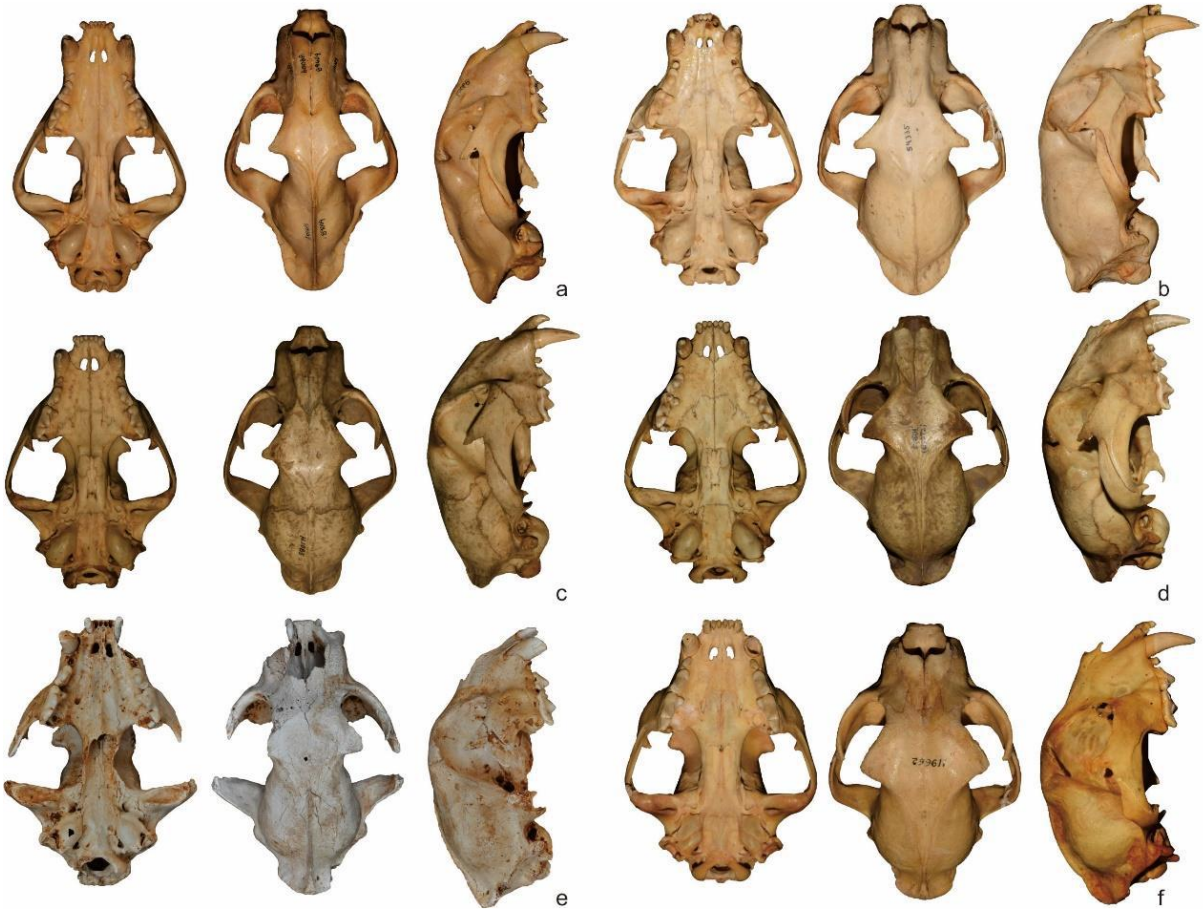


Fig. S1. **Comparison of African, Asiatic leopard, fossil snow leopard and modern snow leopard in ventral, dorsal and lateral views**. a. *P. pardus* Africa, AMNH89009; b. *P. pardus* Africa, AMNH M54335; c. *P. pardus* Asia, IOZ H1085; d. *P. pardus* Asia, IOZ07805; e. *P. u. lusitana* MG1355.0001; f. *P. uncia* AMNH M116952. Not to scale.

Brief review of fossil records of *P. pardus* in Eurasia

Europe

P. pardus has a rich fossil record in Europe. The earliest records, ~1 Ma, from Vallonet Cave, by some isolated teeth (Sauqué & Cuenca-Bescós, 2013; Moullé et al., 2006; Diedrich, 2013). The earliest skull of *P. pardus* from Europe is from Monte Sacro (Kotsakis & Palombo, 1979), and is assigned to *P. p. sickenbergi* (Diedrich, 2013). This skull is low and long, similar to the modern African leopard (Fig. S1) in general morphology (Diedrich, 2013). Our geometric morphometric analyses suggest its lateral view fully falls into the variation of modern African leopard in lateral view, but shows some differences in dorsal and ventral views. This subspecies is contemporary with *P. pyrenaica*. The other materials of this age are largely represented by isolated or broken

jaw or teeth (Kurtén & Poulianos, 1981). The material from Stránská skála, including a partial mandible with short c p3 diastemata, and vertical symphysis, has also been suggested to show affinity with P. uncia lineage (Hemmer, 1971; Thenius, 1969), but later assigned to *Puma*/*Viretailurus* (Hemmer, 2001). The p3 of Stránská skála specimen has a very low crown and strong anterior accessory cuspids, unlike that of *P. pyrenaica*. Its true affinity is obscure due to material limitations.

The late Middle and Late Pleistocene leopard remains were assigned to different subspecies, i.e., *P. p. antiqua*, *P. p. spelaea*, *P. p. vraonensis*, and these may represent the same subspecies *P. p. spelaea* (Ghezzo & Rook, 2015; Nagel, 1999; Sauqué & Cuenca-Bescós, 2013; Diedrich, 2013). In general, this subspecies is characteristic by having a relatively short and high cranium, as represented by the remains from Equi, Allekoaitze, and Aintzulo caves, Vjeternica Cave, Abric Romaní (Ghezzo & Rook, 2015; Diedrich, 2013; Cáceres et al., 1993), though the crania from Equi shows some variation in cranium shape. The short and high cranium is generally thought to be close to the modern Asian leopard (Diedrich, 2013), as shown in Fig. S1, but in the geometric morphometric analysis, the crania from these localities occupy a slightly different morphospace from that of the modern Asian leopard, though with overlap. Especially in the dorsal view, the morphospace of the Late Pleistocene European leopard is slightly closer to that of modern P. uncia, but this is not reflected in other views. Some Late Pleistocene P. pardus fossils have a relatively vertical symphysis, especially represented by the mandible from Geinsheim (Koenigswald et al., 2006). However, this mandible has a long c-p3 diastema, and the cheek teeth are relatively small, thus different from P. uncia. The postcranial bones from Vraona Cave are more robust than those of modern leopard, probably correlated with adaptation to mountainous regions, but still different from that of the modern snow leopard (Nagel, 1999). In summary, the late Middle and Late Pleistocene leopards show some similarity in morphology and possibly ecological to modern snow leopards, in agreement with the intensive glacial period. However, they still lack some key snow leopard traits and are clearly different from the Manga Larga skull (see discussion below).

Asia

The fossil records of Asian leopards are scarce. In China, many remains were identified as P. pardus, from Early Pleistocene to Late Pleistocene. However, most of them, e.g., from *Gigantopithecus* Cave, Gongwangling, Zhoukoudian Loc.1, are much larger than modern *P. pardus* (Pei, 1987; Hu & Qi, 1978; Pei, 1934), and should in fact represent *P. palaeosinensis* or *P. gombaszogensis* (Jiangzuo et al., 2023). The earliest records of *P. pardus* are dated to the early Middle

Pleistocene, in Zhoukoudian Loc.1 (based on personal observation) and Bailong Cave (Tong et al., 2019). Only incomplete mandibles are known from these sites, and they are generally similar to modern leopards. The late Middle and Late Pleistocene fossil records of fossil *P. pardus* from China are abundant, especially in the southern China cave deposits, but these materials are highly fragmented, nearly all isolated teeth (Pei, 1987; Zhang et al., 2017; Jiangzuo et al., 2018; Liu et al., 2015; Liu et al., 2006; Zhang et al., 2014; Pan et al., 2023). Some records of fossil *P. pardus* has been documented in Japan, e.g., the Kuzuu Ossuaries (Shikama, 1949) and Isa (Shikama & Okafuji, 1963), but these materials are larger than modern and known Pleistocene *P. pardus*. The affinity of these materials needs further study.

A single P4 was identified as P. pardus from Trinil and was identified as P. pardus (Hemmer & Schütt, 1973), with a very narrow metacone, which is different from modern leopard (Hemmer & Schütt, 1973). The late Middle and Late Pleistocene records are mainly based on postcranial (Hemmer & Schütt, 1973). From mainland southeastern Asia, the fossil P. pardus were known by isolated teeth (Filoux et al., 2013; Bacon et al., 2008; Harrison, 1996), much like the condition in southern China.

Paleoenvironmental and chronological background of the studied localities

Among the four localities, the two Middle Pleistocene ones have a good faunal background. The remains from early Middle Pleistocene (MIS 14, 0.53-0.57 Ma) Arago Cave suggest a typical cold condition fauna, represented by now arctic *Rangifer tarandus* and two bovids, *Hemitragus bonali* and *Ovis ammon antiqua*, both of which are now endemic to Tibet. In contrast, the Loc. 3 of Zhoukoudian shows a mixed condition based on faunal composition. There is no precise dating of Loc.3. Kurtén (1960) suggested the age of the fauna is probably correlated to the European Saale glaciation of the late Middle Pleistocene based on the faunal comparison. A recent study of fossil canids from this locality suggests that the large canid there has a similar evolutionary level to that of *Canis lupus lunellensis* of Europe and therefore probably has a similar age (Jiangzuo et al., 2018), 0.3-0.4 Ma. This locality does not have any typical high-altitude or arctic elements but is represented by the general forms of northern China, which is not much different from the current condition. Especially, the presence of diverse cervids, and the Asiatic black bear suggests the presence of abundant trees, not a typical environment for a modern snow leopard.

The two Late Pleistocene localities do not have good faunal composition information. The Manga Larga Cave has no associated fauna with the snow leopard, except a wild cat and a bird

(Regala & Cardoso, 2007). The age is estimated to be between 20-35 Ka, so from LGM, but without firm evidence (Regala & Cardoso, 2007). The Niuyan Cave has only three other mammals that coexisted with the snow leopard, P. pardus as mentioned above, and two bovids *Ovis nahoor* and *Pseudois nayaur*. Pseudois is a typical mountain-lived animal, now endemic to Tibet and the surrounding area. There is no dating of the fauna other than the Late Pleistocene, but the faunal composition suggests a potential age of LGM. The presence of the leopard suggests that the environment was not very cold.

In summary, the paleoenvironment of these fossil localities is close to but not totally the same as the modern living environment of the snow leopard. As the major prey of the snow leopard, ovine bovids are present in all these faunas except Manga Larga Cave, which has no associated fauna. This suggests that the prey type is probably important for the snow leopard.

B.2 Addenda to Materials and Methods

Material

The fossil specimens from the Algar da Manga Larga are housed in the Geological Museum of Lisbon (Portugal). In turn, the Longdan specimen is housed at the Institute of Vertebrate Paleontology and Paleoanthropology of Beijing (China). For comparison, living felid specimens (including all living species of *Panthera*, *Neofelis*, *Puma* and *Acinonyx*) housed at the American Museum of Natural History (AMNH, NYC, USA), Smithsonian National Museum of Natural History (USNM, Washington DC, USA), Museum of Comparative Zoology (MCZ, Boston, USA), Institute of Vertebrate Paleontology and Paleoanthropology, Chinese Academy of Sciences (IVPP, Beijing, China), Institute of Zoology, Chinese Academy of Sciences (IOZ, Beijing, China), and Kunming Institute of Zoology, Chinese Academy of Sciences (KIZ, Kunming, China) were used for comparison.

Methods

The cranial anatomical terms of Jayne (1898) on felids are followed with additional modifications by Qiu et al. (2014). The craniodental measurements are shown in Fig. S2.

Postcranial elements abbreviations—Scapular total length, **ScL**; humerus total length, **HL**; humerus proximal width, **HPrW**; humerus distal maximum width, **HDW**; humerus distal dorsoventral height, **HDH**; radius total length, **RL**; MC3 maximum distal width, **MC3DW**; MC3 length, **MC3 L**; ratio of DW/L of MC3, **MC3ip**; pelvis length, **PL**; femur proximal width, **FPW**; femur total length, **FL**; femur distal width, **FDW**; femur distal medial height, **FDMH**; femur distal lateral

height, **FDLH**; tibia total length, **TL**; MT3 maximum distal width, **MT3DW**; MT3 length, **MT3L**; ratio of DW/L of MT3, **MT3ip**. These measurements were used in the locomotion study of pantherine cats.

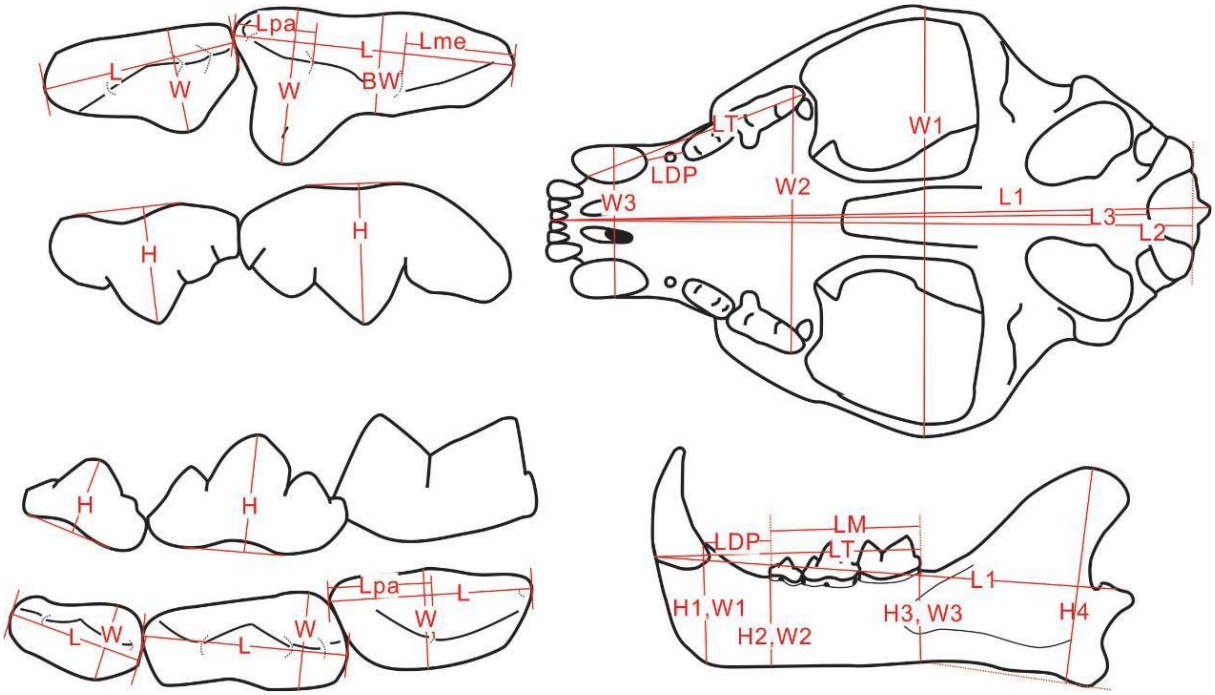


Figure S2. **Craniodental measurements of felids.**

B.3 Addenda to results

Manga Larga cranium

The specimen represents a full adult, judging by the nearly fused cranial sutures, and moderately worn dentition. The cranium is high, short, and wide. The forehead is wide and dorsally convex in lateral view. There is a slight concavity in the dorsal profile mesial to the forehead (lateral view). The nasal is short and wide, and its posterior limit does not reach the level of the maxilla-frontal suture. The postorbital constriction is short and similar to the interorbital width. The zygomatic arch is wide and deep. The braincase is wider in its posterior part. The temporal ridge units into a weakly developed sagittal crest at the level of the anterior part of the braincase.

The palate is wide and widens backwards. The major posterior palatine foramen is large and located at the level of the P4 paracone. The bony choana extends only slightly posterior to the M1. There is a small blur near the sagittal plane on each side of the bony choana. The glenoid fossa is antero-posteriorly wide. It forms a small angle from the horizontal plane. The oval

foramen is located slightly posterior to the glenoid fossa and is closely attached to the auditory bulla. The auditory bulla is flat. The ectotympanic is greatly enlarged and slightly inflated. The mastoid process is well-developed and transversely wide. The shelf between the mastoid process and the paroccipital process is strongly concave. The hypoglossal foramen is located in the same fossa as the posterior lacerated foramen. This fossa is small and only occupies half the length of the posteromedial border of the bulla. The occipital shield is wide and has a triangular shape. The lambdoidal crest is not smooth, with a zigzag shape. The medial wall of the condyle is nearly vertical.

The mandible is robust and has a very deep corpus. The symphysis has a high angle but is not completely vertical. The height of the corpus behind the lower canine is high, distinctly higher than that behind the m1. There are three mental foramina. The two anterior ones are located between the c1 and p3, with the lower one larger. The posterior one is located at the level of p3. The coronoid process is relatively small. The ventral border of the masseteric fossa is poorly laterally expanded.

The upper incisor row is straight. The I3 has no accessory cusp. The upper canine has a rounded cross-section. The C-P3 diastema is short, with a rounded P2 alveolus occupying much of this distance. The P3 is robust, with a small anterior accessory cusp, located medial to the main cusp. The posterior cingulum is distinct. The P4 has a straight buccal border. The protocone is located at the level between the parastyle and paracone. The M1 is small, single-rooted, and transversely short. The lower incisor is small, without accessory cusps. The p3 is low-crowned, with distinct and blunt anterior and posterior accessory cuspid. There is no posterior cingulid. The p4 has a similar basic structure as the p3 but is more elongated, with better-defined accessory cuspids and a weak posterior accessory cusp. The m1 is elongated, with a massive paraconid. There is no distinct m1 metaconid.

Longdan mandible

The specimen IVPP V31895 comes from the bottom of the Wucheng loess in the Linxia Basin, Gansu Province. The mandible is nearly complete, but the lateral corner of the condyle is broken. The incisors and the p3 are not preserved, and the canine is broken. The corpus is moderately deep and has a nearly uniform depth from the symphysis to the m1. The lower border of the corpus is distinctly convex. The symphysis is relatively vertical, with its angle lying within the variation of both modern *P. uncia* and *P. tigris*. The coronoid process is moderately large. The anterior border of the masseteric fossa does not extend anterior to the distal border of

the m1. The ventral border of the masseteric fossa is not laterally expanded as in modern *P. uncia*. The angular process is not ventrally extended as in modern *P. tigris*.

The p3 is not preserved. Judging from the partial absorption of the anterior root, it is probably broken during life. The p4 is elongated, with the mesial accessory cuspid broken or worn during life and experiencing subsequent wear. The main cuspid also has distinct apical wear. The m1 is rather robust and stout. The buccal border is rounded, and the medial border is convex. A small talonid is indistinctly distinguished from the protoconid.

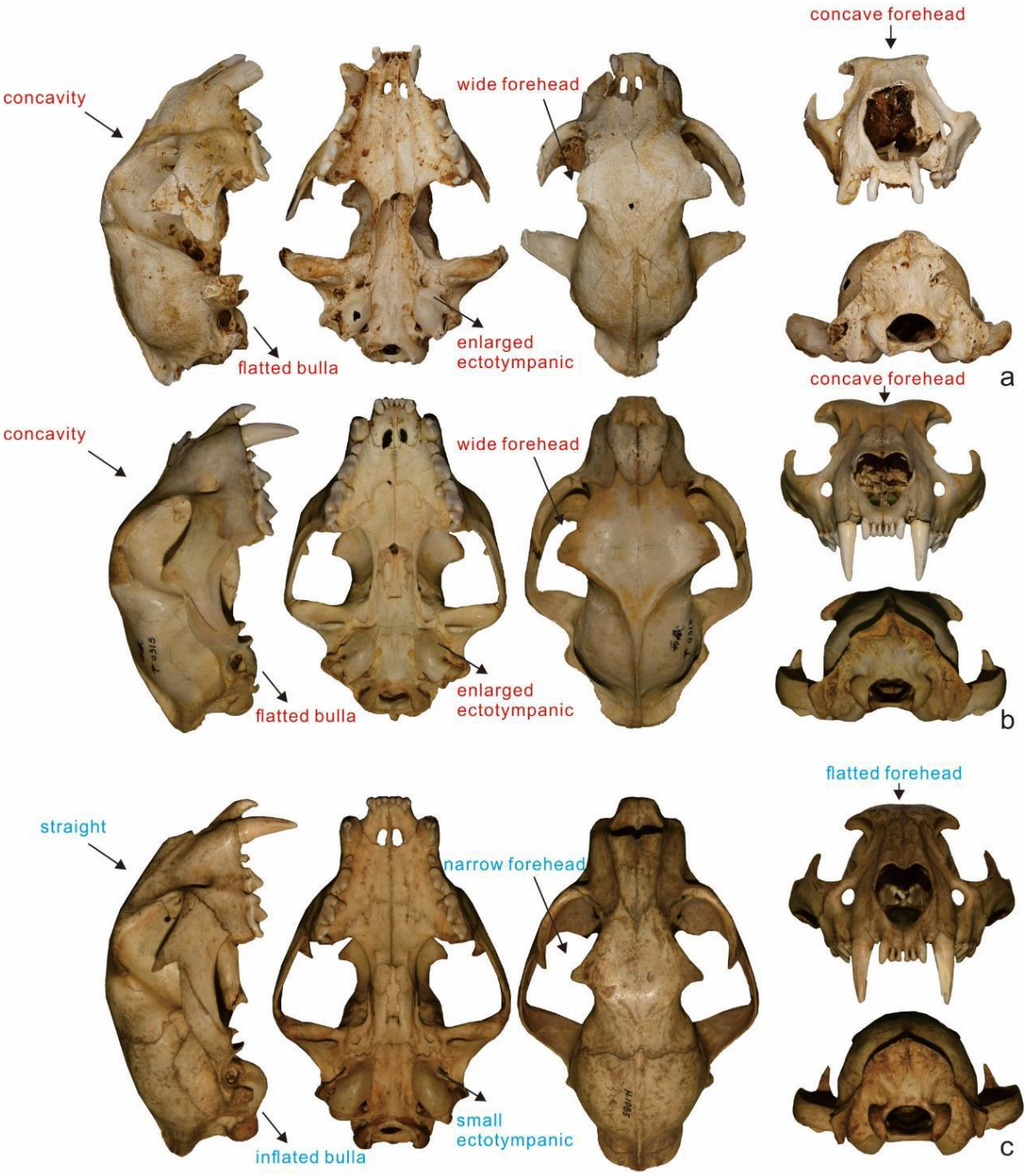


Figure S3. **Cranial comparison of Manga Larga specimen, and modern *P. uncia* and Asiatic *P. pardus*.** a. *P. u. lusitana* MG1355.0001; b. *P. uncia* IOZ T0315; c. *P. pardus* IOZ H1085. Lateral, ventral, dorsal, anterior, and posterior views.

The snow leopard affinity of Manga Larga skull

The skull from the Manga Larga Cave shows a predominant *P. uncia* trait: the cranium is broad and high, with a short rostrum. There is concavity in the forehead in lateral view, which is nearly

only present in *P. uncia* and *P. onca*. The forehead is also very broad, to the extent only seen in modern *P. uncia*. The unique flatted bulla, with enlarged ectotympanic, is also only seen in *P. uncia*. Only some fossil *P. atrox* and *P. spelaea* also have a flatted bulla and enlarged ectotympanic, which, however, seldom reaches the extent seen in Manga Larga cranium. The mandible also shows some clear snow leopard affinity. The symphysis is verticalized, and the c-p3 diastema is short. The coronoid process is relatively small, and the ventral border of the masseteric fossa is not laterally expanded. The cheek teeth are enlarged compared with the cranium size. The m1 shows a typical *P. uncia* trait, i.e., relatively narrow, with an antero-buccal corner.



Figure S4. **Comparison of mandibles of Manga Larga snow leopard, and modern *P. uncia* and *P. pardus*.** Not to scale. a, *P. u. lusitana* MG1355.0002, from Manga Larga; b1-3, *P. uncia*, AMNH M54205, AMNH M166952 (reversed), IOZ T0315 (reversed); c1-2, *P. pardus* Asia, IOZ 09634 (reversed); IOZ H1085 (reversed); d1-2, *P. pardus* Africa, AMNH M89009, AMNH 81845 (reversed).

The Manga Larga skull shows clear differences from *P. pardus*. Even though the Asian and some late Middle to Late Pleistocene European *P. pardus* indeed have relatively short and high cranium (Diedrich, 2013), they never reach the level seen in Manga Larga skull and modern *P. uncia* (Fig. S3). Moreover, P. pardus never has flat bulla and greatly enlarged ectotympanic, enlarged cheek teeth, and short rostrum seen in Manga Larga skull and modern *P. uncia*. The extent of such differences can be clearly seen in our geometric morphometric analysis.

Puma (or *Viretailurus*) is another taxon that could be misidentified as a snow leopard (Hemmer, 2023). It has a relatively rounded cranium and short rostrum, yet does not reach the level of Manga Larga skull and modern *P. uncia*. The bulla is also not flattened, and the ectotympanic is never enlarged. The cheek teeth are also not enlarged as seen in the Manga Larga skull and modern *P. uncia*.

Other species of felid are generally easily distinguished from Manga Larga one. *P. onca* and *P. gombaszogensis* are distinctly larger and lack the unique cranial, bulla, and cheek teeth traits mentioned above. *Acinonyx* has an even wider forehead, and its cheek teeth are characteristic by having a well-developed accessory cuspid and reduced P4 protocone, not seen in Manga Larga skull. *Neofelis* has a clearly narrower forehead and lower cranium, and a much larger canine and higher mandibular symphysis. *Lynx* is smaller in size, having a more pointed supraorbital process, more inflated bulla, and slenderer mandible. The P3/p3 of *Lynx* is also higher-crowned.

On the other hand, the Manga Larga cranium also shows some differences that clearly fall outside the variation range of the modern species. The forehead has a less concave profile than in modern *P. uncia*. The bony choana of the Manga Larga skull is relatively narrower than that of modern *P. uncia*. The mandibular corpus is also much deeper than in modern *P. uncia* (Fig. S4). The dentition is generally similar, but in the Manga Larga specimen, the buccal border of the P4 is straight, which nearly never occurs in modern *P. uncia*, whose P4 buccal border has one or two concavities. These differences suggest there is still a clear distance between the Manga Larga skull and modern *P. uncia*, and the fossil here cannot be assigned to the modern species.

The snow leopard affinity of Longdan mandible

The specimen from Longdan is generally similar to *P. pyrenaica*. Both specimens have a weak ventral border of the masseteric fossa, and a moderately to distinctly verticalized symphysis. In this aspect, the Longdan *Panthera* shows less vertical symphysis as in *P. pyrenaica*, but still falls into the variation of the modern species. Longdan material exhibits two primitive traits shared with *P. pyrenaica*, i.e., the relatively long rostrum (c-p3 diastema), and relatively high coronoid process. These two traits in both species represent the symplesiomorphic characters of *Panthera*.

Previously, two large *Panthera* species, *P. palaeosinensis* and *P. zdanskyi* were identified from Longdan Fauna (Qiu, Deng, & Wang, 2004; Mazak, Christiansen, & Kitchener, 2011). Mazak et al. (2011) proposed that *P. zdanskyi* is different from *P. palaeosinensis* in having a larger size, longer nasal bone, and larger canine, and then interpreted these as traits that unite *P. zdanskyi* with modern *P. tigris*. After the cumulation of more material from Longdan fauna, we proposed that these traits are variable within the population, and are often correlated with sexual dimorphism (Fig. S5, 6). However, the new mandible found from the Longdan clearly falls out of the variation range of *P. palaeosinensis* from the same locality. The new specimen is distinctly smaller than *P. palaeosinensis* from the same site, and also smaller than the type of *P. palaeosinensis*, which is slightly smaller than the *P. palaeosinensis* population from Longdan. Most significantly, the Longdan mandible has a shallower symphysis (with a significant difference of ratio of mandibular depth behind the canine and behind the m1, P value $<<0.01$ in single case t-test) (Fig. S5-6). It further differs from *P. palaeosinensis* in having a less ventrally expanded angular process and a none-laterally expanded ventral border of the masseteric fossa. These two traits are key characters units it with the snow leopard lineage (Hemmer, 2023), and are quite different from *P. palaeosinensis-P. tigris* lineage. The studied specimen is also different from *P. pardus* in having more erected symphysis, more robust m1, and weaker expansion of the ventral border of the masseteric fossa. Especially, the early *P. pardus* from Africa, represented by those from Burgi Member and KBS Member of Koobi Fora and Ahl Al Oughlam has a rather shallow symphysis (Werdelin & Lewis, 2013; Geraads, 1997) and is clearly different from Longdan studied specimen. *Viretailurus pardoides* from Europe (Viret, 1954) has a slightly smaller size, shorter p4, and distinctly less robust m1.

A summary table of Pleistocene and modern *P. uncia* and *P. pardus* is given in Table S7.

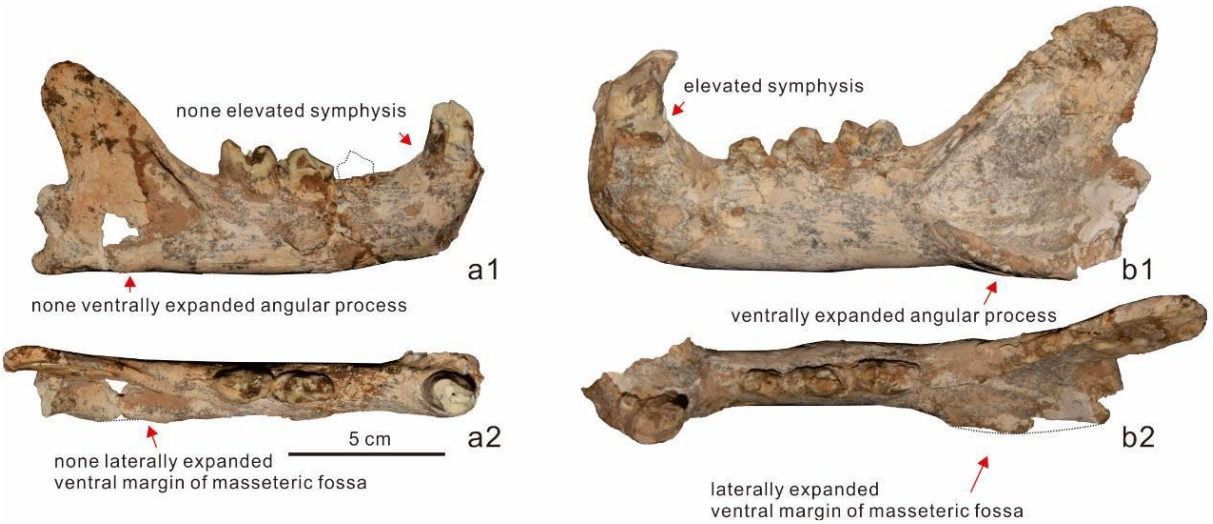


Fig. S5. **Comparison of two *Panthera* species from Longdan.** a1-2. *P.* aff. *pyrenaica* IVPP V31895, lateral and ventral views; b1-2. *P. palaeosinensis* HMV 2029 from Longdan, lateral and ventral views. Note on the different characters marked in the figure.

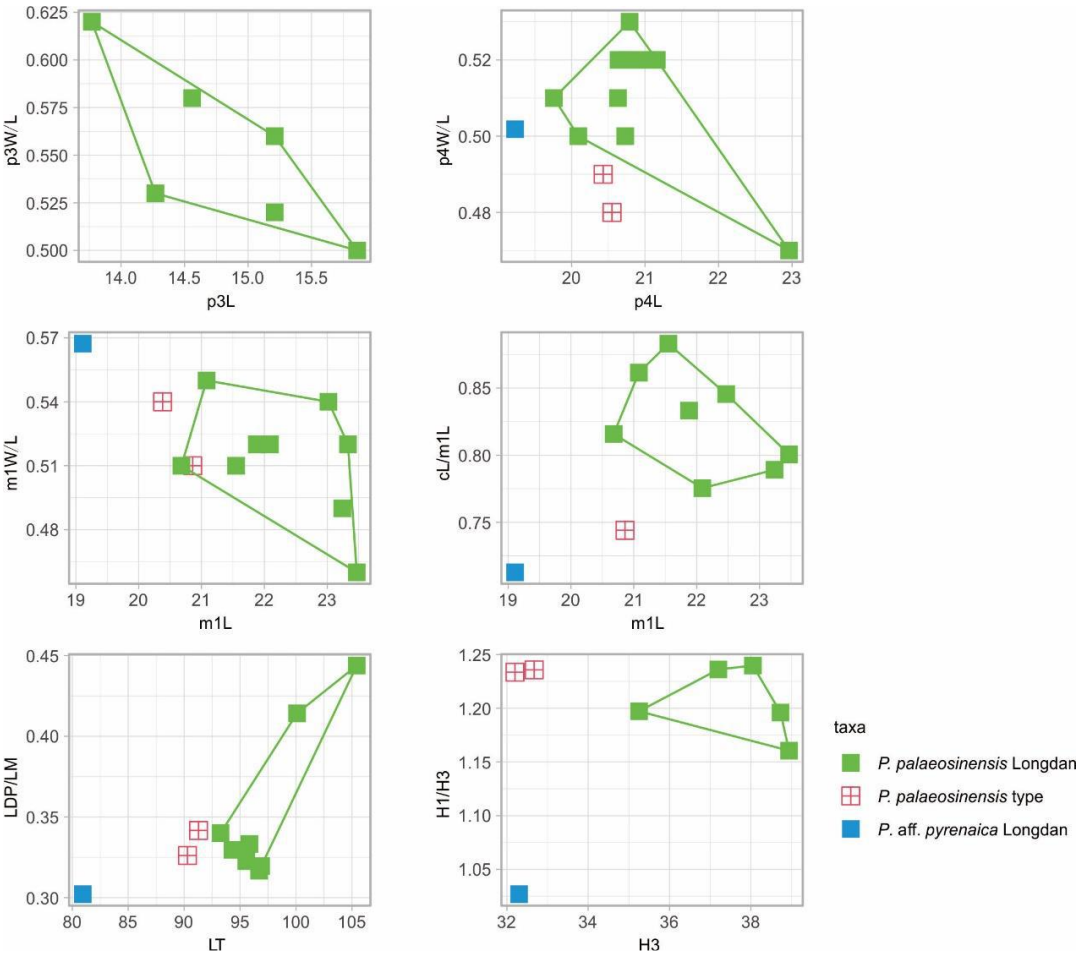


Fig. S6. Metric comparison of *P.* aff. *pyrenaica* and *P. palaeosinensis* from Longdan and type locality.

Remarks on *"Panthera" blytheae*

Tseng, Wang, Slater, Takeuchi, Li, Liu, and Xie (2014) published a Pliocene potential ancestor of the snow leopard as *P. blytheae*. The *Panthera* affinity of this species, however, was questioned by several recent studies (Hemmer, 2023; Geraads & Peigné, 2016; Chatar, Michaud, & Fischer, 2022; Hemmer, 2023). Recently, Hemmer (2023) suggested that this species has an anterior jugal process, and is unlikely to be a member of *Panthera*, and erected a new genus *Palaeopanthera*, regarding it as a basal pantherine. We further found *Panthera* always has a low-crowned p3, the anterior border of the jugal is generally moderately anteriorly inclined, and the postorbital process of the frontal is blunt. In *P. blytheae*, however, the p3 is high-crowned, the anterior border of the jugal is strongly anteriorly inclined, and the postorbital process of the frontal is pointed (Fig. S7-8). These traits are not fitted with *Panthera*. Moreover, there are strong buccal grooves in the buccal sides of the P4 (Fig. S8), which is never present in *Panthera*, but quite distinct in Plio-Pleistocene *Lynx* (Jiangzuo et al., 2022). Therefore, *P. blytheae* is not regarded as a member of or closely related to the snow leopard and is not discussed here. Its affinity needs further study and in light of more material.



Fig. S7. **The cranium of *"P." blytheae*, marking the important characters mentioned in text**. a. lateral view; b. ventral view; c. dorsal view.

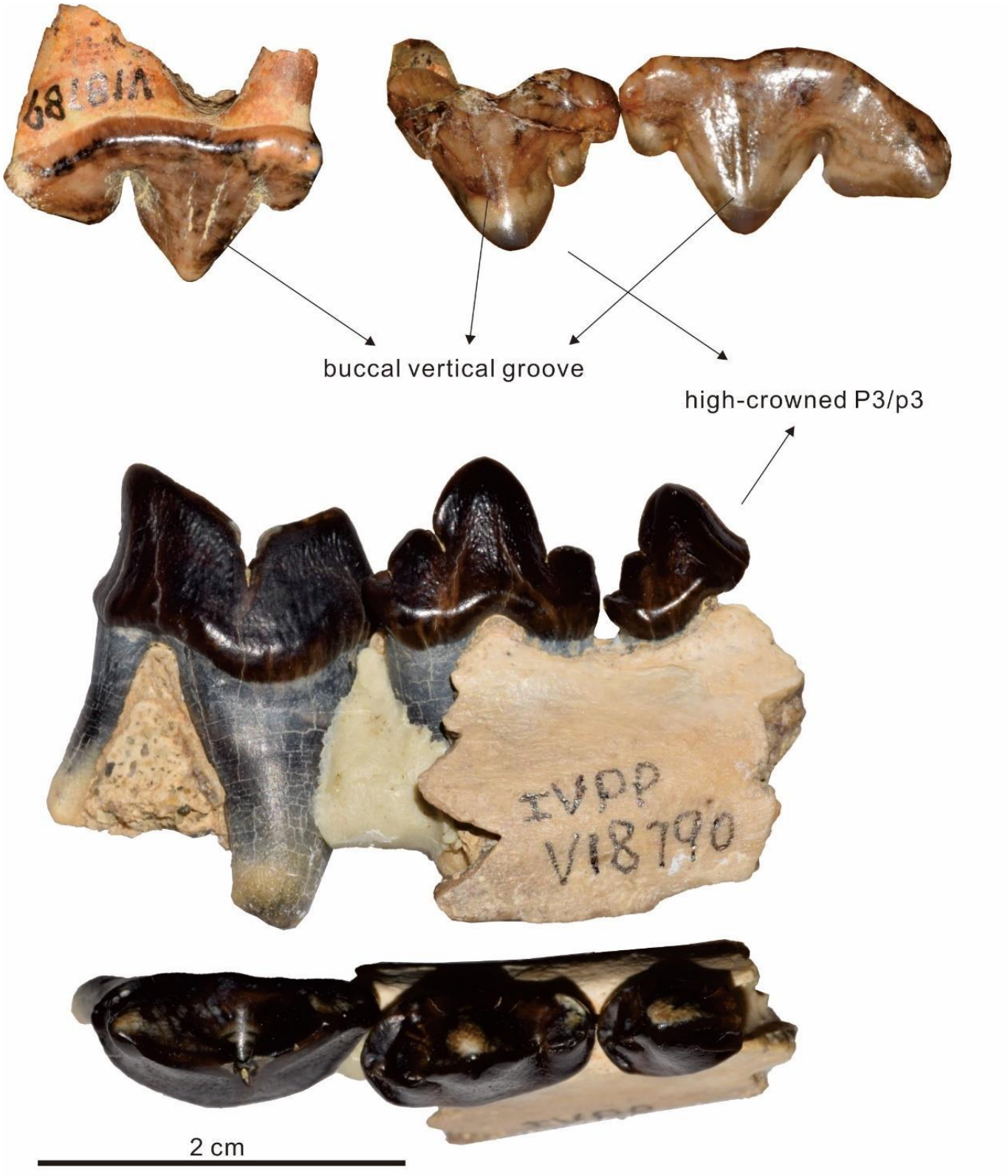


Fig. S8. **The dentition of *"P." blytheae*, marking the important characters mentioned in text.**

B.4 Addenda to discussion

About the coexistence of *Panthera pardus* and *Panthera uncia* in the Niuyan Cave, Beijing. The materials from the Niuyan Cave have both basicranium (Fig. S9) and mandible (Fig. S10). All pantherine specimens from the Niuyan Cave were assigned to *P. pardus* (Tao, Wanbo, & Hongjie, 1999). Our metric analyses (Fig. S11) support that one pair of mandibles from this locality is close to or falls into the variation of modern snow leopards. Especially the vertical symphysis and large m1, and very short c-p3 diastema are characteristic of *P. uncia*. The other pantherine specimens, including a basicranium and a mandible, do not possess key traits of *P. uncia* and are referable to *P. pardus*. The basicranium V11798 has a narrow forehead, and a very small ectotympanic chamber of the bulla. Both traits are seen in *P. pardus*, whereas in *P. uncia*, the forehead is greatly widened, and the ectotympanic chamber of the bulla is enlarged to a similar size to the ectotympanic chamber (Haltenorth, 1936; Salles, 1992; Sims, 2012). The mandible has a low and inclined symphysis and long c-p3 diastema. The metric analyses also support it within the variation of modern *P. pardus* (Fig. S11).

The coexistence of both *P. uncia* and *P. pardus* in the same site is intriguing, suggesting the environment is not too harsh for *P. pardus*, and not very humid to exclude *P. uncia*. In modern ecosystems, the two species also have marginal overlap (Lovari, Ventimiglia, & Minder, 2013; Buzzard, Li, & Bleisch, 2017; Koju et al., 2024; Lovari et al., 2024). This suggests that the paleoenvironment of the Niuyan Cave is in the boundary of different types of vegetation cover.

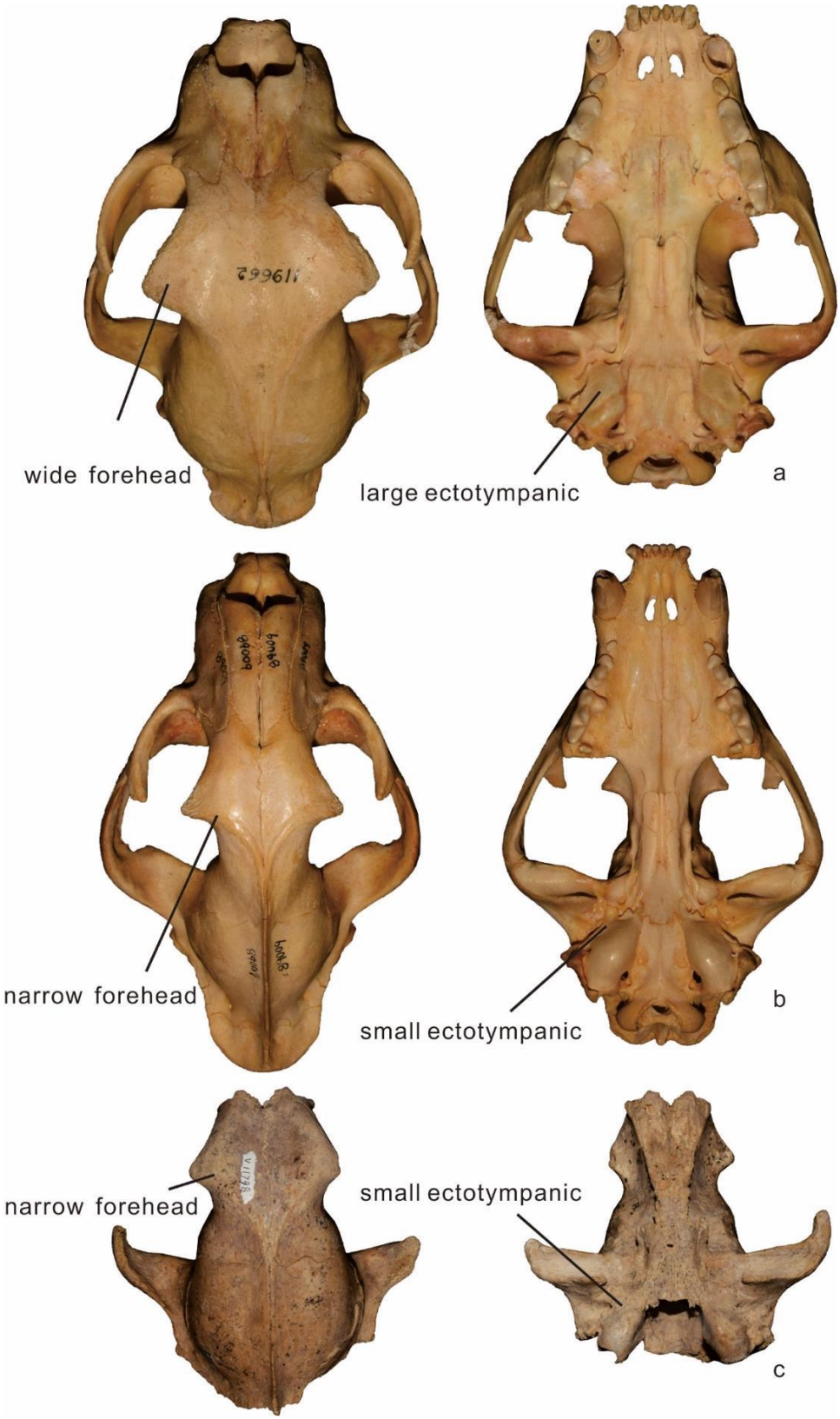


Figure S9. **Cranial comparison of braincase with *P. uncia* and *P. pardus*.** a. modern *P. uncia* AMNH M116952; b. modern *P. pardus*, AMNH M89009; c. *P. pardus* the from Niuyan Cave, V11798.

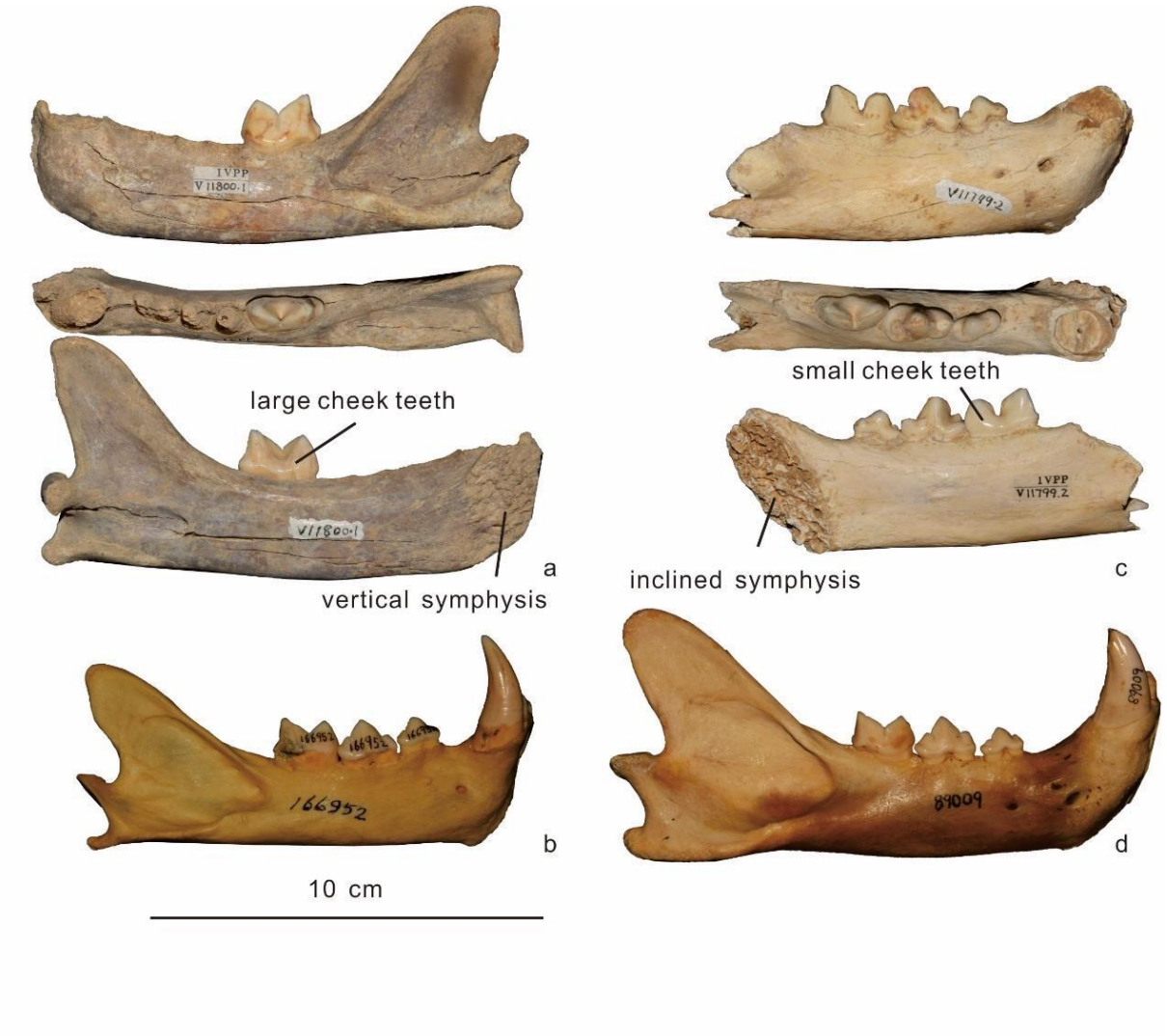


Figure S10. **Mandibles from the Niuyan Cave, and modern comparative specimens**. a. *P. uncia* the from Niuyan Cave, V11800.1; b. *P. pardus* from Niuyan Cave, V11799.2; c. modern *P. uncia* AMNH M116952; d. modern *P. pardus*, AMNH M89009.

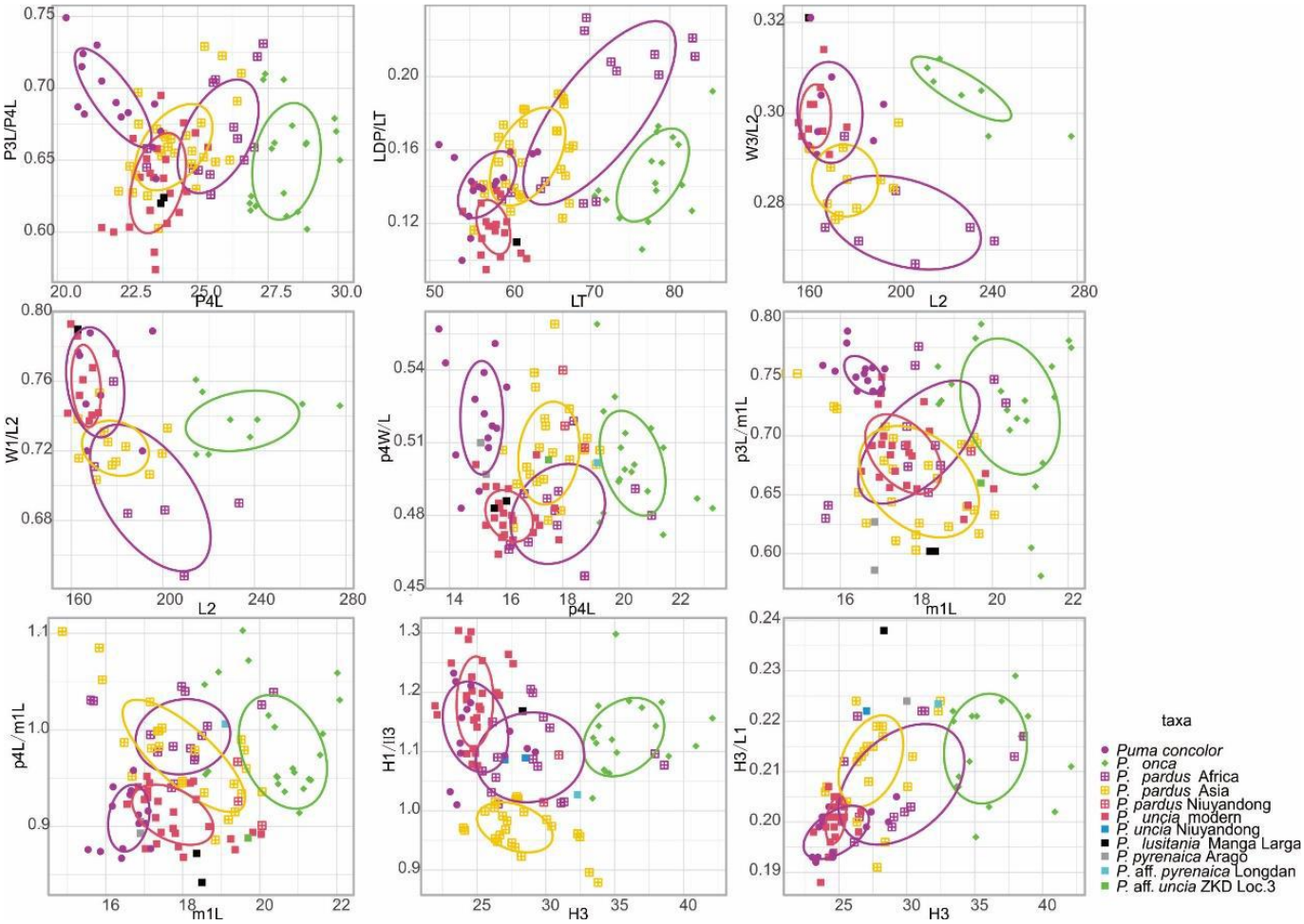


Figure S11. **Metric comparison of P. uncia fossil records and selected living species.**

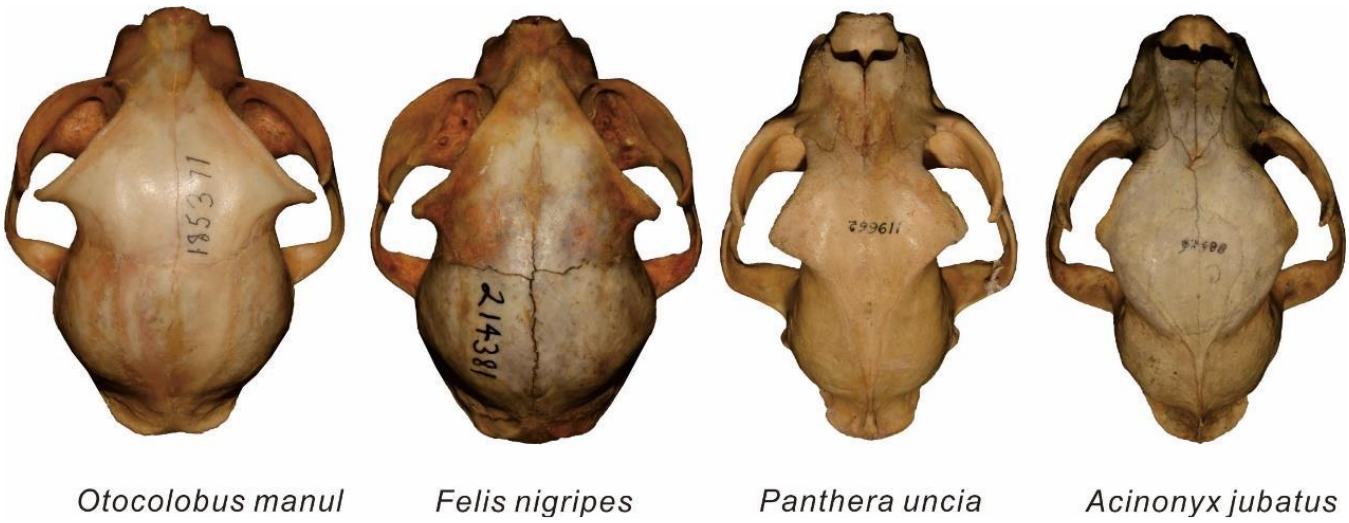


Figure S12. **Comparison of crania**. *Otocolobus manul* AMNH M185371, *Felis nigripes* AMNH M214381, *Panthera uncia* AMNH M119662 and *Acinonyx jubatus* AMNH M88626.

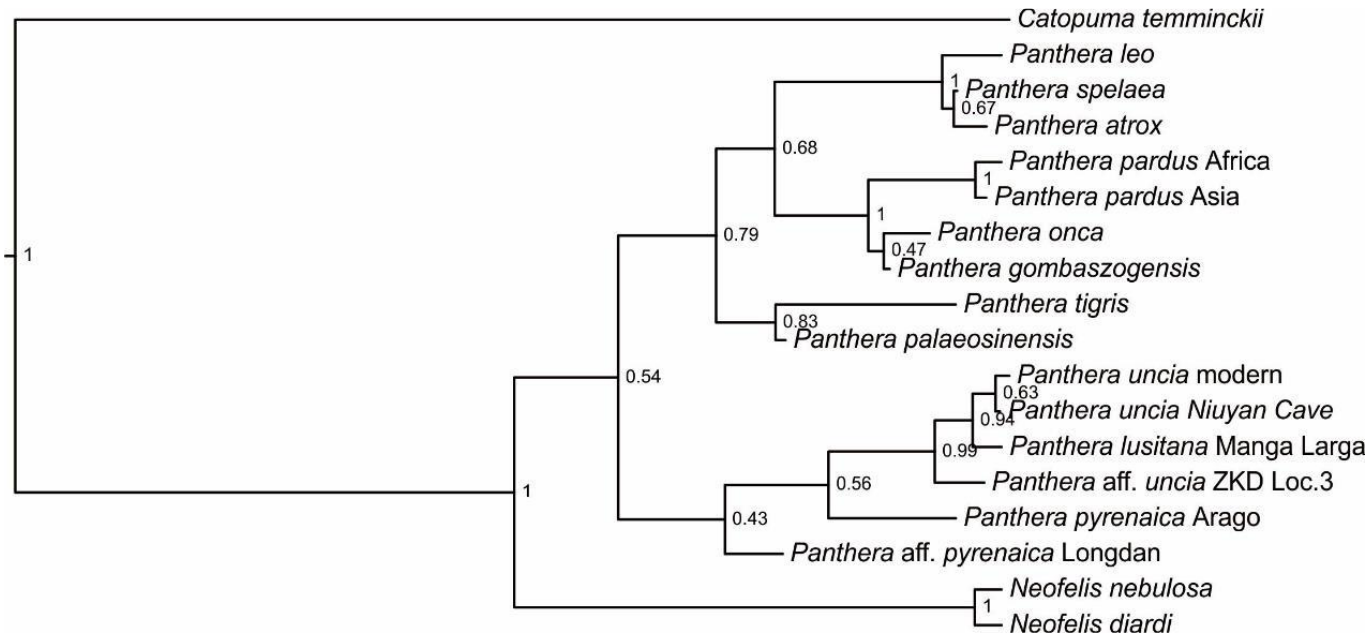


Fig. S13. **The Bayes Inferences using pure morphological data**. The posterior probability is shown in the nodes.

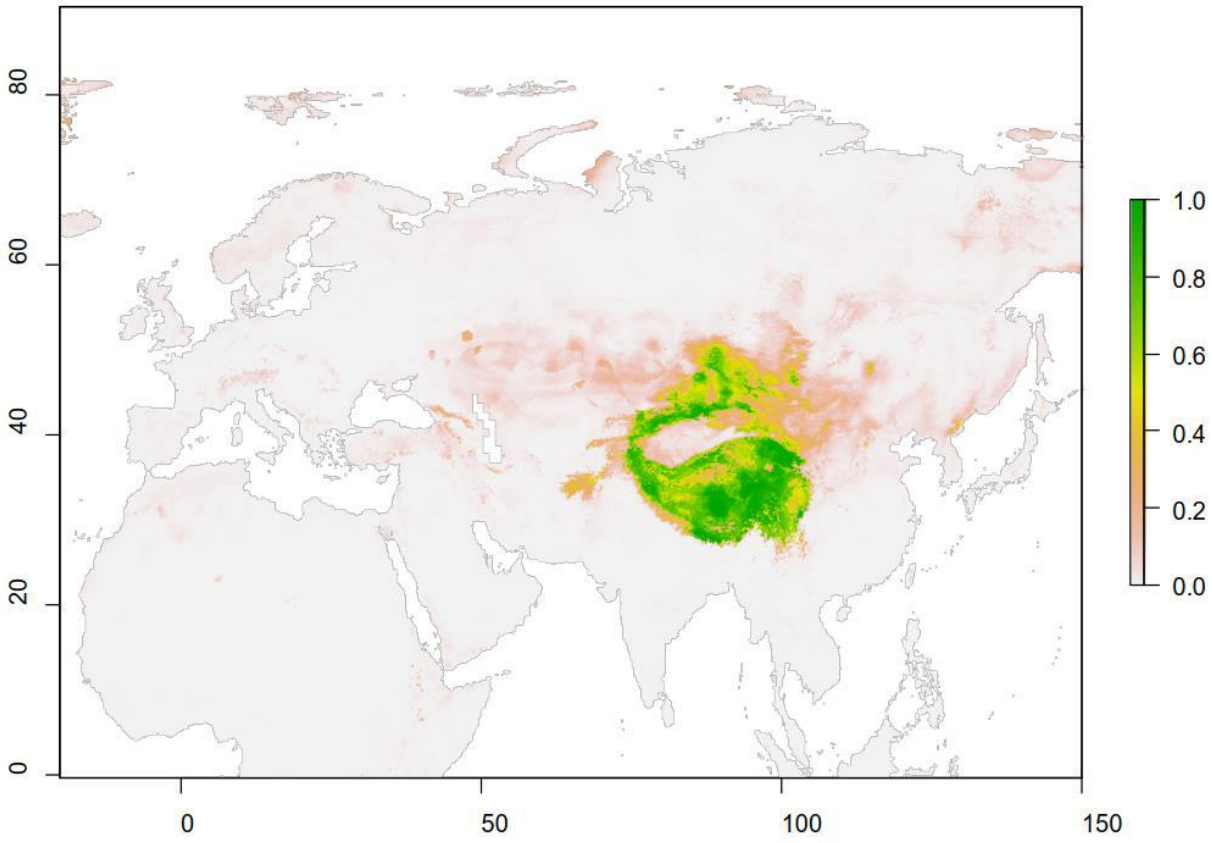


Fig. S14. **The predicted probability of snow leopard presence under the current climate conditions**.

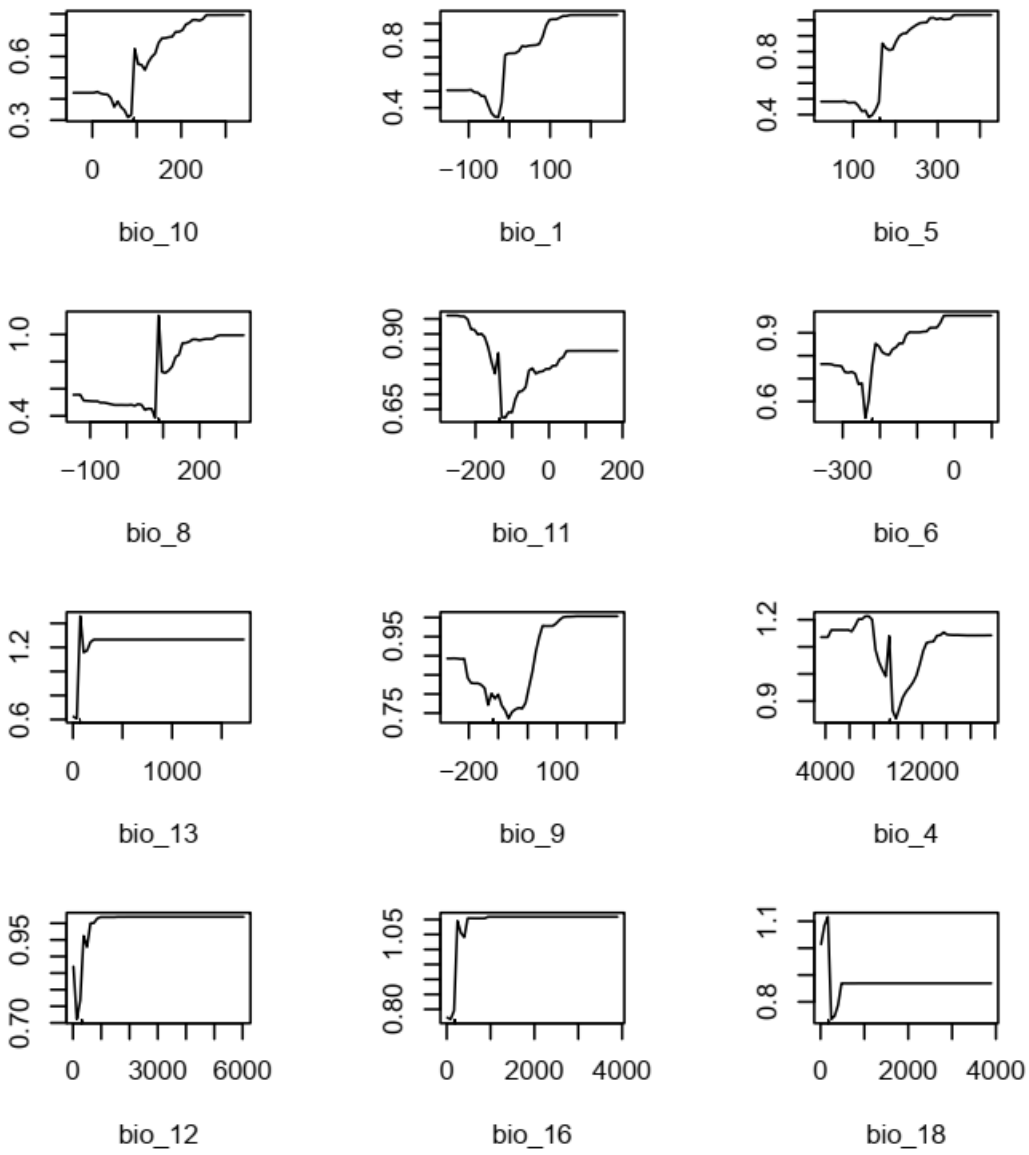


Fig. S15. **The partial effects of the 12 most important elements in the RF analyses.**

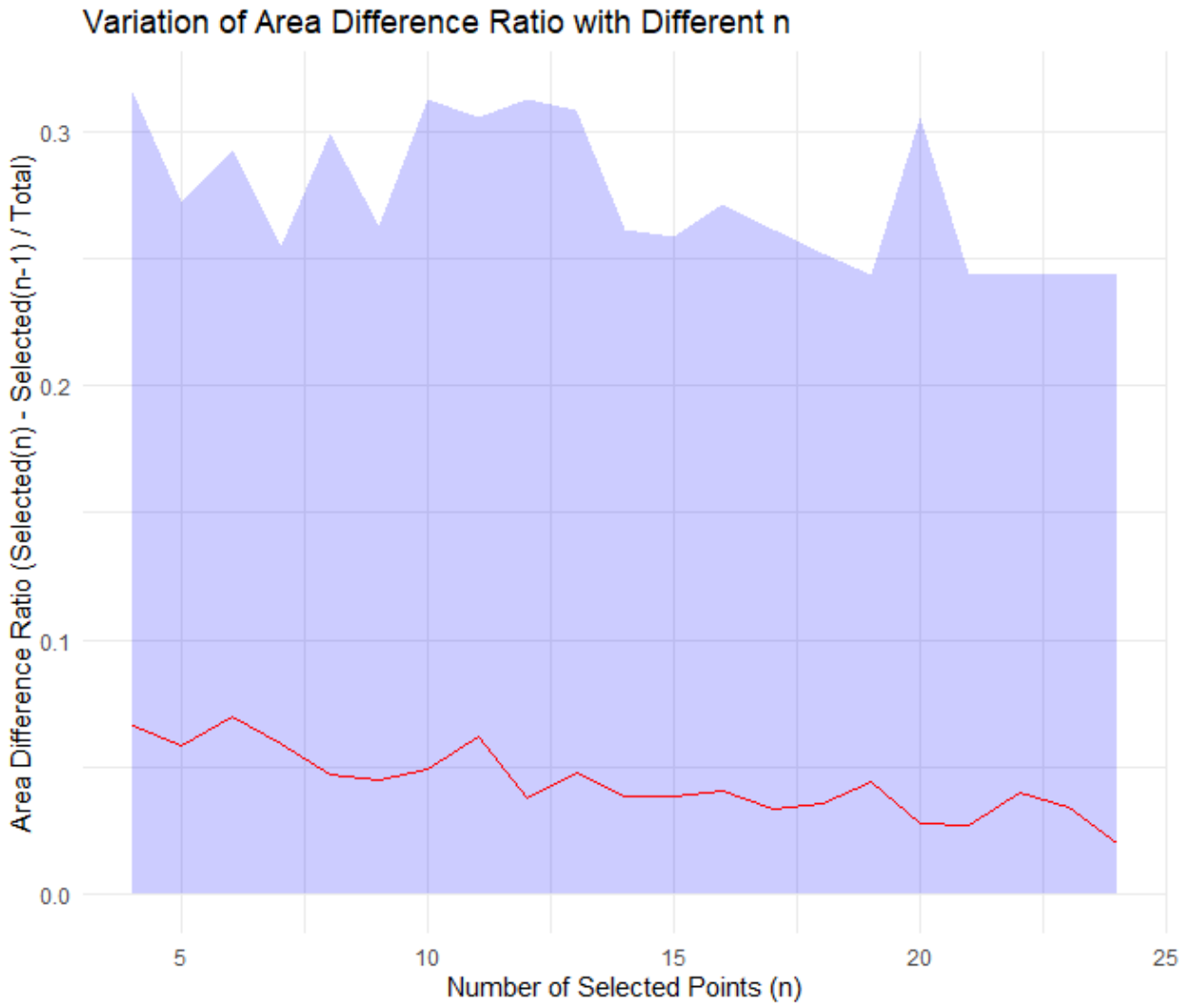


Fig. S16 . Increased area of morphospace of modern *P. uncia* as the specimen number increase, showing a clear tendency of slowing increase.

Table S1. **The muscle angle used in the finite element analyses.** Fossil *Panthera uncia lusitana* and *Panthera* sp. ZKD Loc. 3 use *P. uncia* model, and *Panthera pyrenaica* and *Panthera* aff. *pyrenaica* use *P. pardus* model, based on their mandibular morphology.

Muscle	Species	Angle with Vertical	Vertical Vector of Bite Force	Horizontal Vector of Bite Force	Vertical Component of Bite Force	Horizontal Component of Bite Force
Temporal	*P. uncia*	82,884	0,124	0,992	247,757	2976,892
Temporal	*P. pardus*	90	0	1	0	3000
Masseteric	*P. uncia*	24,095	0,913	0,408	912,87	408,251
Masseteric	*P. pardus*	28,32	0,88	0,474	880,312	474,396

Table S2. **Craniodental measurements of the fossil snow leopard from Longdan, Manga Larga, and Niuyan Cave.**

Nº	**Locality**	**taxa**	**CL**	**CW**	**CW/L**	**P3L**	**P3W**	**P3W/L**	**P4L**	**P4W**	**P4BW**	**P4PaL**	**P4MeL**	**P4W/L**	**P4BW/L**	**P4PaL/L**	**P4MeL/L**
	M. Larga	*P. u. lusitana*				14.7	7.3	0.5	23.7	11.9	7.9	5.9	9.0	0.5	0.3	0.3	0.4
	M. Larga	*P. u. lusitana*	12.3	9.8	0.8	14.9	7.6	0.5	23.8	11.9	8.5	5.3	9.1	0.5	0.4	0.2	0.4
Nº	**Locality**	**taxa**	**M1L**	**M1W**	**M1W/L**	**CL/P4L**	**P3L/P4L**	**M1W/P4L**									
	M. Larga	*P. u. lusitana*	4.4	7.8	1.8		0.6	0.3									
	M. Larga	*P. u. lusitana*				0.5	0.6										
Nº	**Locality**	**taxa**	**L1**	**L2**	**LT**	**W1**	**W2**	**W3**	**LDP**	**LDP/P4**	**LDP/LT**	**W3/W2**	**W2/L2**	**W3/L2**	**W1/L2**	**LP4/L2**	
	M. Larga	*P. u. lusitana*	176.9	162.8	60.9	128.7	73.5	52.2	6.5	0.3	0.1	0.7	0.5	0.3	0.8	0.4	
	M. Larga	*P. u. lusitana*															
Nº	**Locality**	**taxa**	**cL**	**cW**	**cW/L**	**p3L**	**p3W**	**p3W/L**	**p4L**	**p4W**	**p4W/L**						
	M. Larga	*P. u. lusitana*	13.0	10.0	0.8	11.1	6.1	0.6	15.6	7.5	0.5						
	M. Larga	*P. u. lusitana*		10.2		11.1	6.1	0.5	16.0	7.8	0.5						
V11799.1	Niuyan	*P. pardus*							18.1	9.4	0.5						
V11799.2	Niuyan	*P. pardus*				13.4	6.7	0.5	18.0	9.7	0.5						
V11801	Niuyan	*P. pardus*							18.8	9.5	0.5						
V11800.1	Niuyan	*P. pardus*															
V11800.2	Niuyan	*P. pardus*															
V31895	Longdan	*P.* aff. *pyrenaica*	13.6	11.1	0.8				19.2	9.7	0.5						
Nº	**Locality**	**taxa**	**m1L**	**m1PL**	**m1W**	**m1PL/L**	**m1W/L**	**c/m1**	**p3/m1**	**p4/m1**							
	M. Larga	*P. u. lusitana*	18.5	8.6	7.9	0.5	0.4	0.7	0.6	0.8							
	M. Larga	*P. u. lusitana*	18.4	8.9	7.8	0.5	0.4		0.6	0.9							

V11799.1	Niuyan	*P. pardus*	20.1	8.9	9.2	0.4	0.5			0.9							
V11799.2	Niuyan	*P. pardus*	19.4	8.9	9.1	0.5	0.5		0.7	0.9							
V11801	Niuyan	*P. pardus*	19.4	9.5	9.0	0.5	0.5			1.0							
V11800.1	Niuyan	*P. uncia*	20.0	9.6	9.0	0.5	0.5										
V11800.2	Niuyan	*P. uncia*	19.2	9.5	8.8	0.5	0.5										
V31895	Longdan	*P.* aff. *pyrena-ica*	19.1	9.0	10.8	0.5	0.6			1.0							
Nº	**Locality**	**taxa**	**L1**	**LT**	**LDP**	**LM**	**H1**	**W1**	**H2**	**W2**	**H3**	**W3**					
	M. Larga	*P. u. lusitana*	118.9	68.8	11.4	43.7	33.1	15.6	28.4	14.0	28.3	12.5					
	M. Larga	*P. u. lusitana*															
V11799.1	Niuyan	*P. pardus*				49.1	30.3		28.4	16.3	29.9	13.7					
V11799.2	Niuyan	*P. pardus*		78.7	14.9	48.6	33.9	19.2	29.6	15.4	30.9	14.1					
V11801	Niuyan	*P. pardus*			12.3	49.0	31.9	17.6	27.5	15.2							
V11800.1	Niuyan	*P. uncia*	121.9	70.3	7.1	47.6	29.4	12.7	27.7	13.1	27.0	13.1					
V11800.2	Niuyan	*P. uncia*		76.9	11.2	49.6	31.1	17.6	27.9	15.2	28.5	13.6					
V31895	Longdan	*P.* aff. *pyrena-ica*	144.6	80.9	15.1	49.9	33.2	19.5	28.8	14.0	32.3	14.4					
Nº	**Locality**	**taxa**	**LDP/LM**	**H1/H3**	**L3/L1**	**mL/H3**	**H4/L1**	**mL/L1**									
	M. Larga	*P. u. lusitana*	0.3	1.2	0.2	0.7		0.2									
	M. Larga	*P. u. lusitana*															
V11799.1	Niuyan	*P. pardus*		1.0		0.7											
V11799.2	Niuyan	*P. pardus*	0.3	1.1		0.6											
V11801	Niuyan	*P. pardus*	0.3														
V11800.1	Niuyan	*P. uncia*	0.1	1.1	0.2	0.7	0.5	0.2									
V11800.2	Niuyan	*P. uncia*	0.2	1.1		0.7											
V31895	Longdan	*P.* aff. *pyrena-ica*	0.3	1.0	0.2	0.6	0.5	0.1									

Table S3. **Postcranial proportions of *Panthera* spp. and related taxa.**

Taxa	HPrW/HL	HDW/HL	HDH/DW	MC3ip	FPrW/FL	FDW/FL	FDMH/FDLH	MT3ip	ScL/FL	HL/FL	RL/FL	MC3/FL	PL/FL	TL/FL	CL/FL	MT3L/FL
Panthera leo	0.23	0.26	0.65	0.20	0.25	0.21	1.04	0.20	0.76	0.91	0.81	0.31	0.84	0.84	0.29	0.31
Panthera leo	0.24	0.25	0.68	0.20	0.23	0.20	1.05	0.18	0.73	0.89	0.80	0.31	0.82	0.87	0.29	0.34
Panthera leo	0.22	0.25	0.68	0.20	0.24	0.20	1.04	0.18	0.72	0.90	0.82	0.31	0.85	0.85	0.30	0.35
Panthera leo				0.20	0.24	0.19	1.04	0.18	0.72		0.82	0.31	0.84	0.86	0.30	0.36
Panthera leo	0.23	0.27	0.66	0.20	0.24	0.21	1.09	0.18	0.71	0.89	0.83	0.32	0.84	0.87	0.30	0.36
Panthera leo	0.23	0.27	0.66	0.20	0.23	0.20	1.06	0.18	0.71	0.90	0.83	0.31	0.84	0.87	0.29	0.36
Panthera leo	0.23	0.26	0.67	0.19	0.23	0.20	1.06	0.18	0.69	0.86	0.81	0.30	0.81	0.86	0.29	0.35
Panthera leo	0.22	0.26	0.66	0.19	0.23	0.20	1.05	0.17	0.69	0.86	0.81	0.30	0.81	0.86	0.29	0.35
Panthera leo				0.20	0.24	0.20	1.05	0.17	0.73		0.82	0.30	0.83	0.84	0.29	0.34
Panthera leo	0.21	0.25	0.67	0.20	0.24	0.19	1.05	0.17	0.72	0.92	0.83	0.31	0.83	0.84	0.29	0.34
Panthera tigris	0.21	0.26	0.64		0.21	0.20	1.01	0.20	0.65	0.86	0.73		0.83	0.88	0.29	0.33
Panthera tigris	0.22	0.26	0.65	0.21	0.22	0.19	1.01	0.21	0.66	0.86	0.73	0.29	0.85	0.88	0.29	0.33
Panthera tigris	0.24	0.27	0.66	0.22	0.22	0.21	1.02	0.20	0.69	0.86	0.72	0.31	0.84	0.86	0.28	0.35
Panthera tigris	0.23	0.28	0.65	0.22	0.22	0.20	0.99	0.20	0.70	0.86	0.73	0.31	0.85	0.87	0.28	0.35
Panthera tigris	0.24	0.26	0.69	0.22	0.23	0.21	1.04	0.20	0.64	0.87	0.74	0.27	0.83	0.82	0.29	0.33
Panthera tigris	0.24	0.26	0.68	0.22	0.23	0.21	1.03	0.20	0.64	0.87	0.74	0.28	0.84	0.82	0.29	0.33
Panthera tigris	0.22	0.26	0.67	0.20	0.22	0.19	1.02	0.18	0.68	0.87	0.75	0.29	0.84	0.86	0.27	0.34
Panthera tigris	0.21	0.26	0.67	0.20	0.22	0.20	1.02	0.18		0.87	0.74	0.29	0.84	0.87	0.27	0.35
P. pardus	0.18	0.22	0.63	0.18	0.19	0.18	1.00	0.16	0.64	0.90	0.76	0.30	0.78	0.91	0.25	0.36
P. pardus	0.19	0.22	0.63	0.18	0.19	0.17	0.99	0.16	0.65	0.90	0.76	0.30	0.78	0.91		0.36
P. pardus	0.20	0.23	0.66	0.22	0.20	0.19	1.02	0.18	0.70	0.89	0.77	0.28	0.84	0.89	0.26	0.35
P. pardus	0.19	0.24	0.64	0.21	0.21	0.19	1.00	0.18	0.71	0.90	0.76	0.29	0.83	0.89		0.34
P. pardus			0.62	0.20	0.20	0.19	0.96	0.17			0.76	0.29	0.84	0.91	0.27	0.35
P. pardus	0.19	0.22	0.62	0.21	0.20	0.18	0.94	0.17	0.67	0.91	0.76	0.29	0.84			0.35

P. pardus	0.20	0.23	0.64	0.19	0.20	0.19	1.00	0.17	0.64	0.88	0.76	0.31	0.79	0.92	0.28	0.38
P. pardus	0.20	0.23	0.63	0.19	0.20	0.19	0.98	0.17	0.65	0.88	0.76	0.30	0.79	0.92		0.38
P. pardus	0.23	0.25	0.58	0.21	0.22	0.21	1.01	0.18	0.64	0.88	0.71	0.29	0.84	0.93	0.28	0.36
P. pardus	0.23	0.25	0.60	0.21	0.22	0.19	0.94	0.19	0.66	0.90	0.70	0.30	0.83	0.94	0.28	0.36
Neofelis nebulosa	0.20	0.26	0.54		0.21	0.19	1.01	0.17	0.60	0.91	0.72		0.74	0.97	0.26	0.35
Neofelis nebulosa	0.21	0.26	0.57	0.23	0.21	0.19	0.98	0.17	0.61	0.92	0.73	0.27	0.73	0.97	0.26	0.35
Neofelis nebulosa	0.21	0.26	0.52	0.24	0.20	0.20	1.00	0.17	0.58	0.89	0.72	0.26	0.77	0.97		
Neofelis nebulosa	0.22	0.27	0.55	0.24	0.21	0.19	1.02	0.18	0.60	0.89	0.72	0.26	0.77	0.97		0.35
Neofelis nebulosa	0.18	0.24	0.53	0.21	0.20	0.18	0.99	0.17	0.63	0.89	0.71	0.26		0.94	0.28	0.38
Neofelis nebulosa		0.23	0.53	0.21	0.20	0.18	0.93	0.17	0.63	0.89	0.71	0.27		0.95	0.27	0.34
Panthera uncia	0.20	0.25	0.54	0.21	0.22	0.21	0.96	0.16	0.68	0.91	0.79	0.31	0.77	0.99	0.27	0.38
Panthera uncia	0.20	0.25	0.57	0.19	0.23	0.21	0.91	0.16	0.70	0.93	0.81	0.32	0.79	1.02	0.28	0.39
Panthera uncia	0.21	0.24	0.59	0.20	0.23	0.21	0.96	0.16	0.68	0.91	0.80	0.31	0.81	0.99	0.27	0.38
Panthera uncia	0.21	0.24	0.57	0.20	0.22	0.21	0.89	0.16	0.69	0.89	0.80	0.30	0.80	0.98	0.26	0.37
Panthera uncia	0.20	0.25	0.58	0.19	0.22	0.21	1.00	0.16	0.67	0.90	0.82	0.31	0.77	1.01	0.28	0.39
Panthera uncia		0.21	0.58	0.19	0.19	0.17	0.95	0.16	0.70	0.92	0.83	0.31	0.77	1.01	0.27	0.38
Panthera uncia		0.20	0.59	0.19	0.19	0.17	0.94	0.16	0.70	0.92	0.82	0.31	0.78	1.01	0.26	0.38
Panthera onca	0.20	0.26	0.63	0.21	0.21	0.19	1.06	0.18	0.70	0.88	0.75	0.29		0.87	0.27	0.34
Panthera onca	0.21	0.25	0.66	0.21	0.22	0.18	1.03	0.18	0.70	0.88	0.75	0.29		0.87	0.27	0.34
Panthera onca	0.22	0.26	0.65	0.22	0.23	0.19	1.05	0.19	0.74	0.89	0.76	0.29	0.88	0.87	0.28	0.33
Panthera onca	0.22	0.26	0.66	0.23	0.23	0.19	1.00	0.19	0.74	0.89	0.75	0.28	0.88	0.87	0.28	0.33
Panthera onca		0.26	0.63	0.21	0.22	0.20	0.96	0.17	0.72	0.90	0.76	0.29		0.87		0.34
Panthera onca	0.22	0.25	0.63	0.21	0.22	0.19	0.99	0.17	0.72	0.90	0.75	0.29		0.87	0.26	0.34

Table S4. **Occurrences (selected from 758 original records) for snow leopards used in the study**. * "Survey" refers to a line transect survey. ** Including occurrences in India (20 points), Mogolia (9 points), Nepal (5 points), China (5 points), Kyrgyzstan (2 Points), Afghanistan (1 point), and Russia (1 point). *** The regions are national parks in China.

Number of Occurrences	Type	Region	Source
43	Direct observation or camera trapping	All habitats**	GBIF.org. (2021)
164	Survey or camera trapping*	China	Liu et al. (2019)
47	Feces collection or camera trapping	Sanjiangyuan***	Xiao et al. (2019)
15	Survey*	Sanjiangyuan***	Li et al. (2022)
53	Camera trapping	Qilianshan***	Li et al. (2022)
27	Survey*	Qilianshan***	Li et al. (2022)
19	Camera trapping	Wolong***	Wolong National Nature Reserve (2019)
30	Camera trapping	India	Watts et al. (2019)
8	Direct observation	India	Watts et al. (2019)
164	Survey or camera trapping*	Xizang, China	Our data
570	Total	All	All

Table S5: **List of the 19 bioclimatic variables.**

Variable	Description
BIO1	Annual Mean Temperature
BIO2	Mean Diurnal Range
BIO3	Isothermality
BIO4	Temperature Seasonality
BIO5	Max Temperature of Warmest Month
BIO6	Min Temperature of Coldest Month
BIO7	Temperature Annual Range
BIO8	Mean Temperature of Wettest Quarter
BIO9	Mean Temperature of Driest Quarter
BIO10	Mean Temperature of Warmest Quarter
BIO11	Mean Temperature of Coldest Quarter
BIO12	Annual Precipitation
BIO13	Precipitation of Wettest Month
BIO14	Precipitation of Driest Month
BIO15	Precipitation Seasonality
BIO16	Precipitation of Wettest Quarter
BIO17	Precipitation of Driest Quarter
BIO18	Precipitation of Warmest Quarter
BIO19	Precipitation of Coldest Quarter

Table S6. **Basic evaluation parameter of the SDM model.**

AUC	Accuracy (%)	Kappa	Specificity	Sensitivity	Thresh-old	TSS
91,774	87,382	0,49	84	87,931	0,565	71,931

Table S7. **Craniodental differences between the modern and fossil leopard and snow leopard.**

	P. pardus (modern Africa)	*P. pardus* (modern Asia)	*P. pardus* (late Middle and Late Pleistocene Europe)	*P. pardus* (early Middle Pleistocene Europe)	*P. uncia* (modern)	*P. u. lusitana* (Manga Larga)	*P. pyrenaica* (Aragó Cave)	*P.* aff. *pyrenaica* (Longdan)
cranium	long and low	high and short	high and short	long and low	high and short	high and short		
forehead (dorsal view)	narrow	narrow or moderate	narrow or moderate	narrow	wide	wide		
forehead (lateral view)	not concave	not concave	not concave	not concave	concave	concave		
rostrum length	long	long	long or short	long or short	short	short	long	long
auditory bulla flat or inflated	inflated	inflated	inflated	inflated	flat	flat		
ectotympanic chamber	small	small or moderate	small or moderate	small	large	large		
symphysis height	low	low	low	low	high	high	high	low
symphysis orientation	inclined	inclined or vertical	inclined or vertical	vertical	vertical	vertical	vertical	vertical
coronoid process	high	high	high		low	low	high	high
lower border of masseteric fossa	expanded	expanded	expanded		not expanded	not expanded	not expanded	not expanded

Additional dataset: https://www.science.org/doi/10.1126/sciadv.adp5243

Supplementary references

Bacon, A.-M., Demeter, F., Duringer, P., Helm, C., Bano, M., Long, V. T., Thuy, N. T. K., Antoine, P.-O., Mai, B. T., Huong, N. T. M., Dodo, Y., Chabaux, S., & Rihs, S. (2008). The Late Pleistocene Duoi U'Oi cave in northern Vietnam: Palaeontology, sedimentology, taphonomy and palaeoenvironments. Quaternary Science Reviews, 27, 1627–1654.

Bibi, F., Vrba, E., & Fack, F. (2012). A new African fossil caprin and a combined molecular and morphological Bayesian phylogenetic analysis of Caprini (Mammalia: Bovidae). Journal of Evolutionary Biology, 25, 1843–1854.

Breiman, L. (2001). Random forests. Machine Learning, 45, 5–32.

Buzzard, P. J., Li, X., & Bleisch, W. V. (2017). The status of snow leopards Panthera uncia, and high altitude use by common leopards P. pardus, in north-west Yunnan, China. Oryx, 51, 587–589.

Chatar, N., Michaud, M., & Fischer, V. (2022). Not a jaguar after all? Phylogenetic affinities and morphology of the Pleistocene felid Panthera gombaszogensis. Papers in Palaeontology, 8, e1464.

Diedrich, C. G. (2013). Late Pleistocene leopards across Europe–northernmost European German population, highest elevated records in the Swiss Alps, complete skeletons in the Bosnia Herzegowina Dinarids and comparison to the Ice Age cave art. Quaternary Science Reviews, 76, 167–193.

Filoux, A., Lespes, C., Wattanapituksakul, A., & Thongcharoenchaikit, C. (2013). Note about new Pleistocene faunal remains from Tham Prakai Phet, Chaiyaphum Province, Thailand. Journal of Science and Technology, 33, 378.

GBIF.org. (2021). GBIF Occurrence Download. https://doi.org/10.15468/dl.sn4azx

Geraads, D. (1997). Carnivores du Pliocene terminal de Ahl al Oughlam (Casablanca, Maroc) [Carnivores of the terminal Pliocene Ahl al Oughlam (Casablanca, Morocco)]. Geobios, 30, 127–164.

Geraads, D., & Peigné, S. (2016). Re-Appraisal of 'Felis' paniri Ozansoy, 1959 (Carnivora, Felidae) from the Upper Miocene of Turkey: The Earliest Pantherin Cat? Journal of Mammalian Evolution, 24, 415–425.

Ghezzo, E., & Rook, L. (2015). The remarkable Panthera pardus (Felidae, Mammalia) record from Equi (Massa, Italy): Taphonomy, morphology, and paleoecology. Quaternary Science Reviews, 110, 131–151.

Hemmer, H. (1971). Zur Kenntnis pleistozäner mitteleuropäischer Leoparden (Panthera pardus) [On Pleistocene Central European Leopards (Panthera pardus)]. Neues Jahrbuch für Geologie und Paläontologie Abhandlungen, 138, 15–36.

Hemmer, H. (2023). The evolution of the palaeopantherine cats, Palaeopanthera gen. nov. blytheae (Tseng et al., 2014) and Palaeopanthera paniri (Ozansoy, 1959) comb. nov. (Mammalia, Carnivora, Felidae). Palaeobiodiversity and Palaeoenvironments, 103, 827–839.

Jiangzuo, Q., Liu, J., Wagner, J., Dong, W., & Chen, J. (2018). Taxonomical revision of fossil Canis in Middle Pleistocene sites of Zhoukoudian, Beijing, China and a review of fossil records of Canis mosbachensis variabilis in China. Quaternary International, 482, 93–108.

Jiangzuo, Q., Werdelin, L., & Sun, Y. (2022). A dwarf sabertooth cat (Felidae: Machairodontinae) from Shanxi, China, and the phylogeny of the sabertooth tribe Machairodontini. Quaternary Science Reviews, 284, 107517.

Koju, N. P., Buzzard, P., Shrestha, A., Sharma, S., He, K., Li, J., Kyes, R. C., Chen, C., & Beisch, W. V. (2024). Habitat overlap and interspecific competition between snow leopards and leopards in the Central Himalayas of Nepal. Global Ecology and Conservation, 52, e02953.

Li, X., Ma, L., Hu, D., Ma, D., Li, R., Sun, Y., & Gao, E. (2022). Potential range shift of snow leopard in future climate change scenarios. Sustainability, 14, 1115.

Liu, Y., Li, X., Liang, X., Liu, Y., Cheng, C., Li, J., Tang, P., Qi, H., Bian, X., He, B., Xing, R., Li, S., Shi, X., Yang, C., Xue, Y., Lian, X., Awangjiumei, Xierannima, Song, D., Xiao, L., & Lu, Z. (2019). Where and how many? The status of snow leopard (Panthera uncia) density surveys and knowledge gaps in China. Biodiversity Science, 27, 919–931.

Lovari, S., Ventimiglia, M., & Minder, I. (2013). Food habits of two leopard species, competition, climate change and upper treeline: A way to the decrease of an endangered species? Ethology Ecology & Evolution, 25, 305–318.

Lovari, S., Kachel, S., Xueyang, L., & Ferretti, F. (2024). Snow leopard, common leopard, and wolf: Are they good neighbors? In D. Mallon & T. McCarthy (Eds.), Biodiversity of World: Conservation from Genes to Landscapes, Snow Leopards (Second Edition) (pp. 137–147). Academic Press.

Mazak, J. H., Christiansen, P., & Kitchener, A. C. (2011). Oldest known pantherine skull and evolution of the tiger. PLOS ONE, 6, e25483.

Nagel, D. (1999). Panthera pardus vraonensis n. ssp., a new leopard from the Pleistocene of Vraona/ Greece. Neues Jahrbuch für Geologie und Paläontologie Monatshefte, 1999, 129–150.

Pei, W. (1934). On the Carnivora from Locality 1 of Choukoutien. Palaeontologia Sinica, 8, 1–217.

Pei, W. (1987). Carnivora, Proboscidea and Rodentia from Lücheng Gigantopithecus Cave and other caves in Guangxi. Memoirs of Institute of Vertebrate Palaeontology and Palaeoanthropology, Academia Sinica, 18, 1–119.

Qiu, Z., Deng, T., & Wang, B. (2004). Early Pleistocene mammalian fauna from Longdan, Dongxiang, Gansu, China. Palaeontologia Sinica, Science Press.

Salles, L. O. (1992). Felid phylogenetics: Extant taxa and skull morphology (Felidae, Aeluroidea). American Museum Novitates, 3047, 1–67.

Sauqué, V., & Cuenca-Bescós, G. (2013). The Iberian Peninsula, the last European refugium of Panthera pardus Linnaeus 1758 during the Upper Pleistocene. Quaternaire, 24, 13–24.

Sims, M. E. (2012). Cranial morphology of five felids: Acinonyx jubatus, Panthera onca, Panthera pardus, Puma concolor, Uncia uncia. Russian Journal of Theriology, 11, 157–170.

Tao, D., Wanbo, H., & Hongjie, W. (1999). The late Pleistocene mammalian fossils from Niuyan Cave in Mentougou, Beijing, China. Vertebrata PalAsiatica, 37, 156–164.

Tseng, Z. J., Wang, X., Slater, G. J., Takeuchi, G. T., Li, Q., Liu, J., & Xie, G. (2014). Himalayan fossils of the oldest known pantherine establish ancient origin of big cats. Proceedings of the Royal Society B: Biological Sciences, 281, 20132686.

Viret, J. (1954). Le leess à bancs durcis de Saint–Vallier (Drôme) et sa faune de mammifères villafranchiens [The hardened loess of Saint-Vallier (Drôme) and its fauna of Villafranchian mammals]. Nouvelles Archives du Muséum d'Histoire Naturelle de Lyon, 4, 3–67.

Watts, S. M., McCarthy, T. M., & Namgail, T. (2019). Modelling potential habitat for snow leopards (Panthera uncia) in Ladakh, India. PLOS ONE, 14, e0211509.

Werdelin, L., & Lewis, M. E. (2013). Koobi Fora Research Project Volume 7 The Carnivora. California Academy of Sciences.

Wolong National Nature Reserve. (2019). Ten-year monitoring of snow leopard at Wolong.

C

APPENDIX: "3D DIGITAL AND BIOGEOCHEMICAL ANALYSIS OF THE ALGAR DA MANGA LARGA PANTHERINE (*PANTHERA UNCIA LUSITANA*)"

On this appendix the full results of the molecular analyses performed to the type specimen of *Panthera uncia lusitana* are shown as presented by the laboratories.

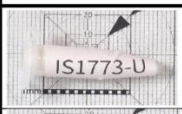
C.1 U-Th dating

isobar science

Sample Tracking Sheet

Submitter Name: Dr. Darío Estraviz-López,NOVA school of Science and Technology (FCT NOVA)
Isobar Client ID: **IS000279**
Sample Submission No.: **IS-207**
Isotopic analysis: U-Th Geocgronology

Progress Summary	
Tasks	**Date Completed**
Received	9/13/2024
Sample Login	9/16/2024
Preparation	9/27/2024
Digestion	10/10/2024
Extraction Chromatography	10/10/2024
Measurement	10/18/2024-10/19/2024
Data reduction	10/21/2024
Data Quality Control	10/21/2024
Report Preparation	10/21/2024
Final Quality Control	10/22/2024
Report Submission	10/22/2024

	Lab Identification	Submitter ID	Material	Image
1	IS-1773	MA.LA01	Bones (Not-ashed)	
2	IS-1774	MA.LA02	Tooth Enamel	
3				
4				
5				
6				
7				
8				
9				
10				

U-Th Test Results

Report Date: 10/22/2024

Please find enclosed the U-Th geochronology results for two bone and tooth enamel samples submitted by Dr. Darío Estraviz-López, NOVA school of Science and Technology (FCT NOVA) on 9/13/2024.

Samples were screened for uranium and thorium after digestion. Uranium and thorium were isolated from the samples by extraction chromatography and analyzed by MC-ICP-MS (Thermo Fisher Neptune Plus™) following the methods described by Pourmand et al., 2013 and Pourmand and Dauphas, 2010.

U-Th dates are reported as years before present (y B.P.). The analytical accuracy and precision for uranium and thorium were assessed by multiple measurements of certified reference material CRM-112A and IRMM-035 respectively during the analysis. Uncertainties on the U-Th ages are reported at the 95% confidence interval (CI).

As always, if you have any questions or would like to discuss the results, don't hesitate to contact us.

Arash Sharifi, Ph.D.
Vice President of Laboratory Operations

Signature

Analysis Details

Submitter: Dr. Darío Estraviz-López,NOVA school of Science and Technology (FCT NOVA)
Client Isobar ID: IS000279
Sample Submission No.: IS-207
Material submitted: Bone and Tooth Enamel
Date received: 09/13/2024
Date reported: 10/22/2024
Isotopic analysis: U-Th geochronology
Method: Extraction chromatography using *Eichrom* UTEVA resin followed by multi-collector inductively coupled plasma mass spectrometry (MC-ICP-MS) (Pourmand et al., 2013 and Pourmand and Dauphas 2010).
Instrument: Thermo Fisher Neptune Plus™ MC-ICP-MS with an Apex-Q desolvation nebulizer

Results

Lab ID	Submitter ID	Material	Uncorrected Age (y BP)	± 95% CI	Corrected Age (y BP)	± 95% CI
IS-1773*	MA.LA01	Bones (Not-ashed)	>500,000	-	-	-
IS-1774*	MA.LA02	Tooth Enamel	>500,000	-	-	-

** Calculated age exceeds the U-Th permissible clock. Samples show open system behavior, see the graph.*

Lab ID	Submitter ID	Material	U ng/g	± 95% CI	Th ng/g	± 95% CI
IS-1773	MA.LA01	Bones (Not-ashed)	3203.26	7.70	298.03	3.46
IS-1774	MA.LA02	Tooth Enamel	4658.22	24.47	777.16	5.12

Lab ID	Submitter ID	^{234}U ng/g	± 95% CI	^{235}U ng/g	± 95% CI	^{238}U ng/g	± 95% CI
IS-1773	MA.LA01	0.2949	0.0012	22.79	0.06	3180.18	7.69
IS-1774	MA.LA02	0.4412	0.0033	33.15	0.23	4624.62	24.47

Lab ID	Submitter ID	^{230}Th ng/g	± 95% CI	^{232}Th ng/g	± 95% CI
IS-1773	MA.LA01	0.11942	0.00275	297.91	3.46
IS-1774	MA.LA02	0.16777	0.00361	776.99	5.12

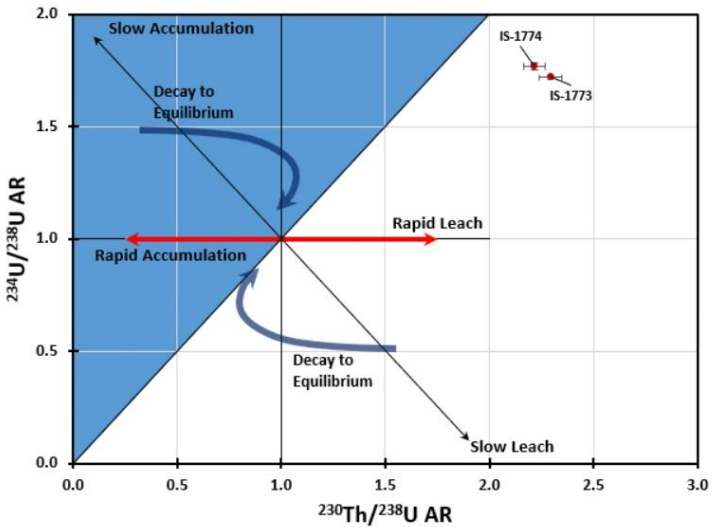
Lab ID	$\delta^{234}U_{initial}$§	± 95% CI	$^{234}U/^{238}U$ Activity Ratio*	± 95% CI	$^{230}Th/^{238}U$ Activity Ratio*	± 95% CI
IS-1773	719.02	8.94	1.71902	0.00894	2.29402	0.05364
IS-1774	768.62	16.67	1.76862	0.01667	2.21605	0.04945

§ $\delta^{234}U = ([^{234}U/^{238}U]_{initial} - 1)*1000$

* *Measured ratios corrected for acid blank, abundance sensitivity, hydride, and spike contribution. The activity ratios are from Monte Carlo Simulation.*

Lab ID	Submitter ID	Material	$^{230}Th/^{232}Th$ Activity Ratio*	± 95% CI	$^{232}Th/^{238}U$ Activity Ratio*	± 95% CI
IS-1773	MA.LA01	Bones (Not-ashed)	74.84848	1.93564	0.03065	0.00037
IS-1774	MA.LA02	Tooth Enamel	40.31415	0.91419	0.05497	0.00050

* *Measured ratios corrected for acid blank, abundance sensitivity, hydride, and spike contribution. The activity ratios are from Monte Carlo Simulation.*



Plot of $^{234}U/^{238}U$ activity ratios against $^{230}Th/^{238}U$ activity ratios, modified after Osmond and Ivanovich (1992). This graphical representation is for reference only and should not be construed as an interpretation of these test results.

Methods

The samples are received in the form of homogenized powder. Around 20 mg of homogenized sample was dissolved in 0.45 M HNO_3 to minimize leaching of uranium and thorium from detrital materials.

Isolation of uranium and thorium from each sample was achieved by extraction chromatography using *Eichrom* UTEVA resin following the methods of Pourmand et al., 2013 and Pourmand and Dauphas, 2010. High precision uranium and thorium isotope analysis was performed on a Thermo Fisher Neptune Plus™ MC-ICP-MS with an Apex-Q desolvation nebulizer. Each sample measurement was bracketed with measurements of two wash solutions and two certified reference materials (CRM-112A and IRMM-035 for uranium and thorium respectively)

Uncertainties on the U-Th ages are reported at the 95% confidence interval (CI) and include propagation of systematic and random uncertainties by Monte Carlo simulation of measured analytical uncertainties on isotope ratios, and those associated with U and Th isotope decay constants.

Age calculation and propagation of the uncertainties were performed by using Monte Carlo simulation (Pourmand et al., 2013) and by taking into account the measured isotopic ratios of U and Th derived along with other variables such as the spike mass and concentration, sample mass, the decay constants of U and Th isotopes along with their associated uncertainties. The average initial $^{230}Th/^{232}Th$ activity ratio of 0.6±0.2 is used to correct for contribution of the detrital fraction to ^{230}Th.

References

Pourmand, A. and Dauphas, N., 2010. Distribution coefficients of 60 elements on TODGA resin: Application to Ca, Lu, Hf, U and Th isotope geochemistry. Talanta 81, 741-753.

Pourmand, A.; Tissot, F.L.H.; Arienzo, M. and Sharifi, A., 2013: Introducing a Comprehensive Data Reduction and Uncertainty Propagation Algorithm for U-Th Geochronometry with Extraction Chromatography and Isotope Dilution MC-ICP-MS. Geostandards and Geoanalytical Research, DOI: 10.1111/j.1751-908X.2013.00266.x.

Osmond, J. K. & Ivanovich, M. (1992). Uranium-series mobilization and surface hydrology. In (M. Ivanovich & R. S. Harmon, Eds), Uranium-series disequilibrium: applications to earth. marine and environmental sciences. Clarendon Press 2nd edition, Oxford, Chap. 8, pp. 259–289.

C.2 Nitrogen quantification

Servizos de Apoio á Investigación
Edificio de Servizos Centrais de Investigación
Campus de Elviña, s/n
15071 A Coruña

Unidade de Técnicas Instrumentais de Análise (UTIA)
utia.sai@udc.gal | 981 167 067 ext. 2074/2123

Ensaio solicitado:	Determinación de nitróxeno e carbono mediante análise elemental (combustión)
Período de realización:	do 10/xul/2024 ao 12/xul/2024
Usuario A-0003-IUX:	Aurora Grandal D'Anglade
Autorizado:	Aurora Grandal D'Anglade
Depto./Área:	Instituto Universitario de Xeoloxía Instituto Universitario de Xeoloxía
Enderezo:	UNIVERSIDADE DA CORUÑA Edificio de Servizos Centrais de Investigación Campus de Elviña, s/n 15071 A Coruña
Data de entrada:	8/xul/2024
Núm. SAI:	2024/23654
Descrición:	Polvo de hueso.
Nome das mostras:	MA.LA.1 ELE
Mostraxe:	Realizado polo/a cliente/usuario/a. Os SAI fanse responsables dos resultados obtidos nas análises das mostras recibidas nos seus laboratorios, sen mediar ningunha responsabilidade sobre a validez ou representatividade de ditas mostras

Método de ensaio

A análise realizouse empregando un analizador elemental FlashEA112 (ThermoFinnigan). A mostra, pésase con precisión nunha cápsula de estaño nunha balanza MX-5 (Mettler Toledo). Posteriormente analízase mediante combustión instantánea nun tubo de cuarzo recheo de WO_3 e cobre, mantido a 1020º C.

Resultados

Mostra	N.º SAI	Peso (mg)	% N	% C
MA.LA.1 ELE	2024/23654	3.051	< 0,05	12.58

Informe emitido por: Servicios de Apoyo a la Investigación de la Universidad de A Coruña

Responsable do informe

María Lema Grille
Técnico dos SAI

UNIVERSIDADE DA CORUÑA

Non debe reproducirse este informe excepto na súa totalidade, sen a aprobación por escrito deste laboratorio
Este documento unicamente será valido se nel aparece a sinatura do técnico responsable do ensaio
Teléfono 981 167 067 - Fax 981 167 068 - ucla.sai@udc.es

C.3 δ 18O and δ 13C in bioapatite

Servizos de Apoio á Investigación
Edificio de Servizos Centrais de Investigación
Campus de Elviña, s/n
15071 A Coruña

Unidade de Técnicas Instrumentais de Análise (UTIA)
utia.sai@udc.gal | 981 167 067 ext. 2074/2123

Ensaio solicitado:	Determinación de δ13C e δ18O en carbonato
Período de realización:	do 8/xan/2025 ao 20/xan/2025
Usuario A-0003-IUX:	Aurora Grandal D'Anglade
Autorizado:	Aurora Grandal D'Anglade
Depto./Área:	Instituto Universitario de Xeoloxía Instituto Universitario de Xeoloxía
Enderezo:	UNIVERSIDADE DA CORUÑA Edificio de Servizos Centrais de Investigación Campus de Elviña, s/n 15071 A Coruña
Data de entrada:	7/xan/2025
Núm. SAI:	2025/00127
Información aportada polo cliente:	Carbonato de esmalte dental O laboratorio non se responsabiliza da información aportada polo cliente. Os nomes das mostras e as referencias do cliente son sempre información aportada polo cliente.
Nome das mostras:	MA.LA.1.CO
Mostraxe:	Realizado polo/a cliente/usuario/a. Os SAI fanse responsables dos resultados obtidos nas análises das mostras recibidas nos seus laboratorios, sen mediar ningunha responsabilidade sobre a validez ou representatividade de ditas mostras

Método de ensaio

Determinación nun analizador GasBench II (ThermoFinnigan) unido a un espectrómetro de masas de relacións isotópicas de isótopos estables MAT253 (ThermoFinnigan). Pesáronse 2 mg de mostra en viais de 12 mL que posteriormente se evacuaron con helio. Sumáronse100 µL de ácido ortosfosfórico do 99% (H_3PO_4) a cada mostra e mantiveronse a 26ºC,durante 24 horas ate o momento da análise. O CO_2 xerado separouse doutros gases nunha columna PoraplotQ (25m,0.32 mm, Varian) mantida a 70ºC. O sistema calibrouse con NBS19 , NBS18, CO-8 e LSVEC (IAEA, Viena, Austria). Os resultados exprésanse como δ13C (‰) vs. VPDB e δ18O (‰) vs.VPDB.

Resultados

Muestra	Nº SAI	δ 13CVPDB(‰)	δ 18OVPDB(‰)
MA.LA.1.CO	2025/00127	-10.79	-4.06
		-10.81	-4.48

Responsable do informe

María Lema Grille

Técnico dos SAI
Informe emitido por: Servicios de Apoyo a la Investigación de la Universidad de A Coruña

UNIVERSIDADE DA CORUÑA

Non debe reproducirse este informe excepto na súa totalidade, sen a aprobación por escrito deste laboratorio
Este documento unicamente será valido se nel aparece a sinatura do técnico responsable do ensaio
Teléfono 981 167 067 - Fax 981 167 068 - ucla.sai@udc.es

D

APPENDIX: "PLEISTOCENE FOSSIL URSIDAE FROM PORTUGAL: MORPHOMETRY AND PALEOBIOLOGICAL INFERENCES"

D.1 Census of remains from different Portuguese sites

Overall census of remains

Site	Elements with at least one usable measurement	MNI	Notes
Furninha	454	20	MNI calculated for different layers
Oliveira	2	2	Many more bones under study, MNI calculated for different layers
Caldeirão	6	3	Two m1 very worn, missing; MNI calculated in base of layers
Escoural	3	2	More inventoried, but uncatalogued bones in storage
Fontainhas	58	2	Most of remains from just one individual
Serra de Molianos	12	2	Absolute lack of context
Total	535	35	

Furninha

Part of the body	Number of elements	MNI
Skull and mandible	9	
Teeth	123	
Axial bones	13	
Anterior long bones	28	
Posterior long bones	17	
Carpus	8	
Tarsus	22	
Metacarpals	37	

Metatarsals	33	
Phalanges	163	
Other bones	1	
TOTAL	**454**	**20 (different layers)**

Oliveira

Part of the body	Number of elements
Posterior long bones	1
Phalanges	1
TOTAL	**2**
MNI	**2 (different layers)**

Caldeirão

Part of the body	Number of elements
Teeth	1
Metatarsals	1
Phalanges	4
TOTAL	**6**
MNI	**3 (different layers)**

Escoural

Part of the body	Number of elements
Teeth	3
TOTAL	**3**
MNI	**2 (two m2s)**

Fontainhas

Part of the body	Number of elements
Skull and mandible	2
Teeth	23
Axial bones	5
Anterior long bones	6
Posterior long bones	7
Carpus	2
Tarsus	2
Metacarpals	1
Metatarsals	3
Phalanges	7

TOTAL	**58**
MNI	**2 (three m3s)**

Serra de Molianos

Part of the body	Number of elements
Teeth	6
Axial bones	1
Anterior long bones	4
Metacarpals	1
TOTAL	**12**
MNI	**2 (2 left radii)**

Number of elements per body part and site and MNI (this number does not include at least four extra juveniles).

	Furninha	Fontainhas	Serra de Molianos	Caldeirão	Escoural	Oliveira		TOTAL
Skull and mandible	9	2						11
Teeth	123	23	6	1	3			156
Axial bones	13	5	1					19
Anterior long bones	28	6	4					38
Posterior long bones	17	7				1		25
Carpus	8	2						10
Tarsus	22	2						24
Metacarpals	37	1	1					39
Metatarsals	33	3		1				37
Phalanges	163	7		4		1		175
Other bones	1							1
TOTAL	454	58	12	6	3	2		535
NMI	20	2	2	3	2	2		31

D.2 Measurements of the material

Canine: Length vs breadth

Specimen	Site	L	B
SM219.34	Serra de Molianos	17,41	12,61
FO.I-87	Fontainhas	24,21	16,14
FO.I-88	Fontainhas	23,52	17,67
FO.I-84	Fontainhas	22,73	18,11
FO.I-85	Fontainhas	23,38	17,95
GFP-No nº 62 2/2	Furninha	22,05	15,87
GFP-1373	Furninha	20,88	16,52
GFP-1525.1	Furninha	15,46	12,64
GFP-1339	Furninha	21,44	18,4
FO.I-81	Fontainhas	27,32	16,02
FO.I-83	Fontainhas	23,31	17,71
FO.I-86	Fontainhas	17,83	18,05
GFP-1382	Furninha	23,18	17,11
GFP-25665.1	Furninha	23,6	17,2
GFP-1354	Furninha	19,33	14,91
GFP-1356.1	Furninha	24,28	18,68
GFP-No Nº Exhibit	Furninha	20,54	16,17
GFP-1328	Furninha	21,9	15,32
ARLU-38	Pleistocene Galicia	20,78	14,02
ARLU-38	Pleistocene Galicia	21,28	14,36
SIPA-16	Pleistocene Galicia	16,47	13,25
SIPA-56	Pleistocene Galicia	18	13,31
SIPA-20	Pleistocene Galicia	19,37	17,04
SIPA-134	Pleistocene Galicia	21,42	15,68
ARLU-54	Pleistocene Galicia	19,45	13,6
ARLU-66	Pleistocene Galicia	20,69	14,3
SIPA-19	Pleistocene Galicia	17,73	13,37
SIPA-14	Pleistocene Galicia	17,58	13,29
SIPA-54	Pleistocene Galicia	19,76	15,03
SIPA-55	Pleistocene Galicia	19,55	14,59
SIPA-129	Pleistocene Galicia	21,79	15,87
SIPA-128	Pleistocene Galicia	21,4	15,92
LCF-003-1996	Holocene Galicia	25,46	17,86
LCF-002-1996	Holocene Galicia	26,56	18,01
LCF-154	Holocene Galicia	19,8	13,09
LCF-155	Holocene Galicia	19,44	13,06
EIX-019	Holocene Galicia	20,11	14,05

GP-4	Holocene Galicia	16,97	12,73
GP-5	Holocene Galicia	17,33	12,46
PUR-Lu-41	Holocene Galicia	22,94	16,86
SH5-97-U29-7	Holocene Galicia	19,68	12,91
SH5-97-U29-6	Holocene Galicia	20,01	13,26
SH5-98-V29-7	Holocene Galicia	21,22	16,16
SH5-98-S30-6	Holocene Galicia	21,63	15,88
SH5-97-N19-4	Holocene Galicia	19,04	11,98
SH5-98-T30-016	Holocene Galicia	20,57	14,08
TA-109	Holocene Galicia	19,62	13,82
TA-192	Holocene Galicia	19,37	13,69
TA-199	Holocene Galicia	22,67	16,15
PVR-013	Holocene Galicia	25,45	17,69
PVR-014	Holocene Galicia	24,3	17,46
CB-010	Holocene Galicia	20,46	18,2
LCF-169	Holocene Galicia	17,94	12,15
LCF-170	Holocene Galicia	18,55	12,29
LCF-001-1996	Holocene Galicia	23,64	17,91
LCF-001-1996	Holocene Galicia	22,81	18
CCV-000	Holocene Galicia	20,55	16,57
CCV-007	Holocene Galicia	18,05	15,31
CGLL-003	Holocene Galicia	21,14	16,57
PUR-Lu-39	Holocene Galicia	21,78	16,94
PUR-Lu-38	Holocene Galicia	21,01	17,01
PVR-012	Holocene Galicia	18,16	13,18
PVR-004	Holocene Galicia	19,06	13,14
PVR-016	Holocene Galicia	20,24	15,17
PVR-008	Holocene Galicia	22,21	16,42
RT-002	Holocene Galicia	19,45	14,48
RT-002	Holocene Galicia	20,05	15,81
Ca-Le-2	Holocene Galicia	18,56	12,45
SH5-98-U30-001	Holocene Galicia	18,57	13,43
SH5-98-U30-001	Holocene Galicia	18,49	13,7
TA-110	Holocene Galicia	17,14	13,88
VA/87/13E/1	Holocene Galicia	19,48	13,21
VA87/PROSP/12D/9	Holocene Galicia	21,21	15,54
VA88/16E/391	Holocene Galicia	20,06	16,02
AC1	Modern	17,34	12,16
AC1	Modern	18,74	12,6
LE1	Modern	21,08	16,39
LE1	Modern	21,36	16,4
QU	Modern	18,5	11,2
QU	Modern	18	11,4
AC1	Modern	17	12,22
AC1	Modern	17,53	12,25

AC2	Modern	14,68	10,98
AC2	Modern	14,86	11,04
LE1	Modern	19,6	16,39
LE2	Modern	19,96	16,04
QU	Modern	15,8	11
QU	Modern	16,7	10,5
CEZ-151	A Ceza	21,3	16,65
CEZ-776	A Ceza	27,32	19,2
EI-1149	Eirós	21,9	17,9
EI-1541	Eirós	23	18,1
EI-1542	Eirós	24	18,5
EI-1222	Eirós	24,7	18,7
EI-1811	Eirós	21,6	18,7
EI-999	Eirós	24,1	19,1
EI-1120	Eirós	22,8	19,2
EI-1104	Eirós	24,6	20,1
EI-999	Eirós	26,6	20,4
EI-6	Eirós	24,2	21,4
EI-1242	Eirós	24,1	22,5
EI-1543	Eirós	28,1	23
EI-1392	Eirós	32,3	24,2
EI-1392	Eirós	30,3	25,4
EI-1394	Eirós	19,2	14,3
EI-1101	Eirós	19,2	14,7
EI-1105	Eirós	19,7	14,7
EI-1618	Eirós	21,3	15
EI-809	Eirós	21,7	15,1
EI-814	Eirós	21,3	15,2
EI-1119	Eirós	20,7	15,3
EI-1394	Eirós	19,8	15,3
EI-1043	Eirós	20,9	15,8
EI-1395	Eirós	24,5	16,5
EI-1004	Eirós	22,1	16,8
EI-1811	Eirós	20	17
LI-272	Liñares	25,91	18,84
LI-273	Liñares	24,5	19,16
LI-271	Liñares	26,46	17,71
LI-1	Liñares	23,58	16,59
LI-1100	Liñares	21,2	15,4
LI-1000	Liñares	22,3	17,3
LI-273	Liñares	24,13	18,45
LI-272	Liñares	27,21	19,69
LI-271	Liñares	25,11	17,52
LI-1100	Liñares	20,6	15,8
LI-841	Liñares	23,8	16,6

P4: Length vs breadth

Specimen	Site	L	B
FO.I-157	Fontainhas	19,15	12,85
FO.I-155	Fontainhas	19,15	14,02
GFP-104	Furninha (Holocene)	16,08	11,556
GFP-1366.2	Furninha (7,5)	17,24	13,98
GFP-1363.1	Furninha (7,5)	18,43	15,01
GFP-1363.2	Furninha (7,5)	16,75	13,24
GFP-1363.4	Furninha (7,5)	17,94	15,72
GFP-1363.5	Furninha (7,5)	15,65	12,32
ARLU-38	Pleistocene Galicia	16,9	13,62
ARLU-38	Pleistocene Galicia	17,47	13,65
SIPA-16	Pleistocene Galicia	14,8	12,22
SIPA-56	Pleistocene Galicia	16,2	12,3
SIPA-57	Pleistocene Galicia	16,27	12,92
SIPA-135	Pleistocene Galicia	16,83	12,82
SIPA-140	Pleistocene Galicia	17,57	13,39
CB-010	Holocene Galicia	17,61	14,55
CB-010	Holocene Galicia	17,49	14,6
LCF-001-1996	Holocene Galicia	15,5	13,31
LCF-001-1996	Holocene Galicia	16,31	13,03
LCF-169	Holocene Galicia	14,92	11,96
CGCH-015	Holocene Galicia	16,7	14,37
CGCH-016	Holocene Galicia	17,18	13,92
RT-001	Holocene Galicia	17,43	10,95
Pur-Lu-47	Holocene Galicia	16,32	12,8
Pur-Lu-48	Holocene Galicia	16,67	12,91
SAB-82	Holocene Galicia	17,17	12,33
SH5-98-T28-013	Holocene Galicia	15,02	9,45
SH5-97-N20-2	Holocene Galicia	15,05	12,17
SH5-97-N20-2	Holocene Galicia	15,33	11,81
SH5-98-U30-001	Holocene Galicia	14,55	12,37
SH5-98-U30-001	Holocene Galicia	14,34	13,12
LE1	Modern	14,98	13,65
LE1	Modern	14,1	12,59
MZB82-7005	Modern	14,23	13,21
MZB82-7005	Modern	13,15	12,64

P4: PCA

Specimen	Site	L	B	Hpa	Hme	Hde	Lpa-me	Lpa-de	Lme-de
FO.I-157	Fontainhas	19,15	12,85	10,39	7,16	5,77	7,9	9,23	7,26
FO.I-155	Fontainhas	19,15	14,02	10,81	7,56	6,55	8,91	11,53	8,71
GFP-104	Furninha (Holo-cene)	16,08	11,556	8,93	6,67	6,14	6,2	6,76	5,62
GFP-1366.2	Furninha (7,5)	17,24	13,98	11,28	9,37	7,33	5,88	6	5,2
GFP-1363.1	Furninha (7,5)	18,43	15,01	8,93	8,92	7,82	7,74	6,5	7,59
GFP-1363.2	Furninha (7,5)	16,75	13,24	9,01	6,21	5,08	8,65	10,19	6,93
GFP-1363.4	Furninha (7,5)	17,94	15,72	10,15	9,18	6,88	5,82	6,58	6,23
GFP-1363.5	Furninha (7,5)	15,65	12,32	8,74	6,69	4,13	4,82	6,39	5,01
ARLU-38	Pleistocene Galicia	16,9	13,62	10,37	8,81	5,29	7,02	7,61	7,26
ARLU-38	Pleistocene Galicia	17,47	13,65	10,43	8,74	7,08	7,54	8,97	8,18
SIPA-16	Pleistocene Galicia	14,8	12,22	9,29	6,15	4,93	6,14	6,88	5,81
SIPA-56	Pleistocene Galicia	16,2	12,3	6,82	5,55	5,39	6,53	7,17	5,67
SIPA-57	Pleistocene Galicia	16,27	12,92	7,94	4,98	5,41	6,59	7,07	6,29
SIPA-135	Pleistocene Galicia	16,83	12,82	9,01	6,38	6,43	6,25	7,68	6,16
SIPA-140	Pleistocene Galicia	17,57	13,39	9,49	7,52	6,04	6,1	7,46	6,04
CB-010	Holocene Galicia	17,61	14,55	12,38	8,85	8,61	5,36	7,62	6,17
CB-010	Holocene Galicia	17,49	14,6	12,41	8,95	8,4	6,03	6,77	6,66
LCF-001-1996	Holocene Galicia	15,5	13,31	8,27	7,24	7,72	7,48	8,07	6,75
LCF-001-1996	Holocene Galicia	16,31	13,03	9,5	7,4	6,82	6,94	8,52	5,38
LCF-169	Holocene Galicia	14,92	11,96	7,22	6,36	7,35	5,67	6,49	5,68
CGCH-015	Holocene Galicia	16,7	14,37	11,83	7,37	6,6	5,54	7,85	5,73
CGCH-016	Holocene Galicia	17,18	13,92	11,34	5,98	7	6,03	8,18	6,15
RT-001	Holocene Galicia	17,43	10,95	8,53	7,02	4	6,41	8,65	4,52
Pur-Lu-47	Holocene Galicia	16,32	12,8	9,18	6,91	6,32	6,95	8,05	6,97
Pur-Lu-48	Holocene Galicia	16,67	12,91	9,09	6,72	6,36	7,21	7,5	5,95
SAB-82	Holocene Galicia	17,17	12,33	9,7	7,6	5,81	6,88	9,76	6,54
SH5-98-T28-013	Holocene Galicia	15,02	9,45	10,05	6,45	6,6	4,86	7,16	3,83
SH5-97-N20-2	Holocene Galicia	15,05	12,17	9,51	6,19	6,99	4,8	6,09	5,64
SH5-97-N20-2	Holocene Galicia	15,33	11,81	8,87	7,59	6,9	4,41	7,82	6,51
SH5-98-U30-001	Holocene Galicia	14,55	12,37	10	8,3	8,48	6,62	8,15	6,7
SH5-98-U30-001	Holocene Galicia	14,34	13,12	10,57	8,86	8,22	6,23	7,38	7,42
LE1	Modern	14,98	13,65	8	5,07	4,94	6,87	9,64	6,84
LE1	Modern	14,1	12,59	8,14	5,35	6,19	6,58	9,22	5,89
MZB82-7005	Modern	14,23	13,21	8,25	7,1	7,15	5,56	6,6	5,52
MZB82-7005	Modern	13,15	12,64	8,54	6,47	6,94	5,74	6,61	5,03

M1: Length vs breadth

Specimen	Site	L	B
P11-886 (309)	Caldeirão	21,9	16,73
FO.I-151	Fontainhas	20,82	16,35
FO.I-154	Fontainhas	22,74	18,46
GFP-1140.37.21	Furninha (7,5)	24,2	17,65
GFP-1140.37.22	Furninha (7,5)	24,71	18,13
GFP-1140.37.23	Furninha (7,5)	24,25	16,97
GFP-1140.37.24	Furninha (7,5)	24,17	17,59
GFP-1140.37.25	Furninha (7,5)	25,17	20,1
GFP-1140.37.26	Furninha (7,5)	24,29	17,84
GFP-1140.37.31	Furninha (7,5)	23,69	19,4
GFP-1374	Furninha (7,5)	26,61	19
GFP-1371.1	Furninha (7,5)	26,04	18,74
GFP-1355.3.3	Furninha (7,5)	21,97	16,57
GFP-1518.3	Furninha (7,5)	25,81	18,14
ARLU-38	Pleistocene Galicia	21,99	17,07
ARLU-38	Pleistocene Galicia	21,67	17,23
SIPA-16	Pleistocene Galicia	21,27	15,96
SIPA-56	Pleistocene Galicia	23,26	16,43
SIPA-33	Pleistocene Galicia	25,21	17,87
SIPA-136	Pleistocene Galicia	23,85	17,71
SIPA-141	Pleistocene Galicia	24,18	17,9
CB-010	Holocene Galicia	25,62	19,46
CB-010	Holocene Galicia	25,14	19,81
LCF-001-1996	Holocene Galicia	25,05	18,38
LCF-001-1996	Holocene Galicia	25,07	18,18
LCF-169	Holocene Galicia	22,54	16,48
CGCH-015	Holocene Galicia	23,83	18,2
CGCH-016	Holocene Galicia	23,56	18,52
Pur-Lu-49	Holocene Galicia	22,61	17,23
RT-001	Holocene Galicia	23,33	18,29
RT-001	Holocene Galicia	23,09	18,12
SH5-98-T28-013	Holocene Galicia	20,43	15,01
SH5-97-N20-2	Holocene Galicia	21,39	16,17
SH5-97-N20-2	Holocene Galicia	21,68	15,94
SH5-98-U30-001	Holocene Galicia	22,68	16,21
SH5-98-U30-001	Holocene Galicia	22,57	16,12
SH5-97-AO34-39	Holocene Galicia	21,19	15,08
SH5-97-AO34-36	Holocene Galicia	20,79	14,68
TA-196	Holocene Galicia	22,02	17,92
LE1	Modern	23,11	17,25

LE1	Modern	22,98	17,25
QU	Modern	21,85	15,9
QU	Modern	21,5	16,2
MZB82-7005	Modern	21,74	15,14
CEZ-135	A Ceza	27,89	20,54
CEZ-154	A Ceza	27,7	19,95
CEZ-159	A Ceza	28,88	20,9
CEZ-833	A Ceza	28,5	20,93
CEZ-834	A Ceza	26,05	19,03
LI-273	Liñares	28,41	19,85
LI-272	Liñares	26,88	19,46
LI-273	Liñares	27,96	20,31
LI-272	Liñares	27,07	20
LI-271	Liñares	26,86	19,87
LI-1	Liñares	28,16	20,06
LI-1100	Liñares	26,6	19,1
LI-841	Liñares	28,7	20,8
LI-271	Liñares	26,84	19,2
LI-1	Liñares	28,2	19,84
LI-1100	Liñares	27,2	18,3
LI-841	Liñares	28,6	20,8

M1: PCA

Speci-men	Site	L	B	Lant(lin.)	Bant.	Bpost.	Bcons.	Lpa	Lme	Hpa	Hme	Lpa-pr	Lpa-hy	Lpr-me	Lme-hy
P11-886 (309)	Caldeirão	21,9	16,73	10,11	16,43	15,21	15,16	9,08	9,31	10,49	10,38	6,79	10,75	12,06	7,24
FO.I-154	Fontain-has	22,74	18,46	10,34	16,08	17,96	16,86	7,56	9,96	10,25	10,5	7,28	11,88	12,41	8,39
GFP-1140.37.22	Furninha (7,5)	24,71	18,13	10,68	16,17	17,84	16,9	8,63	8,95	10,76	9,97	8,05	13,37	12,51	8,75
GFP-1140.37.23	Furninha (7,5)	24,25	16,97	10,94	16,88	17,77	16,95	8,58	5,78	9,71	10,2	7,95	13,22	11,86	9,89
GFP-1140.37.24	Furninha (7,5)	24,17	17,59	10,98	16	17,48	17,14	9,42	9,08	10,05	10,45	8,35	14	12,29	9,77
GFP-1140.37.25	Furninha (7,5)	25,17	20,1	12,47	19,58	17,38	17,79	7,53	8,15	10,55	10,86	8,65	12,95	12,98	10,18
GFP-1371.1	Furninha (7,5)	26,04	18,74	11,65	18,22	18,6	18,05	9,09	10,5	12,1	12,16	8,75	15,25	13,61	9,85
GFP-1518.3	Furninha (7,5)	25,81	18,14	11,86	17,73	16,69	16,93	8,64	9,18	10,16	9,47	9,24	11,6	13,16	8,63
ARLU-38	Pleisto-cene Gali-cia	21,99	17,07	10,3	15,7	16,8	15,89	8,24	9,45	7,57	6,89	7,29	13,03	11,29	8,15
ARLU-38	Pleisto-cene Gali-cia	21,67	17,23	10,39	15,84	17,16	16,15	8,35	9,45	7,59	7,95	8,07	13,6	11,03	9,22

SIPA-16	Pleistocene Galicia	21,27	15,96	9,86	14,99	15,98	17,71	8,88	8,07	7,76	8,26	7,28	12,15	11,97	8,1
SIPA-56	Pleistocene Galicia	23,26	16,43	11,91	15,9	16,71	16,12	7,98	8,08	7,42	7,8	8,85	11,73	12,73	9,03
SIPA-33	Pleistocene Galicia	25,21	17,87	13,64	16,45	17,84	16,06	10,75	10,99	12,45	12,43	8,9	15,47	12,06	8,72
SIPA-136	Pleistocene Galicia	23,85	17,71	10,99	16,04	17,66	16,55	9,35	9,47	9,51	10,27	7,99	14,75	11,62	8,55
SIPA-141	Pleistocene Galicia	24,18	17,9	11,21	16,15	17,73	16,77	9,25	9,42	9,54	9,61	8,65	14,32	11,75	8,84
CB-010	Holocene Galicia	25,62	19,46	12,08	18,82	19,28	18,6	10,32	10,17	11,18	11,47	9,23	15,08	13,29	9,66
CB-010	Holocene Galicia	25,14	19,81	11,59	19,13	19,82	19,11	10,33	9,97	10,94	10,74	9,75	14,56	13,57	9,88
LCF-001-1996	Holocene Galicia	25,05	18,38	12,69	17,31	18,21	17,73	9,1	10,16	10,1	9,91	8,67	14,88	11,37	9,42
LCF-001-1996	Holocene Galicia	25,07	18,18	12,21	17,09	18,2	17	9,45	9,75	9,99	9,37	8,41	15,16	11,58	8,87
LCF-169	Holocene Galicia	22,54	16,48	10,97	15,21	16,46	15,75	8,47	9,34	7,72	8,01	7,07	12,74	9,7	5,99
CGCH-015	Holocene Galicia	23,83	18,2	10,22	17,16	18,39	17,24	9,04	9,32	9,95	10,11	7,42	13,27	11,2	7,12
CGCH-016	Holocene Galicia	23,56	18,52	10,71	17,2	18,61	17,55	8,92	9,25	10,06	9,9	7,14	13,62	11,76	7,59
Pur-Lu-49	Holocene Galicia	22,61	17,23	10,99	16,56	17,26	16,27	9,53	9,41	9,27	9,15	8,75	14,4	12,53	8,8
RT-001	Holocene Galicia	23,33	18,29	11,55	17,06	18,69	16,38	8,72	9,11	8,42	9,09	8,03	12,69	10,31	7,57
RT-001	Holocene Galicia	23,09	18,12	11,6	16,07	18,24	16,85	8,6	9,04	8,93	9,54	7,35	13,53	10,79	7,54
SH5-98-T28-013	Holocene Galicia	20,43	15,01	10,96	14,87	14,69	14,86	8,17	8,19	9,93	9,47	7,27	12,5	10,91	7,76
SH5-97-N20-2	Holocene Galicia	21,39	16,17	10,96	15,67	15,44	16,61	8,74	8,61	8,72	8,2	6,62	12,21	10,76	7,99
SH5-97-N20-2	Holocene Galicia	21,68	15,94	10,95	15,36	14,92	15,42	8,05	8,38	8,08	8,67	7,37	12,88	9,82	8,02
SH5-98-U30-001	Holocene Galicia	22,68	16,21	12,22	16,98	15,19	16,35	9,71	9,26	8,27	8,29	7,19	12,26	12,28	8,65
SH5-98-U30-001	Holocene Galicia	22,57	16,12	12,1	16,5	14,13	15,51	10,08	9,48	8,94	8,26	7,31	13,2	12,76	8,29
SH5-97-AO34-39	Holocene Galicia	21,19	15,08	11,48	14,99	13,85	13,87	7,39	7,59	8,35	9,26	7,91	11,54	11,74	7,48
SH5-97-AO34-36	Holocene Galicia	20,79	14,68	10,76	15,19	13,55	13,76	7,99	8,49	8,1	8,79	7,99	11,32	12,39	6,12
TA-196	Holocene Galicia	22,02	17,92	10,85	17,51	17,29	17,58	9,67	9,24	9,71	9,57	8,04	13,17	11,86	8,56
LE1	Modern	23,11	17,25	10,46	16,37	17,27	16,58	9,49	9,17	8,85	7,97	8,95	14,76	13,76	8,92
LE1	Modern	22,98	17,25	11,54	16,43	17,28	16,78	9,11	9,04	8,91	8,15	9,03	14,98	12,32	9,03
MZB82-7005	Modern	21,74	15,14	10,04	13,63	15,17	13,96	8,21	8,99	8,29	9,08	7,38	12,12	11,2	7,01
CEZ-135	A Ceza	27,89	20,54	13,34	20,17	19,41	19,85	9,7	10,9	11,4	10,82	11,78	19,7	16,07	12,6
CEZ-154	A Ceza	27,7	19,95	13,94	20,2	20,38	19,6	10,7	10	10,75	10,51	12,15	19,22	16,5	11,35
CEZ-833	A Ceza	28,5	20,93	14,75	20,25	20,47	19,6	10,4	11,02	11,47	12,06	13,2	16,25	20,43	11,6

CEZ-834	A Ceza	26,05	19,03	12,38	18,85	18,45	18,4	10,03	8,74	10,7	9,36	11,09	17,74	15,02	10,37

M2: Length vs breadth

Specimen	Site	L	B
GFP-25665.2	Furninha (7,5)	38,15	20,99
GFP-1341	Furninha (7,5)	35,82	18,27
GFP-1342	Furninha (7,5)	37,93	21,04
GFP-1140.37.27	Furninha (7,5)	35	19,72
GFP-1140.37.28	Furninha (7,5)	35,14	15,06
GFP-1140.37.29	Furninha (7,5)	36,84	20,68
GFP-1140.37.30	Furninha (7,5)	32,46	18,64
GFP-1140.37.32	Furninha (7,5)	34,31	19,2
GFP-1140.37.33	Furninha (7,5)	36,22	19,71
GFP-1365.2	Furninha (7,5)	38,26	18,7
GFP-1360.2	Furninha (7,5)	36,86	18,21
ARLU-38	Pleistocene Galicia	34,99	18,33
ARLU-38	Pleistocene Galicia	35,27	18,31
SIPA-16	Pleistocene Galicia	31,1	17,02
SIPA-56	Pleistocene Galicia	39,19	18,68
SIPA-137	Pleistocene Galicia	36,93	20,21
SIPA-142	Pleistocene Galicia	36,97	20,52
Ca-Le-3	Pleistocene Galicia	33,02	20,04
CB-010	Holocene Galicia	42,38	22,45
CB-010	Holocene Galicia	42,41	21,7
LCF-001-1996	Holocene Galicia	34,21	20,28
LCF-001-1996	Holocene Galicia	36,05	19,8
LCF-148	Holocene Galicia	32,56	17,53
LCF-169	Holocene Galicia	32,97	17,74
CGCH-015	Holocene Galicia	36,58	19,52
CGCH-016	Holocene Galicia	36,14	19,32
RT-001	Holocene Galicia	35,07	20,37
RT-001	Holocene Galicia	34,19	20,22
Pur-Lu-50	Holocene Galicia	34,19	18,81
SH5-97-N20-2	Holocene Galicia	32,77	17,88
SH5-97-N20-2	Holocene Galicia	33,48	17,84
SH5-98-U30-001	Holocene Galicia	33,99	18,37
SH5-98-U30-001	Holocene Galicia	34,4	18,89
SH5-97-N19-3	Holocene Galicia	35,34	18,33
VA88/14D/4.1	Holocene Galicia	42,7	21,87
LE1	Modern	29,31	18,82
LE1	Modern	30,29	17,49
QU	Modern	31,55	16,25
QU	Modern	31,5	15,7
MZB82-7005	Modern	30,85	16,87

MZB82-7005	Modern	31,25	17,14
LI-1100	Liñares	43,5	23,6
LI-273	Liñares	44,76	24,28
LI-272	Liñares	44,94	22,66
LI-271	Liñares	46,17	24,05
LI-273	Liñares	45,85	23,86
LI-272	Liñares	44,18	22,92
LI-271	Liñares	47,21	24,39
LI-1	Liñares	46,08	23,21
LI-1000	Liñares	43,9	23,2
LI-841	Liñares	46,4	24,6
LI-1	Liñares	45,66	23,44
LI-1000	Liñares	44,6	24,3
LI-841	Liñares	45,8	24,3
LI-1100	Liñares	42,2	23,1
CEZ-155	A Ceza	43,9	24,3

M2: PCA

Specimen	Site	L	B	Bant.	Bpost.	Bcons.	Lpa	Lme	Hpa	Hme	Lpa-pr	Lpa-hy	Lpr-me	Lme-hy
GFP-25665.2	Furninha (7,5)	38,15	20,99	21,16	20,52	20,34	20,05	9,11	9,06	9,32	11,03	13,37	15,25	9,01
GFP-1341	Furninha (7,5)	35,82	18,27	19,96	19,14	17,75	11,96	8,37	7,95	7,93	9,47	15,07	10,97	9,6
GFP-1342	Furninha (7,5)	37,93	21,04	20,51	20,18	19,89	10,02	7,77	8,54	8,24	10,4	15,71	12,36	8,92
GFP-1365.2	Furninha (7,5)	38,26	18,7	17,21	18,05	17,16	9,93	10,34	9,2	9,75	10,5	15,47	9,93	9,82
ARLU-38	Pleistocene Galicia	35,27	18,31	18,92	17,59	17,57	11,01	8,36	8,38	8,78	10,16	8,96	15,99	12,97
SIPA-16	Pleistocene Galicia	31,1	17,02	16,42	16,59	16,73	7,42	5,43	7,43	9,35	10,13	16,17	12,59	9,49
SIPA-56	Pleistocene Galicia	39,19	18,68	18,73	18,94	17,87	11,61	8,31	7,52	7,89	9,45	16,16	12,17	10,1
SIPA-137	Pleistocene Galicia	36,93	20,21	19,65	19,4	19,63	11,78	10,03	8,19	6,47	9,17	17,96	11,72	10,69
SIPA-142	Pleistocene Galicia	36,97	20,52	20,51	19,93	19,94	11,94	12,11	7,62	7,53	11,19	18,22	14,29	10,42
CB-010	Holocene Galicia	42,38	22,45	22,66	22,09	21,5	12,41	13,29	9,75	10,28	13,36	18,14	16,25	10,7
CB-010	Holocene Galicia	42,41	21,7	21,67	21,06	20,23	12,26	12,2	9,56	9,13	11,36	18,48	13,27	12,08
LCF-001-1996	Holocene Galicia	34,21	20,28	19,97	17,88	18,52	12,28	11,12	8,45	9,37	11,78	18,1	14,06	12
LCF-001-1996	Holocene Galicia	36,05	19,8	20,18	19,22	18,55	11,49	10,69	8,85	7,98	11,93	16,63	11,44	10,23
LCF-148	Holocene Galicia	32,56	17,53	17,4	17,37	17,18	9,71	9,08	6,91	8,25	10,19	16,64	12,26	9,88
LCF-169	Holocene Galicia	32,97	17,74	17,2	17,5	17,17	9,96	10,18	6,96	7,14	10,56	15,29	11,77	8,84
CGCH-015	Holocene Galicia	36,58	19,52	19,5	18,78	18,89	9,71	10,07	8,72	6,79	9,8	14,99	10,94	8,95

CGCH-016	Holocene Galicia	36,14	19,32	19,25	19,02	18,56	9,88	9,97	9,11	9,28	9,47	15,41	13,72	9,64
RT-001	Holocene Galicia	35,07	20,37	20,4	19,38	18,57	11,92	9,68	7,87	6,83	12,11	18,41	14,88	11,26
RT-001	Holocene Galicia	34,19	20,22	20,27	19,52	19,13	11,44	9,94	8,27	8,38	10,15	14,73	13,45	10,09
Pur-Lu-50	Holocene Galicia	34,19	18,81	18,47	18,69	18,54	11,57	10,98	8,67	8,28	10,29	15,75	13,78	9,2
SH5-97-N20-2	Holocene Galicia	33,48	17,84	17,19	17,31	17,05	10,14	10,44	8,22	9,38	9,48	15,09	12,67	10,26
SH5-98-U30-001	Holocene Galicia	33,99	18,37	17,86	18,3	15,19	11,65	9,39	7,86	9,47	9,41	15,34	12,47	10,1
SH5-98-U30-001	Holocene Galicia	34,4	18,89	18,02	18,46	15,14	11,32	9,13	8,45	7,25	10,35	17,13	12,1	10,21
SH5-97-N19-3	Holocene Galicia	35,34	18,33	18,43	17,42	17,78	10,81	9,92	8,66	7,5	10,39	15,23	12,82	9,18
VA88/14D/4.1	Holocene Galicia	42,7	21,87	20,19	21,31	20,69	13,47	11,06	10,69	7,27	10,61	16,37	14,39	9,35
LE1	Modern	29,31	18,82	18,74	17,68	17,97	10,9	8,09	6,55	6,63	11,35	14,81	12,99	8,43
MZB82-7005	Modern	30,85	16,87	16,82	16,93	16,64	11,56	8,77	7,81	8,24	10,38	14,8	13,4	9,6
MZB82-7005	Modern	31,25	17,14	16,94	17,01	16,82	9,11	10,16	7,75	8,28	9,92	14,85	14,07	9,98
CEZ-155	A Ceza	43,9	24,3	22,72	22,02	21,5	13,75	11,56	11,5	11,44	12,82	20,64	18,15	13,6

p4: Length vs breadth

		L	B
FO.I-33	Fontainhas	15,15	8,44
GFP-1366.1	Furninha	11,56	7,14
GFP-1517.2	Furninha	14,61	8,77
GFP-1517.3	Furninha	13,63	8,97
GFP-1517.4	Furninha	14,56	9,45
GFP-1517.5	Furninha	13,8	9,05
GFP-1328	Furninha	13,72	7,91
SIPA-15	Pleistocene Galicia	11,09	7,15
SIPA-53	Pleistocene Galicia	12,79	7,6
SIPA-55	Pleistocene Galicia	13	7,83
SIPA-129	Pleistocene Galicia	13,04	7,94
LCF-003-1996	Holocene Galicia	13,05	8,42
LCF-002-1996	Holocene Galicia	13,2	8,37
LCF-154	Holocene Galicia	11,44	7,57
LCF-155	Holocene Galicia	10,62	7,18
CGLL-012	Holocene Galicia	13,14	7,65
CGLL-011	Holocene Galicia	12,5	7,54
SH5-97-U29-7	Holocene Galicia	13,02	6,4
SH5-97-U29-6	Holocene Galicia	13,41	6,48
SH5-97-T29-090	Holocene Galicia	10,97	6,94
SH5-98-V29-7	Holocene Galicia	13,09	8,01
SH5-98-S30-6	Holocene Galicia	13,14	7,97
SH5-97-N19-4	Holocene Galicia	12,03	6,66

SH5-98-U28-010	Holocene Galicia	12,34	6,5
TA-108	Holocene Galicia	10,93	6,62
TA-109	Holocene Galicia	10,6	6,91
TA-192	Holocene Galicia	11,89	7,75
LE1	Modern	12,75	7,98
QU	Modern	10,3	6
QU	Modern	10,4	6,2
MZB82-7005	Modern	11,6	6,77
MZB82-7005	Modern	10,85	6,74

p4: PCA

Specimen	Site	L	B	Hprd
FO.I-33	Fontainhas	15,15	8,44	8,36
GFP-1517.2	Furninha	14,61	8,77	7,62
GFP-1517.3	Furninha	13,63	8,97	7,65
GFP-1517.4	Furninha	14,56	9,45	7,25
GFP-1517.5	Furninha	13,8	9,05	8,61
GFP-1328	Furninha	13,72	7,91	6,23
SIPA-15	Pleistocene Galicia	11,09	7,15	6,69
SIPA-53	Pleistocene Galicia	12,79	7,6	7,47
SIPA-55	Pleistocene Galicia	13	7,83	7,24
SIPA-129	Pleistocene Galicia	13,04	7,94	8,76
LCF-003-1996	Holocene Galicia	13,05	8,42	7,68
LCF-002-1996	Holocene Galicia	13,2	8,37	7,54
LCF-154	Holocene Galicia	11,44	7,57	6,82
LCF-155	Holocene Galicia	10,62	7,18	6,82
CGLL-012	Holocene Galicia	13,14	7,65	8,16
CGLL-011	Holocene Galicia	12,5	7,54	7,96
SH5-97-U29-7	Holocene Galicia	13,02	6,4	6,37
SH5-97-U29-6	Holocene Galicia	13,41	6,48	6,3
SH5-97-T29-090	Holocene Galicia	10,97	6,94	7,88
SH5-98-V29-7	Holocene Galicia	13,09	8,01	7,58
SH5-98-S30-6	Holocene Galicia	13,14	7,97	8,08
SH5-97-N19-4	Holocene Galicia	12,03	6,66	7,33
SH5-98-U28-010	Holocene Galicia	12,34	6,5	4,82
TA-108	Holocene Galicia	10,93	6,62	8,12
TA-109	Holocene Galicia	10,6	6,91	8,16
TA-192	Holocene Galicia	11,89	7,75	5,99
LE1	Modern	12,75	7,98	7,3
MZB82-7005	Modern	11,6	6,77	7,38
MZB82-7005	Modern	10,85	6,74	7,85

m1: Length vs breadth

Specimen	Site	L	B
P-11 714	Caldeirão	27,9	14
Escral121966	Escoural	26,39	14,3
SM219.36	Serra de Molianos	24,61	10,31
FO.I-156	Fontainhas	26,31	13,39
GFP-1328	Furninha (7,5)	25,55	12,13
GFP-1381.1	Furninha (7,5)	26,75	13,16
GFP-1140.37.15	Furninha (7,5)	25,97	12,65
GFP-1140.37.16	Furninha (7,5)	25,41	13,42
GFP-1140.37.17	Furninha (7,5)	23,24	11,36
GFP-1140.37.18	Furninha (7,5)	25,4	11,95
GFP-1140.37.19	Furninha (7,5)	25,14	12,47
GFP-1140.37.20	Furninha (7,5)	25,26	12,44
GFP-1365.1	Furninha (7,5)	27,71	13,78
GFP-1424	Furninha (7,5)	26,47	12,75
GFP-1383.1	Furninha (7,5)	26,85	13,58
GFP-1358.1	Furninha (7,5)	25,47	12,4
GFP-1360.1	Furninha (7,5)	29,39	12,03
GFP-1522	Furninha (7,5)	26,74	12,96
SIPA-15	Pleistocene Galicia	22,88	11,59
SIPA-14	Pleistocene Galicia	23,34	11,67
SIPA-129	Pleistocene Galicia	25,05	12,86
SIPA-132	Pleistocene Galicia	25,03	12,65
LCF-003-1996	Holocene Galicia	26,11	12,49
LCF-154	Holocene Galicia	23,37	11,43
LCF-155	Holocene Galicia	23,16	11,11
CGLL-011	Holocene Galicia	23,93	11,47
CGLL-001	Holocene Galicia	24,45	11,87
Pur-Lu-51	Holocene Galicia	24,34	12,22
SH5-97-U29-6	Holocene Galicia	22,88	10,92
SH5-98-V29-7	Holocene Galicia	24,66	13,23
SH5-98-S30-6	Holocene Galicia	25,33	13,13
SH5-97-N19-4	Holocene Galicia	23,47	11,08
SH5-97-AO34-38	Holocene Galicia	22,11	10,85
TA-109	Holocene Galicia	23,87	12
TA-192	Holocene Galicia	23,75	12,07
TA-194	Holocene Galicia	23,88	12,02
LE1	Modern	23,55	13,05
LE1	Modern	23,45	12,45
MZB82-7006	Modern	21,67	10,39
CEZ-660	A Ceza	27,44	13,32
CEZ-156	A Ceza	31,11	14,1
EI-1558	Eirós	31,2	14,3

EI-851	Eirós	31,3	14,9
EI-850	Eirós	31,1	14,8
EI-1552	Eirós	31,2	15,2
EI-1555	Eirós	31,5	15,1
EI-299	Eirós	31,6	15,5
EI-852	Eirós	31,4	14,5
EI-844	Eirós	31,5	14,9
EI-1553	Eirós	30,5	14
EI-1193	Eirós	29	14,6
EI-1556	Eirós	29,3	13,7
EI-1296	Eirós	28	13,7
EI-845	Eirós	28,8	13,3
EI-626	Eirós	30	14,2
EI-225	Eirós	30,5	14,1
EI-1551	Eirós	29,5	13,6
EI-1125	Eirós	29,7	14,7
EI-1183	Eirós	31,7	14,4
EI-846	Eirós	32,5	15
EI-853	Eirós	32,6	15,1
EI-1549	Eirós	32,3	15,1
EI-847	Eirós	32,4	14,4
EI-488	Eirós	33	15,7
EI-727	Eirós	33,1	15,6
EI-1564	Eirós	32,6	15,7
EI-1563	Eirós	33	15,4
EI-848	Eirós	32,3	14,6
EI-1562	Eirós	32,1	16,1
EI-1557	Eirós	32,1	16
EI-1092	Eirós	32	15,2
EI-229	Eirós	32,1	15,5
EI-1554	Eirós	32,3	14,7
EI-484	Eirós	32,3	14,8
EI-224	Eirós	32,1	16
EI-1559	Eirós	32,2	15,2

m1: PCA

Speci-men	Site	L	B	Ltrd	Btrd	Btld	Bcons	Lpad	Lprd	Lmed	Lend	Lhyd	Hpad	Hprd	Hmed	Hend	Hhyd	Lprd-med	Lpad-prd	Lpad-med	Lmed-hyd	Lprd-end	Lhyd-en
GFP-1381.1	Furninha (7,5)	26,75	13,16	15,98	11,9	13,73	12,11	6,17	12,44	11,44	9,64	10,03	7,48	11,21	8,5	9,55	10,07	4,75	8,66	10,43	13,68	14,92	8,21
GFP-1140.37.15	Furninha (7,5)	25,97	12,65	13,8	10,54	12,11	10,18	4,63	10,64	5,82	9,73	8,28	7,96	10,42	6,93	8,6	9,64	5,09	7,57	9,83	10,89	13,99	7,15
GFP-1140.37.18	Furninha (7,5)	25,4	11,95	13,94	10,46	12,56	10,19	5,13	9,28	9,85	9,78	8,71	7,18	10,51	7,31	8,38	8,31	5,51	7,88	5,35	9,24	11,7	6,21
GFP-1140.37.19	Furninha (7,5)	25,14	12,47	13,63	9,72	12,07	10,41	4,57	9,04	9,99	9,12	8,47	6,74	11,47	6,9	8,34	5,8	4,48	8,22	9,21	11,21	12,37	6,57
GFP-1140.37.20	Furninha (7,5)	25,26	12,44	14,55	8,98	12,31	10,82	4,35	9,85	11,86	7,91	8,48	8,22	7,19	7,05	7,84	10,19	3,92	7,65	7,26	10,12	12,25	6,41
GFP-1365.1	Furninha (7,5)	27,71	13,78	16,41	12,3	14,2	12,19	4,51	10,6	7,19	7,94	6,84	6,85	9,3	7,32	8,15	9,36	5,69	7,96	10,47	10,82	13,46	7,59
GFP-1424	Furninha (7,5)	26,47	12,75	14,61	11,33	12,63	10,22	4,13	9,1	9,11	7,8	7,25	8,35	10,13	7,45	8,75	9,18	6,09	6,63	8,36	9,86	13,83	6,2
GFP-1383.1	Furninha (7,5)	26,85	13,58	15,95	12,03	13,17	11,65	5,22	8,57	10,21	9,33	8,04	6,37	9,65	6,92	8,05	9,5	4,43	7,7	9,29	11,42	13,75	6,14
GFP-1360.1	Furninha (7,5)	29,39	12,03	10,99	9,66	12,52	9,61	4,14	10,52	9,57	8,23	7,35	7,03	11,17	7,1	8,45	9,87	4,15	7,1	9,62	10,8	12,87	6,5
GFP-1522	Furninha (7,5)	26,74	12,96	14,28	10,93	13,13	10,83	4,24	8,94	8,91	8,65	7,16	6,77	10,26	8,23	7,84	9,35	3,78	6,48	9,22	11,64	12,94	6,66
SIPA-15	Pleisto-cene Gali-cia	22,88	11,59	13,1	9,79	11,51	9,86	3,5	8,51	9,4	7,25	5,95	6,46	8,31	7,41	7,37	7,61	4,91	7,74	8,51	10,81	12,08	6,43
SIPA-14	Pleisto-cene Gali-cia	23,34	11,67	13,42	10,15	11,46	10,25	3,34	10,01	10,44	9,27	6,73	6,24	8,48	7,32	6,43	7,57	4,67	7,82	9,24	10,77	12,8	5,4
SIPA-129	Pleisto-cene Gali-cia	25,05	12,86	13,86	10,36	12,66	10,65	4,7	10,79	10,1	9,63	7,01	7,05	9,3	6,55	7,79	8,53	4,49	7,14	9,73	10,54	12,99	6,82
SIPA-132	Pleisto-cene Gali-cia	25,03	12,65	13,93	10,29	12,63	10,56	5,04	10,55	10	9,64	7,17	6,7	8,73	6,72	7,83	8,35	5,3	7,4	9,52	9,71	13,09	6,67

LCF-003-1996	Holocene Galicia	26,11	12,49	16,14	10,6	12,27	10,6	5,25	12,13	9,8	9,46	7,51	7,07	8,84	6,55	7,39	8,33	5,53	8,29	10,54	11,59	14,8	5,36
LCF-154	Holocene Galicia	23,37	11,43	13,28	9,78	11,79	9,68	4,27	8,13	8,35	6,76	8,09	6,75	8,83	6,25	6,93	7,7	5,22	7,67	9	9,88	12,35	6,04
LCF-155	Holocene Galicia	23,16	11,11	12,9	9,39	11,34	9,25	4,48	7,15	8,42	6,88	8,72	5,64	9,22	6,44	7,41	8,76	4,41	6,87	9,05	9,54	12,48	6,61
CGLL-011	Holocene Galicia	23,93	11,47	14,9	10,56	12,04	10,57	3,83	8,02	8,86	9,13	7,14	8,91	10,64	7,27	8,4	9,52	5,64	7,89	8,99	10,37	13,84	6,27
CGLL-001	Holocene Galicia	24,45	11,87	13,59	10,33	12,39	10,1	4,89	8,96	8,94	9,26	6,91	7,22	9,2	6,88	8,38	9,09	4,77	6,77	8,44	10,9	13,62	6,33
Pur-Lu-51	Holocene Galicia	24,34	12,22	12,44	9,81	12,35	9,75	4,36	10,03	9,83	8,15	7,01	7,45	7,49	6,45	7,1	7,22	5,38	6,44	8,7	11,46	13,81	5,8
SH5-97-U29-6	Holocene Galicia	22,88	10,92	12,33	9,26	11,18	8,82	2,92	10,71	9,39	8,83	7,38	7,44	7,97	6,12	6,64	8,06	4,75	6,66	7,09	10,22	13,09	6,31
SH5-98-V29-7	Holocene Galicia	24,66	13,23	14,32	10,92	12,92	10,74	5,01	9,07	11,5	10,02	7,72	7,1	10,66	7,2	8,18	8,92	5,52	7,43	9,35	11,23	14	7,29
SH5-98-S30-6	Holocene Galicia	25,33	13,13	15,21	10,94	13,04	10,1	4,8	12,44	9,71	9,62	8,31	7,34	10,46	7,13	8,47	9,91	4,89	8,03	9,92	12,46	14,33	8,29
SH5-97-N19-4	Holocene Galicia	23,47	11,08	14,16	9,55	10,93	9,25	4,52	10,72	9,13	8,91	7,35	7,46	7,62	6,93	7,4	6,89	4,96	7,67	9,02	10,5	12,21	6,07
SH5-97-AO34-38	Holocene Galicia	22,11	10,85	12,89	9,35	11,47	9,1	3,11	7,02	8,88	6,89	7,51	6,82	8,15	6,37	7,44	8,42	4,64	7,03	8,2	9,59	11,47	6,37
TA-109	Holocene Galicia	23,87	12	15,43	9,08	11,19	9,48	3,98	11,47	9,68	8,95	6,39	5,03	7,67	6,14	7,78	6,15	4,48	7,61	9,6	12,3	13,79	6,47
TA-192	Holocene Galicia	23,75	12,07	14,81	9,9	11,69	10,4	4,36	8,51	8,98	8,35	6,9	6,83	9,13	7,27	8,04	8,52	5,32	7,95	9,04	10,52	13,08	6,44
TA-194	Holocene Galicia	23,88	12,02	14,55	9,82	11,86	10,13	4,71	8,39	8,72	8,39	7,11	8,05	9,96	7,15	7,46	8,71	5,01	8,51	8,71	11,07	13,64	6,48
LE1	Modern	23,55	13,05	14,29	11,36	12,63	10,33	4,34	9,78	8,73	7,38	7,21	7,82	8,08	7,26	7,06	6,83	4,03	7,35	7,8	10,59	13,36	5,78
LE1	Modern	23,45	12,45	14,24	10,34	12,5	10,54	4,39	8,6	9,12	7,64	7,68	6,36	8,01	7,03	6,99	6,14	4,28	6,16	7,61	10,82	13,76	6,09
MZB82-7006	Modern	21,67	10,39	14,01	8,61	10,45	8,57	4,68	8,15	8,2	6,6	5,87	6,63	8,16	5,36	6,9	6,62	5,51	6,4	9,51	8,76	12,68	6,69

m2: Length vs breadth

Specimen	Site	L	B
EscGalEntrad1964	Escoural	24,66	16,84
EscGal2Tal7C1	Escoural	23,49	12,85
SM219.38	Serra de Molianos	25,82	16,57
FO.I-153	Fontainhas	27,91	19,25
GFP-1420	Furninha (7,5)	26,11	16,8
GFP-1140.37.11	Furninha (7,5)	24,46	15,97
GFP-1140.37.12	Furninha (7,5)	25,83	17,97
GFP-1140.37.13	Furninha (7,5)	25,91	16,23
GFP-1140.37.14	Furninha (7,5)	25,32	16,47
GFP-1356.2	Furninha (7,5)	27,05	15,68
GFP-1358.2	Furninha (7,5)	22,81	14,35
GFP-1361.1	Furninha (7,5)	27,37	17,14
GFP-1361.2	Furninha (7,5)	28,77	17,74
GFP-1361.3	Furninha (7,5)	25,6	19,35
GFP-1361.4	Furninha (7,5)	26,08	16,36
GFP-1519.1	Furninha (7,5)	26,16	16,1
GFP-1521	Furninha (7,5)	27,11	16,56
GFP-1518.1	Furninha (7,5)	29,05	18,65
GFP-1518.2	Furninha (7,5)	27,33	17,57
GFP-1328	Furninha (7,5)	24,5	15,68
SIPA-15	Pleistocene Galicia	22,67	14,11
SIPA-129	Pleistocene Galicia	26,03	16,42
SIPA-133	Pleistocene Galicia	25,93	16,64
LCF-003-1996	Holocene Galicia	27,26	15,72
LCF-002-1996	Holocene Galicia	27,89	15,79
LCF-154	Holocene Galicia	23,44	14,71
LCF-155	Holocene Galicia	23,43	15,22
EIX-018	Holocene Galicia	24,59	14,9
CGLL-011	Holocene Galicia	24,74	14,59
CGLL-004	Holocene Galicia	25,19	15,32
Pur-Lu-52	Holocene Galicia	25,53	15,91
Pur-Lu-53	Holocene Galicia	25,09	15,17
SH5-97-U29-6	Holocene Galicia	23,11	14,51
SH5-98-V29-7	Holocene Galicia	26,15	15,62
SH5-98-S30-6	Holocene Galicia	26,77	15,95
SH5-97-N19-4	Holocene Galicia	23,56	13,62
SH5-98-U30-014	Holocene Galicia	23,23	13,85
SH5-98-U30-025	Holocene Galicia	23,36	13,98
TA-109	Holocene Galicia	25,28	14,09
TA-192	Holocene Galicia	24,31	16,15
TA-195	Holocene Galicia	24,62	16,03
VA87/16F/37	Holocene Galicia	25,37	15,42

LE1	Modern	22,7	15,2
LE1	Modern	22,71	16,01
QU	Modern	20,8	13,1
QU	Modern	21,5	12,75
MZB82-7005	Modern	21,05	12,28
MZB82-7006	Modern	21,2	12,91
CEZ-518	A Ceza	32,79	18,48
CEZ-144	A Ceza	31,7	18,44
CEZ-142	A Ceza	31,38	17,71
CEZ-518	A Ceza	32,92	19,1
CEZ-517	A Ceza	32,32	18,68
CEZ-801	A Ceza	30,88	18,03

m2: PCA

Specimen	Site	L	B	Ltrd(lind.)	Ltrd(lab.)	Btrd	Btld	Bcons.(min)	Hprd	Hmed	Hend	Hhyd	Lprd-med	Lmed-hyd	Lprd-end	Lhyd-end
EscGalEn-trad1964	Escoural	24,66	16,84	11,24	12,57	16,21	15,68	15,86	8,67	6,55	6,93	8,41	7,16	13,27	14,77	6,95
EscGal2Tal7C1	Escoural	23,49	12,85	13,72	11,9	12,51	13,58	12,56	7,83	6,04	6,44	7,77	6,79	12,31	11,81	7,56
SM219.38	Serra de Molianos	25,82	16,57	13,06	12,66	14,55	16,81	14,96	8,76	7,12	7,15	8,2	6,18	16,64	14,41	8,87
GFP-1420	Furninha (7,5)	26,11	16,8	11,56	13,18	16,2	17,04	15,25	9,97	7,66	7,57	8,95	8,32	15,44	15,22	10,78
GFP-1140.37.13	Furninha (7,5)	25,91	16,23	11,11	13,21	16,13	16,21	15,86	9,08	7,38	6,53	7,73	10,35	16,7	16,19	11
GFP-1356.2	Furninha (7,5)	27,05	15,68	13,59	14,55	16,8	17,9	15,86	10,82	8,4	8,83	10,05	8,72	13,83	15,6	10,48
GFP-1361.2	Furninha (7,5)	28,77	17,74	13,91	14,17	18,44	16,3	16,52	10,36	8,81	7,03	9,51	8,41	16,79	17,94	10,47
GFP-1361.3	Furninha (7,5)	25,6	19,35	15,3	14,43	18,4	18,75	16,84	10,48	8,24	8,22	10,31	8,23	14,05	15,63	10,78
GFP-1361.4	Furninha (7,5)	26,08	16,36	15,72	14,42	16,77	17,53	15,06	8,79	8,67	7,79	9,64	8	15,15	15,62	11,06
GFP-1521	Furninha (7,5)	27,11	16,56	15,3	14,38	17,1	17,3	15,68	9,33	8,54	7,59	7,95	7,75	14,56	15,51	9,51
GFP-1518.1	Furninha (7,5)	29,05	18,65	15,83	14,82	16,25	19,58	16,61	9,85	8,06	7,78	10,87	7	12,98	14,66	11,25
GFP-1518.2	Furninha (7,5)	27,33	17,57	15,9	14,91	16,77	16,91	16,06	9,53	8,82	7,56	9,44	8,8	15,53	15,22	9,24
GFP-1328	Furninha (7,5)	24,5	15,68	15,54	13,22	16,08	15,82	15,19	9,34	7,6	6,85	6,88	8,61	14,6	16,08	10,39
SIPA-15	Pleisto-cene Gali-cia	22,67	14,11	13,93	15,61	13,66	13,5	13,72	8,49	7,55	7,03	9,13	7,41	16,55	13,53	9,07
SIPA-129	Pleisto-cene Gali-cia	26,03	16,42	11,93	15,89	16,23	16,5	15,64	9,81	7,41	6,44	8,22	6,12	15,04	14,05	8,16
SIPA-133	Pleisto-cene Gali-cia	25,93	16,64	12,83	15,05	16,37	16,54	15,4	8,99	7,98	7,71	8,7	8,13	15,63	17,46	9,63
LCF-003-1996	Holocene Galicia	27,26	15,72	14,97	12,21	16,6	15,7	14,76	8,29	7,78	7,16	8,68	8,49	16,3	16,8	8,58

LCF-002-1996	Holocene Galicia	27,89	15,79	15,07	13,03	15,24	15,4	14,43	8,2	6,88	6,34	8,09	7,69	14,02	16,25	8,45
LCF-154	Holocene Galicia	23,44	14,71	13,11	11,87	13,79	14,75	13,87	7,46	7,02	6,93	7,82	8,32	14,67	16,8	8,51
LCF-155	Holocene Galicia	23,43	15,22	13,77	11,46	13,77	14,78	13,39	7,89	9,18	7,43	8,4	7,62	13,16	14,35	7,7
EIX-018	Holocene Galicia	24,59	14,9	11,78	13,45	13,81	14,57	13,81	7,91	8,19	7,87	8,21	7,43	13,06	14,04	8,21
CGLL-011	Holocene Galicia	24,74	14,59	14,7	12,28	14,7	15,33	14,79	10,11	7,56	7,3	8,24	8,09	15,55	19,7	10,22
CGLL-004	Holocene Galicia	25,19	15,32	14,46	11,22	15,74	15,2	15,07	9,28	7,73	7,92	9,43	8,8	14,07	16,14	8,02
Pur-Lu-52	Holocene Galicia	25,53	15,91	12,12	14,77	15,81	15,33	15,19	8,48	6,8	7,12	8,45	8,19	15,34	17,1	9,34
Pur-Lu-53	Holocene Galicia	25,09	15,17	12,9	14,71	15,16	15,6	14,96	8,12	7,43	7,76	8,11	8,88	14,09	16,63	7,79
SH5-97-U29-6	Holocene Galicia	23,11	14,51	10,65	12,49	13,55	14,4	13,88	7,7	7,62	7,57	8,35	7,99	15,42	13,56	9,58
SH5-98-V29-7	Holocene Galicia	26,15	15,62	13,9	14,8	15,64	14,84	15,82	9,88	9,13	8,76	7,33	7,88	14,98	14,42	9,67
SH5-98-S30-6	Holocene Galicia	26,77	15,95	15,86	13,22	15,54	15,56	15,45	11,19	8,06	7,92	9,83	8,57	15,49	17,24	8,42
SH5-97-N19-4	Holocene Galicia	23,56	13,62	14,04	11,33	13,49	13,94	12,38	8,9	7,8	8,87	10,71	8,24	15,84	15,96	8,33
SH5-98-U30-014	Holocene Galicia	23,23	13,85	14,07	11,56	12,55	13,59	13,09	9,51	7,76	7,74	8,58	6,63	8,69	14,96	14,34
SH5-98-U30-025	Holocene Galicia	23,36	13,98	13,92	11,18	12,91	14,25	13,06	9,1	7,17	5,87	8,44	6,98	14,82	15,62	9,01
TA-109	Holocene Galicia	25,28	14,09	13,6	15,94	13,47	14,05	12,23	9,18	7,85	6,36	8,62	6,71	14,32	16,58	8,51
TA-195	Holocene Galicia	24,62	16,03	10,72	13,01	15,38	15,76	15,69	9	7,16	7,3	8,45	8,27	14,84	16,08	8,88
VA87/16F/37	Holocene Galicia	25,37	15,42	11,04	12,02	14,27	14,93	15,23	7,42	7,41	8,1	8,33	6,91	12,66	14,69	6,51
LE1	Modern	22,7	15,2	12,58	12,64	14,59	15,2	14,45	7,05	7,54	6,21	6,91	8,44	15,39	17,29	7,96
LE1	Modern	22,71	16,01	11,81	13,06	14,3	15,26	14,51	7,11	7,01	6,55	6,62	7,59	12,81	14,44	7,88
MZB82-7005	Modern	21,05	12,28	14,62	9,36	12,82	12,26	12,16	9,29	7,57	6,29	8,13	7,72	14,51	11,95	7,05
MZB82-7006	Modern	21,2	12,91	14,68	10,03	12,62	12,26	12,87	9,35	7,12	7,07	7,93	7,02	13,2	12,93	6,68
CEZ-518	A Ceza	32,79	18,48	18,53	16,92	18,67	19,48	17,65	10,3	9,48	9,3	11,65	11,61	19,21	21,75	13,62
CEZ-144	A Ceza	31,7	18,44	15,79	14,8	18,35	18,79	16,95	11,15	8,25	8	11,4	11,71	18,8	20,39	12,62
CEZ-142	A Ceza	31,38	17,71	15,64	15,31	18,3	19,53	16,94	11,26	9,34	9,25	10,51	11,02	18,9	20,8	12,57
CEZ-518	A Ceza	32,92	19,1	15,16	14,82	19,17	19,75	17,82	10,5	8,71	9,34	11,73	11,54	18,92	21,67	13,86
CEZ-517	A Ceza	32,32	18,68	14,87	15,63	17,95	18,95	16,08	10,57	7,9	7,5	10,62	11,32	18,88	20,22	14,58
CEZ-801	A Ceza	30,88	18,03	14,43	15,75	16,86	18,46	15,01	9,37	8,2	8,67	9,33	10,59	16,78	19,45	13,32

m3: Length vs breadth

Specimen	Site	L	B
SM219.40	Serra de Molianos	20,53	15,41
FO.I-35	Fontainhas	22,88	15,52
FO.I-152	Fontainhas	22,66	15,2
FO.I-37	Fontainhas	23,52	17,8
GFP-1423	Furninha (8,8)	22,78	15,44
GFP-1381.3	Furninha (7,5)	22,75	16,61
GFP-1140.37.1	Furninha (7,5)	21,53	17,05
GFP-1140.37.2	Furninha (7,5)	21,45	15,1
GFP-1140.37.3	Furninha (7,5)	22,27	15,1
GFP-1140.37.4	Furninha (7,5)	18,65	13,52
GFP-1140.37.5	Furninha (7,5)	22,66	16,74
GFP-1140.37.6	Furninha (7,5)	18,19	13,9
GFP-1140.37.7	Furninha (7,5)	25,84	18,68
GFP-1140.37.8	Furninha (7,5)	21,45	16,05
GFP-1140.37.9	Furninha (7,5)	21,68	17,12
GFP-1140.37.10	Furninha (7,5)	22,12	15,93
GFP-1362.1	Furninha (7,5)	22,31	17,56
GFP-1362.2	Furninha (7,5)	21,29	16,25
GFP-1356.3	Furninha (7,5)	22,73	16,12
GFP-1358.3	Furninha (7,5)	19,65	14,82
GFP-1519.2	Furninha (7,5)	23,99	16,07
GFP-1520	Furninha (7,5)	20,17	15,88
GFP-1328	Furninha (7,5)	21,32	15,93
SIPA-23	Pleistocene Galicia	15,21	13,45
SIPA-53	Pleistocene Galicia	19,59	15,68
SIPA-17	Pleistocene Galicia	21,8	16,1
SIPA-130	Pleistocene Galicia	21,54	16,53
LCF-003-1996	Holocene Galicia	17,96	15,21
LCF-002-1996	Holocene Galicia	18,38	15,5
LCF-147	Holocene Galicia	18,51	14,49
LCF-155	Holocene Galicia	19,32	14,76
EIX-018	Holocene Galicia	19,25	14,6
CGLL-006	Holocene Galicia	20,52	15,68
CGLL-011	Holocene Galicia	20,24	15,59
SH5-97-U29-7	Holocene Galicia	19,42	14,39
SH5-97-U29-6	Holocene Galicia	19,37	13,88
SH5-98-V29-7	Holocene Galicia	20,97	15,87
SH5-98-S30-6	Holocene Galicia	21,15	15,98
TA-192	Holocene Galicia	19,73	15,26
TA-200	Holocene Galicia	19,52	14,68
LE1	Modern	16,25	13,77
LE1	Modern	16,71	13,93

QU	Modern	12,85	11,6
QU	Modern	13,2	11,4
MZB82-7005	Modern	16,99	14,35
MZB82-7006	Modern	17,27	14,36
CEZ-153	A Ceza	25,31	17,91
CEZ-163	A Ceza	23,87	17,8
CEZ-146	A Ceza	26,4	20,3
CEZ-801	A Ceza	22,17	17,1
CEZ-144	A Ceza	25,42	19,44
CEZ-518	A Ceza	28,78	20,66

m3: Length vs breadth including *Ursus thibetanus*.

Specimen	Site	L	B
SM219.40	Serra de Molianos	20,53	15,41
FO.I-35	Fontainhas	22,88	15,52
FO.I-152	Fontainhas	22,66	15,2
FO.I-37	Fontainhas	23,52	17,8
GFP-1423	Furninha (8,8)	22,78	15,44
GFP-1381.3	Furninha (7,5)	22,75	16,61
GFP-1140.37.1	Furninha (7,5)	21,53	17,05
GFP-1140.37.2	Furninha (7,5)	21,45	15,1
GFP-1140.37.3	Furninha (7,5)	22,27	15,1
GFP-1140.37.4	Furninha (7,5)	18,65	13,52
GFP-1140.37.5	Furninha (7,5)	22,66	16,74
GFP-1140.37.6	Furninha (7,5)	18,19	13,9
GFP-1140.37.7	Furninha (7,5)	25,84	18,68
GFP-1140.37.8	Furninha (7,5)	21,45	16,05
GFP-1140.37.9	Furninha (7,5)	21,68	17,12
GFP-1140.37.10	Furninha (7,5)	22,12	15,93
GFP-1362.1	Furninha (7,5)	22,31	17,56
GFP-1362.2	Furninha (7,5)	21,29	16,25
GFP-1356.3	Furninha (7,5)	22,73	16,12
GFP-1358.3	Furninha (7,5)	19,65	14,82
GFP-1519.2	Furninha (7,5)	23,99	16,07
GFP-1520	Furninha (7,5)	20,17	15,88
GFP-1328	Furninha (7,5)	21,32	15,93
SIPA-23	Pleistocene Galicia	15,21	13,45
SIPA-53	Pleistocene Galicia	19,59	15,68
SIPA-17	Pleistocene Galicia	21,8	16,1
SIPA-130	Pleistocene Galicia	21,54	16,53
LCF-003-1996	Holocene Galicia	17,96	15,21
LCF-002-1996	Holocene Galicia	18,38	15,5
LCF-147	Holocene Galicia	18,51	14,49
LCF-155	Holocene Galicia	19,32	14,76

EIX-018	Holocene Galicia	19,25	14,6
CGLL-006	Holocene Galicia	20,52	15,68
CGLL-011	Holocene Galicia	20,24	15,59
SH5-97-U29-7	Holocene Galicia	19,42	14,39
SH5-97-U29-6	Holocene Galicia	19,37	13,88
SH5-98-V29-7	Holocene Galicia	20,97	15,87
SH5-98-S30-6	Holocene Galicia	21,15	15,98
TA-192	Holocene Galicia	19,73	15,26
TA-200	Holocene Galicia	19,52	14,68
LE1	Modern	16,25	13,77
LE1	Modern	16,71	13,93
QU	Modern	12,85	11,6
QU	Modern	13,2	11,4
MZB82-7005	Modern	16,99	14,35
MZB82-7006	Modern	17,27	14,36
CEZ-153	A Ceza	25,31	17,91
CEZ-163	A Ceza	23,87	17,8
CEZ-146	A Ceza	26,4	20,3
CEZ-801	A Ceza	22,17	17,1
CEZ-144	A Ceza	25,42	19,44
CEZ-518	A Ceza	28,78	20,66
V6059	U. thibetanus	15,5	12
V6061	U. thibetanus	16,7	12,3
min Europe	U. thibetanus	14,6	10,9
avg Europe	U. thibetanus	16	12,18
max Europe	U. thibetanus	17,4	13
min modern	U. thibetanus	11,4	9,9
avg modern	U. thibetanus	14,21	11,08
max modern	U. thibetanus	17,8	12,09

m3: PCA

Specimen	Site	L	B	Ltrd(in.)	Bant.	Bpost.	Hprd	Hmed	Hend	Hhyd	Lprd-med	Lmed-hyd	Lprd-end	Lhyd-end
SM219.40	Serra de Molianos	20,53	15,41	10,77	15,12	12,84	6,38	6,92	5,02	5,26	9,57	14,26	13,3	7,55
FO.I-35	Fontainhas	22,88	15,52	11,77	15,48	13,65	6,1	6,76	5,5	4,95	10,66	13,42	16,6	9,52
FO.I-152	Fontainhas	22,66	15,2	10,83	15,46	14,05	6,59	6,49	4,55	4,56	11,39	14,01	16,4	9,61
GFP-1423	Furninha (8,8)	22,78	15,44	11,68	15,66	14,14	7,21	8,66	6,36	6,05	8,36	15,91	13,41	7,41
GFP-1140.37.1	Furninha (7,5)	21,53	17,05	11,22	16,97	14,65	6,67	7	5,34	6,54	10,14	14,82	16,21	10,54
GFP-1140.37.3	Furninha (7,5)	22,27	15,1	10,13	14,74	13,64	5,57	5,3	4,21	6,04	10,11	16,3	17,42	10,72
GFP-1140.37.5	Furninha (7,5)	22,66	16,74	12,23	16,19	14,84	5,27	6,45	5,03	6,25	9,7	16,25	14,6	8,66
GFP-1140.37.7	Furninha (7,5)	25,84	18,68	12,81	18,07	17,33	6,62	6,98	7,25	5,75	10,85	17,42	18,51	10,8

GFP-1140.37.8	Furninha (7,5)	21,45	16,05	11,54	15,95	13,83	6,05	5,85	5,16	4,95	10,21	15,42	14,87	9,44
GFP-1140.37.9	Furninha (7,5)	21,68	17,12	11,26	17,29	15,5	6,91	6,24	4,07	6,83	10,26	14,46	14,51	10,31
GFP-1140.37.10	Furninha (7,5)	22,12	15,93	12,07	15,95	14,31	6,72	6,58	5,95	5,6	9,85	13,96	15,8	10,24
GFP-1362.1	Furninha (7,5)	22,31	17,56	12,68	17,4	15,63	6,09	7,41	5,99	6,78	10,3	16	15,42	8,39
GFP-1362.2	Furninha (7,5)	21,29	16,25	12,13	16,29	14,33	5,27	5,99	4,79	4,45	9,71	14,61	16,11	8,86
GFP-1520	Furninha (7,5)	20,17	15,88	12,11	15,59	13,38	5,1	5,49	5,58	3,78	11,3	14,59	14,37	7,66
GFP-1328	Furninha (7,5)	21,32	15,93	12,51	15,97	12,92	5,11	5,72	4,92	4,89	10,15	14,66	18,39	8,02
SIPA-23	Pleistocene Galicia	15,21	13,45	9,75	13,51	10,64	5,31	4,79	3,8	4,03	10,5	13,19	13,58	8,68
SIPA-53	Pleistocene Galicia	19,59	15,68	11,4	15,72	13,49	5,86	5,18	5,15	3,62	10,5	12,85	12,82	7,8
SIPA-17	Pleistocene Galicia	21,8	16,1	12,89	16,39	14,73	5,94	5,82	5,34	3,51	9,61	12,85	13,34	8,53
SIPA-130	Pleistocene Galicia	21,54	16,53	12,76	16,49	15,53	6,64	5,69	4,38	3,74	9,69	13,34	12,83	8,31
LCF-003-1996	Holocene Galicia	17,96	15,21	9,5	15,35	13,4	6,11	5,99	4,87	4,26	9,95	12,79	14,54	9,03
LCF-002-1996	Holocene Galicia	18,38	15,5	8,04	15,42	14,29	5,16	5,45	4,01	5,57	9,75	14,77	14,28	9,66
LCF-147	Holocene Galicia	18,51	14,49	7,57	14,52	13,72	5,66	5,87	5,1	5,91	9,12	14,77	14,68	9,4
LCF-155	Holocene Galicia	19,32	14,76	9,95	14,61	13,78	5,65	5,72	4,75	3,77	9,75	12,05	12,53	7,12
EIX-018	Holocene Galicia	19,25	14,6	9,25	14,21	13,23	5,69	5,64	4,23	4,46	10,44	17,19	13,03	9,52
CGLL-006	Holocene Galicia	20,52	15,68	8,8	15,6	14,34	6,02	6,41	5,92	4,71	11,43	15,97	13,96	9,28
CGLL-011	Holocene Galicia	20,24	15,59	10,02	14,87	14,98	6,1	6,61	5,52	4,56	11,74	16,1	14,8	10,09
SH5-97-U29-7	Holocene Galicia	19,42	14,39	9,12	14,29	12,85	6,16	5,86	5,33	4,73	9,87	12,42	14,76	9,16
SH5-98-V29-7	Holocene Galicia	20,97	15,87	10,12	16,28	14,82	6,78	7,58	5,93	5,97	10,1	16,81	13,98	9,8
SH5-98-S30-6	Holocene Galicia	21,15	15,98	10,6	16,13	14,84	8,02	6,74	5,88	5,97	10,02	16,55	14,48	9,54
TA-200	Holocene Galicia	19,52	14,68	10,25	14,68	12,91	6,11	6,03	4,73	5,22	8,74	12,54	13,59	6,36
LE1	Modern	16,25	13,77	9,93	13,53	10,55	3,37	4,59	4,67	3,22	8,71	11,78	12,24	7,28
LE1	Modern	16,71	13,93	10,33	14,47	11,38	3,78	4,96	3,68	3,18	9,96	10,62	11,45	5,69
CEZ-163	A Ceza	23,87	17,8	12,08	16,9	16,4	7,23	6,09	6,98	4,03	12,01	16,06	16,16	10,51
CEZ-146	A Ceza	26,4	20,3	12,75	19,93	18,1	7,35	8,53	7,97	5,58	11,99	18,71	18,49	10,65
CEZ-801	A Ceza	22,17	17,1	11,9	16,67	16,6	6,49	6,34	6,02	4,25	11,42	16,43	14,73	10,14
CEZ-144	A Ceza	25,42	19,44	12,99	19,28	17,97	6,9	7,05	6,6	5,17	13,6	18,25	19,31	11,27
CEZ-518	A Ceza	28,78	20,66	15,45	19,39	20,4	6,84	7,8	7,67	4,3	13,61	20,28	20,67	13,84

Cranium: PCA

Specimen	Site	LA-F	DTot-ot	DTproc.	DTf.m.	HB-O	DTEu-Eu	DTcons.ncr.	DTEco-Eco	HA-B
GFP-1338	Furninha	202,22	101,12	136,13	31,49	18,31	101,72	75,4	102,92	84,75
ARLU-38	Pleistocene Galicia	193,3	62,85	147,22	33,38	21,37	86,39	73,19	115,29	82,56
LCF-001-1996	Holocene Galicia	208,7	131,56	179,28	34,59	23,58	111,75	75,22	126,08	87,01
GP-2	Holocene Galicia	176,25	117,01	138,63	33,6	20,97	95,5	74,36	105,07	94,25
RT-002	Holocene Galicia	212	130,92	185,28	29,35	19,49	105,54	78,52	134,37	137,1
RT-001	Holocene Galicia	220,6	134	183,47	33,88	20,74	106,16	76,57	118,4	108,5
SH5-97-N20-2	Holocene Galicia	191,66	102,3	135,78	33,5	21,56	93,3	72,48	103,41	79,29
SH5-98-U30-001	Holocene Galicia	170,57	127,93	134,49	38,89	19,89	99,47	73	97,46	83,94
PVR-012	Holocene Galicia	171,3	96,57	137,27	33,92	19,96	98,57	67,47	89,09	92,75
AC2	Modern	157,02	85,86	105,98	32,37	19,11	92,74	70,24	75,32	83,59
AC1	Modern	158,9	91,14	105,92	32,54	22,28	95,03	66,55	71,18	77,6

Hemimandible: Height condyle vs Diameter condyle

Specimen	Site	Hcond	DTcond
GFP-1086	Furninha (8,8)	17,24	40,37
GFP-1328	Furninha (7,5)	19,35	51,9
GFP-1667.1	Furninha (7,5)	18,8	48,55
LCF-003-1996	Holocene Galicia	21,59	61,56
LCF-002-1996	Holocene Galicia	21,16	61,67
LCF-167	Holocene Galicia	19,7	59,96
CCV-003	Holocene Galicia	25,05	69,22
PVR-013	Holocene Galicia	22,65	47,64
PVR-014	Holocene Galicia	23,35	51,64
SH5-97-U29-7	Holocene Galicia	16,37	43,71
SH5-97-U29-6	Holocene Galicia	16,48	42,99
AC1	Modern	16,23	31,82
AC1	Modern	14,83	33,97
AC2	Modern	15,39	34,49
LE1	Modern	15,54	61,01
CEZ-141	A Ceza	26,7	66,45

Hemimandible: Height mandible vs Diameter mandible

Specimen	Site	Hmd(M2p.)(li.)	DTmd(M2,M3)
FO.I-36	Fontainhas	58,48	22,84
FO.I-37	Fontainhas	63,98	21,11
GFP-1358	Furninha (7,5)	56,94	24,37
GFP-1328	Furninha (7,5)	55,73	24,7
LCF-003-1996	Holocene Galicia	52,1	23,31
LCF-002-1996	Holocene Galicia	52,73	23,86
LCF-155	Holocene Galicia	40,92	19,47

CCV-003	Holocene Galicia	51,43	25,03
CCV-004	Holocene Galicia	54,38	22,8
GP-1	Holocene Galicia	41,48	16,07
CGLL-012	Holocene Galicia	40,61	18,39
CGLL-011	Holocene Galicia	41,26	18,16
PVR-013	Holocene Galicia	50,64	20
PVR-014	Holocene Galicia	46,99	19,57
SH5-97-U29-7	Holocene Galicia	36,41	14,35
SH5-97-U29-6	Holocene Galicia	37,13	14,25
SH5-98-V29-7	Holocene Galicia	49,89	23,26
SH5-98-S30-6	Holocene Galicia	50,71	22,49
TA-109	Holocene Galicia	44,3	19,95
TA-108	Holocene Galicia	41,65	18,76
AC1	Modern	35,62	16,16
AC1	Modern	34,08	16,07
AC2	Modern	36,58	14,99
LE1	Modern	47,53	19,93
LE1	Modern	49,91	18,85
CEZ-141	A Ceza	67,62	25,88

Atlas: PCA

Specimen	Site	H	DTart.prox.	DAPart.dist.	DAParts.max.	DAParts.min.(dors.)	DAParts.min.(vent.)	H foramen magnum
FO.I-164	Fontainhas	55,31	83,83	76,12	69,23	34,46	28,49	31,32
GFP-No Nº 62 2/2	Furninha (7,5)	38,57	45,14	42,19	48,12	25,91	18,26	21,29
SIPA-25	Pleistocene Galicia	41,92	77,05	57,28	55,42	29,31	19,94	23,45
LCF-151	Holocene Galicia	52,3	78,87	68,68	61,15	32,7	27,63	30,01
GP-3	Holocene Galicia	48,01	72,34	65,45	59,82	27,74	24,32	31,1
TA-112	Holocene Galicia	46,36	70,06	56,31	57,62	29,38	23,26	27,49
TA-Lu-c-10	Holocene Galicia	40,76	71,87	55,66	55,95	30,05	21,52	25,63
LE1	Modern	45,66	70,75	64,33	62,31	33,95	25	37,19

Atlas: Dorsal diameter vs ventral diameter.

Specimen	Site	DAParts.min.(dors.)	DAParts.min.(vent.)
FO.I-164	Fontainhas	34,46	28,49
GFP-No Nº 62 2/2	Furninha (7,5)	25,91	18,26
SIPA-25	Pleistocene Galicia	29,31	19,94
SIPA-143	Pleistocene Galicia	29,7	22,57
LCF-151	Holocene Galicia	32,7	27,63
GP-3	Holocene Galicia	27,74	24,32
TA-112	Holocene Galicia	29,38	23,26
TA-Lu-c-10	Holocene Galicia	30,05	21,52
LE1	Modern	33,95	25
EI-977	Eirós	41,8	31,7

EI-1044	Eirós	44,4	32,4
EI-1290	Eirós	54,9	31,5
EI-314	Eirós	46,6	29,3
EI-1401	Eirós	37,7	36,2
EI-1402	Eirós	34,3	27,8
EI-1403	Eirós	39,8	40,2
LI-1104	Liñares	56,8	31,7

Scapula: PCA

Specimen	Site	DTdist.	DTart.	DAPart.
GFP-1405	Furninha (7,5)	76,76	62,33	43,33
GFP-1134.16.6	Furninha (7,5)	77,33	63,09	40,49
GFP-1505	Furninha (7,5)	74,19	62,98	42,37
LCF-153	Holocene Galicia	80,9	67,64	44,23
LCF-057	Holocene Galicia	78,92	64,05	40,83
LCF-160	Holocene Galicia	77,74	59,85	35
LCF-161	Holocene Galicia	78,35	59,5	36,28
LCF-162	Holocene Galicia	82,31	69,58	44,32
SH5-97-N19-5	Holocene Galicia	70,37	53,27	34,03
SH5-97-U29-15	Holocene Galicia	74,33	50,19	33,7
SH5-98-U28-011	Holocene Galicia	71,32	54,73	37,82
SH5-97-T30-1	Holocene Galicia	65,19	53,3	33,78
TA-113	Holocene Galicia	67,78	60,22	37,92
TA-Lu-c-10	Holocene Galicia	70,38	58,42	38,77
LE1	Modern	73,76	57,24	41,55
LE1	Modern	71,1	55,34	40,63
LE2	Modern	69,03	53,66	35,78
EI-442	Eirós	88,3	66,3	39,5
EI-372	Eirós	85,8	63,3	41,1
EI-301	Eirós	109	78	50
EI-1640	Eirós	99,4	77,3	53,9
EI-1642	Eirós	105,9	84,7	59
EI-1643	Eirós	85,7	70,2	48,6
EI-1644	Eirós	82,6	68	43,4
EI-1645	Eirós	85,1	71,3	45
EI-1647	Eirós	85,7	68,3	43,4
EI-1650	Eirós	102,1	80,4	55,1

Scapula: Anteroposterior articular diameter vs transverse articular diameter

Specimen	Site	DTart.	DAPart.
GFP-1405	Furninha (7,5)	62,33	43,33
GFP-1134.16.6	Furninha (7,5)	63,09	40,49
GFP-1505	Furninha (7,5)	62,98	42,37

LCF-153	Holocene Galicia	67,64	44,23
LCF-057	Holocene Galicia	64,05	40,83
LCF-160	Holocene Galicia	59,85	35
LCF-161	Holocene Galicia	59,5	36,28
LCF-162	Holocene Galicia	69,58	44,32
SH5-97-N19-5	Holocene Galicia	53,27	34,03
SH5-97-U29-15	Holocene Galicia	50,19	33,7
SH5-98-U28-011	Holocene Galicia	54,73	37,82
SH5-97-T30-1	Holocene Galicia	53,3	33,78
TA-113	Holocene Galicia	60,22	37,92
TA-Lu-c-10	Holocene Galicia	58,42	38,77
LE1	Modern	57,24	41,55
LE1	Modern	55,34	40,63
LE2	Modern	53,66	35,78
EI-442	Eirós	66,3	39,5
EI-372	Eirós	63,3	41,1
EI-301	Eirós	78	50
EI-1640	Eirós	77,3	53,9
EI-1642	Eirós	84,7	59
EI-1643	Eirós	70,2	48,6
EI-1644	Eirós	68	43,4
EI-1645	Eirós	71,3	45
EI-1647	Eirós	68,3	43,4
EI-1650	Eirós	80,4	55,1
EI-1652	Eirós	70,8	46,5

Humerus: Length vs transverse distal diameter

Specimen	**Site**	**L**	**DTdist.**
FO.I-34	Fontainhas	390	110,19
SIPA-24	Pleistocene Galicia	298	82,72
CB-006	Holocene Galicia	271,15	89,88
LCF-005-1996	Holocene Galicia	366,5	106,6
LCF-004-1996	Holocene Galicia	367,8	106,72
LCF-96-036	Holocene Galicia	321,75	87,59
Pur-Lu-16	Holocene Galicia	334,5	101,54
SH5-97-T29-26	Holocene Galicia	319,9	84,13
SH5-97-T29-35	Holocene Galicia	231,65	85,09
TA-Lu-c-2	Holocene Galicia	307,8	87,65
TA-Lu-c-3	Holocene Galicia	310,65	86,5
PVR-015	Holocene Galicia	335,55	94,17
LE1	Modern	317	87,09
LE1	Modern	314,75	90,87
LE2	Modern	301,3	89,06
EI-949	Eirós	361,6	111,7

EI-371	Eirós	377,2	110,5
LI-805	Liñares	372,3	109,3
LI-812	Liñares	356,3	107,3
LI-814	Liñares	372,2	107,8

Humerus: Diaphysis transverse diameter vs diaphysis anteroposterior diameter

Specimen	Site	DTdia.	DAPdia.
FO.I-34	Fontainhas	46,93	43,23
FO.I-55	Fontainhas	44,13	43,2
GFP-1537	Furninha (8,8)	17,44	23,18
GFP-1376	Furninha (7,5)	40,42	38,35
GFP-1375	Furninha (7,5)	40,42	47,72
GFP-1373	Furninha (7,5)	50,97	46,02
GFP-1130.7	Furninha (7,5)	35,88	43,45
GFP-142	Furninha (7,5)	22,75	30,1
SIPA-24	Pleistocene Galicia	27,6	30,94
CB-006	Holocene Galicia	24,65	31,59
LCF-005-1996	Holocene Galicia	37,38	41,99
LCF-004-1996	Holocene Galicia	37,34	41,69
LCF-96-036	Holocene Galicia	31,35	35,75
LCF-055	Holocene Galicia	31,98	34,66
CGLL-048	Holocene Galicia	26,82	32,76
CGLL-049	Holocene Galicia	25,67	33,45
Pur-Lu-16	Holocene Galicia	38,18	40,48
SH5-97-T29-26	Holocene Galicia	26,01	29,97
SH5-97-T29-35	Holocene Galicia	26,68	29,71
SH5-98-S28-095	Holocene Galicia	32,97	38,91
SH5-97-AD26-001	Holocene Galicia	27,12	28,43
TA-117	Holocene Galicia	33,23	35,19
TA-Lu-c-2	Holocene Galicia	30,24	33,82
TA-Lu-c-3	Holocene Galicia	30,03	35,7
LE1	Modern	31,01	34,42
LE1	Modern	31,99	34,6
LE2	Modern	32,08	33,87

Humerus: transverse distal diameter vs transverse distal articular diameter

Specimen	Site	DTdist.	DTart.dist.
FO.I-34	Fontainhas	110,19	86,06
GFP-1379	Furninha (7,5)	114,09	83,31
ARLU–39(2102)	Pleistocene Galicia	106,41	65,74
SIPA-24	Pleistocene Galicia	82,72	56,58
CB-006	Holocene Galicia	89,88	71,4
LCF-005-1996	Holocene Galicia	106,6	71,82

LCF-004-1996	Holocene Galicia	106,72	71,93
LCF-96-036	Holocene Galicia	87,59	59,75
Pur-Lu-16	Holocene Galicia	101,54	71,22
SH5-97-T29-26	Holocene Galicia	84,13	58,99
SH5-97-T29-35	Holocene Galicia	85,09	58,45
SH5-98-S28-095	Holocene Galicia	110,16	75,03
TA-Lu-c-2	Holocene Galicia	87,65	62,56
TA-Lu-c-3	Holocene Galicia	86,5	61,44
PVR-015	Holocene Galicia	94,17	67,38
LE1	Modern	87,09	62,27
LE1	Modern	90,87	66,65
LE2	Modern	89,06	65,18
CEZ-118	A Ceza	105,41	84,03
EI-949	Eirós	111,7	70,8
EI-371	Eirós	110,5	71,3
EI-1661	Eirós	108,6	75,5
EI-1	Eirós	107,3	64,4
EI-951	Eirós	107,5	74
EI-950	Eirós	124	78
LI-6	Liñares	120,86	86,05
LI-805	Liñares	109,3	74,4
LI-812	Liñares	107,3	74,3
LI-813	Liñares	102,6	67,4
LI-814	Liñares	107,8	77,2
LI-815	Liñares	124,4	84,5
LI-816	Liñares	116,2	77,4

Humerus: Transverse distal diameter vs anteroposterior distal diameter

Specimen	Site	DTdist.	DTart.dist.
FO.I-34	Fontainhas	110,19	86,06
GFP-1379	Furninha (7,5)	114,09	83,31
ARLU–39(2102)	Pleistocene Galicia	106,41	65,74
SIPA-24	Pleistocene Galicia	82,72	56,58
CB-006	Holocene Galicia	89,88	71,4
LCF-005-1996	Holocene Galicia	106,6	71,82
LCF-004-1996	Holocene Galicia	106,72	71,93
LCF-96-036	Holocene Galicia	87,59	59,75
Pur-Lu-16	Holocene Galicia	101,54	71,22
SH5-97-T29-26	Holocene Galicia	84,13	58,99
SH5-97-T29-35	Holocene Galicia	85,09	58,45
SH5-98-S28-095	Holocene Galicia	110,16	75,03
TA-Lu-c-2	Holocene Galicia	87,65	62,56
TA-Lu-c-3	Holocene Galicia	86,5	61,44
PVR-015	Holocene Galicia	94,17	67,38

LE1	Modern	87,09	62,27
LE1	Modern	90,87	66,65
LE2	Modern	89,06	65,18
CEZ-118	A Ceza	105,41	84,03
EI-949	Eirós	111,7	70,8
EI-371	Eirós	110,5	71,3
EI-1661	Eirós	108,6	75,5
EI-1	Eirós	107,3	64,4
EI-951	Eirós	107,5	74
EI-950	Eirós	124	78
LI-6	Liñares	120,86	86,05
LI-805	Liñares	109,3	74,4
LI-812	Liñares	107,3	74,3
LI-813	Liñares	102,6	67,4
LI-814	Liñares	107,8	77,2
LI-815	Liñares	124,4	84,5
LI-816	Liñares	116,2	77,4

Radius: Length vs Transverse distal diameter

Specimen	Site	L	DTdist.
FO.I-59	Fontainhas	347	62,54
FO.I-58	Fontainhas	345	63,44
GFP-1332	Furninha (7,5)	294	64,66
GFP-1333	Furninha (7,5)	300,9	66,35
GFP-1134.16.11	Furninha (7,5)	250,08	55,83
CB-004	Holocene Galicia	251,5	54,45
LCF-008-1996	Holocene Galicia	331,1	66,13
LCF-009-1996	Holocene Galicia	332,2	66,84
LCF-96-038	Holocene Galicia	276,8	53,98
CGLL-043	Holocene Galicia	261,45	55,91
Pur-Lu-19	Holocene Galicia	306,5	62,82
Pur-Lu-20	Holocene Galicia	303	58,73
1996-SH5-001	Holocene Galicia	292,4	52,76
SH5-97-V28-001	Holocene Galicia	290,95	52,49
SH5-98-S28-035	Holocene Galicia	320,55	65,81
SH5-98-U30-012	Holocene Galicia	291,1	57,61
TA-Lu-c-5	Holocene Galicia	276,05	54,92
TA-Lu-c-6	Holocene Galicia	274,85	55,41
LE1	Modern	275,2	56,53
LE2	Modern	274	50,34
CEZ-112	A Ceza	266	63,67
CEZ-113	A Ceza	272	56,65
CEZ-553	A Ceza	262	61,13
CEZ-554	A Ceza	258	59,22

EI-250	Eirós	274,8	64,8
EI-1673	Eirós	274,9	66,3
EI-959	Eirós	280,6	68,9
EI-1679	Eirós	287,4	67,4
EI-1680	Eirós	289,9	68,5
EI-1674	Eirós	290,6	68,8
EI-1672	Eirós	292,2	61,7
EI-960	Eirós	293,4	68,7
EI-1677	Eirós	296,8	63,8
EI-1681	Eirós	298,7	65,6
EI-1671	Eirós	323	79,6
EI-1670	Eirós	323,9	79,1
EI-1678	Eirós	327,3	78
EI-1675	Eirós	329,1	85,3
EI-1676	Eirós	331,6	81,7
EI-1378	Eirós	333,4	82
EI-1265	Eirós	338,9	81
LI-821	Liñares	278,6	68,3
LI-822	Liñares	291,3	72,4
LI-823	Liñares	279,8	57,8
LI-825	Liñares	277	66,2
LI-826	Liñares	263,3	65,55

Radius: Transverse proximal diameter vs anteroposterior proximal diameter.

Specimen	Site	DTprox.	DAPprox.
SM219.2	Serra de Molianos	42,94	33,54
SM219.32.2	Serra de Molianos	42,69	31,16
FO.I-59	Fontainhas	42,61	35,05
FO.I-58	Fontainhas	47,73	35,72
GFP-1427	Furninha (8,8)	47,64	44,01
GFP-1333	Furninha (7,5)	39,59	41,23
GFP-1133.21.3	Furninha (7,5)	41,73	43,06
GFP-1134.16.9	Furninha (7,5)	47,06	34,69
GFP-1134.16.10	Furninha (7,5)	40,27	35,84
GFP-1134.16.11	Furninha (7,5)	36,31	37,38
CB-004	Holocene Galicia	40,77	31,24
CB-005	Holocene Galicia	40,28	32,38
LCF-008-1996	Holocene Galicia	46,37	36,96
LCF-101	Holocene Galicia	47,45	35,64
LCF-009-1996	Holocene Galicia	44,89	37,23
LCF-96-038	Holocene Galicia	38,52	29,06
CGLL-043	Holocene Galicia	40,76	27,63
Pur-Lu-19	Holocene Galicia	43,74	39,52
Pur-Lu-20	Holocene Galicia	43,56	37,88

1996-SH5-001	Holocene Galicia	35,34	32,04
SH5-97-V28-001	Holocene Galicia	35,46	31,05
SH5-98-S28-035	Holocene Galicia	44,45	36,01
SH5-98-U30-012	Holocene Galicia	37,33	33,79
TA-Lu-c-5	Holocene Galicia	37,21	30,28
TA-Lu-c-6	Holocene Galicia	37,18	28,4
LE1	Modern	33,67	39,1
LE2	Modern	34,21	36,15

Radius: Transverse distal diameter vs anteroposterior distal diameter

Specimen	Site	DTdist.	DAPdist.
SM219.32.1	Serra de Molianos	59,23	35,86
FO.I-59	Fontainhas	62,54	39,7
FO.I-58	Fontainhas	63,44	35,99
GFP-1332	Furninha (7,5)	64,66	34,95
GFP-1333	Furninha (7,5)	66,35	37,35
GFP-1133.21.4	Furninha (7,5)	57,44	33,86
GFP-1134.16.11	Furninha (7,5)	55,83	34,88
GFP-1666.2	Furninha (7,5)	61,13	33,18
SIPA-3	Pleistocene Galicia	55,25	32,19
CB-004	Holocene Galicia	54,45	34,98
LCF-008-1996	Holocene Galicia	66,13	41,14
LCF-009-1996	Holocene Galicia	66,84	40,65
LCF-96-037	Holocene Galicia	65,68	39,59
LCF-96-038	Holocene Galicia	53,98	31,58
CGLL-043	Holocene Galicia	55,91	35,42
Pur-Lu-19	Holocene Galicia	62,82	38,25
Pur-Lu-20	Holocene Galicia	58,73	40,43
1996-SH5-001	Holocene Galicia	52,76	32,56
SH5-97-V28-001	Holocene Galicia	52,49	32,05
SH5-98-S28-035	Holocene Galicia	65,81	41,75
SH5-98-S29-011	Holocene Galicia	55,29	32,95
SH5-98-U30-012	Holocene Galicia	57,61	33,88
TA-Lu-c-6	Holocene Galicia	55,41	32,77
LE1	Modern	56,53	36,19
LE2	Modern	50,34	32,48

Ulna: PCA

Specimen	Site	DTol.	DAPol.	Dint.sem.	Dext.sem.	DTdia.
SM219.4	Serra de Molianos	34,55	62,45	33,06	69,27	21,55
GFP-1378	Furninha (7,5)	32,62	71,81	33,08	82,07	25,15
SIPA-4	Pleistocene Galicia	39,37	53,46	29,85	61,19	18,45
LCF-010-1996	Holocene Galicia	37,72	71,94	36,01	78,69	23,07

EIX-009	Holocene Galicia	33,86	63,44	37,38	62,75	19,26
SH5-97-T29-11	Holocene Galicia	30,28	57,03	30,27	64,97	15,51
SH5-97-AB25-002	Holocene Galicia	41,54	72,82	32,64	75,97	30,79
SH5-97-T29-27	Holocene Galicia	30,19	55,75	32,45	71,34	16,21
CEZ-101	A Ceza	51,58	95,33	48,33	93,02	38,34

Ulna: Diaphysis transverse diameter vs diaphysis anteroposterior diameter

Specimen	Site	DTdia.	DAPdia.
SM219.4	Serra de Molianos	21,55	34,11
GFP-1535	Furninha (8,8)	18,66	30
GFP-1527	Furninha (8,8)	20,09	31,7
GFP-1377	Furninha (7,5)	25,72	38,08
GFP-1378	Furninha (7,5)	25,15	35,02
SIPA-4	Pleistocene Galicia	18,45	29,81
SIPA-62	Pleistocene Galicia	17,96	25,08
CB-001	Holocene Galicia	15,18	24,94
CB-002	Holocene Galicia	15,12	22,61
LCF-010-1996	Holocene Galicia	23,07	34,09
LCF-163	Holocene Galicia	23,84	32,47
LCF-164	Holocene Galicia	14,15	27,7
EIX-009	Holocene Galicia	19,26	28,64
CGLL-053	Holocene Galicia	16,61	28,29
CGLL-054	Holocene Galicia	17,13	27,51
Pur-Lu-18	Holocene Galicia	23,47	39,29
SH5-97-T29-11	Holocene Galicia	15,51	24,55
SH5-97-T29-091	Holocene Galicia	20,38	26,65
SH5-97-AB25-002	Holocene Galicia	30,79	30,96
SH5-97-T29-27	Holocene Galicia	16,21	24,58
TA-Lu-c-4	Holocene Galicia	20,89	28,69
LE1	Modern	20,07	29,99
LE1	Modern	20,07	28,2
LE2	Modern	20,22	29,35
CEZ-101	A Ceza	38,34	51,65

Ulna: Transverse articular proximal diameter vs Interior articular diameter

Specimen	Site	DTart.prox.	Dint.sem.
FO.I-57	Fontainhas	57,58	39,7
FO.I-56	Fontainhas	60,21	35,38
GFP-1535	Furninha (8,8)	41,99	25,96
GFP-1527	Furninha (8,8)	54,29	33,64
GFP-1425	Furninha (8,8)	54,86	33,6
GFP-1426	Furninha (8,8)	60,58	33,91
GFP-1378	Furninha (7,5)	59,68	33,08

ARLU-14	Pleistocene Galicia	48,69	27,55
SIPA-4	Pleistocene Galicia	37,54	29,85
LCF-010-1996	Holocene Galicia	54,33	36,01
EIX-009	Holocene Galicia	41,86	37,38
CGLL-050	Holocene Galicia	48,02	26,36
CGLL-051	Holocene Galicia	48,83	26,57
CGLL-053	Holocene Galicia	52,71	39,02
SH5-97-T29-11	Holocene Galicia	46,54	30,27
SH5-97-T29-091	Holocene Galicia	45,67	28,81
SH5-97-AB25-002	Holocene Galicia	59,56	32,64
SH5-97-T29-27	Holocene Galicia	45,48	32,45
CEZ-101	A Ceza	69,38	48,33
EI-954	Eirós	56,8	39,4
EI-955	Eirós	56	36,3
EI-957	Eirós	50,4	33,5
EI-20	Eirós	63	42,2
EI-24	Eirós	68,3	43,5
EI-1664	Eirós	62,7	49,7
EI-1663	Eirós	58,8	39
EI-1662	Eirós	58,8	39,3
EI-1665	Eirós	67,5	45,2
EI-1666	Eirós	62,7	44,9
EI-1667	Eirós	56,3	38,1
EI-1668	Eirós	68,9	46,3
LI-253	Liñares	49,1	43,37
LI-818	Liñares	39,7	48

Scapholunate: Length vs transverse diameter

Specimen	Site	L	DT
FO.I-74	Fontainhas	33,99	52,27
GFP-1133.21.7	Furninha	29,79	50,1
SIPA-52	Pleistocene Galicia	26,27	43,59
SIPA-118	Pleistocene Galicia	31,3	51,12
PUR-80	Holocene Galicia	27,69	49,08
LCF-137	Holocene Galicia	26,79	49,43
SH5-98-S28-089	Holocene Galicia	33,14	50,86
SH5-98-S28-100	Holocene Galicia	33,23	51,51
SH5-97-T29-25	Holocene Galicia	25,83	42,62
SH5-97-U29-079	Holocene Galicia	24,34	42,35
TA-Lu-c-34	Holocene Galicia	26,65	44,33
CIPA-922	Modern	30,18	49,54
CEZ-42	A Ceza	36,49	58,8
CEZ-171	A Ceza	25,45	48,24
CEZ-729	A Ceza	28,9	49,84

CEZ-730	A Ceza	28,42	49,8
CEZ-731	A Ceza	40,36	64,61

Pisiform: PCA

Specimen	Site	L	Lmin.	Dtuber.	DTart.	DAPart.	DTdia.min
FO.I-166	Fontainhas	46,76	45,55	26,83	29,21	16,38	16,65
GFP-1551	Furninha (8,8)	43,07	40,74	24,22	27,1	13,57	17,32
GFP-1620.1	Furninha (7,5)	42,65	38,08	24,53	28,21	16,6	15,39
GFP-1123.1	Furninha (7,5)	39,72	35,75	22,32	28,28	14,42	16,05
GFP-1123.2	Furninha (7,5)	46,65	42,45	23,28	29,48	19,64	15,05
GFP-1123.3	Furninha (7,5)	46,46	41,8	24,24	30,03	17,28	15,49
GFP-1123.4	Furninha (7,5)	45,41	40,03	26,25	27,48	15,13	15,52
LCF-139	Holocene Galicia	49,76	43,44	24,84	29,51	16,38	17,44
PUR-83	Holocene Galicia	48,32	40,27	24,77	27,39	17,04	15,16
SH5-98-S28-072	Holocene Galicia	50,23	45,89	26,73	31,54	19,93	18,31
SH5-97-T29-32	Holocene Galicia	35,81	32,45	18,28	24,63	16,5	14,98
SH5-98-T30-006	Holocene Galicia	35,66	32,86	18,67	24,11	15,7	13,94
LE1	Modern	42,67	33,6	24,81	26,91	18,82	17,85
CEZ-49	A Ceza	45,87	39,41	26,36	30,54	16,89	21,08
CEZ-50	A Ceza	43,62	40,36	29,77	30,22	17,43	20,11
CEZ-51	A Ceza	50,9	42,71	30,13	36,15	18,56	24,64
CEZ-52	A Ceza	49,75	45,47	28,57	38,38	24,4	22,54
CEZ-745	A Ceza	51,33	44,78	32,13	34,21	19,05	19,43

Pisiform: Length vs tubercle diameter

Specimen	Site	L	Dtuber.
FO.I-166	Fontainhas	46,76	26,83
GFP-1551	Furninha (8,8)	43,07	24,22
GFP-1620.1	Furninha (7,5)	42,65	24,53
GFP-1123.1	Furninha (7,5)	39,72	22,32
GFP-1123.2	Furninha (7,5)	46,65	23,28
GFP-1123.3	Furninha (7,5)	46,46	24,24
GFP-1123.4	Furninha (7,5)	45,41	26,25
LCF-139	Holocene Galicia	49,76	24,84
PUR-83	Holocene Galicia	48,32	24,77
SH5-98-S28-072	Holocene Galicia	50,23	26,73
SH5-97-T29-32	Holocene Galicia	35,81	18,28
SH5-98-T30-006	Holocene Galicia	35,66	18,67
LE1	Modern	42,67	24,81
CEZ-49	A Ceza	45,87	26,36
CEZ-50	A Ceza	43,62	29,77
CEZ-51	A Ceza	50,9	30,13
CEZ-52	A Ceza	49,75	28,57

CEZ-745	A Ceza	51,33	32,13

First metacarpal: PCA

Specimen	Site	L	DTprox.	DAPprox.	DTdia.min.	DAPdia.	DTdist.	DAPdist.
PUR-65	Holocene Galicia	72,34	23,35	19,18	11,65	10,07	19,68	16,78
SH5-98-S28-053	Holocene Galicia	81,33	24,73	21,68	11,52	11,08	20,8	18,59
SH5-97-T29-23	Holocene Galicia	69,05	20,68	16,63	10,32	10,51	16,26	14,07
SH5-97-AB25	Holocene Galicia	63,13	19,87	18,95	9,05	10,15	15,96	13,33
SH5-97-U29-3	Holocene Galicia	70,15	20,28	17,56	10,07	8,34	16,13	14,36
SH5-97-T29-5	Holocene Galicia	62,9	17,96	21,37	9,52	9,91	16,49	13,23
TA-Lu-c-26	Holocene Galicia	67,51	21,07	17,64	8,77	8,61	16,15	15,3
TA-201	Holocene Galicia	73,99	20,58	10,74	11,2	17,88	13,92	13,52
Modern 2	Modern	68,38	21,96	19,57	10,53	10,28	17,06	13,89
FO.I-64	Fontainhas	80,04	26,1	20,23	12,86	10,37	20,08	15,72
GFP-1603	Furninha (7,5)	72,65	23,83	20,82	11,43	11,09	19,13	16,33
GFP-1602	Furninha (7,5)	75,14	25,99	23,69	12,88	11,57	19,11	15,81
GFP-1601	Furninha (7,5)	68,26	21,98	19,85	9,89	10,38	17,11	15,27
GFP-1605	Furninha (7,5)	85,65	26,6	27,59	17,7	14,72	24,28	19,08
GFP-1138.21.1	Furninha (7,5)	75,13	26,03	20,93	12,45	12,12	19,38	15,89
GFP-1138.21.3	Furninha (7,5)	66,88	20,6	18,61	9,33	10,8	19,43	15,84
GFP-1618.2	Furninha (7,5)	68,9	21,99	17,26	10,11	10,65	16,96	15,42
CIPA-922	Modern	78,12	21,87	20,31	9,35	9,32	17,85	15,71
CEZ-881	A Ceza	46,59	19,12	19,89	9,03	11,04	13,95	13,4
CEZ-513	A Ceza	61,61	22,5	16,69	13,07	10,35	18,38	16,71
EI-133	Eirós	49	19,3	19	9,8	11	14,2	13,8
EI-644	Eirós	59,3	22	18,3	12,3	12,8	16	14,2
EI-645	Eirós	59,9	24,5	21,2	15	11,7	19,6	17
EI-764	Eirós	60,6	24,8	23	14,3	14,6	18,3	17,4
EI-776	Eirós	56,9	20,9	17,5	11,6	11,4	17	16
EI-789	Eirós	67,6	29,6	24,6	16	14	22,4	21,1
EI-1046	Eirós	63,7	26,4	22,5	14	14,7	19,2	18,2
EI-1082	Eirós	68	26,8	21,4	16,8	13	21	19,4
EI-1087	Eirós	68,7	20,9	21,2	12	13,5	17,7	14,9
EI-1220	Eirós	59,3	21,3	19,9	11,7	11,4	17,2	15,8
EI-1238	Eirós	66	26,7	24,2	15,4	16,6	19,1	21,2
EI-1308	Eirós	63,8	33	22,1	17,5	12	22,2	18,7
EI-1755	Eirós	60,4	24,2	25,5	14,7	13,8	18,7	18,1
EI-1756	Eirós	59,7	22	19,9	12,4	10,2	16,4	16,6

First metacarpal: Modified PCA with Serra de Molianos specimen

Specimen	Site	L	DTprox.	DTdia.min.	DTdist.
PUR-65	Holocene Galicia	72,34	23,35	11,65	19,68
SH5-98-S28-053	Holocene Galicia	81,33	24,73	11,52	20,8

SH5-97-T29-23	Holocene Galicia	69,05	20,68	10,32	16,26
SH5-97-AB25	Holocene Galicia	63,13	19,87	9,05	15,96
SH5-97-U29-3	Holocene Galicia	70,15	20,28	10,07	16,13
SH5-97-T29-5	Holocene Galicia	62,9	17,96	9,52	16,49
TA-Lu-c-26	Holocene Galicia	67,51	21,07	8,77	16,15
TA-201	Holocene Galicia	73,99	20,58	11,2	13,92
Modern 2	Modern	68,38	21,96	10,53	17,06
FO.I-64	Fontainhas	80,04	26,1	12,86	20,08
GFP-1603	Furninha	72,65	23,83	11,43	19,13
GFP-1602	Furninha	75,14	25,99	12,88	19,11
GFP-1601	Furninha	68,26	21,98	9,89	17,11
GFP-1605	Furninha	85,65	26,6	17,7	24,28
GFP-1138.21.1	Furninha	75,13	26,03	12,45	19,38
GFP-1138.21.3	Furninha	66,88	20,6	9,33	19,43
GFP-1618.2	Furninha	68,9	21,99	10,11	16,96
CIPA-922	Modern	78,12	21,87	9,35	17,85
Postes-4	Postes	78,2	24,5	12	19,7
SM219.33.1	Serra de Molianos	73,57	21,29	10,45	15,08
CEZ-881	A Ceza	46,59	19,12	9,03	13,95
CEZ-513	A Ceza	61,61	22,5	13,07	18,38
EI-133	Eirós	49	19,3	9,8	14,2
EI-644	Eirós	59,3	22	12,3	16
EI-645	Eirós	59,9	24,5	15	19,6
EI-764	Eirós	60,6	24,8	14,3	18,3
EI-776	Eirós	56,9	20,9	11,6	17
EI-789	Eirós	67,6	29,6	16	22,4
EI-1046	Eirós	63,7	26,4	14	19,2
EI-1082	Eirós	68	26,8	16,8	21
EI-1087	Eirós	68,7	20,9	12	17,7
EI-1220	Eirós	59,3	21,3	11,7	17,2
EI-1238	Eirós	66	26,7	15,4	19,1
EI-1308	Eirós	63,8	33	17,5	22,2
EI-1755	Eirós	60,4	24,2	14,7	18,7
EI-1756	Eirós	59,7	22	12,4	16,4

First metacarpal: Robustness

Specimen	Group	Robustness
CEZ-881	*U. spelaeus*	29,94
CEZ-513	*U. spelaeus*	29,83
EI-133	*U. spelaeus*	28,98
EI-644	*U. spelaeus*	26,98
EI-645	*U. spelaeus*	32,72
EI-764	*U. spelaeus*	30,20
EI-776	*U. spelaeus*	29,88

EI-789	*U. spelaeus*	33,14
EI-1046	*U. spelaeus*	30,14
EI-1082	*U. spelaeus*	30,88
EI-1087	*U. spelaeus*	25,76
EI-1220	*U. spelaeus*	29,01
EI-1238	*U. spelaeus*	28,94
EI-1308	*U. spelaeus*	34,80
EI-1755	*U. spelaeus*	30,96
EI-1756	*U. spelaeus*	27,47
PUR-65	*U.arctos*	27,20
SH5-98-S28-053	*U.arctos*	25,57
SH5-97-T29-23	*U.arctos*	23,55
SH5-97-AB25	*U.arctos*	25,28
SH5-97-U29-3	*U.arctos*	22,99
SH5-97-T29-5	*U.arctos*	26,22
TA-Lu-c-26	*U.arctos*	23,92
TA-201	*U.arctos*	18,81
Modern 2	*U.arctos*	24,95
FO.I-64	*U.arctos*	25,09
GFP-1603	Furninha	26,33
GFP-1602	Furninha	25,43
GFP-1601	Furninha	25,07
GFP-1605	Furninha	28,35
GFP-1138.21.1	Furninha	25,80
GFP-1138.21.3	Furninha	29,05
GFP-1618.2	Furninha	24,62
CIPA-922	*U.arctos*	22,85

Second metacarpal: PCA

Specimen	Site	L	DTprox.	DAPprox.	DTdia.min.	DAPdia.	DTdist.	DAPdist.
CEZ 13	A Ceza	68,76	16,01	23,7	16,42	13,06	23,71	17,77
CEZ 16	A Ceza	67,22	16,91	25,21	15,18	14,07	23,21	18,24
CEZ 18	A Ceza	68,6	16,46	23,56	16,15	14,34	23,96	17,81
CEZ 30	A Ceza	76,2	21,2	26,64	17,63	16,45	27,56	21,33
CEZ 741	A Ceza	83,19	20,72	36,35	20,06	15,24	29,05	23,63
EI-239	Eirós	68,5	18,1	24,7	16,3	12,3	22,5	17,2
EI 462	Eirós	68,5	19	25,4	16,6	12,5	23,1	18,2
EI 462	Eirós	76,5	21,6	27,7	18	15,2	25,2	19,4
EI 643	Eirós	74,2	19,2	26,6	18,7	16	27,4	21,6
EI 759	Eirós	71,3	21,2	26,7	17	13,9	25,5	20,3
EI 771	Eirós	73	20,3	25,1	16,5	13,4	22,7	17,1
EI 787	Eirós	71,4	21,6	25,4	17,3	13,5	23,6	18,8
EI 1131	Eirós	76,2	22,3	30,2	18,8	15,7	24,6	21,8
EI 1200	Eirós	79,6	23,1	29,5	20,3	15	27	20,9

EI 1245	Eirós	74,9	20	27,2	16,9	13,8	25,6	19,5
EI 1264	Eirós	80,9	24,1	29,5	19,7	15,2	25,9	19,6
EI 1274	Eirós	80,7	22,9	31,4	19,2	15,8	28,6	21,4
EI 1284	Eirós	76,2	24,2	26,4	19,1	15,6	27	19,4
EI 1779	Eirós	71,6	18,9	23,8	16,3	13,7	23	19
EI 1782	Eirós	79	24,7	30	20,6	15,4	27,8	21,6
EI 1783	Eirós	69,1	19,4	25,4	17,2	14	22,5	18,4
EI 1784	Eirós	75,8	24,6	31	19,7	18	27,2	20,6
EI 1785	Eirós	69,1	19,3	25	16,9	13,1	23,8	19
EI 1786	Eirós	72,3	20,8	25,4	16,4	14,1	22,1	19,9
EI 1787	Eirós	77	25,5	29,7	19,4	19	27,8	21,7
LI 966	Liñares	72,5	17,97	25,77	15,45	12,66	23,79	19,25
LI 967	Liñares	75,17	19,09	29,95	18,74	15	28,1	21,26
LI 968	Liñares	74,7	17,5	27,41	17,07	13,32	24,18	21,56
LCF-131	Holocene Galicia	91,44	20,25	26,76	16,3	15,1	25,56	17,89
LCF-132	Holocene Galicia	90,74	16,69	27,64	13,91	15,27	22,59	18,55
LCF-135	Holocene Galicia	86,23	15,53	26,06	14,35	10,99	21,53	16,03
PUR-67	Holocene Galicia	79,65	15,51	25,6	11,88	13,03	20,8	18,17
SH5-98-S28-052	Holocene Galicia	89,43	16,69	25,78	13,1	11,97	22,47	20,34
SH5-97-T29-21	Holocene Galicia	77,18	13,6	20,7	11,38	11,26	18,25	16,93
SH5-97-U29-4	Holocene Galicia	77,15	13,73	21,01	11,74	10,92	18,02	15,18
Modern 2	Modern	74,97	17,95	23,17	13,49	11,24	20,86	18,36
GFP-1544	Furninha	75,1	14,28	24,92	12,42	15,5	15,98	16,63
GFP-1549	Furninha	76,55	15,63	23,43	13,45	12,5	16,71	16,63
GFP-1388	Furninha	78,86	16,64	25,64	13,77	13,31	20,81	18,25
GFP-1599	Furninha	78,77	16,77	24,75	15,26	13,13	22,42	17,92
GFP-1598	Furninha	65,68	12,78	20,33	11,05	9,2	16,16	15,17
GFP-1138.21.4	Furninha	75,6	13,86	23,99	11,95	11,81	19,35	17
GFP-1138.21.5	Furninha	75,83	16,9	23,86	12,61	11,68	19,15	17,22

Second metacarpal: Robustness

Specimen	Group	Robustness
CEZ 13	*U. spelaeus*	34,48
CEZ 16	*U. spelaeus*	34,53
CEZ 18	*U. spelaeus*	34,93
CEZ 30	*U. spelaeus*	36,17
CEZ 741	*U. spelaeus*	34,92
EI-239	*U. spelaeus*	32,85
EI 462	*U. spelaeus*	33,72
EI 462	*U. spelaeus*	32,94
EI 643	*U. spelaeus*	36,93
EI 759	*U. spelaeus*	35,76
EI 771	*U. spelaeus*	31,10
EI 787	*U. spelaeus*	33,05

EI 1131	*U. spelaeus*	32,28
EI 1200	*U. spelaeus*	33,92
EI 1245	*U. spelaeus*	34,18
EI 1264	*U. spelaeus*	32,01
EI 1274	*U. spelaeus*	35,44
EI 1284	*U. spelaeus*	35,43
EI 1779	*U. spelaeus*	32,12
EI 1782	*U. spelaeus*	35,19
EI 1783	*U. spelaeus*	32,56
EI 1784	*U. spelaeus*	35,88
EI 1785	*U. spelaeus*	34,44
EI 1786	*U. spelaeus*	30,57
EI 1787	*U. spelaeus*	36,10
LI 966	*U. spelaeus*	32,81
LI 967	*U. spelaeus*	37,38
LI 968	*U. spelaeus*	32,37
LCF-131	*U.arctos*	27,95
LCF-132	*U.arctos*	24,90
LCF-135	*U.arctos*	24,97
PUR-67	*U.arctos*	26,11
SH5-98-S28-052	*U.arctos*	25,13
SH5-97-T29-21	*U.arctos*	23,65
SH5-97-U29-4	*U.arctos*	23,36
Modern 2	*U.arctos*	27,82
GFP-1544	Furninha	21,28
GFP-1549	Furninha	21,83
GFP-1388	Furninha	26,39
GFP-1599	Furninha	28,46
GFP-1598	Furninha	24,60
GFP-1138.21.4	Furninha	25,60
GFP-1138.21.5	Furninha	25,25

Third metacarpal: PCA

Specimen	Site	L	DTprox.	DAPprox.	DTdia.min.	DAPdia.	DTdist.	DAPdist.
CEZ-11	A Ceza	82,38	22,68	30,75	18,95	16,34	29,01	23,27
CEZ-12	A Ceza	75,82	18,5	26,37	16,86	14,58	24,39	19,27
CEZ-712	A Ceza	73,91	20,19	26,6	16,63	13,15	22,55	19,86
CEZ-733	A Ceza	72,11	18,94	25,84	16,83	13,4	22,98	19,46
EI-96	Eirós	76,7	18,5	26,7	16,8	13,2	23,3	19,3
EI-240	Eirós	83,4	21	30,4	18,9	16,5	27,8	22,3
EI-416	Eirós	78,4	19,3	28,3	15,4	14,3	23	19,5
EI-636	Eirós	78,6	19,5	29,5	16,1	14	25,4	21
EI-637	Eirós	76,2	19,7	28,2	16,7	13,8	26	21,3
EI-760	Eirós	72,8	18,3	25,3	16,2	13,7	23,6	19,5

EI-762	Eirós	78,3	21,9	30,2	19,1	18,9	26,7	19,7
EI-786	Eirós	77,8	18,7	27,3	15,6	13,5	22,6	19
EI-790	Eirós	73,5	19,3	26,7	17	13,2	23,5	19,4
EI-1055	Eirós	81,2	23	21,1	18,8	15	27,3	19,6
EI-1280	Eirós	84	22	30,3	17,9	15,2	27	21,3
EI-1298	Eirós	81,1	20,7	32	17	14	26,2	22
EI-1766	Eirós	79,2	21,9	31,7	18,6	16,8	27,1	20
LI-972	Liñares	75	21,1	28,2	15,7	13,3	24,8	20
LCF-133	Holocene Galicia	82,48	20,08	24,17	17,26	10,89	18,4	14,97
LCF-134	Holocene Galicia	82,87	20,44	25,97	12,5	10,47	18,24	16,32
SH5-98-S28-062	Holocene Galicia	92,98	22,62	26,26	14,78	12,28	22,8	22,03
SH5-97-T29-082	Holocene Galicia	78,26	15,81	22,53	11,92	9,92	17,97	15,62
SH5-97-U29-2	Holocene Galicia	79,84	16,21	22,66	11,83	10,03	17,57	16,04
GFP-1387	Furninha	81,96	18,59	27,06	14,55	12,88	21,78	20,12
GFP-1597	Furninha	76,53	16,42	23,43	12,69	11,07	20,26	17,98
GFP-1595	Furninha	81,86	17,16	24,87	15,27	13,46	22,74	19,75
GFP-1596	Furninha	80,55	18,68	26,06	15,05	13,54	22,4	19,17
GFP-1138.21.6	Furninha	82,28	19,31	27,13	15,78	14,01	22,75	19,07
GFP-1138.21.7	Furninha	78,22	17,5	25,08	12,24	11,22	19,33	18,24
GFP-1138.21.8	Furninha	77,99	16,66	24,25	12,51	10,94	18,87	17,77
CIPA-922	Modern	89,39	14,16	24,58	11,35	10,79	19,72	18,25

Third metacarpal: Robustness

Specimen	Group	Robustness
CEZ-11	*U. spelaeus*	35,21
CEZ-12	*U. spelaeus*	32,17
CEZ-712	*U. spelaeus*	30,51
CEZ-733	*U. spelaeus*	31,87
EI-96	*U. spelaeus*	30,38
EI-240	*U. spelaeus*	33,33
EI-416	*U. spelaeus*	29,34
EI-636	*U. spelaeus*	32,32
EI-637	*U. spelaeus*	34,12
EI-760	*U. spelaeus*	32,42
EI-762	*U. spelaeus*	34,10
EI-786	*U. spelaeus*	29,05
EI-790	*U. spelaeus*	31,97
EI-1055	*U. spelaeus*	33,62
EI-1280	*U. spelaeus*	32,14
EI-1298	*U. spelaeus*	32,31
EI-1766	*U. spelaeus*	34,22
LI-972	*U. spelaeus*	33,07
LCF-133	*U.arctos*	22,31
LCF-134	*U.arctos*	22,01

SH5-98-S28-062	*U.arctos*	24,52
SH5-97-T29-082	*U.arctos*	22,96
SH5-97-U29-2	*U.arctos*	22,01
GFP-1387	Furninha	26,57
GFP-1597	Furninha	26,47
GFP-1595	Furninha	27,78
GFP-1596	Furninha	27,81
GFP-1138.21.6	Furninha	27,65
GFP-1138.21.7	Furninha	24,71
GFP-1138.21.8	Furninha	24,20
CIPA-922	*U.arctos*	22,06

Fourth metacarpal: PCA

Specimen	Site	L	DTprox.	DAPprox.	DTdia.min.	DAPdia.	DTdist.	DAPdist.
CEZ-19	A Ceza	82,84	23,58	32,27	19,4	17,07	28,56	23,17
CEZ-22	A Ceza	85,33	24,43	32,42	20,84	19,07	31,12	24,11
CEZ-28	A Ceza	85,42	25,43	30,25	19,55	18,11	29,95	23,46
EI-30	Eirós	77,8	22,5	28	16,7	14,2	24,1	19,2
EI-97	Eirós	83,5	25	29,5	19,6	15,6	28,2	21,7
EI-238	Eirós	86,5	26,3	31	20,8	16,5	28	22
EI-441	Eirós	76,2	21,4	27,1	18	14,1	25	19,4
EI-518	Eirós	79,5	21,4	28	18	14	24,3	19,8
EI-765	Eirós	84,6	24,1	31,4	19,4	18,6	28,4	20,7
EI-770	Eirós	81	20,7	28,4	17,5	11,3	20,4	19,7
EI-1075	Eirós	82	22,4	31	16,5	15,1	25,3	21,2
EI-1089	Eirós	89,2	23,7	33,2	20,4	18	26,6	21,3
EI-1156	Eirós	86,5	25,3	34,5	19,9	17,5	31,8	23,7
EI-1221	Eirós	87,6	25,7	33,9	21	17,1	29,1	22,8
EI-1767	Eirós	81,2	24,4	35	20,4	18,2	28	20,7
EI-1769	Eirós	86,4	26,3	33,4	22,7	19,8	30	23,8
EI-1770	Eirós	76,2	21,9	28	18,1	14,7	25,1	20,1
EI-1771	Eirós	85,6	26,3	33,3	22,9	19,4	29,6	23,7
LI-5	Liñares	80,5	21,65	30,9	18,23	14,65	26,18	21,33
SH5-98-S28-061	Holocene Galicia	89,3	20,23	25,49	13,81	11,8	21,2	20,64
SH5-98-U30-004	Holocene Galicia	79,34	14	21,81	11,52	9,58	17,94	16,17
SH5-98-T28-016	Holocene Galicia	82,36	15,63	23,34	13,66	10,97	20,05	18
SH5-97-U29-5	Holocene Galicia	79,09	14,44	22,09	11,59	9,46	17,55	15,98
TA-Lu-c-21	Holocene Galicia	77,28	16,12	22,08	12,46	10,18	19,37	17,26
GFP-1386	Furninha	85,25	18,64	28,75	15,48	12,74	22,23	18,97
GFP-1591	Furninha	76,67	19,3	23,98	13,15	11,68	19,69	18,17
GFP-1593	Furninha	76,21	16,87	25,4	12,69	10,47	19,29	15,14
GFP-1594	Furninha	88,23	20,38	27,47	17,93	13,97	24,37	20,96
GFP-1619.1	Furninha	75	16,77	26,24	13,85	11,05	20,35	17,83
CIPA-922	Modern	92,7	17,4	24,31	13,24	11,42	20,83	18,84

Fourth metacarpal: Robustness

Specimen	Group	Robustness
CEZ-19	*U. spelaeus*	34,48
CEZ-22	*U. spelaeus*	36,47
CEZ-28	*U. spelaeus*	35,06
EI-30	*U. spelaeus*	30,98
EI-97	*U. spelaeus*	33,77
EI-238	*U. spelaeus*	32,37
EI-441	*U. spelaeus*	32,81
EI-518	*U. spelaeus*	30,57
EI-765	*U. spelaeus*	33,57
EI-770	*U. spelaeus*	25,19
EI-1075	*U. spelaeus*	30,85
EI-1089	*U. spelaeus*	29,82
EI-1156	*U. spelaeus*	36,76
EI-1221	*U. spelaeus*	33,22
EI-1767	*U. spelaeus*	34,48
EI-1769	*U. spelaeus*	34,72
EI-1770	*U. spelaeus*	32,94
EI-1771	*U. spelaeus*	34,58
LI-5	*U. spelaeus*	32,52
SH5-98-S28-061	*U.arctos*	23,74
SH5-98-U30-004	*U.arctos*	22,61
SH5-98-T28-016	*U.arctos*	24,34
SH5-97-U29-5	*U.arctos*	22,19
TA-Lu-c-21	*U.arctos*	25,06
GFP-1386	Furninha	26,08
GFP-1591	Furninha	25,68
GFP-1593	Furninha	25,31
GFP-1594	Furninha	27,62
GFP-1619.1	Furninha	27,13
CIPA-922	*U.arctos*	22,47

Fifth metacarpal: PCA

Specimen	Site	L	DTprox.	DAPprox.	DTdia.min.	DAPdia.	DTdist.	DAPdist.
EI-88	Eirós	76,1	25	29,2	18	15,4	24,1	17,8
EI-94	Eirós	76,6	25,7	29,9	17,8	16,3	25,6	19,8
EI-641	Eirós	80,2	29,7	31,1	19,8	17,4	26,4	21,1
EI-766	Eirós	83,2	29	34,9	19,4	18,6	28,1	20,8
EI-1015	Eirós	86,6	31,4	35,9	23,2	19	29,5	21,8
EI-1033	Eirós	88,6	32,1	34,4	21,9	18,5	30,2	22,4

EI-1232	Eirós	77	26	29,1	18,5	15,3	25,6	17,6
EI-1772	Eirós	76,2	26,4	30,5	17,5	15,2	26,2	19,3
EI-1774	Eirós	76,9	27	29,3	18,4	15,4	26,1	19,7
EI-1775	Eirós	83	29,9	33,6	20,1	18,9	29,3	20,6
EI-1776	Eirós	75,9	26	30,9	17,7	15,2	26	18,9
SH5-98-S28-063	Holocene Galicia	95,87	29,34	29,45	15,67	12,93	24,5	21,32
SH5-97-T29-24	Holocene Galicia	80,1	21,38	23,92	12,04	10,08	20,93	16,58
SH5-98-T30-004	Holocene Galicia	80,22	21,22	24,55	12,24	10,27	20,6	16,47
SH5-96-008	Holocene Galicia	79,77	27,37	26,25	14,42	11,88	22,63	17,63
VA87/14E/3	Holocene Galicia	73,16	21,01	22,73	13,07	10,23	20,13	17,7
LE1	Modern	80,19	23,27	20,26	13,63	12,99	22,43	18,14
GFP-1385	Furninha	86,58	25,66	25,36	17,03	12,6	24,66	18,56
GFP-1619.2	Furninha	87,46	25,28	27,37	16,05	12,18	24,42	18,51
GFP-1619.3	Furninha	81,65	23,91	25,34	14,67	11,25	21,45	17,45
GFP-1618.1	Furninha	80,53	29,08	24,04	15,48	11,22	23,15	17,7
CIPA-922	Modern	91,96	25,88	28,64	14,78	11,95	24,75	18,55

Fifth metacarpal: Robustness

Specimen	Group	Robustness
EI-88	*U. spelaeus*	31,67
EI-94	*U. spelaeus*	33,42
EI-641	*U. spelaeus*	32,92
EI-766	*U. spelaeus*	33,77
EI-1015	*U. spelaeus*	34,06
EI-1033	*U. spelaeus*	34,09
EI-1232	*U. spelaeus*	33,25
EI-1772	*U. spelaeus*	34,38
EI-1774	*U. spelaeus*	33,94
EI-1775	*U. spelaeus*	35,30
EI-1776	*U. spelaeus*	34,26
SH5-98-S28-063	*U.arctos*	25,56
SH5-97-T29-24	*U.arctos*	26,13
SH5-98-T30-004	*U.arctos*	25,68
SH5-96-008	*U.arctos*	28,37
VA87/14E/3	*U.arctos*	27,52
LE1	*U.arctos*	27,97
GFP-1385	Furninha	28,48
GFP-1619.2	Furninha	27,92
GFP-1619.3	Furninha	26,27
GFP-1618.1	Furninha	28,75
CIPA-922	*U.arctos*	26,91

Pelvis: Acetabulum transverse diameter

	Dacet.
FO.I-46	56,76
FO.I-47	57,6
GFP-1336	53
GFP-1507	51,56
GFP-1503	52,66
ARLU-42	48,92
SIPA-106	56,17
LCF-SN	51,72
LCF-SN	53,86
LCF-172	53,71
LCF-172	54,09
EIX-007	46,79
CGLL-024+CGLL-025	53,15
PUR-Lu-1	53,64
SH5-97-T29-2	49,63
SH5-98-U30-010	52,16
SH5-98-Q30-003	48,37
SH5-98-Q30-003	44,41
TA-Lu-c-1	45,48
TA-Lu-c-1	44,85
LE1	46,94
LE1	46,51
LE2	45,49
LE2	45,37

Femur: PCA

Specimen	Site	DTprox	DAPcaput	Ltroc.	Lcollum	Dtdia.	DAPdia.
FO.I-51	Fontainhas	115,25	51,96	79,84	58,76	40,86	34,34
FO.I-49	Fontainhas	115,14	51,25	81,64	62,82	41,05	34,4
GFP-1142	Furninha (7,5)	105,33	45,57	80,54	57,5	35,02	34,03
LCF-006-1996	Holocene Galicia	98,8	49,9	69,87	68,44	36,81	32,29
LCF-007-1996	Holocene Galicia	100,5	50,69	70,73	62,04	37,1	31,97
LCF-173	Holocene Galicia	92,72	44,58	57,16	50,28	29,77	25,61
EIX-010	Holocene Galicia	89,57	41,94	49,26	43,97	29,57	25,34
Pur-Lu-21	Holocene Galicia	100,56	46,86	74,93	65,44	36,96	31,13
Pur-Lu-22	Holocene Galicia	100,31	48,32	72,89	64,77	37,81	31,47
SH5-97-T28-12	Holocene Galicia	94,01	43,61	62,26	49,77	35,14	27,58
SH5-98-T30-008	Holocene Galicia	86,9	39,39	52,94	41,92	31,16	25,94
SH5-97-T29-58	Holocene Galicia	86,78	39,65	66,73	50,04	26,89	22,89
TA-Lu-c-7	Holocene Galicia	89,42	40,67	65,88	45,55	28,45	24,61
TA-Lu-c-8	Holocene Galicia	86,56	41,1	69,65	45,51	28,52	25,39
LE2	Modern	87,94	42,34	59,92	40,4	32,26	28,43

LE2	Modern	88,87	40,76	59,06	40	32,76	27,67

Femur: Length vs transverse proximal diameter

Specimen	Site	L	DTprox
FO.I-51	Fontainhas	461	115,25
FO.I-49	Fontainhas	459	115,14
LCF-006-1996	Holocene Galicia	444,8	98,8
LCF-007-1996	Holocene Galicia	443,4	100,5
LCF-173	Holocene Galicia	375,25	92,72
EIX-010	Holocene Galicia	377	89,57
Pur-Lu-21	Holocene Galicia	417,5	100,56
Pur-Lu-22	Holocene Galicia	417	100,31
SH5-98-T30-008	Holocene Galicia	355,85	86,9
SH5-97-T29-58	Holocene Galicia	380,6	86,78
TA-Lu-c-7	Holocene Galicia	367,1	89,42
TA-Lu-c-8	Holocene Galicia	364,3	86,56
LE2	Modern	358,05	87,94
LE2	Modern	355,9	88,87
EI-968	Eirós	378,9	100,9
EI-46	Eirós	395,5	97,5
EI-967	Eirós	401,1	110,7
EI-43	Eirós	403	101,4
EI-1686	Eirós	404,3	105,1
EI-1682	Eirós	407,6	103,3
EI-1684	Eirós	455,7	121,6
EI-1683	Eirós	456,3	121,6
EI-966	Eirós	475,8	134,9
LI-792	Liñares	400,1	111,5
LI-793	Liñares	379,7	102
LI-794	Liñares	407,3	107,2

Patella: Length vs transverse diameter

Specimen	Site	L	DT
FO.I-60	Fontainhas	59,23	41,64
FO.I-73	Fontainhas	59,09	42,09
GFP-1569	Furninha (7,5)	48,34	38,18
GFP-1628.2	Furninha (7,5)	48,02	39,41
GFP-1628.3	Furninha (7,5)	48,58	39,31
TA-Lu-c-31	Holocene Galicia	51,11	34,88
TA-Lu-c-30	Holocene Galicia	52,67	38,07
SH5-97-U29-42	Holocene Galicia	45,01	31,23
SH5-97-U29-41	Holocene Galicia	45,89	31,28
LCF-140	Holocene Galicia	59,17	38,33

LE1	Modern	44,79	38,09
LE1	Modern	45,78	36,03
LE2	Modern	46,92	32,14
LE2	Modern	45,75	35,18
EI-619	Eirós	66,2	49,3
EI-757	Eirós	55,3	39,1
EI-1184	Eirós	71,5	51
EI-501	Eirós	57,9	39,5
EI-324	Eirós	60	39
EI-25	Eirós	61,3	40,4
EI-1703	Eirós	56,9	38,7
EI-1704	Eirós	61,1	40,5
EI-1705	Eirós	68,9	49,6
EI-1706	Eirós	66,3	50,5
EI-1707	Eirós	73,3	52
EI-1708	Eirós	68,7	51
EI-1709	Eirós	70,2	50
EI-1710	Eirós	63,5	47,6

Tibia: Transverse proximal diameter vs anteroposterior proximal diameter

Specimen	Site	DTprox.	DAPprox.
OLV-016-766	Oliveira	77,16	66,31
FO.I-54	Fontainhas	90,99	69,43
FO.I-50	Fontainhas	95,81	76,08
GFP-1134.16.4	Furninha	82,54	66,74
GFP-1334	Furninha	77,35	70,74
Postes-156	Postes	73,2	65,6
LCF-010-1996	Holocene Galicia	89,91	85,57
LCF-166	Holocene Galicia	76,56	58,84
Pur-Lu-23	Holocene Galicia	90,5	80,37
Pur-Lu-24	Holocene Galicia	89,19	82,6
SH5-98-S28-066	Holocene Galicia	87,34	65,89
SH5-98-530-002	Holocene Galicia	71,64	53,07
SH5-97-U29-10	Holocene Galicia	71,32	56,19
SH5-98-U30-007	Holocene Galicia	71,72	64,28
SH5-97-729-1	Holocene Galicia	73,28	52,61
TA-Lu-c-11	Holocene Galicia	78,2	66,1
TA-Lu-c-12	Holocene Galicia	78,29	69,86
LE1	Modern	78,82	77,03
LE1	Modern	78,87	78,22
LE2	Modern	76,79	70,27
LE2	Modern	75,23	70,02
EI-1690	Eirós	90,6	68
EI-1113	Eirós	84,9	58,4

EI-1688	Eirós	87,9	64,5
EI-1691	Eirós	102,4	70,7
EI-99	Eirós	84,7	61
EI-413	Eirós	84,3	60,5
EI-294	Eirós	89,5	60,5
EI-1689	Eirós	100,1	77,9
EI-1693	Eirós	107	78,9
EI-457	Eirós	106,8	76,2

Fibula: PCA

Specimen	Site	Dprox.max.	Dprox.min.	Ddia.max. (mid.)	Ddia.min. (mid.)
FO.I-62	Fontainhas	28,9	20,42	12,35	11,7
GFP-1624	Furninha (7,5)	23,4	24,39	14,32	13,86
LCF-102	Holocene Galicia	21,22	26,88	13,6	13,94
SH5-98-S29-001	Holocene Galicia	20,91	16,35	10,14	11,41
SH5-97-T29-48	Holocene Galicia	18,98	15,97	8,06	8,18
SH5-97-T29-37	Holocene Galicia	18,79	15,17	8,02	8,9
Ta-Lu-c-41	Holocene Galicia	23,45	16,27	10,38	9,81
LE1	Modern	24,16	21,89	12,22	10,78
LE1	Modern	23,41	22,76	11,87	10,34
LE2	Modern	15,79	22,15	11,55	10,46

Astragalus: PCA

Specimen	Site	L	DT	DAP	DAPmin.	DTtr.	DTcollum	DTcaput.	Ddiag.prox.
FO.I-52	Fontainhas	52,78	47,47	34,73	29,36	43,11	24,34	36,12	55,85
GFP-1572	Furninha (7,5)	50,92	44,53	31,31	24,19	41,07	32,36	35,74	55,63
GFP-1576	Furninha (7,5)	44,85	47,71	35,6	26,88	40,55	31,63	36,35	55,38
GFP-1575	Furninha (7,5)	44,31	51,8	32,6	25,53	36,71	25,91	32,38	51,32
GFP-1573	Furninha (7,5)	49,32	47,96	36,55	23,65	40,48	31,76	35,66	57,56
GFP-1570	Furninha (7,5)	48,21	51,68	34,43	25,29	39,05	30,37	35,75	57,11
SIPA-120	Pleistocene Galicia	45,63	51,33	27,62	20,12	34,61	33,34	36,48	51,5
VA87/14D/162	Holocene Galicia	43,93	47,49	31,65	19,88	38,97	29,74	32,38	55,07
CGLL-032	Holocene Galicia	45,59	49,67	34,24	21,02	38,72	28,92	33,69	52,14
CGLL-033	Holocene Galicia	47,03	50,6	32,94	20,57	40,5	28,26	34,34	53,08
SH5-98-S29-005	Holocene Galicia	42,42	44,23	31,65	22,96	34,13	28,68	29,61	44,41
SH5-98-S28-005	Holocene Galicia	41,58	44,09	32,13	23,17	34,92	30,26	31,08	45,91
SH5-97-T29-55	Holocene Galicia	40,6	45,34	30,1	21,31	34,97	25,25	29,67	46,97
SH5-97-T29-46	Holocene Galicia	39,68	45,33	29,92	22,1	32,45	24,61	29,49	46,28
SH5-98-S28-088	Holocene Galicia	52,36	58,19	39,59	29,69	42,47	32,82	36,64	60,39
SH5-98-S28-038	Holocene Galicia	54,4	57,18	39,68	28,61	42,39	32,89	36,95	59,68
CIPA-922	Modern Finland	45,98	48,53	30,07	19,23	39,57	31,08	34,8	50,87

CIPA-922	Modern Finland	46,37	48,67	31,07	20,73	38,9	31,48	34,12	53,15
CIPA-923	Modern Finland	39,61	43,88	30,54	16,86	36,85	27,41	29,43	45,96
CEZ-40	A Ceza	60,23	63,03	36,22	30,97	46,7	35,7	39,44	67,51
CEZ-755	A Ceza	51,03	53,23	32,04	27,43	41,67	25,96	31,7	54,41

Astragalus: Length vs transverse diameter

Specimen	Site	L	DT
FO.I-52	Fontainhas	52,78	47,47
GFP-1572	Furninha (7,5)	50,92	44,53
GFP-1576	Furninha (7,5)	44,85	47,71
GFP-1574	Furninha (7,5)	49,04	51,09
GFP-1575	Furninha (7,5)	44,31	51,8
GFP-1573	Furninha (7,5)	49,32	47,96
GFP-1570	Furninha (7,5)	48,21	51,68
GFP-1461	Furninha (7,5)	47,45	45,3
GFP-1134.16.2	Furninha (7,5)	44,38	45,35
SIPA-120	Pleistocene Galicia	45,63	51,33
VA87/14D/162	Holocene Galicia	43,93	47,49
CGLL-032	Holocene Galicia	45,59	49,67
CGLL-033	Holocene Galicia	47,03	50,6
SH5-98-S29-005	Holocene Galicia	42,42	44,23
SH5-98-S28-005	Holocene Galicia	41,58	44,09
SH5-97-T29-55	Holocene Galicia	40,6	45,34
SH5-97-T29-46	Holocene Galicia	39,68	45,33
SH5-98-S28-088	Holocene Galicia	52,36	58,19
SH5-98-S28-038	Holocene Galicia	54,4	57,18
TA-Lu-a-39	Holocene Galicia	51,56	44,73
CIPA-922	Modern Finland	45,98	48,53
CIPA-922	Modern Finland	46,37	48,67
CIPA-923	Modern Finland	39,61	43,88
Postes-242	Postes	37,4	42,2
Postes-243	Postes	38,6	45,5
CEZ-40	A Ceza	60,23	63,03
CEZ-755	A Ceza	51,03	53,23

Calcaneus: PCA

Specimen	Site	L	DT	DAP	DTtuber	DAPtuber	Ls.t.
FO.I-?	Fontainhas	101,61	62,19	47,92	35,71	39,22	32,02
GFP-1567	Furninha (7,5)	82,62	45,27	43,06	30,77	34,95	31,49
GFP-1566	Furninha (7,5)	79,81	48,82	46,44	25,9	35,75	35
GFP-1565	Furninha (7,5)	81,74	49,88	44,1	28,81	36,07	31,12
GFP-1577	Furninha (7,5)	62,66	33,98	31,25	18,33	23,7	23,57
GFP-1462	Furninha (7,5)	70,57	47,5	44,47	31,82	32,33	31,84

GFP-1133.21.5	Furninha (7,5)	74,23	46,87	39,83	31,14	33,6	27,6
GFP-1133.21.6	Furninha (7,5)	83,03	53,19	47,48	30,51	33,58	32,49
GFP-1126.1	Furninha (7,5)	85,09	47,2	47,41	28,54	33,35	41,84
GFP-1690	Furninha (4,5)	81,16	56,3	45,04	31,53	34,43	30,41
SH5-97-T29-4	Holocene Galicia	75,13	46,93	40,67	25,9	31,89	26,38
SH5-97-T29-51	Holocene Galicia	75,2	47,46	40,4	26,02	30,62	28,99
SH5-98-S28-099	Holocene Galicia	95,92	61,16	49,76	32,07	38,3	41,01
TA-Lu-c-29	Holocene Galicia	79,87	51,01	41,45	26,38	32,8	31,77
TA-Lu-c-28	Holocene Galicia	79,26	51,72	41,84	27,21	32,75	30,72
CIPA-922	Modern Finland	84,58	50,97	41,41	31,97	34,67	29,83
CEZ-35	A Ceza	107,09	74,35	42,7	41,31	40	51,17
CEZ-37	A Ceza	80,93	56,89	41,1	29,8	29,6	40,95
CEZ-38	A Ceza	86,57	57,41	43,86	33,61	32,42	37,27
CEZ-39	A Ceza	97,64	65,03	45,26	39,29	38,73	46,65

Calcaneus: Length vs transverse diameter.

Specimen	Site	L	DT
FO.I-?	Fontainhas	101,61	62,19
GFP-1567	Furninha (7,5)	82,62	45,27
GFP-1566	Furninha (7,5)	79,81	48,82
GFP-1565	Furninha (7,5)	81,74	49,88
GFP-1568	Furninha (7,5)	87,97	55,45
GFP-1577	Furninha (7,5)	62,66	33,98
GFP-1462	Furninha (7,5)	70,57	47,5
GFP-1133.21.5	Furninha (7,5)	74,23	46,87
GFP-1133.21.6	Furninha (7,5)	83,03	53,19
GFP-1488	Furninha (7,5)	87,72	60,95
GFP-1126.1	Furninha (7,5)	85,09	47,2
GFP-1690	Furninha (4,5)	81,16	56,3
SH5-97-T29-4	Holocene Galicia	75,13	46,93
SH5-97-T29-51	Holocene Galicia	75,2	47,46
SH5-98-S28-099	Holocene Galicia	95,92	61,16
TA-Lu-c-29	Holocene Galicia	79,87	51,01
TA-Lu-c-28	Holocene Galicia	79,26	51,72
CIPA-922	Modern Finland	84,58	50,97
Postes-307	Postes	72,5	40
CEZ-35	A Ceza	107,09	74,35
CEZ-37	A Ceza	80,93	56,89
CEZ-38	A Ceza	86,57	57,41
CEZ-39	A Ceza	97,64	65,03

First metatarsal: PCA

Specimen	Site	L	DTprox.	DAPprox.	DTdia.min.	DAPdia.	DTdist.	DAPdist.
CEZ-880	A Ceza	48,23	20,12	20,23	9,66	12,66	16,31	14,41
CEZ-26	A Ceza	56,7	25,61	28,3	14,74	16,43	18,03	16,1
CEZ-514	A Ceza	57,92	23,62	26,77	13,9	15,59	18,2	18,12
CEZ-658	A Ceza	51,71	21,53	19,51	9,75	11,82	16,04	14,81
CEZ-738	A Ceza	50,16	21,38	23,62	11	12,04	16,9	15,03
CEZ-739	A Ceza	49,06	19,64	21,45	10,76	12,92	16,34	14,42
EI-495	Eirós	48,6	18,5	18,5	9	9,5	15,4	14
EI-775	Eirós	50,8	20,9	19,4	10,2	10,3	14,6	14,7
EI-777	Eirós	50,5	21,3	27	12,2	13,5	18,3	15,2
EI-1085	Eirós	54,5	23,2	22,8	11,8	12,6	17	16,2
EI-1173	Eirós	59,4	25,4	25,9	13,2	13,8	19,9	17,2
EI-1211	Eirós	55,3	23,7	26,8	12,5	12,8	18,4	15,1
EI-1235	Eirós	51,1	23	25,9	11,5	13,1	16,7	15,6
EI-1281	Eirós	55,7	23,9	25,6	11,3	14,2	17,2	16,4
EI-1285	Eirós	55,3	23,8	25,9	11,7	13,2	18	16,5
EI-1777	Eirós	52,6	22,1	22,2	12,7	14,5	17,7	15,5
EI-1778	Eirós	52,5	22,7	23,1	12,3	14,5	17,4	15,6
LI-957	Liñares	49,4	20,7	23,4	12,4	11,3	16,9	14,5
VA87/17F/8	Holocene Galicia	65,53	21,99	19,13	9,89	12,07	16,95	13,1
LCF-124	Holocene Galicia	68,43	21,7	16,03	10,26	10,62	16,92	16,1
LCF-125	Holocene Galicia	68,7	22,14	17,09	10,45	9,35	17,45	15,87
LCF-126	Holocene Galicia	72,97	18,15	23,56	11,57	11,17	18,08	16,02
LCF-128	Holocene Galicia	65,25	19,84	17,18	9,14	11,52	15,48	14,15
CCV-009	Holocene Galicia	69,77	22,87	25,16	10,39	13,24	16,44	14,13
SH5-98-S28-045	Holocene Galicia	74,76	24,33	25,01	10,82	12,22	18,87	16,53
SH5-98-S29-012	Holocene Galicia	69,86	19,94	20,14	9,32	10,6	16,96	14,24
SH5-98-S28-028	Holocene Galicia	72,64	21,54	18,95	9,33	10,74	17,72	15,47
SH5-97-T29-39	Holocene Galicia	62,63	18,59	21,53	9,68	10,09	15,59	12,9
SH5-98-S28-058	Holocene Galicia	81,36	25,05	24,31	11,64	11,31	20,54	18,93
TA-Lu-c-25	Holocene Galicia	61,27	21,79	22,49	9,27	10,88	15,33	13,32
GFP-1542	Furninha	70,38	24,25	26,25	14,57	13,52	18,65	16,18
GFP-1543	Furninha	67,52	22,05	20,24	12,26	13,85	16,93	14,92
GFP-1548	Furninha	64,58	22,73	20,32	10,63	12,02	16,58	14,56
GFP-1138.21.2	Furninha	65,05	22,85	21,33	11,24	11,31	17,68	13,88
CIPA-922	Modern	67,62	20,36	23,95	9,45	11,37	15,91	13,65

First metatarsal: PCA including a specimen from Caldeirão

Specimen	Site	L	DTprox.	DAPprox.	DTdia.min.	DAPdia.	DAPdist.
CEZ-880	A Ceza	48,23	20,12	20,23	9,66	12,66	14,41
CEZ-26	A Ceza	56,7	25,61	28,3	14,74	16,43	16,1
CEZ-514	A Ceza	57,92	23,62	26,77	13,9	15,59	18,12
CEZ-658	A Ceza	51,71	21,53	19,51	9,75	11,82	14,81

CEZ-738	A Ceza	50,16	21,38	23,62	11	12,04	15,03
CEZ-739	A Ceza	49,06	19,64	21,45	10,76	12,92	14,42
EI-495	Eirós	48,6	18,5	18,5	9	9,5	14
EI-775	Eirós	50,8	20,9	19,4	10,2	10,3	14,7
EI-777	Eirós	50,5	21,3	27	12,2	13,5	15,2
EI-1085	Eirós	54,5	23,2	22,8	11,8	12,6	16,2
EI-1173	Eirós	59,4	25,4	25,9	13,2	13,8	17,2
EI-1211	Eirós	55,3	23,7	26,8	12,5	12,8	15,1
EI-1235	Eirós	51,1	23	25,9	11,5	13,1	15,6
EI-1281	Eirós	55,7	23,9	25,6	11,3	14,2	16,4
EI-1285	Eirós	55,3	23,8	25,9	11,7	13,2	16,5
EI-1777	Eirós	52,6	22,1	22,2	12,7	14,5	15,5
EI-1778	Eirós	52,5	22,7	23,1	12,3	14,5	15,6
LI-957	Liñares	49,4	20,7	23,4	12,4	11,3	14,5
VA87/17F/8	Holocene Galicia	65,53	21,99	19,13	9,89	12,07	13,1
LCF-124	Holocene Galicia	68,43	21,7	16,03	10,26	10,62	16,1
LCF-125	Holocene Galicia	68,7	22,14	17,09	10,45	9,35	15,87
LCF-126	Holocene Galicia	72,97	18,15	23,56	11,57	11,17	16,02
LCF-128	Holocene Galicia	65,25	19,84	17,18	9,14	11,52	14,15
CCV-009	Holocene Galicia	69,77	22,87	25,16	10,39	13,24	14,13
SH5-98-S28-045	Pleistocene Galicia	74,76	24,33	25,01	10,82	12,22	16,53
SH5-98-S29-012	Pleistocene Galicia	69,86	19,94	20,14	9,32	10,6	14,24
SH5-98-S28-028	Pleistocene Galicia	72,64	21,54	18,95	9,33	10,74	15,47
SH5-97-T29-39	Pleistocene Galicia	62,63	18,59	21,53	9,68	10,09	12,9
SH5-98-S28-058	Pleistocene Galicia	81,36	25,05	24,31	11,64	11,31	18,93
TA-Lu-c-25	Pleistocene Galicia	61,27	21,79	22,49	9,27	10,88	13,32
P-11 666	Caldeirão	63,45	21,38	20,49	10,82	9,13	12,92
GFP-1542	Furninha	70,38	24,25	26,25	14,57	13,52	16,18
GFP-1543	Furninha	67,52	22,05	20,24	12,26	13,85	14,92
GFP-1548	Furninha	64,58	22,73	20,32	10,63	12,02	14,56
GFP-1138.21.2	Furninha	65,05	22,85	21,33	11,24	11,31	13,88
CIPA-922	Modern	67,62	20,36	23,95	9,45	11,37	13,65

First metatarsal: Robustness

Specimen	Group	Robustness
CEZ-880	*U. spelaeus*	33,82
CEZ-26	*U. spelaeus*	31,80
CEZ-514	*U. spelaeus*	31,42
CEZ-658	*U. spelaeus*	31,02
CEZ-738	*U. spelaeus*	33,69
CEZ-739	*U. spelaeus*	33,31
EI-495	*U. spelaeus*	31,69
EI-775	*U. spelaeus*	28,74
EI-777	*U. spelaeus*	36,24

EI-1085	*U. spelaeus*	31,19
EI-1173	*U. spelaeus*	33,50
EI-1211	*U. spelaeus*	33,27
EI-1235	*U. spelaeus*	32,68
EI-1281	*U. spelaeus*	30,88
EI-1285	*U. spelaeus*	32,55
EI-1777	*U. spelaeus*	33,65
EI-1778	*U. spelaeus*	33,14
LI-957	*U. spelaeus*	34,21
VA87/17F/8	*U. arctos*	25,87
LCF-124	*U. arctos*	24,73
LCF-125	*U. arctos*	25,40
LCF-126	*U. arctos*	24,78
LCF-128	*U. arctos*	23,72
CCV-009	*U. arctos*	23,56
SH5-98-S28-045	*U. arctos*	25,24
SH5-98-S29-012	*U. arctos*	24,28
SH5-98-S28-028	*U. arctos*	24,39
SH5-97-T29-39	*U. arctos*	24,89
SH5-98-S28-058	*U. arctos*	25,25
TA-Lu-c-25	*U. arctos*	25,02
GFP-1542	Furninha	26,50
GFP-1543	Furninha	25,07
GFP-1548	Furninha	25,67
GFP-1138.21.2	Furninha	27,18
CIPA-922	*U. arctos*	23,53

Second metatarsal: PCA

Specimen	Site	L	DTprox.	DAPprox.	DTdia.min.	DAPdia.	DTdist.	DAPdist.
CEZ-882	A Ceza	61,14	12,33	21,01	11,4	8,37	19,17	14,32
CEZ-24	A Ceza	61,74	13,74	21,76	12,13	9,77	19,28	15,13
CEZ-657	A Ceza	70,12	16,67	25,64	16,09	13,7	22,9	17,93
EI-447	Eirós	67,3	15,3	24,4	16,1	12,9	23,3	17,1
EI-514	Eirós	64,5	13,5	22,5	13,2	11,5	19,1	15,4
EI-774	Eirós	74,2	19,2	26,6	18,7	15	27,4	21,6
EI-778	Eirós	68,8	18,7	24,9	16,8	12,9	23,7	19,4
EI-780	Eirós	63,5	13	20,4	13,5	10	18,2	14,1
EI-791	Eirós	65,3	15,2	24,8	16,1	12,3	22,2	15,6
EI-1088	Eirós	64,3	12,7	21	12,6	9,7	19,4	13,8
EI-1213	Eirós	72,2	16,6	26,4	15,3	13,5	24,6	17,9
EI-1757	Eirós	65,6	15,9	24	16,2	11,8	22,1	15,7
EI-1758	Eirós	60	14,2	21,5	12,8	9,9	18,4	13,9
EI-1759	Eirós	61,1	13,4	21,2	12,8	10,8	18,1	14,4
EI-1760	Eirós	62	14	21,3	12,9	10,5	18	14,6

EI-1761	Eirós	63,8	15,1	22,2	13,2	11,2	18,6	13,7
EI-1762	Eirós	61,6	13,8	21	12,9	10,7	19	14,3
EI-1763	Eirós	68,4	16,4	26,2	14,8	12,5	22,6	16,2
LI-966	Liñares	72,2	17,4	25,8	15,5	12,3	23,6	18,9
LI-967	Liñares	75	22,2	30	18,8	15,5	28,3	21,6
LI-968	Liñares	73,7	20,2	27,4	17,1	13,3	24,2	20,6
SH5-98-97-S29-009	Holocene Galicia	76,25	13,53	22,78	12,92	9,04	18,19	15,02
SH5-97-T29-7	Holocene Galicia	71,99	11,31	20,1	12,3	8,14	17,11	14,04
SH5-98-S28-044	Holocene Galicia	83,73	16,7	27,17	13,91	11,3	21,08	18,5
SH5-97-T29-088	Holocene Galicia	71,84	13,32	20,64	12,13	8,28	17,51	14,31
SH5-98-S28-006	Holocene Galicia	75,59	15,17	22,39	12,88	8,82	18,52	14,81
TA-Lu-c-23	Holocene Galicia	69,28	13,06	21,63	11,01	7,75	18,07	15,25
TA-Lu-c-24	Holocene Galicia	69,74	12,68	21,98	11,16	8,05	18,38	14,96
FO.I-69	Fontainhas	78,17	13,97	25,46	14,92	9,68	21,21	16,88
GFP-1138.21.10	Furninha	70,6	11,77	23,24	11,63	9,36	17,2	14,9
GFP-1138.21.11	Furninha	71,52	20,44	21,86	11,3	9,23	18,82	14,38
GFP-1138.21.12	Furninha	76,13	13,92	25,73	13,01	10,75	18,42	16,39
GFP-1645.2	Furninha	61,53	11,62	20,58	10,7	8,54	15,83	13,92

Second metatarsal: Robustness

Specimen	Group	Robustness
CEZ-882	*U. spelaeus*	31,35
CEZ-24	*U. spelaeus*	31,23
CEZ-657	*U. spelaeus*	32,66
EI-447	*U. spelaeus*	34,62
EI-514	*U. spelaeus*	29,61
EI-774	*U. spelaeus*	36,93
EI-778	*U. spelaeus*	34,45
EI-780	*U. spelaeus*	28,66
EI-791	*U. spelaeus*	34,00
EI-1088	*U. spelaeus*	30,17
EI-1213	*U. spelaeus*	34,07
EI-1757	*U. spelaeus*	33,69
EI-1758	*U. spelaeus*	30,67
EI-1759	*U. spelaeus*	29,62
EI-1760	*U. spelaeus*	29,03
EI-1761	*U. spelaeus*	29,15
EI-1762	*U. spelaeus*	30,84
EI-1763	*U. spelaeus*	33,04
LI-966	*U. spelaeus*	32,69
LI-967	*U. spelaeus*	37,73
LI-968	*U. spelaeus*	32,84
SH5-98-97-S29-009	*U. arctos*	23,86
SH5-97-T29-7	*U. arctos*	23,77

SH5-98-S28-044	*U. arctos*	25,18
SH5-97-T29-088	*U. arctos*	24,37
SH5-98-S28-006	*U. arctos*	24,50
TA-Lu-c-23	*U. arctos*	26,08
TA-Lu-c-24	*U. arctos*	26,36
FO.I-69	*U. arctos*	27,13
GFP-1138.21.10	Furninha	24,36
GFP-1138.21.11	Furninha	26,31
GFP-1138.21.12	Furninha	24,20
GFP-1645.2	Furninha	25,73

Third metatarsal: PCA

Specimen	Site	L	DTprox.	DAPprox.	DTdia.min.	DAPdia.	DTdist.	DAPdist.
CEZ-883	A Ceza	69,67	14,41	26,74	14,2	11,74	21,68	15,14
CEZ-27	A Ceza	77,25	19,4	29,84	18,22	14,94	23,62	18,59
EI-768	Eirós	83	21	33	20,1	15,4	25,2	17,4
EI-779	Eirós	76,2	18,9	28,5	16,8	13,5	22,8	17,5
EI-782	Eirós	73,3	16,4	28	15	12,4	20,8	15,8
EI-1178	Eirós	76,2	18,6	26,5	16,4	12,1	20,6	14,7
EI-1195	Eirós	69,2	15,4	25,5	14,4	11	18,8	15,6
EI-1260	Eirós	71,4	14,9	27,6	13,2	11,1	19,9	15,5
EI-1789	Eirós	69,6	17,6	25,4	16	12,3	19,7	15,3
EI-1790	Eirós	78	18,6	29,5	16,9	14,5	22,7	17
EI-1791	Eirós	73,4	20,4	31,2	17,5	14,3	23,2	17,1
EI-1792	Eirós	77,3	17,2	29,9	16,8	13,4	22,1	16,5
EI-1793	Eirós	73,9	16,4	29,1	14,6	12,3	20,4	16,3
EI-1794	Eirós	70,4	15,9	25,8	12,6	11,1	16,8	15,3
LI-261	Liñares	75,95	19,43	31,47	16,9	12,95	23,1	19,01
LI-965	Liñares	73,5	20	29,8	14,9	12,3	21,4	16,8
LCF-129	Holocene Galicia	72,45	13,05	21,44	11,6	9,01	17,69	15,37
LCF-130	Holocene Galicia	80,13	17,13	24,68	12,89	12,76	20,02	17,69
SH5-97-T29-42	Holocene Galicia	76,67	16,13	23,05	12,43	9,29	16,7	14,22
SH5-98-V30-016	Holocene Galicia	82,3	16,04	26,57	13,78	11,19	18,12	16,63
SH5-98-R29-001	Holocene Galicia	81,36	17,06	25,03	12,95	9,49	18,16	14,64
SH5-97-T29-59	Holocene Galicia	74,86	14,8	23,73	12,34	9,84	18,1	14,2
SH5-98-S28-075	Holocene Galicia	88,95	20,26	30,67	13,98	13,04	20,67	18,99
SH5-98-T31-002	Holocene Galicia	80,56	16,71	25,57	13,21	9,36	18,8	14,62
TA-Lu-c-22	Holocene Galicia	76,29	15,61	23,37	12,11	9,44	18,13	16,89
FO.I-71	Fontainhas	83,93	21,14	27,17	14,94	11,35	19,69	17,21
FO.I-67	Fontainhas	83,52	19,34	27,53	14,86	11,25	21,03	17,68
GFP-1545	Furninha	83,23	17,93	24,62	12,88	12,28	18,95	15,32
GFP-1539	Furninha	79,15	17,72	28,63	15,85	13,73	19,65	17,28
GFP-1593	Furninha	76,21	16,87	25,4	12,69	10,47	19,29	15,14
GFP-1138.21.13	Furninha	81,84	20,06	28,27	14,26	11,93	19,59	17,15

GFP-1138.21.14	Furninha	84,66	16,75	29,35	13,82	10,94	21,19	18,24
GFP-1138.21.15	Furninha	76,93	15,49	25,77	12,34	10,93	18,61	15,38
GFP-1645.3	Furninha	66,68	14,37	12,33	10,25	16,13	14,04	12,61

Third metatarsal: Robustness

Specimen	Group	Robustness
CEZ-883	*U. spelaeus*	31,12
CEZ-27	*U. spelaeus*	30,58
EI-768	*U. spelaeus*	30,36
EI-779	*U. spelaeus*	29,92
EI-782	*U. spelaeus*	28,38
EI-1178	*U. spelaeus*	27,03
EI-1195	*U. spelaeus*	27,17
EI-1260	*U. spelaeus*	27,87
EI-1789	*U. spelaeus*	28,30
EI-1790	*U. spelaeus*	29,10
EI-1791	*U. spelaeus*	31,61
EI-1792	*U. spelaeus*	28,59
EI-1793	*U. spelaeus*	27,60
EI-1794	*U. spelaeus*	23,86
LI-261	*U. spelaeus*	30,41
LI-965	*U. spelaeus*	29,12
LCF-129	*U. arctos*	24,42
LCF-130	*U. arctos*	24,98
SH5-97-T29-42	*U. arctos*	21,78
SH5-98-V30-016	*U. arctos*	22,02
SH5-98-R29-001	*U. arctos*	22,32
SH5-97-T29-59	*U. arctos*	24,18
SH5-98-S28-075	*U. arctos*	23,24
SH5-98-T31-002	*U. arctos*	23,34
TA-Lu-c-22	*U. arctos*	23,76
FO.I-71	*U. arctos*	23,46
FO.I-67	*U. arctos*	25,18
GFP-1545	Furninha	22,77
GFP-1539	Furninha	24,83
GFP-1593	Furninha	25,31
GFP-1138.21.13	Furninha	23,94
GFP-1138.21.14	Furninha	25,03
GFP-1138.21.15	Furninha	24,19
GFP-1645.3	Furninha	21,06

Fourth metatarsal: PCA

Specimen	Site	L	DTprox.	DAPprox.	DTdia.min.	DAPdia.	DTdist.	DAPdist.
CEZ-884	A Ceza	75,4	19,01	27,37	14,61	11,51	21,54	15,72
CEZ-21	A Ceza	76,92	19,7	24,85	14,28	11,1	21,89	15,99
CEZ-23	A Ceza	87,39	20,19	30,06	16,45	14,56	23,95	17,99
CEZ-515	A Ceza	77,13	16,59	28,53	13,95	12,71	21,65	16,91
CEZ-557	A Ceza	73,75	19,08	27,26	13,83	12,26	21,49	16,4
CEZ-740	A Ceza	92,5	22,07	30,01	17,55	15,86	26,59	19,05
EI-181	Eirós	78,3	22	33	17,7	14,8	24,2	18,7
EI-210	Eirós	78,1	19,5	25,5	15,3	14,2	21,3	16,2
EI-540	Eirós	85,2	22,2	29	17,4	15,5	25,6	18,3
EI-638	Eirós	81,5	17,8	31,6	15,8	14,4	24,1	18,2
EI-761	Eirós	83,4	23,6	29,5	18,1	16,2	25,9	17,2
EI-784	Eirós	82,4	18,9	28,3	16,1	14,7	22,3	16,6
EI-1017	Eirós	89,6	24,2	32,5	18,6	17,6	25,8	20
EI-1029	Eirós	84,3	21,1	29,9	16,2	14,8	23,9	16,3
EI-1234	Eirós	80,7	21	28,5	16	15,4	23,2	17,1
EI-1277	Eirós	85,3	22,8	30,7	17,9	18	24,8	18,3
EI-1797	Eirós	76,6	17,9	26	13,9	13,3	20	14,2
EI-1798	Eirós	77,7	19,1	27	16,8	15,4	23,4	16,6
EI-1799	Eirós	88,2	22,5	33,1	19,2	16,3	26,1	19,2
EI-1801	Eirós	85,2	22,6	30,8	20,7	16,6	27,6	21,5
LI-5	Liñares	80,2	21,58	29,79	18,31	14,13	26,42	21,12
LI-260	Liñares	84,73	22,85	32,17	15,89	15,02	24,32	19,8
LI-970	Liñares	80,8	19,9	27,7	14,2	13,3	22,8	17,7
LI-1343	Liñares	77,5	16,2	25,8	14,9	12,6	22,1	16,5
LCF-127	Holocene Galicia	78,13	16,82	25,1	11,7	9,9	17,23	15,57
SIPA-58	Holocene Galicia	76,58	15,9	22,53	10,5	9,86	17,57	17,37
PUR-66	Holocene Galicia	87,32	21,05	25	13,77	12,81	21,18	18,5
SH5-97-T29-34	Holocene Galicia	83,76	17,06	23,31	12,11	9,82	17,74	14,41
SH5-S29-003	Holocene Galicia	87,84	18,35	24,14	12,55	10,86	18,28	15,06
SH5-97-U29-21	Holocene Galicia	89,2	20,56	26,33	13,89	12,82	19,36	17,31
SH5-98-S28-010	Holocene Galicia	95,13	26,41	28,6	14,97	12,33	22,59	18,75
SH5-98-S28-060	Holocene Galicia	96,43	26	29,27	14,7	12,91	21,89	18,31
GFP-1541	Furninha	83,79	19,25	26,92	15,1	13,97	16,46	14,34
GFP-1607	Furninha	89,06	18,97	26,22	14,89	12,22	20,79	17,52
GFP-1610	Furninha	89,29	20,01	25,21	14,07	12,55	20,74	16,46
GFP-1609	Furninha	81,43	18,68	24,45	13,11	12,66	19,44	16,1
GFP-1608	Furninha	92,58	16,75	26,85	15,93	12,76	21,85	18,79
GFP-1138.21.16	Furninha	90,84	16,02	26,27	14,41	12,76	19,33	15,31
GFP-1138.21.18	Furninha	81,78	17,05	24,85	13,29	10,55	19,29	15,76

Fourth metatarsal: Robustness

Specimen	Group	Robustness
CEZ-884	*U. spelaeus*	28,57
CEZ-21	*U. spelaeus*	28,46
CEZ-23	*U. spelaeus*	27,41
CEZ-515	*U. spelaeus*	28,07
CEZ-557	*U. spelaeus*	29,14
CEZ-740	*U. spelaeus*	28,75
EI-181	*U. spelaeus*	30,91
EI-210	*U. spelaeus*	27,27
EI-540	*U. spelaeus*	30,05
EI-638	*U. spelaeus*	29,57
EI-761	*U. spelaeus*	31,06
EI-784	*U. spelaeus*	27,06
EI-1017	*U. spelaeus*	28,79
EI-1029	*U. spelaeus*	28,35
EI-1234	*U. spelaeus*	28,75
EI-1277	*U. spelaeus*	29,07
EI-1797	*U. spelaeus*	26,11
EI-1798	*U. spelaeus*	30,12
EI-1799	*U. spelaeus*	29,59
EI-1801	*U. spelaeus*	32,39
LI-5	*U. spelaeus*	32,94
LI-260	*U. spelaeus*	28,70
LI-970	*U. spelaeus*	28,22
LI-1343	*U. spelaeus*	28,52
LCF-127	*U. arctos*	22,05
SIPA-58	*U. arctos*	22,94
PUR-66	*U. arctos*	24,26
SH5-97-T29-34	*U. arctos*	21,18
SH5-S29-003	*U. arctos*	20,81
SH5-97-U29-21	*U. arctos*	21,70
SH5-98-S28-010	*U. arctos*	23,75
SH5-98-S28-060	*U. arctos*	22,70
GFP-1541	Furninha	19,64
GFP-1607	Furninha	23,34
GFP-1610	Furninha	23,23
GFP-1609	Furninha	23,87
GFP-1608	Furninha	23,60
GFP-1138.21.16	Furninha	21,28
GFP-1138.21.18	Furninha	23,59

Fifth metatarsal: PCA

Specimen	Site	L	DTprox.	DAPprox.	DTdia.min.	DAPdia.	DTdist.	DAPdist.
CEZ-885	A Ceza	75,86	26,2	27,48	12,84	14,07	21,55	16,33
CEZ-10	A Ceza	76,4	23,96	28,1	12,64	13,89	21,79	16,14
CEZ-17	A Ceza	79,79	26,09	29,39	14,01	15,66	23,88	17,28
CEZ-20	A Ceza	86,59	29,55	32,53	16,72	17,29	24,44	19,32
CEZ-57	A Ceza	90,36	33,01	33,4	16,07	17,7	25,61	20,05
EI-80	Eirós	82,5	26,5	30,3	14,1	15,1	23,5	17,1
EI-87	Eirós	78,1	27,1	30,5	13	17,1	24	16,8
EI-178	Eirós	80,6	27,3	26	12,4	15,2	21,7	15,3
EI-634	Eirós	87,7	32,3	29,9	16,2	17,2	20,3	20
EI-773	Eirós	83,8	26,3	29	13,7	15,7	22,7	16,3
EI-781	Eirós	79,1	26,6	29,3	13,1	15,7	23,8	16,3
EI-783	Eirós	82,2	28,1	30,5	12,8	14,6	22,4	15,1
EI-785	Eirós	86,5	31,8	35,2	16,1	17,5	26,4	18,6
EI-1099	Eirós	82,5	24,4	27	13,2	17	23,8	15,9
EI-1198	Eirós	88	31,4	38,3	16,2	18,8	25,2	18,1
EI-1256	Eirós	85,1	30,9	32,6	15,7	18,6	28,2	18
EI-1379	Eirós	87,6	28,7	30,3	15,6	19,7	27,3	18,7
EI-1803	Eirós	89	31,8	35,2	16	17,8	25,8	17,5
EI-1804	Eirós	90,7	33	34,8	16,1	18,6	26,1	19,2
EI-1805	Eirós	90,6	32	33,8	16,2	18,3	26,1	18,8
EI-1806	Eirós	91,3	32,5	33,1	15,4	18,9	27,3	19,4
EI-1807	Eirós	84,5	32,4	34,9	15,6	18	26,7	18,1
EI-1808	Eirós	83	28,1	29,6	14,7	15,9	24,1	16,8
EI-1809	Eirós	80,5	30,3	28,6	14,5	16,3	24,5	17
EI-1810	Eirós	89,1	35,8	38	15,5	18,5	27,7	18,8
LI-259	Liñares	84,37	28,06	28,02	12,73	14,26	25,17	17,93
LI-969	Liñares	85,8	27,6	31,7	12,8	16,7	27,2	19,4
LCF-136	Holocene Galicia	88,9	23,54	24,29	11,42	10,33	20,33	16,74
SH5-97-T29-36	Holocene Galicia	88,04	23,01	24,17	11,57	10,29	20,17	15,19
SH5-97-T29-087	Holocene Galicia	87,46	22,44	24,36	11,82	9,91	19,97	14,95
SH5-98-S28-076	Holocene Galicia	98,69	29,08	31,56	14,51	13,29	23,45	19,28
TA-Lu-c-20	Holocene Galicia	81,53	24,25	24,58	11,18	10,61	20,42	16,49
LE1	Modern	91,79	26,38	25,85	11,23	14,23	18,37	15,83
GFP-1592	Furninha	85,04	27,61	27,79	13,52	12,36	21,18	15,39
GFP-1604	Furninha	83,33	27,46	26,7	14,48	12,82	21,49	15,47
GFP-1645.4	Furninha	83,66	27,81	26,13	14,1	12,15	21,81	17,39
GFP-1645.5	Furninha	77,18	20,64	22,93	11,11	10,71	17,47	14,33

Fifth metatarsal: Robustness

Specimen	Group	Robustness
CEZ-885	*U. spelaeus*	28,41
CEZ-10	*U. spelaeus*	28,52

CEZ-17	*U. spelaeus*	29,93
CEZ-20	*U. spelaeus*	28,22
CEZ-57	*U. spelaeus*	28,34
EI-80	*U. spelaeus*	28,48
EI-87	*U. spelaeus*	30,73
EI-178	*U. spelaeus*	26,92
EI-634	*U. spelaeus*	23,15
EI-773	*U. spelaeus*	27,09
EI-781	*U. spelaeus*	30,09
EI-783	*U. spelaeus*	27,25
EI-785	*U. spelaeus*	30,52
EI-1099	*U. spelaeus*	28,85
EI-1198	*U. spelaeus*	28,64
EI-1256	*U. spelaeus*	33,14
EI-1379	*U. spelaeus*	31,16
EI-1803	*U. spelaeus*	28,99
EI-1804	*U. spelaeus*	28,78
EI-1805	*U. spelaeus*	28,81
EI-1806	*U. spelaeus*	29,90
EI-1807	*U. spelaeus*	31,60
EI-1808	*U. spelaeus*	29,04
EI-1809	*U. spelaeus*	30,43
EI-1810	*U. spelaeus*	31,09
LI-259	*U. spelaeus*	29,83
LI-969	*U. spelaeus*	31,70
LCF-136	*U. arctos*	22,87
SH5-97-T29-36	*U. arctos*	22,91
SH5-97-T29-087	*U. arctos*	22,83
SH5-98-S28-076	*U. arctos*	23,76
TA-Lu-c-20	*U. arctos*	25,05
LE1	*U. arctos*	20,01
GFP-1592	Furninha	24,91
GFP-1604	Furninha	25,79
GFP-1645.4	Furninha	26,07
GFP-1645.5	Furninha	22,64

First phalanx: PCA

Specimen	Site	L	Dtprox.	DTdia.min.	DTdist.
Caldeirão min	Caldeirão	32,79	16,21	10,27	11,84
Caldeirão avg	Caldeirão	35,45	16,78	11,03	12,95
Caldeirão max	Caldeirão	40,91	17,82	11,96	13,93
Fontainhas min	Fontainhas	44,66	21,93	12,69	15,75
Fontainhas avg	Fontainhas	46,41	23,13	14,67	16,84
Fontainhas max	Fontainhas	48,70	24,54	15,72	17,63

Furninha (8,8) min	Furninha (8,8)	28,95	14,27	10,41	11,56
Furninha (8,8) avg	Furninha (8,8)	38,36	19,59	13,46	14,17
Furninha (8,8) max	Furninha (8,8)	44,96	24,56	17,36	15,86
Furninha (7,5) min	Furninha (7,5)	31,10	14,85	9,59	11,96
Furninha (7,5) avg	Furninha (7,5)	40,53	20,19	12,74	15,11
Furninha (7,5) max	Furninha (7,5)	52,90	24,57	16,13	17,90
Pleistocene Galicia min	Pleistocene Galicia	41,26	14,85	9,59	11,96
Pleistocene Galicia avg	Pleistocene Galicia	44,14	19,92	12,52	14,82
Pleistocene Galicia max	Pleistocene Galicia	45,28	24,57	16,13	17,90
Holocene Galicia min	Holocene Galicia	23,18	13,78	10,12	11,05
Holocene Galicia avg	Holocene Galicia	35,08	17,46	12,17	13,99
Holocene Galicia max	Holocene Galicia	53,30	21,34	14,88	16,69
Modern min	Modern	32,14	15,54	10,92	11,66
Modern avg	Modern	38,45	18,02	12,52	15,79
Modern max	Modern	43,72	21,03	16,09	21,33
A Ceza min	A Ceza	35,30	17,65	12,02	14,09
A Ceza avg	A Ceza	41,06	21,38	14,43	16,56
A Ceza max	A Ceza	49,02	26,52	18,88	20,27
Postes min	Postes	28,8	11,9	9,7	10,7
Postes avg	Postes	33,43	15,05	10,77	12,17
Postes max	Postes	37,70	17,80	12,10	13,50

Second phalanx: PCA

Specimen	Site	L	Dtprox.	DTdia.min.	DTdist.
N14-Sc341	Caldeirão	22,86	14,65	9,94	13,36
FO.I-172	Fontainhas	30,89	19,31	13,77	14,99
GFP-1555	Furninha (8,8)	32,83	18,96	14,18	16,41
GFP-1560	Furninha (8,8)	30,99	17,92	12,82	14,50
Furninha (7,5) min	Furninha (7,5)	21,19	13,54	7,24	8,57
Furninha (7,5) avg	Furninha (7,5)	28,00	16,85	11,67	13,83
Furninha (7,5) max	Furninha (7,5)	35,62	19,68	14,58	16,45
Pleistocene Galicia min	Pleistocene Galicia	23,02	13,48	10,55	12,83
Pleistocene Galicia avg	Pleistocene Galicia	29,45	15,82	11,36	14,34
Pleistocene Galicia max	Pleistocene Galicia	33,53	16,38	11,93	15,10
Holocene Galicia min	Holocene Galicia	20,35	13,76	9,39	11,35
Holocene Galicia avg	Holocene Galicia	37,84	18,36	12,15	14,55
Holocene Galicia max	Holocene Galicia	55,24	23,66	17,60	17,51
Modern min	Modern	19,01	14,49	9,77	11,78
Modern avg	Modern	26,61	16,18	11,49	13,82
Modern max	Modern	32,82	18,77	14,16	15,62
CEZ-525	A Ceza	33,52	20,72	15,57	16,62
CEZ-725	A Ceza	26,07	16,15	12,49	13,89
Postes-243	Postes	21,20	13,70	9,50	11,30
Postes-289	Postes	22,50	14,90	9,80	11,60

Third phalanx: PCA

Specimen	Site	L	H	DT	Hart.	Dtart.
O17-226	Oliveira	48,88	27,45	14,99	17,34	14,00
FO.I-165	Fontainhas	47,70	30,31	15,73	22,68	14,57
Furninha (8,8) min	Furninha (8,8)	27,45	17,74	8,47	8,92	7,49
Furninha (8,8) avg	Furninha (8,8)	39,17	22,67	12,00	11,45	9,62
Furninha (8,8) max	Furninha (8,8)	50,26	29,15	15,96	13,68	11,45
Furninha (7,5) min	Furninha (7,5)	13,33	11,50	6,53	5,16	5,05
Furninha (7,5) avg	Furninha (7,5)	40,97	23,83	13,48	13,70	11,93
Furninha (7,5) max	Furninha (7,5)	60,05	30,64	17,45	26,78	16,76
SIPA-147	Pleistocene Galicia	35,40	20,92	12,39	14,77	11,76
SIPA-148	Pleistocene Galicia	34,59	19,90	13,25	14,92	10,83
Holocene Galicia min	Holocene Galicia	31,04	17,87	12,64	11,93	10,40
Holocene Galicia avg	Holocene Galicia	40,97	22,27	14,46	14,04	12,73
Holocene Galicia max	Holocene Galicia	47,06	26,48	16,54	15,74	15,23
Modern min	Modern	29,29	17,20	13,89	9,38	10,61
Modern avg	Modern	33,90	19,75	16,73	11,94	11,46
Modern max	Modern	40,21	23,81	20,30	14,55	12,67
CEZ-1	A Ceza	42,77	27,52	17,10	17,92	15,24
CEZ-2	A Ceza	40,95	25,72	14,79	15,18	13,61

D.3 Estimated masses of bears

Mass of modern Iberian bears

Reference	Area	Period	Sex	N	Average mass (kg)	Min. mass (kg)	Max. mass (kg)
Couturier, (1954)	Pyrenees	1848-1951	Male	16	174,06	100	350
Notario, (1964)	Cantabrian mountains	1957-1964	Male	13	113,50	73	163
Couturier, (1954)	Pyrenees	1911-1948	Female	9	118,11	75	245
Notario, (1964)	Cantabrian mountains	1957-1964	Female	15	85,40	53	140
This work	Whole Iberian Peninsula	1848-1964	Male	29	143,78	73	350
This work	Whole Iberian Peninsula	1848-1964	Female	24	101,76	53	245

Masses of mainly Holocene bears from NW Iberia, García-Vázquez (2015)

Site	Specimen	Sex	Age	Mass	Estimation Method
Arcoia	ARLU – 39 (2102)	Male	Pleisto-cene	256,922	Average for specimen (Viranta, 1994 & Christiansen, 1999)
Cuetu Blanco	CB-006	Female	Holocene	111,693	Average for specimen (Viranta, 1994 & Christiansen, 1999)
O Eixe	EIX-010	Female	Holocene	148,212	Average for specimen (Viranta, 1994 & Christiansen, 1999)
La Canal Fuerte	LCF-004-1996	Male	Holocene	290,024	Average for specimen (Viranta, 1994 & Christiansen, 1999)
La Canal Fuerte	LCF005-1996	Male	Holocene	286,602	Average for specimen (Viranta, 1994 & Christiansen, 1999)

La Canal Fuerte	LCF-006-1996	Male	Holocene	297,814	Average for specimen (Viranta, 1994 & Christiansen, 1999)
La Canal Fuerte	LCF-007-1996	Male	Holocene	296,995	Average for specimen (Viranta, 1994 & Christiansen, 1999)
La Canal Fuerte	LCF-173	Female	Holocene	150,107	Average for specimen (Viranta, 1994 & Christiansen, 1999)
La Canal Fuerte	LCF-96-036	Female	Holocene	183,458	Average for specimen (Viranta, 1994 & Christiansen, 1999)
Purruñal	Pur-Lu-16	Male	Holocene	219,829	Average for specimen (Viranta, 1994 & Christiansen, 1999)
Purruñal	Pur-Lu-21	Male	Holocene	251,841	Average for specimen (Viranta, 1994 & Christiansen, 1999)
Purruñal	Pur-Lu-22	Male	Holocene	254,933	Average for specimen (Viranta, 1994 & Christiansen, 1999)
Pozu La Veiga el Retuertu	PVR-015	Male	Holocene	237,952	Average for specimen (Viranta, 1994 & Christiansen, 1999)
Somiedo	SH5-97-T29-26	Female	Holocene	134,888	Average for specimen (Viranta, 1994 & Christiansen, 1999)
Somiedo	SH5-97-T29-35	Female	Holocene	139,532	Average for specimen (Viranta, 1994 & Christiansen, 1999)
Somiedo	SH5-97-T29-58	Female	Holocene	136,105	Average for specimen (Viranta, 1994 & Christiansen, 1999)
Somiedo	SH5-98-S28-095	Male	Holocene	306,279	Average for specimen (Viranta, 1994 & Christiansen, 1999)
Somiedo	SH5-98-T30-008	Female	Holocene	139,645	Average for specimen (Viranta, 1994 & Christiansen, 1999)
Pena Paleira	SIPA-24	Female	Holocene	120,483	Average for specimen (Viranta, 1994 & Christiansen, 1999)
Tarelo	TA-Lu-c-2	Female	Holocene	152,803	Average for specimen (Viranta, 1994 & Christiansen, 1999)
Tarelo	TA-Lu-c-3	Female	Holocene	151,065	Average for specimen (Viranta, 1994 & Christiansen, 1999)
Tarelo	TA-Lu-c-7	Female	Holocene	127,160	Average for specimen (Viranta, 1994 & Christiansen, 1999)
Tarelo	TA-Lu-c-8	Female	Holocene	126,049	Average for specimen (Viranta, 1994 & Christiansen, 1999)
Univ. León	LE1	Male	Modern	161,303	Average for specimen (Viranta, 1994 & Christiansen, 1999)
Univ. León	LE2	Male	Modern	166,166	Average for specimen (Viranta, 1994 & Christiansen, 1999)

Mass estimated based on teeth following Van Valkenburgh (1990)

Site	Specimen	L m1	Log. Mass	Estimated mass (kg)
Caldeirão	P-11 714	27,90	1,97	92,97
Escoural	Escral121966	26,39	1,96	90,47
Serra de Molianos	SM219.36	24,61	1,94	87,43
Fontainhas	FO.I-156	26,31	1,96	90,34
Furninha	GFP-1328	25,55	1,95	89,05
Furninha	GFP-1381.1	26,75	1,96	91,07
Furninha	GFP-1140.37.15	25,97	1,95	89,76
Furninha	GFP-1140.37.16	25,41	1,95	88,81
Furninha	GFP-1140.37.17	23,24	1,93	85,01
Furninha	GFP-1140.37.18	25,40	1,95	88,79
Furninha	GFP-1140.37.19	25,14	1,95	88,34
Furninha	GFP-1140.37.20	25,26	1,95	88,55
Furninha	GFP-1365.1	27,71	1,97	92,66
Furninha	GFP-1424	26,47	1,96	90,60
Furninha	GFP-1383.1	26,85	1,96	91,24
Furninha	GFP-1358.1	25,47	1,95	88,91
Furninha	GFP-1360.1	29,39	1,98	95,37
Furninha	GFP-1522	26,74	1,96	91,06
Furninha	GFP-1514.1	12,16	1,79	61,89
Furninha	GFP-1514.2	12,82	1,80	63,51
Furninha	GFP-148	10,52	1,76	57,65

Mass estimated based on teeth following Legendre & Roth (1988)

Site	Specimen	L m1	B m1	Area m1 (mm2)	Log. Mass	Estimated mass (Kg)
Caldeirão	P-11 714	27,90	14,00	390,60	5,02	151,85
Escoural	Escral121966	26,39	14,30	377,38	4,97	144,45
Serra de Molianos	SM219.36	24,61	10,31	253,73	4,91	135,66
Fontainhas	FO.I-156	26,31	13,39	352,29	4,97	144,05
Furninha	GFP-1328	25,55	12,13	309,92	4,94	140,31
Furninha	GFP-1381.1	26,75	13,16	352,03	4,99	146,22
Furninha	GFP-1140.37.15	25,97	12,65	328,52	4,96	142,38
Furninha	GFP-1140.37.16	25,41	13,42	341,00	4,94	139,62
Furninha	GFP-1140.37.17	23,24	11,36	264,01	4,86	128,86
Furninha	GFP-1140.37.18	25,40	11,95	303,53	4,94	139,57
Furninha	GFP-1140.37.19	25,14	12,47	313,50	4,93	138,29
Furninha	GFP-1140.37.20	25,26	12,44	314,23	4,93	138,88
Furninha	GFP-1365.1	27,71	13,78	381,84	5,02	150,92
Furninha	GFP-1424	26,47	12,75	337,49	4,98	144,84
Furninha	GFP-1383.1	26,85	13,58	364,62	4,99	146,71
Furninha	GFP-1358.1	25,47	12,40	315,83	4,94	139,91
Furninha	GFP-1360.1	29,39	12,03	353,56	5,07	159,12
Furninha	GFP-1522	26,74	12,96	346,55	4,98	146,17
Furninha	GFP-1514.1	12,16	5,44	66,15	4,28	72,01
Furninha	GFP-1514.2	12,82	5,60	71,79	4,32	75,52
Furninha	GFP-148	10,52	4,54	47,76	4,15	63,23

Average masses of Portuguese bears based on teeth, following Van Valkenburgh (1990) and Legendre & Roth (1988)

Site	Specimen	Van Valkenburgh, (1990)	Legendre & Roth, (1988)	Average mass based on teeth
Furninha	GFP-1328	89,05	140,31	114,68
Furninha	GFP-1381.1	91,07	146,22	118,64
Furninha	GFP-1140.37.15	89,76	142,38	116,07
Furninha	GFP-1140.37.16	88,81	139,62	114,21
Furninha	GFP-1140.37.17	85,01	128,86	106,93
Furninha	GFP-1140.37.18	88,79	139,57	114,18
Furninha	GFP-1140.37.19	88,34	138,29	113,31
Furninha	GFP-1140.37.20	88,55	138,88	113,71
Furninha	GFP-1365.1	92,66	150,92	121,79
Furninha	GFP-1424	90,60	144,84	117,72
Furninha	GFP-1383.1	91,24	146,71	118,97
Furninha	GFP-1358.1	88,91	139,91	114,41
Furninha	GFP-1360.1	95,37	159,12	127,24
Furninha	GFP-1522	91,06	146,17	118,61
Furninha	GFP-1514.1	61,89	72,01	66,95

Furninha	GFP-1514.2	63,51	75,52	69,51
Furninha	GFP-148	57,65	63,23	60,44
Fontainhas	FO.I-156	90,34	144,05	117,19
Caldeirão	P-11 714	92,97	151,85	122,41
Escoural	Escral121966	90,47	144,45	117,46
Serra de Molianos	SM219.36	87,43	135,66	111,55

Masses of Portuguese bears based on limb measurements, following Viranta (1994)

Site	Specimen	Bone	Type of measurement	Measurement (mm)	Estimated mass (Kg)
Furninha	GFP-1537	Humerus	DTdia.	17,44	11,53*
Furninha	GFP-1376	Humerus	DTdia.	40,42	1070,42**
Furninha	GFP-1379	Humerus	DTdist.	114,09	224,65
Furninha	GFP-1375	Humerus	DTdia.	40,42	1070,42**
Furninha	GFP-1373	Humerus	DTdia.	50,97	3736,16**
Furninha	GFP-1130.7	Humerus	DTdia.	35,88	244,80
Furninha	GFP-142	Humerus	DTdia.	22,75	48,32*
Furninha	GFP-1427	Radius	DTprox.	47,64	317,47
Furninha	GFP-1332	Radius	L	294	123,31
Furninha	GFP-1332	Radius	DTprox.	43,74	256,22
Furninha	GFP-1332	Radius	DTart.dist.	46,86	606,16**
Furninha	GFP-1333	Radius	L	300,9	132,10
Furninha	GFP-1333	Radius	DTprox.	39,59	199,50
Furninha	GFP-1333	Radius	DTart.dist.	45,63	547,16**
Furninha	GFP-1133.21.3	Radius	DTprox.	41,73	227,68
Furninha	GFP-1133.21.4	Radius	DTart.dist.	41,55	381,50
Furninha	GFP-1134.16.9	Radius	DTprox.	47,06	307,86
Furninha	GFP-1134.16.10	Radius	DTprox.	40,27	208,21
Furninha	GFP-1134.16.11	Radius	L	250,08	76,26
Furninha	GFP-1134.16.11	Radius	DTprox.	36,31	160,57
Furninha	GFP-1134.16.11	Radius	DTart.dist.	38,94	297,18
Furninha	GFP-1666.2	Radius	DTart.dist.	44,42	493,38**
Furninha	GFP-1142	Femur	Dtdia.	35,02	226,19
Furninha	GFP-1471	Femur	DTdist.	88,48	4642,11**
Furninha	GFP-1538	Tibia	DTdia.min.	24,17	184,55
Furninha	GFP-1134.16.4	Tibia	DTprox.	82,54	163,11
Furninha	GFP-1135.11.1	Tibia	DTdia.min.	25,17	217,56
Furninha	GFP-1621	Tibia	DTdia.min.	24,88	207,56
Furninha	GFP-1334	Tibia	L	285	156,70
Furninha	GFP-1334	Tibia	DTprox.	77,35	128,36
Furninha	GFP-1334	Tibia	DTdia.min.	30,23	457,70
Furninha	GFP-1334	Tibia	DTdist.	60,32	142,11
Fontainhas	FO.I-34	Humerus	L	390	411,10
Fontainhas	FO.I-34	Humerus	DTdia.	46,93	2393,97**
Fontainhas	FO.I-34	Humerus	DTdist.	110,19	198,77

Fontainhas	FO.I-55	Humerus	L	390	411,10
Fontainhas	FO.I-55	Humerus	DTdia.	44,13	1718,37**
Fontainhas	FO.I-59	Radius	L	347	201,73
Fontainhas	FO.I-59	Radius	DTprox.	42,61	239,92
Fontainhas	FO.I-59	Radius	DTart.dist.	51,04	842,28**
Fontainhas	FO.I-58	Radius	L	345	198,30
Fontainhas	FO.I-58	Radius	DTprox.	47,73	318,98
Fontainhas	FO.I-58	Radius	DTart.dist.	50,6	814,67**
Fontainhas	FO.I-51	Femur	L	461	416,37
Fontainhas	FO.I-51	Femur	Dtdia.	41,05	379,67
Fontainhas	FO.I-51	Femur	DTdist.	95,71	5996,82**
Fontainhas	FO.I-49	Femur	L	459	408,00
Fontainhas	FO.I-49	Femur	Dtdia.	41,05	379,67
Fontainhas	FO.I-49	Femur	DTdist.	94,76	5804,94**
Fontainhas	FO.I-54	Tibia	L	321	276,03
Fontainhas	FO.I-54	Tibia	DTprox.	90,99	233,72
Fontainhas	FO.I-54	Tibia	DTdia.min.	31,28	525,75
Fontainhas	FO.I-50	Tibia	L	331	319,43
Fontainhas	FO.I-50	Tibia	DTprox.	95,81	282,75
Fontainhas	FO.I-50	Tibia	DTdia.min.	27,14	295,43
Fontainhas	FO.I-50	Tibia	DTdist.	67,22	172,89
Serra de Molianos	SM219.2	Radius	DTprox.	42,94	244,62
Serra de Molianos	SM219.32.2	Radius	DTprox.	42,69	241,06
Serra de Molianos	SM219.32.1	Radius	DTart.dist.	36,12	222,50
Serra de Molianos	Average from site	Radius			236,06
Juvenile	*				
Unrealistically high mass	**				

Masses of Portuguese bears based on limb measurements, following Christiansen (1999)

Site	**Specimen**	**Bone**	**L humerus (mm)**	**DT distal humerus (mm)**	**Circumference humerus (mm)**	**L femur (mm)**	**Circumference femur (mm)**	**LN measurement**	**Estimated mass average (Kg)**
Furninha	GFP-1376	Humerus		114,09				4,736987611	430,81
Furninha	GFP-1376	Humerus			115			4,744932128	253,97
Furninha	GFP-1376	Humerus						**Average:**	342,39
Furninha	GFP-1337	Humerus			71			4,262679877	70,93*
Furninha	GFP-1375	Humerus			162			5,087596335	628,65**
Furninha	GFP-1373	Humerus			160			5,075173815	608,33**
Furninha	GFP-1130.7	Humerus			140			4,941642423	427,32

Furninha	GFP-142	Humerus			100			4,605170186	175,49
Furninha	GFP-1142	Femur					123	4,812184355	451,73
Furninha	GFP-1622	Femur					93	4,532599493	197,68
Fontainhas	FO.I-34	Humerus	390					5,966146739	346,98
Fontainhas	FO.I-34	Humerus		110,19				4,702206148	381,71
Fontainhas	FO.I-34	Humerus			140			4,941642423	427,32
Fontainhas	FO.I-34	Humerus						**Average:**	385,33
Fontainhas	FO.I-55	Humerus	390					5,966146739	346,98
Fontainhas	FO.I-55	Humerus			140			4,941642423	427,32
Fontainhas	FO.I-55	Humerus						**Average:**	385,94
Fontainhas	FOI.I-51	Femur				461		6,133398043	302,85
Fontainhas	FOI.I-51	Femur					125	4,828313737	473,79
Fontainhas	FOI.I-51	Femur						**Average:**	388,32
Fontainhas	FOI.I-49	Femur				459		6,12905021	298,68
Fontainhas	FOI.I-49	Femur					125	4,828313737	473,79
Fontainhas	FOI.I-49	Femur						**Average:**	386,24
Juvenile	*								
Unrealistically high mass	**								

Average of Portuguese specimens based on Viranta (1994) and Christiansen (1999).

Specimen	**Viranta, (1994)**	**Christiansen, (1999)**	**Average mass based on long bones**		**Site**	**Average mass for the site (long bones)**
GFP-1130.7	244,80	427,32	336,06		**Furninha**	337,51
GFP-1142	226,19	451,73	338,96		**Fontainhas**	386,96
Humeri and femora from one individual	376,97	396,95	386,96			

Masses of Iberian brown bears, Pleistocene-Modern day

Site	**Number**	**Mass**	**Age**	**Method**
Furninha	GFP-1130.7	336,06	Pleistocene	Average specimen; Viranta, (1994) & Christiansen, (1999)
Furninha	GFP-1142	338,96	Pleistocene	Average specimen; Viranta, (1994) & Christiansen, (1999)
Fontainhas	FO.I-Several numbers, same individual	386,96	Pleistocene	Average specimen; Viranta, (1994) & Christiansen, (1999)

Arcoia	ARLU – 39 (2102)	256,92	Pleisto-cene	Average specimen; Viranta, (1994) & Christiansen, (1999)
Cuetu Blanco	CB-006	111,69	Holocene	Average specimen; Viranta, (1994) & Christiansen, (1999)
O Eixe	EIX-010	148,21	Holocene	Average specimen; Viranta, (1994) & Christiansen, (1999)
La Canal Fuerte	LCF-004-1996	290,02	Holocene	Average specimen; Viranta, (1994) & Christiansen, (1999)
La Canal Fuerte	LCF005-1996	286,60	Holocene	Average specimen; Viranta, (1994) & Christiansen, (1999)
La Canal Fuerte	LCF-006-1996	297,81	Holocene	Average specimen; Viranta, (1994) & Christiansen, (1999)
La Canal Fuerte	LCF-007-1996	297,00	Holocene	Average specimen; Viranta, (1994) & Christiansen, (1999)
La Canal Fuerte	LCF-173	150,11	Holocene	Average specimen; Viranta, (1994) & Christiansen, (1999)
La Canal Fuerte	LCF-96-036	183,46	Holocene	Average specimen; Viranta, (1994) & Christiansen, (1999)
Purruñal	Pur-Lu-16	219,83	Holocene	Average specimen; Viranta, (1994) & Christiansen, (1999)
Purruñal	Pur-Lu-21	251,84	Holocene	Average specimen; Viranta, (1994) & Christiansen, (1999)
Purruñal	Pur-Lu-22	254,93	Holocene	Average specimen; Viranta, (1994) & Christiansen, (1999)
Pozu La Veiga el Retuertu	PVR-015	237,95	Holocene	Average specimen; Viranta, (1994) & Christiansen, (1999)
Somiedo	SH5-97-T29-26	134,89	Holocene	Average specimen; Viranta, (1994) & Christiansen, (1999)
Somiedo	SH5-97-T29-35	139,53	Holocene	Average specimen; Viranta, (1994) & Christiansen, (1999)
Somiedo	SH5-97-T29-58	136,10	Holocene	Average specimen; Viranta, (1994) & Christiansen, (1999)
Somiedo	SH5-98-S28-095	306,28	Holocene	Average specimen; Viranta, (1994) & Christiansen, (1999)
Somiedo	SH5-98-T30-008	139,64	Holocene	Average specimen; Viranta, (1994) & Christiansen, (1999)
Pena Paleira	SIPA-24	120,48	Holocene	Average specimen; Viranta, (1994) & Christiansen, (1999)
Tarelo	TA-Lu-c-2	152,80	Holocene	Average specimen; Viranta, (1994) & Christiansen, (1999)
Tarelo	TA-Lu-c-3	151,07	Holocene	Average specimen; Viranta, (1994) & Christiansen, (1999)
Tarelo	TA-Lu-c-7	127,16	Holocene	Average specimen; Viranta, (1994) & Christiansen, (1999)
Tarelo	TA-Lu-c-8	126,05	Holocene	Average specimen; Viranta, (1994) & Christiansen, (1999)
Univ. León	LE1	161,30	Modern	Average specimen; Viranta, (1994) & Christiansen, (1999)
Univ. León	LE2	166,17	Modern	Average specimen; Viranta, (1994) & Christiansen, (1999)
Cantabrian mountains	1957-1965 Avg Cantabrian Female	85,40	Modern	Direct weighting
Cantabrian mountains	1957-1965 Avg Cantabrian Male	113,50	Modern	Direct weighting
Pyrenees	1911-1948 Avg Pyrenean Female	118,11	Modern	Direct weighting
Pyrenees	1848-1951 Avg Pyrenean Male	174,10	Modern	Direct weighting

E

APPENDIX: "PALEOBIODIVERSITY OF PLEISTOCENE VERTEBRATES FROM PORTUGAL "

E.1 Taxa present in the Pleistocene of Portugal. localities where they appear and references used.

TAXA	LOCALITIES	REFERENCES
Salamandra salamandra (Linnaeus, 1758)	Lagar Velho, Figueira Brava	Moreno-García & Pimenta 2002; Crespo et al. 2000
Triturus marmoratus (Latreille, 1800)	Lagar Velho	Moreno-García & Pimenta 2002
Pelodytes sp. Daudin, 1802	Aroeira	López-García et al. 2018
Bufo spinosus (Daudin, 1803)	Lapa do Picareiro, Guia, Aroeira, Escoural	Antunes et al. 1989; Gautier 1996; Hockett & Haws 2009; López-García et al. 2018; Haws et al. 2021
Pelobates cultripes Cuvier, 1829	Lapa do Picareiro, Figueira Brava, Guia, Escoural	Gautier 1996; Crespo et al. 2000; Hockett & Haws 2009; Haws et al. 2021
Pleurodeles waltl (Michahelles, 1830)	Guia	Antunes et al. 1989
Epidalea calamita (Laurenti, 1768)	Guia	Antunes et al. 1989
Pelophylax perezi (Seoane, 1885)	Guia, Lapa do Picareiro	Antunes et al. 1989; Haws et al. 2021
Rana iberica Boulenger, 1979	Lapa do Picareiro	Haws et al. 2021
Timon lepidus (Daudin, 1802)	Figueira Brava, Guia, Escoural	Gautier 1996; Crespo et al. 2000 Antunes et al. 1989
Psammodromus manuelae Busack *et al.*, 2006	Figueira Brava	Crespo et al. 2000
*Podarcis*sp. Wagler, 1830	Figueira Brava	Crespo et al. 2000
Acanthodactylus erythrurus (Schinz, 1833)	Guia	Antunes et al. 1989
Rhinechis scalaris (Schinz, 1822)	Figueira Brava	Crespo et al. 2000
Hemorrhois hippocrepis (Linnaeus, 1758)	Figueira Brava	Crespo et al. 2000
Coronella girondica Daudin, 1803	Aroeira, Figueira Brava	Crespo et al. 2000 López-García et al. 2018
Vipera lastei Bosca, 1878	Figueira Brava	Crespo et al. 2000
Natrix maura (Linnaeus, 1758)	Aroeira	López-García et al. 2018
Blanus cinereus (Vandelli, 1797)	Figueira Brava	Crespo et al. 2000

Testudo hermanni Gmelin, 1789	Aroeira, Oliveira, Furninha, Figueira Brava, Gruta Nova da Columbeira, Escoural, Gruta de Ibn Amar	Jiménez Fuentes et al.1998; Crespo 2000; Bicho 2004; Morales-Pérez & Sanchís-Serra 2009; Nabais & Zilhão 2019; Jiménez et al. 2023
Mauremys leprosa (Schweiger, 1812)	Mealhada, Caldeirão, Gruta Nova da Columbeira, Escoural	Jiménez Fuentes et al.1998; Lapparent de Broin & Antunes 2000; Morales Pérez & Serra 2009 Nabais & Zilhão 2019; Jiménez et al. 2023a; Jiménez et al. 2023b
Emys orbicularis (Linnaeus, 1758)	Mealhada, Figueira Brava, Gruta Nova da Columbeira	Lapparent de Broin & Antunes 2000; Nabais & Zilhão 2019; Jiménez et al. 2023a; Jiménez et al. 2023b
Tetrao urogallus Linnaeus, 1758	Lapa da Rainha	Figueiredo 2010
Alectoris rufa (Linnaeus, 1758)	Lapa do Picareiro, Furninha, Lapa do Suão, Gruta Nova da Columbeira, Escoural, Figueira Brava	Pimenta et al. 2015; Figueiredo et al. 2017; Figueiredo et al. 2018; Zilhão et al. 2020; Haws et al. 2021
Perdix perdix (Linnaeus, 1758)	Lapa do Picareiro, Furninha, Gruta Nova da Columbeira, Caldeirão	Figueiredo 2010; Pimenta et al. 2015; Figueiredo et al. 2018; Haws et al. 2021
Coturnix coturnix (Linnaeus, 1758)	Furninha, Gruta Nova da Columbeira	Figueiredo 2010; Figueiredo et al. 2017; Figueiredo et al. 2018
Phasianus colchicus Linnaeus, 1758	Pego do Diabo	Figueiredo 2010
Lagopus lagopus (Linnaeus, 1758)	Lapa da Rainha	Figueiredo 2010
Lagopus muta (Montin, 1781)	Gruta Nova da Columbeira	Figueiredo 2010; Figueiredo et al. 2018
Anas platyrhynchos Linnaeus, 1758	Lapa do Suão, Escoural, Figueira Brava, Gruta Nova da Columbeira	Pimenta et al. 2015 Figueiredo et al. 2018; Zilhão et al. 2020
Anas crecca Linnaeus, 1758	Furninha	Pimenta et al. 2015; Figueiredo et al. 2017
Melanitta nigra (Linnaeus, 1758)	Furninha, Gruta Nova da Columbeira, Figueira Brava	Figueiredo 2010; Pimenta et al. 2015; Figueiredo et al. 2017; Figueiredo et al. 2018; Zilhão et al. 2020
Melanitta fusca (Linnaeus, 1758)	Figueira Brava	Pimenta et al. 2015
Aythya sp. Boie, 1822	Aroeira	Marks et al. 2002
Clangula hyemalis (Linnaeus, 1758)	Figueira Brava	Pimenta et al. 2015
Tadorna tadorna (Linnaeus, 1758)	Furninha	Figueiredo 2010; Figueiredo et al. 2017
Tadorna ferruginea (Pallas, 1761)	Furninha	Figueiredo 2010; Figueiredo et al. 2017
Somateria mollisima (Linnaeus, 1758)	Furninha	Figueiredo 2010; Figueiredo et al. 2017
Mergus merganser (Linnaeus, 1758)	Escoural	Pimenta et al. 2015
Mergellus albellus (Linnaeus, 1758)	Aroeira	Marks et al. 2002
Anser albifrons (Scopoli, 1769)	Pego do Diabo	Figueiredo 2010
Cygnus olor (Gmelin, 1789)	Aroeira, Furninha	Pimenta et al. 2015; Figueiredo et al. 2017
Scolopax rusticola Linnaeus, 1758	Aroeira, Figueira Brava, Lapa do Picareiro	Pimenta et al. 2015 Zilhão et al. 2020; Haws et al. 2021
Gallinago sp.	Furninha	Figueiredo et al. 2017
Numenius phaeopus (Linnaeus, 1758)	Furninha, Figueira Brava	Pimenta et al. 2015; Figueiredo et al. 2017
Tringa totanus (Linnaeus, 1758)	Lapa do Picareiro	Haws et al. 2021
Calidris canutus (Linnaeus, 1758)	Lapa do Picareiro, Figueira Brava	Pimenta et al. 2015; Haws et al. 2021
Calidris pugnax (Linnaeus, 1758)	Lapa do Picareiro	Haws et al. 2021

Sterna hirundo Linnaeus, 1758	Figueira Brava	Zilhão et al. 2020
Larus fuscus Linnaeus, 1759	Figueira Brava	Pimenta et al. 2015
Pinguinus impennis (Linnaeus, 1758)	Furninha, Figueira Brava	Pimenta et al. 2015 Zilhão et al. 2020
Fratercula arctica (Linnaeus, 1758)	Figueira Brava	Zilhão et al. 2020
Alca torda Linnaeus, 1758	Figueira Brava	Pimenta et al. 2015 Zilhão et al. 2020
Vanellus vanellus (Linnaeus, 1758)	Fontainhas	Figueiredo 2010
Pluvialis squatarola (Linnaeus, 1758)	Gruta Nova da Columbeira	Figueiredo et al. 2018
Pluvialis apricaria (Linnaeus, 1758)	Lapa do Picareiro	Pimenta et al. 2015 Haws et al. 2021
Podiceps nigricollis Brehm, 1831	Figueira Brava	Figueiredo 2010
Otis tarda Linnaeus, 1758	Gruta de Casa da Moura	Figueiredo 2010
Grus grus (Linnaeus, 1758)	Gruta de Casa da Moura	Figueiredo 2010
Grus primigenia (Milne-Edwards, 1869)	Figueira Brava	Figueiredo 2010
Puffinus puffinus (Brünnich, 1764)	Furninha, Figueira Brava	Figueiredo et al. 2017; Zilhão et al. 2020
Puffinus holeae Walker *et al.*, 1990	Figueira Brava	Pimenta et al. 2015
Phalacrocorax aristotelis (Linnaeus, 1761)	Furninha, Figueira Brava	Pimenta et al. 2015; Figueiredo et al. 2017; Zilhão et al. 2020
Phalacrocorax carbo (Linnaeus, 1758)	Figueira Brava	Pimenta et al. 2015; Zilhão et al. 2020
Morus bassanus (Linnaeus, 1758)	Figueira Brava	Pimenta et al. 2015; Zilhão et al. 2020
Phoenicopterus roseus Pallas, 1811	Furninha	Figueiredo 2010; Figueiredo et al. 2017
Gavia stellata (Pontoppidan, 1763)	Figueira Brava	Pimenta et al. 2015; Zilhão et al. 2020
Accipiter nisus (Linnaeus, 1758)	Figueira Brava	Pimenta et al. 2015; Zilhão et al. 2020

Aquila chrysaetos (Linnaeus, 1758)	Figueira Brava, Vale Boi, Gruta Nova da Columbeira, Furninha, Lapa do Picareiro	Manne et al. 2012; Pimenta et al. 2015; Figueiredo et al. 2017; Figueiredo et al. 2018; Haws et al. 2021
Aquila adalberti (Brehm, 1861)	Lapa da Rainha, Lapa do Picareiro	Figueiredo 2010; Haws et al. 2021
Aquila fasciata (Viellot, 1822)	Figueira Brava	Pimenta et al. 2015
Milvus migrans (Boddaert, 1783)	Figueira Brava	Pimenta et al. 2015 Zilhão et al. 2020
Buteo buteo (Linnaeus, 1758)	Aroeira	Marks et al. 2002
Haliaeetus albicilla (Linnaeus, 1758)	Aroeira	Marks et al. 2002
Gypaetus barbatus (Linnaeus, 1758)	Caldeirão, Lagar Velho	Davis et al. 2007; Sanz et al. 2023
Aegypius monachus (Linnaeus, 1766)	Caldeirão	Davis 2002
Gyps fulvus (Hablizl, 1783)	Furninha, Caldeirão, Figueira Brava	Pimenta et al. 2015; Figueiredo et al. 2017; Zilhão et al. 2020
Falco tinnunculus Linnaeus, 1758	Lagar Velho, Figueira Brava, Furninha, Gruta Nova da Columbeira	Pimenta et al. 2015; Figueiredo et al. 2017; Figueiredo et al. 2018
Falco rusticolus Linnaeus, 1758	Gruta de Casa da Moura	Figueiredo 2010
Bubo bubo (Linnaeus, 1758)	Aroeira, Caldeirão, Furninha, Casa da Moura, Figueira Brava, Lapa do Picareiro	Figueiredo 2010; Pimenta et al. 2015; Figueiredo et al. 2017; Haws et al. 2021
Athene noctua (Scopoli, 1769)	Aroeira, Caldeirão, Lapa do Picareiro, Gruta Nova da Columbeira, Lapa da Rainha, Escoural, Figueira Brava	Pimenta et al. 2015; Zilhão et al. 2020
Strix aluco Linnaeus, 1758	Gruta Nova da Columbeira; Lapa do Picareiro	Figueiredo 2010; Figueiredo 2018; Haws et al. 2021
Tyto alba (Scopoli, 1769)	Furninha	Figueiredo et al. 2017
Asio flammeus (Potoppidan, 1763)	Lapa do Picareiro, Furninha	Pimenta et al. 2015; Haws et al. 2021
Pterocles orientalis (Linnaeus, 1758)	Lapa do Picareiro	Haws et al. 2021
Streptopelia turtur (Linnaeus, 1758)	Escoural	Pimenta et al. 2015
Columba livia Gmelin, 1789	Aroeira, Lapa do Picareiro, Lapa da Rainha, Gruta das Salemas, Furninha, Gruta Nova da Columbeira, Figueira Brava	Figueiredo 2010 Pimenta et al. 2015; Figueiredo et al. 2017; Figueiredo et al. 2018; Haws et al. 2021
Columba palumbus Linnaeus, 1758	Aroeira, Caldeirão, Escoural, Figueira Brava, Gruta Nova da Columbeira	Figueiredo 2010 Pimenta et al. 2015; Figueiredo et al. 2018
Ciconia sp. Linnaeus, 1758	Gruta da Aroreira	Marks et al. 2002
Egretta garzetta (Linnaeus, 1766)	Figueira Brava	Zilhão et al. 2020
Ardea alba Linnaeus, 1758	Aroeira	Marks et al. 2002
Pyrrhocorax pyrrhocorax (Linnaeus, 1758)	Caldeirão, Lapa do Picareiro, Furninha, Lapa do Suão, Gruta Nova da Columbeira, Fontainhas, Lapa da Rainha, Figueira Brava, Gruta das Salemas	Pimenta et al. 2015; Figueiredo et al. 2017; Figueiredo et al. 2018; Zilhão et al. 2020; Haws et al. 2021

Pyrrhocorax graculus (Linnaeus, 1766)	Aroeira, Lapa da Rainha, Lapa do Picareiro, Furninha, Gruta de Casa da Moura, Fontainhas, Caldeirão, Gruta Nova da Columbeira	Figueiredo 2010; Pimenta et al. 2015; Figueiredo et al. 2017; Figueiredo et al. 2018; Haws et al. 2021
Coloeus monedula (Linnaeus, 1758)	Aroeira, Lagar Velho, Lapa do Picareiro, Furninha, Lapa do Suão, Gruta Nova da Columbeira, Fontainhas, Lapa da Rainha, Figueira Brava	Pimenta et al. 2015; Figueiredo et al. 2017; Figueiredo et al. 2018; Haws et al. 2021
Corvus corax (Linnaeus, 1758)	Caldeirão, Gruta Nova da Columbeira, Lapa da Rainha, Casa da Moura, Figueira Brava, Lapa do Picareiro	Figueiredo 2010; Pimenta et al. 2015; Figueiredo et al. 2018; Zilhão et al. 2020; Haws et al. 2021
Corvus corone Linnaeus, 1758	Aroeira, Lapa do Picareiro, Furninha, Figueira Brava, Gruta Nova da Columbeira	Pimenta et al. 2015; Figueiredo et al. 2017; Figueiredo et al. 2018; Zilhão et al. 2020
Corvus frugilegus Linnaeus, 1758	Furninha, Escoural, Gruta Nova da Columbeira	Pimenta et al. 2015; Figueiredo et al. 2017; Figueiredo et al. 2018
Corvus antecorax Mourer-Chauviré, 1975	Aroeira	Trinkaus et al. 2003; Figueiredo 2010
Pica pica (Linnaeus, 1758)	Aroeira, Caldeirão, Furninha, Escoural, Gruta Nova da Columbeira, Lapa do Picareiro	Pimenta et al. 2015; Figueiredo et al. 2017; Figueiredo et al. 2018; Haws et al. 2021
Garrulus glandarius (Linnaeus, 1758)	Lapa do Picareiro, Lapa do Suão, Gruta Nova da Columbeira	Pimenta et al. 2015; Figueiredo et al. 2018; Haws et al. 2021
Turdus iliacus Linnaeus, 1766	Furninha, Gruta Nova da Columbeira	Figueiredo 2010; Figueiredo et al. 2017; Figueiredo et al. 2018
Turdus pilaris Linnaeus, 1758	Furninha, Gruta Nova da Columbeira, Lapa do Picareiro	Figueiredo 2010; Figueiredo et al. 2017; Figueiredo et al. 2018; Haws et al. 2021
Turdus philomelos Brehm, 1831	Gruta Nova da Columbeira, Lapa do Picareiro	Figueiredo 2010; Figueiredo et al. 2018; Haws et al. 2021
Turdus merula Linnaeus, 1758	Furninha, Gruta Nova da Columbeira, Lapa do Picareiro	Figueiredo 2010; Figueiredo et al. 2017; Figueiredo et al. 2018; Haws et al. 2021
Picus sharpei (Saunders, 1872)	Aroeira, Gruta Nova da Columbeira	Figueiredo 2010 Pimenta et al. 2015; Figueiredo et al. 2018
Cyanopica cooki Bonaparte, 1850	Gruta Nova da Columbeira	Figueiredo 2010; Figueiredo et al. 2018
Sturnus unicolor Temminck, 1820	Lapa do Picareiro	Haws et al. 2021
Sturnus vulgaris Linnaeus, 1758	Lagar Velho, Lapa do Picareiro	Pimenta et al. 2015
Carduelis carduelis (Linnaeus, 1758)	Gruta Nova da Columbeira	Figueiredo 2010; Figueiredo et al. 2018
Passer sp.	Lapa do Picareiro	Haws et al. 2021
Ptyonoprogne rupestris (Scopoli, 1769)	Gruta Nova da Columbeira	Figueiredo 2010; Figueiredo et al. 2018
Motacilla alba Linnaeus, 1758	Lapa da Rainha	Figueiredo 2010
Caprimulgus europaeus Linnaeus, 1758	Aroeira, Gruta Nova da Columbeira	Pimenta et al. 2015
Cuculus canorus Linnaeus, 1758	Furninha, Gruta de Casa da Moura, Figuira Brava	Figueiredo 2010; Figueiredo et al. 2017; Zilhão et al. 2020
Erinaceus europaeus Linnaeus, 1758	Casa da Moura, Furninha, Figueira Brava, Lagar Velho, Lapa do Picareiro, Escoural	Harlé 1910/11;Gautier 1996; Mein & Antunes 2000; Moreno-García & Pimenta 2002; Bicho et al. 2003; Brugal et al. 2012; Haws et al. 2021; López-García et al. 2021

Crocidura russula Hermann, 1780	Aroeira, Figueira Brava, Lapa do Picareiro, Lagar Velho, Goldra, Guia, Oliveira	Antunes et al. 1986c; Antunes et al. 1989; Mein & Antunes 2000; Marks et al. 2002; Moreno-García & Pimenta 2002; Bicho et al. 2003; López-García et al. 2022
Crocidura suaveolens Pallas, 1811	Figueira Brava, Lapa do Picareiro, Lagar Velho	Mein & Antunes 2000; Bicho et al. 2003; López-García et al. 2021
Sorex sp.	Oliveira	López-García et al. 2022
Sorex granarius Miller, 1910	Lagar Velho	López-García et al. 2021
Sorex araneus Linnaeus, 1758	Goldra	Antunes et al. 1986c
Talpa occidentalis Cabrera, 1907	Goldra, Figueira Brava, Lapa do Picareiro, Escoural, Oliveira, Lagar Velho	Antunes et al. 1986c; Gautier 1996; Mein & Antunes 2000; Bicho et al. 2003; Haws et al. 2021; López-García et al. 2021; López-García et al. 2022
Galemys kormosi (Shereuder, 1940)	Morgadinho	Antunes et al. 1986b
Galemys pyrenaicus Geoffroy, 1811	Aroeira, Lapa do Picareiro	Marks et al. 2002; Bicho et al. 2003
Rinolophus ferrumequinun (Shereber, 1774)	Aroeira, Furninha, Figueira Brava, Oliveira	Mein & Antunes 2000; Brugal et al. 2012; López-García et al. 2018; López-García et al. 2022
Rinolophus hipposideros (Bechstein, 1800)	Figueira Brava, Oliveira	Mein & Antunes 2000; López-García et al. 2022
Rinolophus meheleyi Matschie, 1901	Oliveira	López-García et al. 2022
Rinolophus euryale Blasius, 1853	Figueira Brava, Oliveira	Mein & Antunes 2000 López-García et al. 2022
Myotis myotis (Borkhausen, 1797)	Aroeira, Figueira Brava, Lapa do Picareiro, Oliveira	Mein & Antunes 2000; Marks et al. 2002; Bicho et al. 2003; López-García et al. 2018; López-García et al. 2022
Myotis blythi (Tomes, 1857)	Figueira Brava	Mein & Antunes 2000
Myotis nattereri (Khul, 1818)	Figueira Brava	Mein & Antunes 2000
Myotis mystacinus Khul, 1817	Lapa do Picareiro	Bicho et al. 2003
Nyctalus sp. Bowdich, 1825	Oliveira	López-García et al. 2022
Plecotus sp. Geoffroy, 1818	Oliveira	López-García et al. 2022
Miniopterus schreibersi (Khul, 1819)	Aroeira, Figueira Brava, Oliveira	Mein & Antunes 2000; López-García et al. 2018; López-García et al. 2022
Vespertilio murinus Linnaeus, 1758	Furninha	Brugal et al. 2012
Pipistrellus sp. Kaup, 1829	Aroeira, Oliveira	Marks et al. 2002; López-García et al. 2022
Apodemus sylvaticus (Linnaeus, 1758)	Goldra, Guia, Caldeirão, Lagar Velho, Lapa do Picareiro, Santa Margarida, Oliveira	Antunes et al. 1986c; Antunes et al. 1989; Póvoas et al. 1992; Moreno-García & Pimenta 2002; Bicho et al. 2003; Estraviz-López & Mateus 2019; López-García et al. 2020; López-García et al. 2021; López-García et al. 2022

Apodemus flavicollis (Melchior, 1834)	Aroeira, Figueira Brava	Jeannet 2000; López-García et al. 2018
Sciurus vulgaris Linnaeus, 1758	Figueira Brava, Lagar Velho, Fariseu	Jeannet 2000; Moreno-García & Pimenta 2002; Gabriel & Béarez 2009
Eliomys quercinus Linnaeus, 1766	Aroeira, Goldra, Guia, Caldeirão, Figueira Brava, Lapa do Suão, Pego do Diabo, Santa Margarida, Oliveira	Antunes et al. 1986c; Antunes et al. 1989; Póvoas et al. 1992; Jeannet 2000; Marks et al. 2002; Valente 2004; Valente & Haws 2006; López-García et al. 2018; Estraviz-López & Mateus 2019; López-García et al. 2020; López-García et al. 2022; Estraviz-López et al. 2024
Glis glis (Linnaeus, 1766)	Lapa do Picareiro, Oliveira	Bicho et al. 2003; López-García et al. 2022
Allocricetus bursae Schaub., 1930	Aroeira, Caldeirão, Santa Margarida, Oliveira	Póvoas et al. 1992; López-García et al. 2018; López-García et al. 2020; López-García et al. 2022; Estraviz-López et al. 2024
*Mimomys*sp. Forsyth-Major, 1902	Morgadinho	Antunes et al. 1986b
Pliomys sp. Méhely, 1914	Oliveira	López-García et al. 2022
Pliomys episcopalis Méhely, 1914	Aroeira	Marks et al. 2002 López-García et al. 2018
Chionomys nivalis Martins, 1842	Caldeirão, Lapa do Picareiro	Póvoas et al. 1992; Bicho et al. 2003
Arvicola sapidus Miller, 1908	Caldeirão, Figueira Brava, Lagar Velho, Oliveira	Póvoas et al. 1992; Jeannet 2000; Moreno-García & Pimenta 2002; López-García et al. 2020; López-García et al. 2021; López-García et al. 2022
Arvicola amphibious (Linnaeus, 1758)	Lapa do Suão; Oliveira	Valente & Haws 2006; López-García et al. 2022
Arvicola cantiana Hinton, 1910	Figueira Brava	Jeannet 2000
Victoriamys chalinei (Alcalde et al., 1981)	Santa Margarida	Estraviz-López & Mateus 2019
Microtus lusitanicus (Gerbe, 1879)	Caldeirão, Lapa do Suão, Lagar Velho, Guia, Pego do Diabo, Oliveira	Antunes et al. 1989; Póvoas et al. 1992; Moreno-García & Pimenta 2002; Valente 2004; Valente & Haws 2006; López-García et al. 2020; López-García et al. 2021; López-García et al. 2022
Microtus duodecimcostatus (de Selys-Longchamps, 1839)	Figueira Brava, Caldeirão, Lapa do Picareiro, Goldra	Antunes et al. 1986c; Póvoas et al. 1992; Jeannet 2000; Moreno-García & Pimenta 2002; Bicho et al. 2003; Valente & Haws 2006; López-García et al. 2020; López-García et al. 2024
Microtus arvalis (Pallas, 1778)	Figueira Brava, Caldeirão, Lagar Velho	Póvoas et al. 1992; Jeannet 2000; Moreno-García & Pimenta 2002; López-García et al. 2020; López-García et al. 2021
Microtus agrestis (Linnaeus, 1761)	Caldeirão, Lapa do Picareiro, Lagar Velho, Oliveira	Póvoas et al. 1992; Moreno-García & Pimenta 2002; Bicho et al. 2003; López-García et al. 2020; López-García et al. 2021; López-García et al. 2022
Iberomys huescarensis Ruiz-Bustos, 1988	Santa Margarida	Estraviz-López et al. 2024
Iberomys brecciensis Forsyth Major, 1905	Aroeira, Figueira Brava, Goldra, Santa Margarida	Antunes et al. 1986c; Póvoas et al. 1992; Jeannet 2000; Marks et al. 2002; López-García et al. 2018; Estraviz-López et al. 2024
Iberomys cabrerae (Thomas, 1906)	Caldeirão, Oliveira, Lagar Velho	Póvoas et al. 1992; López-García et al. 2020; López-García et al. 2021; López-García et al. 2022
Hystrix cristata Linnaeus, 1758	Figueira Brava	Zilhão et al. 2020 Cardoso et al. 2021
Castor fiber Linnaeus, 1758	Oliveira, Caldeirão, Aroeira	Antunes 1989; Zilhão et al. 2010a; Cuenca-Bescós et al. 2021
Prolagus calpensis Major, 1905	Morgadinho	Antunes et al. 1986b
Lepus granatensis Rosenhauer, 1856	Caldeirão, Pego do Diabo, Lapa do Suão, Figueira Brava, Lapa do Picareiro, Lapa dos Coelhos	Davis 2002; Valente 2004; Gameiro et al. 2017; Zilhão et al. 2020; Haws et al. 2021

Oryctolagus cuniculus (Linnaeus, 1758)	Aroeira, Fariseu, Buraca Escura, Buraca Grande, Foz do Enxarrique, Pego do Diabo, Lapa do Suão, Lapa do Picareiro, Caldeirão, Vale Boi, Lagar Velho, Furninha, Algar de João Ramos, Fontainhas, Figueira Brava, Ibn Amar, Goldra, Escoural**,** Santa Margarida, Lapa dos Coelhos	Harlé 1910/11; Antunes et al. 1986c; Aubry et al. 1992; Gautier 1996; Brugal & Raposo 1999; Antunes 2000; Hockett & Bicho 2000; Aubry et al. 2001; Davis 2002; Marks et al. 2002; Moreno-García & Pimenta 2002; Bicho 2004; Valente & Haws 2006; Brugal et al. 2012; Manne et al. 2012; Gameiro et al. 2017; Haws et al. 2021; Estraviz-López et al. 2024
Macaca sylvanus (Linnaeus, 1758)	Aroeira	Marks et al. 2002; Alba et al. 2019
Paleoloxodon antiquus (Falconer & Cautley, 1847)	Mealhada, Condeixa, Foz do Enxarrique, Praia dos bifaces (Almonda), Furninha, Meirinha, Algés, Carregado, Santa Cruz, Santo Antão do Tojal, Figueira Brava	Antunes & Cardoso 1992; Figueiredo 2012 Estraviz-López & Mateus 2018c; Zilhão et al. 2020
Mammuthus primigenius Blumebach, 1799	Algar de João Ramos, Oeiras sea floor	Antunes & Cardoso 1992; Cardoso & Regala 2002; Zilhão et al. 2020
Stephanorhinus hemitoechus (Falconer, 1859)	Lorga de Dine, Aroeira, Oliveira, Furninha, Gruta Nova da Columbeira, Lapa da Rainha, Salemas, Escoural, Figueira Brava, Serra de Molianos, Correio-Mor	Veiga Ferreira 1975; Cardoso 1993; Marks et al. 2002; Zilhão et al. 2010a
Equus hydruntinus Regalia, 1905	Pedreira das Salemas, Caldeirão, Vale Boi	Cardoso 1995b; Davis 2002; Manne et al. 2012
Equus ferus (Linnaeus, 1758)	Lorga de Dine, Mealhada, Buraca Grande, Buraca Escura, Lagar Velho, Caldeirão, Foz do Enxarrique, Aroeira, Oliveira, Algar de João Ramos, Furninha, Casa da Moura, Gruta Nova da Columbeira, Lapa do Suão, Fontainhas, Salemas, Pego do Diabo, Algar de Cascais, Escoural, Figueira Brava, Vale Boi, Ibn Amar, Serra de Molianos, Casais Robustos, São Antão do Tojal, Lapa do Picareiro	Aubry et al. 1992; Cardoso 1993; Aubry et al. 2001; Davis 2002; Zilhão et al. 2010a; Manne et al. 2012; Estraviz-López & Mateus 2018c; Zilhão et al. 2020; Haws et al. 2021
Hippopotamus amphibious Linnaeus, 1758	Mealhada	Choffat 1895; Antunes et al. 1988; Martino et al. 2022
Hippopotamus antiquus Desmaret, 1822	Algoz, Condeixa	Antunes et al. 1986a; Martino et al. 2022
Sus scrofa Linnaeus, 1758	Fariseu, Fontainhas, Pedreira das Salemas, Gruta das Salemas, Escoural, Lapa do Picareiro, Furninha, Figueira Brava, Caldeirão, Vale Boi, Goldra, Lagar Velho, Pego do Diabo, Buraca Grande, Oliveira, Lapa dos Coelhos	Antunes et al. 1986c; Aubry et al. 1992; Cardoso 1993; Antunes 2000; Davis 2002; Moreno-García & Pimenta 2002; Gabriel & Béarez 2009; Hockett & Haws 2009; Zilhão et al. 2010b; Brugal et al. 2012; Manne et al. 2012; Gameiro et al. 2017; Haws et al. 2021; Angelucci et al. 2023

Cervus elaphus Linnaeus, 1758	Lorga de Dine, Fariseu, Mealhada, Buraca grande, Buraca escura, Lagar Velho, Caldeirão, Foz do Enxarrique, Lapa do Picareiro, Aroeira, Oliveira, Algar de João Ramos, Furninha, Casa da Moura, Gruta Nova da Columbeira, Lapa do Suão, Fontainhas, Lapa da Rainha, Salemas, Pego do Diabo, Porto Covo, Algar de Cascais, Escoural, Figueira Brava, Ibn Amar, Goldra, Vale Boi, Casais Robustos, Lapa dos Coelhos, Serra de Molianos	Harlé 1910/1911; Antunes et al. 1989; Aubry et al. 1992; Cardoso 1993; Aubry et al. 2001; Marks et al. 2002; Moreno-García & Pimenta 2002; Bicho 2004; Bicho et al. 2006; Haws & Valente 2006; Gabriel & Béarez 2009; Zilhão et al. 2010a; Manne et al. 2012; Estraviz-López & Mateus 2018b; Gameiro et al. 2017; Haws et al. 2021
Capreolus capreolus Linnaeus, 1758	Lagar Velho, Caldeirão, Gruta Nova da Columbeira, Lapa da Rainha, Pedreira das Salemas, Lapa do Picareiro, Porto Covo, Escoural, Lapa dos Coelhos	Cardoso 1993; Gautier 1996; Moreno-García & Pimenta 2002; Hockett & Haws 2009; Gameiro et al. 2017; Haws et al. 2021
Dama dama Linnaeus, 1758	Algar de João Ramos, Fontainhas, Gruta Nova da Columbeira, Pedreira das Salemas	Cardoso 1993
*Dama vallonnetensis*De Lumley *et al.*, 1988	Aroeira	Marks et al. 2002
Haploidoceros mediterraneus (Bonifay, 1967)	Aroeira	Croitor et al. 2019
Praedama savini (Dawkins, 1887)	Aroeira	Croitor et al. 2019
Metacervocerus rhenanus (Dubois, 1904)	Algoz	Antunes et al. 1986a; Estraviz-López et al. 2024
Eucladoceros sp. Falconer, 1868	Algoz	Antunes et al. 1986a; Estraviz-López et al. 2024
Bos primigenius Bojanus, 1827	Lorga de Dine, Gruta Nova da Columbeira, Pedreira das Salemas, Algar de Cascais, Figueira Brava, Escoural, Lapa da Rainha, Foz do Enxarrique, Furninha, Lapa do Picareiro, Vale Boi, Guia, Lagar Velho, Buraca Escura, Pampilhosa do Botão	Antunes et al. 1989; Cardoso 1993; Aubry et al. 2002; Moreno-García & Pimenta 2002; Manne et al. 2012; Arceredillo et al. 2018

Capra pyrenaica Schinz, 1838	Buraca grande, Buraca escura, Caldeirão, Lapa do Picareiro, Aroeira, Oliveira, Algar de João Ramos, Gruta Nova da Columbeira, Fontainhas, Pedreira das Salemas, Pego de Diabo, Figueira Brava, Vale Boi, Escoural, Casais Robustos, Lapa dos Coelhos	Aubry et al. 1992; Cardoso 1993; Otte & Silva 1996; Antunes 2000; Aubry et al. 2001; Marks et al. 2002; Zilhão et al. 2002; Hockett & Haws 2009; Manne et al. 2012; Estraviz-López & Mateus 2018b; Gameiro et al. 2017; Haws et al. 2021
Rupicapra pyrenaica Bonaparte, 1845	Fariseu, Gruta das Salemas, Caldeirão, Pego do Diabo, Lapa do Picareiro	Cardoso 1993; Gabriel & Béarez 2009; Hockett & Haws 2009; Haws et al. 2021
Canis lupus Linnaeus, 1758	Fontainhas, Casa da Moura, Algar de João Ramos, Lapa da Rainha, Pego do Diabo, Gruta Nova da Columbeira, Salemas, Caldeirão, Escoural, Lagar Velho, Vale Boi, Furninha, Buraca Escura, Aroeira, Oliveira, Lapa do Picareiro, Lapa dos Coelhos	Cardoso 1993; Aubry et al. 2002; Marks et al. 2002; Moreno-García & Pimenta 2002; Zilhão et al. 2010a; Brugal et al. 2012; Manne et al. 2012; Gameiro et al. 2024; Haws et al. 2024
Cuon priscus Thenius, 1954	Aroeira	Trinkaus et al. 2003
Cuon alpinus Pallas, 1811	Escoural	Cardoso 1992
Vulpes vulpes (Linnaeus, 1758)	Buraca Escura, Oliveira, Furninha, Casa da Moura, Pedreira das Salemas, Gruta das Salemas, Pego do Diabo, Figueira Brava, Caldeirão, Escoural, Vale Boi, Lagar Velho, Foz do Enxarrique, Lapa do Picareiro, Lapa dos Coelhos	Cardoso 1993; Brugal & Raposo 1999; Aubry et al. 2001; Moreno-García & Pimenta 2002; Zilhão et al. 2010a; Manne et al. 2012; Gameiro et al. 2017; Haws et al. 2021
Ursus deningeri Von Reichenau, 1904	Aroeira	Sanz et al. 2024
Ursus arctos Linnaeus, 1758	Lorga de Dine, Furninha, Gruta Nova da Columbeira, Fontainhas, Pedreira das Salemas, Gruta das Salemas, Algar de Cascais, Escoural, Figueira Brava, Aroeira, Oliveira, Pego do Diabo, Caldeirão, Serra de Molianos, Algar do Vale da Pena, Gruta São Bartolomeu, Lapa do Picareiro, Lapa dos Coelhos	Furtado et al. 1974; Cardoso 1993; Marks et al. 2002; Davis 2002; Zilhão et al. 2010a; Zilhão et al. 2010b; Estraviz-López & Mateus 2019a; Gameiro et al. 2017; Haws et al. 2021; Angelucci et al. 2024
Mustela sp. Linnaeus, 1758	Vale Boi, Furninha	Brugal et al. 2012; Manne et al. 2012
Martes foina (Erxeleben, 1777)	Lapa dos Coelhos	Gameiro et al. 2024
Martes sp. Pinel, 1792	Vale Boi, Furninha, Figueira Brava	Brugal et al. 2012; Manne et al. 2012; Zilhão et al. 2020
Meles meles Linnaeus, 1758	Furninha, Caldeirão, Lapa do Suão, Escoural	Gautier 1996; Davis 2002; Haws & Valente 2006; Brugal et al. 2012
"Hyaena" prisca de Serres, 1828	Furninha	Brugal et al. 2012
Crocuta crocuta (Erxleben, 1777)	Lorga de Dine, Caldeirão, Gruta Nova da Columbeira, Fontainhas, Lapa da Rainha, Gruta das Salemas, Algar de Cascais, Porto Covo, Figueira Brava, Escoural, Buraca Grande, Oliveira, Foz do Enxarrique, Lapa dos Coelhos	Aubry et al. 1992; Cardoso 1996; Brugal & Raposo 1999; Valente 2004; Zilhão et al. 2010a; Gameiro et al. 2017
Felis silvestris Schreber, 1777	Escoural, Figueira Brava, Pego do Diabo, Gruta das Salemas, Pedreira das Salemas, Fontainhas, Furninha, Caldeirão, Lapa da Rainha, Gruta Nova da Columbeira, Vale Boi, Buraca Escura, Oliveira, Algar da Manga Larga, Lapa do Picareiro, Lapa dos Coelhos	Aubry et al. 2001; Cardoso & Regala 2006; Zilhão et al. 2010a; Manne et al. 2012; Villaluenga 2016; Gameiro et al. 2017; Haws et al. 2021; Angelucci et al. 2024

Lynx sp. Kerr, 1792	Escoural, Pego do Diabo, Pedreira das Salemas, Gruta das Salemas, Furninha, Caldeirão, Lapa da Rainha, Gruta Nova da Columbeira, Casa da Moura, Algar de João Ramos, Algar de Cascais, Oliveira, Buraca Escura, Vale Boi, Lapa do Picareiro, Casais Robustos, Figueira Brava, Aroeira	Aubry et al. 2001; Hockett & Haws; 2009; Zilhão et al. 2010; Manne et al. 2012; Villaluenga 2016; Estraviz-López & Mateus 2018b; Zilhão et al. 2020; Haws et al. 2021; Angelucci et al. 2024
Panthera pardus Linnaeus, 1758	Escoural, Pego do Diabo, Pedreira das Salemas, Figueira Brava, Fontainhas, Furninha, Casa da Moura, Oliveira, Caldeirão, Lorga de Dine	Villaluenga 2016
Panthera spelaea Goldfuss, 1810	Escoural, Figueira Brava, Pedreira das Salemas, Lorga de Dine, Vale Boi, Oliveira	Manne et al. 2012; Villaluenga 2016; Angelucci et al. 2023
Panthera uncia Goldfuss, 1811	Algar da Manga Larga	Jiangzuo et al. 2025
Homotherium latidens Owen, 1846	Mealhada	Antunes 1986

E.2 Output from Palaeobiology database

identified_name	accepted_name	ref_author	ref_pubyr	collection_name	class
Pinguinus impennis	*Pinguinus impennis*	Mourer-Chauvire and Antunes	1991	Figueira Brava	Aves
Tadorna tadorna	*Tadorna tadorna*	Figueiredo et al.	2017	Gruta da Furninha	Aves
Tadorna ferruginea	*Tadorna ferruginea*	Figueiredo et al.	2017	Gruta da Furninha	Aves
Somateria mollissima	*Somateria mollissima*	Figueiredo et al.	2017	Gruta da Furninha	Aves
Somateria sp.	*Somateria*	Figueiredo et al.	2017	Gruta da Furninha	Aves
Cygnus olor	*Cygnus olor*	Figueiredo et al.	2017	Gruta da Furninha	Aves
Anas crecca	*Anas crecca*	Figueiredo et al.	2017	Gruta da Furninha	Aves
Melanitta nigra	*Melanitta nigra*	Figueiredo et al.	2017	Gruta da Furninha	Aves
Columba livia	*Columba livia*	Figueiredo et al.	2017	Gruta da Furninha	Aves
Numenius phaeopus	*Numenius phaeopus*	Figueiredo et al.	2017	Gruta da Furninha	Aves
Pinguinus impennis	*Pinguinus impennis*	Figueiredo et al.	2017	Gruta da Furninha	Aves
Gallinago sp.	*Gallinago*	Figueiredo et al.	2017	Gruta da Furninha	Aves
Larus sp.	*Larus*	Figueiredo et al.	2017	Gruta da Furninha	Aves
Puffinus puffinus	*Puffinus puffinus*	Figueiredo et al.	2017	Gruta da Furninha	Aves
Phoenicopterus roseus	*Phoenicopterus roseus*	Torres et al.	2014	Gruta da Furninha	Aves
Phalacrocorax aristotelis	*Phalacrocorax aristotelis*	Figueiredo et al.	2017	Gruta da Furninha	Aves
Tyto alba	*Tyto alba*	Figueiredo et al.	2017	Gruta da Furninha	Aves
Bubo bubo	*Bubo bubo*	Figueiredo et al.	2017	Gruta da Furninha	Aves
Asio flammeus	*Asio flammeus*	Figueiredo et al.	2017	Gruta da Furninha	Aves
Falco tinnunculus	*Falco tinnunculus*	Figueiredo et al.	2017	Gruta da Furninha	Aves
Aquila chrysaetos	*Aquila chrysaetos*	Figueiredo et al.	2017	Gruta da Furninha	Aves
Aquila sp.	*Aquila*	Figueiredo et al.	2017	Gruta da Furninha	Aves
Gyps fulvus	*Gyps fulvus*	Figueiredo et al.	2017	Gruta da Furninha	Aves
Pyrrhocorax pyrrhocorax	*Pyrrhocorax pyrrhocorax*	Figueiredo et al.	2017	Gruta da Furninha	Aves

Pyrrhocorax graculus	*Pyrrhocorax graculus*	Figueiredo et al.	2017	Gruta da Furninha	Aves
Corvus corone	*Corvus corone*	Figueiredo et al.	2017	Gruta da Furninha	Aves
Corvus frugilegus	*Corvus frugilegus*	Figueiredo et al.	2017	Gruta da Furninha	Aves
Corvus monedula	*Corvus monedula*	Figueiredo et al.	2017	Gruta da Furninha	Aves
Turdus merula	*Turdus merula*	Figueiredo et al.	2017	Gruta da Furninha	Aves
Turdus philomelos	*Turdus philomelos*	Figueiredo et al.	2017	Gruta da Furninha	Aves
Turdus pilaris	*Turdus pilaris*	Figueiredo et al.	2017	Gruta da Furninha	Aves
Turdus iliacus	*Turdus iliacus*	Figueiredo et al.	2017	Gruta da Furninha	Aves
Turdus sp.	*Turdus*	Figueiredo et al.	2017	Gruta da Furninha	Aves
Pica pica	*Pica pica*	Figueiredo et al.	2017	Gruta da Furninha	Aves
Cuculus canorus	*Cuculus canorus*	Figueiredo et al.	2017	Gruta da Furninha	Aves
Calonectris diomedea	*Calonectris diomedea*	Tyrberg	1999	Grotte de Fuminha	Aves
Phalacrocorax aristotelis	*Phalacrocorax aristotelis*	Tyrberg	1999	Grotte de Fuminha	Aves
Alectoris rufa	*Alectoris rufa*	Figueiredo et al.	2017	Gruta da Furninha	Aves
Coturnix coturnix	*Coturnix coturnix*	Figueiredo et al.	2017	Gruta da Furninha	Aves
Palaeoloxodon antiquus	*Palaeoloxodon antiquus*	Antunes and Cardoso	1992	Condeixa-a-Velha	Mammalia
Elephas antiquus	*Palaeoloxodon antiquus*	Antunes and Cardoso	1992	Conimbriga	Mammalia
Elephas antiquus	*Palaeoloxodon antiquus*	Antunes and Cardoso	1992	Foz do Enxarrique	Mammalia
Elephas antiquus	*Palaeoloxodon antiquus*	Antunes and Cardoso	1992	Casal do Torquato	Mammalia
Elephas antiquus	*Palaeoloxodon antiquus*	Antunes and Cardoso	1992	auto-estrada do Norte, Carregado	Mammalia
Elephas antiquus	*Palaeoloxodon antiquus*	Antunes and Cardoso	1992	Santa Cruz	Mammalia
Hippopotamus antiquus	*Hippopotamus antiquus*	Antunes et al.	1986	Algoz	Mammalia
Cervus sp.	*Cervus*	Antunes et al.	1986	Algoz	Mammalia
Eucladoceros cf. dicranios	*Eucladoceros dicranios*	Antunes et al.	1986	Algoz	Mammalia
Oryctolagus lacosti	*Oryctolagus*	Antunes et al.	1986	Algoz	Mammalia
Equus sp.	*Equus*	Antunes et al.	1986	Goldra	Mammalia
Cervus elephas	*Cervus*	Antunes et al.	1986	Goldra	Mammalia
Sus cf. scrofa	*Sus scrofa*	Antunes et al.	1986	Goldra	Mammalia
Sorex araneus	*Sorex araneus*	Antunes et al.	1986	Goldra	Mammalia
Crocidura russula	*Crocidura russula*	Antunes et al.	1986	Goldra	Mammalia
Talpa europaea	*Talpa europaea*	Antunes et al.	1986	Goldra	Mammalia
Oryctolagus cuniculus	*Oryctolagus cuniculus*	Antunes et al.	1986	Goldra	Mammalia
Apodemus sylvaticus	*Mus sylvaticus*	Antunes et al.	1986	Goldra	Mammalia
Microtus brecciensis	*Microtus brecciensis*	Antunes et al.	1986	Goldra	Mammalia
Pitymys duodecimcostatus	*Microtus*	Antunes et al.	1986	Goldra	Mammalia
Eliomys quercinus	*Eliomys quercinus*	Antunes et al.	1986	Goldra	Mammalia
Galemys kormosi	*Galemys kormosi*	Antunes et al.	1986	Morgadinho	Mammalia
Prolagus cf. calpensis	*Prolagus*	Antunes et al.	1986	Morgadinho	Mammalia
Mimomys sp.	*Mimomys*	Antunes et al.	1986	Morgadinho	Mammalia
Homotherium latidens	*Homotherium latidens*	Serangeli et al.	2015	Mealhada	Mammalia
Ursus arctos	*Ursus arctos*	Figueiredo et al.	2022	Gruta da Furninha	Mammalia
Panthera pardus	*Panthera pardus*	Figueiredo et al.	2022	Gruta da Furninha	Mammalia
Felis silvestris	*Felis silvestris*	Figueiredo et al.	2022	Gruta da Furninha	Mammalia
Lynx pardina	*Lynx pardinus*	Figueiredo et al.	2022	Gruta da Furninha	Mammalia

Canis lupus	*Canis lupus*	Figueiredo et al.	2022	Gruta da Furninha	Mammalia
Vulpes vulpes	*Vulpes vulpes*	Figueiredo et al.	2022	Gruta da Furninha	Mammalia
Meles meles	*Meles meles*	Figueiredo et al.	2022	Gruta da Furninha	Mammalia
Martes sp.	*Martes*	Figueiredo et al.	2022	Gruta da Furninha	Mammalia
Cervus elaphus	*Cervus elaphus*	Figueiredo et al.	2022	Gruta da Furninha	Mammalia
Dama ? sp.	*Dama*	Figueiredo et al.	2022	Gruta da Furninha	Mammalia
Sus scrofa	*Sus scrofa*	Figueiredo et al.	2022	Gruta da Furninha	Mammalia
Bos primigenius	*Bos primigenius*	Figueiredo et al.	2022	Gruta da Furninha	Mammalia
Dicerorhinus hemitoechus	*Stephanorhinus hemitoechus*	Figueiredo et al.	2022	Gruta da Furninha	Mammalia
Equus caballus	*Equus caballus*	Figueiredo et al.	2022	Gruta da Furninha	Mammalia
Palaeoloxodon sp.	*Elephas*	Figueiredo et al.	2022	Gruta da Furninha	Mammalia
Erinaceus europaeus	*Erinaceus europaeus*	Figueiredo et al.	2022	Gruta da Furninha	Mammalia
Oryctolagus sp.	*Oryctolagus*	Figueiredo et al.	2022	Gruta da Furninha	Mammalia
Arvicola sp.	*Arvicola*	Figueiredo et al.	2022	Gruta da Furninha	Mammalia
Rhinolophus ferrumequinum	*Rhinolophus ferrumequinum*	Figueiredo et al.	2022	Gruta da Furninha	Mammalia
Delphinus sp.	*Delphinus*	Figueiredo et al.	2022	Gruta da Furninha	Mammalia
Crocuta crocuta	*Crocuta crocuta*	Boneta Jiménez et al.	2023	Gruta Nova da Columbeira	Mammalia
Felis sylvestris	*Felis*	Boneta Jiménez et al.	2023	Gruta Nova da Columbeira	Mammalia
Lynx pardina	*Lynx pardinus*	Boneta Jiménez et al.	2023	Gruta Nova da Columbeira	Mammalia
Canis lupus	*Canis lupus*	Boneta Jiménez et al.	2023	Gruta Nova da Columbeira	Mammalia
Ursus arctos	*Ursus arctos*	Boneta Jiménez et al.	2023	Gruta Nova da Columbeira	Mammalia
Dicerorhinus hemitoechus	*Stephanorhinus hemitoechus*	Boneta Jiménez et al.	2023	Gruta Nova da Columbeira	Mammalia
Equus caballus	*Equus caballus*	Boneta Jiménez et al.	2023	Gruta Nova da Columbeira	Mammalia
Cervus elaphus	*Cervus elaphus*	Boneta Jiménez et al.	2023	Gruta Nova da Columbeira	Mammalia
Capreolus capreolus	*Capreolus capreolus*	Boneta Jiménez et al.	2023	Gruta Nova da Columbeira	Mammalia
Capra pyrenaica	*Capra pyrenaica*	Boneta Jiménez et al.	2023	Gruta Nova da Columbeira	Mammalia
Bos primigenius	*Bos primigenius*	Boneta Jiménez et al.	2023	Gruta Nova da Columbeira	Mammalia
Homo neanderthalensis	*Homo neanderthalensis*	Boneta Jiménez et al.	2023	Gruta Nova da Columbeira	Mammalia
Cuon europaeus	*Cuon alpinus europaeus*	Cardoso	1992	Escoural Cave	Mammalia
Chersine hermanni	*Testudo hermanni*	Boneta Jiménez et al.	2023	Gruta Nova da Columbeira	Reptilia
Emys orbicularis	*Emys orbicularis*	Boneta Jiménez et al.	2023	Gruta Nova da Columbeira	Reptilia

E.3 Matrix used for statistical analyses

All further statistical analyses are based on the following data matrix, edited to exclude Epivillafranchian taxa, or karstic localities or species known only as fossils, following the classification provided at the main list.

	Lorga de Dine	Fariseu	Mealhada	Condeixa	Buraca Grande	Buraca Escura	Lagar Velho	Caldeirão	Foz do Enxarrique	Lapa do Picareiro	Aroeira	Oliveira	Lapa dos Coelhos	Algar da Manga	Casais Robustos	Algar de João Ramos	Serra de Molianos	Furninha	Casa da Moura	Gruta Nova da	Lapa do Suão	Fontainhas	Lapa da Rainha	Pedreira e Gruta das	Pego do Diabo	Porto Covo	Algar de Cascais	Escoural	Figueira Brava	Gruta de Ibn Amar	Santa Margarida	Algoz	Goldra	Guia	Morgadinho	Vale Boi		Total localities per species
Salamandra salamandra (Linnaeus, 1758)	0	0	0	0	0	0	1	0	0	0	0	0	0	0	0	0	0	0	0	0	0	0	0	0	0	0	0	0	1	0	0	0	0	0	0	0	2
Triturus marmoratus (Latreille, 1800)	0	0	0	0	0	0	1	0	0	0	0	0	0	0	0	0	0	0	0	0	0	0	0	0	0	0	0	0	0	0	0	0	0	0	0	0	1
Pelodytes sp. Daudin, 1802	0	0	0	0	0	0	0	0	0	0	1	0	0	0	0	0	0	0	0	0	0	0	0	0	0	0	0	0	0	0	0	0	0	0	0	0	1
Bufo spinosus (Daudin, 1803)	0	0	0	0	0	0	0	0	0	1	1	0	0	0	0	0	0	0	0	0	0	0	0	0	0	0	0	1	0	0	0	0	0	1	0	0	4
Pelobates cultripes Cuvier, 1829	0	0	0	0	0	0	0	0	0	1	0	0	0	0	0	0	0	0	0	0	0	0	0	0	0	0	0	1	1	0	0	0	0	1	0	0	4
Pleurodeles waltl (Michahelles, 1830)	0	0	0	0	0	0	0	0	0	0	0	0	0	0	0	0	0	0	0	0	0	0	0	0	0	0	0	0	0	0	0	0	0	1	0	0	1
Epidalea calamita (Laurenti, 1768)	0	0	0	0	0	0	0	0	0	0	0	0	0	0	0	0	0	0	0	0	0	0	0	0	0	0	0	0	0	0	0	0	0	1	0	0	1
Pelophylax perezi (Seoane, 1885)	0	0	0	0	0	0	0	0	0	1	0	0	0	0	0	0	0	0	0	0	0	0	0	0	0	0	0	0	0	0	0	0	0	1	0	0	2
Rana iberica Boulenger, 1979	0	0	0	0	0	0	0	0	0	1	0	0	0	0	0	0	0	0	0	0	0	0	0	0	0	0	0	0	0	0	0	0	0	0	0	0	1
Timon lepidus (Daudin, 1802)	0	0	0	0	0	0	0	0	0	0	0	0	0	0	0	0	0	0	0	0	0	0	0	0	0	0	0	1	1	0	0	0	0	1	0	0	3
Psammodromus manuelae Busack et al., 2006	0	0	0	0	0	0	0	0	0	0	0	0	0	0	0	0	0	0	0	0	0	0	0	0	0	0	0	0	1	0	0	0	0	0	0	0	1
Podarcissp. Wagler, 1830	0	0	0	0	0	0	0	0	0	0	0	0	0	0	0	0	0	0	0	0	0	0	0	0	0	0	0	0	1	0	0	0	0	0	0	0	1
Acanthodactylus erythrurus (Schinz, 1833)	0	0	0	0	0	0	0	0	0	0	0	0	0	0	0	0	0	0	0	0	0	0	0	0	0	0	0	0	0	0	0	0	0	1	0	0	1
Rhinechis scalaris (Schinz, 1822)	0	0	0	0	0	0	0	0	0	0	0	0	0	0	0	0	0	0	0	0	0	0	0	0	0	0	0	0	1	0	0	0	0	0	0	0	1
Hemorrhois hippocrepis (Linnaeus, 1758)	0	0	0	0	0	0	0	0	0	0	0	0	0	0	0	0	0	0	0	0	0	0	0	0	0	0	0	0	1	0	0	0	0	0	0	0	1
Coronella girondica Daudin, 1803	0	0	0	0	0	0	0	0	0	0	1	0	0	0	0	0	0	0	0	0	0	0	0	0	0	0	0	0	1	0	0	0	0	0	0	0	2
Vipera lastei Bosca, 1878	0	0	0	0	0	0	0	0	0	0	0	0	0	0	0	0	0	0	0	0	0	0	0	0	0	0	0	0	1	0	0	0	0	0	0	0	1
Natrix maura (Linnaeus, 1758)	0	0	0	0	0	0	0	0	0	0	1	0	0	0	0	0	0	0	0	0	0	0	0	0	0	0	0	0	0	0	0	0	0	0	0	0	1
Blanus cinereus (Vandelli, 1797)	0	0	0	0	0	0	0	0	0	0	0	0	0	0	0	0	0	0	0	0	0	0	0	0	0	0	0	0	1	0	0	0	0	0	0	0	1
Testudo hermanni Gmelin, 1789	0	0	0	0	0	0	0	0	0	0	1	1	0	0	0	0	0	1	0	1	0	0	0	0	0	0	0	1	1	1	0	0	0	0	0	0	7
Mauremys leprosa (Schweiger, 1812)	0	0	1	0	0	0	0	1	0	0	0	0	0	0	0	0	0	0	0	1	0	0	0	0	0	0	0	1	0	0	0	0	0	0	0	0	4
Emys orbicularis (Linnaeus, 1758)	0	0	1	0	0	0	0	0	0	0	0	0	0	0	0	0	0	0	0	1	0	0	0	0	0	0	0	1	0	0	0	0	0	0	0	0	3
Tetrao urogallus Linnaeus, 1758	0	0	0	0	0	0	0	0	0	0	0	0	0	0	0	0	0	0	0	0	0	0	1	0	0	0	0	0	0	0	0	0	0	0	0	0	1
Alectoris rufa (Linnaeus, 1758)	0	0	0	0	0	0	0	0	0	1	0	0	0	0	0	0	0	1	0	1	1	0	0	0	0	0	0	1	1	0	0	0	0	0	0	0	6
Perdix perdix (Linnaeus, 1758)	0	0	0	0	0	0	0	1	0	1	0	0	0	0	0	0	0	1	0	1	0	0	0	0	0	0	0	0	0	0	0	0	0	0	0	0	4
Coturnix coturnix (Linnaeus, 1758)	0	0	0	0	0	0	0	0	0	0	0	0	0	0	0	0	0	1	0	1	0	0	0	0	0	0	0	0	0	0	0	0	0	0	0	0	2

Phasianus colchicus Linnaeus, 1758	0	0	0	0	0	0	0	0	0	0	0	0	0	0	0	0	0	0	0	0	0	0	0	0	1	0	0	0	0	0	0	0	0	0	0		1
Lagopus lagopus (Linnaeus, 1758)	0	0	0	0	0	0	0	0	0	0	0	0	0	0	0	0	0	0	0	0	0	0	1	0	0	0	0	0	0	0	0	0	0	0	0		1
Lagopus muta (Montin, 1781)	0	0	0	0	0	0	0	0	0	0	0	0	0	0	0	0	0	0	0	1	0	0	0	0	0	0	0	0	0	0	0	0	0	0	0		1
Anas platyrhynchos Linnaeus, 1758	0	0	0	0	0	0	0	0	0	0	0	0	0	0	0	0	0	0	0	1	1	0	0	0	0	0	0	1	1	0	0	0	0	0	0		4
Anas crecca Linnaeus, 1758	0	0	0	0	0	0	0	0	0	0	0	0	0	0	0	0	0	1	0	0	0	0	0	0	0	0	0	0	0	0	0	0	0	0	0		1
Melanitta nigra (Linnaeus, 1758)	0	0	0	0	0	0	0	0	0	0	0	0	0	0	0	0	0	1	0	1	0	0	0	0	0	0	0	0	1	0	0	0	0	0	0		3
Melanitta fusca (Linnaeus, 1758)	0	0	0	0	0	0	0	0	0	0	0	0	0	0	0	0	0	0	0	0	0	0	0	0	0	0	0	0	1	0	0	0	0	0	0		1
Aythya sp. Boie, 1822	0	0	0	0	0	0	0	0	0	0	1	0	0	0	0	0	0	0	0	0	0	0	0	0	0	0	0	0	0	0	0	0	0	0	0		1
Clangula hyemalis (Linnaeus, 1758)	0	0	0	0	0	0	0	0	0	0	0	0	0	0	0	0	0	0	0	0	0	0	0	0	0	0	0	1	0	0	0	0	0	0	0		1
Tadorna tadorna (Linnaeus, 1758)	0	0	0	0	0	0	0	0	0	0	0	0	0	0	0	0	0	1	0	0	0	0	0	0	0	0	0	0	0	0	0	0	0	0	0		1
Tadorna ferruginea (Pallas, 1761)	0	0	0	0	0	0	0	0	0	0	0	0	0	0	0	0	0	1	0	0	0	0	0	0	0	0	0	0	0	0	0	0	0	0	0		1
Somateria mollisima (Linnaeus, 1758)	0	0	0	0	0	0	0	0	0	0	0	0	0	0	0	0	0	1	0	0	0	0	0	0	0	0	0	0	0	0	0	0	0	0	0		1
Mergus merganser (Linnaeus, 1758)	0	0	0	0	0	0	0	0	0	0	0	0	0	0	0	0	0	0	0	0	0	0	0	0	0	0	0	1	0	0	0	0	0	0	0		1
Mergellus albellus (Linnaeus, 1758)	0	0	0	0	0	0	0	0	0	0	1	0	0	0	0	0	0	0	0	0	0	0	0	0	0	0	0	0	0	0	0	0	0	0	0		1
Anser albifrons (Scopoli, 1769)	0	0	0	0	0	0	0	0	0	0	0	0	0	0	0	0	0	0	0	0	0	0	0	0	1	0	0	0	0	0	0	0	0	0	0		1
Cygnus olor (Gmelin, 1789)	0	0	0	0	0	0	0	0	0	0	1	0	0	0	0	0	0	1	0	0	0	0	0	0	0	0	0	0	0	0	0	0	0	0	0		2
Scolopax rusticola Linnaeus, 1758	0	0	0	0	0	0	0	0	0	1	1	0	0	0	0	0	0	0	0	0	0	0	0	0	0	0	0	1	0	0	0	0	0	0	0		3
Gallinago sp.	0	0	0	0	0	0	0	0	0	0	0	0	0	0	0	0	0	1	0	0	0	0	0	0	0	0	0	0	0	0	0	0	0	0	0		1
Numenius phaeopus (Linnaeus, 1758)	0	0	0	0	0	0	0	0	0	0	0	0	0	0	0	0	0	1	0	0	0	0	0	0	0	0	0	1	0	0	0	0	0	0	0		2
Tringa totanus (Linnaeus, 1758)	0	0	0	0	0	0	0	0	0	1	0	0	0	0	0	0	0	0	0	0	0	0	0	0	0	0	0	0	0	0	0	0	0	0	0		1
Calidris canutus (Linnaeus, 1758)	0	0	0	0	0	0	0	0	0	1	0	0	0	0	0	0	0	0	0	0	0	0	0	0	0	0	0	1	0	0	0	0	0	0	0		2
Calidris pugnax (Linnaeus, 1758)	0	0	0	0	0	0	0	0	0	1	0	0	0	0	0	0	0	0	0	0	0	0	0	0	0	0	0	0	0	0	0	0	0	0	0		1
Sterna hirundo Linnaeus, 1758	0	0	0	0	0	0	0	0	0	0	0	0	0	0	0	0	0	0	0	0	0	0	0	0	0	0	0	1	0	0	0	0	0	0	0		1
Larus fuscus Linnaeus, 1759	0	0	0	0	0	0	0	0	0	0	0	0	0	0	0	0	0	0	0	0	0	0	0	0	0	0	0	1	0	0	0	0	0	0	0		1
Pinguinus impennis (Linnaeus, 1758)	0	0	0	0	0	0	0	0	0	0	0	0	0	0	0	0	0	1	0	0	0	0	0	0	0	0	0	1	0	0	0	0	0	0	0		2
Fratercula arctica (Linnaeus, 1758)	0	0	0	0	0	0	0	0	0	0	0	0	0	0	0	0	0	0	0	0	0	0	0	0	0	0	0	1	0	0	0	0	0	0	0		1
Alca torda Linnaeus, 1758	0	0	0	0	0	0	0	0	0	0	0	0	0	0	0	0	0	0	0	0	0	0	0	0	0	0	0	1	0	0	0	0	0	0	0		1
Vanellus vanellus (Linnaeus, 1758)	0	0	0	0	0	0	0	0	0	0	0	0	0	0	0	0	0	0	0	0	0	1	0	0	0	0	0	0	0	0	0	0	0	0	0		1
Pluvialis squatarola (Linnaeus, 1758)	0	0	0	0	0	0	0	0	0	0	0	0	0	0	0	0	0	0	0	1	0	0	0	0	0	0	0	0	0	0	0	0	0	0	0		1
Pluvialis apricaria (Linnaeus, 1758)	0	0	0	0	0	0	0	0	0	1	0	0	0	0	0	0	0	0	0	0	0	0	0	0	0	0	0	0	0	0	0	0	0	0	0		1

Podiceps nigricollis Brehm, 1831	0	0	0	0	0	0	0	0	0	0	0	0	0	0	0	0	0	0	0	0	0	0	0	0	0	0	0	0	1	0	0	0	0	0	0	0	1
Otis tarda Linnaeus, 1758	0	0	0	0	0	0	0	0	0	0	0	0	0	0	0	0	0	0	1	0	0	0	0	0	0	0	0	0	0	0	0	0	0	0	0	0	1
Grus grus (Linnaeus, 1758)	0	0	0	0	0	0	0	0	0	0	0	0	0	0	0	0	0	0	1	0	0	0	0	0	0	0	0	0	0	0	0	0	0	0	0	0	1
Grus primigenia (Milne-Edwards, 1869)	0	0	0	0	0	0	0	0	0	0	0	0	0	0	0	0	0	0	0	0	0	0	0	0	0	0	0	0	1	0	0	0	0	0	0	0	1
Puffinus puffinus (Brünnich, 1764)	0	0	0	0	0	0	0	0	0	0	0	0	0	0	0	0	0	1	0	0	0	0	0	0	0	0	0	0	1	0	0	0	0	0	0	0	2
Puffinus holeae Walker et al., 1990	0	0	0	0	0	0	0	0	0	0	0	0	0	0	0	0	0	0	0	0	0	0	0	0	0	0	0	0	1	0	0	0	0	0	0	0	1
Phalacrocorax aristotelis (Linnaeus, 1761)	0	0	0	0	0	0	0	0	0	0	0	0	0	0	0	0	0	1	0	0	0	0	0	0	0	0	0	0	1	0	0	0	0	0	0	0	2
Phalacrocorax carbo (Linnaeus, 1758)	0	0	0	0	0	0	0	0	0	0	0	0	0	0	0	0	0	0	0	0	0	0	0	0	0	0	0	0	1	0	0	0	0	0	0	0	1
Morus bassanus (Linnaeus, 1758)	0	0	0	0	0	0	0	0	0	0	0	0	0	0	0	0	0	0	0	0	0	0	0	0	0	0	0	0	1	0	0	0	0	0	0	0	1
Phoenicopterus roseus Pallas, 1811	0	0	0	0	0	0	0	0	0	0	0	0	0	0	0	0	0	1	0	0	0	0	0	0	0	0	0	0	0	0	0	0	0	0	0	0	1
Gavia stellata (Pontoppidan, 1763)	0	0	0	0	0	0	0	0	0	0	0	0	0	0	0	0	0	0	0	0	0	0	0	0	0	0	0	0	1	0	0	0	0	0	0	0	1
Accipiter nisus (Linnaeus, 1758)	0	0	0	0	0	0	0	0	0	0	0	0	0	0	0	0	0	0	0	0	0	0	0	0	0	0	0	0	1	0	0	0	0	0	0	0	1
Aquila chrysaetos (Linnaeus, 1758)	0	0	0	0	0	0	0	0	0	1	0	0	0	0	0	0	0	1	0	1	0	0	0	0	0	0	0	0	1	0	0	0	0	0	0	1	5
Aquila adalberti (Brehm, 1861)	0	0	0	0	0	0	0	0	0	1	0	0	0	0	0	0	0	0	0	0	0	0	0	1	0	0	0	0	0	0	0	0	0	0	0	0	2
Aquila fasciata (Viellot, 1822)	0	0	0	0	0	0	0	0	0	0	0	0	0	0	0	0	0	0	0	0	0	0	0	0	0	0	0	0	1	0	0	0	0	0	0	0	1
Milvus migrans (Boddaert, 1783)	0	0	0	0	0	0	0	0	0	0	0	0	0	0	0	0	0	0	0	0	0	0	0	0	0	0	0	0	1	0	0	0	0	0	0	0	1
Buteo buteo (Linnaeus, 1758)	0	0	0	0	0	0	0	0	0	0	1	0	0	0	0	0	0	0	0	0	0	0	0	0	0	0	0	0	0	0	0	0	0	0	0	0	1
Haliaeetus albicilla (Linnaeus, 1758)	0	0	0	0	0	0	0	0	0	0	1	0	0	0	0	0	0	0	0	0	0	0	0	0	0	0	0	0	0	0	0	0	0	0	0	0	1
Gypaetus barbatus (Linnaeus, 1758)	0	0	0	0	0	0	1	1	0	0	0	0	0	0	0	0	0	0	0	0	0	0	0	0	0	0	0	0	0	0	0	0	0	0	0	0	2
Aegypius monachus (Linnaeus, 1766)	0	0	0	0	0	0	0	1	0	0	0	0	0	0	0	0	0	0	0	0	0	0	0	0	0	0	0	0	0	0	0	0	0	0	0	0	1
Gyps fulvus (Hablizl, 1783)	0	0	0	0	0	0	0	1	0	0	0	0	0	0	0	0	0	1	0	0	0	0	0	0	0	0	0	0	1	0	0	0	0	0	0	0	3
Falco tinnunculus Linnaeus, 1758	0	0	0	0	0	0	1	0	0	0	0	0	0	0	0	0	0	1	0	1	0	0	0	0	0	0	0	0	1	0	0	0	0	0	0	0	4
Falco rusticolus Linnaeus, 1758	0	0	0	0	0	0	0	0	0	0	0	0	0	0	0	0	0	0	1	0	0	0	0	0	0	0	0	0	0	0	0	0	0	0	0	0	1
Bubo bubo (Linnaeus, 1758)	0	0	0	0	0	0	0	1	0	1	1	0	0	0	0	0	0	1	1	0	0	0	0	0	0	0	0	0	1	0	0	0	0	0	0	0	6
Athene noctua (Scopoli, 1769)	0	0	0	0	0	0	0	1	0	1	1	0	0	0	0	0	0	0	0	1	0	0	1	0	0	0	0	1	1	0	0	0	0	0	0	0	7
Strix aluco Linnaeus, 1758	0	0	0	0	0	0	0	0	0	1	0	0	0	0	0	0	0	0	0	1	0	0	0	0	0	0	0	0	0	0	0	0	0	0	0	0	2
Tyto alba (Scopoli, 1769)	0	0	0	0	0	0	0	0	0	0	0	0	0	0	0	0	0	1	0	0	0	0	0	0	0	0	0	0	0	0	0	0	0	0	0	0	1
Asio flammeus (Potoppidan, 1763)	0	0	0	0	0	0	0	0	0	1	0	0	0	0	0	0	0	1	0	0	0	0	0	0	0	0	0	0	0	0	0	0	0	0	0	0	2
Pterocles orientalis (Linnaeus, 1758)	0	0	0	0	0	0	0	0	0	1	0	0	0	0	0	0	0	0	0	0	0	0	0	0	0	0	0	0	0	0	0	0	0	0	0	0	1
Streptopelia turtur (Linnaeus, 1758)	0	0	0	0	0	0	0	0	0	0	0	0	0	0	0	0	0	0	0	0	0	0	0	0	0	0	0	1	0	0	0	0	0	0	0	0	1

Columba livia Gmelin, 1789	0	0	0	0	0	0	0	0	0	1	1	0	0	0	0	0	0	1	0	1	0	0	1	1	0	0	0	0	1	0	0	0	0	0	0	0		7
Columba palumbus Linnaeus, 1758	0	0	0	0	0	0	0	1	0	0	1	0	0	0	0	0	0	0	0	0	1	0	0	0	0	0	0	0	1	1	0	0	0	0	0	0		5
Ciconia sp. Linnaeus, 1758	0	0	0	0	0	0	0	0	0	0	1	0	0	0	0	0	0	0	0	0	0	0	0	0	0	0	0	0	0	0	0	0	0	0	0	0		1
Egretta garzetta (Linnaeus, 1766)	0	0	0	0	0	0	0	0	0	0	0	0	0	0	0	0	0	0	0	0	0	0	0	0	0	0	0	0	1	0	0	0	0	0	0	0		1
Ardea alba Linnaeus, 1758	0	0	0	0	0	0	0	0	0	0	1	0	0	0	0	0	0	0	0	0	0	0	0	0	0	0	0	0	0	0	0	0	0	0	0	0		1
Pyrrhocorax pyrrhocorax (Linnaeus, 1758)	0	0	0	0	0	0	0	1	0	1	0	0	0	0	0	0	0	0	1	0	1	1	1	1	1	0	0	0	0	1	0	0	0	0	0	0		9
Pyrrhocorax graculus (Linnaeus, 1766)	0	0	0	0	0	0	0	1	0	1	1	0	0	0	0	0	0	1	1	1	0	1	1	0	0	0	0	0	0	0	0	0	0	0	0	0		8
Coloeus monedula (Linnaeus, 1758)	0	0	0	0	0	0	1	0	0	1	1	0	0	0	0	0	0	1	0	1	1	1	1	0	0	0	0	0	1	0	0	0	0	0	0	0		9
Corvus corax (Linnaeus, 1758)	0	0	0	0	0	0	0	1	0	1	0	0	0	0	0	0	0	0	1	1	0	0	1	0	0	0	0	0	1	0	0	0	0	0	0	0		6
Corvus corone Linnaeus, 1758	0	0	0	0	0	0	0	0	0	1	1	0	0	0	0	0	0	1	0	1	0	0	0	0	0	0	0	0	1	0	0	0	0	0	0	0		5
Corvus frugilegus Linnaeus, 1758	0	0	0	0	0	0	0	0	0	0	0	0	0	0	0	0	0	1	0	1	0	0	0	0	0	0	0	1	0	0	0	0	0	0	0	0		3
Corvus antecorax Mourer-Chauviré, 1975	0	0	0	0	0	0	0	0	0	0	1	0	0	0	0	0	0	0	0	0	0	0	0	0	0	0	0	0	0	0	0	0	0	0	0	0		1
Pica pica (Linnaeus, 1758)	0	0	0	0	0	0	0	1	0	1	1	0	0	0	0	0	0	1	0	1	0	0	0	0	0	0	0	1	0	0	0	0	0	0	0	0		6
Garrulus glandarius (Linnaeus, 1758)	0	0	0	0	0	0	0	0	0	1	0	0	0	0	0	0	0	0	0	1	1	0	0	0	0	0	0	0	0	0	0	0	0	0	0	0		3
Turdus iliacus Linnaeus, 1766	0	0	0	0	0	0	0	0	0	0	0	0	0	0	0	0	0	1	0	1	0	0	0	0	0	0	0	0	0	0	0	0	0	0	0	0		2
Turdus pilaris Linnaeus, 1758	0	0	0	0	0	0	0	0	0	1	0	0	0	0	0	0	0	1	0	1	0	0	0	0	0	0	0	0	0	0	0	0	0	0	0	0		3
Turdus philomelos Brehm, 1831	0	0	0	0	0	0	0	0	0	1	0	0	0	0	0	0	0	0	0	1	0	0	0	0	0	0	0	0	0	0	0	0	0	0	0	0		2
Turdus merula Linnaeus, 1758	0	0	0	0	0	0	0	0	0	1	0	0	0	0	0	0	0	1	0	1	0	0	0	0	0	0	0	0	0	0	0	0	0	0	0	0		3
Picus sharpei (Saunders, 1872)	0	0	0	0	0	0	0	0	0	0	1	0	0	0	0	0	0	0	0	1	0	0	0	0	0	0	0	0	0	0	0	0	0	0	0	0		2
Cyanopica cooki Bonaparte, 1850	0	0	0	0	0	0	0	0	0	0	0	0	0	0	0	0	0	0	0	1	0	0	0	0	0	0	0	0	0	0	0	0	0	0	0	0		1
Sturnus unicolor Temminck, 1820	0	0	0	0	0	0	0	0	0	1	0	0	0	0	0	0	0	0	0	0	0	0	0	0	0	0	0	0	0	0	0	0	0	0	0	0		1
Sturnus vulgaris Linnaeus, 1758	0	0	0	0	0	0	1	0	0	1	0	0	0	0	0	0	0	0	0	0	0	0	0	0	0	0	0	0	0	0	0	0	0	0	0	0		2
Carduelis carduelis (Linnaeus, 1758)	0	0	0	0	0	0	0	0	0	0	0	0	0	0	0	0	0	0	0	1	0	0	0	0	0	0	0	0	0	0	0	0	0	0	0	0		1
Passer sp.	0	0	0	0	0	0	0	0	0	1	0	0	0	0	0	0	0	0	0	0	0	0	0	0	0	0	0	0	0	0	0	0	0	0	0	0		1
Ptyonoprogne rupestris (Scopoli, 1769)	0	0	0	0	0	0	0	0	0	0	0	0	0	0	0	0	0	0	0	1	0	0	0	0	0	0	0	0	0	0	0	0	0	0	0	0		1
Motacilla alba Linnaeus, 1758	0	0	0	0	0	0	0	0	0	0	0	0	0	0	0	0	0	0	0	0	0	0	1	0	0	0	0	0	0	0	0	0	0	0	0	0		1
Caprimulgus europaeus Linnaeus, 1758	0	0	0	0	0	0	0	0	0	0	1	0	0	0	0	0	0	0	0	1	0	0	0	0	0	0	0	0	0	0	0	0	0	0	0	0		2
Cuculus canorus Linnaeus, 1758	0	0	0	0	0	0	0	0	0	0	0	0	0	0	0	0	0	1	1	0	0	0	0	0	0	0	0	0	1	0	0	0	0	0	0	0		3
Erinaceus europaeus Linnaeus, 1758	0	0	0	0	0	0	1	0	0	1	0	0	0	0	0	0	0	1	1	0	0	0	0	0	0	0	0	1	1	0	0	0	0	0	0	0		6
Crocidura russula Hermann, 1780	0	0	0	0	0	0	1	0	0	1	1	1	0	0	0	0	0	0	0	0	0	0	0	0	0	0	0	0	1	0	0	0	1	1	0	0		7

Crocidura suaveolens Pallas, 1811	0	0	0	0	0	0	1	0	0	1	0	0	0	0	0	0	0	0	0	0	0	0	0	0	0	0	0	0	0	1	0	0	0	0	0	0	0		3
Sorex sp.	0	0	0	0	0	0	0	0	0	0	0	1	0	0	0	0	0	0	0	0	0	0	0	0	0	0	0	0	0	0	0	0	0	0	0	0	0		1
Sorex granarius Miller, 1910	0	0	0	0	0	0	1	0	0	0	0	0	0	0	0	0	0	0	0	0	0	0	0	0	0	0	0	0	0	0	0	0	0	0	0	0	0		1
Sorex araneus Linnaeus, 1758	0	0	0	0	0	0	0	0	0	0	0	0	0	0	0	0	0	0	0	0	0	0	0	0	0	0	0	0	0	0	0	0	0	1	0	0	0		1
Talpa occidentalis Cabrera, 1907	0	0	0	0	0	0	1	0	0	1	0	1	0	0	0	0	0	0	0	0	0	0	0	0	0	0	0	0	1	1	0	0	0	1	0	0	0		6
Galemys kormosi (Shereuder, 1940)	0	0	0	0	0	0	0	0	0	0	0	0	0	0	0	0	0	0	0	0	0	0	0	0	0	0	0	0	0	0	0	0	0	0	0	1	0		1
Galemys pyrenaicus Geoffroy, 1811	0	0	0	0	0	0	0	0	0	1	1	0	0	0	0	0	0	0	0	0	0	0	0	0	0	0	0	0	0	0	0	0	0	0	0	0	0		2
Rinolophus ferrumequinun (Shereber, 1774)	0	0	0	0	0	0	0	0	0	0	1	1	0	0	0	0	0	1	0	0	0	0	0	0	0	0	0	0	0	1	0	0	0	0	0	0	0		4
Rinolophus hipposideros (Bechstein, 1800)	0	0	0	0	0	0	0	0	0	0	0	1	0	0	0	0	0	0	0	0	0	0	0	0	0	0	0	0	0	1	0	0	0	0	0	0	0		2
Rinolophus meheleyi Matschie, 1901	0	0	0	0	0	0	0	0	0	0	0	1	0	0	0	0	0	0	0	0	0	0	0	0	0	0	0	0	0	0	0	0	0	0	0	0	0		1
Rinolophus euryale Blasius, 1853	0	0	0	0	0	0	0	0	0	0	0	1	0	0	0	0	0	0	0	0	0	0	0	0	0	0	0	0	0	1	0	0	0	0	0	0	0		2
Myotis myotis (Borkhausen, 1797)	0	0	0	0	0	0	0	0	0	1	1	1	0	0	0	0	0	0	0	0	0	0	0	0	0	0	0	0	0	1	0	0	0	0	0	0	0		4
Myotis blythi (Tomes, 1857)	0	0	0	0	0	0	0	0	0	0	0	0	0	0	0	0	0	0	0	0	0	0	0	0	0	0	0	0	0	1	0	0	0	0	0	0	0		1
Myotis nattereri (Khul, 1818)	0	0	0	0	0	0	0	0	0	0	0	0	0	0	0	0	0	0	0	0	0	0	0	0	0	0	0	0	0	1	0	0	0	0	0	0	0		1
Myotis mystacinus Khul, 1817	0	0	0	0	0	0	0	0	0	1	0	0	0	0	0	0	0	0	0	0	0	0	0	0	0	0	0	0	0	0	0	0	0	0	0	0	0		1
Nyctalus sp. Bowdich, 1825	0	0	0	0	0	0	0	0	0	0	0	1	0	0	0	0	0	0	0	0	0	0	0	0	0	0	0	0	0	0	0	0	0	0	0	0	0		1
Plecotus sp. Geoffroy, 1818	0	0	0	0	0	0	0	0	0	0	0	1	0	0	0	0	0	0	0	0	0	0	0	0	0	0	0	0	0	0	0	0	0	0	0	0	0		1
Miniopterus schreibersi (Khul, 1819)	0	0	0	0	0	0	0	0	0	0	1	1	0	0	0	0	0	0	0	0	0	0	0	0	0	0	0	0	0	1	0	0	0	0	0	0	0		3
Vespertilio murinus Linnaeus, 1758	0	0	0	0	0	0	0	0	0	0	0	0	0	0	0	0	0	1	0	0	0	0	0	0	0	0	0	0	0	0	0	0	0	0	0	0	0		1
Pipistrellus sp. Kaup, 1829	0	0	0	0	0	0	0	0	0	0	1	1	0	0	0	0	0	0	0	0	0	0	0	0	0	0	0	0	0	0	0	0	0	0	0	0	0		2
Apodemus sylvaticus (Linnaeus, 1758)	0	0	0	0	0	0	1	1	0	1	0	1	0	0	0	0	0	0	0	0	0	0	0	0	0	0	0	0	0	0	0	0	1	0	1	1	0		7
Apodemus flavicollis (Melchior, 1834)	0	0	0	0	0	0	0	0	0	0	1	0	0	0	0	0	0	0	0	0	0	0	0	0	0	0	0	0	0	1	0	0	0	0	0	0	0		2
Sciurus vulgaris Linnaeus, 1758	0	1	0	0	0	0	1	0	0	0	0	0	0	0	0	0	0	0	0	0	0	0	0	0	0	0	0	0	0	1	0	0	0	0	0	0	0		3
Eliomys quercinus Linnaeus, 1766	0	0	0	0	0	0	0	1	0	0	1	1	0	0	0	0	0	0	0	0	0	1	0	0	0	1	0	0	0	1	0	1	0	1	1	0	0		9
Glis glis (Linnaeus, 1766)	0	0	0	0	0	0	0	0	0	1	0	1	0	0	0	0	0	0	0	0	0	0	0	0	0	0	0	0	0	0	0	0	0	0	0	0	0		2
Allocricetus bursae Schaub., 1930	0	0	0	0	0	0	0	1	0	0	1	1	0	0	0	0	0	0	0	0	0	0	0	0	0	0	0	0	0	0	0	1	0	0	0	0	0		4
Mimomyssp. Forsyth-Major, 1902	0	0	0	0	0	0	0	0	0	0	0	0	0	0	0	0	0	0	0	0	0	0	0	0	0	0	0	0	0	0	0	0	0	0	0	1	0		1
Pliomys sp. Méhely, 1914	0	0	0	0	0	0	0	0	0	0	0	1	0	0	0	0	0	0	0	0	0	0	0	0	0	0	0	0	0	0	0	0	0	0	0	0	0		1
Pliomys episcopalis Méhely, 1914	0	0	0	0	0	0	0	0	0	0	1	0	0	0	0	0	0	0	0	0	0	0	0	0	0	0	0	0	0	0	0	0	0	0	0	0	0		1
Chionomys nivalis Martins, 1842	0	0	0	0	0	0	0	1	0	1	0	0	0	0	0	0	0	0	0	0	0	0	0	0	0	0	0	0	0	0	0	0	0	0	0	0	0		2

Arvicola sapidus Miller, 1908	0	0	0	0	0	0	1	1	0	0	0	1	0	0	0	0	0	0	0	0	0	0	0	0	0	0	0	0	1	0	0	0	0	0	0	0		4
Arvicola amphibious (Linnaeus, 1758)	0	0	0	0	0	0	0	0	0	0	0	1	0	0	0	0	0	0	0	0	1	0	0	0	0	0	0	0	0	0	0	0	0	0	0	0		2
Arvicola cantiana Hinton, 1910	0	0	0	0	0	0	0	0	0	0	0	0	0	0	0	0	0	0	0	0	0	0	0	0	0	0	0	1	0	0	0	0	0	0	0	0		1
Victoriamys chalinei (Alcalde et al., 1981)	0	0	0	0	0	0	0	0	0	0	0	0	0	0	0	0	0	0	0	0	0	0	0	0	0	0	0	0	0	1	0	0	0	0	0	0		1
Microtus lusitanicus (Gerbe, 1879)	0	0	0	0	0	0	1	1	0	0	0	1	0	0	0	0	0	0	0	0	1	0	0	0	1	0	0	0	0	0	0	0	0	1	0	0		6
Microtus duodecimcostatus (de Selys-Longchamps, 1839)	0	0	0	0	0	0	0	1	0	1	0	0	0	0	0	0	0	0	0	0	0	0	0	0	0	0	0	0	1	0	0	0	1	0	0	0		4
Microtus arvalis (Pallas, 1778)	0	0	0	0	0	0	1	1	0	0	0	0	0	0	0	0	0	0	0	0	0	0	0	0	0	0	0	1	0	0	0	0	0	0	0	0		3
Microtus agrestis (Linnaeus, 1761)	0	0	0	0	0	0	1	1	0	1	0	1	0	0	0	0	0	0	0	0	0	0	0	0	0	0	0	0	0	0	0	0	0	0	0	0		4
Iberomys huescarensis Ruiz-Bustos, 1988	0	0	0	0	0	0	0	0	0	0	0	0	0	0	0	0	0	0	0	0	0	0	0	0	0	0	0	0	0	1	0	0	0	0	0	0		1
Iberomys brecciensis Forsyth Major, 1905	0	0	0	0	0	0	0	0	0	0	1	0	0	0	0	0	0	0	0	0	0	0	0	0	0	0	0	1	0	1	0	1	0	0	0	0		4
Iberomys cabrerae (Thomas, 1906)	0	0	0	0	0	0	1	1	0	0	0	1	0	0	0	0	0	0	0	0	0	0	0	0	0	0	0	0	0	0	0	0	0	0	0	0		3
Hystrix cristata Linnaeus, 1758	0	0	0	0	0	0	0	0	0	0	0	0	0	0	0	0	0	0	0	0	0	0	0	0	0	0	0	1	0	0	0	0	0	0	0	0		1
Castor fiber Linnaeus, 1758	0	0	0	0	0	0	0	1	0	0	1	1	0	0	0	0	0	0	0	0	0	0	0	0	0	0	0	0	0	0	0	0	0	0	0	0		3
Prolagus calpensis Major, 1905	0	0	0	0	0	0	0	0	0	0	0	0	0	0	0	0	0	0	0	0	0	0	0	0	0	0	0	0	0	0	0	0	0	0	1	0		1
Lepus granatensis Rosenhauer, 1856	0	0	0	0	0	0	0	1	0	1	0	0	1	0	0	0	0	0	0	0	1	0	0	0	1	0	0	0	1	0	0	0	0	0	0	0		6
Oryctolagus cuniculus (Linnaeus, 1758)	0	1	0	0	1	1	1	1	1	1	1	0	1	0	0	1	0	1	0	0	1	1	0	0	1	0	0	1	1	1	1	0	1	0	0	1		20
Macaca sylvanus (Linnaeus, 1758)	0	0	0	0	0	0	0	0	0	0	1	0	0	0	0	0	0	0	0	0	0	0	0	0	0	0	0	0	0	0	0	0	0	0	0	0		1
Paleoloxodon antiquus (Falconer & Cautley, 1847)	0	0	1	1	0	0	0	0	1	0	0	0	0	0	0	0	0	1	0	0	0	0	0	0	0	0	0	0	1	0	0	0	0	0	0	0		5
Mammuthus primigenius Blumebach, 1799	0	0	0	0	0	0	0	0	0	0	0	0	0	0	0	1	0	0	0	0	0	0	0	0	0	0	0	0	0	0	0	0	0	0	0	0		1
Stephanorhinus hemitoechus (Falconer, 1859)	1	0	0	0	0	0	0	0	0	0	1	1	0	0	0	0	1	1	0	1	0	0	1	1	0	0	0	1	1	0	0	0	0	0	0	0		10
Equus hydruntinus Regalia, 1905	0	0	0	0	0	0	0	1	0	0	0	0	0	0	0	0	0	0	0	0	0	0	0	1	0	0	0	0	0	0	0	0	0	0	0	1		3
Equus ferus (Linnaeus, 1758)	1	0	1	0	1	1	1	1	1	1	1	1	1	0	1	1	1	1	1	1	1	1	0	1	1	0	1	1	1	1	0	0	0	0	0	1		26
Hippopotamus amphibious Linnaeus, 1758	0	0	1	0	0	0	0	0	0	0	0	0	0	0	0	0	0	0	0	0	0	0	0	0	0	0	0	0	0	0	0	0	0	0	0	0		1
Hippopotamus antiquus Desmaret, 1822	0	0	0	1	0	0	0	0	0	0	0	0	0	0	0	0	0	0	0	0	0	0	0	0	0	0	0	0	0	0	1	0	0	0	0	0		2
Sus scrofa Linnaeus, 1758	0	1	0	0	1	0	1	1	0	1	0	1	1	0	0	0	0	1	0	0	0	1	0	1	1	0	0	1	1	0	0	0	1	0	0	1		15
Cervus elaphus Linnaeus, 1758	1	1	1	0	1	1	1	1	1	1	1	1	1	0	1	1	1	1	1	1	1	1	1	1	1	1	1	1	1	1	0	0	1	0	0	1		30
Capreolus capreolus Linnaeus, 1758	0	0	0	0	0	0	1	1	0	1	0	0	1	0	0	0	0	0	0	0	1	0	0	1	1	0	1	0	1	0	0	0	0	0	0	0		9
Dama dama Linnaeus, 1758	0	0	0	0	0	0	0	0	0	0	0	0	0	0	0	1	0	0	0	1	0	1	0	1	0	0	0	0	0	0	0	0	0	0	0	0		4
Dama vallonnetensisDe Lumley et al., 1988	0	0	0	0	0	0	0	0	0	0	1	0	0	0	0	0	0	0	0	0	0	0	0	0	0	0	0	0	0	0	0	0	0	0	0	0		1
Haploidoceros mediterraneus (Bonifay, 1967)	0	0	0	0	0	0	0	0	0	0	1	0	0	0	0	0	0	0	0	0	0	0	0	0	0	0	0	0	0	0	0	0	0	0	0	0		1

Praedama savini (Dawkins, 1887)	0	0	0	0	0	0	0	0	0	0	1	0	0	0	0	0	0	0	0	0	0	0	0	0	0	0	0	0	0	0	0	0	0	0	0		1
Metacervocerus rhenanus (Dubois, 1904)	0	0	0	0	0	0	0	0	0	0	0	0	0	0	0	0	0	0	0	0	0	0	0	0	0	0	0	0	0	0	0	1	0	0	0		1
Eucladoceros sp. Falconer, 1868	0	0	0	0	0	0	0	0	0	0	0	0	0	0	0	0	0	0	0	0	0	0	0	0	0	0	0	0	0	0	0	1	0	0	0		1
Bos primigenius Bojanus, 1827	1	0	0	0	0	1	1	0	1	1	0	0	0	0	0	0	0	1	0	1	0	0	1	1	0	0	1	1	1	0	0	0	0	1	0	1		14
Capra pyrenaica Schinz, 1838	0	0	0	0	1	1	0	1	0	1	1	1	1	0	1	1	0	0	0	1	0	1	0	1	1	0	0	1	1	0	0	0	0	0	0	1		16
Rupicapra pyrenaica Bonaparte, 1845	0	1	0	0	0	0	0	1	0	1	0	0	0	0	0	0	0	0	0	0	0	0	0	1	1	0	0	0	0	0	0	0	0	0	0	0		5
Canis lupus Linnaeus, 1758	0	0	0	0	0	1	1	1	0	1	1	1	1	0	0	1	0	1	1	1	0	1	1	1	1	0	0	1	0	0	0	0	0	0	0	1		17
Cuon priscus Thenius, 1954	0	0	0	0	0	0	0	0	0	0	1	0	0	0	0	0	0	0	0	0	0	0	0	0	0	0	0	0	0	0	0	0	0	0	0	0		1
Cuon alpinus Pallas, 1811	0	0	0	0	0	0	0	0	0	0	0	0	0	0	0	0	0	0	0	0	0	0	0	0	0	0	0	1	0	0	0	0	0	0	0	0		1
Vulpes vulpes (Linnaeus, 1758)	0	0	0	0	0	1	1	1	1	1	0	1	1	0	0	0	0	1	1	0	0	0	0	1	1	0	0	1	1	0	0	0	0	0	0	1		14
Ursus deningeri Von Reichenau, 1904	0	0	0	0	0	0	0	0	0	0	1	0	0	0	0	0	0	0	0	0	0	0	0	0	0	0	0	0	0	0	0	0	0	0	0	0		1
Ursus arctos Linnaeus, 1758	1	0	0	0	0	0	0	1	0	1	0	1	1	0	0	0	1	1	0	1	0	1	0	1	1	0	1	1	1	0	0	0	0	0	0	0		14
Mustela sp. Linnaeus, 1758	0	0	0	0	0	0	0	0	0	0	0	0	0	0	0	0	0	1	0	0	0	0	0	0	0	0	0	0	0	0	0	0	0	0	0	1		2
Martes foina (Erxeleben, 1777)	0	0	0	0	0	0	0	0	0	0	0	0	1	0	0	0	0	0	0	0	0	0	0	0	0	0	0	0	0	0	0	0	0	0	0	0		1
Martes sp. Pinel, 1792	0	0	0	0	0	0	0	0	0	0	0	0	0	0	0	0	0	1	0	0	0	0	0	0	0	0	0	0	1	0	0	0	0	0	0	1		3
Meles meles Linnaeus, 1758	0	0	0	0	0	0	0	1	0	0	0	0	0	0	0	0	0	1	0	0	1	0	0	0	0	0	0	1	0	0	0	0	0	0	0	0		4
"Hyaena" prisca de Serres, 1828	0	0	0	0	0	0	0	0	0	0	0	0	0	0	0	0	0	1	0	0	0	0	0	0	0	0	0	0	0	0	0	0	0	0	0	0		1
Crocuta crocuta (Erxleben, 1777)	1	0	0	0	1	0	0	1	1	0	0	1	1	0	0	0	0	0	0	1	0	1	1	1	0	1	1	1	1	0	0	0	0	0	0	0		14
Felis silvestris Schreber, 1777	0	0	0	0	0	1	0	1	0	1	0	1	1	1	0	0	0	1	0	1	0	1	1	1	1	0	0	1	1	0	0	0	0	0	0	1		15
Lynx sp. Kerr, 1792	0	0	0	0	0	1	0	1	0	1	1	1	0	0	1	1	0	1	1	1	0	0	1	1	1	0	1	1	1	0	0	0	0	0	0	1		17
Panthera pardus Linnaeus, 1758	1	0	0	0	0	0	0	1	0	0	0	1	0	0	0	0	0	1	1	0	0	1	0	1	1	0	0	1	1	0	0	0	0	0	0	0		10
Panthera spelaea Goldfuss, 1810	1	0	0	0	0	0	0	0	0	0	0	1	0	0	0	0	0	0	0	0	0	0	0	1	0	0	0	1	1	0	0	0	0	0	0	1		6
Panthera uncia Goldfuss, 1811	0	0	0	0	0	0	0	0	0	0	0	0	0	1	0	0	0	0	0	0	0	0	0	0	0	0	0	0	0	0	0	0	0	0	0	0		1
Homotherium latidens Owen, 1846	0	0	1	0	0	0	0	0	0	0	0	0	0	0	0	0	0	0	0	0	0	0	0	0	0	0	0	0	0	0	0	0	0	0	0	0		1
																																						3,31
Total species per site	8	5	7	2	6	9	26	40	7	58	49	37	13	2	4	8	4	53	14	45	13	15	18	20	17	3	6	33	86	4	7	3	10	12	3	15	**18,39**	

2025

DARÍO ESTRAVIZ-LÓPEZ

PLEISTOCENE VERTEBRATES FROM PORTUGAL: PALEOBIODIVERSITY, PALEOECOLOGY AND QUALITY OF THE FOSSIL RECORD